Studies in Environmental Science 63

# ATMOSPHERIC DEPOSITION
## IN RELATION TO ACIDIFICATION AND EUTROPHICATION

J.W. Erisman
G. P.J. Draaijers


ELSEVIER

# ATMOSPHERIC DEPOSITION
## IN RELATION TO ACIDIFICATION AND EUTROPHICATION

This Page Intentionally Left Blank

Studies in Environmental Science 63

# ATMOSPHERIC DEPOSITION
## IN RELATION TO ACIDIFICATION AND EUTROPHICATION

**J.W. Erisman**

**G.P.J. Draaijers**

*National Institute of Public Health and the Environment*
*Air Research Laboratory, Bilthoven, The Netherlands*

1995
ELSEVIER
Amsterdam – Lausanne – New York – Oxford – Shannon – Tokyo

ELSEVIER SCIENCE B.V.
Sara Burgerhartstraat 25
P.O. Box 211, 1000 AE Amsterdam, The Netherlands

ISBN 0-444-82247-X



This book is printed on acid-free paper.

Printed in The Netherlands

**Studies in Environmental Science**

Other volumes in this series

1 **Atmospheric Pollution 1978** edited by M.M. Benarie
2 **Air Pollution Reference Measurement Methods and Systems** edited by T. Schneider, H.W. de Koning and L.J. Brasser
3 **Biogeochemical Cycling of Mineral-Forming Elements** edited by P.A. Trudinger and D.J. Swaine
4 **Potential Industrial Carcinogens and Mutagens** by L. Fishbein
5 **Industrial Waste Management** by S.E. Jørgensen
6 **Trade and Environment: A Theoretical Enquiry** by H. Siebert, J. Eichberger, R. Gronych and R. Pethig
7 **Field Worker Exposure during Pesticide Application** edited by W.F. Tordoir and E.A.H. van Heemstra-Lequin
8 **Atmospheric Pollution1980** edited by M.M. Benarie
9 **Energetics and Technology of Biological Elimination of Wastes** edited by G. Milazzo
10 **Bioengineering,Thermal Physiology and Comfort** edited by K. Cena and J.A. Clark
11 **Atmospheric Chemistry. Fundamental Aspects** by E. Mészáros
12 **Water Supply and Health** edited by H. van Lelyveld and B.C.J. Zoeteman
13 **Man under Vibration. Suffering and Protection** edited by G. Bianchi, K.V. Frolov and A. Oledzki
14 **Principles of Environmental Science and Technology** by S.E. Jørgensen and I. Johnsen
15 **Disposal of Radioactive Wastes** by Z. Dlouhý
16 **Mankind and Energy** edited by A. Blanc-Lapierre
17 **Quality of Groundwater** edited by W. van Duijvenbooden, P. Glasbergen and H. van Lelyveld
18 **Education and Safe Handling in Pesticide Application** edited by E.A.H. van Heemstra-Lequin and W.F. Tordoir
19 **Physicochemical Methods for Water and Wastewater Treatment** edited by L. Pawlowski
20 **Atmospheric Pollution 1982** edited by M.M. Benarie
21 **Air Pollution by Nitrogen Oxides** edited by T. Schneider and L. Grant
22 **Environmental Radioanalysis** by H.A. Das, A. Faanhof and H.A. van der Sloot
23 **Chemistry for Protection of the Environment** edited by L. Pawlowski, A.J. Verdier and W.J. Lacy
24 **Determination and Assessment of Pesticide Exposure** edited by M. Siewierski
25 **The Biosphere: Problems and Solutions** edited by T.N. Veziroğlu
26 **Chemical Events in the Atmosphere and their Impact on the Environment** edited by G.B. Marini-Bettòlo
27 **Fluoride Research 1985** edited by H. Tsunoda and Ming-Ho Yu
28 **Algal Biofouling** edited by L.V. Evans and K.D. Hoagland
29 **Chemistry for Protection of the Environment 1985** edited by L. Pawlowski, G. Alaerts and W.J. Lacy
30 **Acidification and its Policy Implications** edited by T. Schneider
31 **Teratogens: Chemicals which Cause Birth Defects** edited by V. Kolb Meyers
32 **Pesticide Chemistry** by G. Matolcsy, M. Nádasy and Y. Andriska
33 **Principles of Environmental Science and Technology (second revised edition)** by S.E. Jørgensen and I. Johnsen

34 **Chemistry for Protection of the Environment 1987** edited by L. Pawlowski, E. Mentasti, W.J. Lacy and C. Sarzanini
35 **Atmospheric Ozone Research and its Policy Implications** edited by T. Schneider, S.D. Lee, G.J.R. Wolters and L.D. Grant
36 **Valuation Methods and Policy Making in Environmental Economics** edited by H. Folmer and E. van Ierland
37 **Asbestos in Natural Environment** by H. Schreier
38 **How to Conquer Air Pollution. A Japanese Experience** edited by H. Nishimura
39 **Aquatic Bioenvironmental Studies: The Hanford Experience, 1944–1984** by C.D. Becker
40 **Radon in the Environment** by M. Wilkening
41 **Evaluation of Environmental Data for Regulatory and Impact Assessment** by S. Ramamoorthy and E. Baddaloo
42 **Environmental Biotechnology** edited by A. Blazej and V. Privarová
43 **Applied Isotope Hydrogeology** by F.J. Pearson Jr., W. Balderer, H.H. Loosli, B.E. Lehmann, A. Matter, Tj. Peters, H. Schmassmann and A. Gautschi
44 **Highway Pollution** edited by R.S. Hamilton and R.M. Harrison
45 **Freight Transport and the Environment** edited by M. Kroon, R. Smit and J.van Ham
46 **Acidification Research in The Netherlands** edited by G.J. Heij and T. Schneider
47 **Handbook of Radioactive Contamination and Decontamination** by J. Severa and J. Bár
48 **Waste Materials in Construction** edited by J.J.J.M. Goumans, H.A. van der Sloot and Th.G. Aalbers
49 **Statistical Methods in Water Resources** by D.R. Helsel and R.M. Hirsch
50 **Acidification Research: Evaluation and Policy Applications** edited by T.Schneider
51 **Biotechniques for Air Pollution Abatement and Odour Control Policies** edited by A.J. Dragt and J. van Ham
52 **Environmental Science Theory. Concepts and Methods in a One-World, Problem-Oriented Paradigm** by W.T. de Groot
53 **Chemistry and Biology of Water, Air and Soil. Environmental Aspects** edited by J. Tölgyessy
54 **The Removal of Nitrogen Compounds from Wastewater** by B. Halling-Sørensen and S.E. Jørgensen
55 **Environmental Contamination** edited by J.-P. Vernet
56 **The Reclamation of Former Coal Mines and Steelworks** by I.G. Richards, J.P. Palmer and P.A. Barratt
57 **Natural Analogue Studies in the Geological Disposal of Radioactive Wastes** by W. Miller, R. Alexander, N. Chapman, I. McKinley and J. Smellie
58 **Water and Peace in the Middle East** edited by J. Isaac and H. Shuval
59 **Environmental Oriented Electrochemistry** edited by C.A.C. Sequeira
60 **Environmental Aspects of Construction with Waste Materials** edited by J.J.J.M. Goumans, H.A. van der Sloot and Th. G. Aalbers.
61 **Caracterization and Control of Odours and VOC in the Process Industries** edited by S. Vigneron, J. Hermia, J. Chaouki
62 **Nordic Radioecology. The Transfer of Radionuclides through Nordic Ecosystems to Man** edited by H. Dahlgaard

# PREFACE

In the early 1980s, the problem of acidification was acknowledged on a governmental level in the Netherlands as posing a major environmental threat. The concern for damage to forests and ecosystems, and materials and monuments, as well as for acidification of soils and moorland pools stimulated research and policy development. Acid deposition was used as a characterisation of the atmospheric input leading to these effects. As such, wet and dry deposition of acids, and dry deposition of acid precursors as sulphur dioxide and nitrogen oxides, were considered. At the same time, the important role of ammonia in the acidification of soils and moorland pools was acknowledged. Ammonia, the most important acid neutralising component in the atmosphere, was shown to be nitrified to an important extent in soil into nitric acid, thereby contributing to acidification. This led to the concept of potential acid deposition, in which the deposition of actual acid ($H^+$) was added to that of potential acid (ammonia + ammonium). Moreover, the role of atmospheric nitrogen input was recognised as a disturbing factor for natural ecosystems and forests growing on poor soils.

In Europe critical loads have been widely accepted as a basis for control strategies for regional air pollution. The use of critical loads for ecosystem studies and abatement strategies requires relevant deposition data to describe the atmospheric input to the ecosystem. The knowledge of deposition processes and the possibility of making relevant and accurate deposition estimates are important issues in the work of long-range transport modelling in Europe. Large-scale dispersion and deposition of air pollution emitted in different countries above Europe needs to be assessed correctly to serve as a relevant basis for abatement strategies. On the local scale, the large variations in deposition to landscape, and in sensitivity between landscape elements, make it essential to compare the actual deposition with the site-specific critical load to determine the exceedance value. This is even more important for those areas where high sensitivity is linked to high inputs.

The Dutch Priority Programme on Acidification Research, which was started in 1985, aimed at the following fields of research:
- the relationship between occurrence and effects of acidification on plants in their natural environments (air, soil), in particular the effects on forests, heather and crops;

- ammonia emissions and the deposition of SOx, NOy and NHx, along with emission abatement techniques;
- derivation of critical loads and levels for forest and heathland ecosystems, and estimation of the effectiveness of abatement measures in decreasing the effects.

In this book the research efforts in this programme directed at atmospheric deposition are summarised. These efforts relate to the approach to generalising deposition estimates using models and measurements to meet the local and large-scale demands. Although most research efforts described are of Dutch origin, it has been our endeavour to put the research into a broader perspective by summarising the state of knowledge on the processes affecting atmospheric deposition in Europe. This has resulted in detailed deposition maps for the Netherlands and Europe. Highlighted are the evaluation and applicability of the programme's results. Although the work described in this book is related to components relevant in the issue of acidification, the methods can be used for other components related to other environmental issues as well.

This book was written to collect the results of a large quantity of research in, for example, the Netherlands, which has already been published as parts of books and as articles in international journals. It is intended for anyone involved in research related to atmospheric deposition; i.e. not only those who measure or model atmospheric deposition or ecologists interested in exposure from atmospheric deposition, but also policy-makers and students.

It was Thomas Way who wrote in 1855[1]:

*'.. the quantity at any time present in the air must merely have relation to the distance of time at which it was last swept from it by rain, and takes no account of that which the soil has in the meanwhile appropriated. To be perfect, these experiments should be made simultaneously on the ammonia in the air and in the rain, and that absorbed by a given extent of surface-soil. This is a labour that we can hardly expect from any one experimenter; and considering the great varieties of soil, the result would even then be but an approximation to the truth.'*

Although we will attempt in this book to provide estimates of the atmospheric input to different types of vegetation and soil, we are forced to conclude that despite 140 years of research the results presented here are even now only an approximation of the truth.

*Acknowledgements*

The work presented in this book is that of many persons working in the field of atmospheric pollution and deposition. Several have contributed directly or indirectly to (parts of) the book. We are very grateful for their contributions and acknowledge specifically Addo van Pul, who contributed to Chapters 4, 5 and 6; Jan Duyzer, Marcel Mennen, Walter Ruigrok and Paul Wyers for their contribution to Chapter 4 and 7; Albert Bleeker, Hans van Jaarsveld, Erik van Leeuwen, and Charlos Potma for their contribution to Chapter 5 and 6; Peter Hofschreuder,

[1] J.T. Way (1855), *J. Roy. Agr. Soc.*,**16**,265-266

Niek van Leeuwen and Ferdinand Römer, who contributed to parts of Chapter 4 and, finally, Bertus van den Beld, Dries Boxman, Harrie van Dijk, Remco van Ek, Bernard van de Elzakker, Jos Hogenkamp, Edith van Putten, Fred Römer, Eveliene Steingröver, Willem Uiterwijk and Wim de Vries for their contribution to Chapter 7.

Although no direct contribution was made by following persons, we are grateful for their support, advice and suggestions, and fine co-operation over the past years: Roel van Aalst, Willem Asman, Dennis Baldocchi, Claus Beier, Erik Berge, Wladimir Bleuten, Fred Bosveld, Ed Buijsman, Peter Burrough, Ludger van der Eerden, Anton Eliassen, David Fowler, Hans van Grindsven, Karin Hansen, Gerrit Heil, Bruce Hicks, Bert-Jan Heij, Wilfried Ivens, Leon Janssen, Steve Lindberg, Gun Lövblad, Harriet Marseille, Rob Meyers, Elsbeth Pinksterboer, Jan Roelofs, Marcel Schaap, Sjaak Slanina, Stan Smeulders, Till Spranger, Mark Sutton, Gijs van Tol, Aart Vermetten and Bo Wiman.

EMEP is kindly acknowledged for providing the EMEP model results which are used in Chapter 5 for modelling the small scale deposition in Europe. The project management of the Dutch Priority Programme on Acidification Research is acknowledged for their financial support and their encouragement during recent years. EUROTRAC is also acknowledged for providing and stimulating the interaction and communication between scientists in Europe in the important field of air pollution.

Ruth de Wijs-Christenson did a fine job editing the book, whereas Dirk Onderdelinden and Frank de Leeuw carefully read through the manuscript and made useful comments and suggestions. Thanks for the final touch!

And last but not least, without the support of Elsbeth and Saskia we probably would never have had the chance to complete this work: thanks!

*To the memory of*
*Nettie Draaijers-Paulussen*

# CONTENTS

**PREFACE** ..... vii

**CONTENTS** ..... xi

**LIST OF FIGURES** ..... xix

**LIST OF TABLES** ..... xxvii

**NOMENCLATURE** ..... xxxi

**CHAPTER 1 GENERAL INTRODUCTION** ..... 1

*Introduction* ..... 1

**1.1 INTRODUCTION TO THE ISSUE OF ACIDIFICATION** ..... 1
*Dutch Priority Programme on Acidification* ..... 3

**1. 2 HISTORY OF ATMOSPHERIC DEPOSITION RESEARCH** ..... 8
1.2.1 NITROGEN COMPOUNDS ..... 9
*Wet deposition* ..... 9
*Dry deposition* ..... 11
1.2.2 SULPHUR COMPOUNDS ..... 12
*Wet deposition* ..... 12
*Dry deposition* ..... 14
1.2.3 THROUGHFALL MEASUREMENTS ..... 15
1.2.4 LONG-RANGE TRANSPORT ..... 15
1.2.5 SYNTHESIS ..... 17

**1.3 ATMOSPHERIC DEPOSITION RESEARCH IN THE NETHERLANDS ..... 18**

**1.4 OBJECTIVES AND OUTLINE OF THE BOOK ..... 20**

**CHAPTER 2 EMISSION, TRANSFORMATION AND TRANSPORT ..... 23**

***Introduction*** ..... **23**

**2.1 EMISSION OF NITROGEN AND SULPHUR COMPOUNDS ..... 23**
2.1.1 ATMOSPHERIC SULPHUR AND NITROGEN COMPOUNDS ..... 24
2.1.2 EMISSIONS ..... 24
2.1.3 EVOLVEMENT OF ANTHROPOGENIC EMISSIONS SINCE 1900 ..... 26
*Emissions between 1900 and 1990* ..... 26
*Emissions in the Netherlands and Europe during recent years* ..... 28

**2.2 ATMOSPHERIC CHEMISTRY ..... 30**
$SO_2$ ..... 32
$NOx$ ..... 32
$NH_3$ ..... 33

**2.3 FACTORS AFFECTING TRANSPORT ..... 34**

**2.4 LONG-RANGE TRANSPORT MODELLING ..... 39**

**2.5 SPATIAL VARIATION IN CONCENTRATION ..... 41**
2.5.1 THE NETHERLANDS ..... 41
2.5.2 EUROPE ..... 43

**CHAPTER 3 DEPOSITION PROCESSES AND MEASUREMENT ..... 49**

***Introduction*** ..... **49**

**3.1 WET DEPOSITION ..... 49**
3.1.1 PROCESS DESCRIPTION ..... 49
3.1.2 MEASURING METHODS ..... 51

**3.2 DRY DEPOSITION ..... 55**
3.2.1 PROCESS DESCRIPTION ..... 55
3.2.2 FRAMEWORKS FOR THE DESCRIPTION OF ATMOSPHERE - SURFACE EXCHANGE ..... 57
*Resistance analogy for trace gases* ..... 57
*Particles* ..... 60

3.2.3 MEASURING METHODS FOR DRY DEPOSITION ..... 62
*Micrometeorological methods for estimating dry deposition* ..... 62
*Surface wash methods to estimate dry deposition* ..... 72
*Watershed mass balance method* ..... 74
*Inferential technique* ..... 74
*Chamber methods* ..... 74

**3.3 CLOUD AND FOG DEPOSITION AND DEW ..... 76**
3.3.1 PROCESS DESCRIPTION ..... 76
3.3.2 MEASURING METHODS ..... 76

**3.4 EVALUATION AND COMPARISON OF DIFFERENT METHODS FOR ESTIMATING DEPOSITION ..... 78**
3.4.1 WET DEPOSITION ..... 78
3.4.2 DRY DEPOSITION ..... 78
*Sulphur* ..... 79
*Nitrogen* ..... 80
*Base cations* ..... 81
3.4.3 CLOUD AND FOG DEPOSITION ..... 82

**3.4.3 SYNTHESIS ..... 83**
*Process-oriented studies* ..... 83
*Evaluation of models* ..... 83
*Detection of trends* ..... 84

**CHAPTER 4 MEASUREMENT RESULTS AND DRY DEPOSITION ..... 85**

***Introduction*** ..... **85**

**4.1 MEASUREMENT RESULTS ..... 85**
4.1.1 $SO_2$ ..... 85
*Physiological Control* ..... 86
*Physico-chemical control* ..... 86
*Deposition to soil and litter* ..... 88
4.1.2 NOx ..... 89
4.1.3 HNOx ..... 90
4.1.4 PAN ..... 91
4.1.5 $NH_3$ ..... 91
4.1.6 HCl ..... 93
4.1.7 PARTICLES ..... 93
4.1.8 METEORITES ..... 94

**4.2 SURFACE RESISTANCE PARAMETRISATIONS ..... 98**
*Introduction* ..... 98
4.2.1 SURFACE RESISTANCE PARAMETERISATION FOR GASES ..... 98
*Stomatal and mesophyll resistance* ..... 99
*External leaf uptake* ..... 100
*In-canopy transport* ..... 104
*Deposition to soil and water surfaces* ..... 105
4.2.2 PARTICLES ..... 107
4.2.3 SYNTHESIS ..... 109
*Uncertainties* ..... 111

**CHAPTER 5 GENERALISATION OF DEPOSITION ..... 113**

***Introduction*** ..... **113**

**5.1 LOCAL-SCALE DEPOSITION MAPS, WHAT'S THE USE? ..... 114**

**5.2 DEPOSITION MODELLING IN THE NETHERLANDS ..... 116**
5.2.1 DEADM ..... 116
5.2.2 WET DEPOSITION ..... 118
*Dry deposition in bulk samplers* ..... 118
*Neutral salts* ..... 118
*Calculation procedure* ..... 119
*Wet deposition estimates* ..... 120
5.2.3 DRY DEPOSITION ..... 122
*Roughness length maps* ..... 122
*Dry deposition of acidifying components* ..... 128
*Dry base cation deposition* ..... 132
5.2.4 TOTAL DEPOSITION ..... 136
*Acidifying components* ..... 136
*Total base cation deposition* ..... 141

**5.3 DEPOSITION MODELLING IN EUROPE ..... 146**
5.3.1 EDACS ..... 146
5.3.2 WET DEPOSITION ..... 147
*Data collection and data quality* ..... 148
*Interpolation* ..... 149
*Description of spatial patterns* ..... 150
5.3.3 DRY DEPOSITION ..... 157
*Acidifying components* ..... 157
*Dry base cation deposition* ..... 161
5.3.4 TOTAL DEPOSITION ..... 164

*Acidifying components* ..... 164
*Base cations* ..... 172

**5.4 VARIATION IN DEPOSITION OVER SEVERAL YEARS ..... 176**
5.4.1 DEPOSITION AS A RESULT OF NATURAL SOURCES ..... 176
5.4.2 HISTORICAL MEASUREMENTS OF WET DEPOSITION ..... 177
*Nitrogen compounds* ..... 177
*Sulphur* ..... 181
*Base cations* ..... 182
*The Netherlands* ..... 183
5.4.3 NON-LINEARITIES IN TEMPORAL VARIATIONS ..... 188

**5.5 SYNTHESIS ..... 193**

**CHAPTER 6 EVALUATION OF DEPOSITION ESTIMATES ..... 195**

***Introduction*** ..... **195**

**6.1 EVALUATION OF SURFACE EXCHANGE PARAMETERS FOR $SO_2$ ..... 196**
6.1.2 EXPERIMENTAL PROCEDURE ..... 196
*Deciduous forest* ..... 196
*Coniferous forest* ..... 196
*Grassland* ..... 197
*Heathland* ..... 197
6.1.3 MODELLED $V_D$ COMPARED WITH MEASUREMENTS ..... 198
6.1.4 DISCUSSION ..... 204
*Uncertainties* ..... 205
*Comparison with other parameterisations* ..... 208
*Representativeness of parameterisation for European pollution climates* ..... 208
6.2.5 SYNTHESIS ..... 209

**6.2 RELATION BETWEEN ATMOSPHERIC DEPOSITION AND SOIL LOADS 211**
*Introduction* ..... 211
6.2.1 THEORETICAL CONSIDERATIONS REGARDING CANOPY EXCHANGE 212
6.2.2 RESEARCH RESULTS FROM THE SPEULDER FOREST SITE ..... 213
*Throughfall fluxes at the Speulder forest* ..... 213
*Atmospheric deposition at the Speulder forest* ..... 213
*Comparison of throughfall fluxes with atmospheric deposition estimates* ..... 216
*Canopy exchange processes in the Speulder forest* ..... 216
*Synthesis* ..... 219
6.2.3 THROUGHFALL FLUXES COMPARED TO DEADM DEPOSITION ESTIMATES ..... 220

*Acidifying components* ..... 220
*Base cations* ..... 222

**6.3 UNCERTAINTY IN DEADM RESULTS ..... 225**
6.3.1 DRY DEPOSITION MEASUREMENTS ..... 225
6.3.2 COMPARISON WITH OTHER MODEL RESULTS ..... 228
6.3.3 ESTIMATION OF UNCERTAINTY RANGES ..... 230
*Wet deposition* ..... 231
*Dry deposition* ..... 233
*Total deposition* ..... 236

**6.4 UNCERTAINTY IN THE EDACS RESULTS ..... 238**
6.4.2 WET DEPOSITION ..... 238
*Total uncertainty in the wet deposition maps* ..... 243
6.4.2 DRY DEPOSITION ..... 244
6.4.3 TOTAL DEPOSITION ..... 245

**6.5 GENERAL SYNTHESIS ..... 248**

**CHAPTER 7 THREE CASE STUDIES ..... 253**

***Introduction*** ..... **253**

**7.1 THE ELSPEETSCHE VELD EXPERIMENT ON SURFACE EXCHANGE OF TRACE GASES ..... 254**
7.1.1 INTRODUCTION ..... 254
7.1.2 STUDY AREA AND METHODS ..... 254
*Study area* ..... 254
*Measurement methods and approach* ..... 255
7.1.3 CALCULATION OF DEPOSITION PARAMETERS ..... 256
$SO_2$ ..... 256
$NO_2$ ..... 259
$NH_3$ ..... 259
*Throughfall and stemflow* ..... 262
*Co-deposition of $SO_2$ and $NH_3$* ..... 264
7.1.4 CONCLUSIONS ..... 265

**7.2 THE UTRECHTSE HEUVELRUG EXPERIMENT ON THE IMPACT OF CANOPY STRUCTURE AND FOREST EDGE EFFECTS ON DEPOSITION ..... 267**
7.2.1 INTRODUCTION ..... 267
7.2.2 METHODS ..... 269
*Study area* ..... 269

*Throughfall and bulk precipitation sampling procedure* ..... 272
*Canopy and edge structure measurements* ..... 274
7.2.3 THE IMPACT OF CANOPY STRUCTURE: RESULTS AND DISCUSSION .. 280
*Evaluation of canopy structure parametrisation* ..... 280
*Relationships between dry deposition and canopy structure* ..... 283
*Predicting net throughfall using simple regression models with canopy structure and information on pollution climate* ..... 288
7.2.4 THE IMPACT OF FOREST EDGES: RESULTS AND DISCUSSION ..... 290
*Evaluation of canopy structure parametrisation* ..... 290
*Dry deposition gradients in the forest edges* ..... 292
*Impact of canopy/edge structure and edge aspect* ..... 298
*The impact of edge effects on dry deposition amounts to forests in the Netherlands* . 303
7.2.5 CONCLUSIONS ..... 307
*The impact of forest canopy structure on deposition amounts* ..... 307
*The impact of forest edge effects on deposition amounts* ..... 308

**7.3 THE SPEULDER FOREST EXPERIMENTS TO DETERMINE THE INPUT AND RELATED IMPACTS TO DOUGLAS FIR ..... 310**
7.3.1 INTRODUCTION ..... 310
*Deposition research* ..... 310
*Assessment of relations between loads/levels and effects* ..... 311
7.3.2 SITE DESCRIPTION ..... 312
7.3.3 RESEARCH PROJECTS ..... 313
7.3.4 DEPOSITION MONITORING OF GASEOUS COMPONENTS ..... 314
*Introduction* ..... 314
*Experimental procedure* ..... 314
*Theory and interpretation* ..... 315
*Dry deposition parameters for the Speulder forest* ..... 316
7.3.5 THE AEROSOL PROJECT ..... 325
*Introduction* ..... 325
*Experimental set-up* ..... 326
*Experimental determination of the acidifying aerosol and base cation input onto Speulder forest* ..... 329
*Modelling particle deposition* ..... 331
7.3.6 ANNUAL AVERAGE GAS AND PARTICLE DEPOSITION AND CHANGES WITH TIME ..... 338
7.3.7 ASSESSMENT OF THE EFFECTS OF ACIDIFICATION, EUTROPHICATION AND OZONE ..... 341
*Critical levels and loads at the Speulder forest site* ..... 341
*Effect parameters and observed effects* ..... 344
*Synthesis* ..... 345

7.3.8 CONCLUSIONS ..... 350
*Gaseous deposition* ..... 350
*Deposition of particles* ..... 351
*Assessment of the relation between loads/levels and effects* ..... 353
7.3.9 EVALUATION ..... 355

**REFERENCES** ..... **357**

**INDEX** ..... **397**

# LIST OF FIGURES

**FIGURE 1.1** Pattern of rainfall acidity in Europe based on EMEP measurements (EMEP, 1988) ..... 2
**FIGURE 1.2** Intensity of defoliation for all species, or conifers only in 1988. Percentage of trees in classes 1-4 (>10% defoliation) ..... 4
**FIGURE 1.3** Cause and effect chain studied in the DPA (Heij and Schneider, 1991). ..... 5
**FIGURE 1.4** Schematic representation of deposition ..... 6
**FIGURE 2.1** Emissions of sulphur dioxide, nitrogen oxides and ammonia in Europe from 1900 to 1990 (mton $a^{-1}$) compiled by De Leeuw (1994) ..... 27
**FIGURE 2.2** Emissions of sulphur dioxide, nitrogen oxides and ammonia in USA from 1900 to 1990 (mton $a^{-1}$) (NAPAP, 1992) ..... 27
**FIGURE 2.3** Annual average total $SO_2$, NOx and $NH_3$ emissions in the Netherlands ..... 29
**FIGURE 2.4** Atmospheric chemistry for trace gases in the troposphere. ..... 31
**FIGURE 2.5** Schematic representation of the main circulation types above western and central Europe. The location of the high pressure area is indicated by dots. The arrows give the tracking direction of depressions as well as the mean direction of the wind in the higher air layers. Generally, the characters represent the main direction of the circulation (e.g. SE = southeast); Ww = bending west circulation, BM = high pressure area above Atlantic ocean - central Europe, HM = high pressure area above central Europe, TM = low pressure area above central Europe (after Van der Ham, 1977). ..... 37
**FIGURE 2.6** Daily variation of the boundary-layer development (Stull, 1988). ..... 38
**FIGURE 2.7** Distribution of annual median $SO_2$ (A) and $NO_2$ (B) concentrations in the Netherlands in 1993 ($\mu g\ m^{-3}$) ..... 42
**FIGURE 2.8** Distribution of annual average $NH_3$ concentrations in the Netherlands in 1993 ($\mu g\ m^{-3}$). ..... 43
**FIGURE 2.9** Annual country average of 50-percentile $SO_2$, $NO_2$, NOx and $O_3$ concentrations, and annual average $NH_3$ ($\mu g\ m^{-3}$) in 1977 - 1993 based on LML measurements (RIVM, 1994) and TREND model calculations (Van Jaarsveld, 1995) ..... 44

**FIGURE 2.10** Annual mean concentration of $SO_2$ (above) and $SO_4^{2-}$ aerosol (below) in 1993 in Europe as calculated by Tuovinen *et al.* (1994) using the EMEP-LTRAP model ..... 45
**FIGURE 2.10** (*continued*) Annual mean concentration of NOx (above) and $HNO_3$ (below) in 1993 in Europe as calculated by Tuovinen *et al.* (1994) using the EMEP-LTRAP model ..... 46
**FIGURE 2.10** (*continued*) Annual mean concentration of $NO_3^-$ aerosol (above) and $NH_3$ (below) in 1993 in Europe as calculated by Tuovinen *et al.* (1994) using the EMEP-LTRAP model ..... 47
**FIGURE 2.10** (*continued*) Annual mean concentration of $NH_4^+$ aerosol in 1993 in Europe as calculated by Tuovinen *et al.* (1994) using the EMEP-LTRAP model ..... 48
**FIGURE 3.1** Wet deposition processes. ..... 50
**FIGURE 3.2** The dry deposition process. ..... 55
**FIGURE 3.3** Schematic representation of four transport mechanisms for particles through the quasi-laminar boundary layer (after Davidson and Wu, 1990). Shaded areas indicate the laminar boundary layer. ..... 61
**FIGURE 3.4** Relationship between the deposition velocity of particles and their mass median diameter for an Eucalyptus forest canopy (after Slinn, 1982). The dashed line indicates the sedimentation velocity (i.e. where the deposition rate is a linear function of the fall velocity of the particles). Canopy height = 27.4 m; friction velocity = 75 cm $s^{-1}$; roughness length = 1.86 m; zero plain displacement height = 21.6 m; particle density = 1 g $cm^{-3}$. ..... 62
**FIGURE 3.5** Illustration of instrumentation used for flux gradient measurements ..... 70
**FIGURE 3.5** (*continued*) Illustration of instrumentation used for flux gradient measurements ..... 71
**FIGURE 5.1** Frequency distribution of deposition on a small scale (5 x 5 km) within an EMEP grid (150 x 150 km) for nitrogen compounds. Using EMEP model results together with the appropriate filtering factor, we estimate total nitrogen deposition to this grid at 1650 mol $ha^{-1}$ $a^{-1}$. ..... 115
**FIGURE 5.2** Distribution of the acidification areas over the Netherlands. ..... 117
**FIGURE 5.3** The spatial distribution of the dry deposition of $SO_4^{2-}$, $NO_3^-$, $NH_4^+$ and total potential acid in 1993 (mol $ha^{-1}$ $a^{-1}$) ..... 121
**FIGURE 5.4** Values for $z_0$ as a function of wind direction sector ($30^0$) and season for the Steeg station (103). ..... 124
**FIGURE 5.5** Values for $z_0$ as a function of wind direction sector ($30^0$) for the Cabauw station (620) estimated by Beljaars (1988) and in this study for summer (A) and winter (B) months ..... 125
**FIGURE 5.6** 1 x 1 km grid average $z_0$ values in the Netherlands: A: 0-60 cm, B: >50 cm. .. 127
**FIGURE 5.7** The spatial distribution of the dry deposition of SOx, NOy, NHx and total potential acid in 1993 (mol $ha^{-1}$ $a^{-1}$) ..... 129
**FIGURE 5.8** Distribution of dry deposition SOx to forest, grassland and water in 1993 in the Netherlands. ..... 130

**FIGURE 5.8** *(continued)* Distribution of dry deposition of NOy and NHx to forest, grassland and water in 1993 in the Netherlands. ..... 131
**FIGURE 5.9** Maps of the dry deposition of $Na^+$ (A), $K^+$ (B), $Mg^{2+}$ (C) and $Ca^{2+}$ (D) in the Netherlands (mol $ha^{-1}$ $a^{-1}$). ..... 133
**FIGURE 5.10** Dry deposition distribution of $Na^+$, $K^+$, $Mg^{2+}$ and $Ca^{2+}$ for forest, grassland and water ..... 134
**FIGURE 5.10** *(continued)* Distribution of dry deposition $Mg^{2+}$ and $Ca^{2+}$ to forest, grassland and water. ..... 135
**FIGURE 5.11** Variation in total SOx, NOy, NHx and potential acid deposition between 1980 and 1993 (mol $ha^{-1}$ $a^{-1}$). ..... 136
**FIGURE 5.12** The spatial distribution of the total deposition of SOx, NOy, NHx and total potential acid in 1980 (mol $ha^{-1}$ $a^{-1}$). ..... 137
**FIGURE 5.13** The spatial distribution of the total deposition of SOx, NOy, NHx and total potential acid in 1993 (mol $ha^{-1}$ $a^{-1}$). ..... 138
**FIGURE 5.14** Contribution of different countries to the deposition in the Netherlands (A) 1980 and (B) 1993. ..... 142
**FIGURE 5.15** Source category contribution to the deposition in the Netherlands (A) 1980 and (B) 1990. ..... 143
**FIGURE 5.16** The spatial distribution of the deposition of Na, K, $Mg^{2+}$ and Ca in 1993 (mol $ha^{-1}$ $a^{-1}$). ..... 145
**FIGURE 5.17** Outline of method to estimate local scale deposition fluxes. ..... 147
**FIGURE 5.18** Location of wet deposition monitoring sites in Europe. ..... 148
**FIGURE 5.19** Wet deposition of $SO_4^{2-}$ in Europe on a 50 x 50 km basis in 1989 in mol $ha^{-1}$ $a^{-1}$ (Van Leeuwen *et al.*, 1995). ..... 151
**FIGURE 5.20** Wet deposition of $NO_3^-$ in Europe on a 50 x 50 km basis in 1989 in mol $ha^{-1}$ $a^{-1}$ (Van Leeuwen *et al.*, 1995) ..... 151
**FIGURE 5.21** Wet deposition of $NH_4^+$ in Europe on a 50 x 50 km basis in 1989 in mol $ha^{-1}$ $a^{-1}$ (Van Leeuwen *et al.*, 1995). ..... 152
**FIGURE 5.22** Wet deposition of $H^+$ in Europe on a 50 x 50 km basis in 1989 in mol $ha^{-1}$ $a^{-1}$ (Van Leeuwen *et al.*, 1995) ..... 152
**FIGURE 5.23** Wet deposition of total base cations ($Ca^{2+}$, $Mg^{2+}$ and $K^+$) in Europe on a 50 x 50 km basis in 1989 in mol $ha^{-1}$ $a^{-1}$ (Van Leeuwen *et al.*, 1995). ..... 153
**FIGURE 5.24** Concentration of $Na^+$ in Europe on a 50 x 50 km basis in 1989 in µmol $l^{-1}$ (Van Leeuwen *et al.*, 1995) ..... 154
**FIGURE 5.25** Concentration of $Cl^-$ in Europe on a 50 x 50 km basis in 1989 in µmol $l^{-1}$ (Van Leeuwen *et al.*, 1995) ..... 155
**FIGURE 5.26** Concentration of $Mg^{2+}$ in Europe on a 50 x 50 km basis in 1989 in µmol $l^{-1}$ (Van Leeuwen *et al.*, 1995) ..... 155
**FIGURE 5.27** Concentration of $Ca^{2+}$ in Europe on a 50 x 50 km basis in 1989 in µmol $l^{-1}$ (Van Leeuwen *et al.*, 1995) ..... 156

**FIGURE 5.28** Concentration of $K^+$ in Europe on a 50 x 50 km basis in 1989 in µmol $l^{-1}$ (Van Leeuwen *et al.*, 1995) ..... 156
**FIGURE 5.29** Land-use map on a $1/6^0$ x $1/6^0$ grid of Europe (Van Velde, 1994) ..... 157
**FIGURE 5.30** Roughness length map (cm) for the summer season (A) and winter season (B) on a $1/6^0$ x $1/6^0$ grid of Europe (Van Pul *et al.*, 1995). ..... 158
**FIGURE 5.31** Dry deposition of SOx in Europe on a $1/6^0$ x $1/6^0$ scale in mol $ha^{-1}$ $a^{-1}$ (Van Pul *et al.*, 1995) ..... 159
**FIGURE 5.32** Dry deposition of NOy in Europe on a $1/6^0$ x $1/6^0$scale in mol $ha^{-1}$ $a^{-1}$ (Van Pul *et al.*, 1995) ..... 160
**FIGURE 5.33** Dry deposition of NHx in Europe on a 1/60 x 1/60 scale in mol ha-1 a-1 (Van Pul et al., 1995) ..... 160
**FIGURE 5.34** Dry deposition of Na+ in Europe on a 1/6 x 1/6o scale in mol ha-1 a-1..... 161
**FIGURE 5.35** Dry deposition of Ca2+ in Europe on a 1/6 x 1/6o scale in mol ha-1 a-1..... 162
**FIGURE 5.36** Dry deposition of Mg2+ in Europe on a 1/6 x 1/6o scale in mol ha-1 a-1..... 162
**FIGURE 5.37** Dry deposition of $K^+$ in Europe on a 1/6 x 1/6° scale in mol $ha^{-1}$ $a^{-1}$. ..... 163
**FIGURE 5.38** Dry deposition of $K^+$ in Europe on a 1/6 x 1/6° scale in mol $ha^{-1}$ $a^{-1}$. ..... 163
**FIGURE 5.39** Total deposition of SOx in Europe on a 1/6 x 1/6° scale in mol $ha^{-1}$ $a^{-1}$ (Van Pul *et al.*, 1995) ..... 164
**FIGURE 5.40** Total deposition of NOy in Europe on a 1/6 x 1/6° scale in mol $ha^{-1}$ $a^{-1}$ (Van Pul *et al.*, 1995) ..... 165
**FIGURE 5.41** Total deposition of NHx in Europe on a 1/6 x 1/6° scale in mol $ha^{-1}$ $a^{-1}$ (Van Pul *et al.*, 1995) ..... 165
**FIGURE 5.42** Total deposition of potential acid in Europe on a 1/6 x 1/6° scale in mol $ha^{-1}$ $a^{-1}$ (Van Pul *et al.*, 1995) ..... 166
**FIGURE 5.43** Emission of SOx, NOy and NHx per country or region in Europe in 1993 expressed in mol $H^+$ $ha^{-1}$ $a^{-1}$ (Tuovinen *et al.*, 1994). ..... 168
**FIGURE 5.44** Deposition of SOx, NOy and NHx per country or region in Europe in 1993 expressed in mol $H^+$ $ha^{-1}$ $a^{-1}$ (Tuovinen *et al.*, 1994). ..... 169
**FIGURE 5.45** Emission and deposition of potential acid per country or region in Europe in 1993 in mol $H^+$ $ha^{-1}$ $a^{-1}$ (Tuovinen *et al.*, 1994) ..... 170
**FIGURE 5.46** Contribution (%) of different source catagories to the total potential acid deposition for different countries in Europe ..... 171
**FIGURE 5.47** Total deposition of $Na^+$ in Europe on a 1/6 x 1/6° scale in mol $ha^{-1}$ $a^{-1}$. ..... 172
**FIGURE 5.48** Total deposition of $Ca^{2+}$ in Europe on a 1/6 x 1/6° scale in mol $ha^{-1}$ $a^{-1}$ ..... 173
**FIGURE 5.49** Total deposition of $Mg^{2+}$ in Europe on a 1/6 x 1/6° scale in mol $ha^{-1}$ $a^{-1}$ ..... 173
**FIGURE 5.50** Total deposition of $K^+$ in Europe on a 1/6 x 1/6° scale in mol $ha^{-1}$ $a^{-1}$ ..... 174
**FIGURE 5.51** Total deposition of base cations ($Ca^{2+}$+$Mg^{2+}$+$K^+$) in Europe on a 1/6 x 1/6° scale in mol $ha^{-1}$ $a^{-1}$ ..... 174
**FIGURE 5.52** Wet deposition of ammonium at Rothamsted (UK) and Montsouris (France) (in kg N $ha^{-1}$ $a^{-1}$) ..... 178

**FIGURE 5.52** *(continued)* Wet deposition of nitrate at Rothamsted (UK) and Montsouris (France) (in kg N $ha^{-1}$ $a^{-1}$ ..... 179
**FIGURE 5.53** Precipitation concentrations of sulphur measured over several years (mg $SO_3$ $l^{-1}$) ..... 181
**FIGURE 5.54** Changes in $Na^+$, $Ca^{2+}$ and $Mg^{2+}$ concentrations in precipitation (mg $l^{-1}$) measured at Leiduin near the Dutch coast. ..... 183
**FIGURE 5.55** Horizontal gradient of wet deposition from the coast land inward as reported by Leeflang (1938). Data are averaged over 5 years (1932 - 1937). ..... 184
**FIGURE 5.56** Time series of $SO_4^{2-}$ concentration measurements in precipitation made at several sites in the Netherlands (mg $l^{-1}$ ..... 185
**FIGURE 5.56** *(continued)* Time series of $NO_3^-$ concentration measurements in precipitation made at several sites in the Netherlands (mg $l^{-1}$ ..... 186
**FIGURE 5.57** Time series of wet deposition measurements made at Witteveen: (A) $SO_4^{2-}$, (B) $NO_3^-$ and (C) $NH_4^+$ (mol $ha^{-1}$ $a^{-1}$). ..... 187
**FIGURE 5.57** Time series of wet deposition measurements made at Witteveen: (A) $SO_4^{2-}$, (B) $NO_3^-$ and (C) $NH_4^+$ (mol $ha^{-1}$ $a^{-1}$). ..... 188
**FIGURE 5.58** Relative change between 1955 and 1990 in measured concentrations of sulphur in air, aerosol and precipitation, and in estimated sulphur emissions in the Netherlands and in Europe, and in ammonia emissions in the Netherlands. ..... 190
**FIGURE 5.59** Temporal variation in wet and dry deposition of sulphur in the Netherlands (mol $ha^{-1}$ $a^{-1}$). ..... 191
**FIGURE 5.60** Ratio of $NH_4^+$ over ($SO_4^{2-}$ plus $NO_3^-$) in precipitation in the Netherlands..... 192
**FIGURE 6.1** Comparison of modelled $V_d$ (m $s^{-1}$) with $V_d$ obtained from measurements: A. Deciduous forest; B. Coniferous forest; C. Grassland and D. Heathland. Solid dots represent average modelled values for class-average measured values. The line represents the 1:1 ratio. Small overbars represent measured class averages ± SD, while large overbars represent modelled averages ± SD. ..... 199
**FIGURE 6.2**. Examples of time series of modelled and measured $V_d$: A. Deciduous forest; B. Coniferous forest ..... 203
**FIGURE 6.2** (*continued*). Examples of time series of modelled and measured $V_d$: C. Grassland and D. Heathland. ..... 204
**FIGURE 6.3** Histograms of modelled (open columns) and measured (dark columns) $V_d$ (m $s^{-1}$): A. Deciduous forest; B. Coniferous forest. ..... 206
**FIGURE 6.3** (*continued*) Histograms of modelled (open columns) and measured (dark columns) $V_d$ (m $s^{-1}$): C. Grassland and D. Heathland ..... 207
**FIGURE 6.4** Throughfall estimates compared to DEADM results for SOx (A), NOy (B), NHx (C) and total potential acid (D) (mol $ha^{-1}$ $a^{-1}$ ) for 21 sites. The 1:1 line is also shown. ..... 221
**FIGURE 6.5** Throughfall estimates compared to DEADM results for SOx (A), NOy (B), NHx (C) and total potential acid (D) (mol $ha^{-1}$ $a^{-1}$ ) for 30 sites. The 1:1 line is also shown. ..... 222

**FIGURE 6.6** Net throughfall estimates compared to DEADM dry deposition estimates for 30 sites for $Na^+$ (A), $Mg^{2+}$ (B), $Ca^{2+}$ (C) and $K^+$ (D) (mol $ha^{-1}$ $a^{-1}$ ). The 1:1 line is also shown. ..... 223
**FIGURE 6.7** Comparison of measured concentrations in Speulder forest (30 m) and those obtained from the model's calculations (50 m). ..... 227
**FIGURE 6.8** Comparison of monthly $V_d$ values calculated with DEADM (50-m height) and measured in Speulder forest (36-m height) (m $s^{-1}$). ..... 227
**FIGURE 6.9** Comparison of TREND model results with estimates from this study (mol $ha^{-1}$ $a^{-1}$). The 1:1 line is shown for comparison. ..... 229
**FIGURE 6.10** Comparison of the country average calculated dry deposition of sulphur using EMEP and EDACS (mol $ha^{-1}$ $a^{-1}$) ..... 245
**FIGURE 6.11** Distribution of the numbered (pollution) regions in Europe in Table 6.13.... 246
**FIGURE 7.1** Time series of parameterized and measured $R_c$ for $SO_2$ at Elspeetsche Veld.. 258
**FIGURE 7.2** Averaged $R_c$ for $NO_2$ over heathland (Elspeetsche Veld) in autumn 1989 (Duyzer *et al.*, 1991). ..... 260
**FIGURE 7.3** Annual average diurnal variations of $F$ and $V_d$ for $NH_3$ ..... 261
**FIGURE 7.4** Surface resistance for $SO_2$ and $NH_3$, relative humidity and surface wetness indicator for the Elspeetsche Veld site, 14-15 September 1991 (Erisman and Wyers, 1993). ..... 262
**FIGURE 7.5** Location of the study area with the 30 throughfall measurement sites and five bulk precipitation measurement sites used to study the impact of canopy structure on dry deposition amounts. ..... 270
**FIGURE 7.6** Location of the study area with the eight forest edge measurement sites and four bulk precipitation measurement sites used to study the impact of edge effects on dry deposition amounts. ..... 271
**FIGURE 7.7** An example of a measurement site showing the area (10 x 10 m) around the throughfall gutter in which tree and stand structure characteristics were determined. The throughfall gutter, indicated as a black bar, is located in the centre of the plot. Grey areas mark the vertical crown projection of individual trees, whereas stem bases are indicated as black circles. The thick line indicates the boundary of the 100 $m^2$ plot. ..... 275
**FIGURE 7.8** Relationship between winter net throughfall fluxes of $SO_4^{2-}$ and the aerodynamic roughness length of the canopy. Douglas fir is indicated by squares, Scots pine by plus signs and oak by dots. The following relationship is valid: [*NTF*- $SO_4^{2-}$ ]=344.9*[$z_o$] +201.3 ($R$=0.84; $p$<0.001). ..... 286
**FIGURE 7.9** Relationship between winter net throughfall fluxes of $NO_3^-$ and the aerodynamic roughness length of the canopy. Douglas fir is indicated by squares, Scots pine by plus signs and oak by dots. The following relationship is valid: [*NTF*-$NO_3^-$]=59.6*[$z_o$] +21.5 ($R$=0.84; $p$<0.001) ..... 286
**FIGURE 7.10** Relationship between winter net throughfall fluxes of $NH_4^+$ and the aerodynamic roughness length of the canopy. Douglas fir is indicated by squares, Scots

pine by plus signs and oak by dots. The following relationship is valid: [*NTF-*$NH_4^+$]=431.0*[$z_o$] +65.5 ($R$=0.88; $p$<0.001) ..... 287
**FIGURE 7.11** Winter net throughfall fluxes of $SO_4^{2-}$ predicted from linear regression models with the roughness length of the canopy, compared to measured winter net throughfall fluxes. Douglas fir is indicated by squares, Scots pine by plus signs and oak by dots... 289
**FIGURE 7.12** Winter net throughfall fluxes of $NO_3^-$ predicted from linear regression models with the roughness length of the canopy, compared to measured winter net throughfall fluxes. Douglas fir is indicated by squares, Scots pine by plus signs and oak by dots... 289
**FIGURE 7.13** Winter net throughfall fluxes of $NH_4^+$ predicted from linear regression models with the roughness length of the canopy, compared to measured winter net throughfall fluxes. Douglas fir is indicated by squares, Scots pine by plus signs and oak by dots... 290
**FIGURE 7.14** Net throughfall flux gradients of $SO_4^{2-}$, $NO_3^-$ and $NH_4^+$ for the eight forest edges. Distance to edge divided by edge height is *x/h* ..... 293
**FIGURE 7.14** *(continued)* Net throughfall flux gradients of $Na^+$, $Cl^-$ and $Mg^{2+}$ for the eight forest edges. Distance to edge divided by edge height is *x/h* ..... 294
**FIGURE 7.14** *(continued)* Net throughfall flux gradients of $Ca^{2+}$ and $K^+$, and gradients of the ratio between throughfall volume and precipitation volume for the eight forest edges. Distance to edge divided by edge height is *x/h* ..... 295
**FIGURE 7.15** 'Ideal' net throughfall flux gradient in a forest edge. ..... 296
**FIGURE 7.16** The percentage to which a particular wind direction contributed to the total pollutant dose of $SO_2$, $SO_4^{2-}$, $NO_2$, NO, $NO_3^-$, and $NH_4^+$ during the measurements, respectively ..... 301
**FIGURE 7.16** *(continued)* The percentage to which a particular wind direction contributed to the total pollutant dose of $Na^+$, $Cl^-$, $Mg^{2+}$, $Ca^{2+}$ and $K^+$, and total air supply during the measurements, respectively ..... 302
**FIGURE 7.17** The percentage to which different size classes contribute to the total number (and area) of forest complexes (left), and to the total number (and area) of individual forest stands in the Netherlands (right). ..... 305
**FIGURE 7.18** Frequency distribution of forest stand heights in the Netherlands. The relatively high percentage observed for height class 0-2 m is the result of the relatively high fraction of timber felling areas and non-afforested silvicultural areas in the Netherlands. ..... 306
**FIGURE 7.19** Relationship between the part of the total area of Dutch forests influenced by edge effects and edge width. The thin line represents this relationship when only edges between forested areas and non-forested areas are taken into account. ..... 307
**FIGURE 7.20** Deposition research at the Speulder forest site. ..... 315
**FIGURE 7.21** Eddy correlation $u*$ measurements at 30 m compared to those measured at 36 m ..... 317
**FIGURE 7.22** Eddy correlation $H$ measure ments at 30 m compared to those measured at 36 m. ..... 318
**FIGURE 7.23** Daily variations of $SO_2$ in $R_c$ for dry and wet surface conditions ..... 320

**FIGURE 7.24** $R_c$ values for $SO_2$ and $NH_3$ from continuous measurements of vertical gradients over the Speulder forest ('Weather' provides information on precipitation: 0=dry; 10=rain). ..... 321
**FIGURE 7.25** Diurnal variation of $V_d$ $NO_2$ and $V_d$ for stomatal uptake for selected measuring periods ..... 323
**FIGURE 7.26** Parameterised values of $V_d$ compared to $V_d$ derived from $NH_3$ gradients for selected measuring periods ($R^2$=0.25 for positive values) ..... 324
**FIGURE 7.27** Experimentally determined $V_d$ versus $u_*$. $V_d$ values were estimated at the following heights: fog at 28 m; $NO_3^-$ and $SO_4^{2-}$ (TNO) at 35 m; $SO_4^{2-}$ (ECN) at 22 m and $^{214}Pb$ at 19 m. ..... 330
**FIGURE 7.28** Summary of modelled deposition velocities versus $u_*$. $V_d$ values were estimated at the following heights: fog at 28 m; $NO_3^-$ and $SO_4^{2-}$ (TNO) at 35 m; $SO_4^{2-}$ (ECN) at 22 m and $^{214}Pb$ at 19 m ..... 336

# LIST OF TABLES

**TABLE 2.1** Total $SO_2$, NOx and $NH_3$ emissions in the world and on European and American scales separated into natural and anthropogenic emissions (Whelpdale, 1987) ..... 25
**TABLE 2.2** Source contribution of sulphur dioxide, nitrogen oxides, and ammonia to anthropogenic emissions (Hov *et al.*, 1987; Asman, 1992) ..... 25
**TABLE 2.3** Emissions of reduced sulphur compounds to the atmosphere in Tg (S) $a^{-1}$ ..... 26
**TABLE 2.4** Dutch total annual emissions 1980 - 1993 expressed in kton $SO_2$, kton $NO_2$ for NOx ..... 28
**TABLE 2.5** Overview of the ammonia emission in the Netherlands from 1980 to 1993 ..... 30
**TABLE 2.6** Annual average concentrations of acidifying components measured for the Netherlands in 1993 ($\mu g\ m^{-3}$) ..... 43
**TABLE 3.1** Ratios of wet deposition fluxes obtained by wet-only and bulk samplers according to Ridder *et al.* (1984) and Van Leeuwen *et al.* (1995) ..... 53
**TABLE 3.2** Precipitation monitoring networks in Europe ..... 54
**TABLE 3.3** Schmidt and Prandtl number correction in Eqn. 6 for several gases (Hicks *et al.*, 1987) ..... 60
**TABLE 4.1** The number of meteorites above a certain mass retrieved by the earth's surface as predicted by Hughes (1992) ..... 95
**TABLE 4.2** Internal resistance, $R_i$, to be used for estimating the stomatal resistance for different seasons and land-use types using Eqn. (4.4), with entities of 9999 indicating no air—surface exchange via that resistance pathway (Adopted from Wesely, 1989) ..... 100
**TABLE 4.3** Average $R_c$ values for $SO_2$ and $NH_3$ observed under different conditions; negative values denote emissions (Erisman and Wyers, 1993) ..... 102
**TABLE 4.4** $R_{ext}$ for $NH_3$ ($s\ m^{-1}$) over different vegetation categories in Europe, negative values for $R_{ext}$ denote emission for estimating a net upward flux ..... 103
**TABLE 4.5** $R_c$ values for soil surfaces, snow-covered surfaces and water surfaces (negative values denote emission) ..... 107
**TABLE 4.6** Parametrisations of $E$ values for different components and conditions ..... 108

**TABLE 4.7** Surface resistances for different gases during daytime under different pollution climates. ..... 110
**TABLE 5.1** Number of grid cells (10 x 10 km) in the Netherlands with median critical loads, divided into classes, and the average and standard deviation of the acid loads for the grid cells in each class ..... 114
**TABLE 5.2** Country average dry, wet and total deposition of SOx, NOy, NHx, total nitrogen and potential acid in 1980 - 1993 (mol $ha^{-1}$ $a^{-1}$) ..... 122
**TABLE 5.3** Individual roughness elements as $z_0$ values, with $h$ = the average tree height in m ..... 127
**TABLE 5.4** Average deposition to forests in the Netherlands in 1993 (mol $ha^{-1}$ $a^{-1}$) ..... 128
**TABLE 5.5** Deposition of SOx, NOy, NHx, total nitrogen and total potential acid deposition for each acidification area in the Netherlands in 1980 (mol $ha^{-1}$ $a^{-1}$) ..... 139
**TABLE 5.6** Deposition of SOx, NOy, NHx, total nitrogen and total potential acid deposition for each acidification area in the Netherlands in 1993 (mol $ha^{-1}$ $a^{-1}$) ..... 140
**TABLE 5.7** Dry, wet and total deposition of base cations for each acidification area in the Netherlands in 1993 (mol $ha^{-1}$ $a^{-1}$) ..... 144
**TABLE 5.8** Background wet, dry and total deposition in the Netherlands (mol $H^+$ $ha^{-1}$ $a^{-1}$). 177
**TABLE 6.1** Average, minimum and maximum measured parameters, and measured and modelled $V_d$, $F$ and $R_c$ values, with correlation coefficients between modelled and measured values, as well as SD (in parentheses ..... 200
**TABLE 6.2** Average dry deposition velocities (m $s^{-1}$) and correlation coefficients between modelled and measured $V_d$ for dry/wet and daytime and night-time periods, with SD in parentheses ..... 202
**TABLE 6.3** Average net throughfall fluxes, and dry and fog deposition estimates for the Speulder forest, along with wet deposition at Speulder Veld (mol $ha^{-1}a^{-1}$) ..... 214
**TABLE 6.4** Comparison of net throughfall fluxes with atmospheric deposition (% difference calculated as in Table 6.1) for four periods for which complete wash-off of deposited material was expected ..... 216
**TABLE 6.5** Canopy uptake or leaching in Speulder forest estimated using results of different experiments (+ = uptake; - = leaching; 0 = inert or negligible; x = not estimated) ..... 218
**TABLE 6.6** Throughfall estimates and total deposition estimates averaged over different locations (mol $ha^{-1}$ $a^{-1}$) ..... 220
**TABLE 6.7** Net throughfall estimates and dry deposition estimates averaged over 30 different locations (mol $ha^{-1}$ $a^{-1}$) ..... 224
**TABLE 6.8** Flux measurements and estimates for different locations in the Netherlands in mol $ha^{-1}$ $a^{-1}$ using different methods ..... 226
**TABLE 6.9** Average dry deposition fluxes ) for the Speulder forest (mol $ha^{-1}$ $a^{-1}$) based on measurements (November 1992 - September 1993) and calculated using DEADM (January 1993 - September 1993 ..... 228
**TABLE 6.10** Total systematic uncertainty (%) in yearly average total deposition flux on different spatial scales for all individual components (1993) ..... 233

**TABLE 6.11** Range in annual average $R_c$ values (s $m^{-1}$) for forests, heathland and agricultural areas ..... 235
**TABLE 6.12** Summary of total uncertainty in wet deposition per average grid cell of 50 x 50 km for different areas in the conservative and the worst cases ..... 243
**TABLE 6.13** Uncertainty of key factors influencing deposition estimates of S and oxidised and reduced N in different pollution regions in Europe ..... 247
**TABLE 7.1** Overview of methods and equipment used during the Elspeetsche Veld experiment. ..... 255
**TABLE 7.2** Criteria for acceptance of observations and no. of observations rejected (total no. of measurements: 5298 two hourly average periods). ..... 256
**TABLE 7.3** Average $SO_2$ $R_c$ (4 m) values (± uncertainty estimates) for selected daytime and night-time and dry and wet conditions at Elspeetsche Veld. ..... 257
**TABLE 7.4** Annual average dry deposition parameters for $SO_2$ at Elspeetsche Veld (4 m height). For the resistances the harmonic averages (± uncertainty estimates) are presented. ..... 259
**TABLE 7.5** Annual average $SO_4$, $NO_3$ and $NH_4$ throughflow fluxes and bulk deposition (mol $ha^{-1}$ $a^{-1}$). The standard deviation is given between brackets (Bobbink *et al.*, 1990). ..... 263
**TABLE 7.6** Overview of stand structure characteristics of the 30 forest stands ..... 281
**TABLE 7.7** Overview of stand structure characteristics of single tree species ..... 282
**TABLE 7.8** Mean dimensions of needles from Douglas fir and Scots pine trees, with *SD* in parentheses (n = 150) ..... 283
**TABLE 7.9** Correlation matrix between net throughfall fluxes and canopy structure characteristics for the 30 forest stands ..... 284
**TABLE 7.10** Interrelationships between the individual canopy structure characteristics of the 30 forest stands ..... 287
**TABLE 7.11** Canopy and edge structure characteristics of the eight forest edges, showing averages of 7 or 8 recordings (structure characteristics were determined around each throughfall gutter) with the exception of porosity and the roughness length of the upwind terrain ..... 291
**TABLE 7.12** Whole-edge integrated net throughfall enhancement (*WEINTE*) factors for the eight forest edges ($x$ = mean of all edges) ..... 297
**TABLE 7.13** Ratio between the net throughfall flux at $x/h = 0.25$ and that at $x/h = 5$ for the eight forest edges ..... 298
**TABLE 7.14** Correlation matrix between whole-edge integrated net throughfall enhancement (*WEINTE*) factors and canopy/edge structure characteristics for the eight forest edges 299
**TABLE 7.15** Whole-edge integrated net throughfall enhancement (*WEINTE*) factors in relation to the edge aspect ..... 303
**TABLE 7.16** Soil chemical and texture data for the Speulder forest (Van Breemen and Verstraten, 1991) ..... 313
**TABLE 7.17** Correction factor for flux profile functions over the Speulder forest (Bosveld, 1991). ..... 316

**TABLE 7.18** Selection criteria for gradients measured over the Speulder forest and the percentage of measurements left after selection (total remaining: 2345 hours of continuous $SO_2$ measurements, 220 hours $NO_2$ measurements and 756 hours continuous $NH_3$) ..... 319
**TABLE 7.19** Average deposition parameters for $SO_2$, with standard deviations in parentheses ..... 320
**TABLE 7.20** Average deposition parameters for $NH_3$, with standard deviations in parentheses ..... 325
**TABLE 7.21** An overview of experiments performed at the Speulder forest site to quantify particle dry deposition ..... 329
**TABLE 7.22** Characteristic features of some models describing the dry deposition of particles to vegetation and water surfaces (Ruijgrok *et al.*, 1994) ..... 331
**TABLE 7.23** Component specific-size distributions (mass median diameter, *MMD*, and geometrical standard deviation, $\sigma_g$) derived from measurements in the Netherlands .... 334
**TABLE 7.24** Model performance indicators[a] and averages for the different comparison studies ..... 335
**TABLE 7.25** Average uptake and leaching amounts at the Speulder forest derived from field experiments and modelling (mol $ha^{-1}$ $a^{-1}$) (Draaijers *et al.*, 1994) ..... 337
**TABLE 7.26** Average fluxes at Speulder forest in 1987-1993 (mol $ha^{-1}$ $a^{-1}$) ..... 339
**TABLE 7.27** Estimates of the deposition of acidifying components between 1950 and 1994 for the Speulder forest site (mol $ha^{-1}$ $a^{-1}$) ..... 340
**TABLE 7.28** Critical levels for forests in Europe ..... 342
**TABLE 7.29** Critical acid loads for Speulder forest based on different effects (mol $ha^{-1}$ $a^{-1}$) ..... 343
**TABLE 7.30** Critical N loads for Speulder forest based on different effects (mol $ha^{-1}$ $a^{-1}$) .. 343
**TABLE 7.31** Possible effects on forest ecosystems of increased atmospheric N+S loading and exposure to $SO_2$, NOx, $NH_3$ and/or $O_3$ ..... 345
**TABLE 7.32** Critical loads, exceedances and effects observed at Speulder forest ..... 347

# NOMENCLATURE

*Symbols*

| | |
|---|---|
| *AOT40* | accumulative exposure over a threshold concentration |
| *BAI* | Bark Area Inex |
| *cpa* | crown projection area |
| $c$ | pollutant concentration |
| $C_D$ | drag coefficient |
| $c_p$ | specific heat of air at constant pressure (cal $g^{-1}$ $°C^{-1}$) |
| $c_v$ | scaling parameter of the standard deviation of the lateral wind fluctuations on $u_*$ |
| $d$ | displacement height (m) |
| *d1-d5* | dry deposition factors for open samplers |
| $D$ | diffusion coefficient ($m^2$ $s^1$) |
| *DOSEEXP* | percentage of the total pollutant dose supplied with wind directions exposed to the forest edge |
| $E$ | particle collection efficiency |
| *ET AL* | edge area |
| $F$ | pollutant flux (mol $ha^{-1}$ $a^{-1}$) |
| *FBM* | fractional bias of mean |
| *FBV* | fractional bias of variance |
| $g$ | accelaration due to gravity (m $s^{-2}$) |
| $H$ | sensible heat flux (W $m^{-2}$) |
| $h$ | vegetation height (m) |
| $K_{m,h,c}$ | turbulent diffusion coefficient (eddy diffusivity): m=momentum; h=heat; c=gas or exchange ($m^2$ $s^{-1}$) |
| $K_H$ | Henry coefficient (mol $l^{-1}$ $atm^{-1}$) |
| $K_i$ | reaction rate |
| $l$ | mixing length or mean eddy size at a given height (m) |
| $L$ | Monin Obukhov length (m) |
| *LAI* | Leaf Area Index ($m^2$ $m^{-2}$) |
| *LWC* | Liquid Water Content |

| | |
|---|---|
| $M$ | molecular weight |
| $MMD$ | Mass Median Diameter (μm) |
| $NMSE$ | normalised mean square error |
| $NTF$ | net throughfall |
| $Pr$ | Prandtl number (=0.72) |
| $Q$ | global radiation (W $m^{-2}$) |
| $Q_a$ | relative errors |
| $rh$ | relative humidity (%) |
| $R$ | correlation coefficient |
| $R_a$ | aerodynamic resistance (s $m^{-1}$) |
| $R_b$ | laminar layer resistance (s $m^{-1}$) |
| $R_c$ | surface resistance (s $m^{-1}$) |
| $R_{cuticle}$ | cuticular resistance (s $m^{-1}$) |
| $R_{ext}$ | external resistance (s $m^{-1}$) |
| $R_i$ | internal leaf resistance (s $m^{-1}$) |
| $R_{inc}$ | in-canopy resistance (s $m^{-1}$) |
| $R_m$ | mesophyll resistance (s $m^{-1}$) |
| $R_{soil}$ | soil resistance (s $m^{-1}$) |
| $R_{stom}$ | stomatal resistance (s $m^{-1}$) |
| $R_{wat}$ | surface water resistance (s $m^{-1}$) |
| $Rn$ | net radiation (W $m^2$) |
| $SA$ | sapwood area ($m^2$) |
| $SD$ | standard deviation |
| $S_a$ | absolute errors |
| $Sc$ | Schmidt number |
| $t$ | time (h) |
| $T$ | temperature (°C) |
| $TNA$ | total needle area ($m^2$) |
| $TA$ | total area |
| $T_s$ | surface temperature (°C) |
| $u$ | wind speed (m $s^{-1}$) |
| $u_h$ | wind speed at canopy height (m $s^{-1}$) |
| $u*$ | friction velocty (m $s^{-1}$) |
| $V_d$ | deposition velocity (m $s^{-1}$) |
| $V_{ds}$ | surface deposition velocity (m $s^{-1}$) |
| $V_{dt}$ | turbulent deposition velocity (m $s^{-1}$) |
| $V_s$ | sedimentation velocity (m $s^{-1}$) |
| $WEINTE$ | whole edge integrated net throughfall enhancement factor |
| $w$ | mean vertical wind speed (m $s^{-1}$) |
| $w'$ | instantaneous fluctuations about the mean wind speed (m $s^{-1}$) |
| $x$ | distance to forest edge |

| | |
|---|---|
| $z$ | height (m) |
| $z_i$ | boudary-layer height (m) |
| $z_0$ | roughness length (m) |
| $z_{0c}$ | roughness length appropriate for a pollutant (m) |
| $z_{0t}$ | grid average $z_0$ value (m) |

*Greek symbols*

| | |
|---|---|
| $\alpha_\eta$ | stability correction factor |
| $\beta$ | number of preceding dry hours |
| $\kappa$ | von Karman constant (=0.41) |
| $\theta$ | wind direction ($^o$) |
| $\rho$ | density of an entity (kg $m^{-3}$) |
| $\rho'$ | fluctuations about the mean |
| $\rho_a$ | air density (kg $m^{-3}$) |
| $\sigma_\theta$ | standard deviation of wind direction (rad) |
| $\sigma_v$ | standard deviation of lateral wind (rad) |
| $\tau$ | momentum flux (N $m^{-1}$) |
| $\psi_c$ | stability correction function: concentration |
| $\psi_h$ | stability correction function: heat |
| $\psi_m$ | stability correction function: momentum |

*Abbreviations*

| | |
|---|---|
| DAS | Dutch Acidification System model |
| DFM | Deposition Filter Method |
| DPA | Dutch Programme on Acidification |
| DEADM | Dutch Emperical Deposition Model |
| ECMWF | European Centre for Medium-range Weather Forecast |
| EDACS | European Deposition of Acidifying Compounds estimated on a Small scale |
| EMEFS | Eulerian Model Evaluation Field Studies |
| GIS | Geographical Information System |
| GPCP | Global Precipitation Chemistry Project |
| LML | National Air Quality Monitoring Network |
| LTRAP | Long Range Transport |
| ODS | Observational Data Set |
| RAINS | Regional Acidification Information and Simulation model |
| RADM | Regional Acid Deposition Model |

*Names of institutes*

| | |
|---|---|
| CBS | Central Bureau for Statistics, Voorburg |
| ECN | Netherlands Energy Research Foundation, Petten |
| EMEP | European Monitoring and Evaluation Program |
| EPA | Environmental Protection Agengy (USA) |
| KEMA | The Electric Power Research Institute, Arnhem |
| KNMI | Royal Dutch Meteorological Institute, de Bilt |
| KUN | Catholic University Nijmegen |
| RIVM | National Institute of Public Health and Environmental Protection, Bilthoven |
| RUU | University of Utrecht, Utrecht |
| TNO | Netherlands Organization for Applied Scientific Research, Delft |
| WAU | Wageningen Agricultural University |

# CHAPTER 1 GENERAL INTRODUCTION

*Introduction*
The deposition of potentially damaging chemicals from the atmosphere to ecosystems is an undesirable consequence of air pollution. In the Netherlands, as elsewhere in Europe and North America, there is great and growing concern about the effects of airborne pollution and the accelerating acidification and or eutrophication of the natural environment. The regional distribution of affected ecosystems provides strong empirical evidence for a causal link to acid deposition (Last and Watling, 1991). There are many hypotheses which attempt to relate air pollution, for example, to forest decline but it has proved difficult to demonstrate cause and effect between acid deposition and ecosystem damage or change due to the co-occurrence of natural stresses (e.g. drought, pathogenic insects and fungi) and anthropogenic stresses (e.g. air pollution, climatic change, management practices). Furthermore, exposure to other gases such as ozone and deposition of, for example, heavy metals might also be important. The mechanisms of damage are insufficiently understood; also, the actual exposure to wet and dry deposited pollutants have been found difficult to define. In this chapter some background information will be given on the issue of acidification, followed by a brief overview of the history of atmospheric deposition research. The chapter will be concluded with the objectives and an outline of this book.

## 1.1 INTRODUCTION TO THE ISSUE OF ACIDIFICATION

The term 'acid rain' or 'acid deposition', which covers the whole range of physical, chemical and biological processes involved in the issue of acidification, has evolved gradually. Strictly speaking, the term 'acid rain' refers to precipitation more acid than in remote areas. The term 'acid rain' was first encountered in 1858, when the effect of the atmosphere on stones, bricks and mortar was described (cf. Smith, 1872):
*'It has often been observed that the stones and bricks of buildings, especially under projecting parts, crumble more readily in large towns, where much coal is burnt, than elsewhere. Although this is not sufficient to prove an evil of the highest magnitude, it is still*

*worthy of observation, first as a fact, and next as affecting the value of property. I was led to attribute this effect to the slow, but constant action of the acid rain. If it affects substances with so great an excess of silica, it will not be expected that calcareous substances will resist it long, and one of the greatest evils in old buildings in Manchester is the deterioration of the mortar.'*

It has been shown from rainfall acidity measurements that precipitation more acid than in remote areas occurs in the industrialised regions of the world. pH values range from 4.0 in central Europe and North America to 6.3 in India and Australia (Figure 1.1). In remote areas of the world, the average pH in rain is about 5.6 (Sisteron *et al.*, 1989).

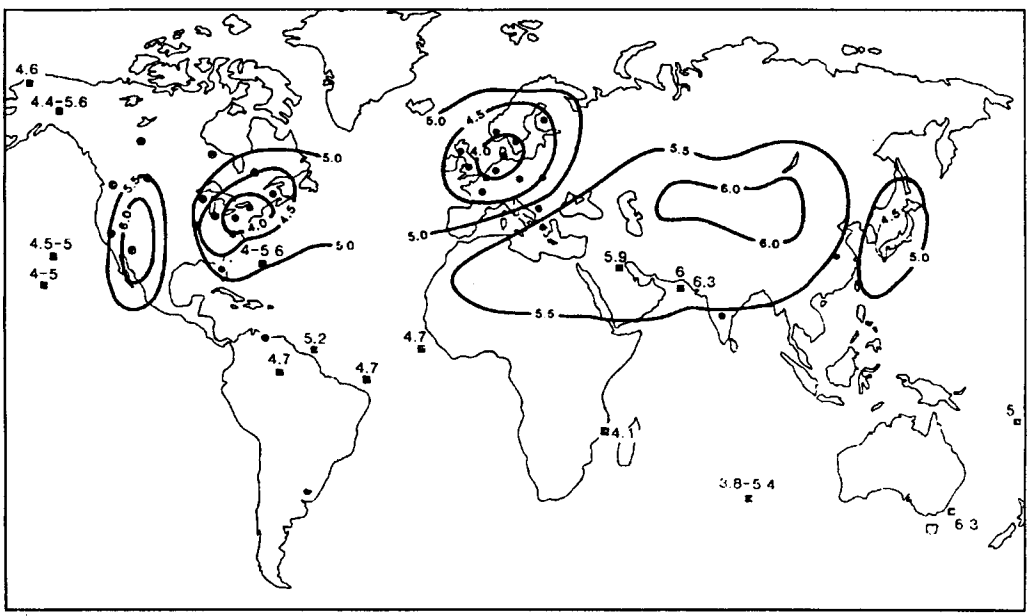


**FIGURE 1.1** Pattern of rainfall acidity in the world (WMO, 1989)

The direct effects of ambient acids to plants were already recognised in 1854, as reported by a Belgium commission (Rapport à M. le Ministre de l'intérieur par la commission d'enquête, Bruxelles, 1856), which reported the influence of hydrochloric acid on trees and bushes. The negative effects to vegetation were found to be related to the size of the exposed area, but mostly to the wind direction. The relation of the sensitivity of species to hydrochloric acid was found for a list of species. In Germany, the direct effects of sulphur dioxide and sulphuric acid on vegetation was observed in and near the cities (Tiegs, 1927). Critical effect levels were defined for sulphuric acid concentrations. An ambient concentration limit of 1:1 000 000 (1 ppm) would be regarded as safe, whereas 1 : 100 000 would lead to mortality on clear

days after several minutes and 1 : 25 000 to death of all vegetation within seconds. It was found that the sensitivity of different species depended on stand conditions and age. Coniferous trees were found more sensitive than deciduous trees (Tiegs, 1927) Acidification of soils was already recognised around 1900 when a German scientist Wieler postulated the theory that the sulphuric acid reaching the soil could dissolve and rinse soil constituents such as chalk, which thus could no longer be used for growth (Tiegs, 1927). Smith (1872) warns for the destruction of roots due to the acid exposures in Belgium, France and Germany.

Scientific research on acidification of rivers and lakes started in the 1920s (cf. Abrahamsen *et al.*, 1989). Experiments had indicated that the trout populations were declining as a result of low pH of the water (Dahl, 1926). The relation between the acidity of freshwater and precipitation was suggested in 1934 (Torgerson, 1934). The public interest in the subject was renewed in Scandinavia about 30 years ago (Odén, 1967). This interest arose from concern regarding freshwater acidification and reduction in fish populations in areas with a low capacity for neutralising acidic inputs. The acidification of the Scandinavian lakes was demonstrated to be the result of long-range transport of air pollution. Acidification of lakes was found to be the result of high inputs of sulphur and nitrogen compounds (Hauhs and Wright, 1988; Brydges and Wilson, 1991). The tall stacks built in the 1960s brought about a considerable reduction in the immediate vicinity of the sources but, in general, it can be stated that when pollutants are emitted at higher levels in the atmosphere, the atmospheric residence time and transport distance increases. The actual transport distance depends on wind, climate and meteorological conditions.

Since about 1975 the novel forest decline in the former Federal Republic of Germany has been observed as extensive and rapid (Brydges and Wilson, 1991). In the last few years interest in the effects of pollutants on crops and materials has grown and, in particular, effects on conservation areas like forests, moorland pools and heathlands. Other effects related to acidification are the result of exposure of humans to acidic gases and aerosols, and reduction in the visibility in the affected areas. Since 1986, most countries have co-ordinated their forest damage surveys on the basis of a system devised in the framework of the International Co-operative Programme on Assessment and Monitoring of Air Pollution Effects on Forests, under the convention on Long Range Transboundary Air Pollution. Figure 1.2 shows the intensity of defoliation resulting from the 1988 inventory (UN ECE/ICP Forest (1989). The percentages show that ailing forests are to be found to a greater or lesser extent in all the countries of Europe.

*Dutch Priority Programme on Acidification*

A programme on the issue of acidification was started in 1985 in the Netherlands as a result of the awakening interest of policy-makers in the effects of air pollution on forests and other vegetation due to dry and wet deposition of sulphur and nitrogen species (Heij and Schneider, 1991). Gradually it became evident that the specific air pollution climate in the Netherlands

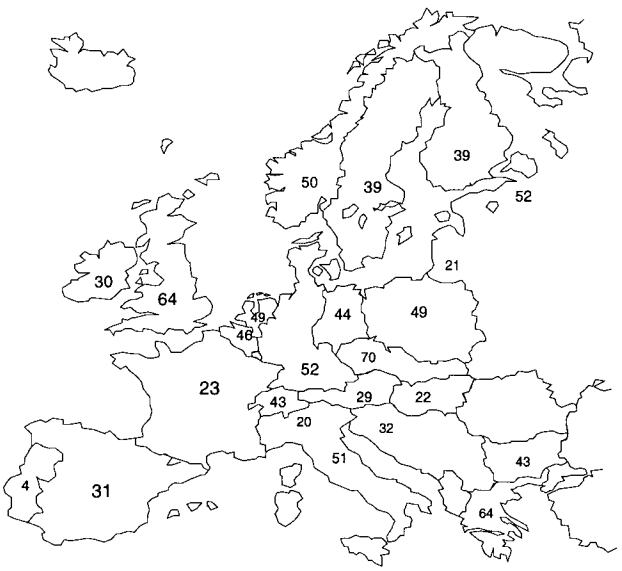


**FIGURE 1.2** Intensity of defoliation for all species, or conifers only in 1988. Percentage of trees in classes 1-4 (>10% defoliation)

deviates from that of other European countries. Severe effects as a result of very high local nitrogen inputs were observed in the Netherlands (Schneider and Bresser, 1988), while in other parts of Europe, effects were attributed to high acid inputs by sulphur and nitrogen species (Scandinavian lakes) or by exposure to ozone (conifers in Germany) (Schlaepfer, 1992).

The causal chain related to these effects, studied in the Dutch Priority Programme on Acidification (DPA), is shown in Figure 1.3. Gases and aerosols can cause damage to vegetation through direct effects on the parts of the vegetation above ground and through indirect effects, via the soil solution, on the parts of the vegetation below the ground (Heij and Schneider, 1991). Effects on the soil solution can be expressed as changes in the concentrations and budgets of sulphur, nitrogen and aluminium in particular. With regard to nitrogen, the acidification problem is closely linked with the problem of N eutrophication. The critical loads and critical levels refer to thresholds, which can serve as a tool to assess the occurrence of effects in natural ecosystems due to acid deposition. A critical load is a quantitative estimate of an exposure to one or more pollutants *below* which significant harmful effects do not occur. A critical level is defined as the concentration of a pollutant in the atmosphere *above* which direct adverse effects on receptors may occur. International co-operation within the framework of the UN Economic Commission for Europe is taking place

to produce maps of critical loads and levels in Europe to create a basis for policy measures (Hettelingh *et al.*, 1991). In this respect, accurate estimates of actual deposition to vegetation, soils and lakes became an important topic in the DPA.

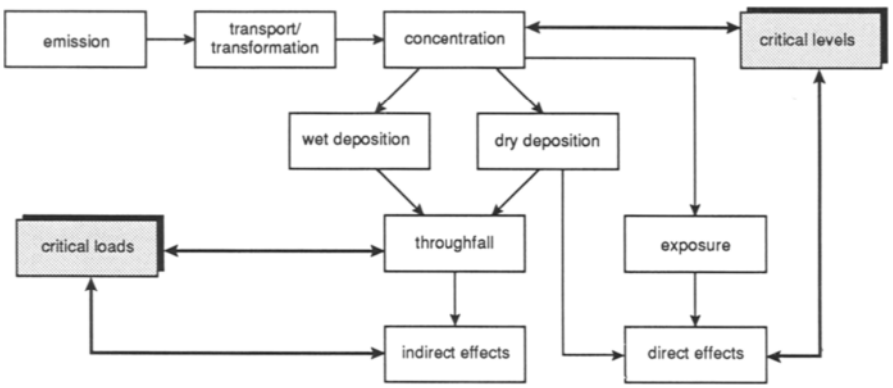


**FIGURE 1.3** Cause and effect chain studied in the DPA (Heij and Schneider, 1991).

Acidification of soils and lakes can be the result of deposition of acidic or acid-forming gases and aerosols, and/or acidic precipitation. The processes of deposition are illustrated in Figure 1.4. Dry deposition is the process where gases and aerosols are deposited directly from the atmosphere onto vegetation, the soil or materials. Wet deposition is the result of rain-out or wash-out by precipitation. Deposition of pollutants by fog and dew is often called occult deposition. Total deposition is the sum of dry, wet and occult deposition. Throughfall and stemflow refer to the water dripping from tree canopies and trunks, respectively. The flux of an ion below the canopy in throughfall provides information on the deposition to the soil.

The acidifying components which play a role in the acidification are gaseous sulphur dioxide ($SO_2$), nitrogen oxides (NO and $NO_2$), nitric acid ($HNO_3$), nitrous acid ($HNO_2$), peroxyacetylnitrate (PAN), hydrochloric acid (HCl), Hydrofluoric acid (HF), organic acids, ammonia ($NH_3$) and ammonium ($NH_4^+$), nitrate ($NO_3^-$) and sulphate ($SO_4^{2-}$) aerosols. These components are emitted mainly by anthropogenic sources such as industry, refineries and power plants ($SO_2$), industry and traffic (NOx), livestock breeding ($NH_3$) and incinerators (HCl), or formed in the atmosphere from these gases ($HNO_3$, $HNO_2$, PAN and aerosol compounds). If HCl is formed by the reaction of acidic gases with sea salt, it is considered to be of quasi-natural origin (Lightowlers and Cape, 1988). On the global scale, acidifying

components are to a large extent originating from natural sources (Welphdale, 1987) such as volcanoes, oceans, soil, burning processes, wildlife, meteorites and lightning.

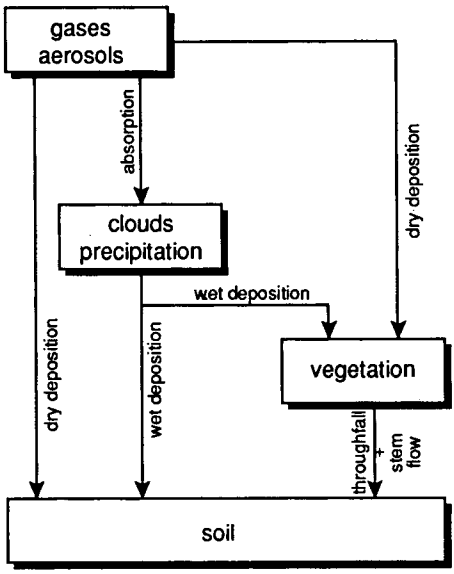


**FIGURE 1.4** Schematic representation of deposition

In the causal chain, soil acidification and nitrogen cycling are the most important processes related to indirect effects (Heij and Schneider, 1991). The total nitrogen deposition can be estimated from the wet and dry deposition of the individual N-containing components. With respect to soil acidification, it is assumed that acid-forming oxides can be oxidised to strong acids in the soil. One mole of $SO_2$ can thus form two equivalents of acid, whereas one mole of NOx or HCl can form one equivalent of acid (Van Aalst, 1983). The soil processes leading to acidification are beyond the scope of this book (see for overviews, Hauhs and Wright, 1988; Van Breemen and Verstraten, 1991). The contribution of $NH_3$ to the acid deposition is related to the rate of soil nitrification. Under the influence of oxygen, nitrifying bacteria may transform ammonia into nitrate and acid according to (see e.g. Van Breemen *et al.*, 1982):

$$NH_4^+ + 2O_2 \longrightarrow NO_3^- + H_2O + 2H^+ \qquad [1.1]$$

Through this process, acids in gaseous form, in aerosols or in rain droplets initially neutralised by $NH_3$ can form two equivalents of acid when deposited: one can be considered as derived from $NH_3$ and one from the neutralised acid. Because of incomplete nitrification in

the soil the contribution of $NH_3$ and/or $NH_4^+$ may be less than one equivalent $H^+$ per mole $NH_3$ deposited. This contribution is dependent on the type of soil and vegetation.

It has been estimated from intensive monitoring studies in forests distributed over the Netherlands (Heij and Schneider, 1991) that the actual acid load of sulphur compounds is generally equal to the potential acid load of sulphur. The actual acid load from nitrogen, however, was found to be only about half the potential load. The difference between potential acid load and actual acidification of the soil (in the sense of a reduced buffer capacity in the soil) is mainly the result of the removal or fixation of N through uptake by plants, denitrification, or immobilisation of N in the soil organic matter (Heij *et al.*, 1991). Furthermore, acids formed from gases in the atmosphere may be neutralised by basic substances before reaching the soil.

The maximum acid load to soils, or the amount of acidifying components removed from the atmosphere by deposition, hereafter referred to as total potential acid deposition, is estimated by:

$$\text{Total potential acid} = 2\text{SOx} + \text{NOy} + \text{NHx} \qquad [1.2]$$

where SOx is the total (dry + wet + occult) deposition of sulphur compounds (one mole of SOx forming two moles of acid), NOy the total deposition of oxidised nitrogen compounds and NHx the total deposition of reduced nitrogen compounds. Other acid or acid-forming species might be added to Eqn. 1.2, such as HCl, organic acids, PAN, $H_2S$ and HF. However, the contribution of these gases to the total acid deposition is considered to be of minor importance relative to other acidifying components. The total potential acid deposition is expressed in mol $H^+$ $ha^{-1}$ $a^{-1}$.

The studies related to atmospheric deposition within the Dutch Priority Programme on Acidification were focused mainly on quantification of the inputs and origin of sulphur and nitrogen compounds to heathland and forests in the Netherlands. The studies comprised experimental research as well as model development and application. The experimental and modelling research was to a large extent conducted within the framework of international programmes such as the EUROTRAC project (BIATEX) and some financed by the European Commission. The work was reviewed by an international review team. They concluded that the atmospheric deposition work conducted in the Netherlands so far was of world class quality (Heij and Schneider, 1995).
In the next section first a brief overview of the evolvement of atmospheric deposition research is given. After this historical overview, the studies conducted in DPA will be elucidated as an introduction to the contents of this book.

## 1. 2 HISTORY OF ATMOSPHERIC DEPOSITION RESEARCH

The study of sulphur and nitrogen deposition in the past had two different purposes. First, research was done in relation to plant nutrition. Both sulphur and nitrogen should be available to some extent for optimal growth of vegetation used in agriculture. That atmospheric nitrogen in the form of ammonia could be of benefit to plant growth was already recognised in 1804 by De Saussure. Ammonia was detected in rain by Von Liebig in samples collected by Zimmermann near Giessen in 1824 (Von Liebig, 1827). In 1825 Von Liebig demonstrated the presence of nitric acid in rain, but it was not until 1852 that Boussingault demonstrated that nitrogen in this form is also beneficial to plant growth. These observations have led to the development of ammonia observations in air and rain, and of nitric acid in precipitation.

Secondly, the relation to atmospheric pollution was studied, with emphasis on human health in relation to exposure of high concentrations of pollutants. In the period before the Second World War atmospheric pollution in the environmental sense was studied mainly because of impacts on human health problems. In the Middle Ages, the relation between human health and smoke from coal burning had already been established. During periods with low wind speeds and/or foggy conditions, the main industrialised cities in Europe experienced high concentrations of smoke, reducing the visibility and increasing the number of deaths each year caused by industrial activities. The most famous example in this respect is the London smog (Brimblecombe, 1987), but observations and statistics on pollution are also available for several cities in Germany (Wernicke, 1927) and in Budapest (Fodor, 1881). The relation between vegetation damage as a result of sulphuric acid and sulphur dioxide in the atmosphere was already studied the 1920s (Tiegs, 1927). The first results in approaching the problem of smoke in relation to human health yielded analyses of wet deposition in or near cities, or individual factories.

The atmospheric measurements dating from around 1800 to early 1900 were mainly analyses of collected precipitation. Ambient concentration measurements of atmospheric components were to a large extent not made. The results of very old measurements are summarised in several reports and papers: Way (1855), Ludwig (1862), Smith (1872), Miller (1905), Liesegang (1927), Eriksson (1952), Brimblecombe and Stedman (1984), Brimblecombe (1987), and Ulrich and Williot (1993). This chapter will present a short overview of the research on atmospheric input measurements. The main focus will be on the old measurements, i.e. before the Second World War. After that time the research on atmospheric input increased gradually, with the main increase in the seventies and eighties.

## 1.2.1 NITROGEN COMPOUNDS

Evelyn, in his *Philosophical Discourse of Earth* (London, 1676), speaks of rains and dews as being *'impregnated .. with Celestial Nitre'*, and of *'nitrous spirits descending with their baulmy pearls'* (cf. Miller, 1905). The presence of ammonia in the atmosphere was noticed by De Saussure (1804) in Geneva. He came to the conclusion that the nitrogen of plants could only be derived from the vegetable and animal matters diffused through the soil, or existed in the form of ammonical vapours in air brought down by rain. That such ammonical vapours do exist in the air was considered by De Saussure to be proven by the change occurring to sulphate of alumina, which, when left exposed to the air, became converted by degrees into double sulphate of alumina and ammonia (cf. Way, 1855). Von Liebig (1827) believed that the nitrogen in soils was derived from the small amount of ammonia in air and rain. As a result, the necessity of applying manure for agricultural purposes was put to question (Lawes and Gilbert, 1851). Von Liebig's theory, therefore, has led to several investigations focused on the benefit of atmospheric nitrogen to plants. Greenhouse experiments were conducted by Ville and Boussingault in France to determine whether the nitrogen used by plants was from nitrogen ($N_2$) itself or occurring in the form of ammonia (cf. Way, 1855). Lawes and Gilbert (1851), and Boussingault (1886), eventually showed atmospheric $N_2$ to be of no benefit to plants.

*Wet deposition*

Precipitation sampling was already a well-known technique to determine the 'atmospheric composition'. Precipitation was sampled in the early days of the development of chemistry. The first analysis date was from 1749-50 when Andreas Sigmund Maggraf sampled with great care the cleanest rainwater and distilled it very carefully using new glass stills (cf Ludwig, 1862). He found hydrochloric acid and nitric acid as well as sodium chloride and lime. He recognised that it was very difficult to sample clean rainwater and snow: it should be sampled 'in the free sky', away from buildings. When he distilled his rainwater, he always found crystals that looked like sodium chloride, but were brown instead of white because they were covered with sticky oil particles. This was not strange because 'you could smell these oil particles after a spring or summer rain' (cf Ludwig, 1862). Later in 1788 in Leipzig Bergman determined the same substances in rain and snow (cf. Miller, 1905). Between 1820 and 1825 several analyses of rain water were made in Giessen and near the Baltic Sea (Germany) and in Utrecht (The Netherlands). Dalton analysed rain water in Manchester for chlorine. Brandes (1825) was probably the first to analyse several components in rain water in Salzuffeln, Germany. He evaporated the rain water and found the residue to contain organic substances, chlorine, sulphuric acid, soda, potash, magnesia, ammonia salts, carbonic acid, lime and oxide of iron (cf. Smith, 1872).

When it was discovered that $NH_3$ in precipitation was used by plants as fertiliser (Von Liebig, 1827), the interest in the ammonium content in precipitation increased. When Boussingault

(1886) showed the importance of nitrate in plant nutrition in 1856, also present in precipitation, this component was determined regularly too.

It was thought that the nitrogen in the form of nitrate in precipitation originated from lightning, because the highest concentrations were observed with measurements made during thunderstorms. Boussingault (1886) made measurements in a forest area under rural conditions during several types of precipitation events, and concluded that the atmosphere was the only source of nitrogen. Marggraf was the first who found nitric acid in rainwater. In several precipitation investigations nitric acid was determined, e.g. by Barral (1852) and Levy (1874) in Paris, Bineau (1855) in Lyon, Filhol (1855) in Toulouse, Gilbert and Lawes (1851) in Rothamsted and Smith (1872) in several sites in Great Britain. Boussingault was the first to sample rime, fog, snow and dew and analysed the samples for ammonium and nitrate concentrations. He was also the first who performed sequential sampling of precipitation (Way, 1855). Boussingault had been led to think, according to his experiments, that rain collected in rural fields contained notably less ammonia than that collected in towns. Most of the precipitation measurements were made in or near towns. Very high concentrations of ammonia in rain water were found by Barral (1852), Boussingault (1886) and Levy (1874) in Paris, by Bineau (1855) in Lyon, Filhol (1855) in Toulouse, Meyrac in Dax (cf Ludwig, 1862) and Pierre (1851) in Caen. Pierre (1851) gives the following explanation:
*'Volcanoes in a state of activity throw out a notable quantity of ammonia salts. They are given off also in calcining organic matter, and in the combustion of coal (an explanation for the enormous concentrations of 130 and 138 mg/l observed by Boussingault, red.). Matters of organic origin, all more or less nitrogenised, decompose, either at the surface of the land or at a very small depth, and among the products of this decomposition we find carbonate of ammonia, a very volatile substance. A portion of this substance remains in the soil, and contributes to the prosperity of the plant; another part is dessiminated in the air. Carbonate of ammonia being very soluble in water, we can understand why it is found in rain.'*

The oldest long-term measurements of wet deposition are those made at Rothamsted in England during 1880 - 1920 (see Brimblecombe and Stedman, 1984) and the measurement taken by Albert Levy in Montsouris near Paris during 1876 - 1907 (see Ulrich and Williot, 1993). These data are used in Chapter 5 to determine trends in atmospheric deposition in Europe. The problem in interpreting these data is that they are sampled near cities and/or in agricultural areas, but are not representative for background concentrations. Furthermore, measurement of nitrogen compounds is sensitive to many sources of errors, such as bird droppings, dry deposition of soil dust, particles and gases, microbial conversion or production and contamination in the laboratory ($NH_3$) (Eriksson, 1952, Galloway and Welphdale, 1980; Buijsman and Erisman, 1988).

*Dry deposition*

Ambient ammonia concentration measurements were made as early as 1840. Grager, a German scientist found 0.42 mg $m^{-3}$; Kemp, an Irishman, 4.78 mg $m^{-3}$ and Fresenius, another German scientist, 0.17 mg $m^{-3}$. Pierre (1851) found during one year of observations in 1851 near Caen 'only' 0.65 mg $m^{-3}$. Smith (1872) analysed several samples for concentrations of $NH_3$ in London in 1870 and found concentrations in the range of 0.11 to 0.27 mg $m^{-3}$. Albert-Levy measured ambient concentrations of 21-29 µg $m^{-3}$ $NH_3$-N during one year sampling in Paris in 1874. Fodor (1881) measured two years continuously in Budapest, Hungary and found an average of 39 µg $m^{-3}$.

Way (1855) was the first to hypothesise the existence of dry deposition. In his paper *The atmosphere as a source of Nitrogen to Plants*, he writes:
*'We have seen then that the form of ammonia or nitric acid the soil receives annually a very large dose of nitrogen in a state to be made use of by plants. That the data yet obtained are not very precise ought not to surprise us, considering the difficulty of the subject. I think, too, that one point has been overlooked in all these inquiries: one experimenter devotes his attention to the ammonia in rain, another to that in air - both independently, at different times, and without concept. But in the meanwhile a cause, and, as I believe, a most active cause of abstraction of ammonia from the calculations of each of them, is at work; - I mean the absorption of ammonia and nitric acid from the air by the soil. Between each shower of rain this cause is continually - to an unknown, but perhaps, a large extent - robbing the air of these compounds; so that the rain when collected really represents that which this agency has not removed.'*

The first dry deposition measurements are probably those made by Ville (1850) and Schlössing (1874) using nitrogen deficient plants in $NH_3$ rich chambers, and those by Bineau (1855) and Bretschneider (1872) using measurements of NHx absorption in dilute acid solutions or soil surfaces exposed to air. Furthermore, the sampling and analysis of snow after different exposure times by Boussingault (1886) might be labelled as dry deposition measurements. He found a 10-fold increase in $NH_3$ concentration in snow after a 36-hour exposure to the ambient air, although he reasoned that the source of ammonia was the soil and not the atmosphere. Similar observations were made by Müller (1888) in Braunsweig Germany. He also showed the dependence of $NH_3$ concentrations in snow on the emission of smoke by sampling outside the city (1 mg $l^{-1}$ $NH_3$) in a sparsely populated area (1.5 mg $l^{-1}$ $NH_3$), and in a densely polluted area (3 mg $l^{-1}$ $NH_3$) of Braunsweig. Schlösing (1875) studied the absorption of ammonia by soil and estimated that about 40 kg $NH_3$-N $ha^{-1}$ was absorbed from the air per year. Hall and Miller (1911) searched for information on whether ammonia was released by soil by exposing shallow dishes of sulphuric acid, some close to the ground and others four feet (1.2 m) above it. They found that the lower dishes generally contained less ammonia than the upper one, which they took as an indication of a steady absorption of ammonia by the soil.

Russell and Richard (1919) were the first to estimate the total flux of nitrogen by rain to Great Britain: the 56,000,000 acres of Great Britain would receive 65,000 tons of combined nitrogen. They found, however, that this was much less than their estimate of the emission from coal consumption.

### 1.2.2 SULPHUR COMPOUNDS

At the end of the seventeenth century Robert Boyle tried to devise sensitive techniques for the estimation of various components in air (cf. Brimblecombe, 1987). He advised the experimenter to hang up clothes or silks died with colours to use the fading or changes in colour as an indicator for the presence of particular nitrous or salino-sulphurous spirits. In 1744 the French chemist Rouelle found sulphur dioxide, or at least sulphate, in air by using a modified version of the technique outlined by Boyle. Van Driessen and Vanhof found in Amsterdam hydrogen sulphite and sulphuric acid (cf Ludwig, 1862). In Copenhagen the existence of hydrogen sulphite was demonstrated because the silver works in the houses near the coast were blackened to a large extent. Sulphuric acid was also determined in London by colouring Litmus paper red.

It took a long time before analytical methods were developed to determine ambient concentrations of trace gases. Smith (1872) measured sulphuric acid in Manchester and London at several places between 1868 and 1869. The sulphuric acid was formed from the burning of sulphur containing coal. He found four times higher concentrations in moist air than under dry conditions. He also reports concentrations measured in the Underground Railway (Metropolitan), which were about a factor of 4 higher than in the city. Witz (1885) identified sulphur in cities (Paris). He compared concentrations outside and inside apartments, in the cities and in the countryside. He was at that time the only one in France interested in sulphur arising from industrial emissions. The direct effects of $H_2SO_4$ and $SO_2$ to vegetation and indirect effects in relation to the loss of chalk as the result of $SO_2$ taken up by the soil (acidification) were recognised at the end of the 18th century (see Tiegs, 1927 for a review). Research was conducted near the main source areas (large cities) to determine acid concentrations, and by determining the sulphur concentrations in needles and leaves from trees grown at several distances from sources and where different wind directions prevailed. A strong relationship was found between sulphur content in needles and the distance from the source or prevailing wind direction.

*Wet deposition*

In 1819 Julia de Fontenelle found sulphates in dew water (cf. Smith, 1872). The first wet deposition measurements of sulphur were probably made in 1868 by Freytag in Essen,

Germany (Hasselhof and Lindau, 1903). Measurements in Manchester, England, were reported by Smith (1872). He describes the sampling and analysis of rain water as follows:
*'A specimen taken in Greenheys field, half a mile from the extreme south-west of Manchester, wind blowing west, had a peculiar oily and bitter taste when freshly caught. A person to whom I gave some of it to taste supposed it had been put into a glass in which castor oil had been put. I had collected the water in a large meat-dish, which had been very carefully cleaned, and was then set on a stand about two feet from the ground during rain. .. Boiling removes all taste, and standing alone removes the taste of the oily matter and leaves only the taste of the smoke. The smoke here shows that it was not out of the range of chimneys, although the wind was west. The taste was that of the flattest and most insipid water, which could not be drunk with pleasure, independently of the nauseous taste.'*

The first large-scale research on rain water composition was reported by R. A. Smith (1872) in his marvellous work: *Air and Rain: The beginnings of a chemical climatology*. Smith was more concerned with polluted air and rain in relation to public health, spreading of diseases and damage to buildings, than in the benefit to agriculture of the substances in it. In 1869 Smith sent glass bottles and funnels all over England for the collection of rain water '*in order to come to satisfactory conclusions, and such as would be useful to those who attended to the influence of air on health'*. The sites comprised several measuring points in 12 large towns (London, Manchester, Liverpool, St. Helen's, Runcorn, New-Castle, Glasgow, Aberdeen, Edinburgh, Dundee, Greenock and Perth), at 12 inland sites in England, 13 inland sites in Scotland and 8 coastal sites on the east coast and another 8 on the west coast. Most of the samples were taken during the winter months (December 1869 to February 1870); at only a few sites was one whole year sampled. Smith had made a list of instructions for the optimal collection and to ascertain the collection of the pure rain water. He advised, for example, not to touch the inside of the funnel after it was cleaned. Furthermore, he advised preventing solid matter, dust, falling leaves, snow and sea spray going into the bottle by using a stopper, or by putting the funnel and bottle inside. The funnel was to be placed somewhat above the ground to prevent splashing from the ground in the sample .

Smith (1872) reported that all the rain was found to contain sulphuric acids in proportion to the distance to the town; the increase in acid also meant an increase in organic matter. Furthermore, he states:
*'In the fields the amount of acid is not sufficient to neutralise the bases which are in union with the organic matter, and the residue is therefore alkaline; but in the town the amount of acid is equal or in excess; what is in excess is driven-off (during heating, ed.), and enough remains to saturate the bases, which become then neutral salts' and 'we may therefore find three kinds of air - that with carbonate of ammonia in the fields at a distance; that with sulphate of ammonia in the suburbs; and that with sulphuric acid, or acid sulphate, in the town'.*

Precipitation was only sporadically analysed for sulphur compounds. Liesegang (1927) and Eriksson (1952b) report some analyses made in Germany, France and Russia between 1860 and 1920. These data are used in Chapter 5 to show the variation over several years. Long-term measurements of sulphur in precipitation are not available in the period before 1930. Since the 1950s interest and research on atmospheric pollution has increased rapidly. This resulted in a strong increase in the number of ambient concentration and precipitation measurements and the formation of monitoring networks. Rodhe and Granat (1984) provide an historical overview of European wet deposition monitoring and an evaluation of $SO_4$ in European precipitation for the period 1955 - 1982, based on data from the European Air Chemistry Network (EACN). EACN was established in the early 1950s by Scandinavian scientists to establish the wet deposition of nutrients to agricultural and forest soils. Later, the emphasis was placed on understanding chemical and meteorological processes and establishing long-term changes in precipitation chemistry associated with human activities. Continuous data on precipitation chemistry became available in 1955. Based on the EACN network data, the first maps of sulphur deposition in Europe were made by Enger and Eriksson (1955) and Bary and Junge (1963). Nowadays, the European network on precipitation chemistry and air concentrations is run by the co-operative programme for monitoring and evaluating the long-range transport of air pollutants in Europe EMEP. Further to this, there are several national networks.

*Dry deposition*

The interest in quantification of sulphur in the atmosphere and its deposition increased in the 1940s when it was recognised that sulphur fertilisation could lead to increased agricultural production. It was suggested by Alway (1940) that part of the sulphur requirements of plants might be supplied by direct adsorption of $SO_2$ by leaves (Chamberlain, 1980). He noted regions where sulphur was deficient due to winds carrying sulphur from sources seldom blowing their way. The first fumigation measurements of alfalfa were reported by Thomas *et al.* (1943) and Chamberlain (1980). The average rate of uptake derived from these experiments was about 1 cm $s^{-1}$. It was found to depend on pH and fumigation time, and $SO_2$ concentration. The work of Thomas *et al.* (1943) is considered one of the starting points of the study of $SO_2$ dry deposition (Chamberlain, 1980). The work of Thomas *et al.* was further extended by, for example, Olsen (1957) and Spedding (1969) for different receptors to determine the rate of uptake. The first gradient measurements of $SO_2$ concentrations over vegetation are probably those by Gilbert (1968). Many experiments determining $SO_2$ dry deposition velocities and resistances in the 1970s are reported (see Chapter 3).

### 1.2.3 THROUGHFALL MEASUREMENTS

Nutrient transfer in throughfall and stemflow is usually substantially larger than that in incident precipitation. The alteration of the composition of water in contact with plant tissues may be attributed to both canopy exchange and atmospheric dry deposition. Hales had already alluded nutrient losses by leaching in his *Vegetable Staticks* in 1727, but De Saussure (1804) remained the first to show experimentally that washed leaves contained less of certain materials than did unwashed leaves (cf. Tukey, 1970). Gaudichaud (1841) and Sachs (1892) observed that water droplets on leaves became alkaline and Garreau (1849) found small amounts of carbonates in washings from leaves (cf. Tukey, 1970). LeClerc and Breazeale (1908) exposed crop plants to artificial rainfall and noted a considerable reduction in cation content within the plants brought about by this treatment. Durant (1932) postulated that throughfall may also contain exudates from the canopy in dry periods. Arens (1934) reviewed papers on particular aspects of canopy exchange published prior to 1930.

That material added to incident precipitation may also originate from dry deposition is a comparatively recent idea postulated by Ingham in 1950. Will (1955) first showed the importance of throughfall relative to the nutrient flux in litterfall for Na, K and Mg. Madgewick and Ovington (1959) were the first to report that different forest types have unique effects in changing the concentration of precipitation (cf. Parker, 1983). Throughfall and stemflow measurements were originally used for the quantification of soil loads. During the last few decades, however, these measurements have been used for studies on atmospheric deposition as well (e.g. Johnson and Lindberg, 1992; Draaijers, 1993).

### 1.2.4 LONG-RANGE TRANSPORT

The first hypotheses of long-range transport of atmospheric components were related to the sea as a source of chloride in rain and at the surface. Maggraf already hypothesised in 1750 that the chloride he found in a precipitation sample must have come from the ocean. Meyrac (1852) in France showed that NaCl could be transported over long distances, with the ocean as the source. Smith (1872) stated: *'One of the uses of storms seems to be to supply the world with salt'*. That components could travel over long distances was also known because Sahara dust and components emitted by volcanoes, which must have been transported over at least 2500 km through the air were identified in several places in Europe. Ehrenberg demonstrated that material which he investigated by his microscope must have been originating from the eruption of the volcano St. Vincent in 1812. Ehrenberg hypothesised in 1850 that material not originating from volcanoes, originates from dust transported from south America by south-westerly winds to Europe (cf. Ludwig, 1862). Freysing analysed material deposited on the snow on the 12th of March 1847 in Tyrol and found similar characteristics as those described

by Ehrenberg. Similar observations were made by Ehrenberg in 1850 in the Gotthard-Alpen, in 1851 in Graubundten and in 1855 in Zurich (cf. Ludwig, 1862).

Brogger (1881) suggested dirt on snow observed in Norway was the result of emissions from Great Britain (Last, 1991). In the Belgium Commission report on damage to vegetation (Rapport à M. le Ministre de l'intérieur par la commission d'enquête, Bruxelles, 1856), so-called 'safe distances' were given for the relation between damage and factories, suggesting transport of pollutants. Smith discussed these distances and hypothesised that they should be a function of wind direction and wind speed, and should not only be related to hydrochloric acid production, but also to smoke stacks producing sulphuric acid.

The first maps of sulphur deposition over large regions, the UK in this case, were made by Meetham (1950). He estimated sulphur and chloride deposition in the UK as the result of smoke emission. The first maps of deposition in Europe were made by Enger and Eriksson (1955). Acidification as a result of deposition of sulphur became of interest in the early sixties (Odén, 1960). In the eighties the concern about the excess nitrogen deposition and its contribution to acidification was recognised as an environmental threat (e.g. Van Breemen *et al.*, 1982). It was only 15 to 20 years ago that air pollution was assumed capable of causing effects not only close to sources. The most feared effects were those to humans because they were exposed to the highest concentrations of pollutants near to source areas (industry, cities). It was thought that the atmosphere was large enough to deal with the relatively low concentrations of pollutants emitted by anthropogenic activity. Furthermore, it was believed that the cleaning capacity of the atmosphere was thus that pollutants would be degraded fast and effectively. The only concern was therefore to keep the concentrations near sources as low as possible. Therefore, high chimneys were built to overcome local pollution. Unfortunately it was not foreseen that long-range transport of pollutants could lead, for instance, to acidification of Scandinavian lakes and destruction of the ozone layer.

The Scandinavian countries hypothesised that the acidification of their lakes was due to acid rain mainly caused by emissions other than their own. To determine whether this was possible, a long-range transport model was developed. This has led to the development of the EMEP (European Monitoring and Evaluation Programme) langrangian long-range transport model which is used under the UN ECE Convention on Long Range Transboundary Air Pollution to determine the concentration and deposition distribution over Europe, to determine the budgets for countries and the so-called blame matrices (Eliassen and Saltbones, 1983; Iversen *et al.*, 1991; Tuovinen *et al.*, 1994). Deposition was treated in this model only as a loss-term. It was thought that the atmospheric deposition had to be known only for large regions as long-term averages. It became clear recently that deposition variation in time and space is very large, and that for determining the relation between effects and deposition, receptor specific estimates are needed (this book).

## 1.2.5 SYNTHESIS

The historical overview of atmospheric deposition research shows that most emphasis has been on wet deposition measurements. The first measurements are a few hundred years old, but only since the beginning of the 20th century measurements of wet deposition were made on a large scale. There are, unfortunately, large uncertainties associated with these measurements (see e.g. Hansen and Hidy, 1982; Cogbill *et al.*, 1984; Ridder, 1978; Buijsman, 1989; and the discussion in section 5.4). This regards the sampling and analytical techniques, handling of samples, but also the representativity of measuring sites, the influence of local sources, etc.. Despite the uncertainties associated with the data, they can still be very useful in the evaluation of the evolvement of emissions and deposition in time (see section 5.4)

.

Techniques for measuring dry deposition have only become available in the seventies. The dry deposition measuring techniques were less suitable for monitoring application than the wet deposition techniques, resulting in a lack of large-scale, long-term dry deposition measurements. Large scale ambient concentration measurements of gases and aerosols were only made since the fifties and sixties. It is therefore not possible to determine the evolvement of dry deposition based on measurements. Although some early studies report measurements of fog composition, these are not accurate and extensive enough to determine the fog deposition.

The long-range transport modelling is well developed during the past twenty years. The emphasis of the studies was on determining the large scale transport and deposition of pollutants. The local scale estimation of deposition was not addressed.

## 1.3 ATMOSPHERIC DEPOSITION RESEARCH IN THE NETHERLANDS

For assessing the wide range of potential effects of air pollution on ecosystems, it is essential to know the actual atmospheric deposition load. Moreover, it is necessary to know where threshold deposition loads are exceeded and which compounds contribute most to the loads. In this way abatement measures on emission controls can be optimised. Critical loads and target loads for ecosystems have been proposed, both internationally (Hettelingh *et al.*, 1991; 1993) and in the Netherlands (Schneider and Bresser 1988; Verzuringsnota, 1990; Heij and Schneider, 1991). These critical loads are defined on a spatial scale that presently does not allow adequate comparison with mapped deposition fields. The spatial resolution for which critical loads are developed is on ecosystem level, whereas deposition fluxes of acidifying components so far have been estimated on a much larger scale (Van Aalst, 1983; Asman *et al.*, 1986; Iversen *et al.*, 1991; Tuovinen *et al.*, 1994).

There are two ways of determining the ecosystem specific critical load exceedances: i.e. by measurement or by modelling. Total deposition at a site can be estimated using wet, dry and fog deposition measurements or surface accumulation measurements. However, because of the limitations of these techniques and because of the large spatial variability in deposition and type and size of receptors, it is impossible to base the deposition to regions or countries merely on measurements. The development of models for generalisation is therefore inevitable. In order to evaluate and increase the accuracy of modelled depositions, experimental work is needed. The focus of the current atmospheric deposition research in the Netherlands is therefore on both experimental and modelling programs. The experimental research deals with determination of the processes involved in deposition and to derive component and receptor specific deposition parameters which can be used in models. Furthermore, monitoring programs were initialised to determine time series for trend detection and to evaluate the changes in deposition parameters. The modelling is focused on understanding the deposition processes and on generalisation of the experimental results. Furthermore, the evolvement of deposition in the past, present and future, and the origin and source contribution is assessed using models. These models therefore form the basis for developing abatement strategies.

To date, critical load exceedance maps of Europe have been made using deposition estimates from large-scale dispersion models, such as the EMEP model (Iversen *et al.*, 1991) and the TREND model (Van Jaarsveld and Onderdelinden, 1991). These models are very useful for linking emission to deposition on a country to country basis. However, for effect-related studies, the grid squares used in these models (150 x 150 km and 50 x 50 km, respectively) are much too large in comparison with local variations in deposition. Within one grid cell, amounts of atmospheric deposition differ considerably between the various ecosystems or receptors. To cope with this receptor dependency, Erisman (1992) has developed an empirical deposition model in which dry deposition of sulphur and nitrogen compounds in the

Netherlands is inferred on a relatively small scale (5 x 5 km) from measured air concentrations, meteorological parameters, surface resistances and surface roughness. Surface roughness is estimated using detailed geographical information on land use. This inferential technique is also used to estimate atmospheric deposition in Europe on a 10 x 20 km scale (Van Pul *et al.*, 1994).

However, to assess the ecological impact of atmospheric pollutants on ecosystems, it is necessary to quantify the input of atmospheric pollutants in even more detail. Within individual land-use categories a considerable deposition variability may exist. For example, assuming an extensive, uniform forest stand, turbulent exchange between atmosphere and vegetation will be controlled to a large extent by the aerodynamic characteristics of the canopy which, in turn, will be determined by tree height and canopy density. Gases and particles transported to the canopy by this kind of turbulence can deposit on needles/leaves, branches and trunks. Actual deposition amounts will depend, for instance, on the local collecting surface area of the canopy elements, and their efficiency and capacity to capture or absorb gases and particles (Wiman *et al.*, 1990; Erisman, 1992; Draaijers, 1993). Because the above-mentioned parameters vary widely, one can expect a large deposition variability between forest stands.

Furthermore, extensive uniform forested areas are not common in northern and western Europe. In Scandinavia forest landscapes consist of a spatial mosaic of several subsystems: forest stands of different composition, height and canopy structure, logging areas, peat bog areas, lakes etc. In the Netherlands, Denmark, Germany, France, the United Kingdom and several other parts of Europe, forests are usually relatively small and surrounded by vast agricultural areas (Bleuten *et al.*, 1989). Consequently, many forest edges and other transitional zones exist as important attributes affecting surface roughness. Compared to deposition of pollutants in forest interiors, this deposition in forest edges may be greater due to local advection and enhanced turbulent exchange. Especially forest edges exposed to prevailing winds and/or high pollutant doses will be subject to enhanced deposition (Draaijers *et al.*, 1994). Up to now, the deposition of air pollutants to forests has been modelled assuming an infinite horizontal shape. There is no technique available to adequately compensate for 'edge effects' as the underlying processes have still scarcely been studied.

As critical loads directly refer to soil loads, atmospheric deposition and forest soil loads must be linked. Furthermore, since most measures to decrease the effects of acidification presently considered are emission abatement measures, it is essential that the relation can be made between emission of various pollutants and the exposure and deposition, as well as the related effects. This relation is formally described in models. Models of the various compartments (air, soil, [ground]water, vegetation) are interconnected, for instance, in the Dutch Acidification System model DAS (Heij and Schneider, 1991) or the RAINS model (Alcamo *et al.*, 1989). In these models, there is, to date, no well-defined sub-model relating the

deposition and the input into the soils below the vegetation. Experimentally, the input to the forest floors and soils below the vegetation has been characterised by measurement of throughfall and stemflow. Due to the interaction with vegetation (e.g. stomatal uptake and leaching), this flux may differ from the deposition flux. Several practical studies have shown that there may be large discrepancies between modelled deposition estimates and forest soil loads measured by throughfall and stemflow (Ivens *et al.*, 1990; Lovett *et al.*, 1992; Erisman, 1992; Cape *et al.*, 1992; Draaijers and Erisman, 1993). Model estimates as well as throughfall deposition estimates are found to be subject to relatively large uncertainties. For components such as $Ca^{2+}$, $K^+$, $Mg^{2+}$ and nitrogen compounds ($NO_3^-$ and $NH_4^+$), canopy exchange processes influence the throughfall composition in such a way that the relation between throughfall and model deposition estimates cannot easily be established. These exchange processes depend on many parameters, e.g. tree vitality, tree age, nutrient status of the soil and pollution climate (Parker, 1983), of which the impact cannot always be quantified adequately with present knowledge. Generally, $SO_4^{2-}$, $Na^+$ and $Cl^-$ in throughfall have been found uninfluenced, to a large extent, by canopy exchange processes relative to the atmospheric input (Garten *et al.*, 1988; Ivens, 1990; Johnson and Lindberg, 1992). For this reason, throughfall measurements of these components may be very useful in establishing a relationship between soil loads and modelled deposition estimates.

## 1.4 OBJECTIVES AND OUTLINE OF THE BOOK

The aim of this book is to describe the current state of knowledge on atmospheric input of acidifying components to ecosystems in Europe. Several issues discussed in the previous section will be addressed; i.e. how to obtain ecosystem-scale deposition estimates using models and measurements, locally but also for Europe as a whole; what is the influence of complex terrain and/or local roughness variation on deposition fluxes; and what is the link between atmospheric deposition estimates and soil loads? The results of these studies provide a quantitative assessment of the actual atmospheric input of acidifying compounds to ecosystems in Europe.

To understand the effects of air pollution to ecosystems, detailed knowledge of concentration and deposition to various parts of the system (e.g. leaves, branches, stems, soil) and the subsequent fate of the pollutants are needed. However, these aspects will not be dealt with in this book. Rather, we will consider deposition as a total input into the system, focusing on deposition on the main target areas, forests, heather and other semi-natural ecosystems in the Netherlands and Europe, although deposition to crops and agricultural areas, and to materials and buildings will also be addressed.

The outline of the book is related to the main lines of atmospheric deposition research conducted in the Netherlands, i.e. first the problems are defined and an overview of the

development and application of methods to tackle the problems is given. Then the methods to determine deposition are explained and results are presented. Finally, the uncertainty in results is assessed.

Following this general introduction, emissions, transport and atmospheric chemistry will be addressed in brief in Chapter 2. The aim of this chapter is to give some background information on the evolvement of emissions in Europe and on factors influencing atmospheric chemistry and transport of pollutants. The long-range transport modelling and spatial variations in concentrations are described. Chapter 3 will elucidate the different deposition processes. Measuring methods for deposition and their use in field campaigns and monitoring programs are described, along with a comparison of results of different methods applied simultaneously, resulting in a synthesis on the applicability of the different methods. An literature review of dry deposition measurement results is given in Chapter 4. The experimental results and knowledge on surface exchange mechanisms are translated into surface exchange parametrisations. The deposition parameters, obtained from the literature and from the studies described in Chapter 4, are used directly as input for the deposition models for generalisation of fluxes over the Netherlands and Europe (Chapter 5). In this chapter, the inferential method for dry deposition is described, and the procedures used to obtain local-scale deposition maps are elucidated. Maps of wet, dry and total deposition of SOx, NOy, NHx and potential acid are presented, along with an overview of the deposition evolvement for several years. Estimates of the natural background deposition are also presented for the sake of comparison. Chapter 6 assesses the uncertainty in deposition estimates by *i)* comparing modelled and measured deposition parameters of $SO_2$ at different sites, *ii)* comparing modelled deposition estimates with throughfall fluxes, and *iii)* by applying an extensive uncertainty analysis of deposition estimates in the Netherlands and Europe. At the end of Chapter 6 the methods and results described in Chapters 1 to 6 will be evaluated in a general synthesis. Three case studies are presented in the last chapter of this book. The first describes a long-term experiment using micrometeorological measurements and throughfall measurements over the heathland called 'Elspeetsche Veld'. The second is a case study on the influence of canopy structure and forest edges on forest deposition using throughfall measurements. The third case study describes the Speulder forest experiment, where micrometeorological measurements, throughfall measurements and measurements of effect parameters have been made to assess the relation between exposure and deposition of pollutants on the one hand and effects on the other.

This Page Intentionally Left Blank

# CHAPTER 2 EMISSION, TRANSFORMATION AND TRANSPORT

*Introduction*

The atmosphere consists mainly of nitrogen (78%), oxygen (21%), argon (1%) and a highly variable amount of water vapour (ranging from less than 0.1% to ca. 4%). Besides these components, the atmosphere contains a large number of so-called trace gases, which play an essential role in preserving life on earth, despite their low concentrations in the order of parts per million (ppm) or less. These trace gases are either emitted into the atmosphere from natural sources (sometimes also as a result of human activities) or they are formed in the atmosphere by chemical processes. Among the air pollutants relevant for acidification and eutrophication are sulphur compounds, and oxidised and reduced nitrogen compounds. Once emitted, gases will be transported and dispersed, leading to long-range transport over several hundred kilometres. Almost all air pollution is emitted at or near the surface of the earth. Transport, transformation and removal are mainly confined to a thin layer of ca. 2-3 km, called the planetary boundary layer (PBL). The understanding of the physics and chemistry of the PBL is important for the development of atmospheric transport models and models for deposition as well as for the interpretation of measurements. In this chapter a comprehensive overview on emission, transformation and transport of gases and aerosols in the PBL and the resulting concentration patterns will be presented.

## 2.1 EMISSION OF NITROGEN AND SULPHUR COMPOUNDS

Sulphur dioxide was one of the first air pollutants recognised as being harmful to humans and ecosystems (see section 1.1 or 1.2). Therefore it is one of the most studied pollutants, with much research being carried out in the early seventies. In the eighties, interest in Europe moved from sulphur compounds to nitrogen compounds. One of the main reasons for that, next to recognising nitrogen as being harmful, is that abatement strategies for sulphur emissions during the last decade have been successful in western Europe, Canada and the USA.

## 2.1.1 ATMOSPHERIC SULPHUR AND NITROGEN COMPOUNDS

Compounds of sulphur found in the atmosphere include sulphur dioxide ($SO_2$), sulphur trioxide ($SO_3$), such aerosol constituents as sulphuric acid ($H_2SO_4$) and different forms of sulphate such as ammonium sulphate ($(NH_4)_2SO_4$), hydrogen sulphide ($H_2S$), dimethyl sulphide (DMS), and, finally, different other forms of sulphur (e.g. COS, $CH_3SH$, $CH_3SCH_3$ and $CS_2$). Sulphur is emitted mainly through human activities in the atmosphere in the form of $SO_2$ (~95%). The most important natural source of $SO_2$ is volcanoes. The oxidation reactions of $SO_2$ eventually all lead to the formation of sulphates in a time period in the order of days. $SO_3$ is emitted together with $SO_2$, however, in very small amounts compared to $SO_2$. $H_2S$ is formed primarily from the natural decay of vegetation on land, marshlands and in the oceans (Welphdale, 1987). DMS is primarily emitted from oceans, whereas organic sulphur compounds might be emitted from oceans and vegetation.

Several nitrogen oxides are known, including nitrous oxide ($N_2O$), nitric oxide (NO), nitrogen dioxide ($NO_2$), nitrogen trioxide ($NO_3$), dinitrogen trioxide ($N_2O_3$), dinitrogen tetroxide ($N_2O_4$) and dinitrogen pentoxide ($N_2O_5$). At normal temperatures and small partial pressures $N_2O_3$ and $N_2O_4$ decompose rapidly to form $NO_2$. Oxidised nitrogen is emitted into the atmosphere mainly by combustion processes and from soils in the form of NO. In the presence of $O_3$, NO is converted rapidly into $NO_2$. As a result of photochemical reactions in the atmosphere or by hydrolyses of $NO_2$, $HNO_3$ and $HNO_2$ can be formed. Also peroxyacetylnitrate (PAN) can be formed from photochemical conversion of $NO_2$. $N_2O$ is emitted from soils under conditions of denitrification (Meszaros, 1987). Nitrate aerosols are formed by the reaction of $HNO_3$ with sea salt or with $NH_3$.

Reduced nitrogen are present in the atmosphere almost entirely as $NH_3$ or particulate $NH_4^+$. $NH_3$ in Europe is primarily emitted from animal manure, whereas $NH_4^+$ is primarily formed in the atmosphere as a reaction of $NH_3$ with $H_2SO_4$, $HNO_3$ or HCl.

## 2.1.2 EMISSIONS

Table 2.1 lists global, European and North American emissions of sulphur dioxide, nitrogen oxides and ammonia separated into anthropogenic and natural sources (Whelpdale, 1987). Anthropogenic emission of $SO_2$ results from fossil fuel combustion. Most important sources are refineries, power plants, domestic heating and traffic (Table 2.2). In addition to these anthropogenic sources, emissions of reduced sulphur compounds have also been quantified. Estimates of the amount emitted by the biosphere from oceans, soils, terrestrial vegetation and from volcanoes and biomass burning range between 35 and 70 Tg S $a^{-1}$ (see Table 2.3). After oxidation and including oxidised sulphur emissions from natural sources, total natural emissions are roughly equivalent to anthropogenic emissions of about 70 - 100 Tg S $a^{-1}$ on a global scale. In Northern America and Europe, however, anthropogenic emissions dominate.

**TABLE 2.1** Total $SO_2$, NOx and $NH_3$ emissions in 1987 in the world and on European and American scales separated into natural and anthropogenic emissions (Whelpdale, 1987; NAPAP, 1989)

| Scale | $SO_2$ Tg S $a^{-1}$ | | NOx Tg N $a^{-1}$ | | $NH_3$ Tg N $a^{-1}$ | |
|---|---|---|---|---|---|---|
| | Anthropogenic | Natural | Anthropogenic | Natural | Anthropogenic | Natural |
| Global | 85 | 82 | 33 | 18 | 77-95 | 32-36 |
| Europe | 26 | 2 | 5.8 | 0.5 | 5.3 | 0.6 |
| North America | 15 | 1 | 6.9 | 1.1 | 1-10 | unknown |

Natural nitrogen emissions form only 10% of total nitrogen emissions in Europe. European emissions form 5 - 8% of the total global nitrogen emissions. Total emissions of nitrogen oxides in Europe from the main source categories are presented in Table 2.2. The most important sources are traffic, power stations and industry. Nitrogen oxides are also emitted from soils by denitrification and formed by conversion of $NH_3$ by OH in the atmosphere. Natural emissions of nitrogen comprise lightning and stratospheric destruction of $N_2O$.

**TABLE 2.2** Source contribution of anthropogenic sulphur dioxide, nitrogen oxides, and ammonia to anthropogenic emissions in 1980 in Europe (Hov *et al.*, 1987; Asman, 1992)

| Source contribution to total emissions in Europe | $SO_2$ | NOx | $NH_3$ |
|---|---|---|---|
| Power stations | 36% | 30% | |
| Refineries | 3% | 1% | |
| Chemical industries | 2% | 3% | 2% |
| Other industries | 42% | 26% | |
| Non-industrial sources | 16% | 5% | |
| Traffic | 1% | 35% | |
| Livestock breeding | | | 81% |
| Fertilisers | | | 17% |

Ammonia sources include livestock farming, fertilisers, coal combustion, human respiration, households, industry, sewage sludge and traffic (Table 2.2). The contribution of different sources is given by Asman (1992). The major sources for ammonia are agricultural activities, i.e. low level sources. More than 80% of ammonia emissions result from intensive pig, cattle and poultry breeding. Natural sources comprise wildlife and oceans. These emissions are, however, very small compared to anthropogenic emissions.

**TABLE 2.3** Emissions of reduced sulphur compounds to the atmosphere in Tg S $a^{-1}$

| Emission sources [a] | Emission |
|---|---|
| Emissions from the oceans, mainly dimethyl sulphide | 16 - 38 |
| Soils and plants | 4.8 - 15 |
| Volcanism | 9 - 13 |
| Coastal wetlands | 2 |
| Biomass burning | >2.4 |
| Sum natural Emissions | 32 - 68 |

[a] Natural emissions as $H_2S$, COS, $CH_3SH$, $CH_3SCH_3$ DMS. and $CS_2$
Data from: Andreae (1991); Andreae and Andreae (1988); Andreae and Jaeschke (1992); Andreae and Raemdonck (1983); Bates *et al.* (1987); Berresheim *et al.* (1989); Cullis and Hirschler (1980).

## 2.1.3 EVOLVEMENT OF ANTHROPOGENIC EMISSIONS SINCE 1900

*Emissions between 1900 and 1990*
Figure 2.1 shows total emissions of sulphur dioxide, nitrogen oxides and ammonia in Europe between 1900 and 1990 (De Leeuw, 1995). Since 1900 all emissions show a distinct upward trend. During the First and second World Wars total sulphur emissions in Europe decreased somewhat. Since 1950 all nitrogen emissions have shown an upward trend. Ammonia emissions doubled between 1950 and 1990, while emissions of nitrogen oxides increased by more than a factor of three. Sulphur dioxide emissions increased by more than a factor of two in these years. After 1985 emissions of both oxidised and reduced nitrogen showed a slight increase, whereas emissions of sulphur dioxide decreased in most countries. Abatement strategies for sulphur emissions during the last decade have been very successful in western Europe (Tuovinen *et al*, 1994), leading to an overall emission reduction of the order of 50%. A comparable trend in emissions has been observed in the USA (National Research Council, 1986; NAPAP, 1992). Figure 2.2 shows the evolvement of sulphur and nitrogen emissions in the USA between 1900 and 1988. Compared to the European estimates a similar evolution of emissions can be observed. Between 1900 and 1970, estimated $SO_2$ emissions increased by a factor of three, and NOx emissions increased almost ten fold (NAPAP, 1992). In the 1970 - 1987 period, US anthropogenic emissions of $SO_2$ decreased 28%. NOx emissions remained at the same level during this period.

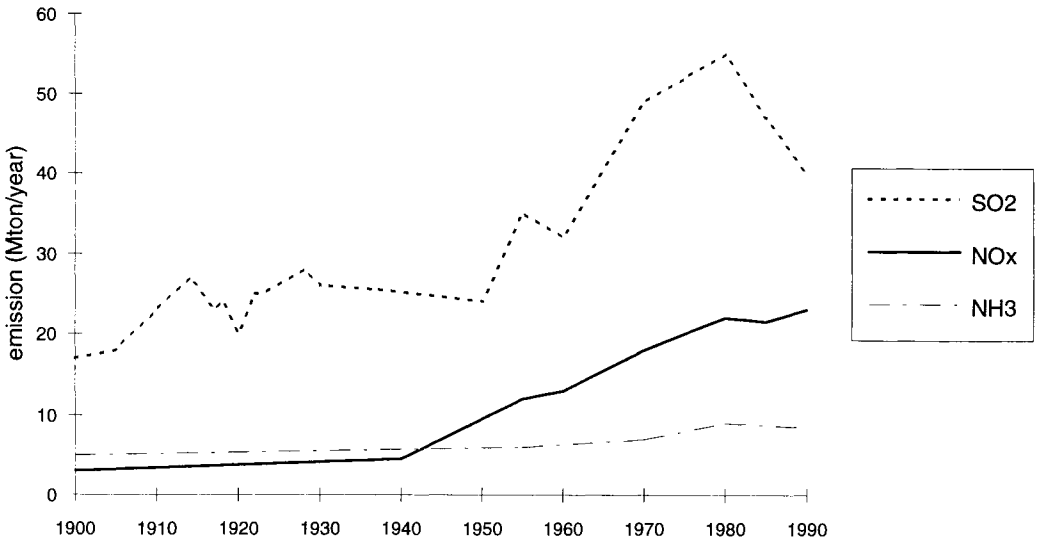


**FIGURE 2.1** Emissions of sulphur dioxide, nitrogen oxides and ammonia in Europe from 1900 to 1990 (mton $a^{-1}$) compiled by De Leeuw (1995)

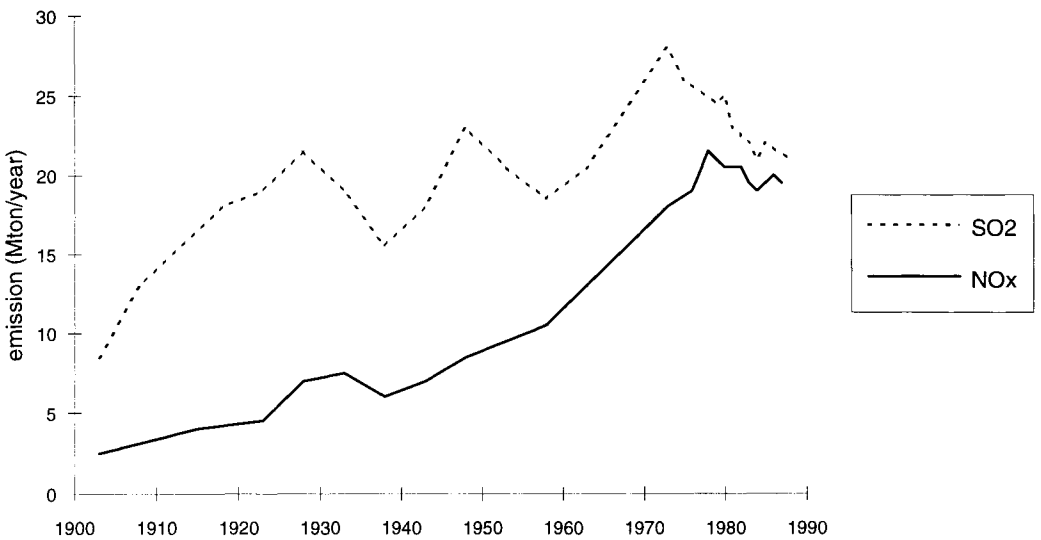


**FIGURE 2.2** Emissions of sulphur dioxide, nitrogen oxides and ammonia in USA from 1900 to 1990 (mton $a^{-1}$) (NAPAP, 1992)

National emissions of sulphur and nitrogen for Europe are compiled by EMEP (Tuovinen *et al*, 1994) (See Appendix A). In most countries nitrogen oxide emissions in 1990 are similar to those in 1985 or a slight (<10%) increase is observed. In contrast to sulphur, a clearly decreasing trend for nitrogen oxides has not been observed in any country. For ammonia, there are few official emission estimates. Estimates have been made for Europe based on animal statistics and emission factors by Buijsman et al. (1984). These estimates were updated by Asman (1992).

*Emissions in the Netherlands and Europe during recent years*
Detailed emissions for different years are used for long-range transport model input to estimate the concentration and deposition distribution over the Netherlands or Europe (see section 2.3).

The Dutch total annual $SO_2$ and NOx emissions for the period 1980 - 1993 are given in Table 2.4 and plotted in Figure 2.3. The spatial distribution of $SO_2$ and NOx emissions in the Netherlands and in Europe shows that the highest emissions are from the industrial areas. For $SO_2$ emissions in the Netherlands this is the Rijnmond area at the west coast, and for NOx the 'Randstad' in the central-west part of the country. In Europe the so-called 'Black triangle', i.e. the border area between Germany, Poland and the Czech Republic, clearly displays the highest emissions of $SO_2$. Highest NOx emissions are found in Germany and the Netherlands. The annual average emissions for the countries in Europe are annually reported by EMEP (Tuovinen *et al.*, 1994).

**TABLE 2.4** Dutch total annual emissions 1980 - 1993 expressed in kton $SO_2$, kton $NO_2$ for NOx

| | 1980 | 1981 | 1982 | 1983 | 1984 | 1985 | 1986 | 1987 | 1988 | 1989 | 1990 | 1991 | 1992 | 1993 |
|---|---|---|---|---|---|---|---|---|---|---|---|---|---|---|
| $SO_2$ | 489 | 463 | 403 | 323 | 299 | 261 | 263 | 262 | 247 | 205 | 201 | 177 | 167 | 168 |
| NOx | 582 | 575 | 561 | 554 | 571 | 573 | 586 | 597 | 599 | 583 | 570 | 561 | 550 | 568 |

The TREND model was used with meteorological statistics obtained from measurements of the National Air Quality Monitoring Network to estimate the concentration and deposition distribution of $NH_3$ and $NH_4^+$ in the Netherlands (Van Jaarsveld, 1994 and Chapter 5). To model this distribution correctly, detailed knowledge on the emission of ammonia in the Netherlands is necessary. Ammonia emissions on a 5 x 5 km grid for 1987 and 1988 were estimated by Erisman (1989). The spatial distribution of the $NH_3$ emissions in 1980 to 1989 was obtained via scaling of the 1987/1988 distribution with the annual average $NH_3$ emission (Erisman, 1992; 1993a). Recently, Van der Hoek (1994) estimated 5 x 5 km grid emissions

for more recent years (1990, 1991 and 1992). His method was also used to estimate emissions for 1993. The annual average emission in the Netherlands during 1980 to 1993 are listed in Table 2.5. The estimates in Table 2.5 are used here to show annual variations, as displayed in Figure 2.3. The highest emissions are found in three areas with intensive livestock breeding, i.e. the Peel area in the southeast, the province of Overijssel in the central-eastern part of the country and the Gelderse Vallei in the centre of the country.

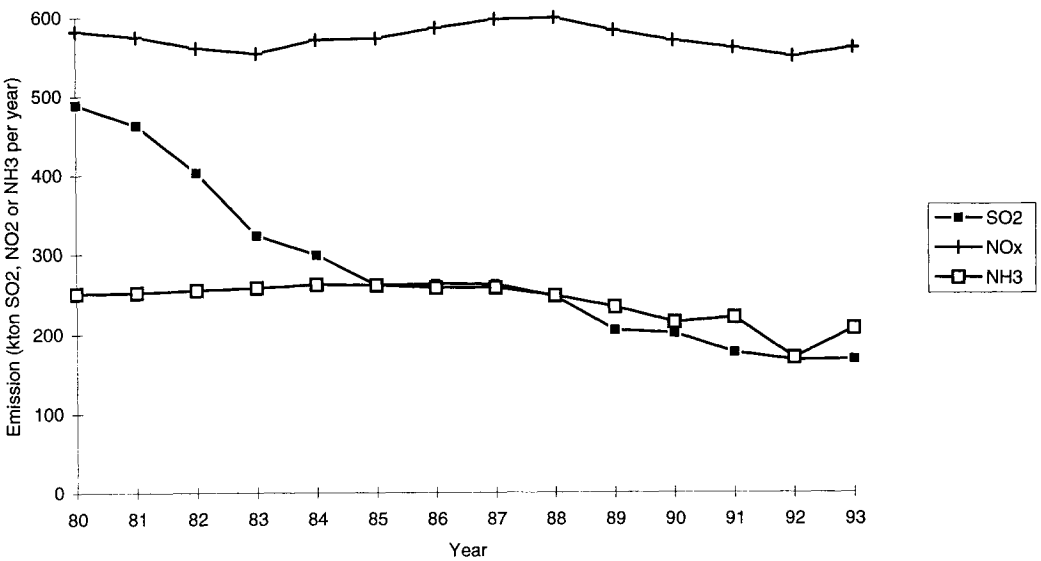


**FIGURE 2.3** Total $SO_2$, NOx and $NH_3$ emissions in the Netherlands (kton $a^{-1}$).

From Table 2.5 and Figure 2.3 it is obvious that after 1987 emissions gradually decreased. In 1992 several emission reduction measures were carried out for the first time on a large scale in the country, such as coverage of manure storage basins, change in nitrogen content of fodder and injection or ploughing of manure into the soil. Especially the injection of manure was expected to lead to large emission reductions (Heij *et al.*, 1991). The ammonia estimates for 1992 and 1993 are based on the assumption that measures implemented for emission reduction were 100% effective (Van der Hoek, 1994). This led to the estimation of 20% emission reduction in these years compared to 1991.

The $NH_3$ emissions for other countries for several years are listed Tuovinen *et al.* (1994). The $NH_3$ emissions reported by EMEP are based on estimates by Asman (1992). The spatial distribution of $NH_3$ emissions in Europe shows that the highest $NH_3$ emissions are found in central Europe with the highest values in the Netherlands, France, Belgium and Denmark.

**TABLE 2.5** Overview of the ammonia emission in the Netherlands from 1980 to 1993

| | 1980[b] | 1981[b] | 1982[b] | 1983[b] | 1984[b] | 1985[b] | 1986[b] | 1987[b] | 1988[b] | 1989[b] | 1990[a] | 1991[a] | 1992[a] | 1993[c] |
|---|---|---|---|---|---|---|---|---|---|---|---|---|---|---|
| Livestock breeding | 235 | 234 | 236 | 240 | 243 | 242 | 242 | 239 | 227 | 211 | 223 | 232 | 174 | 183 |
| Fertiliser | 10 | 10 | 10 | 10 | 10 | 10 | 10 | 10 | 10 | 11 | 11 | 10 | 9 | 9 |
| Industry | 8 | 8 | 8 | 8 | 8 | 8 | 8 | 8 | 8 | 6 | 5 | 5 | 5 | 5 |
| Households | 1 | 1 | 1 | 1 | 1 | 1 | 1 | 1 | 1 | 9 | 10 | 11 | 11 | 11 |
| Total | 254 | 253 | 255 | 258 | 262 | 261 | 260 | 258 | 246 | 237 | 249 | 258 | 199 | 208 |

a Van der Hoek (1994)
b Erisman (1992)
[c] Assumed to be equal to 1992 (Van der Hoek, pers. comm.)

## 2.2 ATMOSPHERIC CHEMISTRY

Atmospheric chemistry is important in relation to atmospheric deposition in two ways. First, conversion of gases in the atmosphere might lead to cleaning the atmosphere of the pollutant gas, or to changes in the physical and chemical properties of the pollutant resulting in changes in deposition characteristics. Second, atmospheric chemistry is important because it might affect the gradient of a pollutant above the surface. This forms a problem when measuring the flux of the component above the surface and when determining its flux with deposition models, assuming a constant flux layer without sources or sinks between the level of determination of the concentration and the receptor surface.

The first case is especially important for all primary emitted gases: $NH_3$, $SO_2$ and NOx. $NH_3$ neutralises acidic gases forming aerosols. These aerosols have much lower deposition velocities, leading to longer transport distances. For $SO_2$ the same is true via the route of oxidisation to sulphuric acid, which in turn might be neutralised by $NH_3$. For NOx the coupling is somewhat more complicated because through formation of $HNO_3$ the deposition velocity of primarily emitted NOx is initially increased to a large extent. However, when neutralised by $NH_3$, the deposition velocity is lowered again by about a factor of about 4. The second case is especially important for equilibrium reactions between $NH_3$ and $HNO_3$, as well as between NOx and $O_3$.

Air pollution chemistry is often rather complicated in the sense that equilibria and higher-order reactions play an important role. Our knowledge of the chemical conversion processes stems in the first place from fundamental kinetic and mechanistic research. Chemical kinetic schemes are built from the kinetic parameters of the reactions that have been shown to be important. However, considerable uncertainty can remain in the results of kinetic parameters.

Therefore the schemes are tested as a whole against smog chamber experiments or in field studies. Validation of chemical schemes by field studies is only possible if an accurate and complete database for chemical and meteorological data is available. Although sophisticated air quality models incorporate updated detailed transport and transformation processes, many areas of uncertainty remain.

Air pollution models can be classified according to the treatment of chemical processes on the one hand and of dispersion and meteorological processes on the other. In most simple dispersion models like, for instance, the Gaussian plume model, chemical conversion can only be specified as a net first-order rate constant. Such an approximation allows for linear combination of the contributions of different sources to local concentrations, thus cutting down computational effort. On the other hand, simple models for chemical air pollution (e.g., box models) have a chemical reaction scheme as their main component, whereas dispersion and meteorology is dealt with in a rather limited way.

In this section the main chemical reactions for $SO_2$, NOx and $NH_3$ are described qualitatively and shown in Figure 2.4. Extensive overviews of chemical reactions can be found in Seinfeld (1986), Finlayson-Pitts and Pitts (1986), Meszaros (1987), and more recently in e.g. EUROTRAC reports (see e.g. Borrel *et al.*, 1995).

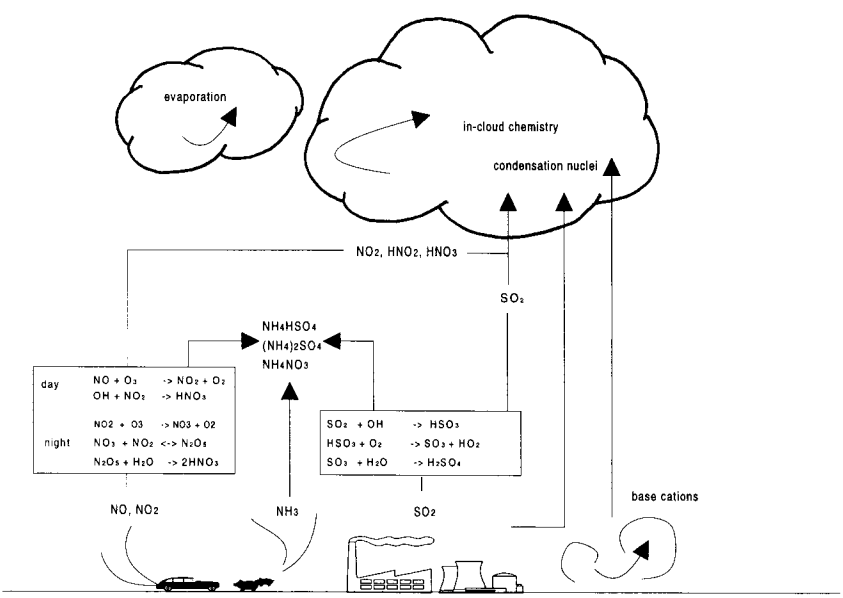


**FIGURE 2.4** Atmospheric chemistry relevant for acidifying species.

*$SO_2$*

Once emitted, $SO_2$ may be oxidised to sulphuric acid aerosols or sulphates by reactions occurring in the gas phase, in the liquid phase, on the surfaces of solids, or combinations of these three. The main gas phase reaction is the reaction of $SO_2$ with OH radicals, first forming $HSO_3$ and subsequently $H_2SO_4$. The latter can be neutralised by $NH_3$ forming $(NH_4)_2SO_4$ or $NH_4HSO_4$. Rates of conversion generally seem to be higher during the day than at night, and in summer compared to winter (Meszaros, 1987). The presence of liquid water in aerosols, clouds and fog is found to be an important factor in determining the rate of conversion of $SO_2$ (Finlayson-Pitts and Pitts, 1986). Furthermore, the reaction rate in liquids is influenced by the pH, metallic catalysts and oxidising pollutants ($O_2$, $O_3$, $H_2O_2$) (Welphdale, 1987). Thus sunlight intensities, presence of oxidants and/or oxidant precursors, humidity and the presence of fog and clouds all appear to affect conversion rates. Because of the influence of these variable factors, a wide range of reaction rates is reported in the literature (see Finlayson-Pitts and Pitts, 1986, for a review). Typical summertime oxidation rates in rural areas cause 0.1 - 1.5% loss of $SO_2$ $a^{-1}$.

*NOx*

The atmospheric chemistry of oxidised nitrogen compounds is complicated because they may be converted into a number of different chemical forms. The main oxidised nitrogen compound emitted is nitrogen monoxide. It is oxidised in the atmosphere to nitrogen dioxide and further to nitrate. During the day, nitrogen dioxide is oxidised in the gas phase to nitric acid by the hydroxyl radical. Nitrogen dioxide reacts with water absorbed on a variety of surfaces to form nitric acid and nitrous acid. Nitrous acid is apparently released from the surface, while nitric acid stays absorbed. This provides a minor pathway for nitrate formation in aerosols (Hov *et al.*, 1987). Nitrous acid can also be formed by the reaction of nitrogen monoxide with OH (Pitts and Pitts, 1986). Although nitrous acid photolyses very rapidly, significant concentration levels can be detected in polluted areas in Europe in the middle of the day (Slanina *et al.*, 1990). PAN (peroxyacetyl nitrate) is formed from the reaction of peroxyacetyl radicals with nitrogen dioxide. Although PAN can be present in significant concentrations, its contribution to nitrogen deposition is expected to be low because of low deposition velocities (Dollard *et al.*, 1990).

During night-time, oxidation of nitrogen dioxide by ozone forming the nitrate radical may be an important source of nitric acid. The residence time in the atmosphere varies due to the different reaction processes involved. Of the gaseous nitrogen compounds, nitric acid has the highest deposition velocity and the shortest residence time in the air.

Particulate nitrate is formed by the reaction of gaseous nitric acid with sea salt, basic particles or gaseous ammonia (Seinfeld, 1986). Conversion of gaseous nitric acid and ammonia to particulate nitrate and ammonium is a process of importance for deposition, since easily deposited gaseous compounds are turned into fine particulate nitrate and ammonium, which are slowly deposited and transported over large distances. Ammonium nitrate and ammonium

sulphate are hygroscopic, and the humidity in the air will to some extent determine the size of the particles in the air and thus influence the rate of deposition. Ammonium nitrate can be converted back to nitric acid at low ammonia concentrations (Stelson and Seinfeld, 1982a-c). The supply of ammonia is therefore an important factor in determining the residence time of nitrogen oxides.

The interpretation of field measurements of the surface exchange of NO, $NO_2$ and $O_3$ are influenced by the photochemical equilibrium between these gases (Duyzer and Fowler, 1994). The reaction rates in this equilibrium system are fast enough to interfere with both measurements of and actual fluxes at the surface. Several methods have been described to correct for the equilibrium reactions to derive the 'real' surface exchange rates. Duyzer and Fowler concluded, however, that none of these methods are accurate enough.

*$NH_3$*

Ammonia has a relatively short residence time in the atmosphere. It is readily water soluble and rapidly converted to ammonium, thereby neutralising acid pollutants in the air as well as in the water phase. Particulate ammonium is formed by the reaction between gaseous ammonia and acid compounds in the air such as sulphur dioxide/sulphuric acid and hydrochloric acid droplets. $NH_3$ can also react with OH radicals, which forms only a minor loss process (Logan, 1982).

$NH_3$ will react irreversibly with $H_2SO_4$ -containing aerosol. A smaller part of atmospheric $NH_3$ will react with $HNO_3$ and HCl to form aerosol compounds such as $NH_4NO_3$ and $NH_4Cl$ (Pio and Harrison, 1987) which can dissociate again. The net conversion rate of $NH_3$ into $NH_4^+$ in the atmosphere is thus the result of various reactions, diffusion to aerosols and vertical exchange processes in the atmosphere. The conversion rate was determined by Erisman *et al.* (1988) using vertical profiles of $NH_3$ and $NH_4^+$ measured at a 200-m meteorological tower in the centre of the Netherlands. For daytime periods a first-order reaction rate of $1 \times 10^{-4}$ $s^{-1}$ and for night-time periods $5 \times 10^{-5}$ $s^{-1}$ were determined. In fact, the reaction mechanism is much more complicated, because many components are involved and different types of reactions take place in both the gas phase and in solution.

The equilibrium between $NH_3$ and $HNO_3$ and HCl can be described using theoretical descriptions of the dissociation constant (Stelson and Seinfeld, 1982). Generally, the theoretical descriptions based on temperature and humidity compare reasonably well with dissociation constants derived from measurements of ambient concentrations of the gases and aerosols. However, at temperatures below 0 °C and at rh > 80% large deviations were found. This might have consequences when the theoretical descriptions are used to correct flux estimates or measurements influenced by the above-mentioned equilibrium reactions.

Because of the frequent predominance of sulphate, nitrate, ammonium and water by total mass, ambient atmospheric aerosol can often be characterised as consisting of a concentrated

aqueous solution of ammonium nitrate, ammonium bisulphate and sulphate, nitric and sulphuric acids and two mixed salts of ammonium sulphate and nitrate. Which of these species predominates depends on ambient conditions. When these aerosols act as condensation nuclei or are incorporated into precipitation by rain-out processes, precipitation characteristics are determined by the chemical aerosol system. Thus the wet deposition flux is determined by the composition of the aerosols. To predict the quantity and composition of the aerosol, a prediction of the formation rate of nitric acid and sulphuric acid from NOx and $SO_2$ precursors, respectively, must be coupled to an equilibrium description of the aerosol. Furthermore, the neutralisation by $NH_3$, and with this its concentration, temperature and relative humidity play an important role. Therefore changes in precursor emissions play an important role in aerosol concentration and thus wet deposition (see also section 5.3).

## 2.3 FACTORS AFFECTING TRANSPORT

The maintenance of a tolerable environment depends very much on the ability of wind and turbulence to disperse pollutants rapidly as they are emitted. When these processes fail, the result is a quick build-up of concentrations. A good example of this is the situation in London in the fifties where people were exposed to enormous concentrations of sulphur in air and fog (Brimblecombe, 1987). There are some locations where natural ventilation is so poor that the emission of pollutants must, at all times, be carefully controlled. Factors affecting the dispersion of gases and particles include:

a) *Source characteristics.* Emissions of small sources usually have relatively little buoyancy, since temperature at the point of emission is not much higher than that of the surrounding air. Such sources are liable therefore to have their greatest impact in the immediate vicinity. Emissions from large-scale industrial installations, on the other hand, may be at higher temperatures, or may, by forced draught, compelled to rise more rapidly. Thus, any major impact in the immediate vicinity may be avoided but weaker effects over a wider area may be produced (Bosanquet, 1957).

Dilution and dispersion over a wide area is also aided by the use of tall stacks. Much is known of the relationship between source strength, stack heights and ground-level concentrations of pollutants through the application of mathematical modelling techniques, coupled with observations around selected sources (e.g. Pasquill, 1971). Introduction of tall stacks was thought to be the solution for problems caused by local build-up of concentrations in the sixties. Tall stacks are widely used for power stations and other major industrial sources. Pollutants emitted from these sources will be carried over great distances, often over national boundaries, and will eventually be deposited far away from their sources

b) *Topography and other landscape features.* The presence of hills and many other features of the landscape, have important effects on the dispersion of plumes from individual sources, or

of the pollution from an area source as a whole. Many industrial cities have developed in river valleys, initially to take advantage of water transport. However, in general, the dispersion of pollutants in such a situation is poorer than it would be from a more exposed location.

c) *Climate and meteorology.* Meteorological factors are of fundamental importance in determining the whole spatial and temporal distribution of pollution. Apart from the general influence of the local climate, the great variability of the weather in any one locality is liable to lead to considerable changes in the concentrations of gases. In particular, temperature inversions can trap pollutants to produce concentrations of up to 100 times the usual concentration.

Large-scale meteorological factors affecting concentration distributions, and with these also deposition distributions, are dispersion, turbulence (transport), humidity and radiation (chemical conversion). Pollutants are mixed or dispersed through the lower atmosphere by turbulent diffusion, vertical wind shear and precipitation processes. Turbulence is generated both mechanically (e.g. wind shear and surface roughness) and thermally (e.g. convective motion from solar radiation heating the surface). The larger the scale and intensity of turbulence, the more efficient the mixing. Atmospheric motions are slowed down due to the surface drag in the boundary layer.

Principle features influencing European climate are the Icelandic low and the Azores high pressure system. They are present at all seasons, although their location and relative intensity can change considerably. The other major pressure system is the Siberian winter anticylone, the occurrence of which is intensified by the extensive winter snow cover and the marked continentality of Eurasia. Atlantic depressions frequently move towards the Norwegian or Mediterranean Seas in winter, but if they travel due east they occlude and fill long before they can penetrate into the heart of Siberia. Thus the Siberian high pressure is quasi-permanent at this season and when it extends westwards severe conditions affect much of Europe. In summer, pressure is low over all of Asia and depressions from the Atlantic tend to follow a more zonal path. Although the depression tracks over Europe do not shift poleward in summer (as a result of a local southwards displacement of the Atlantic Arctic front), the depressions at this season are rather less intense and the diminished airmass contrasts produce weaker fronts. The influence of maritime air masses can extend deep into Europe because there are few major topographic barriers to air flow and because of the presence of the Mediterranean Sea. Hence, the change to a more continental climate regime is relatively gradual except in Scandinavia where the mountain spine produces a sharp contrast between western Norway and Sweden (Barry and Chorley, 1977). Main circulation types above western and central Europe are presented in Figure 2.5.

A large part of western and central Europe is characterised by a relatively warm temperate rainy climate with average temperatures in the coldest month between -3° and 18°C and in the warmest month > 10°C. No distinct dry season can be studied in these areas. Southern Europe

has the same temperate rainy climate but now with a clear dry period in summer. South-eastern Europe has a dry climate with mean temperatures in the warmest month > 18°C. Large parts of northern and eastern Europe have a cold boreal forest climate with mean temperatures in the coldest month < -3°C and in the warmest month > 10°C with no clear dry season. Some parts of Scandinavia have a tundra climate with temperatures in the warmest month < 0°C.

The Dutch climate can be characterised as a maritime climate. Although the wind directions are variable in the regions of the Netherlands, the long-term meteorology can be characterised by several features (KNMI, 1979). Low pressure areas usually move from west to east or from southwest to northeast. These air streams are usually accompanied by moist ocean air and moderate winds. Above the sea, the formation of showers, as a result of convection, is frequently observed. About 60% of the time, wind blows from the south to western directions. The remaining periods can be characterised as variable with regard to wind direction, wind speed and type of weather. One characteristic type of weather is observed during easterly winds, bringing dry air with a low wind speed from the east of the European continent. During such periods, a strong high pressure area is located near Scandinavia. This stable high pressure area persists for several days in a row, leading to episodes of high concentrations of air pollution in the Netherlands and in large other parts of Europe (KNMI, 1979; RIVM, 1990).

The influence of the sea on the climate is large. In summer, the sea brings cool air over the country, whereas in winter it brings warm air. The presence of such a large storage reservoir, not cooled or heated very fast, protects the Netherlands from temperature extremes. Extreme values are therefore nearly always observed in periods with easterly flows. Air coming from an easterly direction can be characterised as polluted because it passes over large industrial areas. Air coming from a (south)westerly direction can be characterised as relatively clean air. The annual amount of precipitation measured in the Netherlands is about 770 mm. The annual average wind speed, measured at a height of 10 m is 4.5 m $s^{-1}$. Average summer and winter temperatures are about 14 °C and 4 °C, respectively.

The deposition processes of interest constitute a complex sequence of atmospheric phenomena. The deposition fluxes, which are the result of these processes, can vary considerably with time and place. Variations in deposition are the result of large-scale and small-scale meteorological processes. In practice, processes in the boundary layer (height < 3 km) are of the most influence for the amount of deposition (Hov *et al.*, 1987; Hicks *et al.*, 1989).

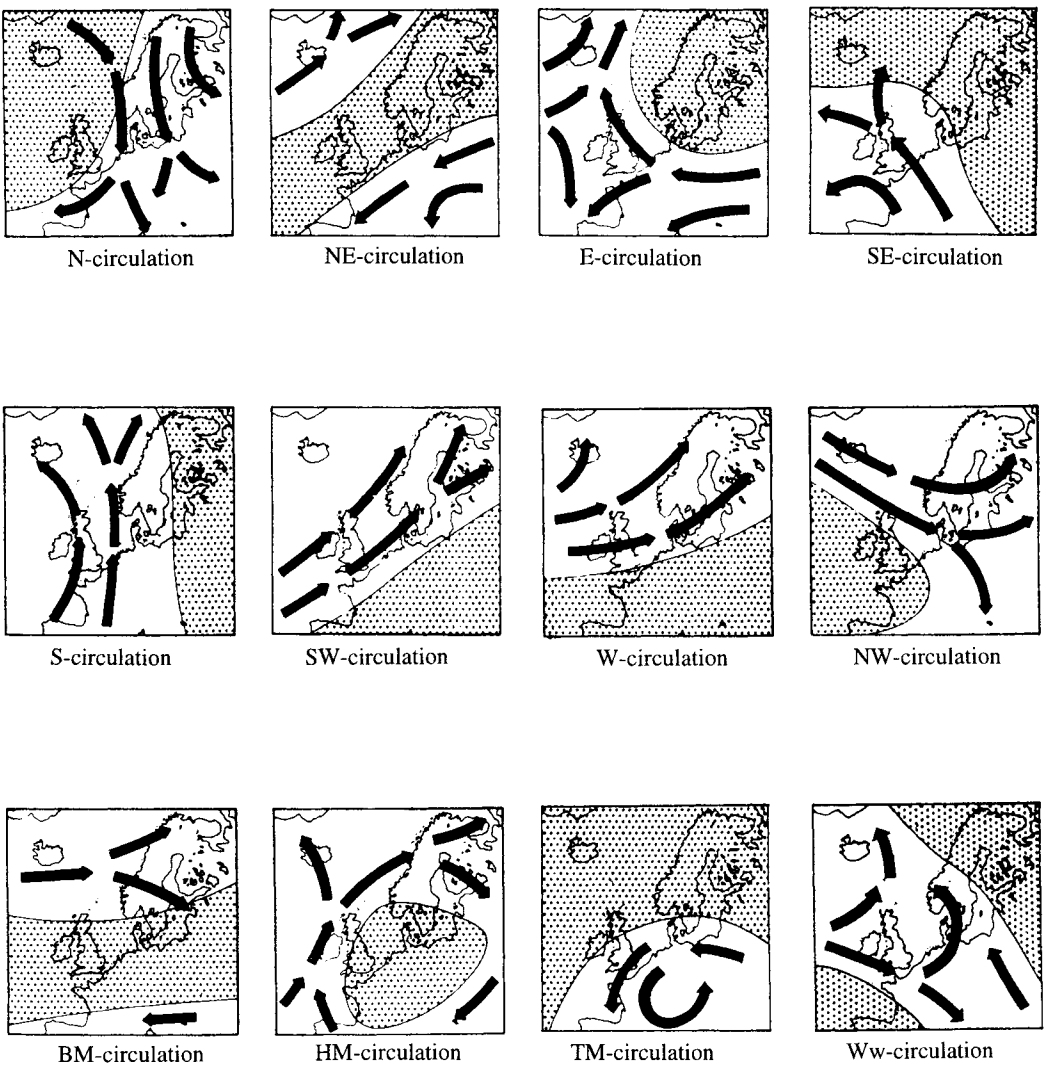


**FIGURE 2.5** Schematic representation of the main circulation types above western and central Europe. The location of the high pressure area is indicated by dots. The arrows give the tracking direction of depressions as well as the mean direction of the wind in the higher air layers. Generally, the characters represent the main direction of the circulation (e.g. SE = southeast); Ww = bending west circulation, BM = high pressure area above Atlantic ocean - central Europe, HM = high pressure area above central Europe, TM = low pressure area above central Europe (after Van der Ham, 1977).

During daytime, the atmospheric boundary layer is usually unstable as a consequence of isolation and convection. During night-time, usually a stable atmosphere is observed because of an upward energy flux due to radiation. The typical boundary-layer development during the day is shown in Figure 2.6. In the morning, during fumigation, the layer breaks open, transporting air from higher levels to ground level. Other meteorological features affecting the transport and deposition of air pollution are snow cover; radiation (influencing the reaction of components and regulating stomatal behaviour); temperature (affecting reaction rates and equilibria, and stomatal behaviour); amount and composition of precipitation; surface wetness by precipitation, dew and fog; wind speed and wind direction. More information on the impact of these features is presented in Chapter 3.

Particles play a crucial role in atmospheric chemistry and atmospheric transport. They can be considered as an important intermediate for gaseous deposition and transport. Furthermore, alkaline particles can increase the buffer capacity of sensitive ecosystems when deposited, thus reducing the effect of acidification due to deposition of acidifying components. The influence of particles in long-range transport, atmospheric chemistry, and wet, dry and fog deposition is gradually becoming clear but is not quantified to a satisfying extent.

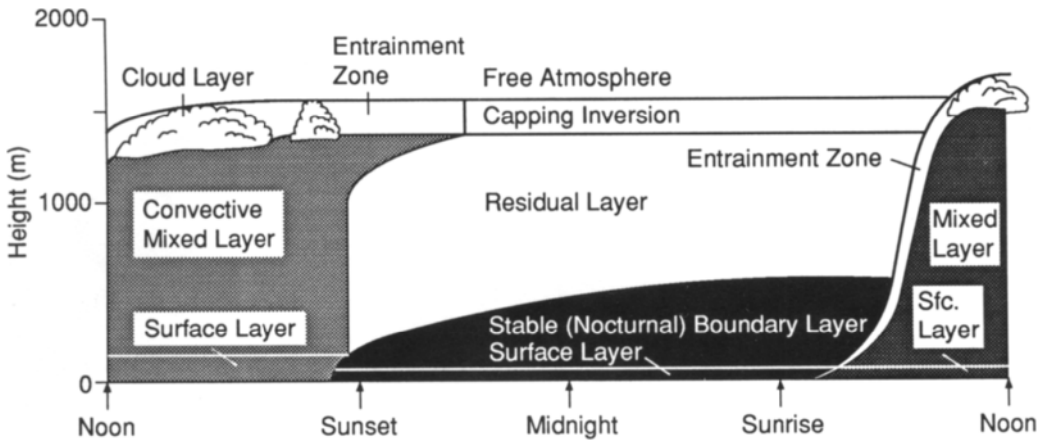


**FIGURE 2.6** Daily variation of the boundary-layer development (Stull, 1988).

Natural sources of particles include 'seaspray', re-suspension, volcanoes, biomass burning and meteorites. The first of these two dominate the natural sources of particles. Seaspray is formed by the outburst of air bubbles in the foam on the sea. The aerosols brought into the atmosphere through this process are large particles of which the composition equals that of the ocean. The

particles emitted into the atmosphere by re-suspension are composed as mineral dust. These are also mainly large particles in which significant concentrations of $Ca^{2+}$, $Mg^{2+}$ and $K^{+}$ can be found. In the Netherlands deposited seaspray can be re-suspended, thus contributing to $Na^{+}$, $Mg^{2+}$, $SO_4^{2-}$ and $Cl^{-}$ concentrations in particles.

Acidifying particles are not directly emitted into the atmosphere but are formed by reactions between gases. Atmospheric transport of gases is influenced by particles by several means. Because the dry deposition velocity of particles is usually much lower than that of the gases, the formation of particles from gases leads to long-range transport of pollutants. Furthermore, deposition of gases is influenced through a shift in gaseous composition of the atmosphere, shifting equilibrium and thus the extent that gases are in gaseous or particle form. Gas deposition, especially of soluble gases, is influenced by the layers of water on top of the vegetation (see Chapter 4). Water layers are the result of direct water input from precipitation, or they are formed by deliquescence of particles deposited on the vegetation (Burkhardt and Eiden, 1994). This might be acidifying particles or base cations. Finally, particles serve as condensation nuclei, forming clouds. Gases and aerosols can be scavenged through precipitation.

## 2.4 LONG-RANGE TRANSPORT MODELLING

The way deposition is modelled depends on its purpose. It may be considered as a loss term in long-range transport modelling, or as an input term in determining the deposition to ecosystems. For the latter it is important to consider the scale on which the deposition is desired. If the scale is comparable to the scale considered in the long-range transport (LTRAP) model, the deposition estimates of this model can be used directly. But if the desirable scale is much smaller than that considered in the LTRAP model, sub-grid processes should be taken into account.

Modelling the dispersion of trace gases in the atmosphere, including their physical and chemical transformations, is an essential element of the general study of trace gas behaviour and in the determination of the functional relationships between emissions and concentration or deposition levels. Measurements and models are strongly intertwined. On the one hand, measurements are necessary for parametrisation and validation of models, while on the other model results may render support in the evaluation, generalisation or extrapolation of measurements. Dispersion models exist in all sizes and complexities. The choice for a model or model concept is determined by the spatial and temporal scale on which air quality and deposition estimates have to be made (cf. Van Dop, 1986). In general, the models can be divided into different categories according to their mathematical framework: Eulerian models with a fixed co-ordinate system, Lagrangian models, where the co-ordinate system moves with the representative parcel of air or hybrid models merging both concepts. Here we will focus on two Lagrangian-type LTRAP models that are used to determine the annual spatial

distribution of pollution in Europe and in the Netherlands related to acidification. These are the EMEP (Eliassen and Salbones 1983, Iversen *et al.*, 1991) and TREND (Van Jaarsveld, 1994) models.

The deterministic Lagrangian EMEP model is a receptor-oriented one-layer trajectory model originally developed at the Norwegian Meteorological Institute (Eliassen and Saltbones, 1983) and operationally applied in the framework of the 'Co-operative programme for monitoring and evaluation of the long-range transmission of air pollutants in Europe'. The European Monitoring and Evaluation Programme (EMEP) under the UN ECE Convention on Long Range Transboundary Air Pollution, consists of a monitoring programme and modelling of atmospheric transport, conversion and deposition. The aim of EMEP is to provide basic information about emissions, levels of concentrations and deposition. The model calculates 96-h trajectories in reverse time on the basis of the 850 hPa wind field from the arrival of an air parcel at a receptor. Receptor points are the grid points of a 150 x 150 km grid system covering Europe. The trajectories arrive at the receptor points four times a day. During the air parcel's travel along the trajectory, the gridded sulphur and nitrogen emissions are immediately mixed in the vertical up to the top of the constant mixed layer. The model is used every year to estimate sulphur and nitrogen pollution in Europe and to determine the country-to-country receptor matrices and country budgets (e.g. Tuovinen *et al*, 1994).

The statistical transport model TREND is able to describe both short- and long-distance transport, and average concentrations and depositions can be computed for time scales from 1 day to more than 10 years (Van Jaarsveld, 1994). It can account for both point sources of various heights and area sources of various shapes and heights. The sources need not be distributed on a regular grid system. It yields realistic results both within area sources and near point sources, as well as at long distances from sources. The receptor system is therefore determined by the resolution of the emissions. The concentrations and depositions in Europe are described on a 50 x 50 km grid system, whereas those in the Netherlands are estimated on a 5 x 5 km grid system. Computations are made for a limited number of meteorological situations (classes) with a representative meteorology for each class. Among the discretisations, a total of 12 wind-direction sectors and 6 atmospheric stability classes are distinguished. The basis for the model is formed by the Gaussian plume formulation for a point source. It is assumed that the plume is reflected only once at the surface and at the top of the boundary layer. Moreover, it is assumed that at larger distances from the source the plume is vertically distributed homogeneously over the whole boundary layer, apart from an attenuation near the surface due to dry deposition (Van Jaarsveld, 1994; Asman and Van Jaarsveld, 1992).

## 2.5 SPATIAL VARIATION IN CONCENTRATION

There is a large difference in residence times for the different constituents of the atmosphere. Residence times range from 5000 years and 1,000,000 years for oxygen and nitrogen, respectively, to less than a day for $SO_2$ and $NH_3$. Gases such as carbon dioxide, methane and nitrous oxide reside 4 to 10 years in the atmosphere, whereas nitrogen dioxide, water and aerosols can stay in the atmosphere for several days before they are lost to the surface. The longer the residence time of a constituent in the atmosphere, the smaller the spatial and temporal variations (Junge, 1974). The spatial and temporal variations of concentrations of constituents also result from the spatial and temporal variations in emission, and from the variation in rates of conversion or deposition to the surface. The concentration of trace constituents in the atmosphere would rise quickly if sink mechanisms did not assure the cleaning of the atmosphere. Oxidised nitrogen compounds are transported over larger distances than reduced. Typical transport distances for oxidised nitrogen and submicron particles may be 750 - 1000 km; for ammonia in the gaseous phase, distances are only 20 - 100 km, for $SO_2$, 50 - 200 km.

### 2.5.1 THE NETHERLANDS

Hourly averaged concentrations of $SO_2$, NO, and $NO_2$ are measured within the framework of the Dutch Air Quality Monitoring Network (LML) on a routine basis. From these measurements an accurate spatial distribution of concentrations over the Netherlands during the period 1980 - 1993 can be obtained. $NH_3$ is introduced in LML in August 1992. Since then continuous hourly averaged $NH_3$ data at eight locations have also become available (Van Elzakker *et al.*, 1994). Daily concentrations of $SO_4^{2-}$, $NO_3^-$ and $NH_4^+$ aerosol are measured at a limited set of stations. In 1989 to 1992 filterpack measurements of total $NO_3^-$ (gaseous $HNO_3$ and particulate $NO_3^-$) and total NHx (gaseous $NH_3$ and particulate $NH_4^+$) were made as daily averages for 1 out of 8 days at six sites. Measurements with the Annual Denuder System (ADS) were made with the same frequency at 4-5 sites by *RIVM* and *University of Wageningen,* yielding concentrations of $SO_2$, $HNO_2$, $HNO_3$, HCl, $NH_3$ and particulate $NH_4^+$, $NO_3^-$, and $SO_4^{2-}$ (Mennen *et al.*, 1993). Current annual average concentrations of acidifying components in the Netherlands are given in Table 2.6. Maps of the $SO_2$ and $NO_2$ concentration distribution derived from LML data over the Netherlands in 1993 are given in Figure 2.7 A and B and of $NH_3$ calculated using the TREND model (Van Jaarsveld, 1995) in Figure 2.8.

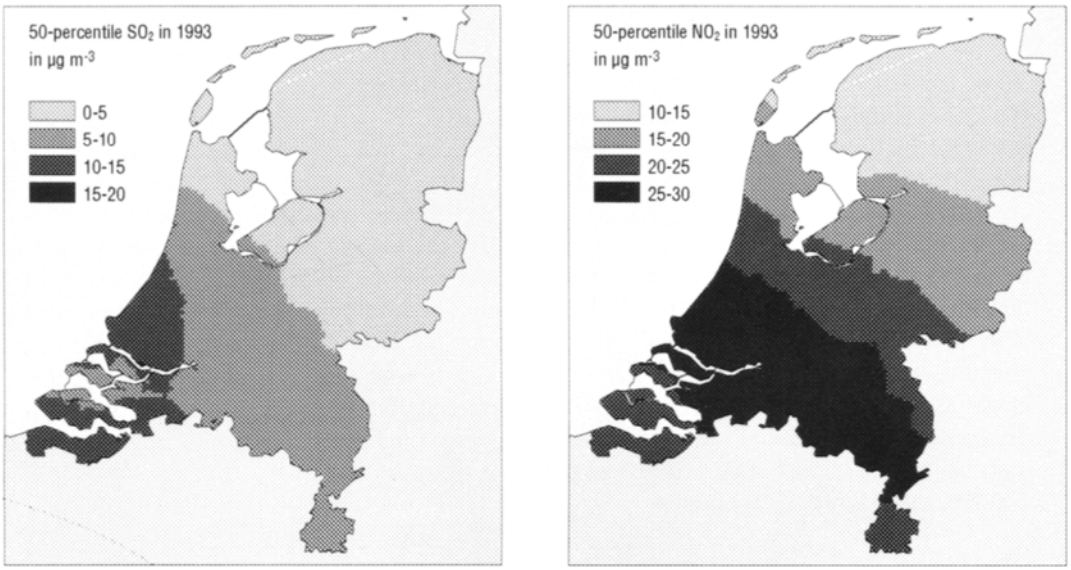


**FIGURE 2.7** Distribution of annual median $SO_2$ and $NO_2$ concentrations in the Netherlands in 1993 (µg $m^{-3}$).

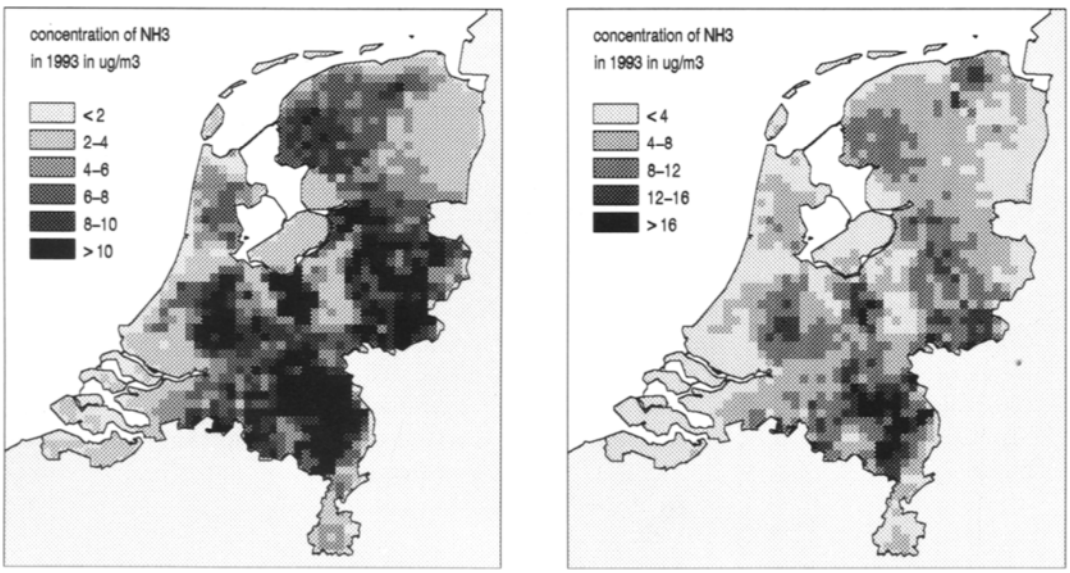


**FIGURE 2.8** Distribution of annual average $NH_3$ concentrations in the Netherlands in 1993 (µg $m^{-3}$).

**TABLE 2.6** Annual average concentrations of acidifying components measured for the Netherlands in 1993 ($\mu g\ m^{-3}$)

| Component | Concentration (4 m) |
|---|---|
| $SO_2$ | 9 |
| $NH_3$ [a] | 6.4 |
| NO | 12 |
| $NO_2$ | 25 |
| $HNO_2$ | 1.1 |
| $HNO_3$ | 0.9 |
| HCl | 0.5 |
| $NH_4^+$ | 5.1 |
| $NO_3^-$ | 5.0 |
| $SO_4^{2-}$ | 5.1 |
| $Cl^-$ | 4.0 |
| $O_3$ | 37 |

[a]Calculated with the TREND model

Figure 2.9 shows the country average of 50 percentile values of $SO_2$, $NO_2$, NOx and $O_3$ measured in the LML (RIVM, 1994), and the calculated annual average concentrations of $NH_3$. Ozone concentrations reach their highest levels in spring and summer, when photochemical production is highest. During episodic conditions in spring or summer, peak levels of $O_3$ above 240 $\mu g\ m^{-3}$ can be reached; examples of this occurred in 1982, 1989 and 1990. $O_3$ concentrations do not show a trend, whereas $SO_2$ concentrations decreased during 1977 to 1993. $NO_2$ concentrations show a slight decrease, whereas NOx concentrations remained the same between 1978 and 1993. $NH_3$ concentrations decreased after 1987, with a strong decrease (20%) after 1991. These estimates are based on emission estimates and TREND model calculations.

### 2.5.2 EUROPE

Concentration measurements of sulphur dioxide, sulphate, nitrogen (di)oxide, total nitrate and total ammonium in the air are available from several locations in Europe within the EMEP programme. In addition to EMEP there are national networks, providing data on nitrogen oxides representative for a smaller scale. Local networks exist, for instance, in the Netherlands, UK, Germany, Belgium, Luxembourg, France, Denmark and Norway. Few or no routine measurements of ammonia, nitrous acid or nitric acid are available in Europe. Measurements of PAN are made at a number of stations within the EUROTRAC project 'Tropospheric Ozone Research' (TOR). Ammonia has been measured using passive samplers

at several locations in the UK during the course of one year (Sutton, 1990), denuders at six locations in the Netherlands for 2 years (Erisman et al., 1986) and wet rotating denuders at eight locations in the Netherlands (Elzakker *et al*, 1994).

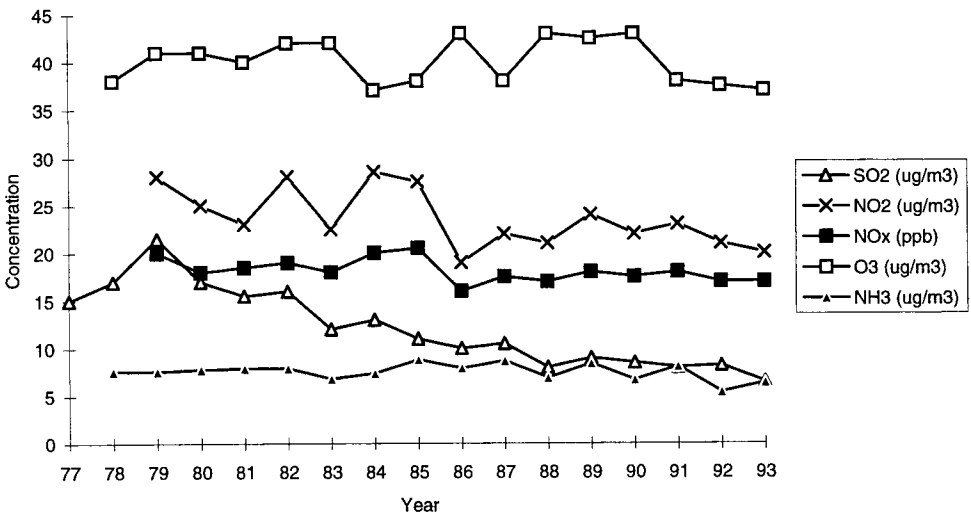


**FIGURE 2.9** Annual country average of 50-percentile $SO_2$, $NO_2$, NOx and $O_3$ concentrations, and annual average $NH_3$ ($\mu g\ m^{-3}$) in 1977 - 1993 based on LML measurements (RIVM, 1994) and TREND model calculations (Van Jaarsveld, 1995).

When local maps are aggregated to a European map, problems may arise due to inconsistency in monitoring methods, quality, time coverage, etc. For this reason, model estimates based on emission inventories and meteorological data have been used to provide concentration maps for $SO_2$, $SO_4^{2-}$, NOx, $HNO_3$ , $NO_3^-$, $NH_3$ and $NH_4^+$ (Iversen *et al.*, 1991; Derwent *et al.*, 1989; van Jaarsveld and Onderdelinden, 1992; Tuovinen *et al.*, 1994). The spatial distribution of the concentrations of these components are given in Figures 2.10 (A - H) (Tuovinen *et al.*, 1994).

The annual mean concentrations of $SO_2$ and $SO_4^{2-}$ are especially high in the border area between Germany, Poland and the Czech Republic (the 'Black Triangle'). The highest concentrations of nitrogen oxides particulate nitrate are calculated for the United Kingdom, the Netherlands, Belgium, Germany and the Czech Republic, whereas nitric acid concentrations are relatively high in the Black Triangle. The highest ammonia concentrations are calculated for the Netherlands. Particulate ammonium concentrations are especially high in the Netherlands, Belgium, parts of Germany and France, Switzerland, Austria and northern Italy.

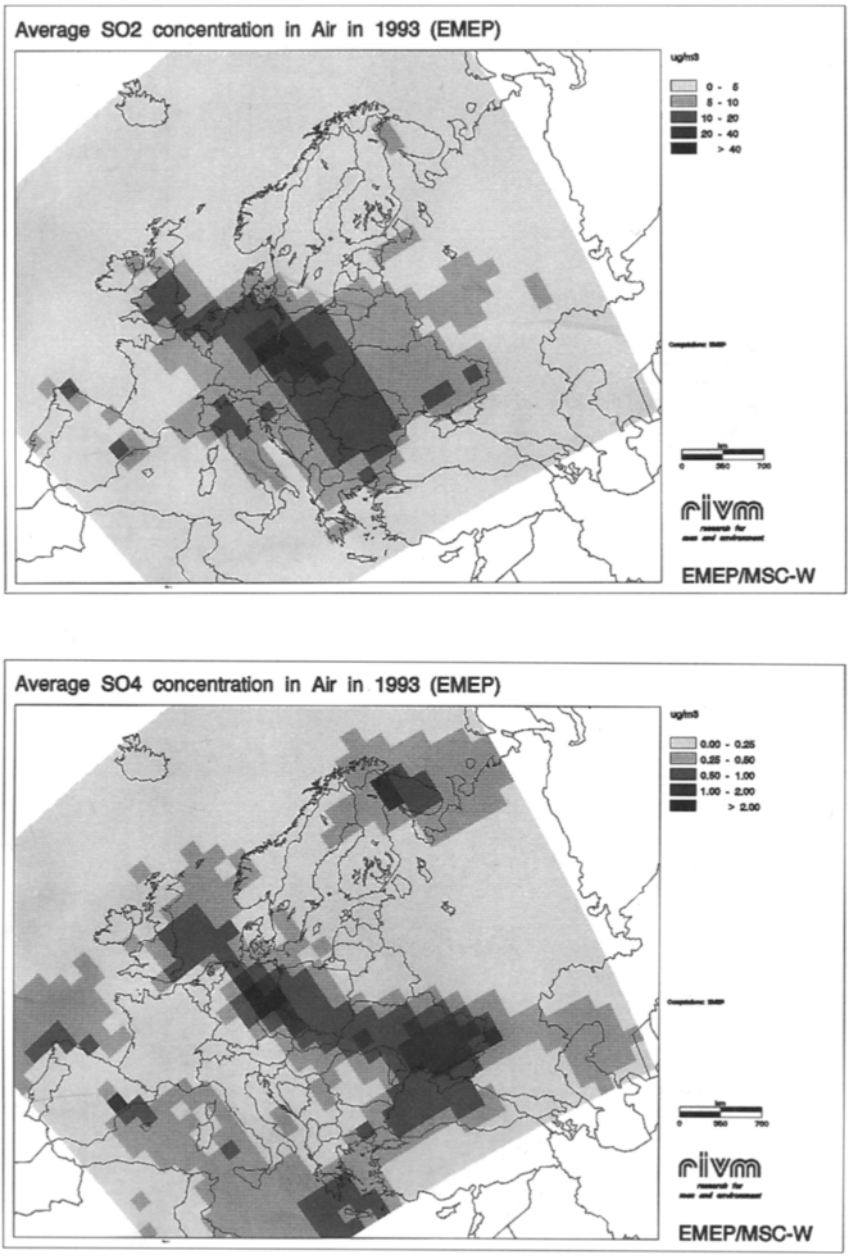


**FIGURE 2.10** Annual mean concentration of $SO_2$ (above) and $SO_4^{2-}$ aerosol (below) in 1993 in Europe as calculated by Tuovinen *et al.* (1994) using the EMEP-LTRAP model

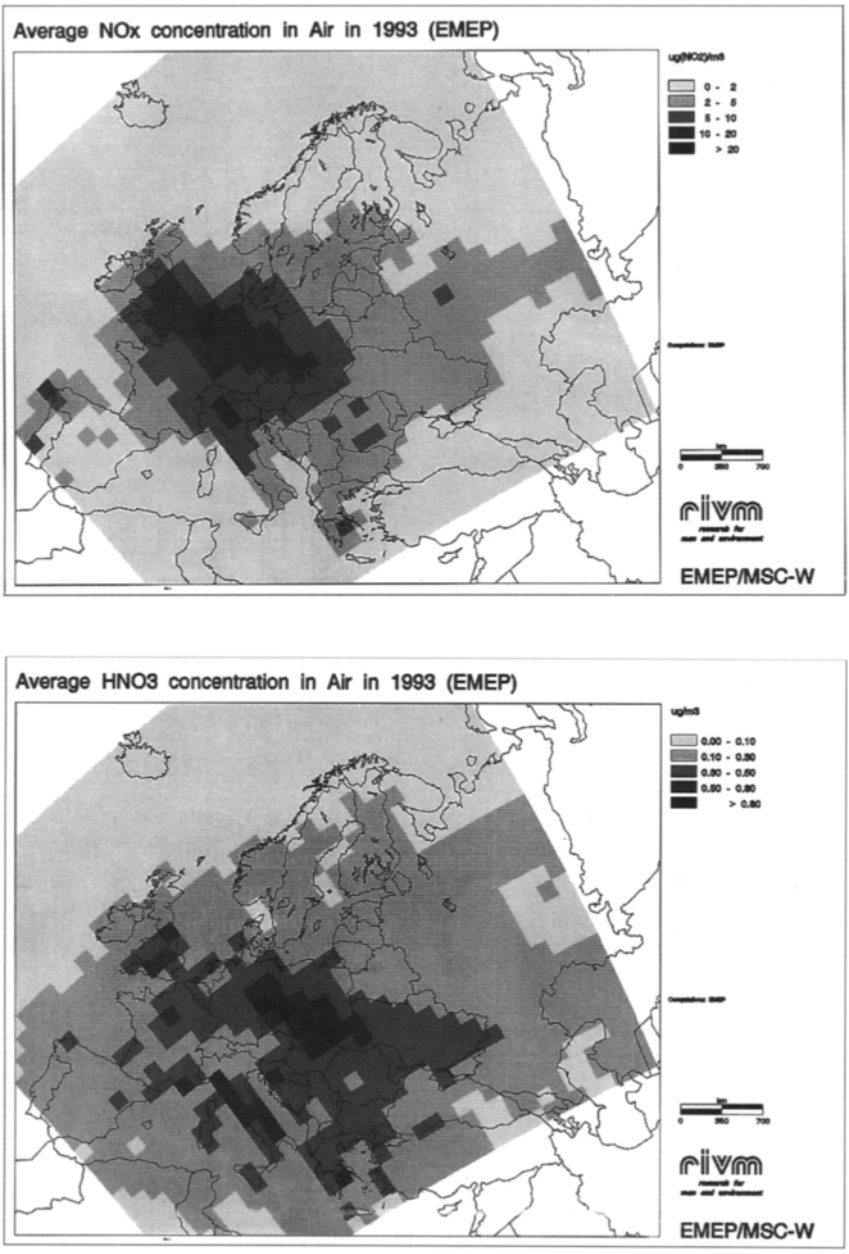


**FIGURE 2.10** (*continued*) Annual mean concentration of NOx (above) and $HNO_3$ (below) in 1993 in Europe as calculated by Tuovinen *et al.* (1994) using the EMEP-LTRAP model

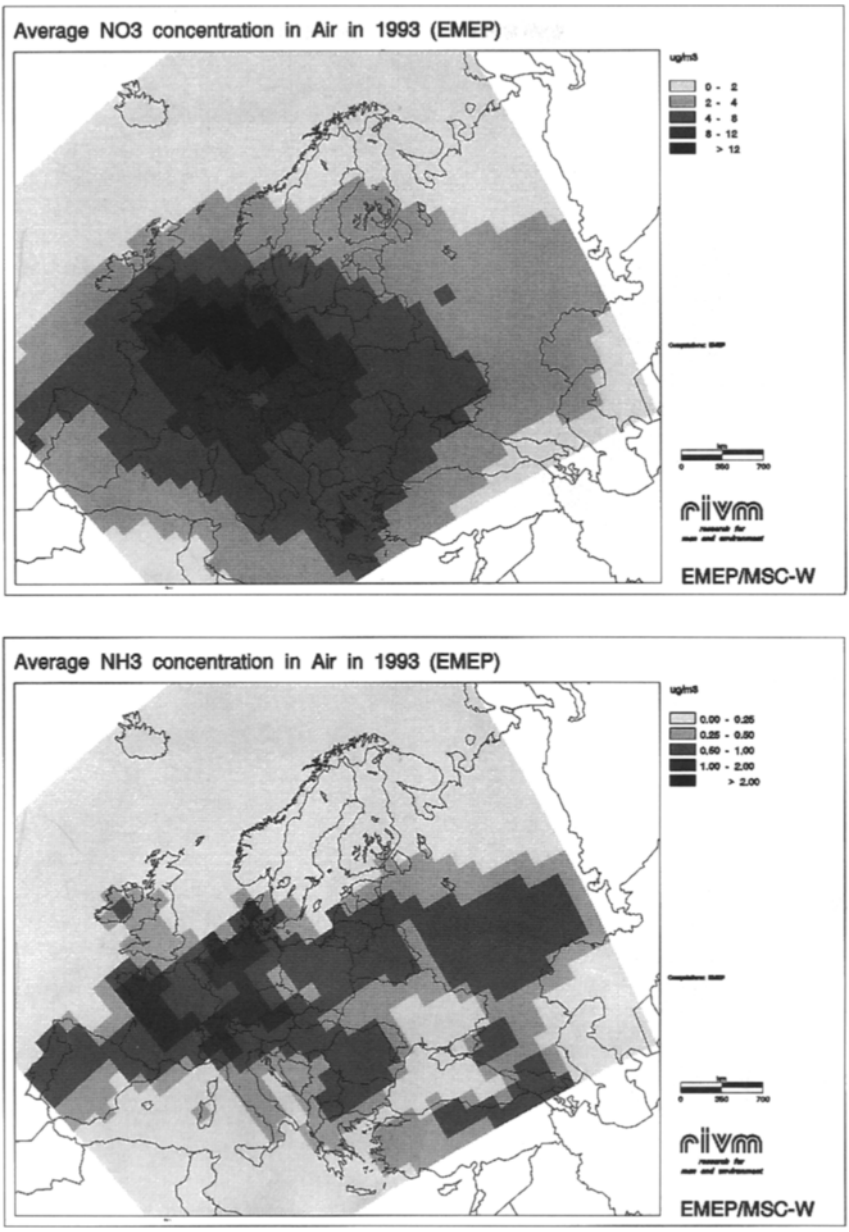


**FIGURE 2.10** *(continued)* Annual mean concentration of $NO_3^-$ aerosol (above) and $NH_3$ (below) in 1993 in Europe as calculated by Tuovinen *et al.* (1994) using the EMEP-LTRAP model

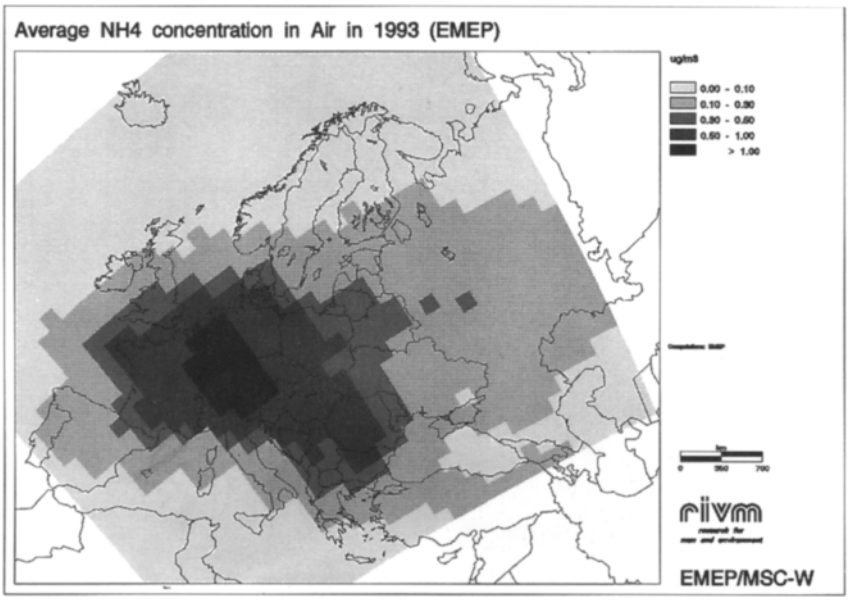


**FIGURE 2.10** (*continued*) Annual mean concentration of $NH_4^+$ aerosol in 1993 in Europe as calculated by Tuovinen *et al.* (1994) using the EMEP-LTRAP model

In addition to the large-scale pollution gradients, there are small-scale concentration variations due to local source impacts. The highest concentrations are expected in or near source regions. As reduced nitrogen compounds are mostly emitted by low-level sources, very steep horizontal gradients in concentration and deposition flux can be observed (Asman *et al.*, 1989). These gradients can lead to serious underestimates in concentrations if large grid averages are used (Asman and Van Jaarsveld, 1992).
Beside the spatial variations in deposition, there is also variation in time. Due to differences in activities leading to variation in emissions and to differences in weather conditions, winds, precipitation, temperature, etc., large temporal variations in concentrations can be observed. There are seasonal variations in the presence of pollutants in air and in precipitation. Concentrations of nitrogen dioxide in the air (with the exception of heavily polluted urban air) is greater during winter than during summer. Concentrations of total ammonium show maxima during spring and autumn. Concentrations in precipitation of reduced as well as oxidised nitrogen are highest in the late spring and lowest in the late autumn.

# CHAPTER 3 DEPOSITION PROCESSES AND MEASUREMENT TECHNIQUES

*Introduction*
After transport and possible transformations, pollutants eventually deposit on a surface by wet, dry, or cloud/fog water deposition. Wet deposition is the process by which atmospheric pollutants are delivered to the earth's surface by rain, hail or snow. Dry deposition is the process where gases and particles are deposited directly from the atmosphere onto vegetation, soil or other surfaces without the hydrometer as medium. Cloud and fog water deposition is the process where cloud and fog water droplets are directly intercepted by the earth's surface. This deposition process is often referred to as 'occult' deposition. In this chapter, deposition processes will be explained and different measurement techniques described.

## 3.1 WET DEPOSITION

In this section the short process description will be followed by an overview of measuring methods for wet deposition and possible contamination of samplers. At the end of this section an overview of European chemical precipitation networks, with some details about sampling procedures, sampling equipment and time coverage, will be presented. The results of the network measurements have been used in Chapter 5 to compile a detailed wet deposition map of Europe.

### 3.1.1 PROCESS DESCRIPTION

Wet scavenging is defined as the natural process by which atmospheric pollutants are attached to and dissolved in cloud and precipitation droplets (or particles), and as a result are delivered to the earth's surface. The amount of compounds thus received per unit of surface area is defined as wet deposition. Figure 3.1 gives an impression of the processes involved.

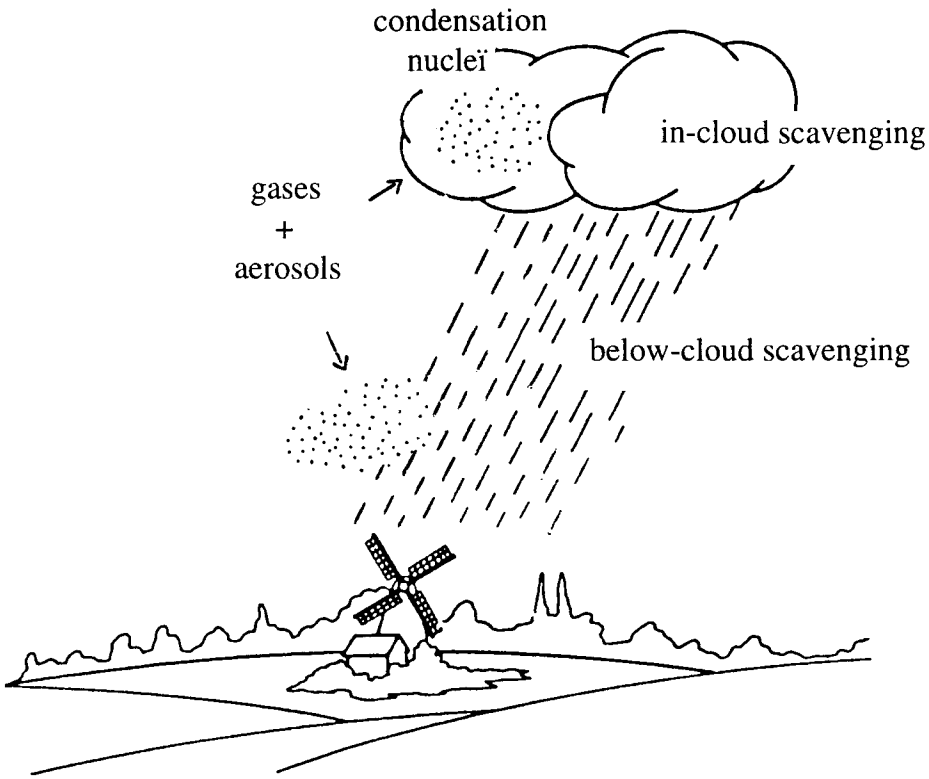


**FIGURE 3.1** Wet deposition processes.

If air is cooled, its relative humidity will increase until the air becomes saturated, and droplets will be formed. Particles containing air will form droplets more rapidly, as the particles act as condensation nuclei. Hygroscopic particles form droplets when the humidity reaches a critical level below 100% rh. After these nuclei become droplets, the air continues to cool, water continues to be condensed onto the droplets that are now growing in size, and the concentration of pollutants in these droplets will tend to decrease with dilution. This process of nucleation scavenging of cloud condensation nuclei is the most important particle incorporation mechanism. Another important mechanism is the absorption, dissolution and subsequent chemical reaction of gases in droplets. Other processes contributing to ion enrichment in clouds are diffusional attachment of particles resulting from the diffusion of small particles through the air to the surface of cloud and raindrops, and inertial attachment of particles due to their collision with falling droplets. The in-cloud processes are referred to as *in cloud scavenging* or *rain-out* scavenging (Hov *et al.*, 1987)

During the downward transport of the droplet in the form of rain, snow, cloud ice, hail, etc. to the earth's surface, uptake of gases and/or particles can occur. This process is referred to as *below-cloud scavenging* or *wash-out*. Wash-out is an efficient removal mechanism for soluble gases and aerosols with a diameter larger than 1 μm (Hicks *et al.*, 1989). Wash-out will play an important role when air concentrations of these gases or aerosols below the cloud are much higher than concentrations in the cloud. This will be the case for plumes close to the source or sources at ground level. On the other hand, the reverse process may occur by evaporation of the droplet and re-volatilisation of the pollutant itself. This is the case only for gases in solution in the droplet not undergoing any reaction inhibiting their escape back to the gaseous phase (Hicks *et al.*, 1989).

It has been estimated that the cloud condensation nuclei removal route for aerosols containing $SO_4^{2-}$, and $NO_3^-$ is responsible for most of the observed $SO_4^{2-}$ and $NO_3^-$ in precipitation (Garland, 1978; Fowler, 1984). The deliquescent nature of these aerosols makes them efficient as cloud condensation nuclei. The other sources are rain-out and wash-out of $SO_2$ and $HNO_3$. For $NH_4^+$ in precipitation, the wash-out of $NH_3$ will be of more importance, for instance, than for $SO_2$ in areas with high $NH_3$ emission found in such countries as the Netherlands, Denmark, Germany and France (Asman, 1992).

The amount of pollutant wet deposition is strongly dependent on the amount of rain and the location of the receptor with respect to sources. Wet deposition patterns depend on the topography (Fowler *et al.* 1991). At high altitudes an enhancement of wet deposition may occur because of increased aerosol scavenging due to so-called seeder-feeder effects (Fowler *et al.*, 1988). Seeder-feeder scavenging results from the incorporation of particles into orographic clouds above hills and the scavenging of the hill cloud droplets by rain droplets falling from a higher level cloud. Such effects are found to be pronounced in northwest Europe and western Scandinavia. Over the central and southern European uplands, where convective processes dominate, the above effect is less important (Fowler *et al.*, 1992; Lövblad and Erisman, 1992). The characteristics of the receptor area do not have much influence on the wet deposition. However, in areas with large roughness elements (like forests or urban areas), the catchment of small droplets could be expected to be possibly more efficient than it would over smooth homogeneous surfaces. This might be due either to increased turbulence or the kinds of scavenging effects associated with forest edges, for example.

### 3.1.2 MEASURING METHODS

Wet deposition is measured by placing samplers in the open field to collect precipitation. Precipitation is collected in bottles for two weeks or a month; after this the sample is analysed for its chemical composition. Wet deposition is the amount of precipitation multiplied by the concentration of the pollutant. The first measured wet deposition fluxes were reported in the

late 19th and early 20th centuries (see section 1.2, for an overview). The first measurements in the Netherlands were made in Utrecht in 1825 (Mulder, 1825), and later in Groningen from 1910 - 1912 and in Hilversum from 1932-1937 (Leeflang, 1938).

Although the measurement of wet deposition seems relatively simple, there are some serious sources of errors (see e.g. Eriksson, 1952; Slanina *et al.*, 1982; Fowler and Cape, 1984; Buijsman and Erisman, 1988; Beier and Rasmussen, 1989). In former days, the most commonly used sampler was the bulk or open sampler, which has no provision to exclude dry deposition during dry periods. Dry deposition of gases and particulate matter may therefore influence the chemical composition of precipitation passing the contaminated funnel (Slanina *et al.*, 1982; Ridder *et al.*, 1984). The use of wet-only samplers, in which the funnel is open to the atmosphere only during precipitation events, is widely recommended. Short exposure periods are also recommended when sample deterioration due to bacterial or chemical action is expected.

Bulk samplers are used in the EMEP network. Wet-only samplers were introduced in the Dutch National Air Quality Monitoring Network after 1988. Before then, bulk samplers were used. Correction factors for the contribution of dry deposition to the funnels of the samplers have been derived from the literature and from parallel measurements with bulk samplers and wet-only samplers (Ridder *et al.*, 1984; Van Leeuwen *et al.*, 1995). Table 3.1 gives these correction factors as the ratio of wet-only and bulk fluxes, averages are given for the Netherlands obtained from Ridder *et al* (1984), whereas ranges are given for several comparison studies in Europe taken from Van Leeuwen *et al.* (1995). Values presented by Ridder *et al.* (1984) correspond well with those found in other experiments in the Netherlands comparing wet-only and bulk precipitation (Ruijgrok *et al.*, 1989; Slanina *et al.*, 1990). Slightly different values have been found by Grennfelt *et al.* (1985) in Sweden, Georgii *et al.* (1986) and Spranger (1992) in Germany, Clark and Lambert (1987) in the United Kingdom and Mosello *et al.* (1988) in Italy. Observed differences in wet-only/bulk ratios may be attributed to the distance to local sources and to the collecting efficiency of the samplers. Differences between bulk and wet-only samplers are different for different components. Ratios are lowest for measurements made near the coast, for components which deposit in the funnels as large particles ($Na^+$, $Ca^{2+}$ and $Mg^{2+}$). Further land inward concentrations of these large particles quickly diminish and ratios become higher. For components which originate from both aerosols and gases ($SO_4^{2-}$, $NO_3^-$ and $NH_4^+$) no clear relationships are found between air concentration and wet-only/bulk ratios. This is because several factors play a role, i.e. distance to sources, particle size, solubility of gases, the time the funnel stays wet, co-deposition, turbulence characteristics at the site, etc.

**TABLE 3.1** Ratios of wet deposition fluxes obtained by wet-only and bulk samplers according to Ridder *et al.* (1984) and Van Leeuwen *et al.* (1995)

| Component | Wet-only/bulk ratio (Ridder *et al.*, 1984) | Range of wet-only/bulk ratio (Van Leeuwen *et al.*, 1995) |
|---|---|---|
| $NH_4^+$ | 0.75 | 0.70 - 1.25 |
| $SO_4^{2-}$ | 0.75 | 0.66 - 0.96 |
| $NO_3^-$ | 0.85 | 0.80 - 0.79 |
| $Ca^{2+}$ | 0.45 | 0.36 - 0.81 |
| $Na^+$ | 0.75 | 0.37 - 0.93 |

Aspects which might influence the composition of the precipitation sample (Buijsman and Erisman, 1988) include:

- transformation of components under the influence of light or enhanced temperature,
- storage conditions or time elapsed before analysis of the samples,
- bird droppings, insects, etc.

Other errors may be introduced by analytical methods and handling of the samples. Usually, these error sources were minimised by using light protected bottles, by minimising the sampling (bi-weekly) and storage periods, and by quality assurance through standardisation in sampling handling and analysis (Schaug *et al.*, 1989; Buijsman, 1989).

Amounts of precipitation show large spatial variation on short time scales. The density of stations used to monitor precipitation for hydrological purposes (e.g. about 300 in the Netherlands, KNMI, 1979) is a clear reflection of this fact. Large variations during the year can be observed. When averaged over the year, precipitation amounts show much smaller spatial variations. When estimating the spatial variation in wet deposition it is recommended to use the precipitation measurements for hydrological purposes for the amount of precipitation, combined with the chemical composition measurements from the air quality monitoring networks (see also discussion in Chapter 6).

At the moment there are several national and international precipitation monitoring networks (EMEP, CaPMoN, NADP). Table 3.2 gives an overview of the networks in Europe with some information about sampling procedures. Most of the data measured in these networks are used in Chapter 5 to describe the wet deposition in Europe in 1989.

**TABLE 3.2** Precipitation monitoring networks in Europe

| Country/ region | Equipement | Sampling period | Number of sites | Period | References |
|---|---|---|---|---|---|
| Europe | bulk/wet-only | varies | 90 | 1978 → | e.g. EMEP (1994) |
| eastern Alps | bulk/wet-only | varies | 107 | varies | Kovar and Puxbaum (1992) |
| Austria | wet-only | unknown | 17 | 1983 → | questionnaire[a] |
| Belgium | wet-only | 1 month | 12 | 1984 → | IHE (1991) |
| Bulgaria | bulk | 1 month | 1 | 1989 → | questionnaire[a] |
| Czech Republic | bulk | varies | 7 | unknown | questionnaire[a] |
| Estonia | bulk | 1 month | 6 | unknown | Kallaste et al (1992) |
| Finland | bulk | 1 month | 61 | 1971-1991 | Leinonen and Junte (1991), Jarvinen and Vanni (1990) |
| France | wet-only | 1 month | 21 | unknown | Codeville *et al* (1993), Dambrine (1992), Ulrich and Williot (1993) |
| Georgia | bulk | unknown | 1 | unknown | questionnaire[a] |
| Germany | bulk/wet-only | varies | 202 | varies | Klockow and Wintermeyer (1990), Bruggeman (1993) |
| Greece | wet-only | unknown | 2 | 1987 → | questionnaire[a] |
| Hungary | wet-only | 1 month | 9 | 1978 → | questionnaire[a] |
| Ireland | bulk | unknown | 17 | unknown | Bowman (1991) |
| Italy | wet-only | unknown | 122 | unknown | Mosello and Morselli (1992) |
| Latvia | bulk | unknown | 7 | 1985 → | questionnaire[a] |
| Moldava | bulk | unknown | 7 | 1989 → | questionnaire[a] |
| the Netherlands | wet-only | 1 month | 14 | 1978-1993 | RIVM (1993) |
| Norway | bulk | 1 month | 38 | 1971 → | SFT (1992) |
| Poland | bulk | unknown | 5 | 1978 → | questionnaire[a] |
| Portugal | wet-only | unknown | 6 | 1979 → | INMG (1989) |
| Russian Federation | bulk | 1 month | 10 | 1958 → | questionnaire[a] |
| Slovak Republic | bulk | unknown | 7 | 1978 → | questionnaire[a] |
| Slovene | bulk | 1 month | 26 | unknown | Hrcek (1992) |
| Sweden | bulk/wet-only | 1 month | 34 | 1975 → | Granat (1989), Persson *et al* (1993) |
| Switzerland | wet-only | unknown | 4 | unknown | NABEL (1992) |
| United Kingdom | bulk | 1 month | 58 | 1986 → | Campbell *et al* (1992), UKRAR (1990) |
| Ukraine | bulk | unknown | 5 | unknown | questionnaire[a] |
| Yugoslavia | bulk | unknown | 5 | unknown | questionnaire[a] |

[a] A questionnaire was send to all authorities responsible for environmental monitoring programmes to obtain wet deposition data (see Van Leeuwen *et al.*, 1995 for more details)

## 3.2 DRY DEPOSITION

This section describes in short the general process, followed by the most important processes and then an overview of measuring methods for dry deposition. At the end of this section an overview of European dry deposition measurements is given, with a few details on sampling procedures, sampling equipment and time coverage. The results of these measurements will be used in the next chapters.

### 3.2.1 PROCESS DESCRIPTION

The dry deposition of gases and particles from the atmosphere to a receptor surface is governed by the concentration in air and by turbulent transport processes in the boundary layer, as well as by the chemical and physical nature of the depositing species and the capability of the surface to capture or absorb gases and particles. The process is illustrated in Figure 3.2.

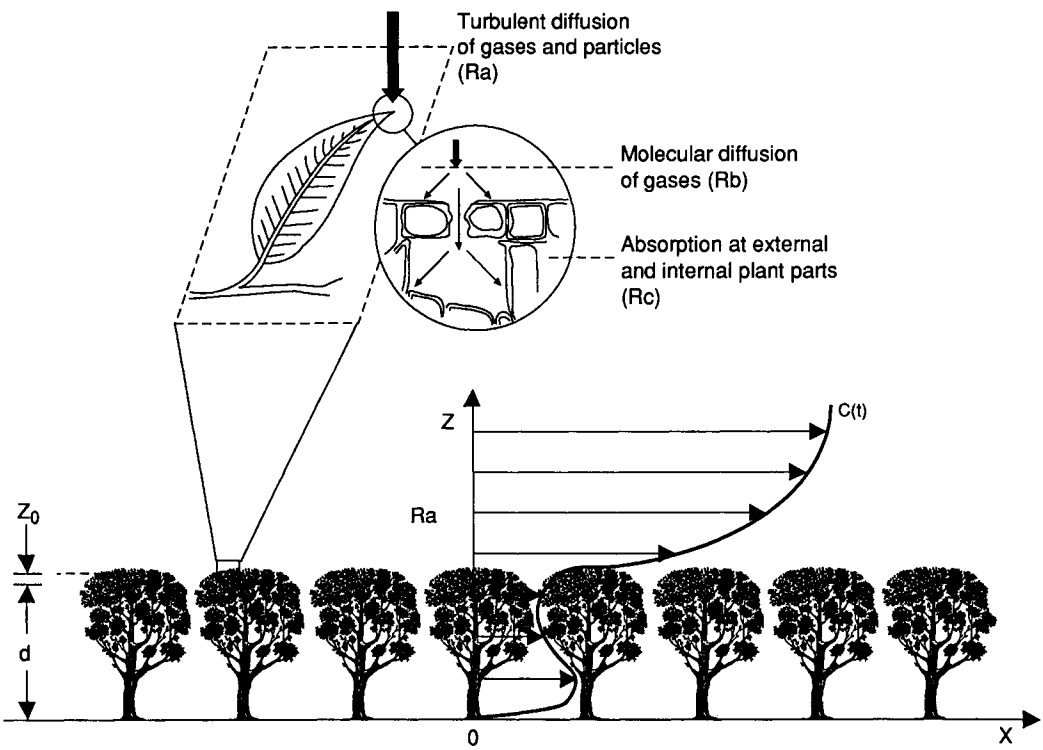


**FIGURE 3.2** The dry deposition process.

The transport of gases and particles from the atmosphere to close to the receptor surface is governed by the level of atmospheric turbulence, generated by both wind shear and buoyancy. The higher the level of atmospheric turbulence, the more efficiently gases and particles are transported to a given receptor surface. Given a constant sink strength for a particular pollutant of interest, the concentration gradients above the receptor will vary according to the intensity of atmospheric turbulence. A well-mixed unstable boundary layer leads to relatively small concentration gradients and to low resistance to vertical transport. For a boundary layer with near neutral stability, buoyancy has essentially no influence on the level of turbulence. Stable stratified boundary layers are associated with much larger gradients, because vertical motions are suppressed.

In the vicinity of sources, the dry deposition is determined primarily by the configuration of the sources, the type of sources and the pollutant's mixing in the atmosphere. For high level sources, the deposition near to the source is small and increases with downwind distance from the source until it reaches a maximum and decreases again. For ground-level sources, dry deposition takes place directly next to the source, where concentrations are highest, decreasing downwind. At some distance, the influence of the sources on the concentration gradient is diminished. At this point, the pollutant is mixed throughout the boundary layer and the concentration gradient is determined primarily by the dry deposition process. If the receptor can act both as a source and sink, the shape of the gradient will be determined by the extent of the source or sink flux. The gradient will then show the shape of the net emission or net deposition flux.

Generally, two layers can be distinguished in the boundary layer for transport of pollutants to the receptor: the fully turbulent layer and the quasi-laminar layer. The quasi-laminar layer is introduced to quantify the way in which pollutant transfer differs from momentum transfer in the immediate vicinity of the surface (Hicks *et al.*, 1987). In this layer, the transport to the receptor surface is dominated by molecular diffusion. Once at the surface, the chemical, biological and physical nature of the surface determines the capture or absorbency of the gases and particles. For gases, surface uptake is frequently controlled by the ability of the surface to absorb the specific chemical species. For reactive trace gases, such as $HNO_3$, molecules are collected immediately upon contact with all surfaces (Huebert and Robert, 1985; Dollard *et al.*, 1986). Less reactive, but soluble, gases, such as $SO_2$ and $NH_3$, tend to be taken up through stomata or through the leaf cuticle (Garland, 1977; Schwela, 1977; Fowler, 1984; Duyzer *et al.*, 1987; Grennfelt, 1987). These gases can also be absorbed in water layers at the leaf surface, or at the soil (Fowler *et al.*, 1991; Hicks *et al.*, 1989). The chemical composition of the surface is important for snow, ice and water (Hicks *et al.*, 1989; see also Chapter 4).

Together with wet deposition, particle dry deposition is responsible for the atmospheric load to ecosystems of such compounds as sulphate, nitrate, chloride and ammonium, and base cations such as calcium, magnesium, sodium and potassium. Deposition of particles containing $SO_4$, $NO_3$, Cl and $NH_4$ contributes to the potential acidification and eutrophication

(nitrogen components) of ecosystems. Compared to gaseous deposition of acidifying compounds onto low vegetation, particle deposition velocities and fluxes are usually found to be small. However, it is believed that the dry deposition velocity of small particles, and with this the fluxes, is currently underestimated for very rough surfaces like forests (Wiman *et al.*, 1990; Erisman, 1993a). Erisman *et al.* (1994) found that deposition of aerosols to the Speulder forest contributed 20 - 40% to the total dry deposition of SOx and total nitrogen, respectively. Current knowledge is not sufficient to give an adequate assessment of the dry deposition of particulate sulphur and nitrogen in the Netherlands and Europe.

For submicron particles, the process of dry deposition is even more complex and the list of potentially determining factors is much longer. Mechanisms of deposition are diffusion, interception, impaction, gravitational settling and phoretic mechanisms (Slinn, 1982). Almost no particles are able to diffuse through stomatal openings (Slinn, 1982). Transfer through the quasi-laminar layer close to the surface presents a considerable restriction on the deposition of 0.1 - 1.0 μm particles. Uptake of particles by surfaces is thus largely controlled by micro-structures and turbulence intensity.

### 3.2.2 FRAMEWORKS FOR THE DESCRIPTION OF ATMOSPHERE - SURFACE EXCHANGE

The dry deposition flux of gases and particles from the atmosphere to a receptor surface is governed by: 1) the concentration in air and turbulent transport processes in the boundary layer; 2) the chemical and physical nature of the depositing species and 3) by the efficiency of the surface to capture or absorb gases and particles.

*Resistance analogy for trace gases*
A common framework is provided to describe the exchange of a range of gases with very different chemical and physical properties. In this framework, three stages in dry deposition to the surface are distinguished. The most widely used is that of the resistance analogy (Thom, 1975, Chamberlain, 1966; Garland, 1977; Fowler, 1978). The analogy of trace gas fluxes to a current in an electrical circuit is described by Ohm's law (resistance = potential difference/current). Assuming one-dimensional transfer over a homogeneous surface, the total resistance $R_t$ is defined by:

$$R_t(z) = \frac{c(z_1) - c(z_2)}{F} \qquad [3.1]$$

where $z_1$ and $z_2$ are two heights above the surface. The flux $F$ is taken as negative when directed towards the surface. The absorbing surface is often assumed to have zero surface concentration; the flux is therefore viewed as being linearly dependent on atmospheric

concentration. In this case, if $z_2$ is considered to be the notional height of the absorbing surface ($z_0$+$d$), the total resistance from a height $z$ to the surface becomes:

$$R_t(z) = -\frac{c(z)}{F} = \frac{1}{V_d} \qquad [3.2]$$

In effect, ($z$-$d$) is the height above the aerodynamic ground level. In Figure 3.2, turbulent boundary layer flow over a receptor surface of uniform height $h$ behaves as if the vertically distributed elements of the receptor were located at a certain distance $d$ from the ground. The bulk effectiveness as a momentum absorber is specified by $z_0$, while the parameter $d$ can be considered to indicate the mean level at which momentum is absorbed by the individual elements of the receptor surface. This concept is valid for the momentum flux, as the wind speed decreases to zero at the receptor surface. For mass transport, however, this does not hold, as surface concentrations might not be zero for gases (or particles). However, the concept of $z_0$ is used for mass transport (Thom, 1975). Values for roughness length, $z_0$, and displacement height, $d$, can be obtained from look-up tables, e.g. those proposed by Davenport (1960), revised by Wieringa (1981) or Voldner *et al.* (1986).

The inverse of the total resistance is the deposition velocity ($V_d$). The latter, providing a measure of conductivity of the atmosphere - surface combination for the gas, is widely used to parametrise gas uptake at the ground surface (Wesely and Hicks, 1977; Hicks *et al.*, 1989; Fowler, 1984; Fowler *et al.*, 1989; Wesely, 1989). $V_d$ is the inverse of three resistances:

$$V_d(z) = \frac{1}{R_a(z) + R_b + R_c} \qquad [3.3]$$

The three resistances represent the three stages of transport: the aerodynamic resistance $R_a$ for the turbulent layer, the laminar layer resistance $R_b$ for the quasi-laminar layer, and the surface or canopy resistance $R_c$ for the receptor itself. The atmospheric resistance to transport of gases across the constant flux layer is assumed to be similar to that of heat (see e.g. Hicks *et al.*, 1989 for an overview). $R_a$ depends mainly on the local atmospheric turbulence intensities. Turbulence may be generated through mechanical forces of friction with the underlying surface (forced convection) or through surface heating (buoyancy or free convection). Unless wind speeds are very low, free convection is small compared to mechanical turbulence. In the case of rough (uneven) surfaces like forest canopies, the aerodynamic characteristics of the canopy and the wind speed control the generation of turbulence to a large extent and regulate vertical mixing of pollutant-laden air layers in the vicinity of the canopy. In this study $R_a$ is approximated following the procedures used by Garland (1978):

$$R_a(z) = \frac{1}{\kappa u_*}\left[\ln\left(\frac{z-d}{z_0}\right) - \psi_h\left(\frac{z-d}{L}\right) + \psi_h\left(\frac{z_0}{L}\right)\right] \qquad [3.4]$$

in which $u*$ is the friction velocity, $L$ the Monin Obukhov length and $\psi[(z-d)/L]$ the integrated stability function for heat. These can be estimated using procedures described in Beljaars and Holtslag (1990) which will be described in section 3.2.3. The second atmospheric resistance component $R_b$ is associated with transfer through the quasi-laminar layer in contact with the surface. $R_b$ quantifies the way in which pollutant or heat transfer differs from momentum transfer in the immediate vicinity of the surface. $R_b$ depends on both turbulence characteristics and the molecular diffusion of the gas considered (Thom, 1975; Garrat and Hicks, 1973; Erisman, 1992). Transport of a pollutant gas through the quasi-laminar layer by molecular diffusion depends on the thickness of the layer, the concentration gradient over the layer, and on a diffusion constant which, in turn, depends on the radius of the gas molecule considered and on temperature. Although a great deal is known about quasi-laminar layer transport to artificial surfaces, the complexity of vegetation limits the accuracy with which the magnitude of this transport mechanism can be estimated in the field. The thickness of the quasi-laminar boundary layer, for example, is found to depend on size, shape and orientation of the receptor surface, and on wind speed. Real-life events like 'fluttering' of leaves make it extremely difficult to model quasi-laminar boundary layer transport accurately (Chamberlain, 1975). The quasi-laminar layer resistance $R_b$ can be approximated by the formulation presented by Hicks *et al.* (1987):

$$R_b = \frac{2}{\kappa u_*}\left(\frac{Sc}{\mathrm{Pr}}\right)^{\frac{2}{3}} \qquad [3.5]$$

where $Sc$ and $Pr$ are the Schmidt and Prandtl numbers, respectively. $Pr$ is 0.72 and $Sc$ is defined as: $Sc = \upsilon/D_i$, with $\upsilon$ the kinematic viscosity of air (0.15 $cm^2\ s^{-1}$) and $D_i$ the molecular diffusivity of pollutant $i$, and thus component specific. The Schmidt and Prandtl number correction in Eqn. 3.5 is listed in Table 3.3 for different gases. Usually $R_b$ values are of less importance than values of $R_a$ and $R_c$, so Eqn. 3.5 can be considered as appropriate. Over very rough surfaces such as forest canopies, however, $R_a$ may approach small values and the accuracy of the $R_b$ estimate becomes important. This is especially the case for trace gases with a small or zero surface resistance.

The surface or canopy resistance, $R_c$, is the most difficult of the three resistances to describe. $R_c$ values can be obtained from theoretical considerations based, for instance, on solubility and equilibrium calculations in combination with simulations of vegetation specific processes, such as accumulation, transfer processes through stomata, mesophyll and cuticles, absorption, etc. (Baldocchi *et al.*, 1987; Wesely, 1989). Many theoretical approaches are, however, hard to validate by measurements because of the complexity of the processes involved. $R_c$ values presented in the literature are primarily based on measurements of $V_d$. By determining $R_a$ and

$R_b$ from the meteorological measurements, $R_c$ can be calculated as the residual resistance using Eqn 3.3. Values of $R_c$ can then be related to surface conditions, time of day, etc., yielding parametrisations (see Chapter 4). Unfortunately, measurements by existing techniques are still neither accurate nor complete enough to obtain $R_c$ values under most conditions. Furthermore, $R_c$ is specific for a given combination of component, type of vegetation and surface conditions; measurements are available for only a limited number of combinations. Bache (1986) demonstrated that in cases of low surface resistances, the $R_c$ values obtained using the resistance analogy are likely to contain aerodynamic factors. In such conditions, the surface and aerodynamic components cannot be fully separated.

**TABLE 3.3** Schmidt and Prandtl number correction in Eqn. 6 for several gases (Hicks *et al.*, 1987)

| Component | $(Sc/Pr)^{2/3}$ |
|---|---|
| $SO_2$ | 1.44 |
| $NO_2$ | 1.30 |
| $HNO_3$ | 1.44 |
| $H_2O$ | 0.96 |
| $O_3$ | 1.30 |

*Particles*

The resistance analogy is not used for particles. Transport from the free atmosphere to the receptor surface is more-or-less similar to gas transport. However, transport processes through the quasi-laminar layer differ considerably between gases and particles. Whereas gases are transported primarily through molecular diffusion, particle transport and deposition basically take place through sedimentation, interception, impaction and/or Brownian diffusion (Figure 3.3). *Sedimentation* under the influence of gravity is especially significant for receptor surfaces with horizontally oriented components. *Interception* occurs if particles moving in the mean air motion pass sufficiently close to an obstacle to collide with it. Like interception, *impaction* occurs when there are changes in the direction of airflow, but unlike interception a particle subject to impaction leaves the air streamline and crosses the laminar boundary layer with inertial energy imparted from the mean airflow. The driving force for *Brownian diffusion* transport is the random thermal energy of molecules. Transport is a function of atmospheric conditions, characteristics of the depositing contaminant and the magnitude of the concentration gradient over the quasi-laminar layer (Davidson and Wu, 1990).

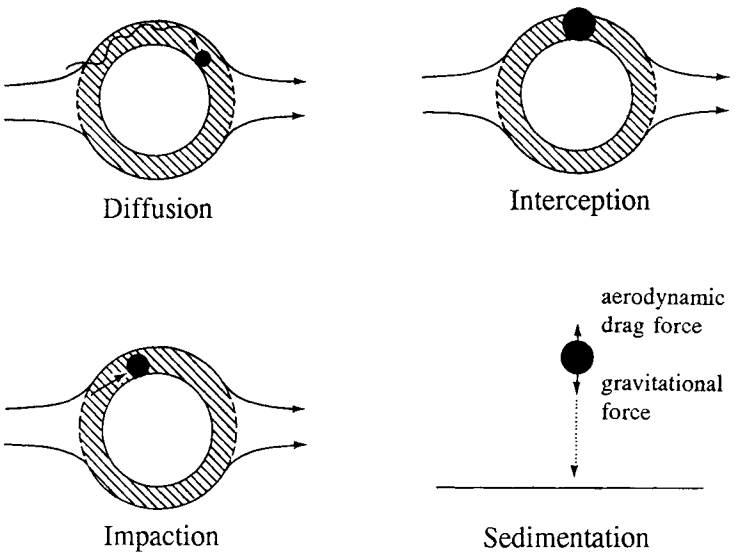


**FIGURE 3.3** Schematic representation of four transport mechanisms for particles through the quasi-laminar boundary layer (adopted from Davidson and Wu, 1990). Shaded areas indicate the laminar boundary layer.

Which type of transport process dominates is largely controlled by the size distribution of the particles (Chamberlain, 1966; Sehmel, 1980; Slinn, 1982). In Figure 3.4, a calculated deposition velocity of particles is plotted against their mass median diameter (*MMD*) for an Eucalyptus forest canopy. This figure clearly demonstrates that deposition of particles with *MMD*s near 0.1-1.0 μm is the least efficient. Deposition of particles falling in this *MMD* range is very much affected by turbulent transfer from the free atmosphere to the receptor surface and, therefore, depends heavily on wind speed and the aerodynamic roughness of the receptor surface (Slinn, 1982). Deposition velocity for particles to low vegetation with a diameter in this range can be obtained from parametrisations on $u_*$ (Eqn. 4.9, Wesely *et al.*, 1989; Erisman *et al.*, 1994). Particles with *MMD*s smaller than 0.1 μm deposit through Brownian diffusion, which efficiency is inversely related to particle size (Fowler, 1980). For particles with *MMD*s between 1 and 10 μm, the deposition velocity increases sharply with the *MMD*. These particles deposit mainly through impaction and/or interception. Here we see relatively efficient removal processes, which depend to a large extent on wind speed and aerodynamic characteristics of the receptor surface. This determines transport from the free atmosphere to the receptor surface. The processes also depend on in-canopy wind speeds controlling inertial impaction through quasi-laminar boundary layers (Thorne *et al.*, 1982). For particles with *MMD*s larger than 10 μm, turbulent transfer is less important and sedimentation is the main

deposition process. Bounce-off or blow-off effects may be important for such large particles (Slinn, 1982; Wu *et al.,* 1992). Sticky or hairy surfaces limit these effects considerably.

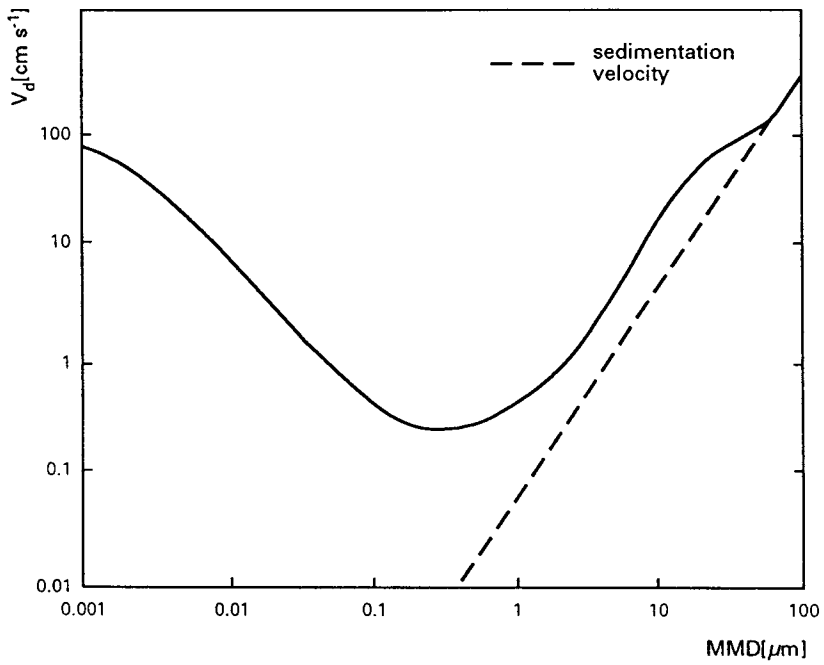


**FIGURE 3.4** Relationship between the deposition velocity of particles and their mass median diameter for an Eucalyptus forest canopy (adopted from Slinn, 1982). The dashed line indicates the sedimentation velocity (i.e. where the deposition rate is a linear function of the fall velocity of the particles). Canopy height = 27.4 m; friction velocity = 75 cm $s^{-1}$; roughness length = 1.86 m; zero plain displacement height = 21.6 m; particle density = 1 g $cm^{-3}$.

### 3.2.3 MEASURING METHODS FOR DRY DEPOSITION

This section contains a summary of measurement methods, mainly based on existing excellent reviews by Hicks *et al.* (1986, 1989) and Davidson and Wu (1989). The applicability of the different methods will be addressed. An overview and assessment of possibilities for measuring deposition of specific substances is presented in Chapter 4.

*Micrometeorological methods for estimating dry deposition*
Among the methods for measuring dry deposition, micrometeorological methods are the most suitable for determining the dry deposition of many gases (Fowler and Duyzer, 1989). The

flux to the total system may be determined with these methods, and the relationship between air concentrations, meteorology and the flux is directly established. In a flat homogeneous terrain, the flux measured at a sampling point above the surface within the constant flux layer represents the average vertical flux over the upwind fetch. A constant flux layer is required to make sure that the flux measured above the surface is that at the surface. Several micro-meteorological measuring methods exist for measuring dry deposition. The flux is derived from measurements of the vertical component of the wind velocity and the gas concentration with the most direct of these methods, the eddy correlation method. With another method, the gradient technique, the flux is derived from measurements of air concentrations at several heights above the receptor surface and from meteorological variables. The principles of the eddy correlation method and gradient technique will be described in this section. Other techniques consist of Bowen ratio approaches, variance and a variety of so-called conditional sampling methods. The latter are not described in this book; information on these techniques can be found in such references as Businger (1986), Hicks *et al.* (1986), Baldocchi *et al.* (1988) or Fowler and Duyzer (1990)

Eddy correlation
The vertical flux density $F$ of an entity is given as

$$F = \overline{\omega\rho} \qquad [3.6]$$

where $\omega$ is the vertical wind velocity and $\rho$ the density of the entity. This may be considered as the sum of two components, the product of mean vertical wind speed $\omega$ and density $\rho$, and fluctuations about the means of the same quantities $\omega'$ and $\rho'$:

$$F = \overline{\omega}\,\overline{\rho} + \overline{\omega'\rho'} \qquad [3.7]$$

where $w'$ and $\rho'$ are the instantaneous vertical wind velocity and the departure from the mean concentration, respectively (Baldocchi *et al.*, 1988). When $\rho$ represents a pollutant concentration, $F$ is simply the flux. When $\rho$ is the momentum, $F$ represents the momentum flux, more commonly denoted as the stress $\tau$. The sensible heat flux $H$ is represented as

$$H = \rho_a c_p \overline{\omega\,\theta} \qquad [3.8]$$

where $\rho_a$ is the air density, $c_p$ the specific heat of air and $\theta$ the potential air temperature. In the constant flux layer, the eddy correlation method provides direct fluxes from measurements of the co-variance of $\omega$ and $\rho$. In order to measure the contribution of all eddies to the flux, fast sensors are necessary. For meteorological quantities such as momentum or sensible heat

fluxes this method has proven to give reliable results (Montheith, 1975; Businger, 1986; Baldocchi *et al.*, 1988; Duyzer and Bosveld, 1988; Fowler and Duyzer, 1990).

When conducting an experiment with the eddy correlation technique, the length of the sampling period must be carefully chosen to ensure that the sampling period accounts for the spectrum of eddies that contribute to the transfer processes. Sampling rates in the order of 5 - 10 Hz are normally required for this method over most surfaces when measurements are made from tower-based systems.

The eddy correlation technique provides a direct measurement of the vertical flux for gases and small particles. The requirement for fast responding chemical instruments limits the application of this technique to just a few chemical species. Relatively fast response analysers are available for $O_3$ and $NO_2$.

Aerodynamic gradient method

Before the measurements required for the aerodynamic gradient method are described, the basic theory will be summarised. In the turbulent layer, transport of heat, momentum and mass are similar (Thom, 1975). The diffusivity $K$ of a property at any point in a particular fluid medium can be defined as the ratio of the property flux through the medium to its concentration gradient (in the same direction) at that point. The flux towards or away from the surface is found as the product of this gradient and the diffusivity.

For the momentum flux ($\tau$):

$$\tau = K_m(z)\frac{\partial(\rho u)}{\partial z} \qquad [3.9]$$

For sensible heat flux ($H$):

$$H = K_h(z)\frac{\partial(\rho_a c_p \theta)}{\partial z} \qquad [3.10]$$

For mass flux ($F$):

$$F = K_c(z)\frac{\partial c}{\partial z} \qquad [3.11]$$

where $u$ is the wind speed, $z$ the vertical distance, $c_p$ the specific heat of air, $\theta$ the potential temperature and $c$ the pollutant concentration.

The approximate similarity of:

$$K_m \approx K_h \approx K_c \qquad [3.12]$$

appears to be valid in neutral and stable conditions (Thom, 1975; Droppo, 1985; Zeller, 1990). In unstable conditions, experiments showed that the equality of $K_h$ and $K_c$ with $K_m$ does not hold (Droppo, 1985). $K_h$ and $K_c$ were observed to be similar in these conditions too (Hicks *et al.* 1989; Droppo, 1985; Zeller *et al.*, 1989).

The shearing stress, or momentum flux $\tau$, is defined as the drag force per unit area of a horizontal plane caused by horizontal air motion (Thom, 1975). $\tau$ is related to the air density and the effectiveness of vertical turbulent exchange in the air flow over the surface:

$$\tau = \rho_a u_*^2 \qquad [3.13]$$

The 'eddy velocity' or friction velocity associated with the momentum flux is $u_*$. The term $u_*$ may be defined in terms of gradient theory, such that:

$$u_* = l\frac{\partial u}{\partial z} \qquad [3.14]$$

where $l$ is the mixing length for momentum, or rather the effective eddy size, at level z. The value for $l$ may be given by:

$$l = \frac{\kappa(z-d)}{\phi_m} \qquad [3.15]$$

where $\kappa$ is the Von Karman constant, established experimentally to be about 0.41 (see discussion in Pasquill and Smith, 1983); $\phi_m$ is the empirically estimated dimensionless correction for stability effects upon this ratio, while $d$ is the zero displacement height.

The eddy diffusivity $K_m$ may be found from Eqns. 3.9, 3.13, 3.14 and 3.15:

$$K_m = \frac{\kappa(z-d)u_*}{\phi_m} \qquad [3.16]$$

This equation may be used to estimate $K_c$, given the similarity between $K_m$, $K_h$ and $K_c$. For $K_c$, $\phi_h$ is used rather than $\phi_m$. Thus given the equality of $\phi_h$ and $\phi_c$:

$$K_c = \frac{\kappa(z-d)u_*}{\phi_h} \qquad [3.17]$$

which may be substituted into the mass flux (Eqn. 3.11), yielding:

$$F = \frac{\kappa(z-d)u_*}{\phi_m}\frac{\partial c}{\partial z} \qquad [3.18]$$

$u_*$ is derived from 3.14 and 3.15:

$$u_* = \frac{\kappa(z-d)}{\phi_m}\frac{\partial u}{\partial z} \qquad [3.19]$$

Similarly, the eddy concentration can be defined as:

$$c_* = \frac{\kappa(z-d)}{\phi_h}\frac{\partial c}{\partial z} \qquad [3.20]$$

and thus the mass flux becomes:

$$F = u_* c_* \qquad [3.21]$$

As a result, the flux of a pollutant may be derived from information on the wind profile, the concentration gradient and the effect of stability. The empirical estimation of $\phi_h$ for different conditions has been the subject of much investigation (Dyer and Hicks, 1970; Pasquill and Smith, 1983). The stability function is a correction for the departure of the neutral profile. Therefore under neutral conditions $\phi_m=\phi_h=\phi_c=1$. The stability correction is a function of height. Therefore $\phi$ should be included in the integration of Eqns. (3.19) and (3.20). In the literature, results obtained by Dyer and Hicks (1970) are widely used (e.g. Thom, 1975; Denmead, 1983). Under stable conditions:

$$\phi_m = \phi_h = \phi_c = 1 + 5.2\frac{(z-d)}{L} \qquad [3.22]$$

and unstable conditions, $\phi_h$ and $\phi_c$ are represented by the square of $\phi_m$:

$$\phi_m^2 = \phi_h = \phi_c = [1 - 16\frac{(z-d)}{L}]^{-0.5} \qquad [3.23]$$

where $L$ is the Monin Obukhov stability length used as stability parameter ($L$>0: stable; $L$<0: unstable; $|L| \to \infty$: neutral), given as:

$$L = \frac{-T\rho_a c_p u_*^3}{\kappa g H} \qquad [3.24]$$

where $T$ is the absolute temperature and $g$, the acceleration of gravity. The sensible heat flux $H$ can be calculated from the net radiation using the Priestly-Taylor model parameterised (modified by Holtslag and De Bruin, 1988). This modified model was tested using experiments at a meteorological mast at Cabauw in the centre of the Netherlands. The model was used in subroutines for the calculation of $H$, $L$ and $u_*$ by Beljaars *et al.* (1987).

Integration of (3.19) and (3.20) between the roughness length $z_0$ and $z$, yields:

$$u_* = \frac{\kappa u(z)}{\ln(\frac{z-d}{z_0}) - \psi_m(\frac{z-d}{L}) + \psi_m(\frac{z_0}{L})} \qquad [3.25]$$

and:

$$c_* = \frac{\kappa c(z)}{\ln(\frac{z-d}{z_0}) - \psi_h(\frac{z-d}{L}) + \psi_h(\frac{z_0}{L})} \qquad [3.26]$$

where

$$\psi_m(\frac{z-d}{L}) = \psi_h(\frac{z-d}{L}) = -5.2\frac{(z-d)}{L} \qquad [3.27]$$

for stable conditions and,

$$\psi_m(\frac{z-d}{L}) = 2\ln(\frac{1+x}{2}) + \ln(\frac{1+x^2}{2}) - 2\arctan(x) + \frac{\pi}{2}$$
$$\psi_h(\frac{z-d}{L}) = 2\ln(\frac{1+x^2}{2}) \qquad [3.28]$$
$$x = [1-16\frac{(z-d)}{L}]^{0.25}$$

for unstable conditions. $\psi_m((z-d)/L)$ is the integrated stability correction for momentum and $\psi_h((z-d)/L)$ is the integrated stability correction for heat.

In this calculation scheme a problem arises in the calculation of $L$, $u_*$ and $H$ because of the interdependence of these variables. Beljaars *et al.* (1987) derived an iterative calculation scheme for the Dutch situation for day and night-time heat fluxes based on publications by Holtslag and Van Ulden (1983), Van Ulden and Holtslag (1985) and Holtslag and De Bruin (1988). The calculation scheme of Beljaars *et al.* (1987) is used here to estimate these values.

An alternative way of estimating $u_*$ values is by using measurements of the standard deviation for wind direction, instead of the wind profile or eddy correlation. According to Hicks *et al.*, (1987), $u_*$ can be estimated from wind speed measurements and the standard deviation of wind direction $\sigma_\theta$. Information both on atmospheric stability and surface roughness is contained in $\sigma_\theta$. Measurements of $\sigma_\theta$ can be used directly as a measure for turbulence. In this method, the value of $u_*$ is estimated directly from $u$ and $\sigma_\theta$ by Hicks *et al.* (1987):

$$u_* = \frac{\sigma_\theta u}{c_v} \qquad [3.29]$$

Here, $c_v$ is a scaling parameter of the standard deviation of the lateral wind fluctuations on $u_*$. This method for calculating $u_*$ relies heavily on estimates of $c_v$, of which the values depend on atmospheric stability and the boundary layer height ($z_i$). The boundary-layer height dependence is the result of a whole variety of large-scale, thermal-like structures in the convective boundary layer. The scaling parameter $c_v$ is independent of height in the surface layer and not heavily affected by terrain irregularities (Beljaars *et al.*, 1983). Various parametrisations of $c_v$ can be found in the literature; a short overview is presented in Erisman *et al.*, (1989A). A $c_v$ value of 2 has been adopted for neutral cases according to Hicks *et al.*, (1987). From the same reference, values of 2 and 3 have been taken for stable and unstable conditions, respectively. These values have been confirmed by experiments performed by Erisman and Duyzer (1991).

An alternative approach for $u_*$ is to first estimate the roughness length of the surroundings from the $\sigma_\theta$ measurements. After that, wind speed measurements at one height are used together with Eqn. 3.25 to estimate $u_*$ values. Values for $z_0$ are commonly derived from measurements of the wind profile (see e.g. Thom, 1975). Under neutral conditions, where the stability correction is negligible, a linear fit of $ln(z)$ against $u(z)$ can provide information on $d$ and $z_0$. Empirically, $z_0$ may be approximated as $0.1h$ (Stull, 1988).

Another way of estimating $z_0$ values is by using measurements of the standard deviation of wind direction, with $\sigma_\theta$ used by other research groups to estimate atmospheric stability and surface fluxes (Erbrink, 1986,1989; Hicks *et al.*, 1987; Erisman *et al.*, 1990) and roughness lengths (Hanna, 1981; Beljaars, 1988; Erisman and Duyzer, 1991). A value for $\sigma_\theta$ is calculated from wind direction measurements and averaged over several minutes to one hour. In order to minimise the effect of systematic change in wind direction, the total measuring period must be as short as possible. However, to minimise statistical errors, a large averaging time is desirable. Erisman and Duyzer (1991) showed that even at 7-min averages, $\sigma_\theta$ can be seriously influenced by change in wind direction at low wind speeds. Beljaars (1988) suggests using 10-min averages in near neutral conditions at high wind speed ($> 4$ m s$^{-1}$ at 10 m height)

to estimate $z_0$ values, thus minimising the effect of a change in wind direction at short averaging times.

Following Hanna (1981), $z_0$ is derived for each wind sector according to:

$$z_0 = zEXP[\frac{-\kappa c_v}{\sigma_\theta}] \qquad [3.30]$$

Under near neutral stability at $u > 4$ m s$^{-1}$, $c_v$ values can be assumed to be independent of stability and Eqn. 3.30 can be applied directly (Beljaars, 1988).

Although the aerodynamic gradient method permits longer sampling times (generally at least one hour) and thus a more accurate measurement of a pollutant concentration, the application of the aerodynamic gradient method is limited by the accuracy of chemical instruments. Concentration differences between two levels in the order of 1 - 5% have to be detected. To avoid systematic differences, gradients are often determined with the same sensor.

Concentrations at two or more heights within about 10 m above a horizontally homogeneous surface (low vegetation) are used to evaluate a local gradient that is assumed to be representative of the area of interest. Next to the concentration gradient, measurements are made to estimate $K_c$ (Eqn. 2.18) and the stability corrections to estimate the pollutant flux. These measurements usually comprise wind profile measurements, sonic anemometer measurements, or measurements on wind speed and standard deviation of wind direction at one level. Typical instrumentation for flux gradient measurements is illustrated in Figure 3.5.

Limitations to the micrometeorological methods

Time-average measurements at a point provide an area-integrated average of the exchange rates between the surface and the atmosphere. The measuring height must be well within the constant flux layer and near to the earth's surface (5 - 10 m). This means that usually only local fluxes can be measured (low measuring heights to meet these demands). Extrapolating these fluxes or derived deposition parameters to larger areas is still a great problem because of varying surface properties and roughness characteristics, and accordingly non-homogeneous turbulent behaviour. Fluxes cannot be measured with these methods in a complex terrain or near to sources where there is no constant flux layer. Measurements must be made over a terrain with an upwind fetch over a homogeneous surface large enough to establish a fully developed constant flux layer. In addition to fetch requirements, the development of the constant flux layer requires that no sources or sinks exist in the atmosphere above the surface, and that the concentration of the constituent does not vary significantly with time (Baldocchi *et al.*, 1988; Hicks *et al.*, 1987; Businger, 1986; Erisman *et al.*, 1990). Sources or sinks might be the result of rapid reactions among reactive species between the point of flux measurement and the surface. The influence of reactions has been suggested for $NH_3$ and acidic gases, such

as $HNO_3$ and HCl (Huebert and Robert, 1985; Erisman *et al.*, 1988; Brost *et al.*, 1988; Allen *et al.*, 1989) and has been demonstrated for the photostationary equilibrium between NO, $NO_2$ and $O_3$ (Lenschow, 1982; Duyzer, 1991; Wesely *et al.*, 1989; Kramm, 1989).

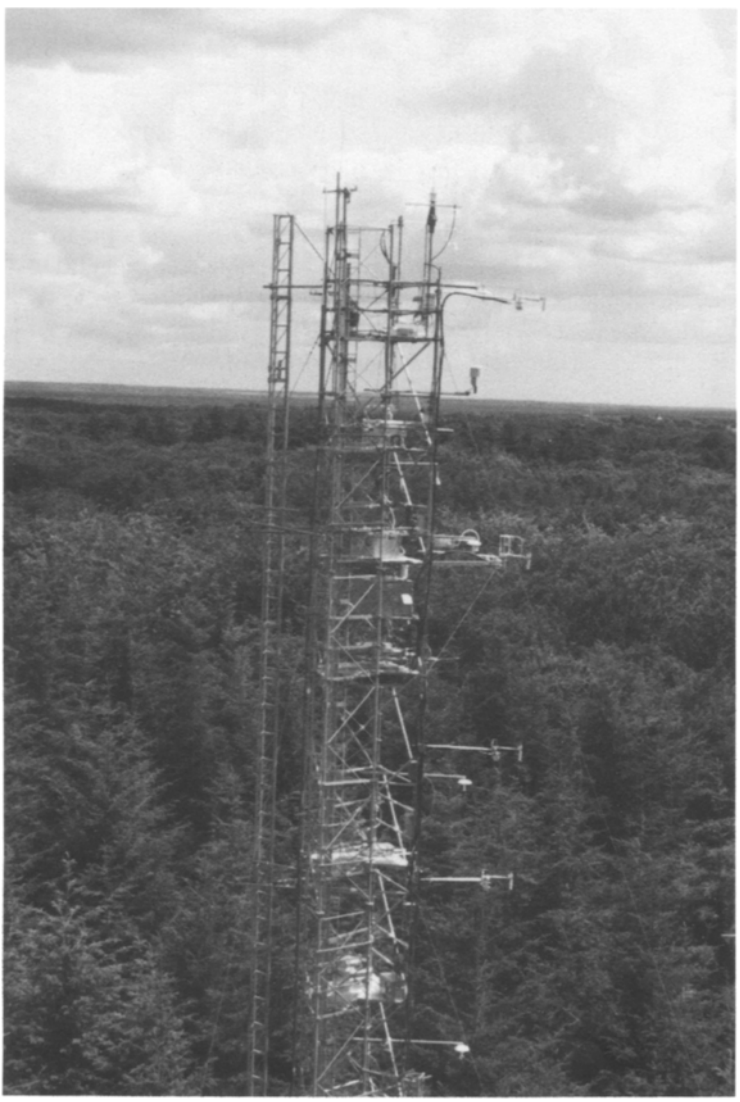

**FIGURE 3.5** Illustration of instrumentation used for flux gradient measurements at the Speulder forest.

**FIGURE 3.5** (*continued*) Illustration of instrumentation used for flux gradient measurements at the Elspeetsche Veld and throughfall measurements at the Speulder forest.

*Surface wash methods to estimate dry deposition*

Measurements of dry deposition can also be made by measuring the deposition at the surface itself directly or indirectly (surface accumulation methods). Direct methods comprise the measurement of deposition to natural surfaces using the throughfall method (see below), or to surrogate surfaces such as dustfall buckets, flat plates, petri dishes or other devices intended to approximate natural surfaces. All these methods may be useful for measuring deposition of large particles. Other direct methods include measurements of accumulated material by electron-microscope counting, laboratory studies (e.g. stomatal conductance), and wind-tunnel and chamber studies. Here the discussion is limited to field experiments. While inert surfaces have provided useful data in process level studies (e.g. Davidson *et al.,* 1985), they do not directly simulate vegetation. The direct method with the most potential in this regard is the throughfall method.

Throughfall method

Throughfall has typically been used for quantification of soil loads with nutrients and not for atmospheric deposition estimates. Throughfall refers to anything from the water dripping from canopies and stemflow to water running down tree trunks. By measuring the amount and quality of the rain water passing through a forest canopy, an estimate of the total (i.e. wet + dry + occult) deposition onto this canopy can be made. Water dripping from leaves/needles and branches, and falling through gaps in the canopy is referred to as throughfall, whereas water running down tree trunks is called stemflow. The contribution of stemflow depends on stem density, bark structure and inclination of branches; it is usually only measured if considered significant for the total flux to the forest floor. The difference between throughfall (+ stemflow) flux and open field wet deposition is often called 'net throughfall'. The net throughfall flux of an ion or insoluble element below the canopy to the extent that deposited material is washed from the canopy by rain provides information on the dry deposition.

Using the throughfall method for the estimation of dry deposition has some important advantages over the micrometeorological methods. First of all, it is not restricted to adequate fetch as micrometeorological methods are, and thus is well suited to monitoring deposition in a complex terrain. Secondly, throughfall contains all gases and particles deposited, including coarse particles. Thirdly, the throughfall method allows fairly easy continuous monitoring, and thus provides the opportunity to study deposition processes. Lastly, the throughfall method is less expensive than micrometeorological measurements and relatively easy to implement. For this reason, the throughfall method is well suited for monitoring at a large number of sites.

However, the throughfall method also has several weak points. Most important are the problems associated with canopy exchange processes. If pollutants are irreversibly taken up or leached by the canopy, throughfall deposition estimates will be obscured. Another problem in using the throughfall method is related to the large spatial variability of throughfall fluxes usually observed within forest stands (e.g. Duijsings *et al.,* 1986; Ivens, 1990; Beier *et al.,* 1992b). Experimental devices used for throughfall measurements should reveal this large

spatial variability so as to obtain representative deposition estimates. Moreover, litterfall, insects, pollen, bird excrements and dry deposition in the throughfall devices, as well as changes in throughfall chemistry during storage due to biological activity may obscure the deposition estimates. To address these problems, throughfall devices and reservoirs must be cleaned regularly. Slanina *et al.* (1990) tested the chemical stability of throughfall samples and concluded that $NO_3^-$, $NH_4^+$, $SO_4^{2-}$ present in throughfall samples stored in opaque bottles stay chemically stable in the field for one full week.

Canopy exchange processes

Throughfall fluxes are found to be influenced by diffusion and ion exchange between the surface water and the underlying apoplast of canopy tissues. Diffusion is found to be the major cause of elevated anionic concentrations in throughfall, while both diffusion and ion exchange contribute to cationic concentrations in throughfall (Schaefer and Reiners, 1990). The rate of canopy exchange depends on tree species and ecological setting. For example, during the growing season deciduous tree species tend to lose more nutrients from the crown foliage through leaching than coniferous tree species. Conifers, however, stay green all year round and continue to lose nutrients throughout the dormant season (Smith, 1981). The age distribution of leaves and soil nutrient status also affect the magnitude of leaching to a large extent. Young immature leaves/needles tend to lose less nutrients compared to older ones (Parker, 1990), and fertilisation is found to enhance canopy leaching considerably (Matzner *et al.,* 1983). Biotic stresses like insect plagues may initiate large canopy leaching. Bobbink *et al.* (1990; 1992) monitored throughfall in a heathland vegetation and observed a marked increase of canopy losses occurring simultaneously with an outbreak of a heather-beetle plague. Furthermore, abiotic stresses like drought and temperature extremes are found to enhance canopy leaching (Tukey and Morgan, 1963). The presence of certain pollutants may also be of importance. Large concentrations of ozone, for example, were found to enhance the permeability of cell membranes in canopy foliage, thereby increasing ion leakage (Evans and Ting, 1973). Moreover, the amount and timing of precipitation is found to be relevant with respect to canopy leaching. Relatively long residence times during drizzle account for relatively high leaching rates compared to short rain periods with large rainfall intensities. Large amounts of rain may deplete leachable pools within the canopy, thereby inhibiting ion leaching (Lovett and Lindberg, 1984). Losses from leachable pools within the canopy are believed to be replenished within 3-4 days after a large storm by increased root uptake or translocation from other parts of the tree (Parker, 1983).

In general the throughfall method provides reasonably good estimates for sulphur, sodium and chloride deposition. Furthermore, the atmospheric deposition of base cations can be estimated using throughfall measurements, provided corrections are made for canopy exchange (see also the results reported in Chapter 6). Nitrogen compounds are found to be retained in the canopy and the throughfall method seems less suitable for estimating atmospheric input. Potentially, part of the deposited inorganic nitrogen retained in the canopy may be converted into organic substances and subsequently leached.

*Watershed mass balance method*
The outflow from catchments is equal to the sum of wet and dry deposition, weathering release and net change in storage in biomass and soil. By measuring the outflow flux, an estimate for the deposition to the catchment is obtained when the latter two are negligible or can be quantified. Up to now, this approach has been applied successfully to the Lake Gårdsjön area in Sweden (Hultberg and Grennfelt, 1992) and the Hubbard Brook forest ecosystem in the USA (Likens *et al.*, 1990); it has given reliable deposition estimates for S, Na and Cl to whole catchments. The possibility of using this method is limited to those areas where the necessary assumptions are valid. Where the facilities (gauged watersheds with routine stream chemistry monitoring) already exist, it is a simple and cheap method for estimating deposition.

*Inferential technique*
As an alternative to the direct measuring methods, knowledge on dry deposition processes can be used to infer dry deposition fluxes from basic information on routinely measured air concentrations and meteorological parameters. The flux is inferred as the product of ambient concentration of the chemical of interest and its dry deposition velocity. The dry deposition velocity is derived using a multiple-resistance transfer model (Hicks *et al.*, 1987). The resistance model provides a framework for coupling individual processes, some being surface-dependent or pollutant-dependent. This resistance analogy is described in section 3.2. The quality of results obtained by this method depends on the availability and quality of data, and on the description of the resistances.

Flux estimations on a routine basis using the inferential technique are made in two networks in the USA (Hicks *et al.*, 1991; Clarke *et al.*, 1992). Weekly mean measurements of $HNO_3$, $SO_2$, $NO_3$, $SO_4$ and $NH_4$ concentrations in these networks are combined with meteorological parameters to obtain weekly average fluxes (Hicks *et al.*, 1985). This technique has also been applied in studies done in the UK (UK Review Group on Acid Rain, 1990), in Sweden (Lövblad and Erisman, 1992) and in the Netherlands (Erisman *et al.*, 1989; Erisman, 1992; 1993a; Chapter 5) and, recently, also for Europe as a whole (Van Pul *et al.*, 1994; 1995; Chapter 5).

Eder and Dennis (1990) developed an inference technique allowing the estimation of the annual and monthly air concentrations of $Ca^{2+}$, $Mg^{2+}$, $Na^{+}$ and $K^{+}$. The technique is based on the strong correlation between concentrations in precipitation and the surface-level air at 23 stations in Ontario, Canada. The technique is used in Chapter 5 to determine concentrations and subsequently the dry deposition of base cations in the Netherlands and Europe.

*Chamber methods*
Chamber methods, in which gas uptake by the depositing surface is measured, are used in the laboratory or in the field. In open-top or closed chambers, deposition is studied in relation to the characteristics of the vegetation. Factors thought to affect deposition are carefully

controlled and measured. The response of different plant species or plant components can be studied in semi-isolation. The deposition to the surfaces (soil or vegetation) in the chambers can estimated by comparing the in and out flux of the chamber over a certain time interval (e.g. Milne *et al.,* 1979; Taylor *et al.,* 1983; Granat and Johansson, 1983). In addition, cuvette and mini-cuvette studies with branches or single leaves provide insight in fundamental physical, chemical and biological processes related to trace gas exchange (see Murphy and Sigmon, 1989).

## 3.3 CLOUD AND FOG DEPOSITION AND DEW

### 3.3.1 PROCESS DESCRIPTION

Vegetation may intercept cloud and fog droplets or directly collect water vapour that forms dew. Hill cloud and lowland fog droplets generally have diameters between 3 and 50 μm, and can be efficiently captured by vegetation (Fowler, 1984; Fowler *et al.*, 1989; Hicks *et al.*, 1989; Fowler *et al.,* 1992). Deposition of such droplets occurs similar to that of coarse particles and thus is only limited by the resistance to aerodynamic transfer (Dollard *et al.*, 1983; Gallagher *et al.,* 1988). As the droplets are rather small, their sedimentation rate is slow, but impaction and interception by foliage, and other obstacles in their path can be effective. Cloud droplets usually contain higher concentrations of pollutants than are found in rain, and cloud water deposition may exceed annual precipitation, especially at high elevation sites (Lovett, 1988). In Europe at altitudes of 400 m above sea level and above, low clouds are present between 500 and 2000 h per year (Fowler *et al.*, 1991). Cloud water deposition might be a significant input mechanism for such regions in Europe. The major limitation for estimating inputs by cloud and fog droplet deposition is the lack of information on cloud and fog water composition, and on liquid water content. In general, concentrations of $SO_4^{2-}$, $NO_3^-$ and $NH_4^+$ in cloud and fog droplets are found to be 10-50 times those in precipitation.

### 3.3.2 MEASURING METHODS

Recently, much research has been conducted on cloud and fog deposition (Fowler *et al.*, 1991; Weathers *et al.*, 1986; Schemenauer, 1986; Mohnen., 1988; Johnson and Lindberg, 1990; Lovett and Kinsman, 1990; Mitchell *et al.*, 1990; Wyers *et al.*, 1995; Vermeulen *et al.*, 1995; Erisman *et al.*, 1994). Several techniques have been applied by which droplet deposition can be separated from wet and dry deposition. Cloud water can be collected by impaction of the droplets on a collection surface (Weathers *et al.*, 1986; Waldman *et al.*, 1982; Mallant and Kos, 1990). Furthermore, estimates of cloud water deposition have been made using throughfall measurements, together with sensors for cloud occurrence and measurements of cloud water amount (Joslin and Wolfe, 1992). Dollard *et al.* (1983) and Gallagher *et al.* (1988) report micrometeorological measurements of cloud water deposition to short vegetation, while Wyers *et al.* (1995) and Vermeulen *et al.* (1994) report similar measurements over the Speulder forest (see also section 7.3). From these studies, it was found that cloud water deposition rates averaged over the droplet size spectrum in these measurements are close to the reciprocal of the aerodynamic resistance for momentum.

The annual input of cloud water in the UK has been determined using annual precipitation chemistry, cloud base and wind statistics, and an average relationship between ionic

composition of precipitation and orographic cloud water obtained at one site (Fowler *et al.*, 1991; Weston and Fowler, 1991).

In the Netherlands about 200 nights per year with one or more hours of dew were observed (Römer *et al.*, 1990). Dew is aqueous vapour condensed on cool bodies (vegetation) and therefore clean, containing very low concentrations of pollutants (Van Aalst and Erisman, 1991; Römer *et al.*, 1991). Dew may play an important role in the process of dry deposition by enhancing surface wetness; in this way, surface resistance to soluble gases will be lowered and dry deposition increased. This process is included in dry deposition estimates.

## 3.4 EVALUATION AND COMPARISON OF DIFFERENT METHODS FOR ESTIMATING DEPOSITION

### 3.4.1 WET DEPOSITION

Comparisons between wet-only and bulk precipitation fluxes have been made by Grennfelt *et al.* (1985), Georgii *et al.* (1986), Clark and Lambert (1987), Mosello *et al.* (1988), Ridder *et al.* (1984), Ruijgrok *et al.*(1989), Slanina *et al.* (1990); Stedman *et al.* (1990) and Richter and Lindberg (1988). In these studies, bulk precipitation of $SO_4^{2-}$, $NO_3^-$ and $NH_4^+$ is found to be between 4 and 34% higher than corresponding wet-only precipitation fluxes (see also Table 3.1). Even larger differences are reported for base cations like $Na^+$, $Ca^{2+}$, $Mg^{2+}$ and $K^+$ (7-75%). Especially coarse particles seem to deposit onto bulk precipitation funnels during dry periods (through sedimentation). The amount of dry deposition onto bulk precipitation funnels is influenced by the distance to local sources, ambient concentrations, wind-shading effects around the funnel, design of sampler, sampling frequency and cleaning protocols.

Intercomparison of wet-only samplers have shown that the results obtained are very sensitive to the type of sensor used for the registration of onset/offset of the precipitation events (Graham *et al.*, 1988).

It used to be thought that bulk samplers could be used to determine the total deposition (wet plus dry and fog deposition). The fog and dry deposition measured with bulk samplers, however, is the fog and dry deposition to the funnels of the samplers and does not have any relation with the fog and dry deposition to ecosystems. The 'extra' deposition is therefore considered as 'contamination' of the wet deposition measured with bulk samplers. Bulk samplers might be useful in specific conditions (high elevation, remote areas). However, wet-only samplers are generally recommended. Sampling procedures need to be designed with great care and sampling locations should be selected to be representative for the area under study (not near sources or obstacles such as fences, trees and buildings). In addition, measures should be taken to preserve the samples if biologically or chemically active species are to be studied; i.e. using light-protected bottles, addition of preservatives, reducing storage temperature or by minimising the storage period in the field.

### 3.4.2 DRY DEPOSITION

Measurement of dry deposition of different pollutants exhibits different difficulties and no single method can probably be regarded as the 'best' for monitoring. In this section we will summarise the results of comparison studies between different measuring methods applied for sulphur, nitrogen and base cations.

*Sulphur*

Detailed long-term comparisons between dry deposition estimates from inferential plus deposition plate methods on the one hand, and dry deposition estimates from the throughfall method on the other, were made by Lindberg and Lovett (1992) during the integrated forest study (IFS). Sulphur was found to behave more-or-less conservatively in the canopy. For a large number of sites scattered over the USA, Canada and Europe, minor $SO_2$ uptake balanced, to some extent, foliar leaching of soil derived sulphate. The estimated total annual deposition of sulphur compounds was found to be within 15% of the measured sulphate fluxes in throughfall plus stemflow in each case ($R^2$=0.97).

Experimental evidence for canopy uptake of $SO_2$ was found by Gay and Murphy (1985), but Schaefer and Reiners (1990) and Granat and Hällgren (1992) concluded that essentially all the dry deposited sulphur dioxide retained by the canopy (taken up via the stomata) is eventually extracted out of the apoplast pools (i.e. aqueous layer on the outside of cell membranes) by rain, and appears in throughfall. Furthermore, several radioactive $^{35}SO_4^{2-}$ studies have shown that, in general, less than 4% of the total throughfall flux of sulphate is caused by foliar leaching of soil-derived sulphate. (Garten *et al.*, 1988; Lindberg and Garten, 1989; Cape *et al.*, 1992).

Comparisons between inferential dry deposition estimates on the one hand, and dry deposition estimates from micrometeorological measurements and/or throughfall data on the other, were made by Ivens (1990), Draaijers and Erisman (1993), Lovett *et al.* (1992) and Erisman (1993B). Ivens (1990) compared $SO_4^{2-}$ throughfall fluxes from all over Europe with deposition estimates of SOx from the long-range transport model RAINS (Eliassen and Saltbones, 1983; Alcamo *et al.*, 1987). For coniferous tree species, sulphate throughfall fluxes were found to be significantly higher (on average, 80%) when compared to sulphur deposition estimates from the RAINS model. For deciduous tree species, neither estimate was significantly different.

Erisman (1993B) compared SOx dry deposition estimates using the inferential technique with throughfall measurements of $SO_4^{2-}$ in 24 forest locations in the Netherlands. The two estimates showed large differences, throughfall fluxes being 45% higher than inference estimates. However, variations in time and space were similar. Draaijers and Erisman (1993) made a detailed comparison of net throughfall measurements of sulphate in 30 different forest stands in a small area in the Netherlands (Van Ek and Draaijers, 1991) and sulphur dry deposition estimates from the same receptor-oriented inferential model (Erisman, 1992; 1993A). Similar results were obtained as those by Erisman (1993B). However, by extending the surface resistance parametrisation for $SO_2$ in the inferential model with results obtained by a field study on co-deposition of $NH_3$ and $SO_2$ (Erisman and Wyers, 1993), the difference between both estimates disappeared. Erisman *et al.* (1993B) and Erisman (1992) compared $SO_4$ throughfall measurements under heathland (Bobbink *et al.*, 1992) with results of the annual average flux of $SO_2$ measured on heathland using the dry deposition monitoring system

for $SO_2$ (sulphate particle deposition was estimated by inference). They found good agreement between the two estimates. For the Hubbard Brook forest ecosystem, Lovett *et al.* (1992) reported higher (65%) sulphur dry deposition estimates from the throughfall method compared to estimates from an inferential model (Hicks *et al.*, 1987). The inferential model is known to underestimate dry deposition in complex terrain (Hicks and Meyers, 1988).

Inference estimates of sulphur dry deposition in the Netherlands compared well with estimates using the LTRAP model TREND (Van Jaarsveld and Onderdelinden, 1992) on a 5 x 5 km scale. Furthermore, inference results compared well with dry deposition measurements using micrometeorological methods (Erisman, 1992; 1993A). Wesely and Lesht (1989) compared RADM $SO_2$ dry deposition results with site-specific estimates using inference. Their results showed some systematic differences between the two techniques due to differences in the algorithms for computing resistances. Weekly averages of the deposition velocities were within approximately 30% of each other.

Comparisons between dry deposition estimates obtained from the throughfall method and dry deposition estimates from the watershed mass balance method are reported by Hultberg and Grennfelt (1992) for the Lake Gårdsjön area in Sweden and by Likens *et al.* (1990) for the Hubbard Brook Forest Ecosystem in the USA. Runoff and throughfall fluxes of sulphate were found to be very similar, suggesting the change in storage in biomass and soil, and weathering release were of minor importance. Sulphate fertilisation in several catchments did not enhance sulphate throughfall fluxes significantly, supporting the hypothesis that foliar leaching is insignificant, and that throughfall provides a reasonably good measure for sulphur ($SO_2$ + $SO_4^{2-}$ aerosol) deposition.

*Nitrogen*

There is considerable experimental evidence for significant uptake of inorganic nitrogen by canopy foliage, stems, epiphytic lichens or other micro-flora. Much insight has been gained from experiments with radio-labelled $^{15}N$. Canopy foliage has been demonstrated to be capable of absorbing and incorporating gaseous $NO_2$ and $HNO_3$, as well as $NO_3^-$ and $NH_4^+$ in solution (Reiners and Olson, 1984; Bowden *et al.*, 1989). In laboratory experiments, $NH_4^+$ in solution was found to be exchanged with base cations present in leaf tissues (Roelofs *et al.*, 1985). Epiphytic lichens have also been shown to be active absorbers of $NO_3^-$ and $NH_4^+$ in solution (Lang *et al.*, 1976; Reiners and Olson, 1984).

The absorption or removal of nitrogen in the canopy will generally cause throughfall measurements to underestimate the total deposition. Based on information available in the literature, Ivens (1990) suggested the above-ground uptake of inorganic nitrogen to be between 150 and 350 eq $ha^{-1}$ $a^{-1}$. Johnson and Lindberg (1992) conclude that, on average, 40% of all inorganic nitrogen input to the IFS forests was retained by the vegetation, whereas 60% is found back in the throughfall data as $NO_3^-$ and $NH_4^+$. Total inorganic nitrogen uptake amounted up to 850 eq $ha^{-1}$ $a^{-1}$, with a strong positive relationship between deposition and

uptake for spruce and spruce-fir stands. Other tree species showed a rather constant inorganic nitrogen uptake (200-300 eq $ha^{-1}$ $a^{-1}$), with only little response to deposition amount (Johnson and Lindberg, 1992). Part of the inorganic nitrogen retained by the canopy may be converted into organic substances and subsequently leached. Total nitrogen (organic + inorganic) in throughfall and stem flow is found to be about 84% of the total inorganic nitrogen deposition (Johnson and Lindberg, 1992). Microbes were assumed to play an important role in the conversion of inorganic to organic N, if it occurs. However, it was recognised that organic N in throughfall also arises from internal pools and surfaces of plant and lichens, and from micro-particulate detritus and pollen (Johnson and Lindberg, 1992).

In comparing throughfall with model estimates of nitrogen input to forests in Europe, Ivens (1990) found no significant difference between $NO_3^-$ throughfall fluxes and NOy (= total oxidised nitrogen) deposition estimates, but $NH_4$ throughfall fluxes were significantly lower (on average, 70%) compared to NHx (= total reduced nitrogen) deposition estimates. The correlation between throughfall fluxes and deposition estimates from the RAINS model were very poor. This was attributed to the large deposition variability introduced by local sources and local differences in aerodynamic and/or surface resistance not accounted for in the RAINS model, and by canopy exchange processes obscuring deposition estimates from the throughfall method.

In a separate study, $NO_3^-$ net throughfall fluxes were found significantly lower (on average, 30%) compared to NOy dry deposition estimates using the inferential model (Erisman, 1992; 1993A). NOx dry deposition estimates from micrometeorological measurements made above forest in the Netherlands were also somewhat lower compared to NOx deposition estimates from this model. $NH_4^+$ net throughfall fluxes were not significantly different from NHx dry deposition estimates, but their correlation was rather poor. $NH_3$ deposition estimates from micrometeorological measurements made over heather and forests in the Netherlands were found both lower and higher compared to inferential model estimates. This is attributed to the large spatial variability in $NH_3$ dry deposition amounts due to the impact of local sources and short atmospheric residence times of $NH_3$ (Erisman, 1992; 1993A). An extensive comparison between throughfall measurements and atmospheric deposition estimates at the Speulder forest and at several locations in the Netherlands can be found in section 6.2.

Nitrogen cycles within ecosystems are very complex. Up to now, no reliable estimates for inorganic nitrogen deposition can be made using the watershed mass balance method.

*Base cations*

Na is normally considered to be more-or-less conservative in the canopy, showing only minor canopy exchange (Parker, 1983; Ivens, 1990; Johnson and Lindberg, 1992). Consequently, Na in throughfall was suggested for use as a substance for modelling particle dry deposition (Ulrich, 1983). This model has been widely used (Freiesleben *et al.*, 1986; Bredemeier, 1988; Horn *et al.*, 1989; Ivens, 1990; Beier, 1991; Beier *et al.*, 1992A; 1992B; Draaijers, 1993; Van

Leeuwen *et al.*, 1994). However, canopy exchange of $Na^+$ may occur; Fassbender (1977) found uptake of $Na^+$ by young Spruce trees. Furthermore, Reiners and Olsson (1984) reported leaching of $Na^+$ from canopies of Balsam Fir in a low input area.

Lovett and Lindberg (1984) developed an approach to estimate dry deposition from net throughfall for a number of ions based on a multiple regression model. Lindberg *et al.* (1988) compared this method with deposition measurements of $Ca^{2+}$ to inert surfaces to develop scaling factors for relating fluxes on scales from small plates to whole canopies. This scaling method has also been applied to the dry deposition of $Na^+$. On the basis of a comparison of throughfall data with deposition measurements of a large number of IFS sites in the United States, Johnson and Lindberg (1992) conclude that $Na^+$ in throughfall may be considered as solely derived from atmospheric deposition. Besides the throughfall method and the surface accumulation method, the mass balance approach in watersheds is also found to provide reliable estimates for atmospheric deposition of $Na^+$ (Hultberg and Grennfelt, 1992).

Unlike $Na^+$, a substantial part of $Mg^{2+}$, $Ca^{2+}$ and $K^+$ in throughfall is normally assumed to be caused by canopy leaching (Parker, 1983). However, a literature compilation made by Parker (1990) indicates that it is not clear to what degree $Mg^{2+}$, $Ca^{2+}$ and $K^+$ present in throughfall originate from atmospheric deposition and foliar leaching, respectively. Canopy leaching contributed between 10 and 80% to the total flux of these base cations reaching the forest floor. However, at coastal forest sites, $Mg^{2+}$ in throughfall may be predominantly caused by atmospheric deposition of sea-salt particles (Parker, 1983; Beier *et al.*, 1992A). Calcium in throughfall may be enhanced at sites located in areas with calcareous soils or near calcium fertilised arable land (Johnson and Lindberg, 1992). For the IFS data, Johnson and Lindberg estimated that leaching represented an average of ~70% of the annual throughfall plus the stem flow flux of $K^+$ below 12 diverse forests, while $Ca^{2+}$ leaching represented about 40% and $Mg^{2+}$ leaching about 50%. Magnesium and calcium may also be irreversibly retained within the canopy in the case of limited supplies from the soil (White and Turner, 1970; Abrahamson *et al.*, 1976; Alcock and Morton, 1981). A new method for estimating the dry deposition of $K^+$, $Ca^{2+}$ and $Mg^{2+}$, based on the $Na^+$ deposition in a forest edge, was recently suggested by Beier *et al.* (1992A). Section 6.2 will report on a comparison between deposition estimates of base cations using the inferential method at the Speulder forest and at other sites in the Netherlands. The canopy exchange of these components is quantified in the Speulder forest.

### 3.4.3 CLOUD AND FOG DEPOSITION

Joslin and Wolfe (1992) concluded that net throughfall may be used as a gross estimate of total cloud S deposition by subtracting precipitation and dry inputs from total throughfall sulphate in high cloud environments. Meuller (1992) compared two techniques for estimating cloud deposition to a high-elevation spruce forest; i.e. throughfall and precipitation chemistry, and a mechanistic cloud deposition model with a cloud event database. The comparison

showed a discrepancy of about 30-35% for sulphate, throughfall being higher than model estimates.

### 3.4.3 SYNTHESIS

As can be concluded from section 3.4, the throughfall method, micrometeorological methods (supplemented/supported by inference) and watershed balance methods (S saturated systems) yield similar estimates of the annual mean total deposition of sulphur within generally acceptable uncertainly limits (~30%). A larger uncertainty exists to estimate reduced or oxidised nitrogen and base cation fluxes.

It is clear that for individual ecosystems deposition in general, and dry deposition in particular, can still not be quantified with sufficient accuracy. The various methods have different advantages and drawbacks and the choice of a certain method for estimation of the flux of a specific pollutant to a specific ecosystem may in many cases depend on the purpose of the study and on requirements on accuracy and costs. For the time being, it is impossible to obtain an accurate annual average deposition map of the Netherlands or of Europe based on actual deposition measurements. Dry, cloud and fog deposition show very strong horizontal gradients due to variations in ambient concentrations in land use, in surface conditions and in meteorology. Therefore deposition maps based on a combination of models and measurements are generated. This is explained in Chapter 5. Regarding spatial and temporal scales, measurements are supplementary to models in such a method. Furthermore, measurements are used for developing process descriptions and for evaluation of model results. Finally, measurements can act as an independent tool for assessing policy targets (trend detection). These issues, outlined below, require different measuring/monitoring strategies.

*Process-oriented studies*
The process-oriented studies are primarily used to provide insight into deposition processes for different components, and to obtain process descriptions and parameters to be used in models. Micrometeorological methods provide the best methods for these purposes. In cases where micrometeorological methods cannot be used, such as complex terrain and within forest stands, the throughfall method is the only one available up to now. Process-oriented studies can be used to test or verify simple/cheap measuring methods, which might be used for other purposes such as monitoring.

*Evaluation of models*
For evaluation or validation of model results, preferably simple and cheap monitoring methods are desired. In general, monthly to annual average fluxes are used for validation. The uncertainty in results obtained by these monitoring methods should be within acceptable limits. Furthermore, results should be representative for areas used as receptor areas in the model. Validation of LTRAP model results can be done using area representative

measurements of wet deposition and of ambient concentrations. Micrometeorological measurements suitable for monitoring might be used for evaluating model dry deposition fluxes (Hicks *et al.*, 1991; Erisman *et al.*, 1993A; Erisman and Wyers, 1993). Throughfall measurements might be used as a validation method for spatial variability in S, $Na^+$ and $Cl^-$ dry (and total) deposition, provided that several criteria on the method and site are met (e.g. Beier and Rasmussen, 1989; Ivens, 1990; Draaijers, 1993). It is advisable to equip several monitoring locations in Europe with dry deposition monitoring systems, wet-only sensors, and cloud and fog deposition measuring methods. These locations should be selected on the basis of pollution climates and type of vegetation. Furthermore, the surroundings should be homogeneous and no sources should be near the site.

*Detection of trends*

If the purpose of measurements is trend detection, the annual averages should be measured as accurately as the magnitude of the trends. Ambient concentration and wet deposition measurements can be used (EMEP monitoring network) for trend detection. The trend in concentrations is representative for the dry deposition trend, which cannot be measured accurately enough at present. The disadvantage of using only concentration measurements is that a change in dry deposition due to ecosystem response (as a result of reduced loads or climatic change) or due to changes in surface conditions (interaction with other gases, etc.) cannot be detected. Extensive deposition monitoring (see previous section) might be useful for trend detection, especially at larger emission reductions.

# CHAPTER 4 MEASUREMENT RESULTS AND DRY DEPOSITION PARAMETRISATIONS

*Introduction*
This chapter will describe experimental results on dry deposition. From these measurements the physical, chemical and biological processes that control deposition fluxes over surfaces are determined and translated in descriptions or parameterisations for modelling dry deposition fluxes. This is done separately for each gas and for particles. Most of the parametrisations have been derived from the literature and from experiments carried out in the Netherlands. These experiments comprise the Elspeetsche Veld three-year experiment to quantify atmospheric fluxes and derive deposition parameters for heathland vegetation; the Speulder forest long-term experiment to determine the input and impact of pollutants to a Douglas fir forest, and the Utrechtse Heuvelrug one-year experiment to determine the influence of complex terrain on deposition. These field experiments are described in some detail in Chapter 7.

## 4.1 MEASUREMENT RESULTS

### 4.1.1 $SO_2$

$SO_2$ dry deposition measurements have been made for several surfaces: coniferous forests (Galbally, 1979; Garland, 1977; Hicks *et al.*, 1982; Fowler and Cape, 1983; Lorenz and Murphy, 1985; McMillen *et al.*, 1987; Vermetten *et al.*, 1992; Erisman *et al.*, 1993d), deciduous forests (Petit et al., 1976; Matt *et al.*, 1987; Meyers and Baldocchi, 1988), heathland (Erisman *et al.*, 1993c), crops (Fowler, 1978), grasslands (Garland, 1977; Platt, 1978; Van Dop *et al.*, 1983; Hicks *et al.*, 1983, 1986; Neumann and den Hartog, 1985; Duyzer and Bosveld, 1988; Davies and Mitchell, 1983; Davies and Wright, 1985; Erisman *et al.*, 1992), water bodies (Welphdale and Shaw, 1974; Garland, 1977), bare soil (Payrissat and Beilke, 1974; Garland, 1977), and snow (Barrie and Warmsley, 1978; Welphdale and Shaw,

1974; Cadle *et al.*, 1985; Granat and Johanssson, 1983; Valdez *et al.*, 1987; Davidson and Wu, 1990; Garland, 1977). In the literature average values for the deposition velocity range from 0.1 to over 2 cm $s^{-1}$ with daytime values usually between 0.8 and 1.2 cm $s^{-1}$ Large values (> 2 cm $s^{-1}$) are observed above water surfaces and forests and relatively small values (< 0.13 cm $s^{-1}$) are measured above snow and bare soil.

Numerous field studies show that the surface resistance $R_c$ controls the $SO_2$ dry deposition velocity. $R_c$ is a function of the canopy stomatal resistance $R_{stom}$, the canopy cuticle resistance $R_{cuticle}$ and the soil resistance $R_{soil}$. In turn, these resistances are affected by leaf area, stomatal physiology, soil pH, and the presence and chemistry of liquid drops and water films on the surface. The stomatal, leaf surface (cuticle) and soil resistances act in parallel.

*Physiological Control*
Most $SO_2$ enter plants through the stomata. As gas molecules enter the leaf, deposition occurs as molecules react with the moist cells in the substomatal chamber and the mesophyll. Stomatal resistance decreases hyperbolically with increasing light and increases linearly with increasing vapour pressure deficits (Jarvis, 1976). Soil water deficits cause stomata to close after some threshold deficit level is exceeded. Low and high temperatures cause stomatal closure and moderate temperatures promotes stomatal opening. Leaf age, nutrition and adaptation are other factors affecting stomatal resistance. Elevated exposure to $SO_2$ causes stomata to close (Black, 1982). Stomatal resistance is different for different types of vegetation. Values of $R_{stom}$ during daytime, range between 30 and 300 s $m^{-1}$ for a variety of herbaceous annuals and woody perennials (Fowler, 1985; Baldocchi *et al.*, 1987; Matt *et al.*, 1987).

The canopy cuticle resistance exceeds by far the canopy stomatal resistance; $R_{cuticle}$ ranges between 3000 and 40000 s $m^{-1}$ (van Hove, 1989). However, it is observed that the surface resistance decreases as relative humidity increases (van Hove *et al.*, 1989; Garsed, 1985; Erisman *et al.*, 1993a; Erisman and Wyers, 1993; Draaijers and Erisman, 1993). Under these circumstances, the surface will become moist e.g. through deliquesence of salts at the external leaf surface. $SO_2$ dry deposition will be enhanced (Garland and Branson, 1977; Fowler and Unsworth, 1979; Fowler, 1985; Vermetten *et al.*, 1992; Erisman *et al.*,1993a; Erisman and Wyers, 1993) and will occur via absorption and chemical oxidation reactions in the water layer.

*Physico-chemical control*
The absorption of $SO_2$ in water layers is associated with a series of reactions (Seinfeld, 1986):

$$SO_2\,(g) + H_2O \Leftrightarrow SO_2 \cdot H_2O \qquad (R0)$$
$$SO_2 \cdot H_2O \Leftrightarrow H^+ + HSO_3^- \qquad (R1) \qquad [4.1]$$
$$HSO_3^- \Leftrightarrow H^+ + SO_3^{2-} \qquad (R2)$$

The total dissolved S(IV) in chemically clean solutions is related to the partial pressure of $SO_2$ over the solution ($p_{SO2}$) and the pH of the solution:

$$[S(IV)] = K_H \cdot p_{SO2}\left(1 + \frac{K_1}{[H^+]} + \frac{K_1 \cdot K_2}{[H^+]^2}\right) \qquad [4.2]$$

where $K_H$ is the Henry coefficient for $SO_2$ (5.4 mol $l^{-1}$ $atm^{-1}$ at 15 °C) and $K_1$ and $K_2$ are the equilibrium coefficients for reactions 1 and 2, respectively. From Equation [4.2] it can be concluded that an increase in acidity will reduce the amount of dissolved $SO_2$. The oxidation of S(IV) to S(VI) by $O_2$, $O_3$ and $H_2O_2$ provides another source of protons. The oxidation of aqueous $SO_2$ by $O_3$ and $H_2O_2$ is fast; oxidation by $O_2$ is slow unless there is a metal catalyst (generally iron or manganese). An increase in acidity due to solution and oxidation of $SO_2$ in water films will reduce $SO_2$ dry deposition to wetted surfaces. The presence of acid-neutralising species, either from the atmosphere (base cations, $NH_3$) or from the inner parts of the leaves, will reduce the acidity of the water film, abolishing the $SO_2$ dry deposition reduction. At present, too little information is available to quantify these processes in terms of the influence on the magnitude of the surface resistance.

As the pH of the wetted surface is the deposition rate limiting factor, the origin of surface wetness through fog, cloud, rain, dew or guttation is important (Fowler and Unsworth, 1979). The pH of rain, cloud and fog is less than that of pure water. The chemistry of wetted surfaces is affected by the uptake of acidic precursors and oxidants, particles on the leaf surface, chemical lifetime, droplet size, leaching of nutrients from leaf and evaporation rate of wetness (Brimblecombe, 1978; Chameides, 1987; Wesely *et al.*, 1990)

Deposition of $NH_3$ will neutralise an acid solution. Thus simultaneous deposition of $SO_2$ and $NH_3$ should show higher $SO_2$ (and $NH_3$) dry deposition rates to water surfaces than would be found by $SO_2$ (or $NH_3$) alone (Wesely *et al.*, 1990; Erisman and Wyers,1993; Erisman *et al.*, 1993c). It has been suggested that the deposition of $NH_3$ can enhance the deposition of $SO_2$. This process, generally referred to as co-deposition, was first suggested by Brimblecombe (1978). Van Breemen *et al.* (1982) measured a 2:1 flux ratio of $NH_4^+$ to $SO_4^{2-}$ in throughfall under a forest canopy. Houdijk (1990) observed that fluxes of both $NH_4^+$ and $SO_4^{2-}$ were much higher in areas with intensive livestock breeding compared to background areas. Both effects were ascribed to co-deposition of $NH_3$ and $SO_2$. The high deposition of $NH_3$ in areas with intensive livestock production was assumed to decrease the acidity of the absorbing

surfaces, thereby increasing the buffering of protons generated in $SO_2$ dissolution. Thus the $SO_2$ deposition increased. Recent measurements of throughfall under forest, heathland and grassland canopies have shown the same phenomena (Van Breemen *et al.*, 1988; Heil *et al.*, 1989; Bobbink *et al.* 1992; Draaijers *et al.*, 1989; Ivens 1990).

The wide range of deposition velocities for $SO_2$ measured during recent years in different locations of the world are ascribed partly to the difference in alkalinity and wetness of vegetation canopies (Fowler *et al.*, 1991). A higher $V_d$ $SO_2$ in areas with high $NH_3$ emissions relative to remote areas was also suggested by Onderdelinden *et al.* (1984) and Lövblad and Erisman (1992).

The process of co-deposition has been demonstrated in laboratory experiments. Adema *et al.* (1986) and Heeres and Adema (1989) showed a clear pH-dependence of $SO_2$ deposition on water layers in a small wind tunnel. Addition of $NH_3$ to the air in the wind tunnel increased the $SO_4^{2-}$ concentration in the water layer. Van Hove (1989) showed stoichiometric adsorption of the two gases in leaf chamber experiments, with the adsorption of $NH_3$ being twice that of $SO_2$ (on a molar basis). At higher relative humidities, adsorption increased and this ratio was maintained. The thickness of water layers on the vegetation was strongly dependent on relative humidity, ranging from 40-200 μm for relative humidities between 60 and 90%.

So far there have only been a limited number of combined micrometeorological measurements of $NH_3$ and $SO_2$, needed to test the importance of this process in the field (Sutton, 1990; Erisman *et al.*, 1991; Erisman 1992; Fowler *et al.*, 1991). Van Hove *et al.* (1989), Fowler *et al.* (1991) and Erisman and Wyers (1993) present evidence showing that the surface $SO_2$ uptake at wet surfaces is enhanced in the presence of $NH_3$. One site of reaction is in the water-filled pores of the cuticle at relative humidities above about 70% and the other site is on the wetted leaf surface.

*Deposition to soil and litter*

Deposition to canopies involves deposition to both vegetation and soil. Early studies assumed that deposition to soils under vegetation was relatively small (5 - 10% of the total flux; Fowler, 1978). Recent work shows that a substantial amount of material can be deposited to the soil below vegetation. Meyers and Baldocchi (1992) report that 20 to 30% of $SO_2$ depositing on a deciduous forest is received at the forest floor. This substantial transfer occurs because large-scale intermittent eddies are able to penetrate through the vegetation and transport material to the soil. Differentiation of deposition to the canopy and to the soil is difficult to measure. Furthermore, it may be variable, both in time and for different canopies. Relatively large deposition amounts to the forest soil are to be expected in forest edges and in deciduous forests in wintertime when gusts can penetrate deeply through the forest canopy.

Deposition to soil decreases at a soil pH below 4 and increases with relative humidity (Garland, 1977; Payrissat and Beilke, 1974). When surface temperatures fall below zero or the

surface is covered with snow, $R_c$ values increase up to 200 - 500 s $m^{-1}$ (Voldner *et al.,* 1986; Erisman and Wyers, 1993). The deposition of $SO_2$ to snow-covered surfaces depends on pH, snow temperature and probably the amount of $SO_2$ already scavenged by the snowpack (Cadle *et al.,*1985; Hicks *et al.,* 1989).

### 4.1.2 NOx

$NO_2$ is absorbed by water, soils and vegetation. However, uptake by water is slow. The conclusion to an analysis by Lee and Schwartz (1981) is that the solubility of $NO_2$ in water and the rate of subsequent reactions in the water are too low to produce deposition velocities of $NO_2$ to water higher than 0.1 cm $s^{-1}$. Gravenhorst and Böttger (1982) and Böttger *et al.* (1980) found values of 0.01 - 0.02 cm $s^{-1}$ for water and sea water using the enclosure technique. For snow, Gravenhorst and Böttger (1982) and Granat and Johansson (1983) report $V_d$ values below 0.03 cm $s^{-1}$.

Hanson *et al.* (1989) conclude that the uptake of $NO_2$ by plants is under stomatal control. Hanson and Lindberg (1991) conclude that the cuticular uptake is 1 or 2 orders of magnitude smaller than the stomatal uptake. Because of the slow uptake of $NO_2$ in water, the uptake on wet leaf surfaces of $NO_2$ is expected to be small. Vegetated surfaces can act either as a source or sink for $NO_2$ and NO. At high concentrations, the deposition of $NO_2$ to vegetation has been shown to be proportional to stomatal conductance, with minimal uptake on the external surfaces of leaves (Johansson, 1987; Fowler *et al.*, 1991; Duyzer *et al.*, 1991). At low concentrations there was hardly any uptake of $NO_2$. Leaf chamber measurements suggest the existence of a 'compensation point' in the order of 2-6 µg $m^{-3}$, below which forests may act as a (minor) source of $NO_2$ (Johansson, 1987). Glass cuvette measurements suggest that deposition of $NO_2$ to the forest floor, based on a soil surface area basis, may be 6- to 7-fold greater than deposition to foliar surfaces (Hanson *et al.*, 1989). However, measurements taken by Williams *et al.* (1987) showed that forest soils may emit $NO_2$ as well. According to Hanson and Lindberg (1991), the deposition velocity of $NO_2$ to broad-leaved forests is greater than to coniferous forests. Whole-canopy measurements of $NO_2$ deposition yield daytime overall deposition velocities between 0.1 and 2.8 cm.$s^{-1}$ (Hanson and Lindberg, 1991).

Since $NO_2$ fluxes are usually small, and because the constant flux layer assumption might be violated by the surface sources and photochemical equilibrium between $O_3$, NO and $NO_2$, micrometeorological measurements have proven to be difficult. Duyzer *et al.* (1983) measured deposition velocities of 1.5 cm $s^{-1}$, with several periods of upward fluxes. Hargreaves *et al.* (1992) measured $NO_2$ deposition to grass and found minimum surface resistances of 60 - 100 s $m^{-1}$, increasing to around 1000 s $m^{-1}$ in the early afternoon, indicating stomatal control. Measurements aboveheathland showed similar results (cf. Erisman *et al*, 1994).

The uptake of NO by vegetation is much more limited than for $NO_2$ due to the low solubility of NO in water. NO uptake is unaffected by the large change in stomatal resistance between day and night conditions (Hanson and Lindberg, 1991). Up to now, no significant downward fluxes of nitric oxide (NO) have been reported. Yet, upward fluxes of NO from soils have been measured and are found to depend on soil temperature, water content and ambient air concentration of NO and $NO_2$ (Hicks *et al.*, 1989). Deposition velocities for NO will be considerably less than for $NO_2$ (Hanson and Lindberg, 1991).

### 4.1.3 HNOx

Among the gases under consideration, $HNO_3$ is the most reactive and readily absorbed by surfaces. All field and laboratory measurements at temperatures above 0 °C show that the surface resistance for $HNO_3$ is zero, and that rates of deposition are determined entirely by atmospheric transfer (Huebert, 1983; Müller *et al*, 1993; Heubert and Robert, 1985; Harrison *et al.*, 1989; Erisman *et al.*, 1989; Hanson and Lindberg, 1991). On the basis of its chemical properties, one would expect deposition of $HNO_3$ to the cuticle to be very efficient and dominant over stomatal uptake. Deposition velocities of $HNO_3$ to forests may therefore become very large. Fowler *et al.* (1989) mentions $V_d$'s of 4.0 $cm.s^{-1}$ for wind speeds near 1 $m.s^{-1}$ and $V_d$'s of 10 $cm.s^{-1}$ when wind speeds are near 4 $m.s^{-1}$. Only at snow surfaces or at temperatures below -5 °C could a surface resistance be detected: 500 s $m^{-1}$ at -18 °C and 100 s $m^{-1}$ at -3 °C (Johansson and Granat, 1987).

If the surface resistance for $HNO_3$ deposition is effectively zero, then calculating rates of deposition onto a wide range of surfaces requires only estimation of the atmospheric resistances ($R_a$ and $R_b$). A major problem then arises in providing an appropriate formulation for $R_b$, the majority of which are based on wind tunnel studies for surfaces not necessarily representative for canopies of vegetation in the field (Brutsaert, 1982). Especially in very turbulent conditions, such as found above a forest, the rate of $HNO_3$ deposition is very sensitive to $R_b$ (Duyzer and Fowler, 1994). In complex terrain near forest edges where turbulence is even more increased, the resistance to transport to these edges will be very small, leading to very high deposition fluxes of $HNO_3$ (Draaijers *et al.*, 1994; Duyzer and Fowler, 1994).

There is almost no knowledge on deposition mechanisms and deposition velocities of $HNO_2$ (Lövblad and Erisman, 1992). The canopy resistance for various seasons under different conditions, estimated by Wesely (1989) from chemical and physical properties of the gas, was assumed to correspond to the canopy resistance for $SO_2$, i.e. mainly stomatal-controlled uptake under dry conditions and efficient uptake to wet surfaces. Wesely (1989) estimated the maximum deposition velocity to a decidious forest at 1 cm $s^{-1}$. The deposition to a canopy wetted by dew or rain was also found te be around this value. Upward fluxes might be

expected due to the formation of $HNO_2$ from $NO_2$ in the water layer on surfaces and the release of nitrous acid from the water phase (Northolt *et al.*, 1992).

### 4.1.4 PAN

Few data are available for PAN deposition. Hill (1971) reports a deposition velocity for PAN to alfalfa of 0.6 cm $s^{-1}$ from his measurements in a recirculating exposure chamber. In a wind tunnel study by Garland and Penkett (1976), values of $V_d$ = 0.21 to 0.3 cm $s^{-1}$ ($R_c$ = 290 - 340 s $m^{-1}$) were found for soil, and $V_d$ = 0.14 to 0.26 ($R_c$ = 380 - 700 s $m^{-1}$) for grass. Deposition to water was very slow ($V_d$ < 0.02 cm $s^{-1}$). Bos *et al.* (1978) reports values for the deposition velocity of PAN to sea water of 0.009 cm $s^{-1}$, to fresh water of 0.011 cm $s^{-1}$, to dune sand of 0.032 cm $s^{-1}$, to agricultural soil of 0.06 cm $s^{-1}$ and to grass of 0.13 cm $s^{-1}$.

### 4.1.5 $NH_3$

Exchange of atmospheric ammonia with various surfaces may be bi-directional, depending on surface type and environmental conditions. Grazed pastures and arable cropland show a net ammonia emission over yearly periods (e.g. Jarvis *et al.*, 1989; Sutton *et al.*, 1989), whereas semi-natural ecosystems show net ammonia deposition (e.g. Duyzer *et al.*, 1987; Schjörring and Byskov, 1991; Erisman, 1992). Ammonia can be taken up efficiently, translocated and metabolised by living plants (Porter *et al.*, 1972; Lockyer and Whitehead, 1986) and by soil (Malo and Purvis, 1964; Hanawalt, 1969; Horvath, 1982).

Deposition of $NH_3$ to semi-natural vegetated surfaces can take place either by stomatal uptake or on external plant parts (Van Hove, 1989). In general, the presence of water layers on vegetation decreases the canopy resistance considerably. However, Van Hove (1989) found large deposition velocities even under dry conditions. With no free water present on the leaf, he found the surface adsorption of $NH_3$ to increase with relative humidity, suggesting that microscale water (which mediates the deposition process) may be present on leaf surfaces, even when the leaves appear dry. Moreover, the presence of $SO_2$ may decrease the canopy resistance of $NH_3$, as its solubility in water is pH-dependent (Adema *et al.*, 1986, see section 4.1.1). Leaf surface interactions with other acid gases such as $HNO_3$ and HCl may also be important. However, because the ammonium salts with these gases ($NH_4NO_3$ and $NH_4Cl$) have significant vapour pressure (Seinfeld, 1986), they may possibly re-dissociate back to the precursor gases, limiting accumulation of salts on leaf surfaces. This is in contrast to ammonium sulphates, which have negligible vapour pressure and may therefore accumulate (Sutton *et al.*, 1993).

Measurements of $NH_3$ deposition to forests have been reported by Duyzer *et al.* (1987), Sutton *et al.* (1989), Slanina *et al.* (1990), Duyzer *et al.* (1992), Wyers *et al.* (1992) and Erisman *et al.* (1994) (see Chapter 7). The low surface resistances (near zero) and accordingly high deposition velocities (1.5-3.6 cm $s^{-1}$) found in these studies suggest that $NH_3$ deposition rates are controlled to a large extent by atmospheric transfer which, in turn, is determined by wind speed and aerodynamic roughness of the canopy. In areas with exceptionally large $NH_3$ air concentrations, the canopy resistance may be substantially enhanced due to saturation of the water layer with $NH_4^+$ (Duyzer and Diederen, 1989). If saturation occurs, net deposition becomes lower and even emission can take place at rising temperatures or decreasing ambient air concentrations (Erisman, 1992) This may be recognised as a compensation point.

Measurements of Langford and Fehsenfeld (1992) in a forest in Colorado show that the forest emits $NH_3$ at low ambient $NH_3$ concentrations, whereas net dry deposition occurs at high $NH_3$ concentrations. Sutton *et al.* (1992) also determined a compensation point using gradient measurements over different types of vegetation. On a daily scale, emission was favoured during warm dry conditions, whereas deposition generally occurred when the surface was wet or frozen. Erisman and Wyers (1993) measured upward fluxes of $NH_3$ during dry conditions in daytime and in conditions where water-layer films on leaves evaporated and the ambient $NH_3$ concentration became small. When interpretating these measurements, however, one has to bear in mind that $NH_3$ is in equilibrium with $HNO_3$ and $NH_4NO_3$ in the atmosphere. Where deposition of both gases occurs it is possible that dissociation of the aerosol can occur. By contrast, a large emission flux of $NH_3$ enhances the concentration product of $NH_3$ and $HNO_3$ and may cause aerosol formation. The major consequence of rapid chemical conversion affecting ammonia exchange is complicating the interpretation of micrometeorological field measurements. Taking such reactions into account represents a substantial increase in complexity of the analysis. While the sum of both phases may be treated as a conserved species, such conversion processes may substantially alter the magnitude of both the component fluxes and their total flux (Sutton *et al.*, 1993).

The compensation point for $NH_3$ is a function of the $NH_4^+$ concentration in the water film at the leaf surface and of the $NH_4^+$ concentration in the substomatal cativity. The processes controlling the concentration of $NH_4^+$ within the cells of growing plants is extremely complicated and the dependence of the compensation point on species and growing conditions is poorly understood. Typical values appear to be in the order of 0.7 $\mu g\ m^{-3}$ for trees (Langford and Fehsenfeld, 1992), 2 - 3.5 $\mu g\ m^{-3}$ for herbaceous crop plants (Dabney and Bouldin, 1990; Farquhar *et al.*, 1980; Lemon and Van Houtte, 1980) and > 7 $\mu g\ m^{-3}$ for wheat and perhaps other cereal-type grasses (Harper *et al.*, 1987; Lemon and Van Houtte, 1980; Morgan and Parton, 1989). The compensation point has an exponential temperature dependence consistent with the presence of a steady-state concentration of dissolved ammonia in the water film present on the mesophyllic surfaces of the substomatal cavities (Farquhar *et al.*, 1980). The compensation point is hypothesised to vary as a function of the balance between $NH_4^+$ releasing reactions (deamination, nitrate reduction and senescence-induced

proteolysis) and $NH_4^+$-consuming reactions (N transport, assimilation via glutamine synthetase). The balance will shift to the former with increasing plant maturity, leading to higher intracellular $NH_3$ concentrations (Morgan and Parton, 1989; Parton *et al.*, 1988). Especially during ripening and senescence of crops high compensation points were found, promoting ammonia emission.

Duyzer *et al.* (1994) show that deposition of ammonia to sea water is only limited by atmospheric transport. Uptake may become limited, however, if significant amounts of $NH_3$ are already present in the sea water. In some cases even emission of $NH_3$ from sea water was observed (Quinn *et al.*, 1987; Asman *et al.*, 1994). The magnitude as well as the direction of the flux may be explained very well with a simple Henry's law equilibrium. The deposition velocity over sea water was as high as 1 cm $s^{-1}$ when wind speed was high. Ammonia concentrations in the air were high and in the water low (Duyzer *et al.*, 1993).

### 4.1.6 HCl

Deposition rates of HCl onto vegetation were determined by Harrison *et al.* (1989). As for $HNO_3$, there was no evidence for surface resistance and the deposition mechanism of HCl is assumed to be identical to that of $HNO_3$.

### 4.1.7 PARTICLES

The dry deposition velocity of particles depends heavily on their diameter. Research on particle size distributions, along with chemical composition of particles, is therefore relevant to determining $V_d$. Milford and Davidson (1985) have summarised size distributions of 38 trace elements reported in the literature. From their review it becomes clear that elements with an MMD smaller than 2 μm (fine particles) generally have bimodal distributions. The dominant peak occurs in the range of 0.5-1 μm. Elements with larger MMDs (coarse particles) usually have a single peak. Most sulphate, nitrate and ammonium containing particles (e.g. $(NH_4)_2SO_4$, $NH_4NO_3$) are found to fall within the 0.1-1.0 μm size range. Coarse particles falling in the range 2-20 μm are mostly derived from alkaline soil dust (e.g. $CaCO_3$, $MgCO_3$) and sea-spray (e.g. NaCl, $MgCl_2$). Fine particles are, due to their low weight, more susceptible to long-range transport than coarse particles. Most soil-derived particles are likely to deposit near the area of origin (Milford and Davidson, 1985), although long-range transport of, for example, desert dust has also been reported (Ganor *et al.*, 1991; Swap *et al.*, 1992). Deposition will alter the mass distribution function of particles remaining airborne. The shift in the distribution is towards particles with small diameters (Ruijgrok and Davidson, 1992). The size distribution is also affected by hygroscopic growth of particles taking place at relative humidities above 80% (Fitzgerald, 1975).

Experiments under controlled conditions in wind tunnels and theoretical models suggest relatively small rates of particle deposition onto vegetation, deposition velocities ranging from 0.1-1 $mm.s^{-1}$ (Chamberlain, 1966; Sehmel, 1980; Nicholson, 1988; Ruijgrok *et al.*, 1992). However, recent field measurements on deposition velocities of particles indicate much higher deposition velocities, especially for forests (e.g. Hicks *et al.*, 1989; Waranghai and Gravenhorst, 1989; Fowler *et al.*, 1992; Sievering *et al.*, 1994; Erisman *et al.*, 1994; Wyers *et al.*, 1994; Duyzer *et al.*, 1994; see also section 7.3). Davidson and Wu (1990) have listed deposition velocities for particulate sulphate to low vegetation and forests derived from the following measurements: micrometeorological, surrogate surface exposure, foliar extraction and throughfall.

It appears that mean dry deposition velocity estimates depend to some extent on the methodology used to derive them. The mean deposition velocity obtained from throughfall measurements is larger than that obtained using other techniques. From the same literature review, Davidson and Wu (1990) conclude that deposition velocities for $NO_3^-$ particles are somewhat higher than corresponding values for $SO_4^{2-}$ particles, which should be attributed to a larger particle size usually associated with $NO_3^-$ particles that are, besides through the reaction of $HNO_3$ and $NH_3$, also formed by the reaction of $HNO_3$ with soil-derived or sea-salt particles). Deposition velocities for particulate $NH_4^+$ are found to be similar to those of particulate $SO_4^{2-}$. The deposition velocity of particulate $Cl^-$ is substantially higher (ranging from 1.0 to 5.1 $cm.s^{-1}$) than encountered for $SO_4^{2-}$ and $NO_3^-$particles, probably reflecting the larger particle size distribution of $Cl^-$. Deposition velocities of $Mg^{2+}$, $Ca^{2+}$ and $K^+$ particles are most likely to fall in the range of 1.0 to 3.0 cm $s^{-1}$ but reliable data on this subject are practically non-existent (Davidson and Wu, 1990).

### 4.1.8 METEORITES

There is not much information about the deposition of meteorites to the surface. It can be speculated that deposition velocities of meteorites are high, but it is questionable if the input of components as the result of meteorite deposition significantly contributes to the total input of these components. In this section meteorite deposition will be described.

Hughes (1992) predicted the actual flux of meteorites to the earth from the flux of meteorite parent bodies to the top of the atmosphere and by using information on atmospheric ablation and fragmentation processes (Table 4.1). Ablation and fragmentation were found to depend on the composition, mass, density, velocity and angle of entry of the incident body.

For incident objects that have an out-of-the atmosphere mass between $10^{-9}$ and $10^3$ g, Hughes (1992) assumes the ablation process to be complete and the incoming particles to be broken up into its constituent atoms and molecules. Moreover, incident objects larger than $10^9$ g are believed to hit the earth's surface with a nearly out-of-the atmosphere velocity and produce

between $10^3$ and $10^9$ g. The annual flux to the top of the atmosphere for incident bodies in this range is 12.4 million kg; this is made up of 871,000 individual bodies. In total 24,000-86,000 meteorites with masses larger than 1 kg are being retrieved by the earth's surface. Their total mass amounts 8-9.4 million kg, corresponding to 1.57-1.84 $10^{-4}$ kg $ha^{-1}$ $a^{-1}$.

**TABLE 4.1** The number of meteorites above a certain mass retrieved by the earth's surface[b] as predicted by Hughes (1992)

| Mass[a] | 5 cm surface layer loss | 10 cm surface layer loss |
|---|---|---|
| $10^{8.5}$ | 2 | 2 |
| $10^8$ | 8 | 7 |
| $10^{7.5}$ | 24 | 22 |
| $10^7$ | 74 | 64 |
| $10^{6.5}$ | 219 | 177 |
| $10^6$ | 626 | 465 |
| $10^{5.5}$ | 1716 | 1141 |
| $10^5$ | 4454 | 2576 |
| $10^{4.5}$ | 10767 | 5271 |
| $10^4$ | 23867 | 9690 |
| $10^{3.5}$ | 47864 | 15964 |
| $10^3$ | 86131 | 23695 |

[a]Only incident objects with masses between $10^3$ and $10^9$ g are considered. It is assumed that from these incident objects a surface layer of 5-10 cm is lost during passage through the atmosphere.

[b]The earth has a surface area of $5.11*10^8$ $km^2$.

The assumption of Hughes (1992) that the ablation of incoming objects with masses smaller than 1 kg (i.e. smaller than approximately 9 cm diameter) is complete, most probably does not hold true. Lindner and Welten (1994), for example, found that more than 90 % of the meteorites collected on Antartica have masses smaller than 100g. As a general rule, ReVelle (1979) mentions ten times as many fall meteorites with masses between $10^n$ and $10^{n+1}$ g as there are with masses between $10^{n+1}$ and $10^{n+2}$ g.

Whipple (1950, 1951) found especially for micrometeoroid particles with masses smaller than $10^{-9}$ g (i.e. smaller than approximately 0.001 cm diameter), the surface area to mass ratio such that the heat produced on entry (by friction with the atmosphere) is radiated away more efficiently than it is generated. In this way these particles are retarded and then floated to the earth's surface essentially unablated. An estimate of the total mass of such particles annually retrieved by the earth's surface was made from stratospheric measurements with cosmic dust collectors. Their total mass was estimated at 20 million kg, corresponding to 3.91 $10^{-4}$ kg $ha^{-1}$ $a^{-1}$ (Priem, personal communication). Micrometeoroid particles are also regularly observed in

collectors. Their total mass was estimated at 20 million kg, corresponding to 3.91 $10^{-4}$ kg $ha^{-1}$ $a^{-1}$ (Priem, personal communication). Micrometeoroid particles are also regularly observed in sediments in the central parts of the oceans (Pannekoek, 1976). The diameter of these particles is generally found to be smaller than 0.01 cm.

The chemical composition of meteorites depends on their origin. The vast majority of the meteorites that have been collected from the surface of the earth have asteroidal parents. Fewer than about 1% have been produced by cratering events on the surfaces of, for example, the moon or Mars. Usually three different kind of meteorites are distinguished on the basis of their iron content: *iron meteorites* with an iron content of more than 90%, *stone-iron meteorites* (approximately 50% iron) and *stone meteorites* with an iron content of less than 10%. The stone fraction of meteorites usually consists of iron and magnesium silicates. Stone meteorites may be seperated in *chondrites* which can be recognised by very small non-Earth like spherical shaped coagulations of silicates, and *achondrites* which do not contain such coagulations and hold only a very small portion of iron (Lindner and Welten, 1994).

Micrometeoroid particles found in sediments in the central parts of the ocean consist mainly of nickel-iron combinations with a crust of magnetite ($Fe_3O_4$), silicates like olivines ($(Mg,Fe)_2SiO_4$) and pyroxenes ($(Na,Ca,Fe,Mg,Al)_2(Si,Al)_2O6$) and micro-tectites (mainly consisting of $SiO_2$ and $Al_2O_3$) (Pannekoek, 1976). Tectites most probably represent molten parts from the moon's surface, which were thrown into space after the impact of large meteorites (Von Koenigswald, 1964).

Deposition of compounds due to meteorites may thus be significant for iron, nickel, silicium and aluminium. Deposition of micrometeoroid particles will thereby be of importance for the whole earth, while large meteorites will have a relatively large impact on only a few 'hot spots'. If we assume a mean iron content of 50%, the deposition of iron through micrometeoroid particles can be calculated to amount to 2 x $10^{-4}$ kg $ha^{-1}$ $a^{-1}$. Van Breemen *et al.* (1988) measured 0.78-1.29 kg $ha^{-1}$ $a^{-1}$ of iron in throughfall in an oak-birch forest stand in the central part of the Netherlands, indicating the contribution of micrometeoroid particles (2 x $10^{-4}$) to the total iron flux to the forest floor to be insignificant. Main sources of iron in throughfall include soil particles and aerosols emitted from the metallurgical industry. Probably the very black coarse particles sometimes seen in precipitation and throughfall samples/filters can be regarded as representing micrometeoroid particles.

Assuming a mean nickel content of 25%, the deposition of nickel through micrometeoroid particles can be calculated to amount to $10^{-4}$ kg $ha^{-1}$ $a^{-1}$. The mean nickel deposition in the Netherlands was estimated 0.3-1.4 $10^{-2}$ kg $ha^{-1}$ $yr^{-1}$ (Van Jaarsveld and Onderdelinden, 1986), suggesting a few per cent contribution of micrometeoroid particles to the total nickel deposition. The main sources of nickel in the Dutch atmosphere will be the combustion of fossil fuel and nickel-containing aerosols emitted from the metallurgical industry (Van

Jaarsveld, personal communication). The contribution of micrometeoroid particles to the total nickel deposition will be considerably larger in non-polluted areas.

No deposition estimates are available for silicium and aluminium but it may be expected that the contribution of micrometeoroid particles to the total deposition of silicium and aluminium is insignificant. The main sources of these components in the atmosphere will be blown-up soil dust and, for aluminium, also aerosol emissions from the metallurgical industry. Moreover, their respective levels in micrometeoroid particles is relatively low.

Despite the large meteorite deposition velocities, it can be concluded that meteorite input to the surface is insignificant for pollutants related to acidification. Although the input of metals can be significant, meteorite deposition is still much lower compared to other inputs.

## 4.2 SURFACE RESISTANCE PARAMETRISATIONS

*Introduction*
The surface exchange parametrisation of acidifying pollutants is based on the resistance analogy outlining the aerodynamic resistance $R_a$, the quasi-laminar layer resistance $R_b$ and the surface resistance $R_c$ (Chapter 3) These parameterisations are derived for use in regional- and local-scale deposition models (Chapter 5). The $R_c$ parameterisation for different gases presented here are based on existing literature (see e.g. previous sections), conclusions from a Workshop on deposition held in Göteborg in November 1992 and a Workshop held in Aveiro in May 1993, and some results of recent dry deposition measurements (e.g. section 7.3).

### 4.2.1 SURFACE RESISTANCE PARAMETERISATION FOR GASES

Values for $R_c$ can be obtained from theoretical considerations based on, for example, solubility and equilibrium calculations in combination with simulations of vegetation specific processes, such as accumulation; transfer processes through stomata, mesophyll and cuticles; absorption, etc. (Baldocchi *et al.*, 1987; Wesely, 1989). Many theoretical approaches are, however, hard to validate using measurements because of the complexity of the processes involved. $R_c$ values presented in the literature are primarily based on measurements of $V_d$ and on chamber studies. By determining $R_a$ and $R_b$ from the meteorological measurements, $R_c$ can be calculated as the residual resistance using Eqn. 3.3. Values for $R_c$ can then be related to surface conditions, time of day, etc., yielding parameterisations. Unfortunately, measurements using existing techniques are still neither accurate nor complete enough to obtain $R_c$ values under most conditions. Furthermore, $R_c$ is specific for a given combination of pollutant, type of vegetation and surface conditions; also, measurements are available for only a limited number of combinations. The $R_c$ parameterisations must be based on routinely available data i.e., ambient temperature, relative humidity, global radiation, wind speed, land-use class, type of soil and vegetation (Van Pul *et al.*, 1992; Erisman *et al.*, 1994).

Equation (4.3) shows a resistance diagram for the transport of gases to various types of surfaces. $R_c$ is a function of the canopy stomatal resistance, $R_{stom}$, and mesophyll resistance $R_m$; the canopy cuticle or external leaf resistance, $R_{ext}$; the soil resistance, $R_{soil}$ and the in-canopy resistance, $R_{inc}$, as well as the resistance to surface waters or moorland pools, $R_{wat}$. In turn, these resistances are affected by leaf area, stomatal physiology, soil pH, and presence and chemistry of liquid drops and films. The stomatal resistance, leaf surface resistance and soil resistance act in parallel:

$$\text{vegetative surface: } R_c = [\frac{1}{R_{stom} + R_m} + \frac{1}{R_{inc} + R_{soil}} + \frac{1}{R_{ext}}]^{-1}$$

$$\text{water surfaces: } R_c = R_{wat} \qquad [4.3]$$

$$\text{bare soil: } R_c = R_{soil}$$

*Stomatal and mesophyll resistance*

Most gases enter plants through the stomata. As gas molecules enter the leaf, deposition occurs as molecules react with the moist cells in the substomatal cavity and the mesophyll. Several conclusions can be drawn on environmental effects and inter-specific differences in pollutant deposition based on known stomatal physiology. Stomatal resistance decreases hyperbolically with increasing light and increases linearly with increasing vapour pressure deficits (Jarvis, 1976). Soil water deficits cause stomata to close after some threshold deficit level is exceeded. Low and high temperatures cause stomatal closure; stomatal opening is optimal at a vegetation-specific temperature. Leaf age, nutrition and adaptation are other factors affecting stomatal resistance (Jarvis, 1976). Elevated exposure to $SO_2$ causes stomata to close, whereas exposure to both $O_3$ and $NH_3$ may increase stomatal opening (Dueck, CABO, the Netherlands, personal communication). Stomatal resistance is different for different types of vegetation. Values of $R_{stom}$ under ideal conditions during daytime are between 30 and 300 s $m^{-1}$ for a range of herbaceous annuals and woody perennials (Fowler, 1985; Baldocchi *et al.*, 1987).

The stomatal resistance can be calculated using a scheme described by Baldocchi *et al.* (1987). This scheme is outlined in Erisman *et al.* (1994). Modelling the stomatal resistance in this manner is only possible if enough information is available. This might be a problem for the water potential and for the leaf area index (*LAI*). For the regions where such data are not available, the parameterisation for the stomatal resistance given by Wesely (1989) may be used. This parameterisation is derived from the method used by Baldocchi *et al.* (1987) and only needs data for global radiation $Q$ and surface temperature $T$:

$$R_{stom} = R_i \{1 + [\frac{200}{Q + 0.1}]^2\} \{\frac{400}{T_s(40 - T_s)}\} \qquad [4.4]$$

Values for $R_i$ can be obtained from a look-up table for different land-use categories and seasons as listed in Table 4.2 (adopted from Wesely, 1989). This general framework for the bulk stomatal resistance can be used to describe stomatal uptake for each gas by correcting the $R_{stom}$ using the ratio of the diffusion coefficient of the gas involved $D_x$ to that of water $D_{H2O}$ and adding the mesophyll resistance:

$$R_{stom,x} = R_{stom} \frac{D_{H_2O}}{D_x} + R_m \qquad [4.5]$$

The mesophyll resistances for different gases are in accordance with the literature (Voldner *et al.*, 1986 and Wesely, 1989) assumed to be zero.

**TABLE 4.2** Internal resistance, $R_i$, to be used for estimating the stomatal resistance for different seasons and land-use types using Eqn. (4.4), with entities of 9999 indicating no air—surface exchange via that resistance pathway (Adopted from Wesely, 1989)

| Land-use type: | 1 | 2 | 3 | 4 | 5 | 6 | 7 | 8 | 9 | 10 | 11 |
|---|---|---|---|---|---|---|---|---|---|---|---|
| Seasonal category: | | | | | | | | | | | |
| Mid-summer with lush vegetation | 9999 | 60 | 120 | 70 | 130 | 100 | 9999 | 9999 | 80 | 100 | 150 |
| Autumn with unharvested cropland | 9999 | 9999 | 9999 | 9999 | 250 | 500 | 9999 | 9999 | 9999 | 9999 | 9999 |
| Late autumn after frost, no snow | 9999 | 9999 | 9999 | 9999 | 250 | 500 | 9999 | 9999 | 9999 | 9999 | 9999 |
| Winter, snow on ground and subfreezing | 9999 | 9999 | 9999 | 9999 | 400 | 800 | 9999 | 9999 | 9999 | 9999 | 9999 |
| Transitional spring with partially green short annuals | 9999 | 120 | 240 | 140 | 250 | 190 | 9999 | 9999 | 160 | 200 | 300 |

(1) Urban land, (2) Agricultural land, (3) Range land, (4) Deciduous forest, (5) Coniferous forest, (6) Mixed forest including wetland, (7) Water, both salt and fresh, (8) Barren land, mostly desert, (9) Non-forested wetland, (10) Mixed agricultural and range land, and (11) Rocky open areas with low-growing shrubs.

*External leaf uptake*

Many studies have shown that the external leaf surface can act as an effective sink, especially for soluble gases at wet surfaces (Hicks *et al.*, 1989; Fowler *et al.*, 1991; Erisman *et al.*, 1993a; b). Under some conditions the external leaf sink can be much larger than the stomatal uptake. When $R_{ext}$ is negligible, $R_c$ in Eqn.4.3 automatically becomes negligible, diminishing the effect of the other resistances in this equation. The external leaf resistance for individual gases will be discussed in the following sections.

$SO_2$

Deposition velocities measured using the enclosure technique in a pine stand in central Sweden showed that during dry conditions the external deposition of $SO_2$ could be as large as stomatal uptake (Richter and Granat, 1993). The canopy cuticle resistance is much larger than the canopy stomatal resistance; $R_{cuticle}$ ranges from 3000 to 40,000 s $m^{-1}$ (Van Hove, 1989). However, the surface resistance is observed to decrease as relative humidity increases (Van Hove, 1989; Garsed, 1985; Erisman *et al.*, 1993a; Erisman and Wyers, 1993; Draaijers and Erisman, 1993). This might indicate that the cuticle resistance is lowered with increasing humidity (Van Hove, 1989) or that the surface becomes moist with increasing humidity, e.g. through deliquescence of salts at the external leaf surface. When the cuticle is wetted, or affected by pre-deposited particles or gases, $SO_2$ deposition to the surface also occurs via absorption and chemical oxidation reactions with the surface.

$SO_2$ dry deposition is enhanced over wet surfaces (Garland and Branson, 1977; Fowler and Unsworth, 1979; Fowler, 1985; Vermetten *et al.*, 1992; Erisman *et al.*, 1993a, 1993c; Erisman and Wyers, 1993). The involved reactions and the possibility of co-deposition with $NH_3$ are described in section 4.1.1. Erisman *et al* (1993b) derived a $R_{ext}$ parameterisation for wet surfaces (due to precipitation and an increase in relative humidity) of heather plants (see section 7.1):

during or just after precipitation: $R_{ext} = 0\ s\ m^{-1}$

in all other cases:

$$R_{ext} = 25000\ EXP[-0.0693\ rh]\ s\ m^{-1} \quad \text{at } rh < 81.3\% \qquad [4.6]$$

$$R_{ext} = 0.58\ 10^{12}\ EXP[-0.278\ rh]\ s\ m^{-1} \text{ at } rh > 81.3\%$$

where $rh$ is the relative humidity. Equation (4.6) is applied to air temperatures above -1 °C. Below this temperature it is assumed that surface uptake decreases and $R_{ext}$ is set at 200 (-1 < $T$ < -5 °C) or 500 ($T$ < -5 °C) s $m^{-1}$. $R_{ext}$ will be zero for some hours after precipitation has stopped. The number of hours will vary with the season and depend on environmental conditions. Drying of vegetation is approximated to take two hours during daytime in summer and four hours in winter. During night-time vegetation is expected to be dry after four hours in summer and after eight hours in winter (Erisman *et al.*, 1993a).

Where rain chemistry will not allow for $SO_2$ uptake, $R_{ext}$ will be significantly different from zero, depending on the extent that rain is saturated with S(IV), on the pH of rain water and on the plant neutralisation capacity. This parameterisation is derived and tested for Dutch environmental conditions in areas with an annual average $NH_3$ concentration approximately equal to that of $SO_2$. For conditions where the neutralisation ability of plants or of $NH_3$ is not sufficient, this parameterisation will probably yield underestimates of $R_c$. Erisman and Wyers (1993) have presented a table with average $R_c$ values observed under different conditions (Table 4.3). Values were obtained for heathland, but are expected to be representative for

other extensively managed low vegetation. This table also shows the influence of $R_c$ under conditions where one gas was in excess of the other in the atmosphere.

**TABLE 4.3** Average $R_c$ values for $SO_2$ and $NH_3$ observed under different conditions; negative values denote emissions (Erisman and Wyers, 1993)

| Condition | $R_c$ $SO_2$ (s $m^{-1}$) | Remark | $R_c$ $NH_3$ (s $m^{-1}$) | Remark |
|---|---|---|---|---|
| *Dry (rh<60)* | | | | |
| Low[a] $NH_3/SO_2$ | 500 (day) 1000 (night) | function of stomatal behaviour | -500 (day) 1000 (night) | emission/ deposition |
| High[a] $NH_3/SO_2$ | 500 (day) 1000 (night) | function of stomatal behaviour | 1000(day) 1000 (night) | |
| *Humid, no rain or fog* | | | | |
| Low[a] $NH_3/SO_2$ | 50 | function of rh and T | 0 | |
| High[a] $NH_3/SO_2$ | 0 | *rh* > 80% | < 100 | increasing to 200 with large excess |
| *Wet, rain* | | | | |
| Low[a] $NH_3/SO_2$ | 5 0 | function of water layer pH, with much rain: 0 | 0 | |
| High[a] $NH_3/SO_2$ | 0 | | < 100 | function of water layer pH, with much rain: 0 |
| *Wet, fog* | | | | |
| Low[a] $NH_3/SO_2$ | 100 - 500 | low pH | 0 | |
| High[a] $NH_3/SO_2$ | 0 | | 200 - 800 | high pH |
| *T* < 0 C | 200 | | 200 | |

[a] Low $NH_3/SO_2$ molar ratio means below 1, high ratio means above 3.

$NH_3$

While most other pollutant gases are consistently deposited, $NH_3$ is both emitted from and deposited to land and water surfaces. For semi-natural vegetation, fluxes are usually directed to the surface, whereas fluxes are directed away from the surface above agricultural grassland treated with manure. For arable cropland, fluxes may be bi-directional, depending on atmospheric conditions and the stage in the cropping cycle (Sutton, 1990). Nitrogen metabolism has been shown to produce $NH_3$ and as a result there is a compensation point (Farquhar *et al.*, 1980) at which deposition might change into emission when ambient concentrations fall below the compensation concentration and vice versa. In this case $c(z_2)$ in Eqn. 3.1 is different from zero.

To describe $NH_3$ exchange it is necessary to consider natural and managed vegetation separately. For managed vegetation the compensation point approach seems to be the most promising for use in models. However, the current state of knowledge is insufficient to define

canopy resistance terms or compensation points reliable over different surface types and under different environmental conditions relevant to model parameterisation (Lövblad *et al.*, 1993). Furthermore, the compensation point is expected to be a function of many (undefined) factors and not a constant value. There are also some difficulties in using the compensation point approach, since it defines emission independent of gridded emission inventories. It was therefore recommended to base the deposition of $NH_3$ on resistance formulation to reflect the systematic variations with meteorological conditions and vegetation or receptor characteristics (Lövblad *et al.*, 1993). There are only a few measurements available on surface exchange of $NH_3$ above different types of vegetation. On the basis of the limited number of data it is not possible to separate the surface resistance into several subresistances. The external leaf resistance is therefore described as matching observed $R_c$ values, taking into account stomatal uptake or emission (see 'External leaf uptake') and in-canopy transport (see 'In-canopy transport').

Ammonia generally deposits rapidly to semi-natural (unfertilised) ecosystems and forests. Results show $R_c$ values mostly in the range of 0-50 s $m^{-1}$ (Duyzer *et al.*, 1987; 1992; Sutton *et al.*, 1992; Erisman *et al.*, 1993b). There is a clear effect of canopy wetness and relative humidity on $R_c$ values (Erisman and Wyers, 1993). Under very dry, warm conditions ($rh$ < 60%, T > 15 °C) deposition to the leaf surface may saturate, so that exchange is limited to uptake through stomata, even allowing for the possibility of emission at low ambient concentrations. In this context, a larger $R_c$ may be appropriate (~ 50 s $m^{-1}$). The influence of co-deposition with acidic species is addressed in the section on $SO_2$ (Table 4.3). $R_c$ values for managed vegetation are given in Table 4.4.

**TABLE 4.4** $R_{ext}$ for $NH_3$ (s $m^{-1}$) over different vegetation categories in Europe, negative values for $R_{ext}$ denote emission for estimating a net upward flux

| Land-use category | Day | | Night | |
|---|---|---|---|---|
| | Dry | Wet | Dry | Wet |
| Pasture during grazing: summer: | -1000 | -1000 | 1000 | 1000 |
| winter: | 50 | 20 | 100 | 20 |
| Crops and ungrazed pasture: summer: | $-R_{stom}$ | 50 | 200 | 50 |
| winter: | $-R_{stom}$ | 100 | 300 | 100 |
| Semi-natural ecosystems and forests (see also Table 4.3 for excess $NH_3$ over $SO_2$) | -500 | 0 | 1000 | 0 |

Winter conditions: T> -1 °C, otherwise $R_{ext}$ =200 s $m^{-1}$ (-1 < T < -5 °C) or $R_{ext}$ =500 s $m^{-1}$ (T < -5 °C)

NOx

A very small stomatal uptake might be observed for NO at ambient concentrations. Fluxes are, however, very low and uptake is therefore neglected (Wesely *et al.*, 1989; Lövblad and Erisman, 1992). $R_{ext}$ is set at 9999 s $m^{-1}$.

Uptake of $NO_2$ seems to be under stomatal control with no internal resistance. At a few sites, a mesophyllic resistance has been observed at concentrations of about 1 ppbv. It is uncertain whether this effect is relevant to other sites (receptors). External uptake of $NO_2$ is negligible (e.g. Fowler *et al.*, 1991). $R_{ext}$ is set at 9999 s $m^{-1}$.

HNOx, HCl, PAN

Data on $HNO_2$ deposition are lacking. On the basis of chemical properties one would expect the same behaviour as for $SO_2$, i.e. mainly stomatal-controlled uptake under dry conditions and efficient uptake to wet surfaces. $R_{ext}$ is assumed to equal that of $SO_2$.

The difficulty of measuring nitric acid and hydrochloric acid concentrations at ambient levels has limited the number of flux measurements for these gases. Recent investigations, however, consistently show that for vegetative surfaces these gases deposit rapidly, with negligible surface resistances (Huebert and Robert, 1985; Erisman *et al.*, 1988; Meixner *et al.*, 1988; 1990; Meyers *et al.*, 1991; Harrison *et al.*, 1989; Dollard *et al.*, 1986, 1990). Deposition of $HNO_3$ and HCl seems to be limited by the aerodynamic resistance only. For these gases the surface resistance is found to be negligible. $R_{ext}$ is set at 0 s $m^{-1}$.

Very little is known about the dry deposition of peroxyacetylnitrate, PAN. The limited number of PAN deposition measurements above various low vegetation types indicate a low uptake rate, with surface resistances in the order of 500-1000 s $m^{-1}$ (Dollard *et al.*, 1990). The deposition velocity showed dependence on the pH of the surface, with lower pH values leading to lower deposition velocities than for surfaces with higher pH values. $R_{ext}$ is set at 9999 s $m^{-1}$.

$O_3$

Ozone is a very strong oxidiser and as such it is destroyed rapidly at various surfaces. The uptake of ozone by vegetation is mainly via the stomata (Rich *et al.*, 1970; Turner *et al.*, 1974). So the uptake can be modelled by parameterising the transpiration of the vegetation. The resistance of the remaining plant parts (the cuticle) to ozone is found in experiments to be larger than 1000 s $m^{-1}$ (Baldocchi *et al.*, 1987; Meyers and Baldocchi, 1988). Ozone is destroyed slowly at a wetted surface due to low water solubility. $R_{ext}$ is set at 1000 s $m^{-1}$.

*In-canopy transport*

Deposition to canopies involves deposition to both vegetation and soil. Early studies assumed that deposition to soils under vegetation was relatively small (5 - 10% of the total flux; Fowler, 1978). Recent work shows that a substantial amount of material can be deposited to

the soil below vegetation. For maize crops about 20-50% of the total $O_3$ flux was found to be deposited to the soil below the canopy (Leuning *et al.*, 1979; Wesely, 1978). Meyers and Baldocchi (1992) report that 20 to 30% of $SO_2$ depositing on a deciduous forest in wintertime is received at the forest floor. This substantial transfer occurs because large-scale intermittent eddies are able to penetrate through the vegetation and transport material to the soil. Differentiation of deposition to the canopy and to the soil is difficult to measure. Furthermore, it may be variable both in time and for different canopies. The in-canopy aerodynamic resistance $R_{inc}$ is modelled tentatively according to data from Van Pul and Jacobs (1993):

$$R_{inc} = \frac{b\,LAI\,h}{u_*} \qquad [4.7]$$

where *LAI* is the one-sided leaf area index, $h$ the vegetation height and $b$ an empirical constant taken as 14 $m^{-1}$. In winter, when deciduous trees are leafless, *LAI* is set at one. In this way the exchange caused by penetration of gusts is accounted for in a very straightforward way. The results obtained with Eqn. (4.7) are in reasonable agreement with those estimated by Wesely (1989). The resistance to uptake at the soil under the canopy $R_{soil}$ is modelled similarly to the soil resistance to bare soils (section 4.2.1). This will probably underestimate uptake to surfaces under forests (partly) covered with vegetation.

*Deposition to soil and water surfaces*

$SO_2$

Deposition of $SO_2$ to soil decreases at a soil pH below 4 and increases with relative humidity (Garland, 1977; Payrissat and Beilke, 1975). When surface temperatures fall below zero or the surface is covered with snow, $R_c$ values increase up to 200-500 s $m^{-1}$ (Voldner *et al.*, 1986; Erisman and Wyers, 1993). The deposition of $SO_2$ to snow-covered surfaces depends on pH, snow temperature and probably the amount of $SO_2$ already scavenged by the snow pack (Caddle *et al.*, 1985; Valdez *et al.*, 1987; Hicks *et al.*, 1989). Onderdelinden *et al.* (1984) and Erisman *et al.* (1993b) found the following relationships for snow-covered surfaces:

$$\begin{aligned} R_{snow} &= 500\ s\,m^{-1} \text{ at } T < -1\ ^oC \\ R_{snow} &= 70\ (2 - T)\ s\,m^{-1} \text{ at } 1 < T \leq -1\ ^oC \end{aligned} \qquad [4.8]$$

$NO_x$

For NO at ambient concentrations, emission from soils is observed more frequently than deposition. This emission, the result of microbial activity in the soil, is dependent on soil temperature, water content and ambient concentrations of NO (Hicks *et al.*, 1989). This has been observed from grassland, agricultural land and forest soils. Wesely *et al.* (1989) concluded that at their measuring site (moist, unsaturated soil overgrown with grass at soil

temperatures of 15 $^{o}$C), emission fluxes are probably most important during daytime. Similar conclusions were obtained from the Halvergate experiment by Fowler *et al.* (1991) and Duyzer *et al.* (1990). Emissions are to be expected at locations with low ambient NO and $NO_2$ concentrations (< 5 ppb). Average $NO_2$ concentrations are higher in most of Europe. The surface resistance for $NO_2$ to soil surfaces was found to be about 1000-2000 s $m^{-1}$. If the soil is covered by snow, the resistance will be even higher (Table 4.5). Resistances of $NO_2$ to water surfaces are also expected to be high due to the low solubility of this gas.

$NH_3$

Deposition of $NH_3$ to soil, snow and water surfaces is similar to that of $SO_2$; only the pH dependence is different (Table 4.5). Resistance's to unfertilised moist soils will be very small provided that the soil pH is below 7. Fertilised soils, or soils with a high ammonium content will show emission fluxes, depending on the ambient concentration of $NH_3$. Resistances to water surfaces will be negligible if the water pH is below 7. Resistances to snow will be similar to that of $SO_2$ at pH<7. Resistance's will increase rapidly above a pH of 7.

HNOx, HCl, PAN

No measurements exist for PAN and $HNO_2$. Resistances for PAN are expected to be high (see section 4.2.1.2), whereas resistance's for $HNO_2$ are assumed to follow those of $SO_2$. Resistances to water surfaces (pH>2) and soils for $HNO_3$ and HCl are assumed to be negligible. A surface resistance for $HNO_3$ and HCl to snow surfaces at temperatures below -5 $^{o}$C is expected (Johansson and Granat, 1986).

$O_3$

Ozone is destroyed slowly at a wetted surface or free water due to its low water solubility. The surface resistance to ozone deduced from measurements above water and snow is about 1000-2000 s $m^{-1}$ (Galbally and Roy, 1980; Wesely *et al.*, 1981). The soil resistance to ozone is largely dependent on the type of soil and the soil water content. This water content dependency is due to the low water solubility of ozone and the reduced effective surface at which ozone can be destructed due to the presence of water films around the soil particles. The soil resistance is typically 100 s $m^{-1}$ under dry soil conditions (Turner *et al.*, 1973; Galbally and Roy, 1980). This value increases typically up to 500 s $m^{-1}$ at a waterlogged stage of the soil (20-30% water content) (Turner *et al.*, 1973; Galbally and Roy, 1980; Van Pul, 1992).

$R_{snow}$ and $R_{wat}$ values for different gases are summarised in Table 4.5.

**TABLE 4.5** $R_c$ values for soil surfaces, snow-covered surfaces and water surfaces (negative values denote emission)

| Gas | Soil surfaces | | Water surfaces | pH | Snow-covered surfaces | Temperature ($^oC$) |
|---|---|---|---|---|---|---|
| | Wet | Dry | | | | |
| $SO_2/HNO_2$ | 0 | 1000 | 0 | >4 | 70(2-$T$) | 1<$T$<-1 |
| | 500 | $R_{ext}$ (Eq. 9) | 500 | <4 | 500 | $T$<-1 |
| $NH_3$ | 250 | -500 | 500 | >8 | 70(2-$T$) | 1<$T$<-1 |
| | 0 | 50 | 0 | <8 | 500 | $T$<-1 |
| NO | -1000 | -1000 | 2000 | - | 2000 | - |
| $NO_2$/PAN | 2000 | 1000 | 2000 | - | 2000 | - |
| $HNO_3$/HCl | 0 | 0 | 0 | >2 | 0 | $T$>-5 |
| | | | | | 100 | $T$<-5 |
| $O_3$ | 500 | 100 | 2000 | - | 2000 | - |

## 4.2.2 PARTICLES

The resistance analogy is not used for particles. Most knowledge on deposition processes and deposition rates of particles has been obtained from studies in wind tunnels (Chamberlain, 1966; Sehmel, 1980). The deposition velocity depends strongly on the particle diameter and surface characteristics (Davidson and Wu, 1989; Ruigrok and Davidson, 1993).

For submicron particles, the transport through the boundary layer is more or less the same as for gases. However, transport of particles through the quasi-laminar layer can differ. For particles with a diameter < 0.1 μm, deposition is controlled by diffusion, whereas deposition of particles with a diameter > 10 μm is more controlled by sedimentation. Deposition of particles with a diameter between 0.1 and 1 μm is determined by the rates of impaction and interception and depends heavily on the turbulence intensity. Deposition velocity for particles with a diameter in this range can be obtained from parameterisations on $u*$, for low vegetation according to Wesely *et al.* (1985):

$$V_d = \frac{u_*}{500} \qquad L > 0$$

$$V_d = \frac{u_*}{500}\left[1 + \left(\frac{300}{-L}\right)^{\frac{2}{3}}\right] \qquad L < 0 \qquad [4.9]$$

Slinn (1982) proposes using a simplification of his model for forests by splitting $V_d$ in a turbulent contribution and a surface deposition velocity, the latter being dependent on the collection efficiency of the surface and thus surface properties:

$$V_d = [V_{dt}^{-1} + V_{ds}^{-1}]^{-1}, \qquad [4.10]$$

where the surface deposition velocity is given as $V_{ds} = E\, u_*^2/u_h$, with $u_h$ the wind speed at canopy height; $E$ is the collection efficiency and $V_{dt}$ is the turbulent contribution, represented by the inverse of the aerodynamic resistance: $R_a(z=50)^{-1}$. The collection efficiency, $E$, is different for different size classes as different processes become important. $E$ is determined by parametrisation of modelled E values for Speulder forest based on data such as $u_*$, $z_0$, $d$, $u_{50}$, $rh$, surface wetness, etc. (Ruigrok *et al.*, 1994). A description of the experiments and model results are extensively described in section 7.3. The following relationships were found.

The general form for $V_d$ at 50 m high is:

$$V_d = \frac{1}{\frac{1}{V_{ds}} + Ra(50)} + V_s \qquad [4.11]$$

where $V_s$ is the deposition velocity due to sedimentation, *Vds* can be estimated from:

$$V_{ds} = \frac{u_*^{\,2}}{u_h} E \qquad [4.12]$$

where $u_h$ is the wind speed at canopy height. Relations for $E$ voor different components and conditions are given in Table 4.6. These were derived from model calculations and multiple regression analysis.

**TABLE 4.6** Parametrisations of $E$ values for different components and conditions

| | Wet surface | | Dry surface | |
|---|---|---|---|---|
| Compound | $rh \le 80\%$ | $rh > 80\%$ | $rh \le 80\%$ | $rh > 80\%$ |
| $NH_4^+$ | $0.066u_*^{0.41}$ | $0.066u_*^{0.41}[1+0.37EXP\left(\frac{rh-80}{20}\right)]$ | $0.05u_*^{0.23}$ | $0.05u_*^{0.23}[1+0.18EXP\left(\frac{rh-80}{20}\right)]$ |
| $SO_4^{2-}$ | $0.08u_*^{0.45}$ | $0.08u_*^{0.45}[1+0.37EXP\left(\frac{rh-80}{20}\right)]$ | $0.05u_*^{0.28}$ | $0.05u_*^{0.28}[1+0.18EXP\left(\frac{rh-80}{20}\right)]$ |
| $NO_3^-$ | $0.10u_*^{0.43}$ | $0.10u_*^{0.43}[1+0.37EXP\left(\frac{rh-80}{20}\right)]$ | $0.063u_*^{0.25}$ | $0.063u_*^{0.25}[1+0.18EXP\left(\frac{rh-80}{20}\right)]$ |
| $Na^+$, $Ca^{2+}$, $Mg^{2+}$ | $0.679u_*^{0.56}$ | $0.679u_*^{0.56}[1+0.37EXP\left(\frac{rh-80}{20}\right)]$ | $0.14u_*^{0.12}$ | $0.14u_*^{0.12}[1-0.09EXP\left(\frac{rh-80}{20}\right)]$ |

For the large particles, represented by Na in Table 4.5 and for low vegetation in Eqn. 4.9, the sedimentation velocity has to be added:

$$V_s = 0.0067\ ms^{-1} \qquad \text{rh} \leq 80\%$$
$$V_s = 0.0067 EXP\left(\frac{0.0066rh}{1.058 - rh}\right) \text{ m s}^{-1} \quad \text{rh} > 80\% \qquad [4.13]$$

The data for $Na^+$ in Table 4.6 are those also representative for $K^+$ if the outcome is halved, because of the smaller MMD.

### 4.2.3 SYNTHESIS

This section gives a short overview of the most important resistances for each component. In Table 4.7, at the end, examples of surface resistances obtained with the parameterisations presented here will be given for three different pollution climates. A short discussion on uncertainties will end this section.

*$SO_2$*
The deposition of $SO_2$ on vegetation has been shown to be regulated mainly by stomatal resistance and the presence of surface water on the foliage. The stomatal uptake can be modelled satisfactory. However, an understanding of the variations of surface resistance with surface wetness chemistry is limited. It is assumed that when the surface is wet, deposition of $SO_2$ is regulated by external leaf uptake. At low $SO_2$ concentrations, the buffering capacities of vegetation leaves are probably sufficient to maintain low $R_c$ values. At high $SO_2$ concentrations other neutralising components, such as $NH_3$, might become important. The surface wetness may be provided by increased relative humidity, dew, guttation, rain or fog, and cloud deposition.

Deposition of $SO_2$ to soil decreases at a soil pH below 4, and increases with relative humidity. When surface temperatures fall below zero or the surface is covered with snow, $R_c$ values increase up to values of 200 - 500 s $m^{-1}$.

*$NO_x$*
NO is not taken into account here as a depositing pollutant. Deposition of $NO_2$ is mainly regulated by stomata. The deposition to external leaf surfaces, water surfaces and soils is one order of magnitude smaller.

*$NH_3$*
$NH_3$ is emitted from fertilised soils and from pasture during grazing. In addition, emission takes place from crops, ungrazed pasture and semi-natural vegetation under dry, warm

conditions during daytime at low ambient concentrations. In other cases $NH_3$ is mainly deposited. Deposition in these cases is regulated by stomatal uptake and by deposition to external leaf surfaces. $R_c$ values for semi-natural vegetation and forests are low (in the range of 0-50 s $m^{-1}$) and dependent on surface wetness.

*HNOx, HCl, PAN*

PAN deposition is slow with an overall surface resistance of 500-1000 s $m^{-1}$. $HNO_2$ is treated like $SO_2$ until more information becomes available. Thus, uptake of $HNO_2$ is regulated by stomata and external leaf surfaces when the surface becomes moist. $HNO_3$ and HCl deposit efficiently to all surfaces with negligible $R_c$ values. Only at low temperatures with a surface covered with snow does $R_c$ increase up to 50-100 s $m^{-1}$.

*$O_3$*

The uptake of ozone by vegetation is mainly via the stomata. The resistance of the remaining plant parts (the cuticle) to ozone is found to be larger than 1000 s $m^{-1}$. Ozone is destroyed slowly at a wetted surface or free water due to its low water solubility. The surface resistance to ozone deduced from measurements above water and snow are about 1000-2000 s $m^{-1}$. The soil resistance to ozone is largely dependent on the type of soil and the soil water content. The soil resistance is typically 100 s $m^{-1}$ under dry soil conditions. This value increases typically up to 500 s $m^{-1}$ at a waterlogged stage of the soil (20-30% water content).

**TABLE 4.7** Surface resistances for different gases during daytime under different pollution climates.

| | Moist (rain or *rh*>90%), moderate temperature | | Winter, snow covered surface | | Dry, warm summer (*rh*<60%), well watered soil | |
|---|---|---|---|---|---|---|
| | Coniferous forest | Grassland | Coniferous forest | Grassland | Coniferous forest | Grassland |
| $R_{stom}$ | 200 | 60 | 400 | - | 150 | 50 |
| $SO_2$ | 0# | 0 | 500 | 500 | 300 | 100 |
| $NH_3$ | 0# | 0 | 500 | 500 | -500* | -500 |
| $NO_2$ | 320 | 100 | 640 | 1000 | 240 | 80 |
| $HNO_2$ | 0# (?) | 0 (?) | 500 | 500 | 300 | 100 |
| $HNO_3$ | 0# | 0 | 10 | 50 | 0# | 0 |
| HCl | 0# | 0 | 10 | 50 | 0# | 0 |
| PAN | 500 | 500 | 1000 | 1000 | 500 | 500 |
| $O_3$ | 320 | 100 | 640 | 1000 | 240 | 80 |

* negative values denote emission.

# $R_c$ values are set to 1 s $m^{-1}$ to avoid unrealistically high deposition velocities at low values of $R_a$ and $R_b$ values.

*Uncertainties*

There are several sources of uncertainty associated with the proposed parameterisations. The main uncertainty arises from the fact that a highly variable and complex process (dry deposition) is captured in a simple scheme. Secondly there are far too little data which can be used for validation. Indications of uncertainty ranges can be obtained from comparison with micrometeorological measurements (Padro *et al.*, 1991; 1992; Wesely and Lesht, 1989; Erisman, 1992; 1994), balance studies using long-range transport models (e.g. van Jaarsveld, 1989; 1990; Erisman, 1993a) or from comparison with throughfall measurements (Ivens *et al.*, 1988; Draaijers and Erisman, 1993; Erisman, 1993b). The uncertainty in the proposed parameterisations was usually found to be large (>40%).

A few important uncertainty sources will be mentioned briefly. In estimating yearly average fluxes for areas or specific sites using the proposed parameterisation, a constant flux layer is assumed through which the resistance analogy can be applied. However, in many situations this assumption is not valid because of advection, nearby sources, chemical reactions, very stable conditions, complex terrain and roughness transition zones. This can lead to large underestimates and overestimates of fluxes. For gases which can react very fast under ambient conditions (e.g. NO, $NO_2$ and $O_3$, Duyzer, 1992; Kramm *et al.*, 1993), the influence of reactions can be very large. Emissions might be of importance for gases with many scattered ground level sources ($NH_3$ and $NO/NO_2$). If area average fluxes are estimated, there is much uncertainty in the way area average $R_c$ and $z_0$ values are derived (Van Pul *et al.*, 1993). For many land-use categories, i.e. for cities, seas, and many types of vegetation and soils, the parameterisation is incomplete. The parameterisation of particle deposition velocities for forests is only based on experiments performed at the Speulder forest. Whether the parameterisation is applicable to other forests remains, up to now, unsure.

This Page Intentionally Left Blank

# CHAPTER 5 GENERALISATION OF DEPOSITION

*Introduction*

There is a difference between deposition modelling and long-range transport modelling, i.e. the focus of the two is different: deposition modelling is aimed at estimating the input to ecosystems as accurately as possible; long-range transport modelling, on the other hand, is aimed at determining the distribution of pollutants (concentration and deposition) based on emission estimates and dispersion calculations. In long-range transport modelling, deposition is a loss term in which the accuracy needed is dependent on the modelled scale. When both the pollution distribution and the deposition needs to be known as accurately as possible, a compromise is required on the detail some of the aspects will be modelled in order to take the main processes determining transport and deposition into account. In applying abatement strategies on a national or European scale, it is desirable to know both the deposition and the distribution of pollution as accurately as possible. When emission abatement strategies are based on the critical load concept, the deposition has to be determined on the ecosystem level. Desired emission reductions based on the target levels should be known per country and/or per individual source or activity. Therefore, long-range transport modelling and ecosystem-scale deposition modelling should be linked. In this chapter we will show two examples of this combination in the Netherlands and in Europe. The deposition model used here to determine the deposition in the Netherlands is DEADM (Dutch Empirical Acid Deposition Model) and in Europe, the EDACS model (Estimation of Deposition of Acidifying Components in Europe). Wet deposition in these models is estimated using interpolation of wet deposition measurements. Dry deposition is determined using the inferential technique (Hicks *et al*, 1987). The dry deposition flux is inferred from interpolated concentrations and land-use-specific dry deposition velocities. The resistance framework used in the inferential technique is already extensively described in Chapter 4 and will not be explained here. First, we will explain the need for local-scale modelling. The application and results for the Netherlands will be given followed by a discussion on the European application and results. At the end of this chapter, a section will be devoted to the variation in deposition over several years. Current deposition estimates will be compared to an estimate of the 'natural background deposition' and to historical deposition measurements.

## 5.1 LOCAL-SCALE DEPOSITION MAPS, WHAT'S THE USE?

The need for small-scale deposition data for many parts of Europe is obvious from the strong variations in deposition observed within a grid due to variation in concentration and receptor characteristics. Concentrations might vary strongly in or near source regions. This is especially the case for gases emitted from low-level sources, such as ammonia and nitrogen oxides. Strong variations in deposition are also a consequence of variation in landscape and surface roughness.

There is a need to identify ecosystems with high local deposition and low critical loads. Most very sensitive ecosystems are located near source areas for the Netherlands. This is illustrated in Table 5.1 where 10 x 10 km grid total acid deposition loads (Erisman, 1992; 1993a) are averaged for each median value critical load for these grids (Hettelingh *et al.*, 1991). The table shows the correlation between critical loads and acid loads. It is obvious that areas in the Netherlands with low critical loads often have the highest acid deposition. For nitrogen species, this situation will be even more pronounced, at least for the Netherlands or other regions with small nature conservation areas and scattered sources or source areas of ammonia.

**TABLE 5.1** Number of grid cells (10 x 10 km) in the Netherlands with median critical loads, divided into classes, and the average and standard deviation of the acid loads for the grid cells in each class

| Median critical load (mol $H^+$ $ha^{-1}$ $a^{-1}$) | Acid deposition (mol $H^+$ $ha^{-1}$ $a^{-1}$) | Standard deviation of acid deposition | Number of grid cells |
|---|---|---|---|
| < 1000 | 4450 | 1180 | 100 |
| 1000 - 1500 | 4730 | 1480 | 167 |
| 1500 - 2400 | 4010 | 970 | 43 |
| 2400 - 3000 | 4000 | 890 | 29 |
| > 3000 | 3540 | 770 | 98 |

If 1 or 5 percentile critical load values are used instead of median values, the anti-correlation between critical loads and actual loads will be even higher. Another similar problem is the correlation between low critical loads for sulphur and nitrogen to forest soils, and the high deposition of these pollutants to forest ecosystems. These problems are not overcome by the use of so-called filtering factors. Filtering factors are estimated as throughfall deposition divided by open field wet deposition, obtained from different throughfall measurements in European forests. This implies that the filtering factor accounts for the dry deposition onto the forest and that there is a relation between dry deposition and wet deposition. Both assumptions are not valid, as is explained in Chapter 6.2. The use of filtering factors can lead to serious errors. This is demonstrated by comparing deposition to ecosystems within EMEP

grids in the Netherlands (obtained using filtering factors) with the small-scale estimates by Erisman (1993a), cf. Figure 5.1. This figure clearly shows the large variation of deposition of sulphur and nitrogen species within an EMEP (150 x 150 km) grid cell. Generally, this will mean that by taking measures based on exceedances estimated on large grids corrected with filtering factors, the deposition reduction will not lead to the necessary reduction.

The appropriate exceedance maps will be obtained when deposition estimates are available at least on the same scale as the critical loads, i.e. generally in the order of 10 x 10 km to 50 x 50 km resolution.

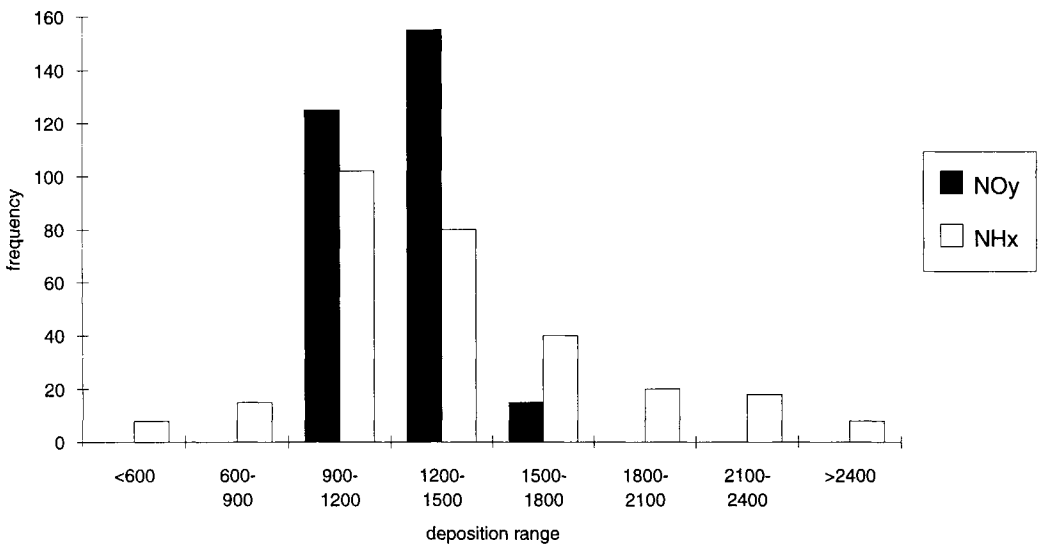


**FIGURE 5.1** Frequency distribution of deposition on a small scale (5 x 5 km) within an EMEP grid (150 x 150 km) for nitrogen compounds. Using EMEP model results together with the appropriate filtering factor, we estimate total nitrogen deposition to this grid at 1650 mol $ha^{-1}$ $a^{-1}$.

## 5.2 DEPOSITION MODELLING IN THE NETHERLANDS

### 5.2.1 DEADM

The Dutch Empirical Acid Deposition Model (DEADM) to describe the deposition of acidifying components on a small scale in the Netherlands has been developed and extensively evaluated (Erisman, 1992; 1993a; 1993b). The model has a wet and dry deposition module. Wet deposition fluxes are obtained directly from precipitation measurements at 14 monitoring locations in the Netherlands. Annual average wet deposition fluxes for each monitoring station are interpolated on a 10 x 10 km grid above the Netherlands. Dry deposition is inferred from measured air concentrations, meteorological parameters, surface resistances and surface roughness. Air concentrations ($SO_2$, NO, $NO_2$, $HNO_2$, $HNO_3$, HCl and aerosols) and meteorological parameters (global radiation, temperature, wind direction/speed, precipitation) are obtained from the National Air Quality Monitoring Network and extended with measurements made by other institutes. For $NH_3$ and $NH_4$ air concentrations, results of model calculations are used (Asman and Van Jaarsveld, 1992). These were calculated for each 5 x 5 km grid over the Netherlands using emission estimates for the Netherlands (Van der Hoek, 1994) and Europe (Asman, 1992) and seasonal and daily variations in the emission (Asman, 1992). Annual average values are used as input for DEADM, together with monthly and daily variations in concentration obtained from the monitoring network (Van Elzakker *et al.*, 1994). Relative monthly variations were estimated for highly polluted areas (annual concentration above 15 $\mu g\ m^{-3}$) and less polluted areas (annual concentration below 15 $\mu g\ m^{-3}$) from data from the eight sites of the ammonia concentration monitoring network. Also, average daily variations were derived for each month. These could be explained by the monthly average concentration, temperature and wind speed variations during the day, again for highly polluted areas (72% variance accounted for) and less polluted areas (83% variance accounted for) (Bleeker and Erisman, 1994). The monthly average concentration and the daily variation in concentration for each grid cell can thus be estimated. The average daily variation in $V_d$ was estimated for each month using the resistance analogy (see below). The average daily variations of $V_d$ were multiplied by the average daily variations in concentration for each grid to estimate monthly and annual average fluxes.

Detailed land-use information is used to characterise roughness lengths and to determine surface resistances, together with other surface conditions. The roughness length for forests is related to tree species, mean tree height and crown coverage of the forest stand; this was estimated separately for summer and winter months (Erisman, 1990; 1992). Wind and concentration fields were obtained for every two hours via extrapolation of the measurements at each individual station, or from model results (in the case of ammonia) to a height of 50 m and subsequent interpolation onto a grid system reaching across the Netherlands. The 50-m height is chosen because it is assumed that at this height concentration and wind speed are not substantially influenced by surface characteristics. For each 1 x 1 km grid, $u_*$ and $L$ are

calculated using the meteorological data and the schemes provided by Beljaars and Holtslag (1990). From $u_*$ and $L$, $R_a$ and $R_b$ can be estimated. With the land-use information and estimation of the surface condition (wet/dry, stomata open or closed, etc.), component-specific surface resistances or surface-exchange parametrisations (see section 4.2) and, subsequently, dry deposition velocities are determined (Erisman, 1993a, Erisman *et al.*, 1994) for each 1 x 1 km grid in the Netherlands. Accordingly, two-hour averaged fluxes are calculated by multiplying $V_d$ with the concentrations. Total annual deposition is calculated by summing the average dry and wet deposition obtained in each time step.

The Netherlands is divided in 20 so-called acidification areas as shown in Figure 5.2. Deposition is determined for each acidification area. These areas are also used in the Dutch Acidification System (DAS) model used for scenario analysis and policy development (Heij and Schneider, 1991).

1 = Groningen
2 = Friesland
3 = Drenthe
4 = W/NO-Overijssel
5 = ZO-Overijssel
6 = NW-Gelderland
7 = NO-Gelderland
8 = Z-Gelderland
9 = Utrecht
10 = N-Noord Holland
11 = Z-Noord Holland, Flevopolder
12 = N-Zuid Holland
13 = Z-Zuid Holland
14 = Zeeland
15 = W-Noord Brabant
16 = Midden-Noord Brabant
17 = NO-Noord Brabant
18 = ZO-Noord Brabant
19 = N-Limburg
20 = Z/Midden Limburg

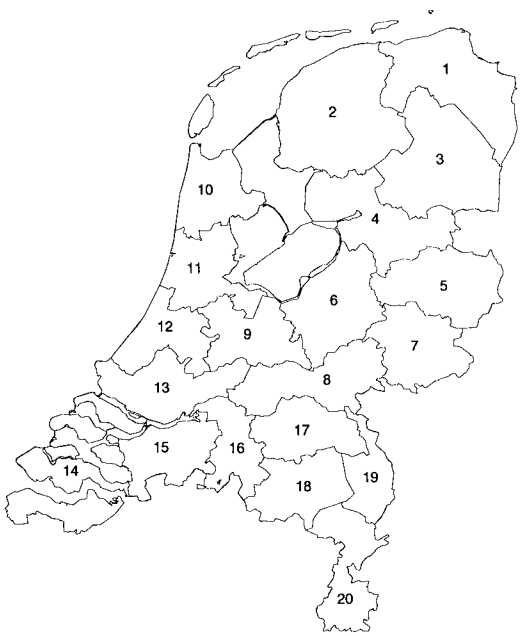


**FIGURE 5.2** Distribution of the acidification areas over the Netherlands.

The deposition of acidifying components in the Netherlands was calculated with the DEADM model for the years 1980 to 1993. Total potential acid, the maximum acid load to soils, or the amount of acidifying components removed from the atmosphere by deposition, is defined as (see also Chapter 1):

$$\text{Total potential acid} = 2\text{SOx} + \text{NOy} + \text{NHx} \qquad [5.1]$$

This is the maximum load as it is assumed that $NH_3$ and $NH_4$ are completely nitrified in the soil (Van Breemen *et al.*, 1982). Furthermore, it is assumed that deposited neutralised aerosols lead to acidification. HCl, organic acids, PAN, $H_2S$ and HF are not taken into account. These are considered of minor importance for the present potential acid deposition loads.

### 5.2.2 WET DEPOSITION

The concentrations of components in precipitation are monitored in the LML on a monthly basis (KNMI/RIVM, 1987; RIVM, 1989). The amount of precipitation is monitored at the same locations using official rain gauges of KNMI. Up to 1988, precipitation samples were collected using bulk samplers. At the beginning of 1988 these were replaced by wet-only samplers. In wet-only samplers dry deposition onto the funnel during dry periods is excluded. Corrections for the dry deposition to bulk samplers have been estimated on the basis of parallel measurements done with the two samplers. In this study the main focus is on the estimation of *potential acid* deposition. As the wet deposition fluxes measured also contain dissolved neutral salts, their contribution to the ion composition of the sample have to be identified and subtracted from the total.

*Dry deposition in bulk samplers*
If open samplers are used, dry deposition onto the funnels of the device influences the results (see section 3.1). For the monthly open field measurements it was found that in the Netherlands an average of 25% of the wet deposition fluxes of $SO_4^{2-}$ and $NH_4$ measured by open samplers was due to dry deposition, whereas for $NO_3^-$ this was only 15% (Ridder *et al.*, 1984). The 1980 - 1987 data from bulk samplers were therefore corrected by these correction factors.

*Neutral salts*
The potential acid deposition from precipitation can be calculated from the volume weighted average deposition of $H^+ + 2\ NH_4^+$, where $NH_4^+$ originates both from gaseous $NH_3$ and particulate $NH_4^+$ dissolved in rain water. Particulate $NH_4^+$ can be associated to both $SO_4^{2-}$ and $NO_3^-$, but their origins in terms of source contributions cannot be ascertained. However, when the molar equivalent ratio of $NH_4^+$ to that of $NO_3^- + SO_4^{2-}$ is near to one, which is the case under Dutch circumstances, the origin can be obtained from the amount of $SO_4^{2-}$ and $NO_3^-$ in the samples. In this procedure, the sulphate levels are corrected for the (neutral) sea salt contribution. Buijsman (1990) in comparing fluxes of potential acid calculated by $H^+ + 2\ NH_4^+$ and $2\ SO_4^{2-} + NO_3^- + NH_4^+$ showed that the agreement was very good, provided a correction was also made for the $Ca^{2+}$ contribution to the neutralisation of the sample:

$$\text{Total potential acid} = NH_4^+ + NO_3^- + 2\ SO_4^{2-} - 2\ Ca^{2+} \qquad [5.2]$$

The $Cl^-$ compound in precipitation is almost completely associated to $Na^+$ and is therefore of sea-salt origin.

In order to determine the relative source contributions to the total potential acid by $SO_4^{2-}$, $NO_3^-$ and $NH_4^+$, the origin of $Ca^{2+}$ in the samples has to be identified. Unfortunately, Buijsman (1990) does not refer to the source or form of $Ca^{2+}$ in the samples. The source of $Ca^{2+}$ can either be dissolved aerosol in rain, or dry deposition of road dust or sea salt onto the funnels. The large correction factor for open samplers of 0.45 (Table 3.1) suggests that dry deposition is the most important source in open samplers. The contribution of $Ca^{2+}$ to $SO_4^{2-}$, $NO_3^-$ and $Cl^-$ in rain water was investigated by Slanina *et al.* (1982) using a cluster analysis on 24-hour averaged rain samples. At two locations, near to the coast and in the centre of the Netherlands, results from eight wet-only samplers were investigated. From the results it was estimated that for the continental location, 11% of $SO_4^{2-}$ and 22% of $NO_3^-$ is related to $Ca^{2+}$. For the coastal site this is 11% and 0%, respectively, for $SO_4^{2-}$ and $NO_3^-$. No $Ca^{2+}$ seems to be connected to $Cl^-$ (Slanina *et al.*, 1990). Information on the contribution of $CaCO_3$ to the amount of $Ca^{2+}$ in precipitation could not be found in the literature. In this study, $Ca^{2+}$ was only attributed to sulphate and nitrate. Taking yearly average fluxes at these sites, as reported by Slanina (1985) for the continental site and by RIVM (1989) for a coastal site, it was estimated that for the coastal site 50% of $Ca^{2+}$ originates from $SO_4^{2-}$ and 50% from $NO_3^-$, whereas all $Ca^{2+}$ originates from $SO_4^{2-}$ at the continental site. These are all results obtained from wet-only measurements not influenced by dry deposition.

*Calculation procedure*

The procedure for correcting fluxes of $SO_4^{2-}$ and $NO_3^-$ for $Ca^{2+}$ and sea salt ($SO_4^{2-}$), as followed here, is first correcting $Ca^{2+}$, $Na^+$, $SO_4^{2-}$ and $NO_3^-$ for dry deposition contribution (open samplers) and then applying the correction to $Ca^{2+}$ and sea salt (0.06 times the $Na^+$ concentration based on the concentration ratio of $SO_4^{2-}$ and $Na^+$ in sea water). This leads to the following equations on molar basis for coastal sites:

$$[SO_4^{2-}]_c = d1 * SO_4^{2-} - 0.5 * d2 * Ca^{2+} - 0.06 * d3 * Na^+ \quad [5.3]$$
$$[NO_3^-]_c = d4 * NO_3^- - 0.5 * d2 * Ca^{2+}$$
$$[NH_4^+]_c = d5 * NH_4^+$$

and for continental sites:

$$[SO_4^{2-}]_c = d1 * SO_4^{2-} - d2 * Ca^{2+} - 0.06 * d3 * Na^+ \quad [5.4]$$
$$[NO_3^-]_c = d4 * NO_3^-$$
$$[NH_4^+]_c = d5 * NH_4^+$$

where the subscript *c* denotes corrected fluxes and *d1* to *d5* the appropriate dry deposition factors listed in Table 3.1. For those years where wet-only samplers were used (from 1988 onwards), the dry deposition factors in Eqn. (5.3) and (5.4) are taken as 1.

*Wet deposition estimates*
The yearly average wet deposition fluxes for each monitoring station in the Netherlands (20 stations in 1980 and 14 in 1987 and successive years) were calculated by multiplying the concentrations by the amount of rain measured with the official KNMI rain gauges. The fluxes were interpolated onto a 10 x 10 km grid reaching across the country. In this way local fluxes were estimated assuming that the amount and composition of precipitation is independent on the structure of the surface. Furthermore, it was assumed that rain-out of gases from local sources is negligible.

The wet deposition maps for the Netherlands in 1993 are shown in Figures 5.3 for SOx, NOy, NHx and potential acid, respectively. Wet deposition fluxes for the years 1980-1993 are presented in Table 5.2. The average wet deposition fluxes for each acidification region in the Netherlands in 1980 and 1993 are listed in Tables 5.5 and 5.6, respectively, shown later in this chapter.

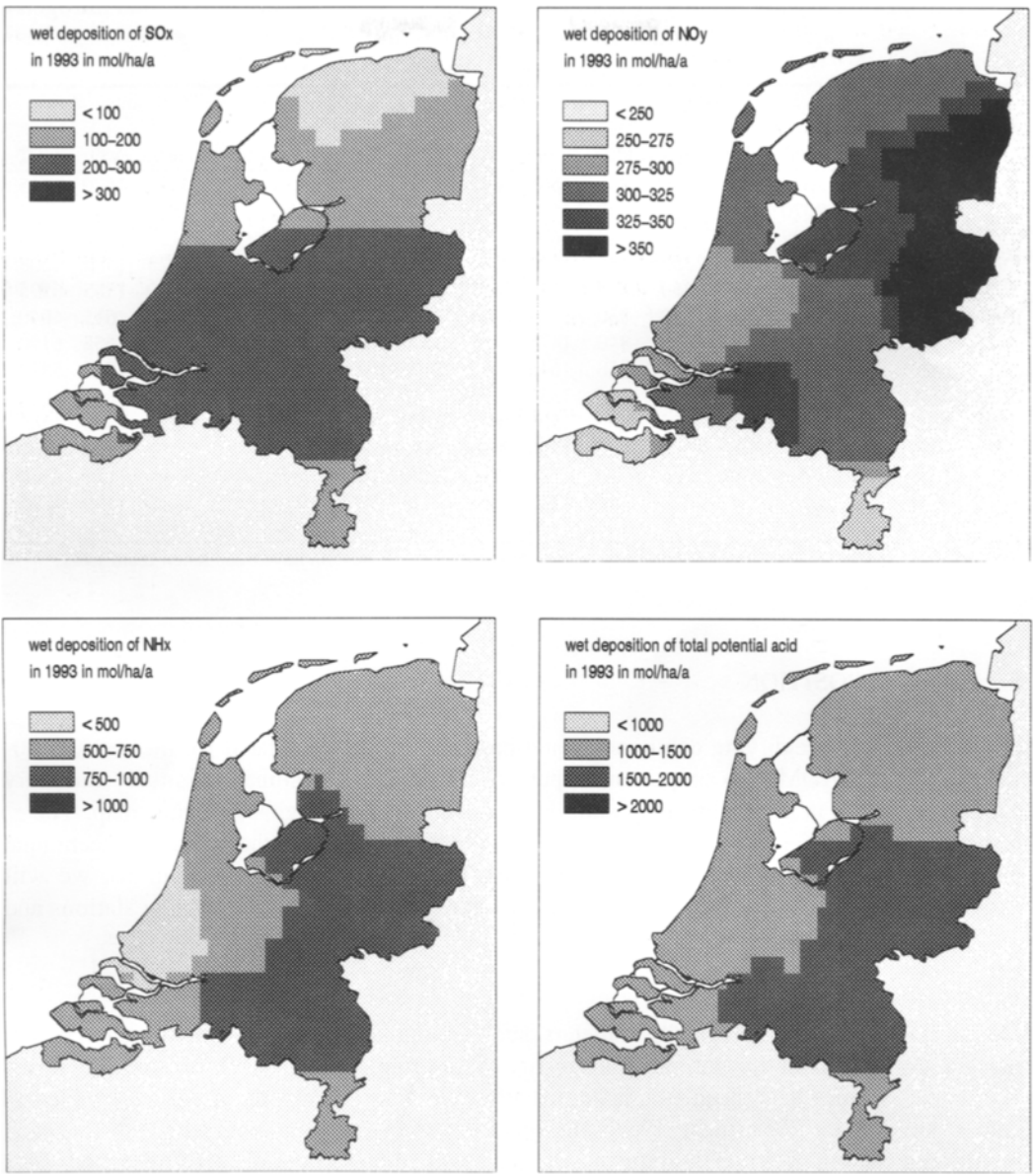


**FIGURE 5.3** The spatial distribution of the wet deposition of SOx, NOy, NHx and potential acid in 1993 (mol $ha^{-1}$ $a^{-1}$).

**TABLE 5.2** Country average dry, wet and total deposition of SOx, NOy, NHx, total nitrogen and potential acid in 1980 - 1993 (mol $ha^{-1}$ $a^{-1}$)

| | SOx | | | NOy | | | NHx | | | Total N | | | Total potential acid | | |
|---|---|---|---|---|---|---|---|---|---|---|---|---|---|---|---|
| | dry | wet | total | dry | wet | total | dry | wet | total | dry | wet | total | dry | wet | total |
| 1980* | 1750 | 320 | 2070 | 480 | 390 | 880 | 1565 | 640 | 2205 | 2045 | 1030 | 3075 | 5545 | 1670 | 7215 |
| 1981 | 1750 | 320 | 2070 | 490 | 390 | 880 | 1565 | 640 | 2205 | 2055 | 1030 | 3085 | 5555 | 1670 | 7225 |
| 1982 | 1510 | 295 | 1805 | 515 | 360 | 875 | 1600 | 630 | 2230 | 2115 | 990 | 3105 | 5135 | 1580 | 6715 |
| 1983 | 1470 | 275 | 1705 | 523 | 355 | 885 | 1560 | 680 | 2240 | 2083 | 1035 | 3118 | 5023 | 1585 | 6608 |
| 1984 | 1430 | 280 | 1830 | 530 | 360 | 870 | 1620 | 665 | 2285 | 2150 | 1025 | 3175 | 5010 | 1585 | 6595 |
| 1985 | 1550 | 275 | 1565 | 510 | 350 | 830 | 1615 | 715 | 2330 | 2125 | 1065 | 3190 | 5225 | 1615 | 6840 |
| 1986 | 1290 | 275 | 1435 | 480 | 370 | 840 | 1475 | 735 | 2210 | 1955 | 1105 | 3060 | 4535 | 1655 | 6190 |
| 1987 | 1030 | 280 | 1310 | 455 | 395 | 850 | 1640 | 760 | 2400 | 2095 | 1155 | 3250 | 4155 | 1715 | 5870 |
| 1988 | 750 | 225 | 975 | 445 | 305 | 750 | 1555 | 625 | 2180 | 2000 | 930 | 2930 | 3500 | 1380 | 4880 |
| 1989 | 620 | 225 | 845 | 455 | 305 | 760 | 1505 | 625 | 2130 | 1960 | 930 | 2890 | 3200 | 1380 | 4580 |
| 1990 | 615 | 225 | 840 | 445 | 290 | 735 | 1490 | 680 | 2170 | 1935 | 970 | 2905 | 3165 | 1420 | 4585 |
| 1991 | 580 | 190 | 770 | 445 | 255 | 700 | 1580 | 540 | 2120 | 2025 | 795 | 2820 | 3185 | 1175 | 4360 |
| 1992 | 555 | 220 | 775 | 420 | 330 | 750 | 1245 | 680 | 1925 | 1665 | 1010 | 2675 | 2775 | 1450 | 4225 |
| 1993 | 570 | 190 | 760 | 420 | 320 | 740 | 1320 | 680 | 2000 | 1740 | 1000 | 2750 | 2900 | 1380 | 4280 |

* Data for 1980 not available for wet deposition, $SO_2$ and $NH_3$; these data have been taken from 1981.

## 5.2.3 DRY DEPOSITION

Dry deposition of acidifying components and base cations are calculated for the years 1980-1993 using DEADM. An important input to DEADM for estimating small scale dry deposition fluxes is a land-use map and, derived from this, a roughness length map. The $z_0$ maps will be used for the dry deposition velocity calculations from the inferential technique on a grid basis. Before describing the results of the dry deposition calculations, we will explain the method to estimate the roughness length for the different monitoring stations and for the Netherlands as a whole.

*Roughness length maps*

Measurements of meteorological parameters, such as wind speed, $u$, and wind direction, $q$, are made at 26 stations in the National Air Quality Monitoring Network LML on a routine basis. To date, $z_0$ values have been estimated, usually by defining landscape classes for which $z_0$ values are known (Wieringa, 1981). In this section, $z_0$ values are estimated for each monitoring station from measurements of the standard deviation of wind direction. The second part of this section describes a method to obtain $z_0$ maps for across the Netherlands from land-use information. Both estimates are used for extrapolating air quality measurements to areas where measurements are lacking.

Values of $z_0$ for meteorological stations
The values for $u$ and $q$ averaged over one hour are available for each station, as well as $\sigma_\theta$ averaged both over one hour and the last 10 minutes of the hour, as calculated from 12-s average wind direction measurements. Most measurements are made at 10 m height, except for four locations, where the measuring height is 20 m. The monitoring stations are extensively described in the Technical Report of the National Air Quality Monitoring Network (Elskamp, 1989).

A dataset of 10-min average measurements for each LML monitoring station is available from the beginning of 1987. The dataset used here contains about 26,000 hours of $\sigma_\theta$ measurements for each station. Data with non-neutral stability and low wind speed ($u < 4$ m s$^{-1}$) were identified and rejected. About 40% of the dataset remained for estimating $z_0$ values. This dataset was subdivided in subsets for four seasons and four wind direction sectors (90°). For each class, $\sigma_\theta$ was averaged. The $z_0$ values for each classification were then calculated from the class average $\sigma_\theta$, using Eqn. (3.30). By first averaging $\sigma_\theta$ and then calculating $z_0$, statistical errors in the results are reduced. Values for each station per season per wind direction sector are listed in Erisman (1990b).

Figure 5.4 shows the calculated $z_0$ values for station 103 (Steeg) as a function of wind direction (in this case in the 30$^0$ sectors) and of season. The seasonal influence on $z_0$ values is clearly demonstrated, with the highest values in spring and summer and lowest in winter. An average $z_0$ value of 7 cm was calculated for this location. From the classification by Wieringa (1981), $z_0$ for this location (agricultural area with homogeneous low crops or pastures with spread roughness elements, like isolated trees, low hedges or isolated farms) should be about 0.1 m, which is in good agreement.

Much research has been done on methods for estimating $z_0$ values at the meteorological tower of Cabauw, KNMI (see e.g. Beljaars, 1988). Beljaars (1988) compared three methods for estimating $z_0$ values (based on $\sigma_\theta$, $\sigma_u$ [standard deviation of wind speed] and wind profile measurements). His estimates for each 30° wind direction sector for summer and winter months are compared to the estimates from the LML dataset in Figure 5.5. Data observed in summer is in very good agreement and in winter in fair, even though data from different years were compared.

Roughness length maps for the Netherlands
Grid average $z_0$ values ($z_{0t}$) have been calculated using the method by Van Dop (1983). This method is based on the assumption that the $z_0$ of a certain area is determined primarily by the roughest subarea within the area considered. Area-weighted averages of the drag coefficient, $c_D$, for each individual subarea assumed to be homogeneous are determined for the whole area. The area average drag coefficient is then used to calculate $z_{0t}$.

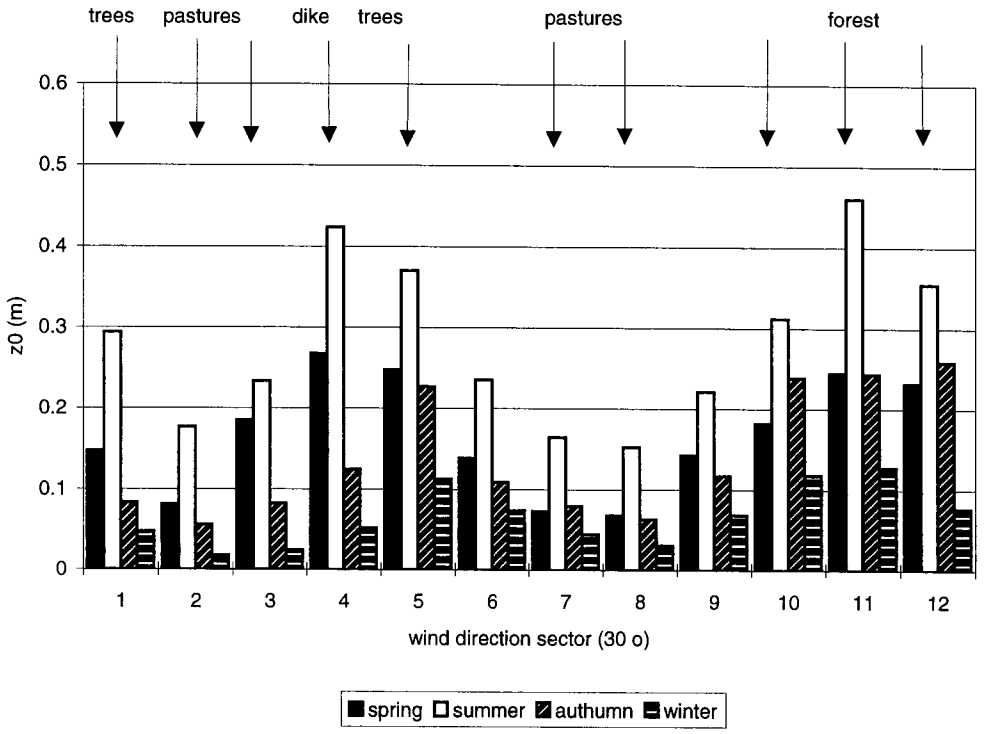


**FIGURE 5.4** Values for $z_0$ as a function of wind direction sector ($30^0$) and season for the Steeg station (103).

The 10-m drag coefficient for each individual subarea, $i$, is related to the $z_{0i}$ by (Van Dop, 1983):

$$C_{D,i} = [\frac{0.4}{\ln(\frac{10}{z_{0i}})}]^2 \qquad [5.5]$$

The weighted average $C_D$ for the whole area is calculated from the individual $C_{D,i}$ and the surface area fraction, $f_i$:

$$C_D = \Sigma_i \; f_i \; C_{D,i} \qquad [5.6]$$

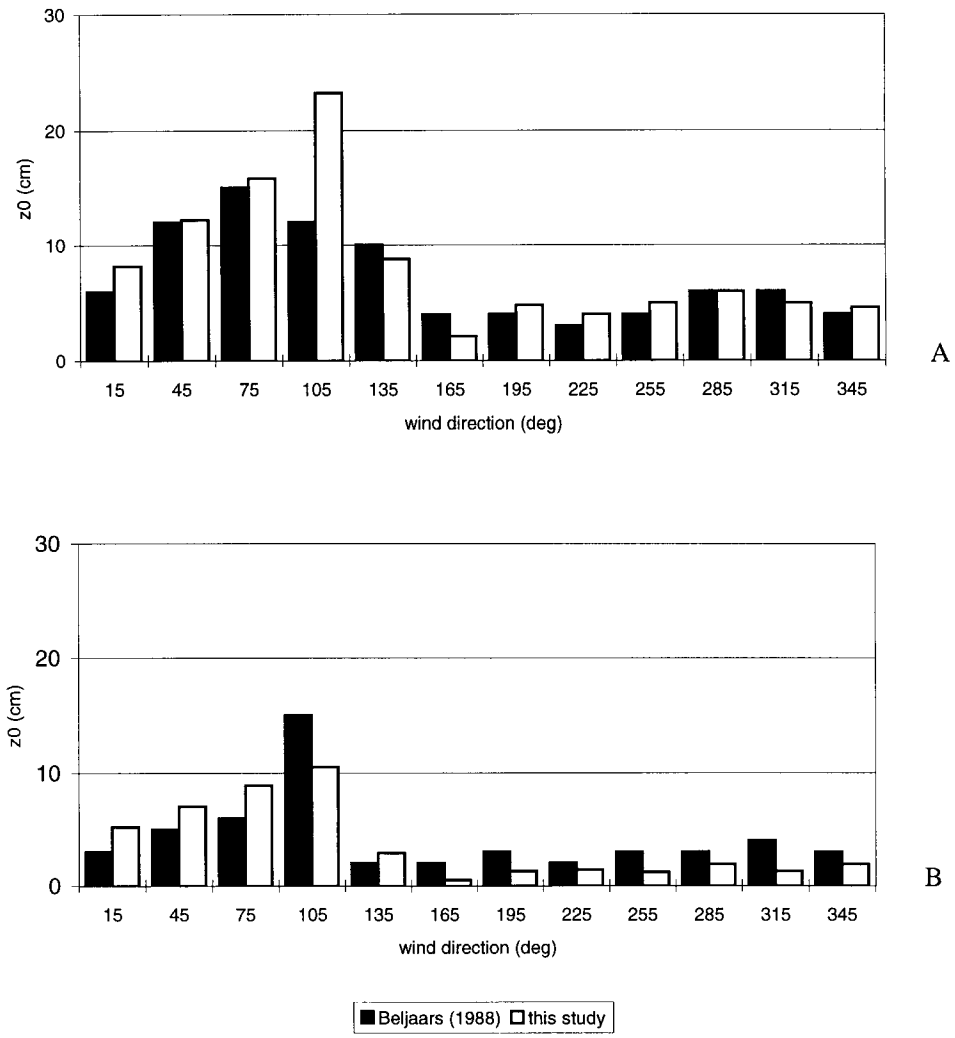


**FIGURE 5.5** Values for $z_0$ as a function of wind direction sector ($30^0$) for the Cabauw station (620) estimated by Beljaars (1988) and in this study for summer (A) and winter (B) months.

By rearranging Equation (5.5), the average $z_0$ for this area at 10 m height can be calculated from $C_D$. The information needed to estimate grid average $z_{0t}$ values from this method are the fraction of the grid covered by the subareas and the $z_0$ values of these subareas.

A detailed inventory of tree species, height, surface area and crown cover of the Dutch forests is available from the Dutch Forestry Service (SBB, 1985). This inventory was revised and aggregated to classes on a 1 x 1 km grid by Meijers (1990). The following classification was used: closed canopy forests (crown cover > 60%) and open forests (crown cover < 60% and > 20%), subdivided into classes of deciduous and coniferous forests with the average height of the trees and the surface area covered by the canopy. Land-use data for the Netherlands on a 25 x 25 m grid (CBS, 1993) were aggregated to classes on the 1 x 1 km grid for the country. These data have been used for estimating grid average surface resistances according to the parametrisations outlined in Chapter 4. Classes used include open water, forest, bare soil, grassland, agricultural crops, heathland, nature conservation areas and remaining categories. The $z_0$ values for each individual class were taken from Verver (1986), and Duijm and Van Aalst (1984). It was assumed that $z_0$ for forests is related to the tree height, $h$, (Stull, 1988). The classification and $z_0$ values for each class are listed in Table 5.3. For deciduous forest and agricultural areas, difference between summer and winter was introduced.

Grid average $z_{0t}$ values were calculated from the Eqns. (5.5) and (5.6) and the values in Table 5.3. The $z_{0t}$ values on a 1 x 1 km grid are plotted in Figure 5.6 A and B for $z_{0t}$ values between 0 and 60 cm and greater than 50 cm, respectively. In these maps the forest areas 'Veluwe' and 'Utrechtse Heuvelrug' in the centre of the Netherlands are clearly shown, as well as the urban areas, like Amsterdam, Rotterdam, The Hague, Groningen, etc.

The $z_0$ values for each LML monitoring station are representative for a measuring height of 10 m and, therefore, represent the roughness characteristics of an area with a radius of about 1 km (100 times the measuring height; Stull, 1988). These values can therefore be compared to the 1 x 1 km averages for the grids in which the LML stations are located (Erisman, 1992). Agreement was found to be reasonable, although large differences can be observed at locations with very small values calculated from $\sigma_\theta$. These locations are surrounded by pastures only. Measurements at these locations show much lower values than estimated from land use. The reason for this is that the value for agricultural areas (average in the Netherlands) is set to 5-15 cm (see Table 5.3). This is an average value for landscapes consisting of pastures with isolated farms and trees or hedges. When these roughness elements are not present in a landscape, this value will be lower. Large discrepancies are also observed for stations which are surrounded by roughness elements in the near vicinity of the measuring location. No LML wind stations are located in forested or urban areas (see Elskamp, 1989).

**TABLE 5.3** Individual roughness elements as $z_0$ values, with $h$ = the average tree height in m

| Classification | | $z_{0t}$ (cm) |
|---|---|---|
| Surface water (> 25 ha) | | 1 |
| Surface water (< 25 ha) | | 8 |
| Agricultural area summer: | | 15 |
| winter: | | 5 |
| Urban area | | 100 |
| Closed canopy forest (> 60% crown coverage): | coniferous: | 0.1 $h$ |
| | deciduous summer: | 0.07 $h$ |
| | winter: | 0.05 $h$ |
| Open canopy forest (> 60% crown coverage): | coniferous: | 0.085 $h$ |
| | deciduous summer: | 0.09 $h$ |
| | winter: | 0.06 $h$ |

The $z_0$ values for the 5 x 5 km grids were calculated by taking the 1 x 1 grid $z_0$ values as individual $z_0$ values, covering 1 km of the larger grid surfaces. For each grid the drag coefficient and, accordingly, the average $z_0$ was calculated as described. It must be emphasised that these values are representative for 10 m height, and can be significantly different for other measuring heights. At other heights, roughness elements within a larger or smaller area will be reflected in $z_0$.

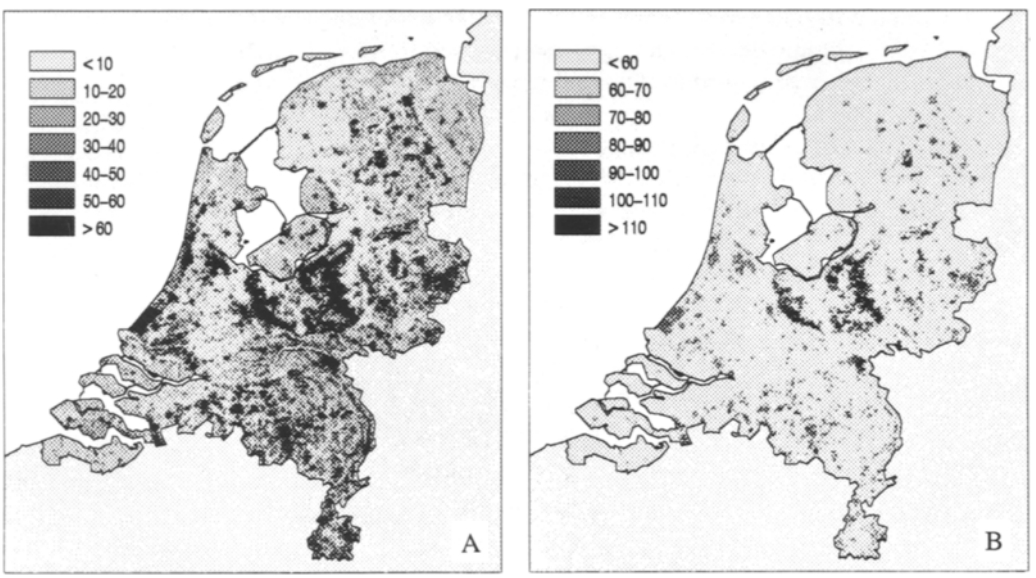


**FIGURE 5.6** 1 x 1 km grid average $z_0$ values in the Netherlands: A: 0-60 cm, B: >50 cm.

*Dry deposition of acidifying components*

The dry deposition of SOx, NOy, NHx, total nitrogen and total potential acid deposition is given in Table 5.2. The spatial distribution of the dry deposition in 1993 is given in Figures 5.7 (A - D) for SOx, NOy, NHx and total potential acid, respectively. These figures show the highest dry deposition of SOx in the large industrial Rijnmond area near the city of Rotterdam on the west coast. Furthermore, there is a gradient with lower dry deposition in the north reaching the highest values in the south of the country. This is mainly the result of the source areas in the neighbouring countries to the east ant the south, such as the Ruhr area in Germany, but also further away in the Black Triangle. Highest dry deposition of NOy is found in the western and central part of the country. Dry deposition of NHx is most pronounced in and near the 'Gelderse Vallei' (in the centre), in the eastern part of the country and in the Peel area to the south.

The average dry deposition of SOx, NOy, NHx in the Netherlands and the total potential acid to deciduous forests, coniferous forests and nature conservation areas are listed in Table 5.4. These estimates are based on 5 x 5 km averages, where the dominant land use is deciduous forest, coniferous forest or nature conservation area. The coverage of deciduous forests over the Netherlands is about 2% of the total land area. For coniferous forests this is 6.2% and for other nature conservation areas, 2.3%. On the average, the dry deposition of SOx to deciduous forests is 28% higher than the average dry deposition of SOx in the Netherlands, whereas the dry deposition to coniferous forests is 42% higher. Dry SOx deposition to forests in the Netherlands is 40% higher than to the 'average' Dutch landscape For NOy, these numbers are 45% higher onto deciduous, 62% higher onto coniferous forests and 58% higher onto forests relative to dry deposition of NOy in the Netherlands. For NHx, the numbers are +2%, +26% and +20%. A higher than country-averaged deposition for forests is caused by the roughness effect on $V_d$. The location of forests to source areas affects concentrations and may also determine the extent that values are higher.

**TABLE 5.4** Average deposition to forests in the Netherlands in 1993 (mol $ha^{-1}$ $a^{-1}$)

| | SOx | | | NOy | | | NHx | | | N | | | Acid | | |
|---|---|---|---|---|---|---|---|---|---|---|---|---|---|---|---|
| | dry | wet | total | dry | wet | total | dry | wet | total | dry | wet | total | dry | wet | total |
| Netherlands | 570 | 190 | 760 | 420 | 320 | 740 | 1320 | 680 | 2000 | 1740 | 1000 | 2750 | 2900 | 1380 | 4280 |
| Deciduous | 730 | 210 | 940 | 610 | 320 | 930 | 1340 | 740 | 2080 | 1950 | 1060 | 3010 | 3420 | 1490 | 4910 |
| Coniferous | 810 | 210 | 1020 | 680 | 320 | 1000 | 1660 | 770 | 2430 | 2350 | 1100 | 3450 | 3980 | 1540 | 5520 |
| Forest (average) | 790 | 210 | 1000 | 660 | 320 | 980 | 1580 | 760 | 2340 | 2240 | 1080 | 3320 | 3820 | 1500 | 5320 |

Figure 5.8 shows histograms of the dry deposition of $SO_x$, $NO_y$ and $NH_x$ to forest, grassland and water. The distribution is determined by taking the deposition to 1 x 1 km grids (5 x 5 km grids for $NH_x$) where the dominating land use is one of these categories. These distributions show that for all three compounds deposition to forest is higher than that to grass and water.

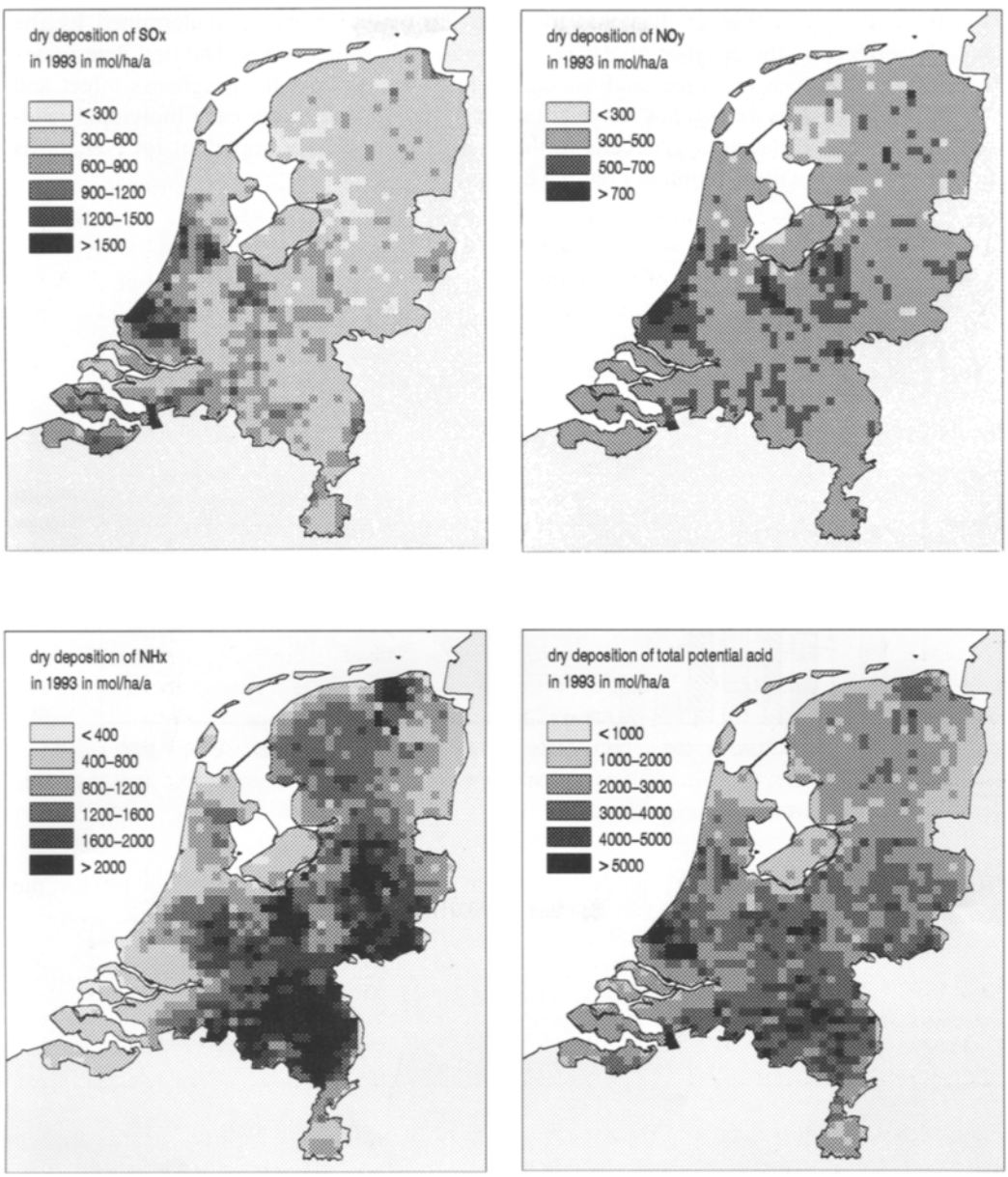


**FIGURE 5.7** The spatial distribution of the dry deposition of SOx, NOy, NHx and total potential acid in 1993 (mol $ha^{-1}$ $a^{-1}$).

Deposition to grass is higher than that to water. The distributions are determined by the roughness effect and the distance of grid cells to sources or source areas. The first determines the difference between the three land-use categories, whereas both the roughness effect and the distance to sources determines the distribution of dry deposition for each individual land-use category. The distance of grid cells to the sources is especially important for $NH_x$. This can be seen from the distribution in Figure 5.8.

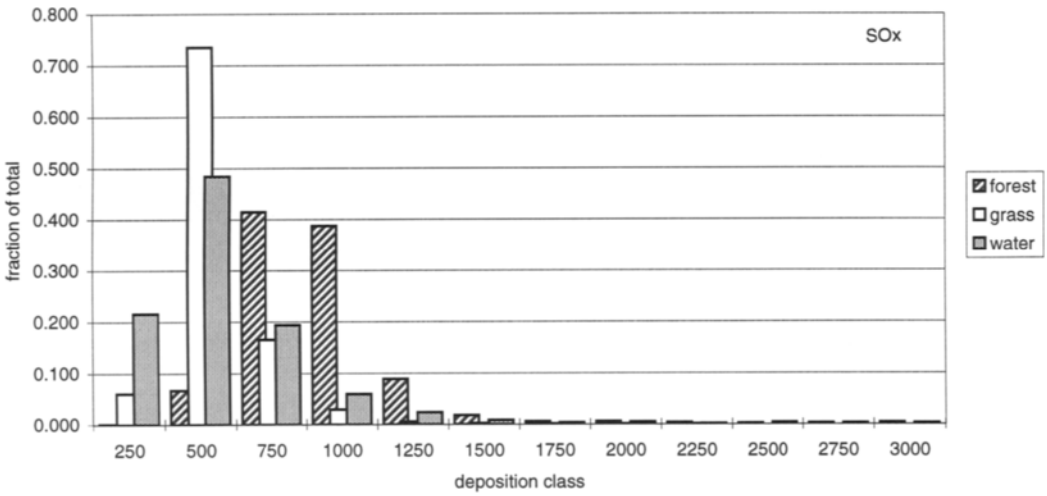


**FIGURE 5.8** Distribution of dry deposition SOx to forest, grassland and water in 1993 in the Netherlands.

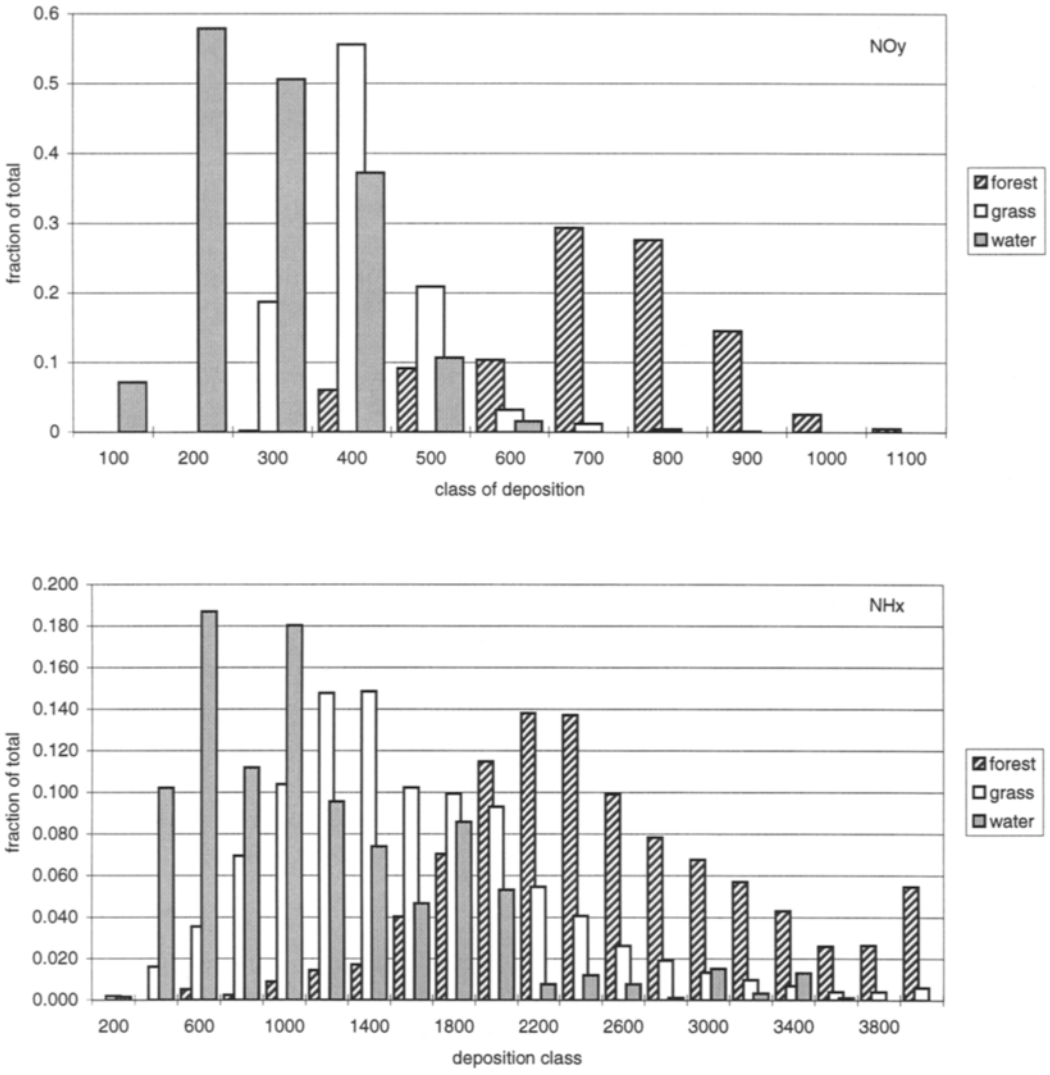


**FIGURE 5.8** *(continued)* Distribution of dry deposition of NOy and NHx to forest, grassland and water in 1993 in the Netherlands.

*Dry base cation deposition*
Up to now there have been no other estimates of the dry deposition of base cations in the Netherlands. The main reason for this is the lack of information on ambient concentrations, both measurements and modelled concentrations. The reason for the lack of the latter is a lack of emission estimates, and the temporal and spatial variation in emissions. Concentrations used here are obtained from wet deposition measurements and scavenging ratios. This method was applied to the Canadian situation (Eder and Dennis, 1990), and evaluated and accordingly applied to the Netherlands and Europe (see section 5.2). An extensive description of this method and the evaluation is found in Erisman *et al.* (1994) and in Chapter 7. Base cation concentrations thus obtained are annual averages on a 10 x 10 km grid across the country. Dry deposition velocities are obtained with DEADM on a 1 x 1 km grid using the parametrisations outlined in section 4.2 for particles.

The first dry deposition results for the Netherlands show the highest input of $Na^+$ over $Ca^{2+}$, $Mg^{2+}$ and $K^+$. Figure 5.9 displays maps of $Na^+$, $K^+$, $Mg^{2+}$ and $Ca^{2+}$ dry deposition. Average dry deposition fluxes of acidifying aerosols and base cations for each acidification area are displayed in Table 5.7. Here it is shown that coastal areas receive the highest base cation inputs. Areas with many forests Veluwe and Brabant also receive high inputs. This is in line with what is expected. Na is of sea-salt origin and inputs are high because of the prevailing southwesterly winds over the Netherlands. A gradient can be seen over the country, with the highest inputs near the coast. High inputs of base cations are caused by periods with southwesterly storms. Such periods dominate annual inputs. Forests receive high base-cation inputs as a result of the high dry deposition velocities for large particles. The estimates are in good agreement with those derived from the experiments and model application at the Speulder forest (Erisman *et al.*, 1994; see section 7.3). It might be concluded that the method used to estimate ambient base cation concentrations is accurate enough to provide concentration estimates. However, there is certainly a need to evaluate the scavenging ratios with simultaneous concentration methods in precipitation and air.

Figure 5.10 shows histograms of the dry deposition of $Na^+$, $K^+$, $Mg^{2+}$ and $Ca^{2+}$ to forest, grassland and water. The distribution is determined by taking the deposition to 1x1 km grids where the dominating land use is one of these categories. These distributions show that for all four compounds deposition to forest is higher than that to grass and water. Deposition to grass is higher than to water. The distributions are determined by the roughness effect and by the distance of grid cells to sources or source areas. The distribution of forests is broader than that of grassland and of water. This is due to the relatively large range in roughness length values in this land-use class compared to the other two.

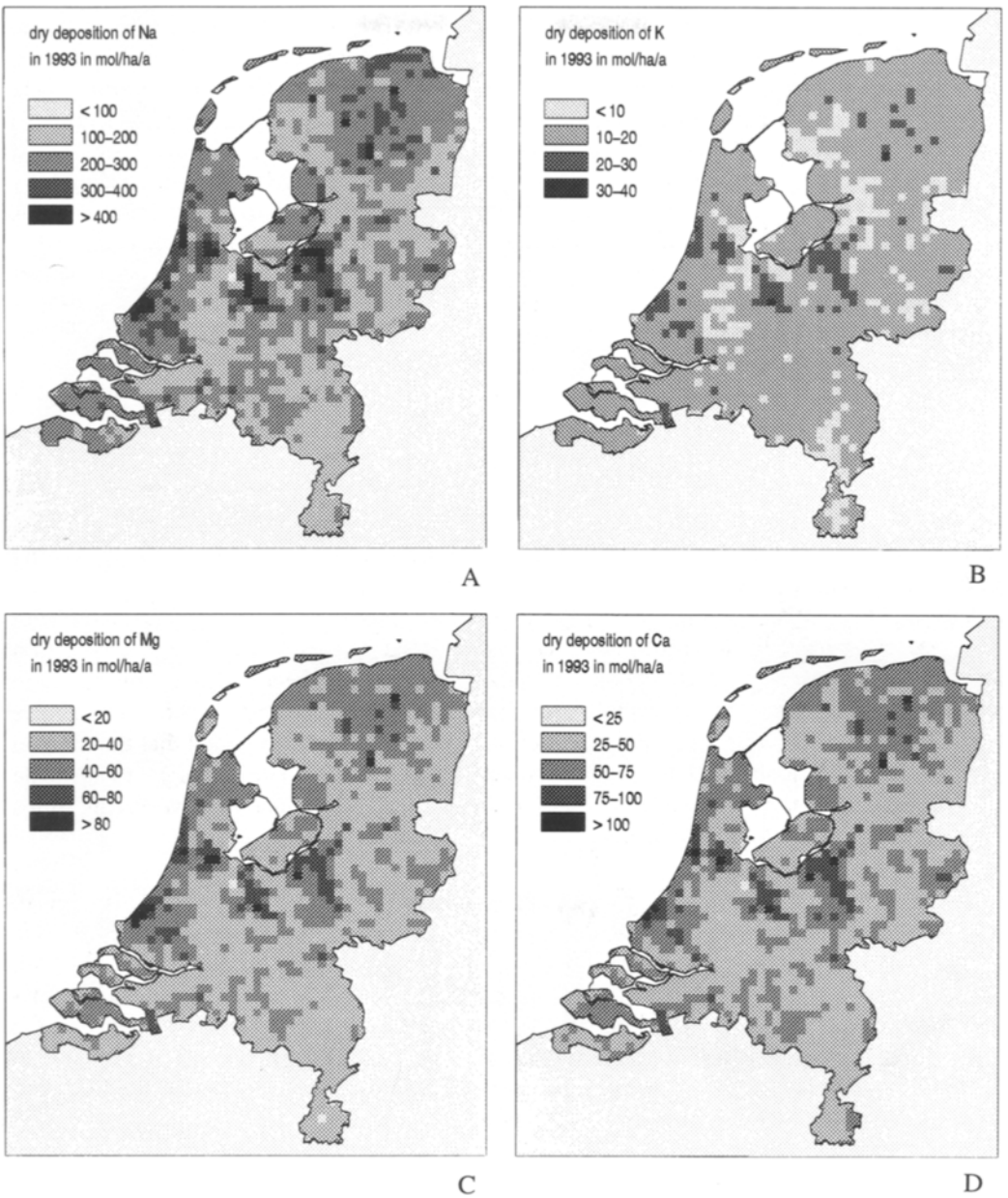


**FIGURE 5.9** Maps of the dry deposition of $Na^+$ (A), $K^+$ (B), $Mg^{2+}$ (C) and $Ca^{2+}$ (D) in the Netherlands (mol $ha^{-1}$ $a^{-1}$).

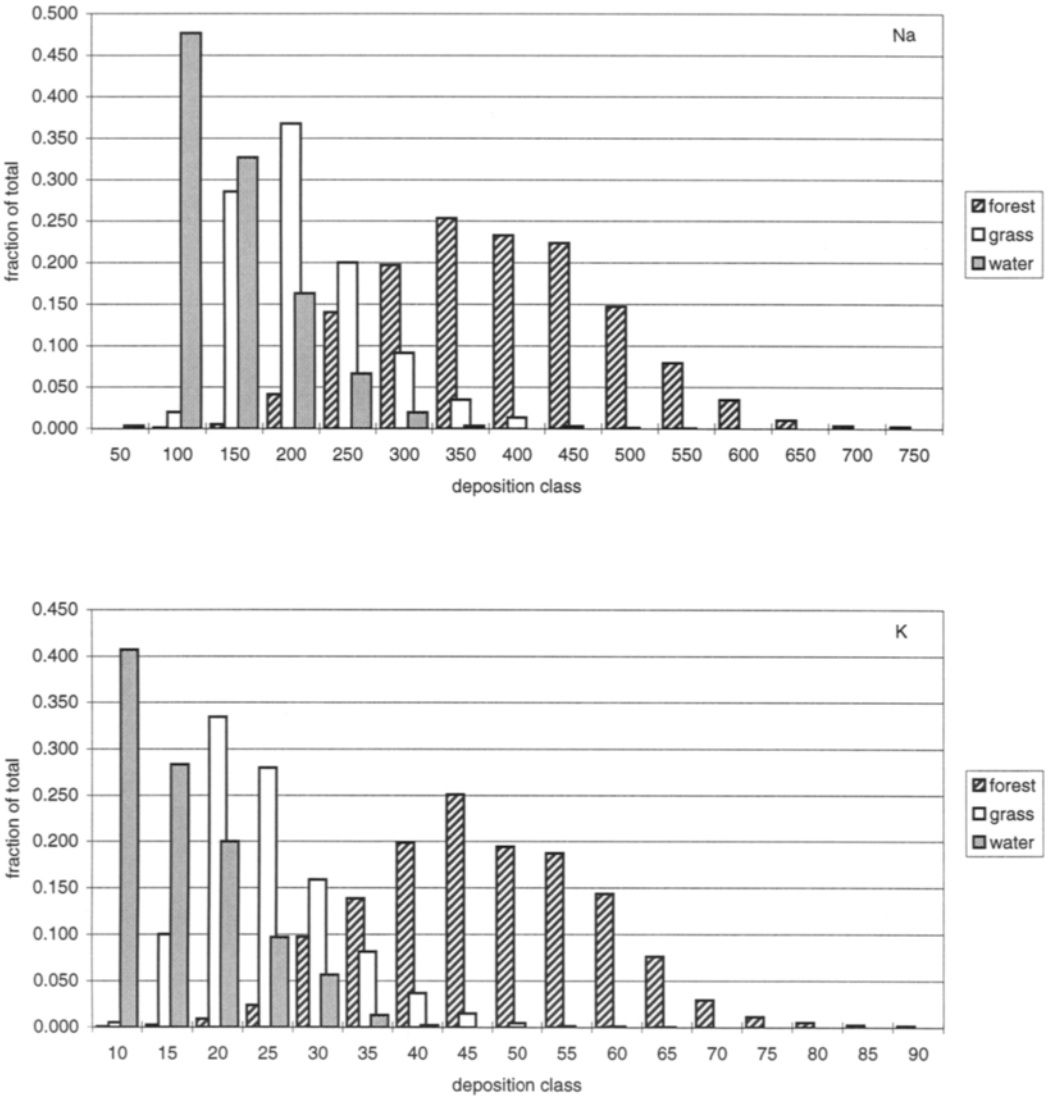


**FIGURE 5.10** Distribution of dry deposition distribution of $Na^+$ and $K^+$ to forest, grassland and water.

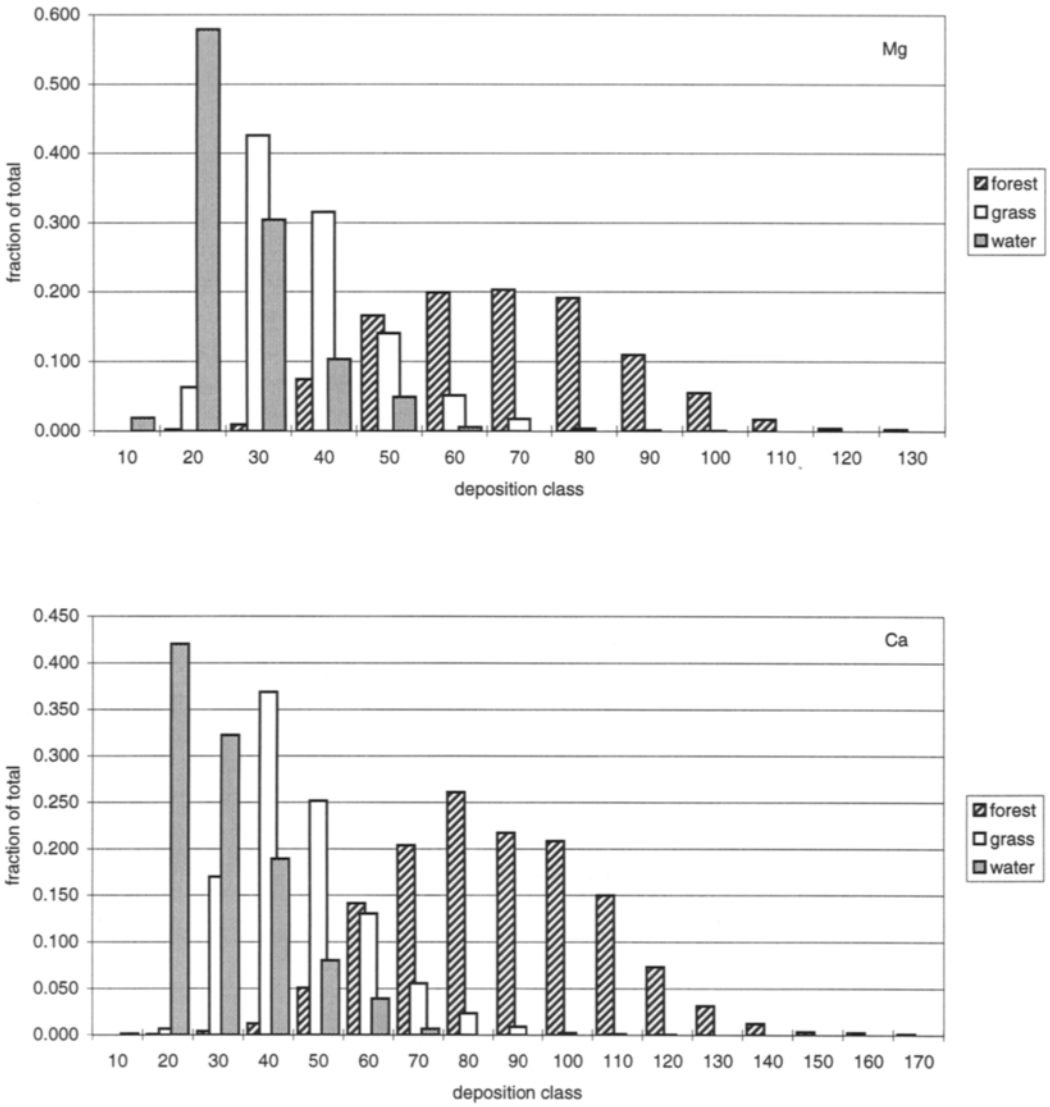


**FIGURE 5.10** *(continued)* Distribution of dry deposition $Mg^{2+}$ and $Ca^{2+}$ to forest, grassland and water.

## 5.2.4 TOTAL DEPOSITION

*Acidifying components*

Table 5.2 lists the dry, wet and total deposition of SOx, NOy, NHx, total nitrogen and total potential acid for each year averaged over the Netherlands. Figure 5.11 shows the variation in total deposition between 1980 and 1993. The deposition of total potential acid decreased from 7215 mol $ha^{-1}$ $a^{-1}$ in 1980 to 4280 mol $ha^{-1}$ $a^{-1}$ in 1993 (-41%). This decrease is mainly the result of the decrease in dry $SO_2$ deposition. The dry $NH_3$ deposition has gradually decreased since 1987, whereas NOy deposition has remained the same over the years. Wet deposition of SOx and NOy has decreased since 1980, whereas that of NHx has remained the same. Trends in wet deposition are lower than those in dry deposition. Over the years wet deposition has become more important in determining total input. This is due to completely different removal mechanisms and source origins. The spatial distribution of the deposition of SOx, NOy, NHx and total potential acid in 1980 and 1993 is shown in Figures 5.12 and 5.13, respectively.

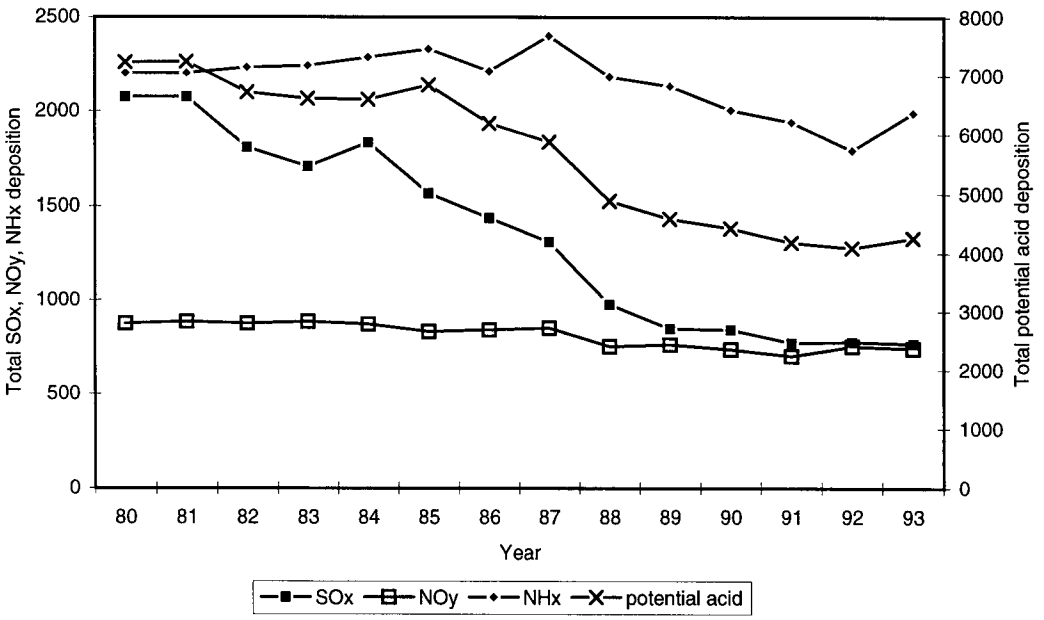


**FIGURE 5.11** Variation in total SOx, NOy, NHx and potential acid deposition between 1980 and 1993 (mol $ha^{-1}$ $a^{-1}$).

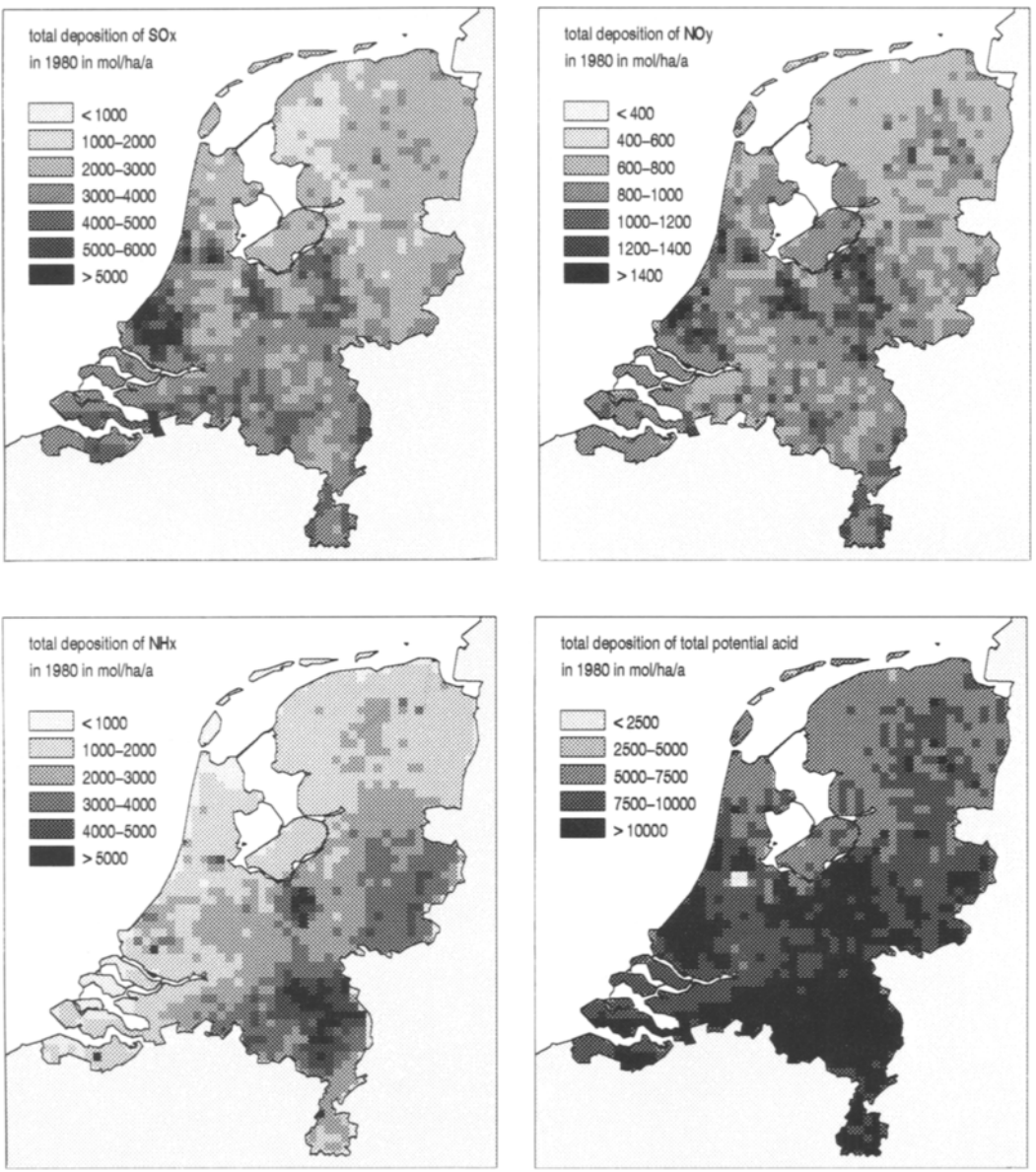


**FIGURE 5.12** The spatial distribution of the total deposition of SOx, NOy, NHx and potential acid in 1980 (mol $ha^{-1}$ $a^{-1}$).

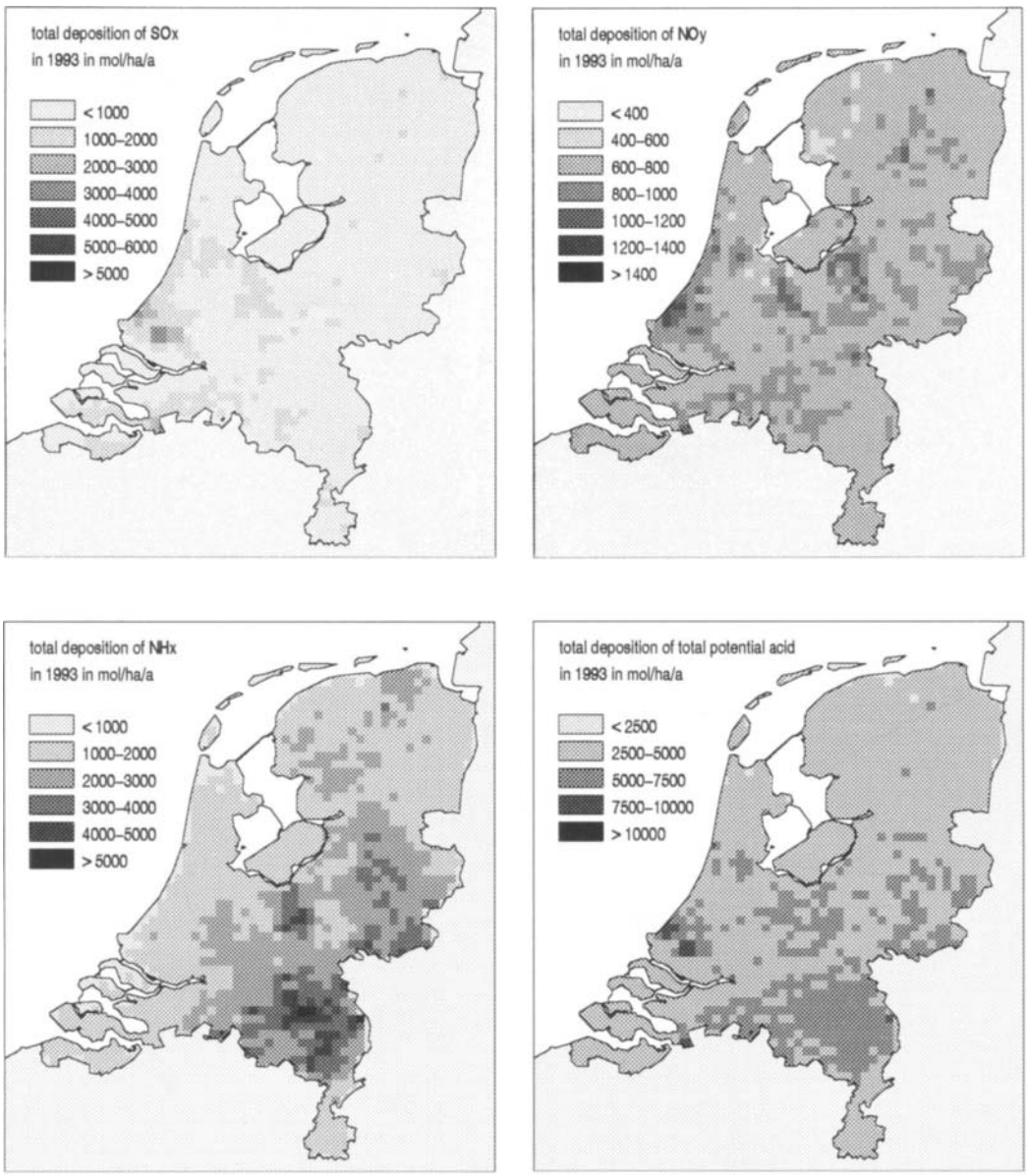


**FIGURE 5.13** The spatial distribution of the total deposition of SOx, NOy, NHx and total potential acid in 1993 (mol $ha^{-1}$ $a^{-1}$).

The deposition for each acidification area in 1980 and 1993 are listed in Tables 5.5 and 5.6, respectively. The total dry deposition accounts for about 68% of the total acid deposition in the Netherlands in 1993; the contribution of dry deposition of the respective components is 75% for SOx, 57% for NOy and 66% for NHx. Local variations are mainly due to variations in dry deposition. These variations are not always fully represented in the figures because of a smoothing introduced by the interpolation of the concentrations from different stations of the monitoring network, and the assumed lack of spatial variation of the $HNO_2$, $HNO_3$ and HCl concentrations, and $SO_4^{2-}$ and $NO_3^-$ aerosols.

**TABLE 5.5** Deposition of SOx, NOy, NHx, total nitrogen and potential acid for each acidification area in the Netherlands in 1980 (mol $ha^{-1}$ $a^{-1}$)

| Acidification area | SOx | | | NOy | | | NHx | | | N | | | Potential acid | | |
|---|---|---|---|---|---|---|---|---|---|---|---|---|---|---|---|
| | dry | wet | total | dry | wet | total | dry | wet | total | dry | wet | total | dry | wet | total |
| The Netherlands | 1750 | 320 | 2070 | 480 | 390 | 880 | 1565 | 640 | 2205 | 2045 | 1030 | 3075 | 5545 | 1670 | 7215 |
| Groningen | 1450 | 270 | 1720 | 410 | 350 | 770 | 955 | 590 | 1545 | 1365 | 940 | 2305 | 4265 | 1480 | 5745 |
| Friesland | 1160 | 230 | 1390 | 380 | 320 | 710 | 960 | 530 | 1490 | 1340 | 850 | 2190 | 3660 | 1310 | 4970 |
| Drenthe | 1510 | 290 | 1800 | 460 | 370 | 830 | 1210 | 620 | 1830 | 1670 | 990 | 2660 | 4690 | 1570 | 6260 |
| W/NE Overijssel | 1320 | 280 | 1600 | 420 | 400 | 820 | 1380 | 640 | 2020 | 1800 | 1040 | 2840 | 4440 | 1600 | 6040 |
| SE Overijssel | 1310 | 320 | 1630 | 460 | 380 | 850 | 2565 | 680 | 3245 | 3025 | 1060 | 4085 | 5645 | 1700 | 7345 |
| NW Gelderland | 1890 | 360 | 2250 | 620 | 420 | 1050 | 2150 | 790 | 2940 | 2770 | 1210 | 3980 | 6550 | 1930 | 8480 |
| NE Gelderland | 1430 | 350 | 1780 | 460 | 400 | 870 | 2695 | 760 | 3455 | 3155 | 1160 | 4315 | 6015 | 1860 | 7875 |
| S Gelderland | 2000 | 370 | 2370 | 560 | 410 | 970 | 1955 | 780 | 2735 | 2515 | 1190 | 3705 | 6515 | 1930 | 8445 |
| Utrecht | 2020 | 340 | 2360 | 610 | 410 | 1030 | 1740 | 660 | 2400 | 2350 | 1070 | 3420 | 6390 | 1750 | 8140 |
| N Noord-Holland | 1610 | 240 | 1850 | 430 | 400 | 830 | 595 | 430 | 1025 | 1025 | 830 | 1855 | 4245 | 1310 | 5555 |
| S Noord-Holland | 1800 | 290 | 2090 | 490 | 420 | 920 | 810 | 630 | 1440 | 1300 | 1050 | 2350 | 4900 | 1630 | 6530 |
| N Zuid-Holland, Flevopl | 2690 | 330 | 3020 | 590 | 420 | 1020 | 1375 | 550 | 1925 | 1965 | 970 | 2935 | 7345 | 1630 | 8975 |
| S Zuid-Holland | 2550 | 340 | 2890 | 510 | 420 | 940 | 1095 | 570 | 1665 | 1605 | 990 | 2595 | 6705 | 1670 | 8375 |
| Zeeland | 2010 | 350 | 2360 | 430 | 460 | 900 | 520 | 510 | 1030 | 950 | 970 | 1920 | 4970 | 1670 | 6640 |
| W Noord-Brabant | 2220 | 400 | 2620 | 470 | 370 | 850 | 1300 | 700 | 2000 | 1770 | 1070 | 2840 | 6210 | 1870 | 8080 |
| Mid-Noord-Brabant | 1940 | 400 | 2340 | 500 | 350 | 860 | 2185 | 720 | 2905 | 2685 | 1070 | 3755 | 6565 | 1870 | 8435 |
| NE Noord-Brabant | 1720 | 350 | 2070 | 500 | 360 | 860 | 3685 | 680 | 4365 | 4185 | 1040 | 5225 | 7625 | 1740 | 9365 |
| SE Noord-Brabant | 1930 | 340 | 2270 | 540 | 350 | 890 | 3225 | 660 | 3885 | 3765 | 1010 | 4775 | 7625 | 1690 | 9315 |
| N Limburg | 1880 | 350 | 2230 | 530 | 370 | 900 | 3845 | 690 | 4535 | 4375 | 1060 | 5435 | 8135 | 1760 | 9895 |
| S-Mid-Limburg | 1870 | 390 | 2260 | 520 | 450 | 980 | 1940 | 770 | 2710 | 2460 | 1220 | 3680 | 6200 | 2000 | 8200 |

**TABLE 5.6** Deposition of SOx, NOy, NHx, total nitrogen and potential acid deposition for each acidification area in the Netherlands in 1993 (mol $ha^{-1}$ $a^{-1}$)

| Acidification areas | SOx | | | NOy | | | NHx | | | N | | | Potential acid | | |
|---|---|---|---|---|---|---|---|---|---|---|---|---|---|---|---|
| | dry | wet | total | dry | wet | total | dry | wet | total | dry | wet | total | dry | wet | total |
| The Netherlands | 570 | 190 | 760 | 420 | 320 | 740 | 1320 | 680 | 2000 | 1740 | 1000 | 2750 | 2900 | 1380 | 4280 |
| Groningen | 480 | 120 | 590 | 370 | 340 | 700 | 1170 | 570 | 1740 | 1540 | 910 | 2440 | 2490 | 1140 | 3630 |
| Friesland | 380 | 110 | 480 | 330 | 320 | 660 | 1160 | 550 | 1710 | 1490 | 880 | 2370 | 2240 | 1090 | 3330 |
| Drenthe | 420 | 180 | 600 | 390 | 350 | 740 | 1040 | 620 | 1650 | 1420 | 970 | 2390 | 2270 | 1320 | 3590 |
| W/NE Overijssel | 380 | 190 | 570 | 370 | 340 | 720 | 1300 | 710 | 2020 | 1680 | 1060 | 2740 | 2430 | 1450 | 3880 |
| SE Overijssel | 470 | 230 | 700 | 410 | 360 | 780 | 1600 | 890 | 2490 | 2010 | 1260 | 3260 | 2950 | 1720 | 4670 |
| NW Gelderland | 510 | 220 | 730 | 500 | 330 | 830 | 1580 | 790 | 2370 | 2080 | 1120 | 3200 | 3110 | 1550 | 4660 |
| NE Gelderland | 400 | 240 | 640 | 380 | 360 | 750 | 2120 | 910 | 3030 | 2500 | 1280 | 3780 | 3300 | 1750 | 5060 |
| S Gelderland | 580 | 230 | 810 | 470 | 310 | 780 | 1610 | 790 | 2400 | 2080 | 1110 | 3190 | 3250 | 1570 | 4810 |
| Utrecht | 690 | 210 | 900 | 500 | 300 | 800 | 1560 | 620 | 2180 | 2050 | 920 | 2970 | 3430 | 1350 | 4780 |
| N Noord-Holland | 510 | 130 | 640 | 380 | 320 | 700 | 720 | 530 | 1250 | 1100 | 850 | 1950 | 2120 | 1110 | 3230 |
| S Noord -Holland | 670 | 190 | 860 | 410 | 320 | 730 | 720 | 640 | 1360 | 1130 | 960 | 2090 | 2470 | 1340 | 3810 |
| N Zuid-Holland, Flevopl | 1030 | 210 | 1240 | 570 | 300 | 870 | 1060 | 480 | 1540 | 1630 | 780 | 2400 | 3690 | 1200 | 4890 |
| S Zuid-Holland | 940 | 210 | 1160 | 490 | 300 | 790 | 890 | 510 | 1400 | 1380 | 810 | 2190 | 3260 | 1230 | 4500 |
| Zeeland | 780 | 190 | 970 | 410 | 270 | 680 | 510 | 570 | 1080 | 910 | 850 | 1760 | 2470 | 1220 | 3700 |
| W Noord-Brabant | 850 | 240 | 1080 | 460 | 310 | 770 | 1050 | 630 | 1690 | 1510 | 950 | 2460 | 3210 | 1420 | 4630 |
| Mid-Noord-Brabant | 640 | 260 | 900 | 470 | 330 | 800 | 1730 | 760 | 2490 | 2200 | 1090 | 3280 | 3480 | 1600 | 5080 |
| NE Noord-Brabant | 510 | 240 | 750 | 450 | 320 | 770 | 2460 | 920 | 3380 | 2910 | 1230 | 4150 | 3930 | 1700 | 5640 |
| SE Noord-Brabant | 610 | 240 | 850 | 450 | 320 | 770 | 2450 | 920 | 3370 | 2900 | 1240 | 4140 | 4130 | 1720 | 5840 |
| N Limburg | 560 | 230 | 790 | 440 | 310 | 750 | 2440 | 990 | 3430 | 2880 | 1310 | 4180 | 4000 | 1770 | 5770 |
| S Mid-Limburg | 550 | 190 | 750 | 400 | 280 | 690 | 1420 | 680 | 2100 | 1820 | 960 | 2780 | 2930 | 1350 | 4270 |

Highest deposition of potential acid, up to 15000 mol $ha^{-1}$ $a^{-1}$ in 1980 and up to 10000 mol $ha^{-1}$ $a^{-1}$ was found in the south of the country in 1993. In the centre of the country, where the largest forested area (the Veluwe) is located, deposition reaches similar values. This is the result of the relatively high roughness of the area but also of the large ammonia emission area situated to the west of the Veluwe (the Gelderse Vallei). The variability in spatial distribution of dry deposition is much more pronounced than that of wet deposition. Whereas the influence of $z_0$ on the deposition velocity is obvious, the influence on the flux is more complex. Regions with high $z_0$ values show significantly higher fluxes for SOx and NOy than, for example, agricultural areas. The $SO_2$ concentration pattern over the whole country happens to be positively correlated with areas having high $z_0$ values, enhancing the correlation between the flux and $z_0$. The highest NHx concentrations are found in the agricultural areas, where $NH_3$ emissions are high. There is a large-scale spatial correlation between concentrations of $NH_3$ and $z_0$. However, the relation of the NHx flux and $z_0$ on a small scale is not univocal because areas with the highest concentration (agricultural) show the smallest $z_0$ values.

The contribution of aerosol to the total deposition in the Netherlands was estimated in the Aerosol project (see also Chapter 2 and section 7.3). Average $SO_4^{2-}$ aerosol input in the

Netherlands is about 9% of the total dry SOx deposition. For forested areas the contribution is much higher; for deciduous forests it is 25% and for coniferous forests, 12%. For $NH_4^+$, these numbers are 24 and 27% respectively, and for $NO_3$, 27% and 29%. The contribution of aerosol deposition to the total deposition in the Netherlands is 7% for $SO_4^{2-}$, 11% for $NH_4^+$ and 9% for $NO_3^-$. For deciduous forests these numbers are 14, 15 and 17%, and for coniferous forests 10, 17 and 20%, respectively. It must be kept in mind that the figures for forests heavily depend on the location of forests to source areas and on forest structure characteristics. Furthermore, the estimates for aerosols and NHx are based on 5 x 5 km calculations.

Source contribution and origin of deposition

The source contribution and origin of deposition in the Netherlands is estimated using the TREND model (Van Jaarsveld, 1995; see also Heij and Schneider, 1991). The most accurate calculation of deposition in the Netherlands with the TREND model can be made for the years 1980 and 1993. For these years accurate estimates of emissions and locations of sources are available for the Netherlands and for Europe. The deposition values derived with the TREND model show a fairly good agreement with those calculated with DEADM (see section 6.2).

Relative contributions of foreign emissions per component and for the total deposition in 1980 and 1993 are show in Figure 5.14. In 1993, the Netherlands contributed almost 57% to the deposition in the Netherlands. The contributions to the deposition in the Netherlands of the surrounding countries (Great Britain, France, Belgium, and Germany) are more or less comparable.

Figure 5.15 shows the contribution of the different Dutch source categories to the total deposition and to the deposition of the different compounds for 1980 and 1993. The largest contribution among Dutch source categories to the total deposition in 1993 is from agriculture (61 %). Traffic is the largest contributor to the NOy deposition in the Netherlands. For SOx, industry, traffic and refineries contribute most to the deposition.

*Total base cation deposition*

Total deposition of base cations, as well as dry and wet deposition, are listed for each acidification area in Table 5.7. In contrast to the acidifying components, dry deposition of base cations is lower than the wet deposition flux. The total base cation flux averaged over the Netherlands relevant to the estimation of buffer capacities or critical loads of ecosystems ($K^+$ + $Ca^{2+}$ + $Mg^{2+}$) is 650 mol $ha^{-1}$ $a^{-1}$. The spatial distribution of $Na^+$, $K^+$, $Mg^{2+}$ and $Ca^{2+}$ deposition is given in Figure 5.16. The highest base cation fluxes are found on the north and west coasts of the country.

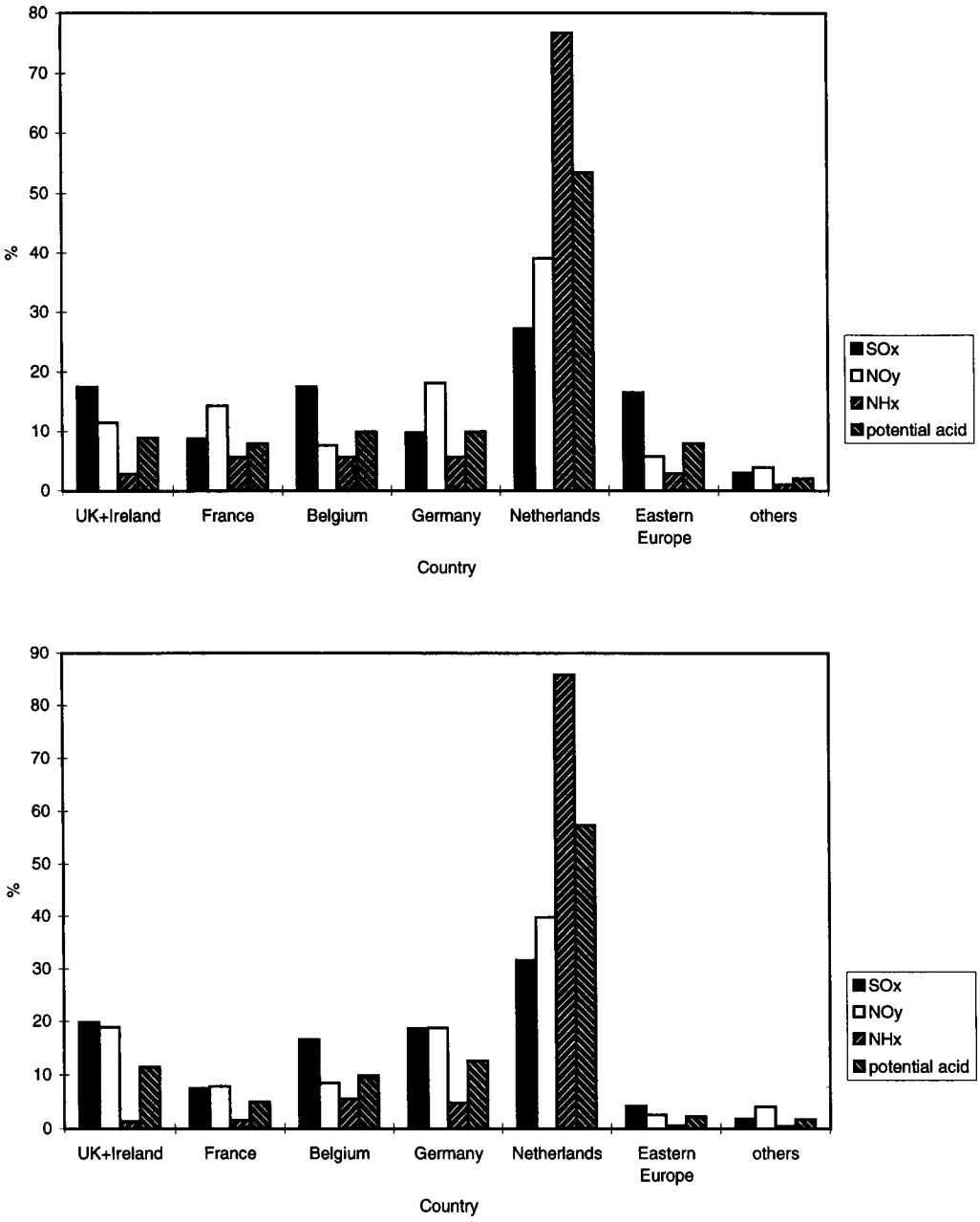


**FIGURE 5.14** Contribution of different countries to the deposition in the Netherlands (A) 1980 and (B) 1993.

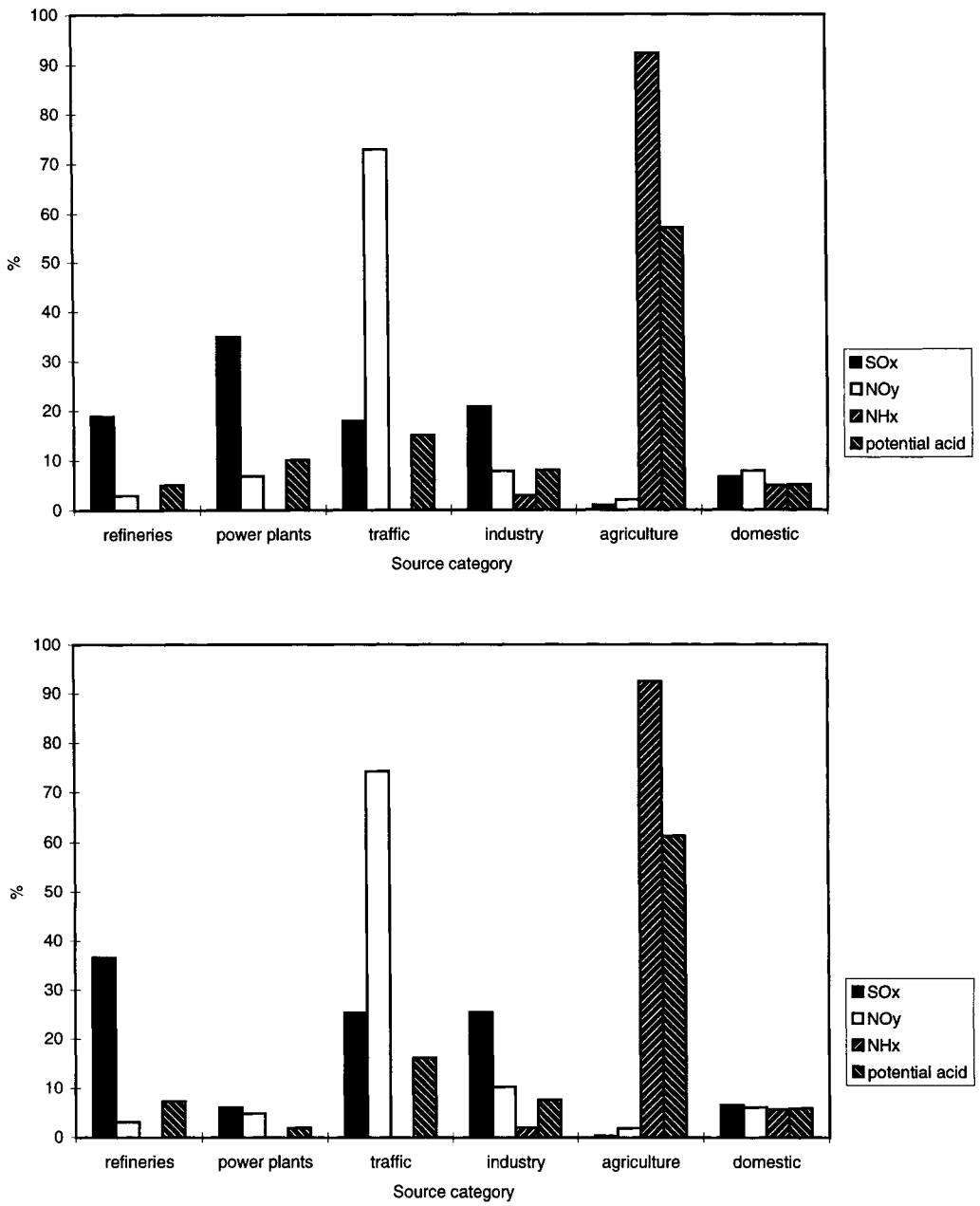


**FIGURE 5.15** Source category contribution to the deposition in the Netherlands (A) 1980 and (B) 1993.

**TABLE 5.7** Dry, wet and total deposition of base cations for each acidification area in the Netherlands in 1993 (mol $ha^{-1}$ $a^{-1}$)

| Acidification area | $Na^+$ | | | $K^+$ | | | $Mg^{2+}$ | | | $Ca^{2+}$ | | | $K^+$+$Ca^{2+}$+$Mg^{2+}$ | | |
|---|---|---|---|---|---|---|---|---|---|---|---|---|---|---|---|
| | dry | wet | total | dry | wet | total | dry | wet | total | dry | wet | total | dry | wet | total |
| The Netherlands | 230 | 690 | 910 | 10 | 40 | 50 | 40 | 80 | 120 | 50 | 130 | 180 | 190 | 460 | 650 |
| Groningen | 260 | 1010 | 1270 | 20 | 50 | 70 | 50 | 130 | 180 | 60 | 130 | 190 | 240 | 570 | 810 |
| Friesland | 230 | 1060 | 1290 | 10 | 50 | 60 | 40 | 130 | 170 | 50 | 130 | 180 | 190 | 570 | 760 |
| Drenthe | 230 | 760 | 1000 | 10 | 40 | 50 | 40 | 90 | 130 | 50 | 60 | 110 | 190 | 340 | 530 |
| W/NE Overijssel | 210 | 580 | 790 | 10 | 40 | 50 | 40 | 70 | 110 | 50 | 50 | 100 | 190 | 280 | 470 |
| SE Overijssel | 210 | 510 | 720 | 10 | 40 | 50 | 40 | 60 | 100 | 50 | 60 | 110 | 190 | 280 | 470 |
| NW Gelderland | 280 | 480 | 750 | 20 | 40 | 60 | 50 | 60 | 110 | 60 | 50 | 110 | 240 | 260 | 500 |
| NE Gelderland | 190 | 480 | 670 | 10 | 40 | 50 | 30 | 60 | 90 | 50 | 60 | 110 | 170 | 280 | 450 |
| S Gelderland | 230 | 500 | 730 | 10 | 40 | 50 | 40 | 60 | 100 | 50 | 60 | 110 | 190 | 280 | 470 |
| Utrecht | 250 | 600 | 850 | 20 | 40 | 60 | 40 | 80 | 120 | 50 | 120 | 170 | 200 | 440 | 640 |
| N Noord-Holland | 250 | 1080 | 1330 | 10 | 50 | 60 | 40 | 130 | 170 | 50 | 90 | 140 | 190 | 490 | 680 |
| S Noord-Holland | 250 | 620 | 870 | 10 | 40 | 50 | 40 | 80 | 120 | 50 | 70 | 120 | 190 | 340 | 530 |
| N Zuid-Holland, Flevopl | 280 | 860 | 1140 | 20 | 50 | 70 | 50 | 110 | 160 | 60 | 80 | 140 | 240 | 430 | 670 |
| S Zuid-Holland | 240 | 870 | 1100 | 10 | 60 | 70 | 40 | 110 | 150 | 50 | 80 | 130 | 190 | 440 | 630 |
| Zeeland | 210 | 790 | 1010 | 10 | 50 | 60 | 40 | 90 | 130 | 50 | 80 | 130 | 190 | 390 | 580 |
| W Noord-Brabant | 210 | 710 | 930 | 10 | 50 | 60 | 40 | 80 | 120 | 50 | 60 | 110 | 190 | 330 | 520 |
| Mid-Noord-Brabant | 210 | 520 | 720 | 10 | 40 | 50 | 40 | 60 | 100 | 50 | 60 | 110 | 190 | 280 | 470 |
| NE Noord-Brabant | 200 | 390 | 580 | 10 | 40 | 50 | 30 | 50 | 80 | 40 | 50 | 90 | 150 | 240 | 390 |
| SE Noord-Brabant | 200 | 350 | 540 | 10 | 40 | 50 | 30 | 40 | 70 | 50 | 50 | 100 | 170 | 220 | 390 |
| N Limburg | 180 | 290 | 470 | 10 | 40 | 50 | 30 | 40 | 70 | 40 | 50 | 90 | 150 | 220 | 370 |
| S/Mid-Limburg | 150 | 250 | 400 | 10 | 30 | 40 | 30 | 30 | 60 | 40 | 70 | 110 | 150 | 230 | 380 |

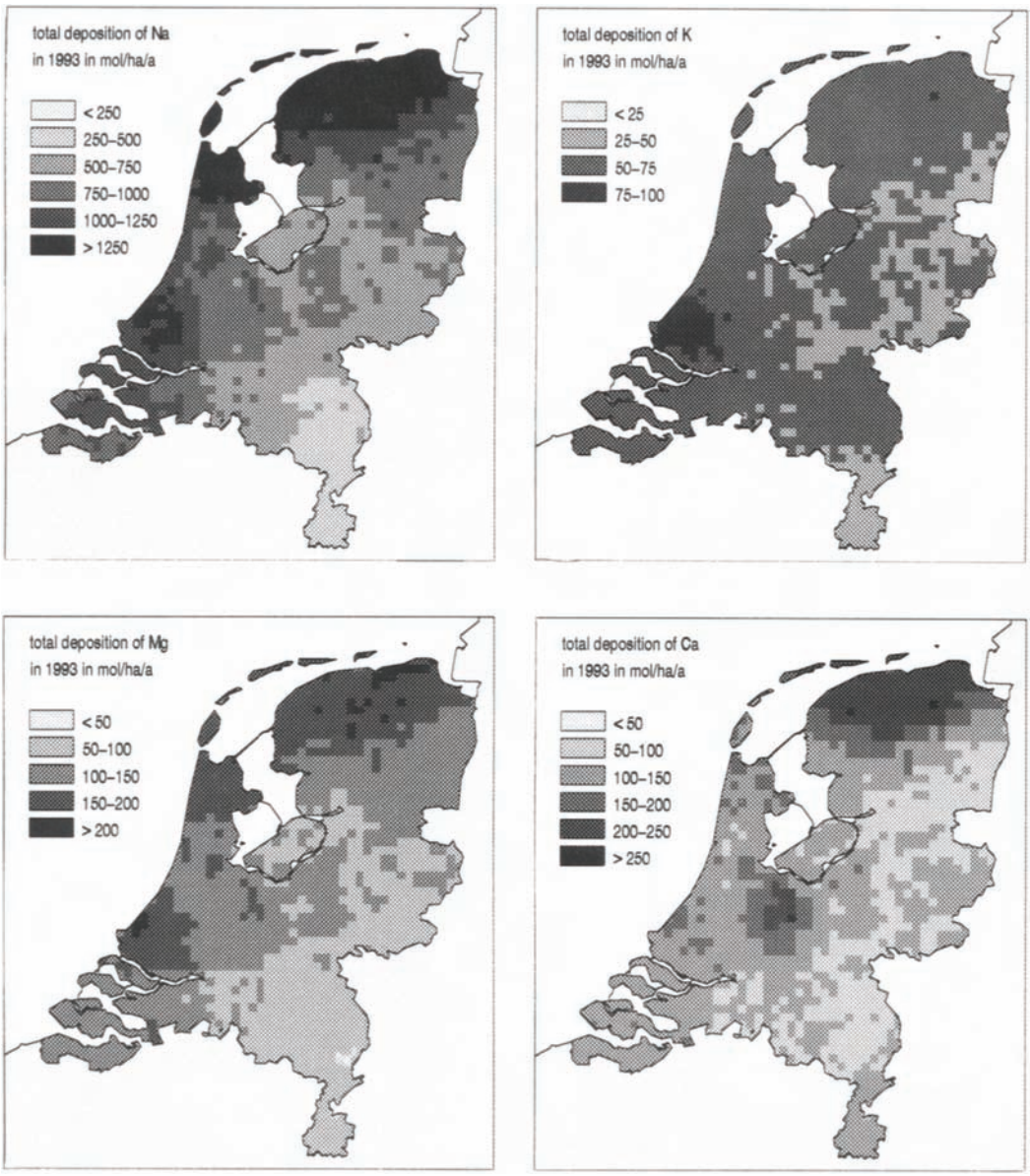


**FIGURE 5.16** The spatial distribution of the deposition of $Na^+$, $K^+$, $Mg^{2+}$ and $Ca^{2+}$ in 1993 (mol $ha^{-1}$ $a^{-1}$).

## 5.3 DEPOSITION MODELLING IN EUROPE

### 5.3.1 EDACS

The outline of the EDACS model to estimate local and regional scale deposition fluxes is presented in Figure 5.17. The basis for the two estimates is formed by calculations with the EMEP long-range transport model. With this model dry, wet and total deposition is estimated on a 150 x 150 km grid over Europe using emission maps for $SO_2$, NOx and $NH_3$ (Eliassen and Saltbones, 1983; Iversen *et al.*, 1991; Tuovinen *et al.*, 1994). The model results are used for estimating country-to-country budgets, as a basis of sulphur and nitrogen protocols, and for assessments. The local-scale approach used by RIVM depends strongly on LTRAP model results. Calculated ambient concentrations of the acidifying components (daily averages) and concentrations in precipitation (monthly averages) are used along with a detailed land-use map and meteorological observations to estimate small-scale dry deposition fluxes (Figure 5.17). By using calculated concentration maps, the relationship between emissions and deposition is maintained and scenario studies, budget studies and assessments can be carried out on different scales. Wet deposition is added to the dry deposition to estimate total local scale deposition in Europe. Wet deposition can either be obtained directly from the EMEP model, or from measurements made in Europe. The latter method is used here and will be described in the next section. The method for estimating dry deposition will be explained in section 5.3.3.

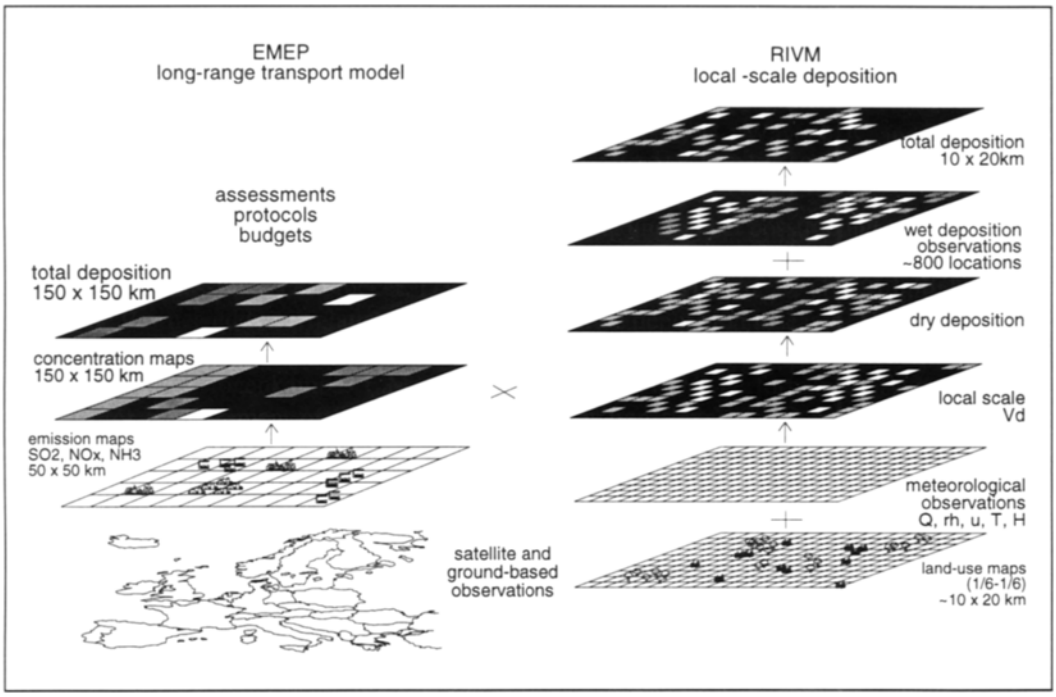


**FIGURE 5.17** Outline of method to estimate local scale deposition fluxes.

### 5.3.2 WET DEPOSITION

Up to now, wet deposition maps on a European scale are based on long-range transport model results (e.g. the EMEP model; Iversen *et al.*, 1991), whereas for most components wet deposition maps based on measurements are only available on national scales. Although wet deposition is not a small-scale process, the resolution of the maps based on models is, for effect-related studies (e.g. the determination of the exceedances of critical loads), generally too small (e.g. 150 x 150 km blocks for the EMEP model) in comparison with local variations in deposition. Maps derived from measurements solve this problem as the resolution of these maps can be larger. Additionally, these measurement-based maps can be used to evaluate the long-range transport models. The first wet deposition map of $NH_4^+$ in Europe based on measurements was compiled by Buijsman and Erisman (1988). Van Leeuwen *et al.* (1995) recently used measurements in Europe to estimate the wet deposition in Europe.

In this section concentration and wet deposition maps of non-marine sulphate, nitrate, ammonium, hydrogen, sodium, chloride, magnesium, potassium and calcium based on the work by Van Leeuwen *et al.* (1995) are presented. These components, based on results of field measurements made at approximately 750 locations (the number of locations differs per

component), are mapped on a 50 x 50 km scale over Europe for 1989. Point observations are interpolated to a field covering the whole of Europe using the Kriging interpolation technique. An extensive uncertainty analysis is performed to assess the quality of the maps.

*Data collection and data quality*

The composition of precipitation is monitored in collectors throughout almost the whole of Europe. Information on concentrations of ions in precipitation in 1989 was obtained from the EMEP database (European Monitoring and Evaluation Programme) and from organisations responsible for wet deposition monitoring in their countries. The map of sites is presented in Figure 5.18; a list of monitoring networks is given in Table 3.2. The figure shows that the measurement sites are not evenly spread over Europe. Not all elements were analysed at all sites: the acidifying components $SO_4^{2-}$, $NO_3^-$ and $NH_4^+$ were most frequently analysed. Concentrations measured with bulk samplers were corrected for the contribution of dry deposition onto the funnels of these samplers. Sulphate concentrations were corrected for the contribution of sea salt, because only non-marine sulphate contributes to the acidification process. By assuming that the ratio of sodium to sulphate in sea-spray is the same as in bulk sea water, and that all the sodium in a sample is of marine origin, it is possible to calculate non-marine sulphate. At about 200 sites only information about the sulphate concentration was available and the sodium concentration was not measured. At those sites interpolated values from the sodium map were used for correction.

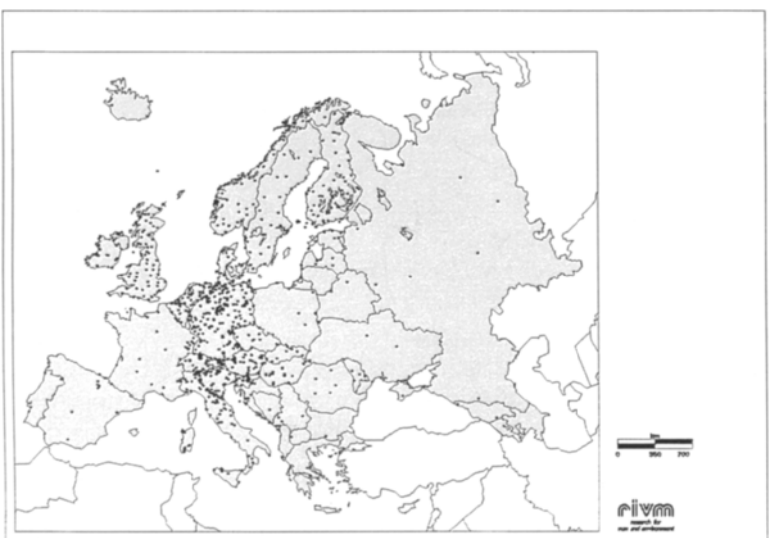


**FIGURE 5.18** Location of wet deposition monitoring sites in Europe.

To obtain an idea on the quality of the data, two checks were carried out. First, a check on the ionic balance of the samples was performed. Of the total 824 measurement sites, all ions studied were measured at 478. About 52% of the 478 samples showed an ionic imbalance > 10%, and 13%, > 25%. In some cases a surplus of cations was observed, while in others anions dominate. The quality of the data was also checked by constructing X-Y plots of two elements that were highly correlated, e.g. $NH_4$-$SO_4$, $NO_3$-$NH_4$, $SO_4$-$NO_3$, Na-Mg, Cl-Mg and Na-Cl. No large outliers were observed.

Because data were skewly distributed, they were transformed to their common logarithms. Spatial structures of the concentration data were analysed using geostatistics based on Regionalised Variable Theory (Matheron, 1965). This spatial analysis revealed autocorrelation in all ions and reasonable bonded models were fitted to the experimental variograms. Data were interpolated using the Kriging interpolation technique. Using this technique, it is assumed that the sample data satisfy the intrinsic hypothesis (Cressie, 1993). A cross validation procedure was carried out to investigate whether the fitted variogram models describe the spatial structure of the data correctly. Generally, results were found to be satisfactory.

*Interpolation*
Because concentrations in precipitation are less variable in space and time than precipitation amounts, interpolation was performed on concentration data instead of fluxes. To obtain wet deposition fluxes, interpolated concentrations were multiplied by long-term mean precipitation amounts compiled by EPA (Environmental Protection Agency, USA). To create maps of all ions, estimates of the concentrations were made on a regular grid of 50 x 50 km by ordinary block Kriging. In some regions of Europe the distance between measurement sites is too large to obtain interpolated fields covering the whole of Europe. In the maps this can be seen in the concentric circles around some data points. Interpolation proceeds until the maximum distance of spatial correlation is reached.

Concentration data originated mainly from 1989. Because concentrations and precipitation amounts are physically linked, in principle, only precipitation amounts from 1989 should be used. As precipitation amounts can vary very much over short distances, a number of several thousands of sites is necessary to describe the variation to a reasonable extent. Therefore actual data measured in 1989 were necessary. For this purpose, data from the Observational Data Set (ODS), which is a product of ECMWF (European Centre for Medium-range Weather Forecasts), were investigated. The ODS dataset contains 1297 measurement sites spread over Europe. At each site amounts of rainfall were measured every 6-hour period. Data are invalidated and therefore highly uncertain (Potma, 1993), making these data not considered suitable for providing a map on amounts of precipitation for Europe.

Another dataset with interpolated values of long-term annual mean amounts of precipitation, based on several thousands of measurements (Legates and Willmott, 1990) was used at

RIVM. This EPA map (compiled at the Environmental Protection Agency, USA) is based on validated monthly mean precipitation amounts measured from 1920 to 1980. Data were corrected for gauge-induced biases to remove systematic errors caused by wind, wetting on the interior walls of the gauge and evaporation from the gauge. These corrected values were interpolated to a 0.5 degree of longitude by 0.5 degree of latitude grid. Areas with large precipitation amounts in coastal regions and in mountainous areas (due to orographic effects) can be recognised. Investigated was whether systematic differences between 1989 (ODS) data and long-term average (EPA) data could be found (Van Leeuwen *et al.*, 1995). As this did not happen, EPA data were used instead to determine wet deposition fluxes.

*Description of spatial patterns*

Several maps are presented in this section. These are flux maps of $SO_4^{2-}$ (Figure 5.19), $NO_3^-$ (Figure 5.20), $NH_4^+$ (Figure 5.21), $H^+$ (Figure 5.22) and total base cations ($Mg^{2+}$, $Ca^{2+}$ and $K^+$) (Figure 5.23), as well as concentration maps of $Na^+$ (Figure 5.24), $Cl^-$ (Figure 5.25), $Mg^{2+}$ (Figure 5.26), $Ca^{2+}$ (Figure 5.27) and $K^+$ (Figure 5.28). The non-marine sulphate, nitrate, ammonium and hydrogen maps clearly resemble European emission and climate patterns. Large emission sources can be recognised in the concentration maps, whereas in the flux maps climate patterns and orographic effects are also observed. In mountainous areas large fluxes due to orographic rains can be seen. Especially in former Yugoslavia the large long-term mean precipitation cause large fluxes in all flux maps. Besides originating from large amounts of rainfall, large fluxes can also arise from high concentrations in precipitation.

Considering the non-marine sulphate maps, large fluxes (400-1000 mol $ha^{-1}$ $a^{-1}$) can be observed in Eastern and Central Europe (Germany, Poland, Czech and Slovak Republics, Austria, Hungary, northern Italy, The Ukraine and former Yugoslavia). Large sulphate concentrations are mainly caused by $SO_2$ emissions from industry and power stations. Concentrations and fluxes obtained in Turkey should be interpreted with care, as they are not based on measurements in Turkey itself but are solely the result of interpolation (in this case extrapolation) from surrounding countries. Nitrate arises mainly from $NO_X$ emissions from industry, power stations and motor vehicle exhausts (i.e. burning processes). Spatial patterns in the nitrate maps resemble patterns found in the sulphate maps, but this time also in the Netherlands and southern Scandinavia rather large fluxes are observed (300-700 mol $ha^{-1}$ $a^{-1}$). Again, large concentrations can be observed in the Black Triangle. In Russia nitrate concentrations and fluxes are low compared to sulphate concentrations and fluxes. Ammonia emissions arise mainly from livestock wastes, with smaller contributions from fertiliser application and the fertiliser-producing industry. Largest ammonium fluxes (400-1000 mol $ha^{-1}$ $a^{-1}$) can therefore be observed in or near areas with intensive agricultural land use, e.g. Central Europe. In the Netherlands, for example, high ammonium fluxes are found due to intensive livestock breeding in this country.

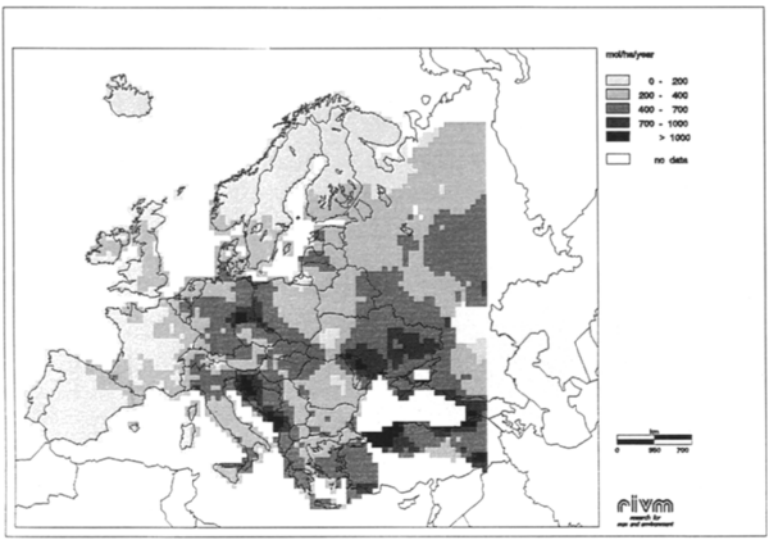


**FIGURE 5.19** Wet deposition of $SO_4^{2-}$ in Europe on a 50 x 50 km basis in 1989 in mol $ha^{-1}$ $a^{-1}$ (Van Leeuwen *et al.*, 1995).

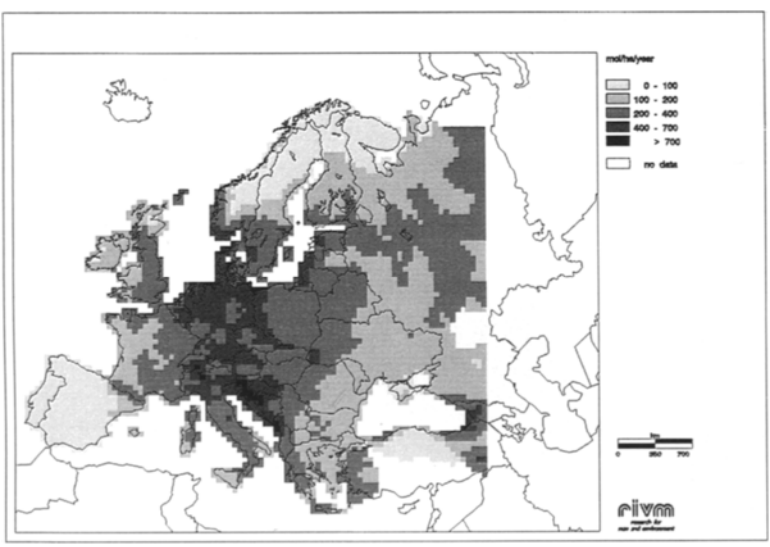


**FIGURE 5.20** Wet deposition of $NO_3^-$ in Europe on a 50 x 50 km basis in 1989 in mol $ha^{-1}$ $a^{-1}$ (Van Leeuwen *et al.*, 1995).

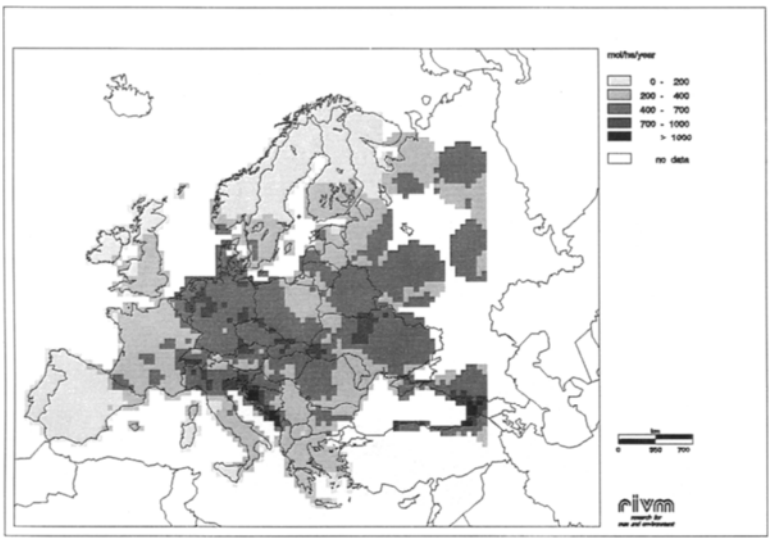


**FIGURE 5.21** Wet deposition of $NH_4^+$ in Europe on a 50 x 50 km basis in 1989 in mol $ha^{-1}$ $a^{-1}$ (Van Leeuwen *et al.*, 1995).

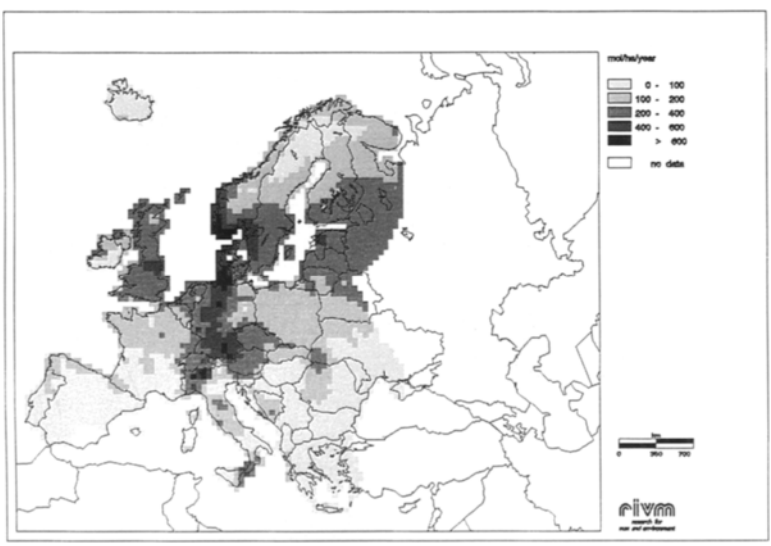


**FIGURE 5.22** Wet deposition of $H^+$ in Europe on a 50 x 50 km basis in 1989 in mol $ha^{-1}$ $a^{-1}$ (Van Leeuwen *et al.*, 1995).

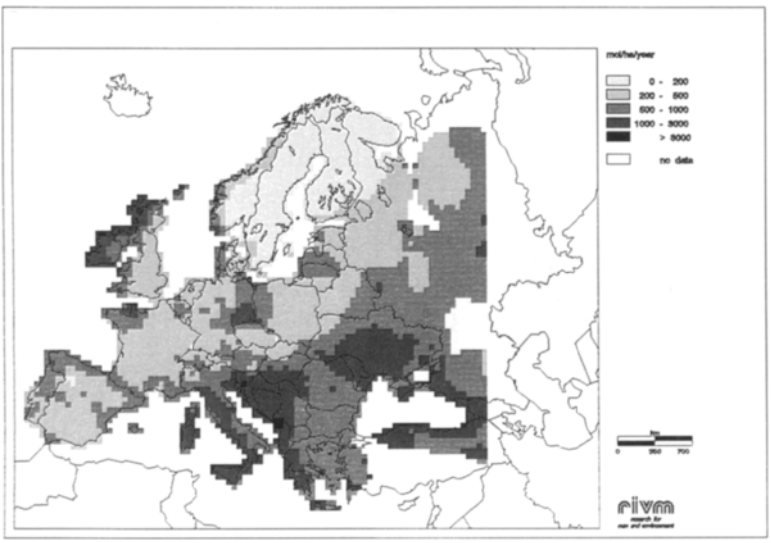


**FIGURE 5.23** Wet deposition of total base cations ($Ca^{2+}$, $Mg^{2+}$ and $K^{+}$) in Europe on a 50 x 50 km basis in 1989 in mol $ha^{-1}$ $a^{-1}$ (Van Leeuwen *et al.*, 1995).

In the hydrogen ion concentration map the largest acidity can be found in a small zone ranging from southern Scandinavia to northern Italy (Po Valley) and in Great Britain. The hydrogen ion concentration is a balancing term corresponding to the concentrations of the other three ions and is not related to any single factor. Lowest fluxes for all four components (< 200 mol $ha^{-1}$ $a^{-1}$) can be found in northern Scandinavia, the Iberian Peninsula, and, to a lesser extent, France and Great Britain (except for the hydrogen ion). Note the spatial patterns of non-marine sulphate, nitrate and ammonium concentrations in Great Britain. The pattern clearly resembles increasing concentrations in eastern part of the country due to the influence of industry in the Midlands and the dominating westerly winds.

For base cations, a division can be made between components of marine origin (sodium, chloride and magnesium) and other elements (potassium and calcium), mainly originating from soils, agricultural activities, road dust and industry, as well as from marine sources. A clear pattern of decreasing fluxes with increasing distance to seas, in particular the Atlantic Ocean, can be observed for the elements of marine origin. This pattern is most distinct for sodium and chloride, especially along the Irish coast and the north coast of Great Britain, where fluxes are larger than 3000 mol $ha^{-1}$ $a^{-1}$, caused by the combined effect of large concentrations with large precipitation amounts. The remainder of the European continent shows a fairly homogeneous pattern (fluxes varying from 0 to 800 mol $ha^{-1}$ $a^{-1}$). The spatial variation in the magnesium fluxes is somewhat more differentiated than the variation in the

sodium and chloride fluxes. Besides near seas, large magnesium fluxes (> 100 mol $ha^{-1}$ $a^{-1}$) can be observed in Hungary, The Ukraine and the former Soviet Union due to large concentrations. Note that the interpolated field in the former Soviet Union is based on only a few measurements. The potassium concentration and flux maps show homogeneous spatial variation almost all over Europe (fluxes varying between 0-75 mol $ha^{-1}$ $a^{-1}$). Large fluxes (200-500 mol $ha^{-1}$ $a^{-1}$) due to large concentrations can be observed in Ukraine and due to large rainfall amounts in Ireland and Great Britain. In the Ukraine large magnesium and calcium concentrations, and fluxes, can also be found. Particularly for calcium, this may be caused by the influence of locally emitted soil dust (especially in areas with alkaline soils), transport of desert dust from the Sahara and emissions of fly ash from the cement and concrete-processing industry. Besides in the Ukraine, the largest calcium fluxes (400-800 mol $ha^{-1}$ $a^{-1}$) are found in Italy, Hungary and the Black Triangle. Calcium fluxes are lowest (0-100 mol $ha^{-1}$ $yr^{-1}$) in Great Britain and Scandinavia.

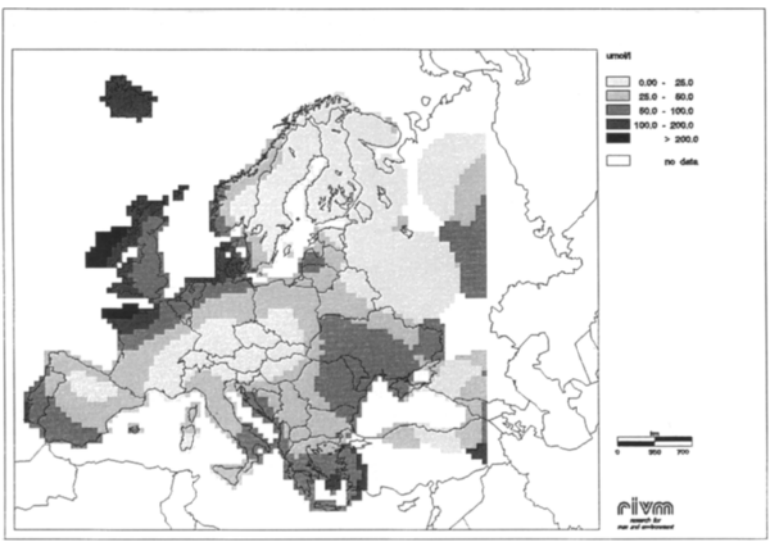


**FIGURE 5.24** Concentration of $Na^+$ in Europe on a 50 x 50 km basis in 1989 in µmol $l^{-1}$ (Van Leeuwen *et al.*, 1995).

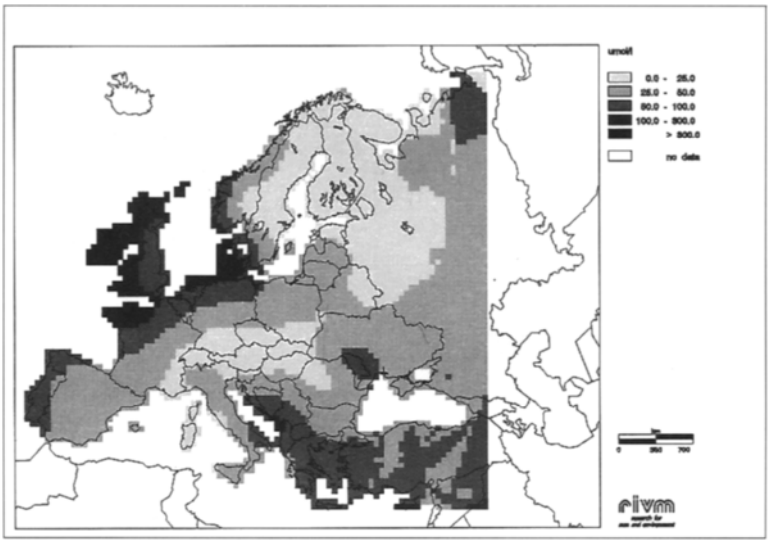


**FIGURE 5.25** Concentration of $Cl^-$ in Europe on a 50 x 50 km basis in 1989 in µmol $l^{-1}$ (Van Leeuwen *et al.*, 1995).

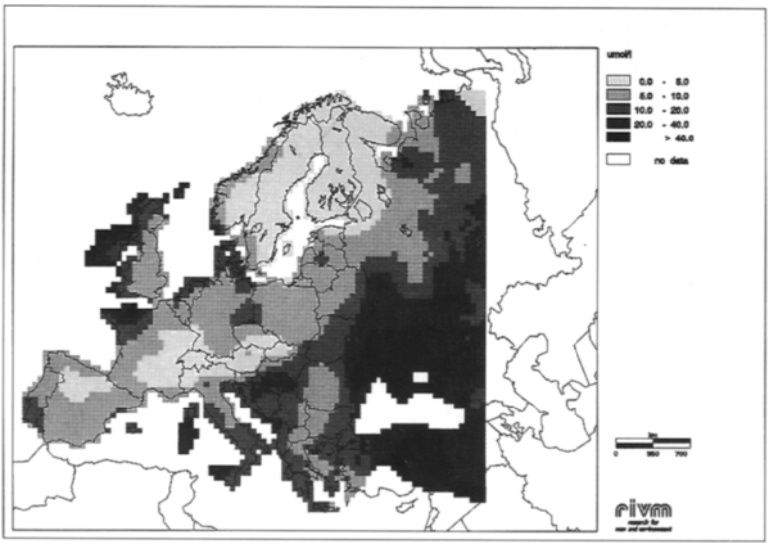


**FIGURE 5.26** Concentration of $Mg^{2+}$ in Europe on a 50 x 50 km basis in 1989 in µmol $l^{-1}$ (Van Leeuwen *et al.*, 1995).

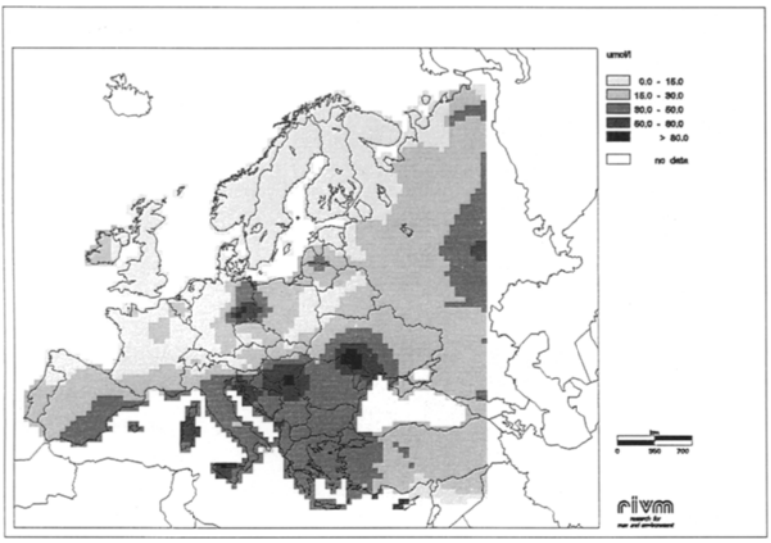


**FIGURE 5.27** Concentration of $Ca^{2+}$ in Europe on a 50 x 50 km basis in 1989 in µmol $l^{-1}$ (Van Leeuwen *et al.*, 1995).

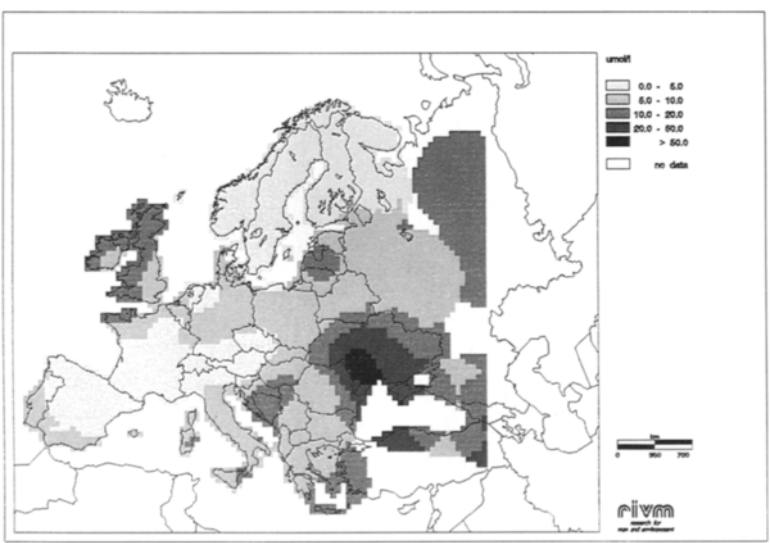


**FIGURE 5.28** Concentration of $K^+$ in Europe on a 50 x 50 km basis in 1989 in µmol $l^{-1}$ (Van Leeuwen *et al.*, 1995).

## 5.3.3 DRY DEPOSITION

*Acidifying components*

The method for dry deposition has been developed by Van Pul *et al.* (1992; 1994; 1995). Details can be found in these references. It is based on that used for the Netherlands and modelled in DEADM (Erisman, 1992; 1993a; see section 5.2.1). The main difference is that DEADM uses concentration measurements to determine the concentration distribution over the country (except for $NH_3$), while in EDACS, modelled concentrations are used. Dry deposition is inferred from the combination of long-range transport model concentrations provided by EMEP and parametrised dry deposition velocities (Hicks *et al.*, 1987; Van Pul *et al.*, 1995). Concentrations at 50 m above the surface (blending height) are used. At this height it is assumed that concentrations and meteorological parameters are not influenced by surface properties to a large extent. Dry deposition velocities of gases and particles at this height are calculated on a small scale using a land-use map, routinely available meteorological data and the inferential technique (Erisman *et al.*, 1994; Van Pul *et al.*, 1995) Resistances are modelled using observations for meteorological parameters in Europe and parametrisation of surface exchange processes. Parametrisations of the surface resistance used for different receptor surfaces and pollution climates in Europe were described in Chapter 4. Meteorological parameters are obtained from the ODS (Observational Data Set: Potma, 1994) every 6 h and interpolated over Europe on a $1/6^0$ x $1/6^0$ grid. Meteorological parameters consist of wind speed, friction velocity, radiation, temperature, humidity and precipitation.

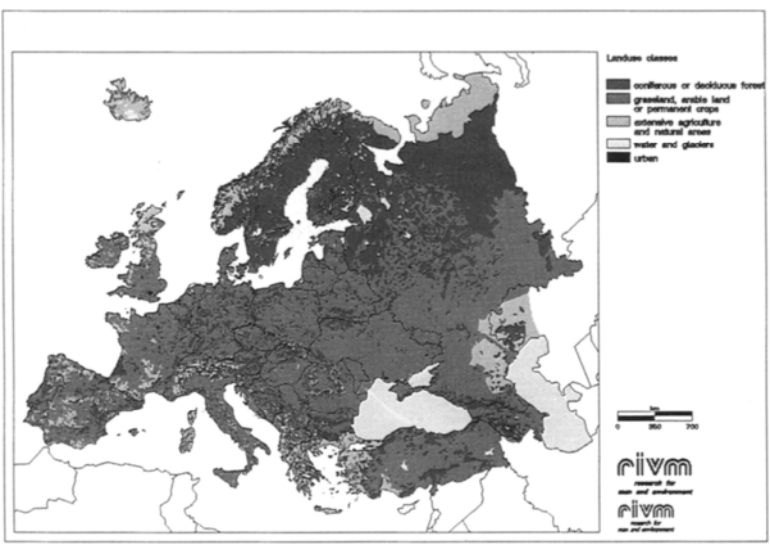


**FIGURE 5.29** Land-use map on a $1/6^0$ x $1/6^0$ grid of Europe (Van Velde, 1994).

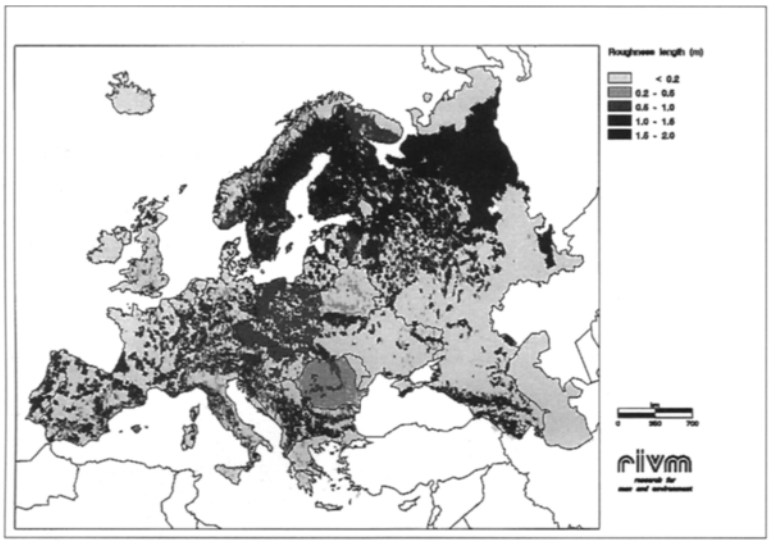


A

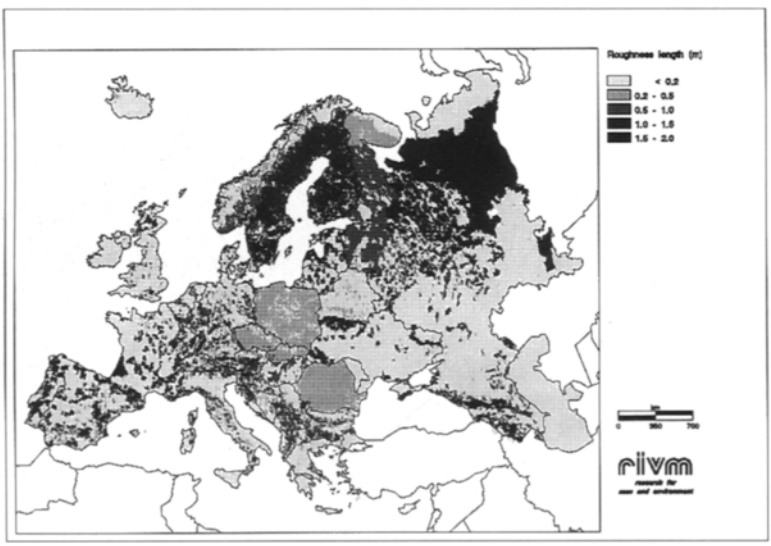


B

**FIGURE 5.30** Summer (A) and winter (B) roughness length map of Europe on a $1/6^0$ x $1/6^0$ grid (in cm) (after Van Pul *et al.*, 1995).

The land-use map for Europe, based on a $1/6^0$ x $1/6^0$ (ca. 10 x 20 km), is constructed by RIVM from ground-based and satellite observations (Van Velde *et al.*, 1994). The map is shown in Figure 5.29. Figure 5.30 shows roughness length maps for the summer and winter seasons as derived from the land-use map. These maps were estimated according to the method described in section 5.2.2. The roughness length is used for estimating atmospheric transport to the surface. For each land-use class, the coverage within a grid cell and the deposition velocity are calculated. The average deposition velocity for a grid cell is then calculated by weighting the land-use specific deposition velocities with the surface area within that specific grid cell. Site-specific dry deposition might be calculated likewise, provided that detailed land-use and surface-roughness data of the site is available. Here aggregated estimates are presented.

Figure 5.31 to 5.33 show maps of the annual average dry deposition on a $1/6^0$ x $1/6^0$ scale of NOy, NHx and SOx in Europe. The effect of land use (roughness) and the difference in $V_d$ is clearly shown. In areas with forested terrain (see Figure 5.29) the dry deposition is increased relative to the EMEP values, and, for example, in dry areas, the dry deposition is decreased as a result of a difference in $V_d$ estimates. There is a clear sub-grid effect. The variation in dry deposition within EMEP grids is determined by variation in land use. This is the result of a variation in the resistance due to atmospheric transport due to differences in roughness (see Figure 5.29), or of a variation of the surface resistance due to differences in vegetation and surface conditions.

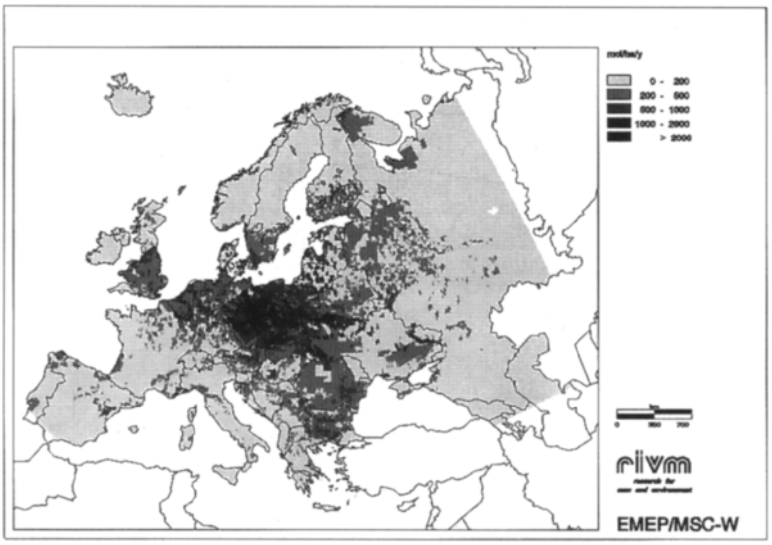


**FIGURE 5.31** Dry deposition of SOx in Europe on a $1/6^0$ x $1/6^0$ scale in mol $ha^{-1}$ $a^{-1}$ (Van Pul *et al.*, 1995)

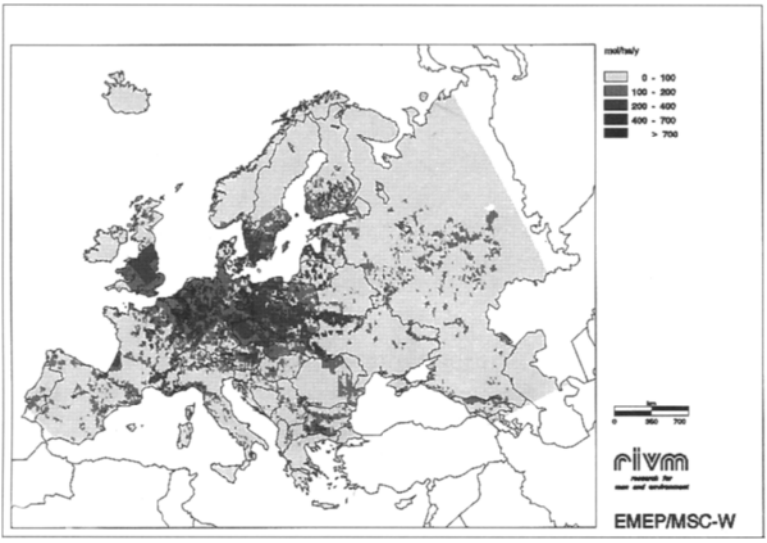


**FIGURE 5.32** Dry deposition of NOy in Europe on a $1/6^0$ x $1/6^0$ scale in mol $ha^{-1}$ $a^{-1}$ (Van Pul *et al.*, 1995)

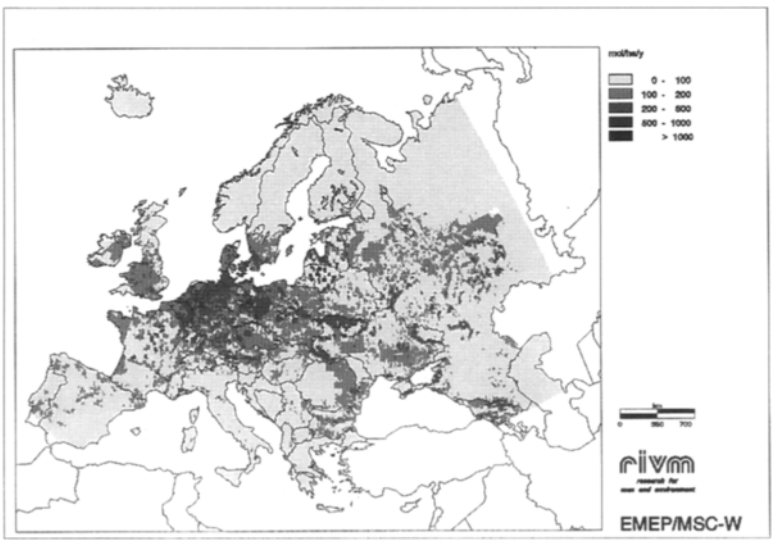


**FIGURE 5.33** Dry deposition of NHx in Europe on a $1/6^0$ x $1/6^0$ scale in mol $ha^{-1}$ $a^{-1}$ (Van Pul et al., 1995)

*Dry base cation deposition*

The EDACS model is used to estimate the dry deposition of base cations in Europe. The dry deposition velocity is calculated for each land use class within the 1/6 x 1/6° grid cells for every six hours and averaged over the year. The deposition velocity is parametrised using the equations given in section 4.2.2. As is the case for the Netherlands, there is a serious lack of measured and modelled base cation concentrations in Europe. Therefore, the same method to estimate concentrations is used as that for the Netherlands (see section 5.2.3). The annual average base cation concentration maps are derived from the interpolated precipitation concentration maps given in Figure 5.24, 5.26, 5.27 and 5.28, and scavenging ratios of Eder and Dennis (1990) extended with the Speulder forest data. Correlations in time are not taken into account, because only annual data are available. Dry deposition maps of $Na^+$, $Ca^{2+}$, $Mg^{2+}$ and $K^+$ are given in Figure 5.34 to 5.37. Figure 5.38 gives the total dry deposition of base cations ($Mg^{2+}$+$Ca^{2+}$+$K^+$), which is relevant for estimating critical loads. The spatial variation of the dry deposition of $Na^+$, $Ca^{2+}$, $Mg^{2+}$ and $K^+$ is similar to that of precipitation concentrations. However, the influence of roughness is clearly shown in the figures. Data have not been compared with measurements because these first estimates for the small scale of Europe have been finished two minutes before printing this book. However, a quick glance at the data representative for the Speulder forest and some other sites in Europe shows that the agreement is reasonably good!

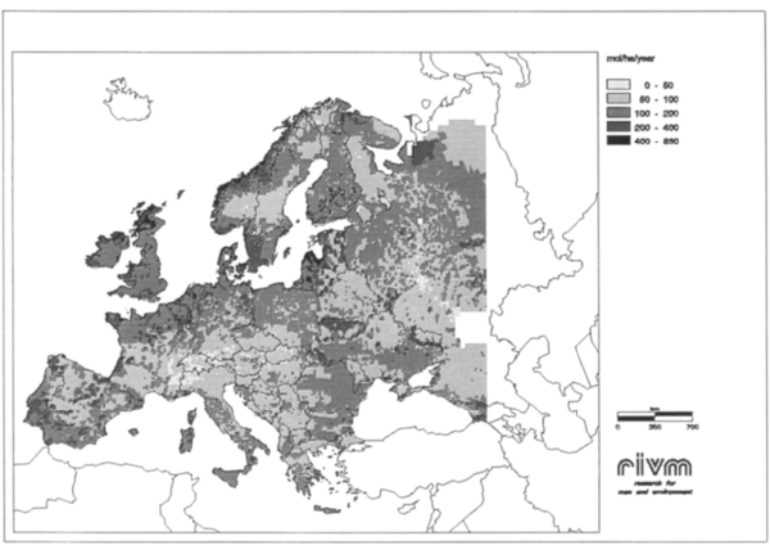


**FIGURE 5.34** Dry deposition of $Na^+$ in Europe on a 1/6 x 1/6° scale in mol $ha^{-1}$ $a^{-1}$.

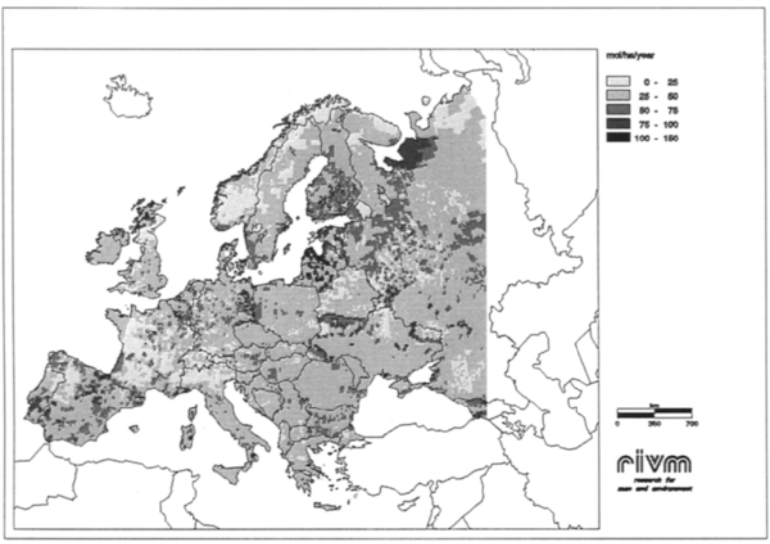


**FIGURE 5.35** Dry deposition of $Ca^{2+}$ in Europe on a 1/6 x 1/6° scale in mol $ha^{-1}$ $a^{-1}$.

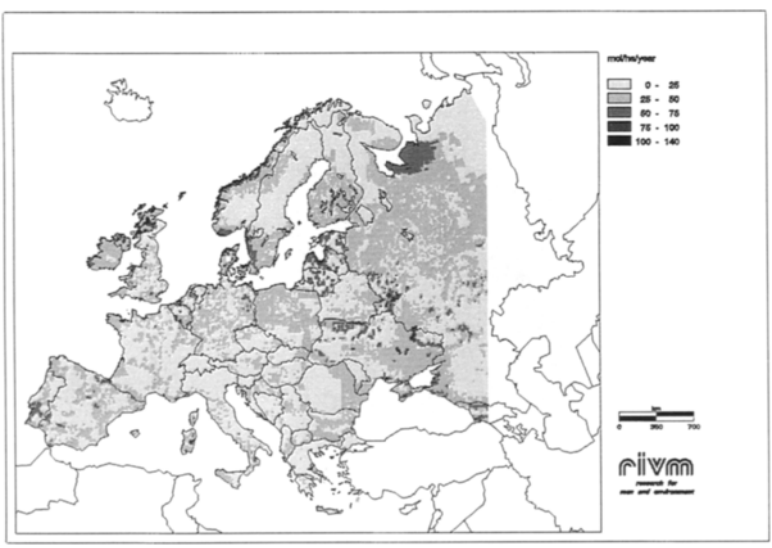


**FIGURE 5.36** Dry deposition of $Mg^{2+}$ in Europe on a 1/6 x 1/6° scale in mol $ha^{-1}$ $a^{-1}$.

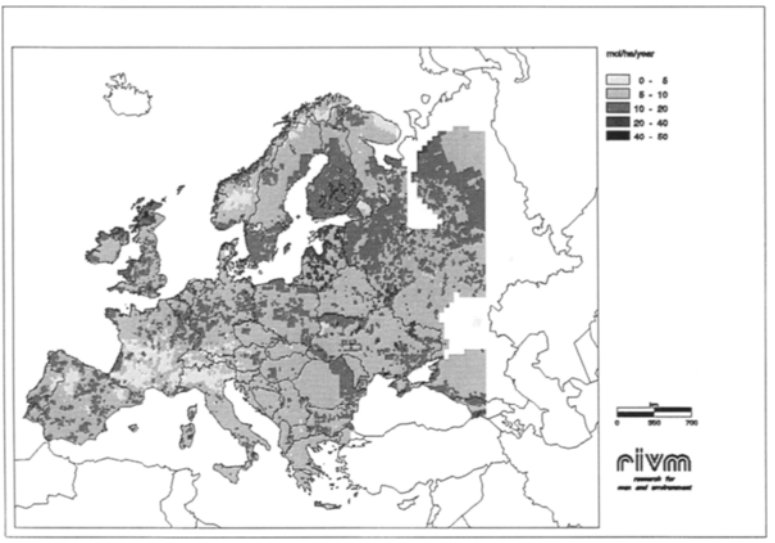


**FIGURE 5.37** Dry deposition of $K^+$ in Europe on a 1/6 x 1/6° scale in mol $ha^{-1}$ $a^{-1}$.

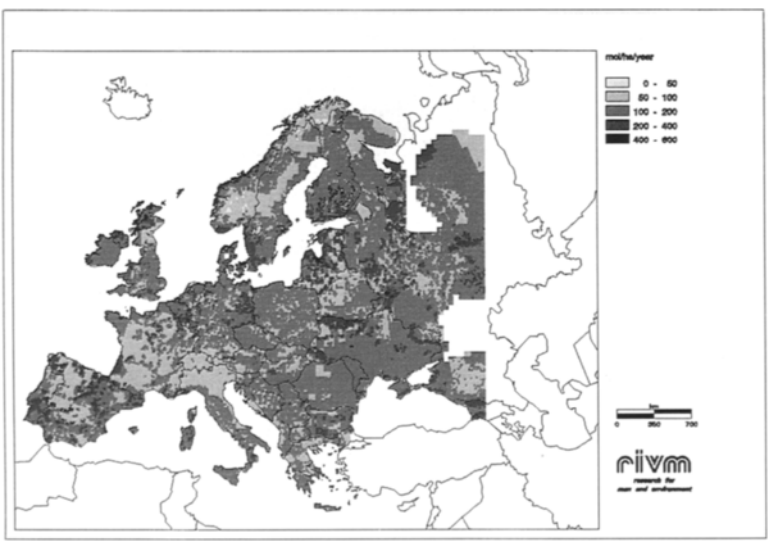


**FIGURE 5.38** Dry deposition of base cations ($Mg^{2+}$+$Ca^{2+}$+$K^+$) in Europe on a 1/6 x 1/6° scale in mol $ha^{-1}$ $a^{-1}$.

## 5.3.4 TOTAL DEPOSITION

*Acidifying components*

Total deposition of these components is given in Figures 5.39 to 5.41. Highest deposition of total sulphur occurs in the 'Black Triangle'. Relatively high sulphur fluxes are also found in parts of the Ukraine and former Yugoslavia. The highest deposition of total nitrogen is observed for the area including northern France, Belgium, The Netherlands, Germany, the Czech and Slovak Republics and Poland. Lower depositions are found over southwestern Europe, Ireland and northern Scandinavia. High deposition of oxidised nitrogen (>0.7 g N $m^{-2}$ $a^{-1}$) is found in an area mainly covering the Netherlands, Germany and large parts of Poland, whereas high deposition of reduced nitrogen is also found over large parts of Ireland, Great Britain, France and Eastern Europe.

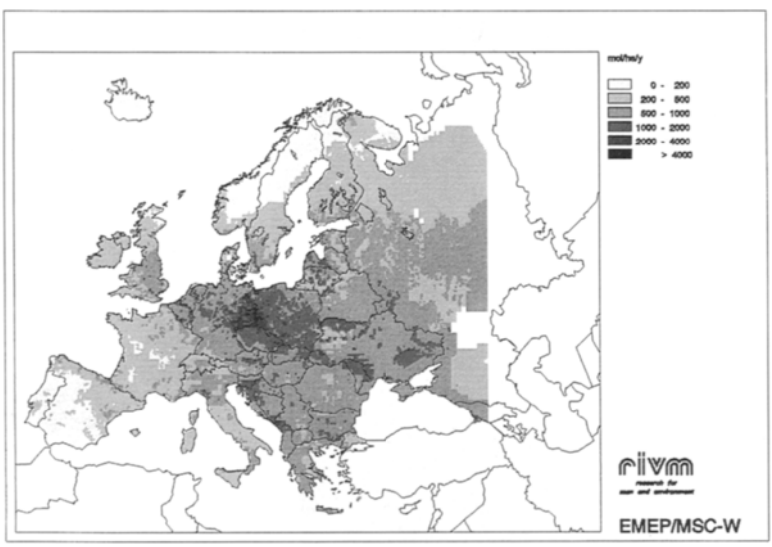


**FIGURE 5.39** Total deposition of SOx in Europe on a 1/6 x 1/6° scale in mol $ha^{-1}$ $a^{-1}$ (Van Pul *et al.*, 1995)

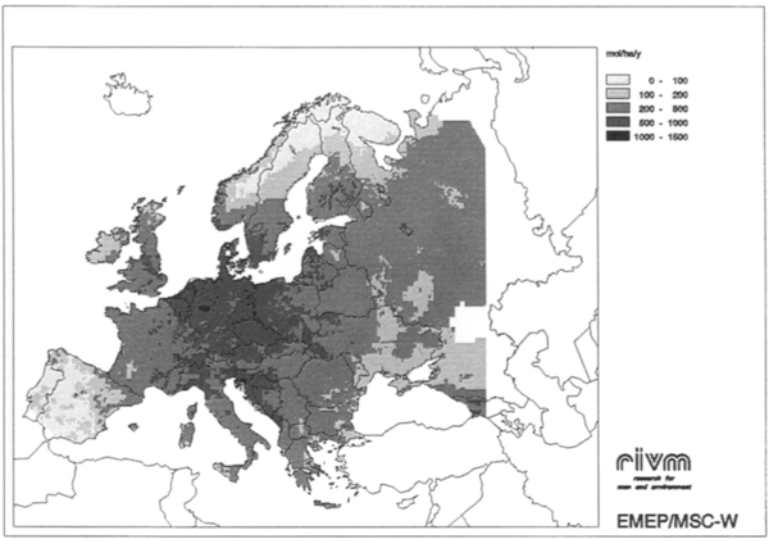


**FIGURE 5.40** Total deposition of NOy in Europe on a 1/6 x 1/6° scale in mol $ha^{-1}$ $a^{-1}$ (Van Pul *et al.*, 1995)

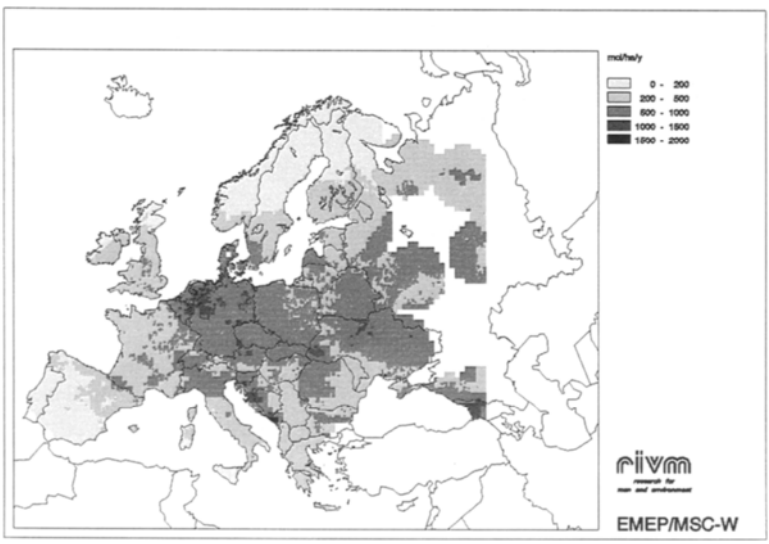


**FIGURE 5.41** Total deposition of NHx in Europe on a 1/6 x 1/6° scale in mol $ha^{-1}$ $a^{-1}$ (Van Pul *et al.*, 1995)

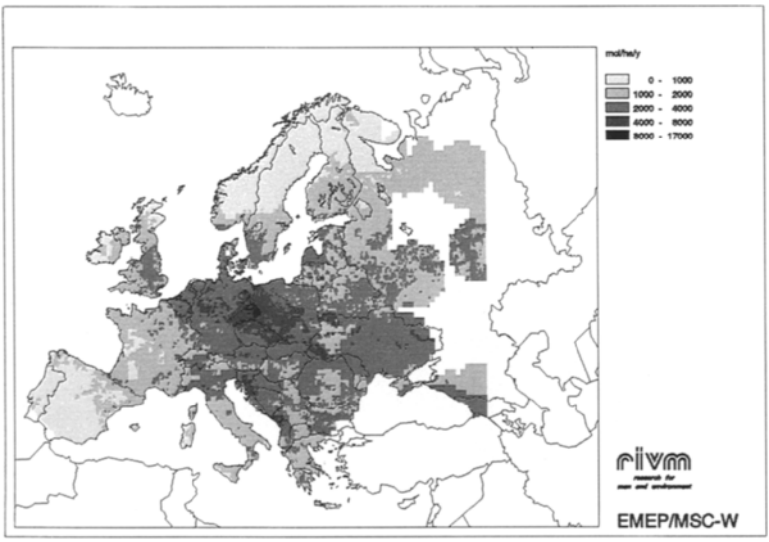


**FIGURE 5.42** Total deposition of potential acid in Europe on a 1/6 x 1/6° scale in mol $ha^{-1}$ $a^{-1}$ (Van Pul *et al.*, 1995)

In all countries in Europe, only a fraction of the total deposition within the country originates from emission sources within the country itself. Figures 5.43 and 5.44 shows the emission and deposition of SOx, NOy and NHx per unit area per country or region in Europe in 1993 (data from Tuovinen *et al.*, 1994). These data may be somewhat different from those presented in this chapter because these are estimated using the long-range transport model results in which different deposition parametrisations are used. Furthermore, because of the large grid cells used as model resolution, the small countries, such as the Netherlands, are covered by grid cells, which also cover part of neighbouring countries. Moreover, the surface area of countries used to determine the average fluxes per unit area is different, leading, for example, to lower fluxes in the Netherlands than reported in section 5.2.

Figures 5.43 and 5.44 show which component contributes most to the potential acid emission or deposition in each country. Furthermore, they show where the potential acid emission or deposition is highest in Europe, and that in many countries of Europe sulphur is the most important component contributing to the potential acid emission and deposition. Nitrogen oxides always have the lowest contribution to the potential acid emission and deposition, only for Belgium, Norway, Sweden, Germany, the Czech Republic and the United Kingdom, the emission of NOx is higher than that of $NH_3$. In the Netherlands, France, Iceland, Ireland, Switzerland, Turkey, Latvia, Lithuania and Macedonia, the $NH_3$ emissions dominate over the other two components. The highest sulphur deposition is found in the Czech Republic, being

about 2700 mol $H^+$ $ha^{-1}$ $a^{-1}$. The lowest sulphur deposition per unit area is found in Iceland (35 mol $H^+$ $ha^{-1}$ $a^{-1}$), except for the oceans and seas. The highest nitrogen oxide and reduced nitrogen deposition per unit area are found in the Netherlands, being 750 and 1770 mol $H^+$ $ha^{-1}$ $a^{-1}$, respectively. The lowest fluxes of NOx and NHx are found in Iceland, being 35 and 16 mol $H^+$ $ha^{-1}$ $a^{-1}$, respectively.

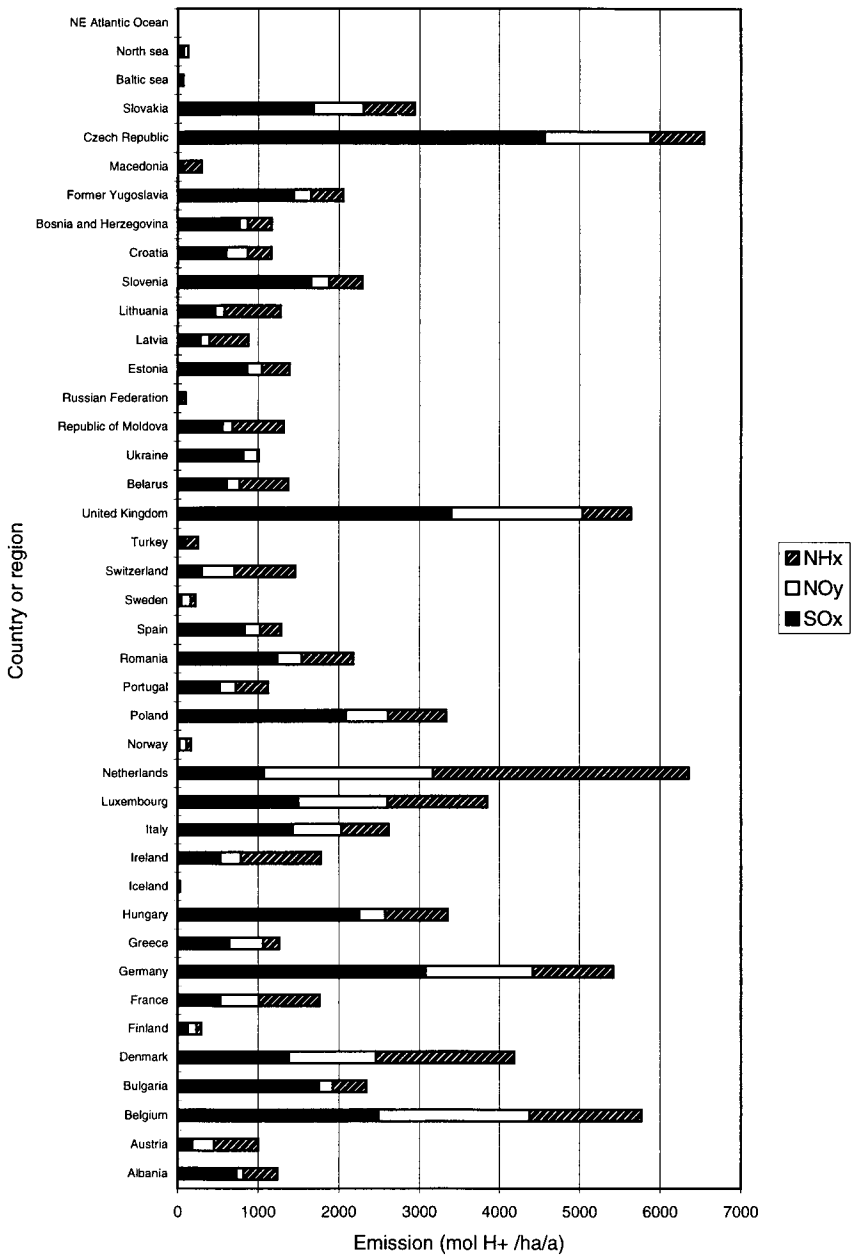


**FIGURE 5.43** Emission of SOx, NOy and NHx per country or region in Europe in 1993 expressed in mol $H^+$ $ha^{-1}$ $a^{-1}$ (Tuovinen *et al.*, 1994).

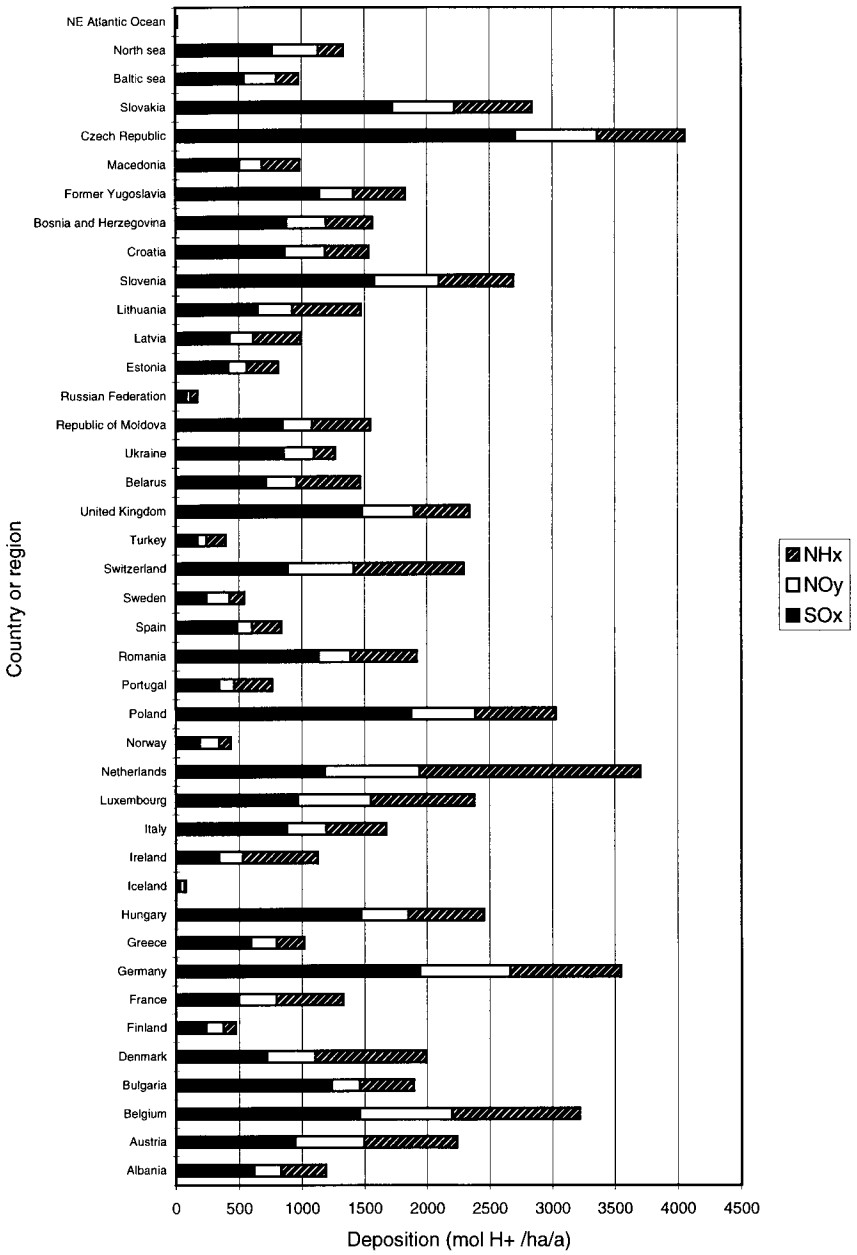


**FIGURE 5.44** Deposition of SOx, NOy and NHx per country or region in Europe in 1993 expressed in mol $H^+$ $ha^{-1}$ $a^{-1}$ (Tuovinen *et al.*, 1994).

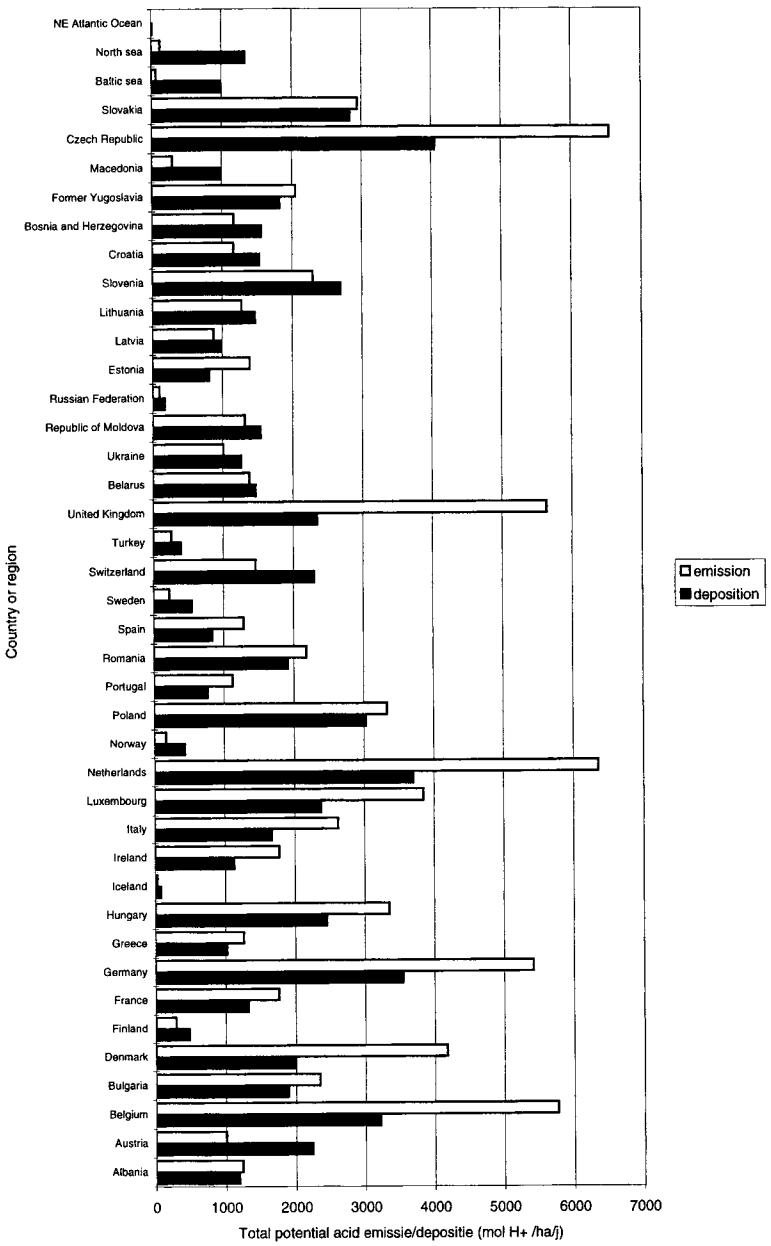


**FIGURE 5.45** Emission and deposition of potential acid per country or region in Europe in 1993 in mol $H^+$ $ha^{-1}$ $a^{-1}$ (Tuovinen *et al.*, 1994).

Figure 5.45 shows the total potential emission next to the deposition in each country, expressed as average flux in the country. From this figure it can be deduced whether a country is a net-importer or exporter of acidic deposition and which country receives the highest fluxes per unit area. The figure shows that the largest emitters are the Czech Republic, the United Kingdom, The Netherlands, Germany, Denmark and Belgium. The largest fluxes are received by the Czech Republic, Poland, The Netherlands, Germany and Belgium. Relatively large net exporters of acidic pollutants are the United Kingdom, Germany, the Czech Republic, The Netherlands, Luxembourg, Italy, Denmark and Belgium. Relatively large net importers are the oceans and sees, Macedonia, Sweden, Norway, Finland, Switzerland and Austria. The extent of transboundary exchange of pollutants is a very complex function of the atmospheric residence time of the pollutant, the relative size of the country, location of emission sources within the country, the relative magnitude of domestic sources and sources outside the country, the strength and direction of dominant winds, and many other factors.

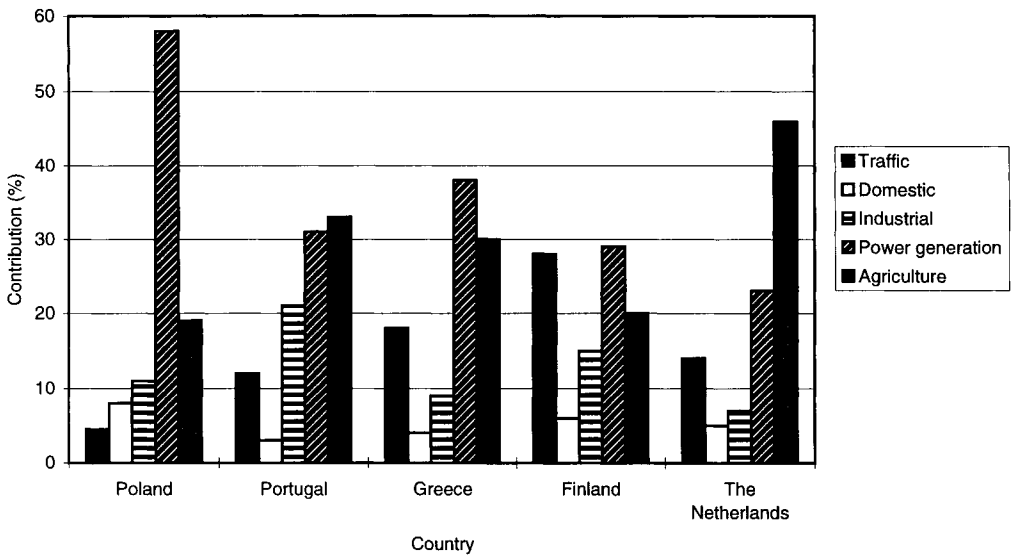


**FIGURE 5.46** Contribution (%) of different source categories to the total potential acid deposition for 5 different countries in Europe in 1990.

Contribution of source categories to the deposition

The contribution of different source categories to the deposition varies to a large extent for different regions in Europe. This can be illustrated with Figure 5.46 where the contribution of different categories to the deposition in different countries is given. These data are calculated with the EMEP model (Tuovinen *et al.*, 1994) and are representative for the situation in 1990. Figure 5.46 shows that for Poland power generation is the main source of deposition, whereas the contribution of agriculture is highest in the Netherlands. Traffic and power generation are the main contributors to the deposition in Finland. In Portugal domestic and power generation is equally important. Industry is not dominating in either of these countries. Highest contribution of industry to deposition is found in Portugal (20%). The data for these 5 countries only serve as an example of differences in source contribution for different regions in Europe. It shows that the abatement strategies will have a different focus in different countries.

*Base cations*

No maps of base cation deposition in Europe have been available up to now. Nevertheless, information on base cation deposition is important as base cations influence the acidity of air and precipitation and in certain areas may significantly neutralise acid deposition. First maps of total base cation deposition are presented in Figure 5.47 to 5.50. Total deposition is estimated as the sum of wet and dry deposition. With the exception of forested areas, the contribution of wet deposition to the total deposition of base cations is higher than dry deposition. Highest sodium fluxes are found in coastal areas, reflecting sea salt being the main source. For $Ca^{2+}$, $Mg^{2+}$ and $K^{+}$ relatively high fluxes are estimated e.g. in the Ukraine, in the former Yugoslavia and the southern and eastern part of Europe. Main sources of high input can be combustion processes, calcareous soils and high rainfall. Figure 5.41 shows the total base cation deposition which to some extent is available for neutralising acid deposition ($Ca^{2+}+Mg^{2+}+K^{+}$). Note that the lowest input is found in regions where the buffering capacity of the soil is already relatively low, e.g. in Scandinavia. Highest fluxes are found near the coast of Ireland and Scotland, in the 'Black Triangle', Ukraine, former Yugoslavia and some parts of Italy.

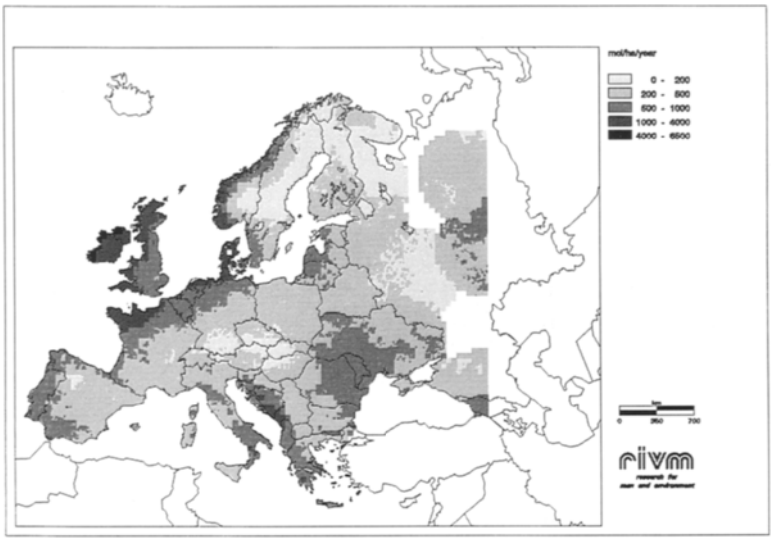


**FIGURE 5.47** Total deposition of $Na^+$ in Europe on a 1/6 x 1/6° scale in mol $ha^{-1}$ $a^{-1}$.

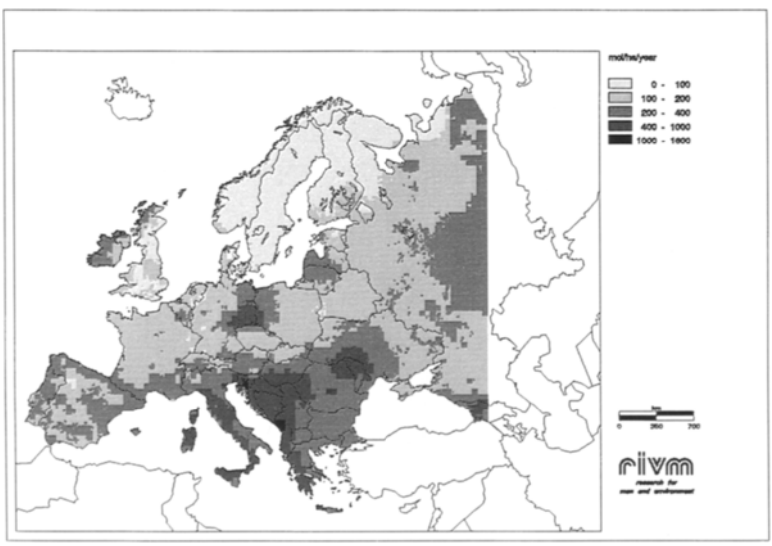


**FIGURE 5.48** Total deposition of $Ca^{2+}$ in Europe on a 1/6 x 1/6° scale in mol $ha^{-1}$ $a^{-1}$.

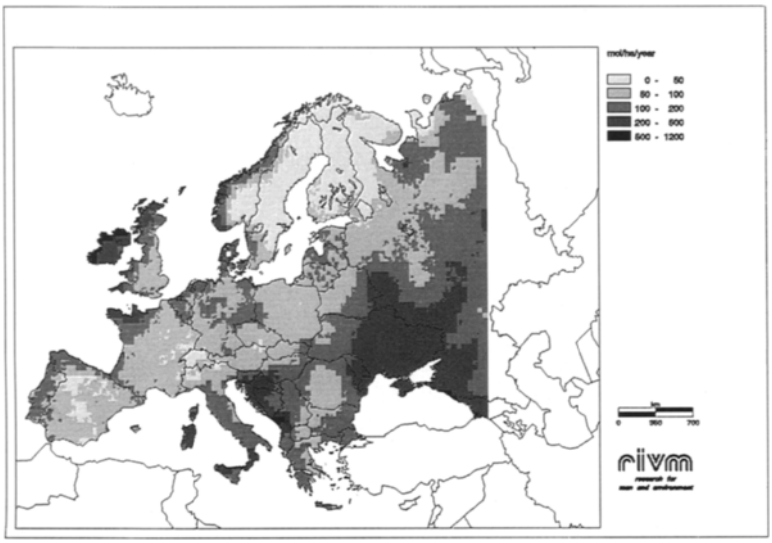


**FIGURE 5.49** Total deposition of $Mg^{2+}$ in Europe on a 1/6 x 1/6° scale in mol $ha^{-1}$ $a^{-1}$.

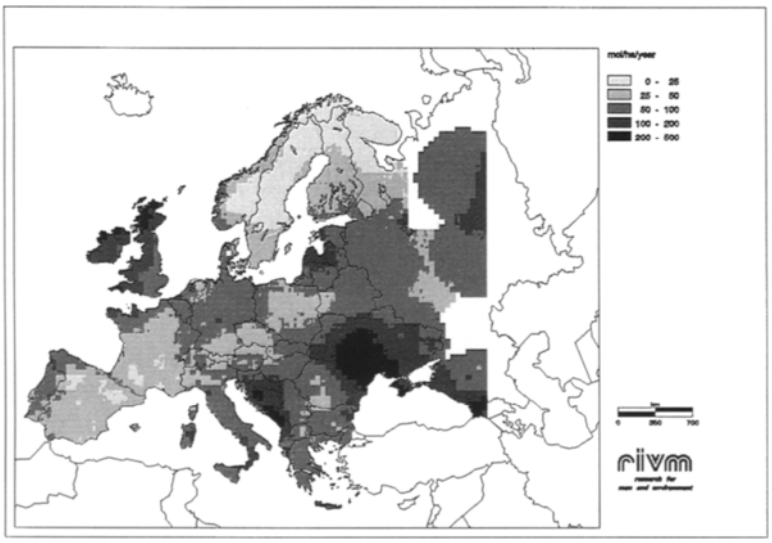


**FIGURE 5.50** Total deposition of $K^{+}$ in Europe on a 1/6 x 1/6° scale in mol $ha^{-1}$ $a^{-1}$.

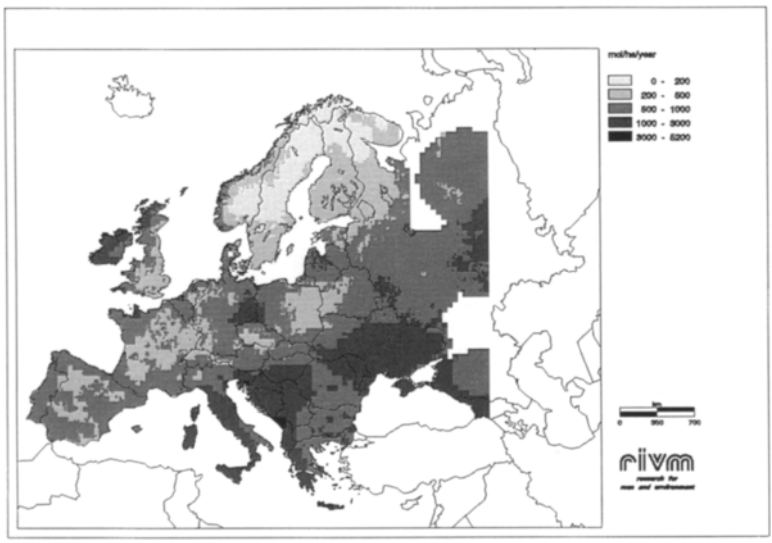


**FIGURE 5.51** Total deposition of base cations ($Ca^{2+}+Mg^{2+}+K^{+}$) in Europe on a 1/6 x 1/6° scale in mol $ha^{-1}$ $a^{-1}$

## 5.4 VARIATION IN DEPOSITION OVER SEVERAL YEARS

There are three ways of determining long-term trends in atmospheric input. First of all, it is possible to estimate trends using estimates of emissions, which in turn are used as input for long-range transport models to estimate atmospheric input using long-term average meteorological statistics (Mylona, 1993). There are several limitations to such a study: it is difficult to accurately determine long-term trends in emissions because usually data are scarce and differ strongly in quality. Furthermore, the long-term average meteorology used in long-range transport models is usually based on the most recent 10 to 30 years and may thus differ from longer-term data. Finally, non-linearities in deposition processes and atmospheric chemistry are not taken into account in current models.

The second option is to use historical measurements to determine long-term trends. The problem with this method is that the quality of data is sometimes not known and/or difficult to assess. Analysis of samples, sample strategy in relation to disturbing factors (sources, obstacles, etc.) are of varying quality and sometimes even unknown. Despite this, historical measurements are of enormous value for obtaining insight in the development in the pollution climates.

A third option is that a combination of long-term emission estimates with long-range transport model calculations and historical measurements are used. With this method, model calculations might be evaluated or calibrated using historical measurements, e.g. to test meteorological statistics and/or non-linearities in processes related to atmospheric input.

### 5.4.1 DEPOSITION AS A RESULT OF NATURAL SOURCES

If stringent emission reductions are realised in the future, the background deposition will become relatively more important. Natural sources of acidifying components can be the soil, volcanoes, oceans, lightning, wild animals and fires.

On the basis of precipitation measurements in remote areas of the world seen in the GPCP network (Global Precipitation Chemistry Project), it was found that the background pH is closer to 5.0 than 5.6, the latter being theoretically derived and assumed up to now (Sisteron *et al.*, 1989). The same data suggest that apart from a sea-salt background, a volume weighted concentration of $SO_4^{2-}$, $NO_3^-$ and $NH_4^+$ of 10.6, 4.5 and 3.4 meq $l^{-1}$, respectively, was found as background. Sisteron *et al.* speculate that these values might be representative for the natural background. These data are somewhat higher than those reported by Locht and Van Aalst (1988), who found ranges for $SO_4^{2-}$, $NO_3^-$ and $NH_4^+$ of, respectively, 2.2 - 7.3, 1.3 - 4.3 and 1.1 - 4.2. Using a long-term average amount of precipitation of 800 mm in the Netherlands, the values from Sisteron *et al.* (1989) would lead to background wet deposition fluxes in the Netherlands as listed in Table 5.8.

For $NO_3^-$ and $NH_4^+$ these fluxes are in agreement with estimations made by Locht and Van Aalst (1988), i.e. 36 mol NOy $ha^{-1}$ $a^{-1}$ and 27 mol NHx $ha^{-1}$ $a^{-1}$. Only the SOx flux is estimated as being lower by Locht and Van Aalst (25 mol $SO_x$ $ha^{-1}$ $a^{-1}$). Locht and Van Aalst (1988) estimated non-anthropogenic fluxes of acidifying components by two methods. A box model, where emissions were taken equal to depositions for a large area was used, and a transport model, along with emission estimates. Their estimates for the dry deposition of acidifying components from natural sources are also listed in Table 5.8. The total potential acid deposition is, in the present-day situation (1993), 1 order of magnitude greater than the background deposition estimates in Table 5.8. The deposition due to natural emissions can therefore presently be neglected. In this estimate, species such as $H_2S$ and PAN have not been taken into account. These may also contribute to background deposition.

**TABLE 5.8** Background wet, dry and total deposition in the Netherlands (mol $H^+$ $ha^{-1}$ $a^{-1}$).

| Component | Wet deposition | Dry deposition | Total deposition |
|---|---|---|---|
| SOx | 74 | 24 | 98 |
| NOy | 32 | 13 | 45 |
| NHx | 24 | 48 | 72 |
| Halogen | 3 | 3 | 6 |
| RCOOH | 300 | 30 | 60 |
| Potential acid | 160 | 120 | 280 |

## 5.4.2 HISTORICAL MEASUREMENTS OF WET DEPOSITION

Section 1.2 provides a short overview of the historical development of atmospheric deposition measurements. Some of the data referred to in that chapter will be used here to assess the development in deposition in the former century up till now. More recent data in the Netherlands and Europe will be used to assess the trend in deposition after the maximum emissions of sulphur occurred in the seventies and nitrogen in the eighties.

*Nitrogen compounds*

The longest time series of wet deposition measurements in Europe to our knowledge were made in Paris (Montsouris) France by Albert Levy in 1876 to 1907 and in Rothamsted (England) between 1850 and 1980. The data from Montsouris comprise wet deposition measurements of oxidised and reduced nitrogen in precipitation. Sulphate was also analysed, but the main (agricultural) interest was focused on nitrogen (Ulrich and Williot, 1993). The data for ammonium and nitrate from Rothamsted and Montsouris are given in Figure 5.52. Also plotted in this figure are the estimates of the natural background deposition (section 5.4.1). These were considered to be representative for the years before 1850. Also shown in

the graph are the data from Eriksson (1952) and Miller (1905) for several locations in Europe. An assessment of the quality of data is reported in Brimblecombe and Pitman (1980) for Rothamsted, and in Ulrich and Williot (1993) for Montsouris and other French data. The data have not been corrected for dry deposition to the funnels of the samplers and other disturbing factors (Eriksson, 1952; Buijsman and Erisman, 1988). The dry deposition contribution could be 25% and 15% for ammonium and nitrate, respectively. The dry deposition contribution to the Montsouris and Rothamsted samples could be even higher because relatively large collecting funnels (3-5 $m^2$) were used in order to collect enough daily sample for analysis.

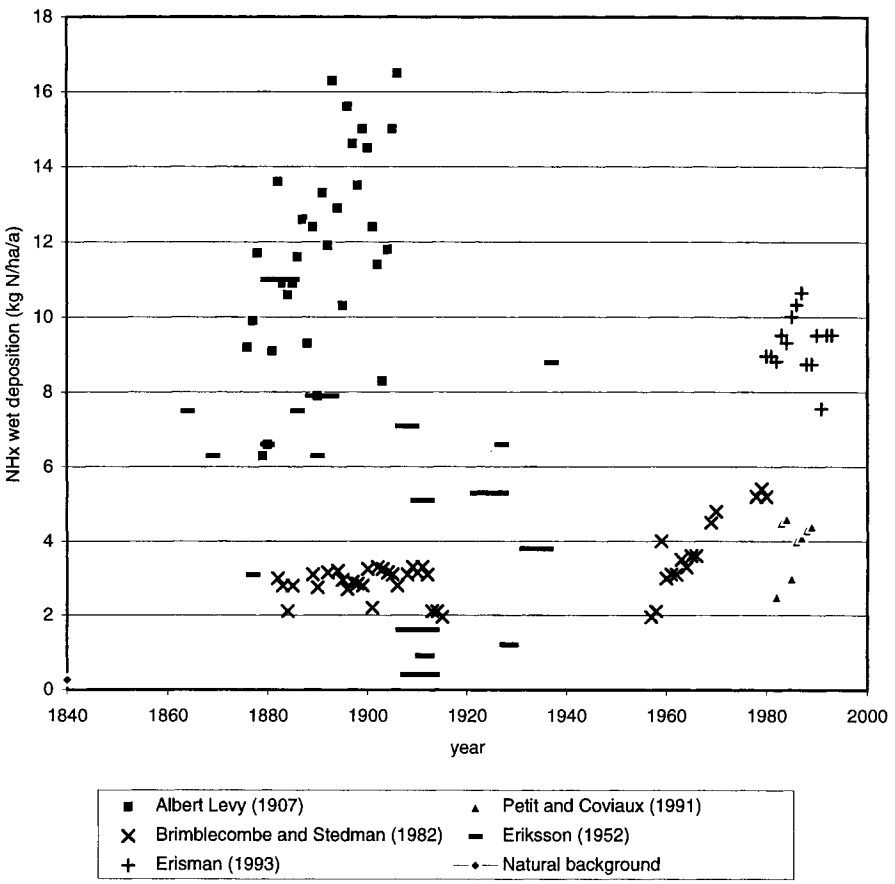


**FIGURE 5.52** Wet deposition of ammonium at Rothamsted (UK) and Montsouris (France) (in kg N $ha^{-1}$ $a^{-1}$)

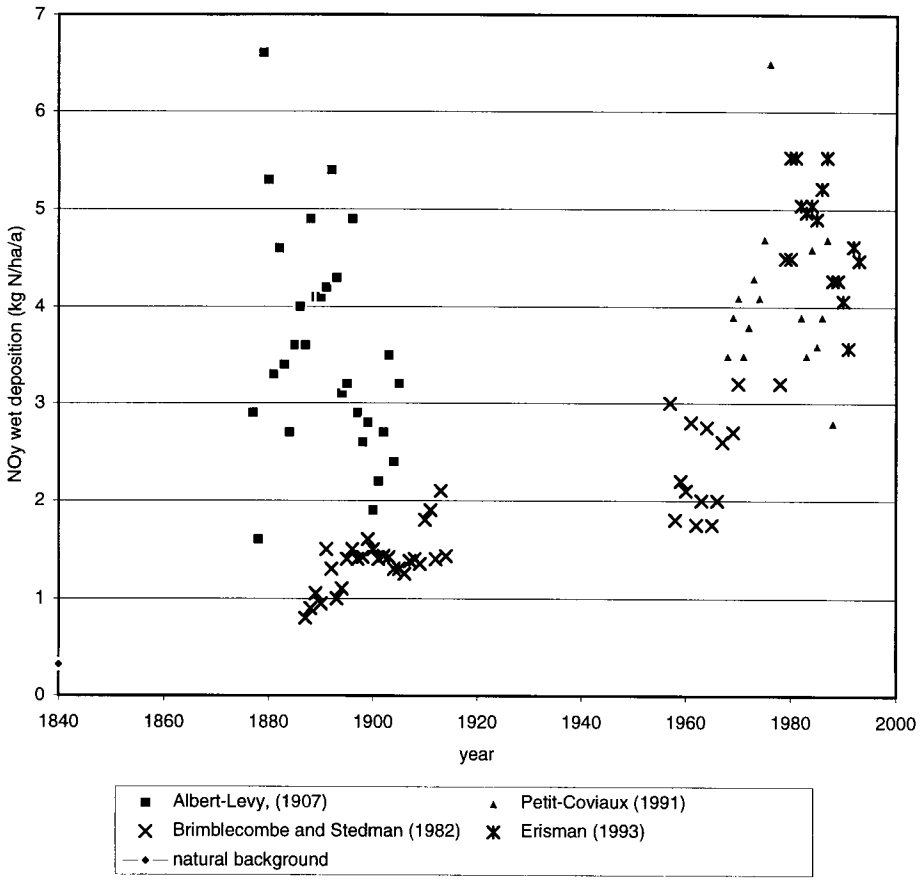


**FIGURE 5.52** *(continued)* Wet deposition of nitrate at Rothamsted (UK) and Montsouris (France) (in kg N $ha^{-1}$ $a^{-1}$

It is striking to see the very high $NH_4^+$ wet deposition values in Montsouris between 1876 and 1907. The values are in the same range of the current wet deposition data in the Netherlands, considered to be the highest in Europe (see Chapter 5). The first reaction is to suspect the measurements. However, this is one of the best documented and executed methods of that time. The quality of data was investigated by Ulrich and Williot (1993) who concluded that the reproducibility of the method was good and that the quality of data was acceptable. It must, however, be noted that ammonia-free laboratories did not exist then and it was not known that both human breath and sweat contains ammonia. Assuming that the data measured

in Montsouris are to some extent influenced by these error sources, the data still show very high values. Another explanation for this could be that the city of Paris, in which the monitoring site was situated, acted as a source of ammonia found in wet deposition. Indeed, Albert Levy, who was the first to make continuous measurements of ambient $NH_3$, measured average concentrations of 17 $\mu g\ m^{-3}$ at the same site. This is comparable to concentrations measured at sites located in high ammonia emission areas in the Netherlands nowadays (Erisman and Boermans, 1995). These high concentrations may be due to the excretion of animals in or near to the city, but also to the emission of $NH_3$ from coal combustion (Smith, 1872, Freyer, 1978). Müller (1888) showed with his snow measurements in and outside the city in Braunsweig (Germany), that the $NH_4^+$ concentration in snow depends on the population density, and more specific, on the flue gas emissions. Furthermore, measurements made by Bineau in 1853 (Bineau, 1855) in and outside Lyon showed that $NH_4^+$ concentrations were higher in winter than in summer in the city, whereas they were higher in summer than in winter in the rural areas outside Lyon. This also suggests that in the city the $NH_4^+$ content in precipitation was mainly determined by burning of coal which was much more intense in winter, whereas outside the city concentrations were mainly determined by emissions from animal waste, because animal waste emissions are higher in summer than in winter (Asman, 1992). The other French, German and British data, collected in the same period as those sampled by Albert-Levy, large variations are shown, with concentrations comparable to or much lower than the Montsouris data.

The recent measurements at Montsouris, made by Petit and Coviaux (1991), show much lower values than those measured in 1876-1907. The $NO_3$ data in Montsouris also seem to be very high, comparable to levels found nowadays. Again, this might be due to the influence of local emissions from Paris. The levels are comparable to those measured by Petit and Coviaux (1991) in Paris nowadays. The sources have changed in and around the city, but this does not necessarily mean that the emission levels have changed.

The Rothamsted $NH_4^+$ data show a gradual increase from 1881 to 1960, and a steeper increase between 1960 to 1980. This is in line with the emission increase during these periods (see Chapter 2). Nitrate at Rothamsted shows a gradual increase from about 1 kg $ha^{-1}\ a^{-1}$ in 1884 to about 3 kg $ha^{-1}\ a^{-1}$ in 1980. The steep increase in nitrate levels after 1960 reflect the change in NOx emissions (see Chapter 2).

The natural background values estimated by Locht and Van Aalst (1988) are much lower than the lowest ammonium and nitrate levels measured, except for the $NH_4$ levels measured around 1910 in Stornaway in the far north of Scotland and at other lighthouses in the Hebrides and in Iceland (Russell and Richards, 1919). When leaving out the Montsouris data, the data in Figure 5.52 indicates that wet deposition of $NO_3^-$ increased from 0.3 kg N $ha^{-1}\ a^{-1}$ in the period before 1850 to about 4 kg N $ha^{-1}\ a^{-1}$ in the 1980s, for $NH_4^+$ these figures are 0.25 to 4 - 10 kg N $ha^{-1}\ a^{-1}$, depending on the location. This is an increase by a factor of 10 - 15 for $NO_3^-$ and 15 to 40 for $NH_4^+$.

*Sulphur*

Average sulphur concentrations in precipitation over several years are displayed in Figure 5.53. Concentrations are given because for most sites no precipitation amounts were given. The data arise from different sources (Liesegang, 1927; Rodhe and Granat, 1984; Smith, 1872; Eriksson, 1952; Lawes, 1883; Locht and Van Aalst, 1988) and are not corrected for dry

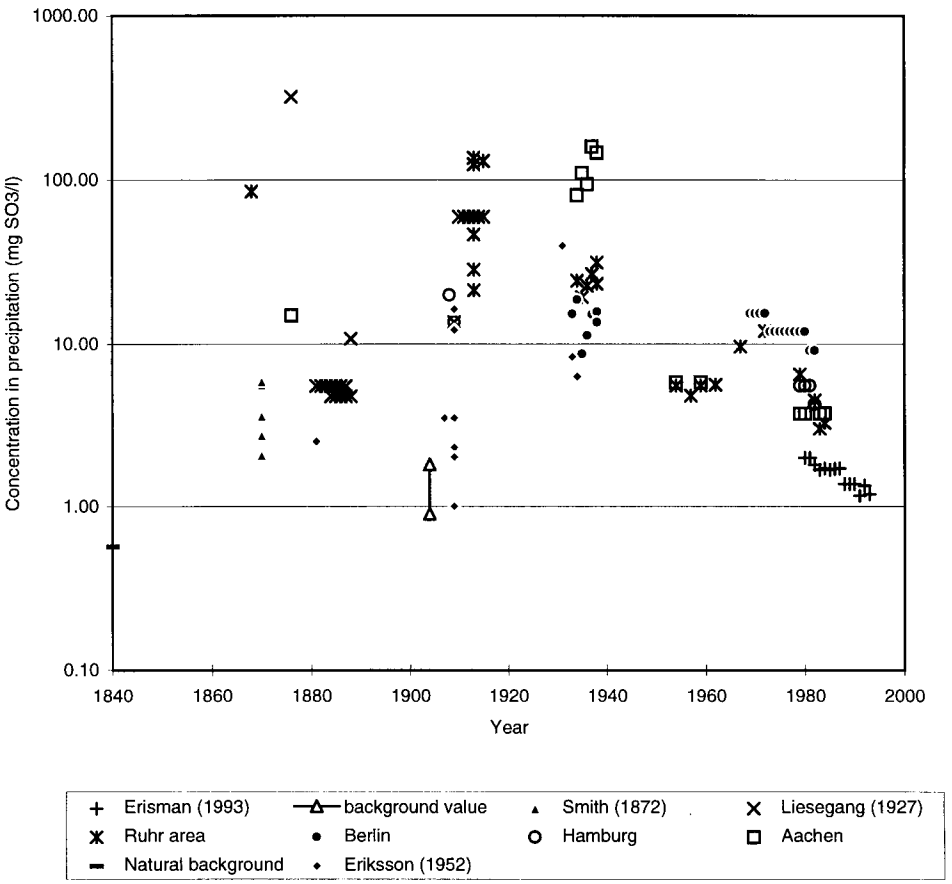


**FIGURE 5.53** Concentrations of sulphur measured in precipitation at several locations in Europe (mg $SO_3$ $l^{-1}$).

deposition to the funnels of the bulk samplers. Most of the measurements were made in different areas in Germany, mostly near industrialised areas, such as the Ruhr area, Hamburg and Berlin. The data after 1960 comprise only those in Germany, in order to allow comparison

deposition to the funnels of the bulk samplers. Most of the measurements were made in different areas in Germany, mostly near industrialised areas, such as the Ruhr area, Hamburg and Berlin. The data after 1960 comprise only those in Germany, in order to allow comparison with other data. The Dutch data from 1980 to 1993 are also given for comparison. The data marked as Smith (1872) represent area averages obtained from measurements at several sites in the UK in the winter of 1870. The natural background is taken from estimates by Locht and Van Aalst (1988) (section 5.4.1). The other 'background values' are obtained from Liesegang (1927). These represent measurements in the rural areas of Tharand and Grillenburg in Germany.

Figure 5.53 displays several enormous concentrations in precipitation, up to 400 mg $l^{-1}$ measured in the Ruhr area in Germany at the end of the eighteenth century. The scale in Figure 5.53 is logarithmic. The German data show an increase in concentration from 1870 to 1920. Between 1920 and 1940 concentrations remained the same, decreased after 1940 and increased again from the sixties to the seventies. After the seventies, the concentrations decreased again. These variations are similar to the variation in emissions in Germany between 1880 and 1990 (Mylona, 1993). Assuming a range of 700 to 1000 mm of precipitation at the sites, the bulk wet deposition of sulphur in Germany ranged from 50 - 70 mol $ha^{-1}$ $a^{-1}$ before 1850, to about 800 - 1100 mol $ha^{-1}$ $a^{-1}$ around 1900, 2000 to 3000 mol $ha^{-1}$ $a^{-1}$ in 1940, and 400 to 600 mol $ha^{-1}$ $a^{-1}$ in 1980.

*Base cations*

Dry deposition of base cations is estimated from wet deposition measurements via scavenging ratios. For those components for which scavenging ratios are obtained from a linear relationships between air concentrations and concentrations in precipitation (i.e. for all base cations at the low concentration ranges generally found in Europe), dry deposition is linear related to wet deposition. Temporal variations in dry deposition are therefore similar to those in wet deposition. Wet deposition of base cations is found to gradually decrease during the last 10 to 20 years in several parts of Europe and North America (Hedin *et al.*, 1994). The decline is related to the decrease in anthropogenic base cation emissions of fuel combustion processes and industrial processes as well as the reduction in emissions from unpaved roads. The decline of total base cation deposition was dominated by $Ca^{2+}$, which contributed about 80% to the total base cation decline (Hedin *et al.*, 1994; Buishand and Montfort, 1989). There is some evidence that in some parts of Europe the decline in base cation deposition have countered the effects of $SO_2$ emission reductions. Figure 5.54 shows the changes in concentrations of $Na^+$, $Ca^{2+}$ and $Mg^{2+}$ relative to the 5 year average concentrations (1932 - 1937) measured at Leiduin as reported by Leeflang (1938). The data in the figure illustrate the decline in $Mg^{2+}$ and $Ca^{2+}$ concentrations which are to some extent influenced by anthropogenic sources. Sodium, which is primarily emitted from the sea shows temporal variations, but no decline. Hedin *et al.* (1994) estimated a decline in base cation concentrations between 30 and 50% for different sites in the Netherlands between 1978 and 1987. Data in Figure 5.54 suggest that the

base cation concentrations decreased with 70% since 1932. The picture might be obscured by measuring errors or uncertainty in analysis in the Leeflang data. However, the Leeflang data are well documented and the uncertainty is expected to be low.

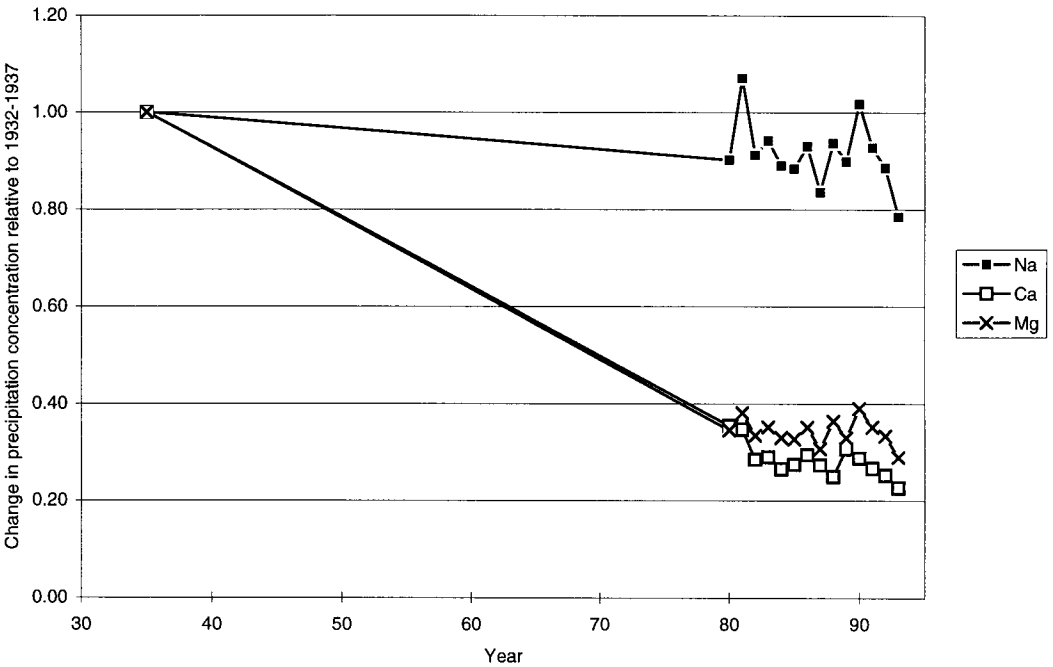


**FIGURE 5.54** Changes in $Na^+$, $Ca^{2+}$ and $Mg^{2+}$ concentrations in precipitation (mg $l^{-1}$) measured at Leiduin near the Dutch coast.

*The Netherlands*

The first rainwater analysis in the Netherlands were made in Utrecht in 1825 by Mulder (1825). Van Ancum determined iodine concentrations somewhere in the Netherlands around 1850 (cf Ludwig, 1862). After these no reports are found on rainwater analysis until about 1900. The first systematic measurements in the Netherlands we found dated from around 1900. They comprise the determination of the chlorine content in precipitation sampled at Den Helder (Jorissen, 1906). Furthermore, Van der Sleen made measurements in the dunes near Haarlem around 1912 (cf. Leeflang, 1938). However, the first extensive research was published by Leeflang (1938). He published results of precipitation sampled every three months at several distances from the North Sea coast from 1932 to 1937. The quality of these measurements can be determined as the methods used are reasonably well described. His

measurements show a gradient from the coast land inward for $Na^+$, $Ca^{2+}$, $Mg^{2+}$ and $Cl^-$, with highest concentrations at the coast and lowest at the Veluwe, about 86 km from the coast (Figure 5.55). The components which are related to inland (anthropogenic) sources, such as $SO_4^{2-}$, $NH_4^+$ and $NO_3^-$ show a different horizontal gradient, with increasing concentrations with distance from the coast.

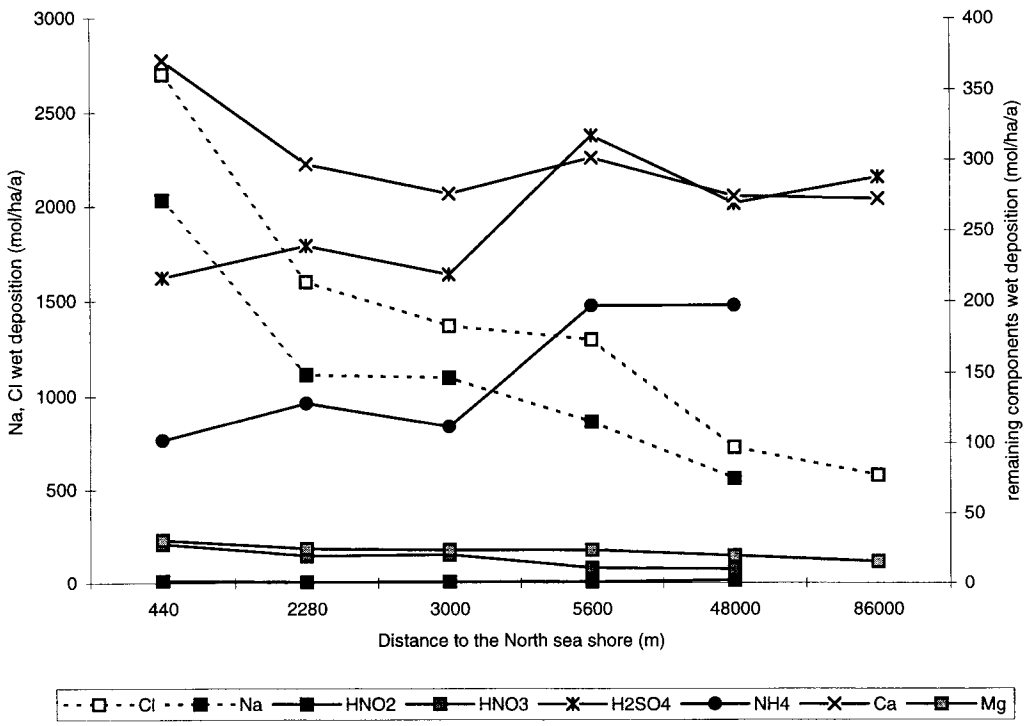


**FIGURE 5.55** Horizontal gradient of wet deposition from the coast land inward as reported by Leeflang (1938). Data are averages of 5 years (1932 - 1937).

After the thirties, the measurements reported date from the fifties up till now. Ridder (1978) presents an overview of all the measurement sites where wet deposition was measured after the fifties in the Netherlands. About 200 different measurement sites were in use, most of them operated simultaneously in the seventies. Long-term measurements are available from the European Rossby monitoring network (1956 - 1970), in which wet deposition was made at three sites in the Netherlands: De Bilt, Den Helder and Witteveen, by KNMI and RIVM. TNO made measurements between 1959 and 1974 at Heijplaat and Oostvoorne. Figure 5.56 shows time series of concentrations measured at the five locations. Concentrations show a gradual

increase in $SO_4^{2-}$, $NH_4^+$ and $NO_3^-$ concentrations during the fifties, sixties and seventies. Values are much lower in the eighties for $SO_4^{2-}$ and $NO_3^-$. $NH_4^+$ levels are highest in the eighties. The values measured in the eighties are obtained from the LMR network which is the precipitation network still operating (Buijsman, 19??; RIVM, 1994). Figure 5.57 shows the deposition as measured at Witteveen during the years 1958 to 1993. Also plotted in this figure are the 5 year average values measured by Leeflang near the coast. The national emissions are also plotted in the figure. For $SO_4^{2-}$ and $NH_4^+$ the variation in emissions and wet depositions are similar, with highest $SO_2$ emission and $SO_4^{2-}$ deposition in the fifties and sixties (see also Figure 5.56), and highest $NH_3$ emission and $NH_4^+$ deposition in the eighties. Lowest emissions and depositions are observed in the thirties. For $NO_3^-$ emission and deposition show different variations. The increase in deposition in the earlier years are similar to the emission increase. However, the measurements in the eighties are lower than those in the sixties and seventies, whereas they are expected to be higher based on the increase in emission.

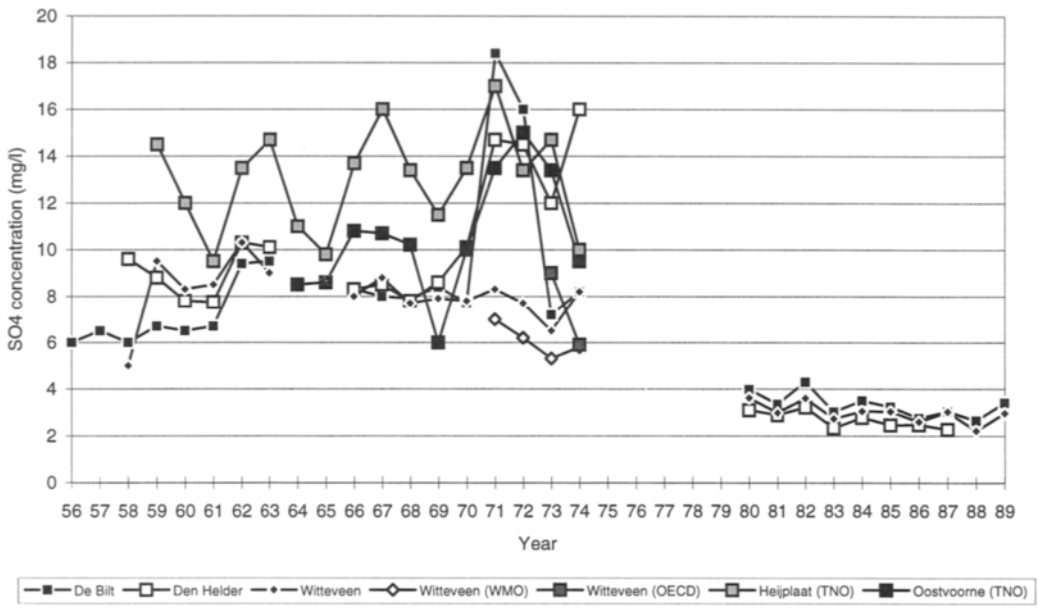


**FIGURE 5.56** Time series of $SO_4^{2-}$ concentration measurements in precipitation made at several sites in the Netherlands (mg $l^{-1}$

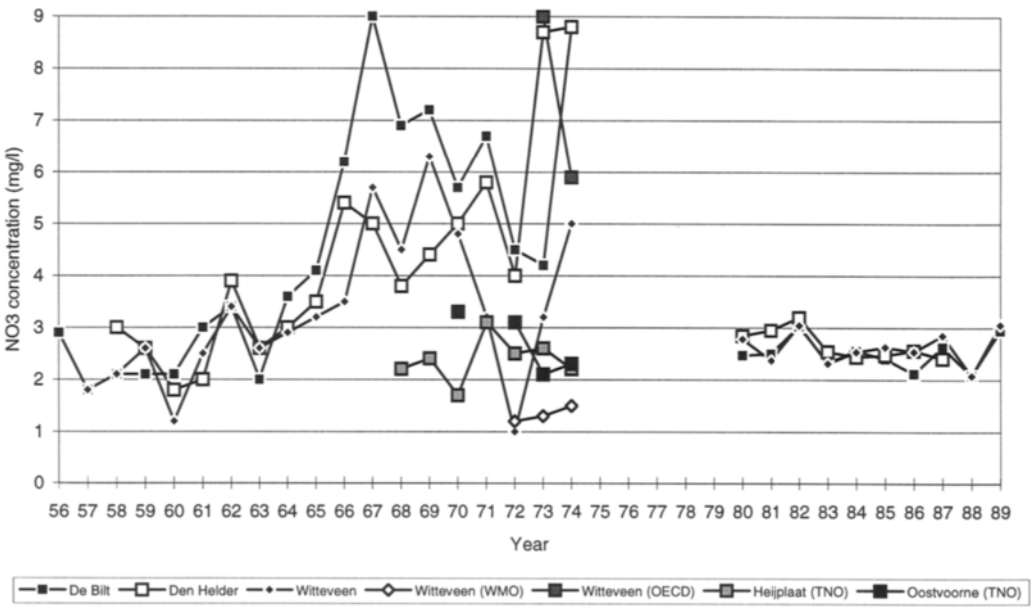


**FIGURE 5.56** *(continued)* Time series of $NO_3^-$ concentration measurements in precipitation made at several sites in the Netherlands (mg $l^{-1}$)

A discussion on the uncertainties in measurements is needed here. Ridder (1978) analysed the data measured at several sites in order to assess the quality of the data. He found several sources of errors, especially related to the Rossby network. He found for example that samples obtained from unrelated sites (i.e. separated several hundreds of kilometres) analysed by the same laboratory showed high correlations, whereas data obtained at nearby sites, analysed by different laboratories showed no correlation at all. Furthermore, he found years where enormous amounts of precipitation were reported, as the result of administrative errors. He also found errors in the conversion of units resulting in reporting of values which are a factor of 20 too high. Furthermore, changes in the application of different sampling methods and procedures or analytical techniques could clearly be identified. The introduction of computers in 1967 did result in erroneous data handling because the punch capacity appeared to be too small.

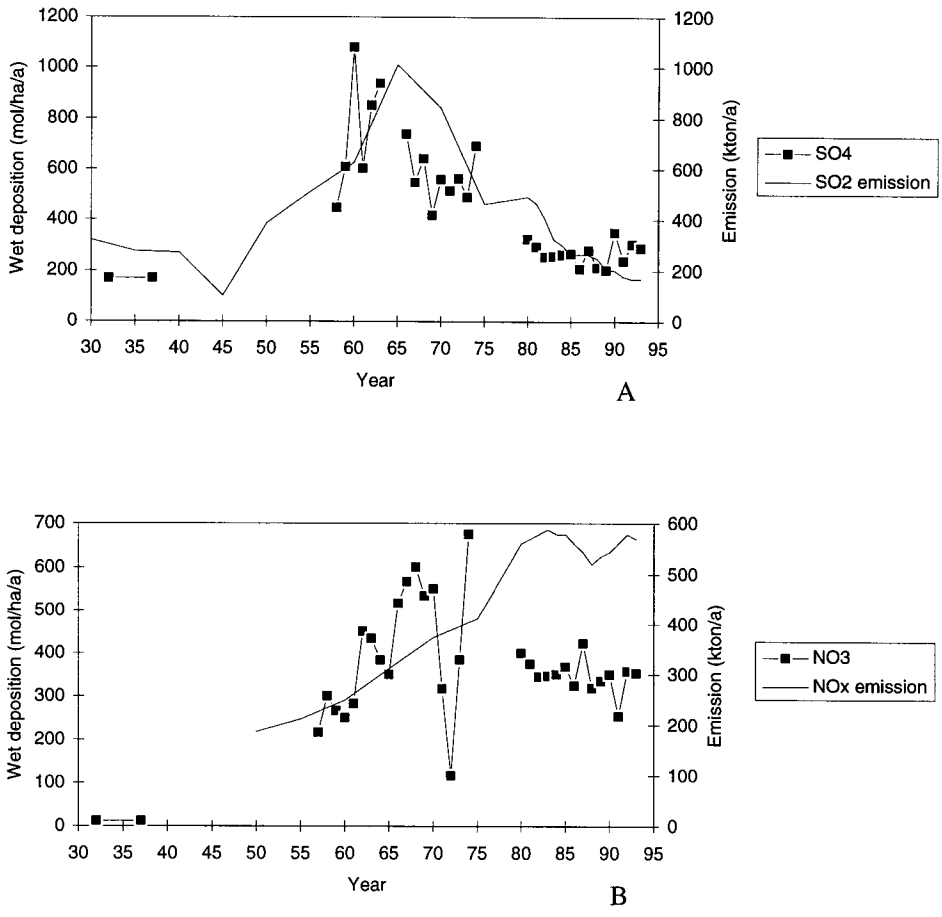


**FIGURE 5.57** Time series of wet deposition measurements for (A) $SO_4^{2-}$ and (B) $NO_3^-$ made at Witteveen (mol $ha^{-1}$ $a^{-1}$).

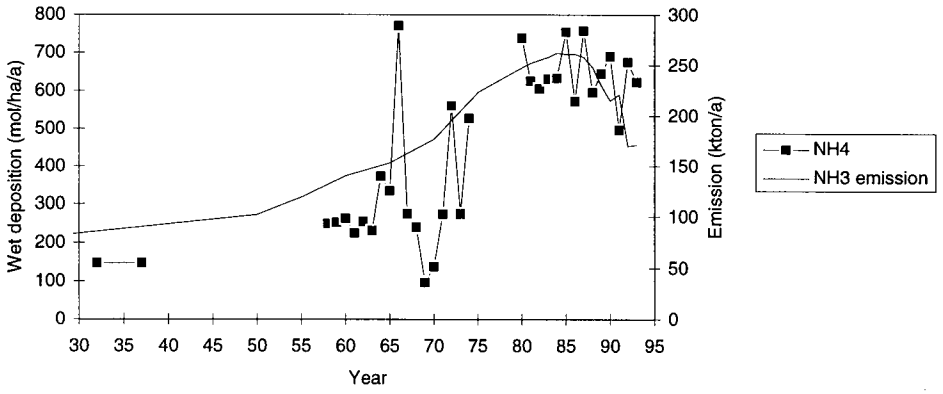


**FIGURE 5.57** *(continued)* Time series of wet deposition measurements for $NH_4^+$ made at Witteveen (mol $ha^{-1}$ $a^{-1}$).

The conclusion of Ridder was that in networks data handling should be done much more careful, that regular intercomparisons should be organised and all sorts of checks should be introduced. Most of the errors just mentioned were corrected for by Ridder when enough information was available to do so. His conclusion regarding the data as presented in Figure 5.56 and 5.57 was that the increase in $NO_3^-$ deposition in the period 1965 - 1972 presumably refers to a real effect, though strongly enlarged by incorrect measurements. Furthermore, he states that the time series of annual average $SO_4^{2-}$ data can be regarded as reasonably accurate. This can be derived from the fact that the variations at different sites are similar. He does not comment on the $NH_4^+$ data. However, Buijsman (1989) states that there is a large uncertainty in these data. This is e.g. shown by comparing data in years where two or more samplers were used at the same location. The fact that the emission variation and deposition variation in Figure 5.57 are similar could be a coincidence, but it could also be that despite the large uncertainty in the data, the increase in deposition is larger than the uncertainty and thus the difference is real.

### 5.4.3 NON-LINEARITIES IN TEMPORAL VARIATIONS

It has been found by Fricke and Beilke (1992) in Germany that the decrease in emissions of sulphur in western Europe from 1980 onwards has resulted in much larger decreases in observed concentrations of $SO_2$ in ambient air compared to the decrease in ambient $SO_4^{2-}$

aerosol concentrations and $SO_4^{2-}$ precipitation concentrations. This result indicate that non-linearities play a role in determining source receptor relations. Non-linearities may be of importance when abatement strategies are based on models in which a linear relationship between emission and deposition changes in time is assumed (Hov *et al.*, 1987). Figure 5.58 shows the relative change in measured ambient $SO_2$ and $SO_4^{2-}$ aerosol concentrations, rainwater $SO_4^{2-}$ concentrations in the southern part of the Netherlands, and the estimated total $SO_2$ emission in the Netherlands and in Europe, between 1955 and 1990. The year 1955 was taken as the reference situation. The figure shows similar results as found by Fricke and Beilke (1992), i.e. the relative decrease in the observed $SO_2$ concentration is larger than that observed in $SO_4^{2-}$ concentrations in aerosol and precipitation. The direction of the changes in sulphur concentrations in air and rain is similar to the changes in $SO_2$ emission but the magnitude is different. The emission in 1990 is only 40% of that in 1955, the $SO_2$ concentration is 54% of that in 1955, the $SO_4$ concentration 69%, the rainwater $SO_4^{2-}$ concentration 76%. The measurements are effected by measuring errors and meteorological variation during the different years. However, these facts cannot explain the systematic difference in magnitude and the difference in $SO_2$ and $SO_4^{2-}$ concentrations (Figure 5.58).

Several explanations for these non-linearities might be given. First of all, the concentrations in air, aerosol and precipitation are of a different origin and transported over different distances (Van Jaarsveld, 1989). The emission in the Netherlands might, therefore, not be representative for the changes in concentrations. It is estimated that only 30% of the concentration of sulphur is determined by sources in the Netherlands, the other 70% coming from abroad, mainly from Germany, Belgium, France and the UK. The changes in European emissions is also displayed in Figure 5.58. This variation, being much different from that in the Netherlands, indicates that the relative change in emission to be used in a comparison like this needs to be derived in another way. The change in emissions determining the concentrations should be compared to the measurements. Van Jaarsveld (1989) explains the difference or non-linearities by the fact that $SO_2$ and $SO_4^{2-}$ (aerosol and precipitation concentrations) originate from different sources in different areas. Non-uniform changes in emissions and source characteristics would thus lead to different changes in $SO_2$ and $SO_4^{2-}$ concentrations with time.

The second explanation might be that there is a non-linearity in atmospheric chemistry and cloud processes (Hov *et al.*, 1987). Cloud processes can be non-linear as the result of the nature of cloud formation but also because of cloud chemistry. Atmospheric or cloud chemistry can cause non-linearities when the components or mechanisms which lead to conversion of $SO_2$ to $SO_4^{2-}$ are limiting, e.g. when the oxidising precursors are exhausted or when clouds are evaporated ($H_2O_2$, $O_3$), the pH of droplets falls below 4. In this respect, the role of ammonia might be of importance. $NH_3$, being an alkaline gas, provides the neutralising capacity of precipitation and aerosols and might provide an 'alkaline environment' when deposited at comparable amounts or in excess over acid-forming components.

The important role of $NH_3$ can clearly be shown in trends of wet and dry deposition of $SO_2$ in the Netherlands. Through a strong decrease in $SO_2$ emission during the past years in western Europe, $SO_2$ concentrations also show a strong decline. In most areas this has led to a decline in dry deposition of $SO_2$ (see Figure 5.59). However, wet deposition does not show the same decline (Figure 5.59). This might be explained by ammonia emissions which did not decrease to a large extent during the period 1955 to 1990. Ammonia can neutralise $SO_2/SO_4^{2-}$ in the atmosphere, forming $(NH_4)_2SO_4$ particles. Before the steep decline of $SO_2$ emissions after 1987, $SO_2$ was in excess over $NH_3$. $NH_3$ was probably then the limiting factor in aerosol formation. After the emission decline, $SO_2$ and $NH_3$ are equally present in the atmosphere (see Figure 5.60), which means that aerosol formation might be limited by one or the other. The aerosol formation has not decreased, thus the availability of condensation nuclei [e.g. $(NH_4)_2SO_4$ particles] and scavenging of aerosols has not decreased. The only decrease in wet deposition of $SO_4^{2-}$ is the decrease in below-cloud scavenging of $SO_2$. This is however not the most important factor determining wet deposition of $SO_4^{2-}$.

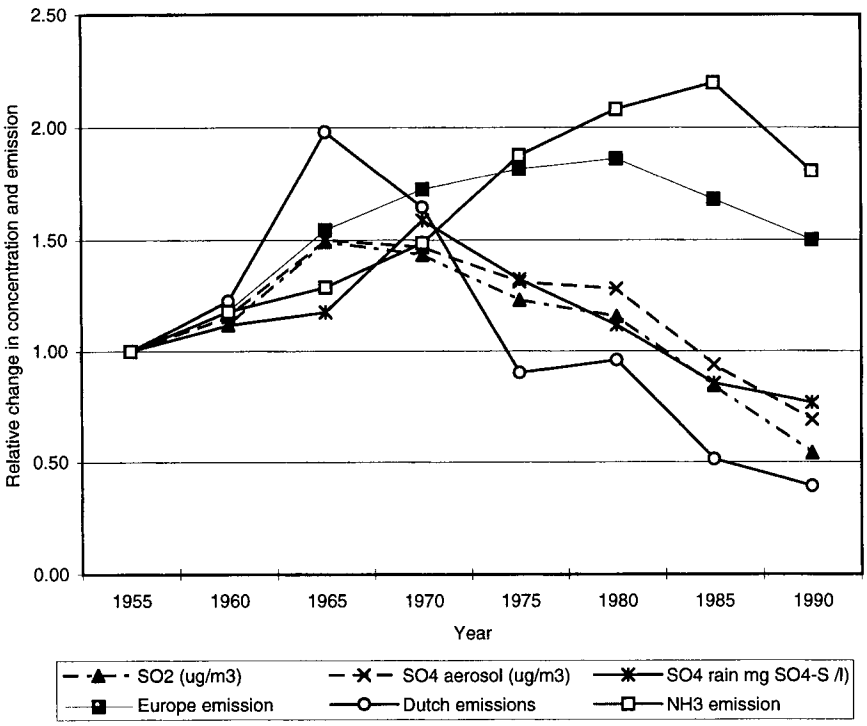


**FIGURE 5.58** Relative change between 1955 and 1990 in measured concentrations of sulphur in air, aerosol and precipitation, and in estimated sulphur emissions in the Netherlands and in Europe, and in ammonia emissions in the Netherlands.

The other role of $NH_3$ is to provide an 'alkaline environment' when deposited. In this respect it is important to know if there is an excess of $SO_2$ over $NH_3$ in terms of deposition fluxes. Again, before the steep emission change in 1987, $SO_2$ was in excess of $NH_3$ in the Netherlands (Onderdelinden *et al.*, 1985; Erisman *et al.*, 1988). In this case, $SO_2$ dry deposition is limited to some extent because the surface becomes acid through which uptake of $SO_2$ in water layers, for example, is limited (see also discussion on co-deposition in Chapter 4). During the years after 1987 $NH_3$ became relatively more important in the Netherlands (see Figure 5.60), thus increasing the effect of co-deposition and increasing the $SO_2$ dry deposition velocity relatively to the $SO_2$ excess situation before 1987. This non-linear effect leads to a relative stronger decrease in $SO_2$ concentrations through the increase in dry deposition velocity and points in the same direction as the aerosol formation.

These results indicate that when simultaneous emission reductions in $SO_2$ and $NH_3$ are implemented, resulting in similar ratios of one gas over the other, non-linearities most probably do not play an important role.

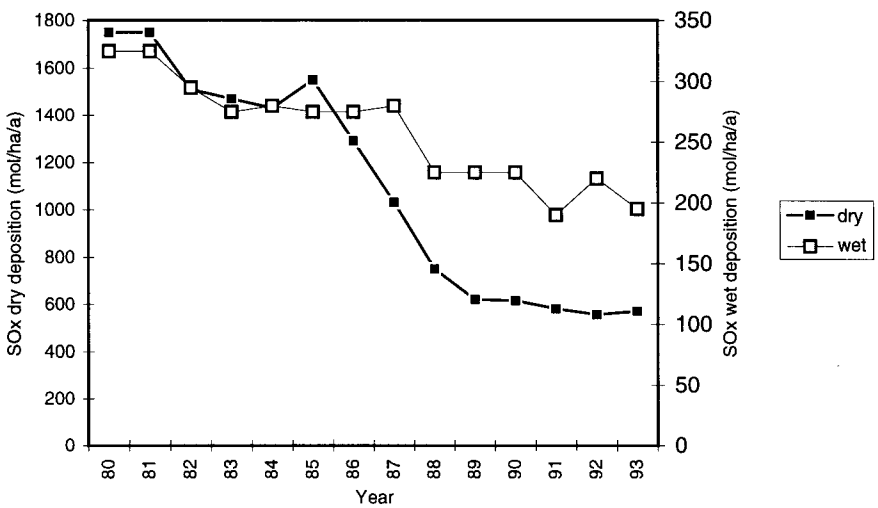


**FIGURE 5.59** Wet and dry deposition of sulphur in the Netherlands over the period 1980-1993 (mol $ha^{-1}$ $a^{-1}$).

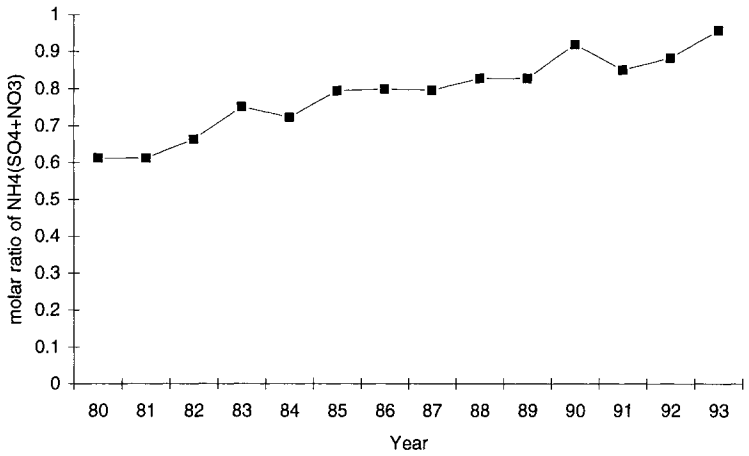


**FIGURE 5.60** Ratio of $NH_4^+$ over ($SO_4^{2-}$ plus $NO_3^-$) in precipitation in the Netherlands over the period 1980-1993.

## 5.5 SYNTHESIS

Inferential models were used to estimate atmospheric deposition of acidifying compounds and base cations in the Netherlands and Europe. In these models wet deposition is estimated using interpolated wet deposition measurement results. Dry deposition is estimated from interpolated air concentration measurement or model results, and land-use specific dry deposition velocities inferred using the resistance analogy. Deposition was estimated on a 5 x 5 km grid scale for the Netherlands and on a 10 x 20 km grid for Europe.

In the Netherlands, total deposition of SOx, NOy, NHx, and potential acid amounted in 1993 on average 760, 740, 2000 and 4280 mol $ha^{-1}$ $a^{-1}$, respectively. Deposition of potential acid was highest in the south of the country, up to 9000 mol $ha^{-1}$ $a^{-1}$. Very high values were also recorded in areas with many forests present. The deposition decreased since 1980 with 41%, mainly as the result of decreasing sulphur emissions in western Europe. Base cation deposition relevant for neutralising the acid input ($Mg^{2+}$, $Ca^{2+}$ and $K^{+}$) amounted on the average 660 mol $ha^{-1}$ $a^{-1}$. In contrast to the deposition of potential acid, base cation fluxes were highest in the north and at the west coast of the country. During recent years the base cation deposition decreased as the result of reductions in industrial emissions.

In Europe, total deposition of SOx, NOy, NHx, and potential acid in 1989 amounted on average 540, 300, 440 and 1820 mol $ha^{-1}$ $a^{-1}$, respectively. Highest deposition of potential acid was found in former eastern Germany and Poland (the Black Triangle) for SOx (7000 mol $ha^{-1}$ $a^{-1}$) and in the eastern part of the Netherlands and the western part of Germany for NOy (1300 mol $ha^{-1}$ $a^{-1}$) and NHx (2500 mol $ha^{-1}$ $a^{-1}$). Deposition of potential acid was highest in the Black Triangle, up to 16.500 mol $ha^{-1}$ $a^{-1}$. Lowest values of deposition are found in the northern part of Europe, including Iceland. Deposition of SOx, NOy, NHx and total potential acid amounts 40, 20, 10 and 110 mol $ha^{-1}$ $a^{-1}$, respectively in these regions. Base cation deposition in Europe relevant for neutralizing acid input amounted 730 mol $ha^{-1}$ on average and ranged between 70 to 5160 mol $ha^{-1}$ $a^{-1}$.

Natural background deposition of SOx, NOy, NHx, and potential acid was estimated around 100, 45, 70 and 280 mol $ha^{-1}$ $a^{-1}$, respectively. In the Netherlands, nowadays these values are exceeded by a factor of 10, 22, 46 and 22, respectively. In some parts of Europe the natural background deposition is exceeded with a factor 20 or more.

Ancient measurements suggest that $NH_4^+$ and $NO_3^-$ concentrations in rain water and ambient $NH_3$ air concentrations were very high in and near the large cities at the end of the 19th century, comparable to those found nowadays. $NH_4^+$ and $NO_3^-$ concentrations in rainwater measured at the more rural site of Rothamsted (UK) show a gradual increase from 1880 to 1960, and a more steep increase between 1960 and 1980. Very high $SO_4^{2-}$ concentrations were found in the (industrial) Ruhr area at the end of the 18th century. Other ancient German

measurements suggest that $SO_4^{2-}$ concentrations in precipitation increased from 1870 to 1920. Between 1920 and 1940 concentrations remained the same, they decreased after 1940 and increased again from 1960 to 1980. After the seventies, $SO_4^{2-}$ concentrations in precipitation decreased again. The temporal variations in wet deposition are similar to those in estimated emissions (see Figure 2.1).

Non-linearities between emission and deposition changes over time have been found. This was attributed to differences in origin, atmospheric chemistry and transport distance of the component.

# CHAPTER 6 EVALUATION OF DEPOSITION ESTIMATES

*Introduction*

Probably as important as the knowledge of the deposition estimates itself, is the knowledge about the uncertainty in the estimates. It is not an easy task to do an accurate and independent uncertainty analysis. Because of the very few field experiments made to determine deposition parameters, the base for generalisation is small, and even worse is the base for evaluation of results, the latter because the same experiments must be used for derivation and evaluation of the parameters. In spite of these difficulties, the evaluation of the $SO_2$ dry deposition parameters has been chosen to open this chapter. For this, three long-term measurements of $SO_2$ gradients, over grassland, heathland and a forest in the Netherlands are used, along with a long-term eddy correlation measurement sequence over the Boden forest in Canada, to compare modelled parameters with those derived from measurements.

The only independent flux measurements which can be used for evaluating model results are throughfall measurements. However, during the past years, there has been discussion on whether throughfall measurements can actually be used to determine atmospheric deposition (Ivens et al., 1989; Johnson and Lindberg, 1990; Erisman, 1993b; Draaijers and Erisman, 1993; Draaijers, 1993). Up to now it has not been possible to quantify the impact of canopy exchange processes on throughfall deposition estimates. In the second part of this chapter, throughfall measurements are compared to flux estimates, canopy exchanges processes are quantified and a relation between the two estimates is determined.

Finally, at the end of this chapter, results of an uncertainty analysis are presented for the DEADM and the EDACS model estimates. The uncertainty analysis for the results in the Netherlands is based on a comparison of flux measurements with modelled values made in recent years in the Netherlands, on a comparison with TREND results and on an error propagation study. Since such a detailed study is not available for EDACS, a more qualitative description of the uncertainty is given.

## 6.1 EVALUATION OF SURFACE EXCHANGE PARAMETERS FOR $SO_2$

The parametrisation scheme for $SO_2$ surface resistance, determined for European pollution climates and receptor surfaces common in Europe (Erisman *et al.*, 1994, outlined in Chapter 4), was tested using $SO_2$ dry deposition measurements over a deciduous forest in Canada (Shaw *et al.*, 1988; Padro *et al.*, 1992; 1993), a coniferous forest (Erisman *et al.*, 1993a); a heathland area (Erisman 1992; Erisman *et al.*, 1993b) and a grassland area in the Netherlands (Erisman *et al.*, 1993b).

### 6.1.2 EXPERIMENTAL PROCEDURE

A short overview of the site characteristics, the methods used, the duration of the experiments and uncertainty estimates will be given for each dataset. The heathland and Douglas fir experiments are extensively described in Chapter 7.

*Deciduous forest*
As part of two Eulerian Model Evaluation Field Studies (EMEFS), measurements were taken over a deciduous forest located on the Borden Canadian Forces Base (44° 19'N, 80° 56'W). $SO_2$ fluxes were measured in the winter of 1990 using the eddy correlation technique (Shaw *et al.*, 1988). Fast-response $SO_2$ measurements were made using a modified Meloy 285 sulphur analyser with a fast-response burner block. The Meloy 285 analyser employs an FPD to sense total sulphur. The FPD is negatively sensitive to water vapour, an effect for which a correction was made. Changes in $SO_2$ concentrations during the half-hourly average measuring periods were accounted for by estimating the storage flux using the concentration measurements before and after the current period. The measured meteorological, concentration and deposition parameters were reported by Padro *et al.* (1993). A description of the forest and dataset of fluxes and deposition velocities can also be found in Padro *et al.* (1993). The one-sided leaf-area index (LAI) varies from 5 in summer to 1 in winter (Bark Area Density, BAI). The average height of the trees in the forest is 18 m. The measurements above the canopy were taken at 33.4 m. The number of half-hourly $V_d$ observations for $SO_2$ amount to 365 for the entire measurement period between March 15, 1990 and April 29, 1990, above the leafless forest. For diurnal patterns, the standard error of the mean for each half-hour was estimated to be about $\pm 0.15$ cm $s^{-1}$ for $V_d$ and $\pm 30\%$ for the flux (Padro *et al.*, 1993).

*Coniferous forest*
Since November 1992 continuous vertical concentration gradients of $SO_2$, $NO_2$ and $NH_3$ as well as relevant meteorological parameters have been measured at a Douglas fir forest site in the Netherlands. The Speulder forest site is located in the national park 'Hoge Veluwe' in the central part of the Netherlands. The measuring site consists of a homogeneous 2.5 ha monoculture of mature Douglas fir of 35 years old, with a stem density of 785 $ha^{-1}$. The mean

tree height is approximately 20 m. The canopy is well closed with the maximum leaf-area density at a height of 10-14 m. The one-sided LAI varies throughout the year from about 8 in early spring to 11 m at the end of the summer. The site is surrounded by a larger forested area of approximately 50 $km^2$; the nearest edge is at a distance of 1.5 km from the site. Directly adjacent to the site are stands of pine, mixed beech/oak, and Douglas fir and larch, with mean tree heights varying from 12 to 25 m, about roughly the same as those of the research area. A small clearing (1 ha) is situated to the north of the stand. The equipment, its performance and experiments to determine measuring errors and accuracy of the measurements are described extensively in Zwart *et al.* (1993). The standard error for each two hourly average $V_d$ was estimated to be about ± 40%.

*Grassland*

A system for $SO_2$ based on the micrometeorological gradient technique has been developed for routine monitoring of dry deposition fluxes. The $SO_2$ dry deposition monitoring system has been described extensively in Mennen *et al.*, (1992) and Erisman *et al.* (1993b). The $SO_2$ concentrations were measured with two UV pulsed-fluorescence monitors (Thermo Environmental Instruments model 43W). One $SO_2$ monitor is used to measure the concentrations at four successive levels (heights of 4, 2, 1 and 0.5 m), while a second monitor continuously measures concentrations at the 4-m level. A change in $SO_2$ concentration during the measuring cycle can thus be detected and corrected for (Erisman *et al.*, 1993b). A measuring cycle lasts 30 min. Selection criteria have been derived to select measuring periods satisfying the demands of the flux-profile theory. Furthermore, a scheme has been developed to calculate yearly average fluxes from the selected and rejected measuring periods.

The dry-deposition monitoring system was placed at a rural site in the centre of the Netherlands from 1987 to 1989. The undisturbed fetch over the grassland is between 700 m and 1 km for the eastern, southern and western directions. The pastures surrounding the location were infrequently used for cattle grazing and irregularly spread with manure during the growing season. The grass height was maintained at 15 cm most of the time. The soil type is so-called wet-peat with an average pH ranging from 4.8 to 5.1; the soil surface was nearly always wet. Eight measuring cycles were averaged to yield 4-h average deposition parameters, in order to minimise (random) measuring errors. The standard error for each four-hourly average $V_d$ was estimated to be about ± 50%.

*Heathland*

A three-year experiment involving several research groups was conducted at the Elspeetsche Veld for the determination of deposition fluxes on heathland. Micrometeorological measurements of $SO_2$, $NH_3$ and $NO_2$ were made using different techniques. Furthermore, throughfall and bulk precipitation fluxes of $SO_4^{2-}$, $NH_4^+$ and $NO_3^-$ were also measured. The experiment was carried out from 1989 to 1992 at a heathland nature reserve in the central part of the Netherlands: i.e. the 'Elspeetsche Veld' (52° 16' N, 5° 45' E) near the village of Elspeet.

The heathland is located in a region with moderate ambient concentrations of $SO_2$ (6 $\mu g\ m^{-3}$) and NOx(20 ppb) (RIVM, 1989). The ammonia emission density in this area is about equal to the average $NH_3$ emission in the Netherlands (Erisman, 1989). The standard error for each two-hourly average $V_d$ was estimated about 30%.

### 6.1.3 MODELLED $V_D$ COMPARED WITH MEASUREMENTS

For the comparison of modelled deposition parameters with those obtained from measurements, only data satisfying theoretical constraints and well above detection limits were employed. Data were rejected for wind speeds below 1 m $s^{-1}$, and for wind directions with no ideal fetch, when one of the measured parameters was below the detection limit and when the concentration changes during a measuring cycle were too large (Padro *et al.*, 1993; Erisman *et al.*, 1993a; 1993b; 1993c). These selection criteria had little influence on the Canadian data. The Speulder forest dataset was reduced by about 50%, mainly as a result of the detection limit of the $SO_2$ monitors and because of technical problems. It has not been estimated whether this has resulted in a systematic bias in the dataset. For Zegveld and Elspeet about 70-80% of the data were rejected, mainly due to a poor fetch and the detection limit of the $SO_2$ monitors used. It was found that for the Zegveld and Elspeet, data selection did not lead to a systematic bias in deposition parameters. The conditions in the remaining dataset were found to be representative for the whole measuring period (Erisman *et al.*, 1993b).

The remaining dataset comprised 364 half-hourly averaged deposition parameters for the deciduous forest, 652 two-hourly averaged data for the coniferous forest, 1391 two-hourly averaged data for heathland and 821 four-hourly averaged data for grassland. For each measuring period, $R_c$ values were calculated according to the parametrisation given in Chapter 4. Furthermore, $R_c$ values were calculated using parametrisations given by Wesely (1989) for comparison. The aerodynamic resistance $R_a$ and the quasi-laminar layer resistance $R_b$ were estimated according to the equations given in Erisman *et al.* (1994, see Chapter 4). The inverse of the sum of the three resistances is the dry deposition velocity $V_d$. In Figures 6.1 A to 1 D, modelled $V_d$ values are compared to those obtained from measurements for the deciduous forest, coniferous forest, heathland and grassland, respectively. In these figures, average modelled values and their standard deviation for each class of measured $V_d$ are plotted against class averages. Classes are formed by placing combinations of measured and modelled $V_d$ values in increasing order of measured deposition and averaging the combinations over an equal number of data. The standard deviation is given as a measure for the variation in each class. This cannot be considered as a measure of the uncertainty in class averages. In Table 6.1, minimum, maximum and average values of some measured parameters are given. This table also gives average deposition parameters and the standard deviation. The correlation coefficient of the modelled $V_d$ against the measured values, and the standard error are also presented here. Averages, standard deviations and correlation coefficients between

measured and modelled $V_d$ obtained with the parametrisation by Wesely (1989) are also given.

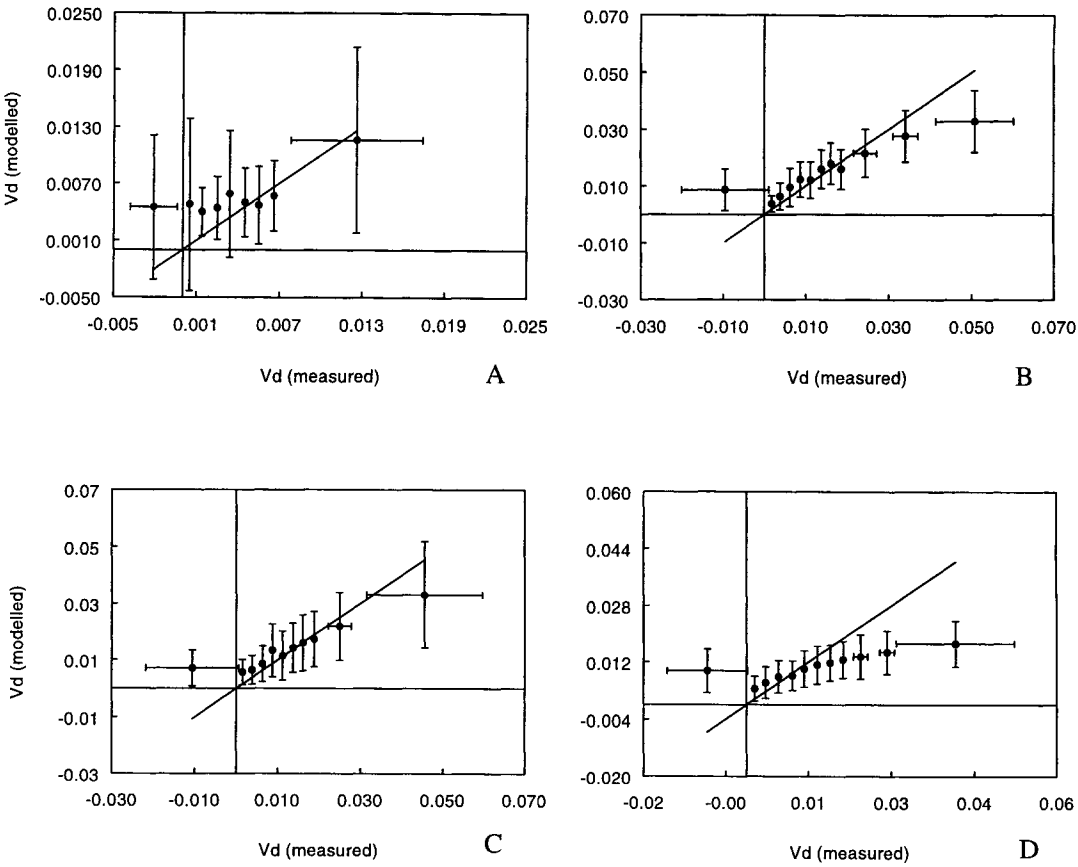


**FIGURE 6.1** Comparison of modelled $V_d$ (m $s^{-1}$) with $V_d$ obtained from measurements: A. Deciduous forest; B. Coniferous forest; C. Grassland and D. Heathland. Solid dots represent average modelled values for class-average measured values. The line represents the 1:1 ratio. Small overbars represent measured class averages ± SD, while large overbars represent modelled averages ± SD.

**TABLE 6.1** Average, minimum and maximum measured parameters, and measured and modelled $V_d$, $F$ and $R_c$ values, with correlation coefficients between modelled and measured values, as well as SD (in parentheses

| Parameter | Deciduous forest | Coniferous forest | Grassland | Heathland |
|---|---|---|---|---|
| C $SO_2$ average | 3.1 | 11.7 | 13.9 | 7.2 |
| min | 1.0 | 4.0 | 3.0 | 0.5 |
| max ($\mu g\ m^{-3}$) | 27.9 | 81.1 | 76.2 | 12.0 |
| T average | 10.5 | 6.4 | 9.7 | 9.6 |
| min | -6.9 | -10.4 | -3.3 | -10.1 |
| max (°C) | 28.2 | 25.2 | 24.3 | 30.1 |
| u average | 3.1 | 4.1 | 4.8 | 3.7 |
| min | 1.0 | 1.0 | 1.1 | 1.0 |
| max ($m\ s^{-1}$) | 7.8 | 9.5 | 13.2 | 9.1 |
| Q average | 190 | 78 | 115 | 145 |
| min | 0 | 0 | 0 | 0 |
| max ($W\ m^{-2}$) | 900 | 860 | 790 | 810 |
| rh average | 59 | 82 | 80 | 85 |
| min | 27 | 20 | 33 | 10 |
| max (%) | 100 | 100 | 99 | 100 |
| No. wet hours | 105 | 487 | 440 | 1013 |
| No. dry hours | 261 | 426 | 381 | 378 |
| Periods | March 15 - April 29, 1990 | November 1992-June 1993 | November 1987-September 1989 | November 1989-Augusts 1992 |
| No. measurements | 365, half-hourly averages | 652, two-hourly averages | 821, four-hourly averages | 1391, two-hourly averages |
| Measured $V_d$[a]: | 0.0028 (0.0056) | 0.0165 (0.0193) | 0.0148 (0.0100) | 0.0115 (0.0135) |
| Modelled $V_d$[a]: | 0.0066 (0.0067) | 0.0168 (0.0152) | 0.0110 (0.0061) | 0.0134 (0.0100) |
| Wesely (1989): ($m\ s^{-1}$) | 0.0010 (0.0001) | 0.0020 (0.0009) | 0.0056 (0.0021) | 0.0071 (0.0034) |
| *modelled versus measured $V_d$:* | | | | |
| Correlation coeff.: | 0.39 | 0.66 | 0.46 | 0.64 |
| Standard error: | 0.007 | 0.011 | 0.010 | 0.010 |
| *Wesely (1989) versus measured $V_d$:* | | | | |
| Correlation coeff.: | 0.39 | 0.17 | 0.30 | 0.21 |
| Standard error: | 0.0001 | 0.0009 | 0.011 | 0.013 |
| Measured $F$[a]: | -0.012 (0.034) | -0.196 (0.239) | -0.199 (0.175) | -0.065 (0.100) |
| Modelled $F$[a]: ($\mu g\ m^{-2}\ s^{-1}$) | -0.021 (0.032) | -0.205 (0.207) | -0.140 (0.109) | -0.074 (0.081) |
| Measured $R_c$[a]: | 4 (6580) | 70 (335) | 20 (195) | 55 (185) |
| Modelled $R_c$[a]: ($s\ m^{-1}$) | 185 (115) | 130 (770) | 50 (85) | 60 (120) |

[a] The estimates have been presented in more significant figures than consistent with their accuracy for intercomparison.

The results in Figures 6.1A to D show that modelled $V_d$ correlate well with the measurements taken in the coniferous forest and heathland, where 44 and 41%, respectively, of the variance was accounted for. The correlation between modelled and measured velocities for the deciduous forest and grassland is lower. Only 15 and 21% , respectively, of the variance was accounted for. The datasets are too large to use statistical tests to test the hypothesis to see if overall averages or variances of measured and modelled values are equal. This can be done for subsets e.g. for each class in Figures 6.1A to D. These results can be roughly extracted from the figures. It can be seen that for the coniferous forest and heathland measurements, averages are about equal for each class except for negative values. For the grassland, average measured values are significantly higher. For the deciduous forest, the lowest modelled values are higher than those measured, whereas the larger values are equal. For each class, Wesely's parametrisation yields significantly lower values than measured or obtained from the parametrisation presented here. Wesely's parametrisation implies too large a value of $R_c$. The correlation between modelled and measured values is lower for Wesely's $R_c$ parametrisation than that given here (Table 6.1).

It is more interesting to see whether modelled and measured values agree for the periods dominated by certain processes than just to compare class averages. Four periods were selected where different resistances are expected to dominate: (1) daytime dry conditions ($R_{stom}$), and (2) wet conditions ($R_{ext}$), (3) night-time dry conditions ($R_{inc}$) and (4) wet conditions ($R_{ext}$). Results of averages and correlation between modelled and measured values for these four periods are presented in Table 6.2.

The results presented in Table 6.2 show the same general features as those obtained for class averages. The modelled $V_d$ values for the deciduous forest are generally higher than those measured. The modelled $V_d$ values for the coniferous forest and heathland are generally in good agreement with measurements. Grassland $V_d$ values agree well for wet periods. However, for dry conditions in daytime and night-time, modelled values are too low. It is not clear from these results which resistance from Eqn. 4.3 is modelled better.

**TABLE 6.2** Average dry deposition velocities (m $s^{-1}$) and correlation coefficients between modelled and measured $V_d$ for dry/wet and daytime and night-time periods, with SD in parentheses.

| | Daytime | | Night-time | |
|---|---|---|---|---|
| | Dry conditions | Wet conditions | Dry conditions | Wet conditions |
| *Deciduous forest* | | | | |
| Measured $V_d$[a] | 0.003 (0.006) | 0.006 (0.007) | 0.001 (0.003) | 0.001 (0.006) |
| Modelled $V_d$[a] | 0.006 (0.007) | 0.011 (0.010) | 0.003 (0.001) | 0.006 (0.010) |
| Cor. coeff. | 0.10 | 0.83 | 0.32 | 0.26 |
| Std. error | 0.007 | 0.005 | 0.001 | 0.010 |
| Number | 195 | 59 | 85 | 26 |
| *Coniferous forest* | | | | |
| Measured $V_d$[a] | 0.007 (0.016) | 0.023 (0.020) | 0.007 (0.008) | 0.025 (0.020) |
| Modelled $V_d$[a] | 0.006 (0.004) | 0.024 (0.014) | 0.006 (0.005) | 0.026 (0.016) |
| Cor. coeff. | 0.47 | 0.57 | 0.56 | 0.60 |
| Std. error | 0.004 | 0.012 | 0.004 | 0.013 |
| Number | 167 | 142 | 123 | 220 |
| *Grassland* | | | | |
| Measured $V_d$[a] | 0.014 (0.010) | 0.015 (0.010) | 0.013 (0.011) | 0.017 (0.013) |
| Modelled $V_d$[a] | 0.007 (0.003) | 0.015 (0.006) | 0.007 (0.004) | 0.014 (0.006) |
| Cor. coeff. | 0.42 | 0.49 | 0.60 | 0.58 |
| Std. error | 0.009 | 0.009 | 0.009 | 0.011 |
| Number | 260 | 268 | 121 | 173 |
| *Heathland* | | | | |
| Measured $V_d$[a] | 0.008 (0.011) | 0.014 (0.015) | 0.009 (0.011) | 0.012 (0.013) |
| Modelled $V_d$[a] | 0.008 (0.005) | 0.019 (0.010) | 0.007 (0.006) | 0.015 (0.010) |
| Cor. coeff. | 0.38 | 0.65 | 0.58 | 0.81 |
| Std. error | 0.005 | 0.012 | 0.006 | 0.008 |
| Number | 403 | 507 | 148 | 333 |

[a]The estimates have been presented in more significant figures than consistent with their accuracy, for intercomparison.

Figures 6.2A to D give examples of time series of measured and modelled $V_d$ values for the four types of vegetation. These figures illustrate comparisons of the diurnal cycles between the model and measurement under different conditions. Again, the model seems to overpredict over the deciduous forest.

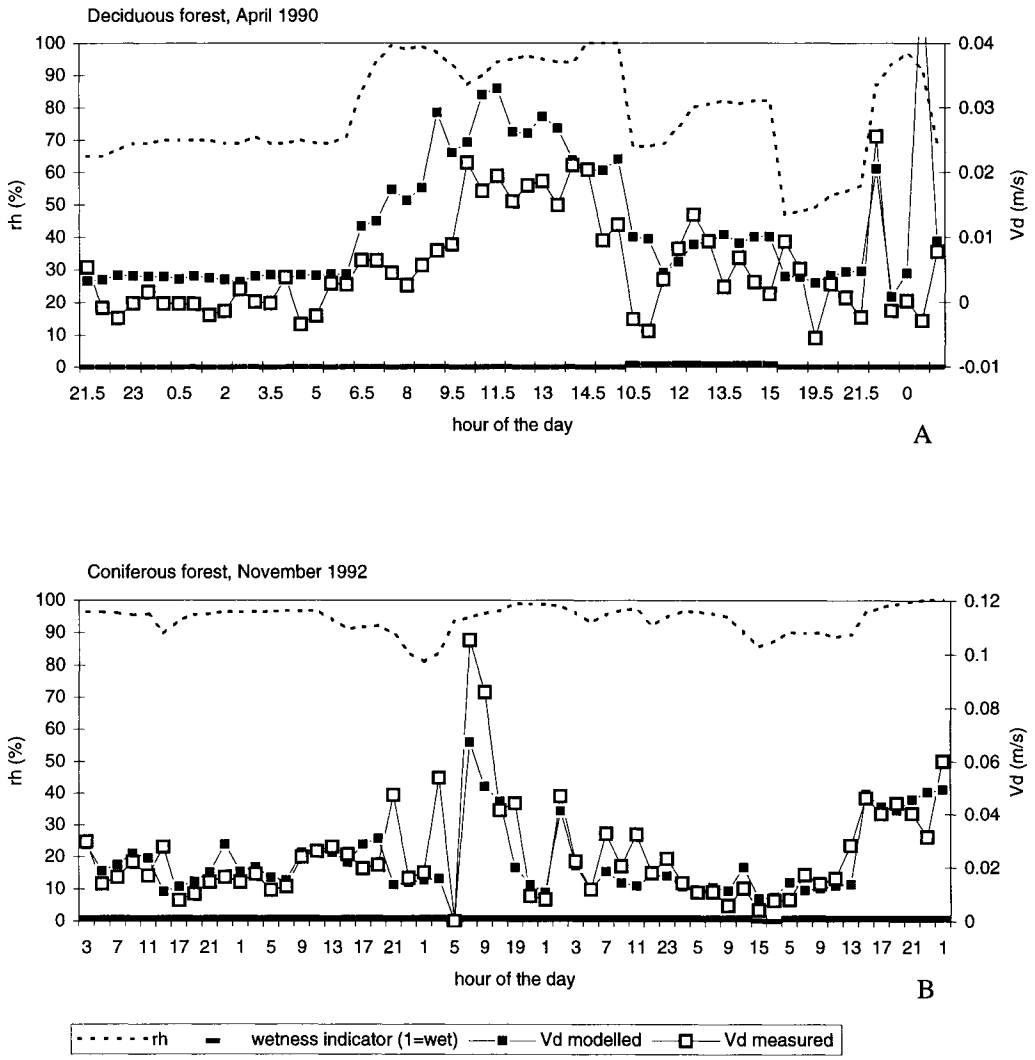


**FIGURE 6.2.** Examples of time series of modelled and measured $V_d$: A. Deciduous forest; B. Coniferous forest.

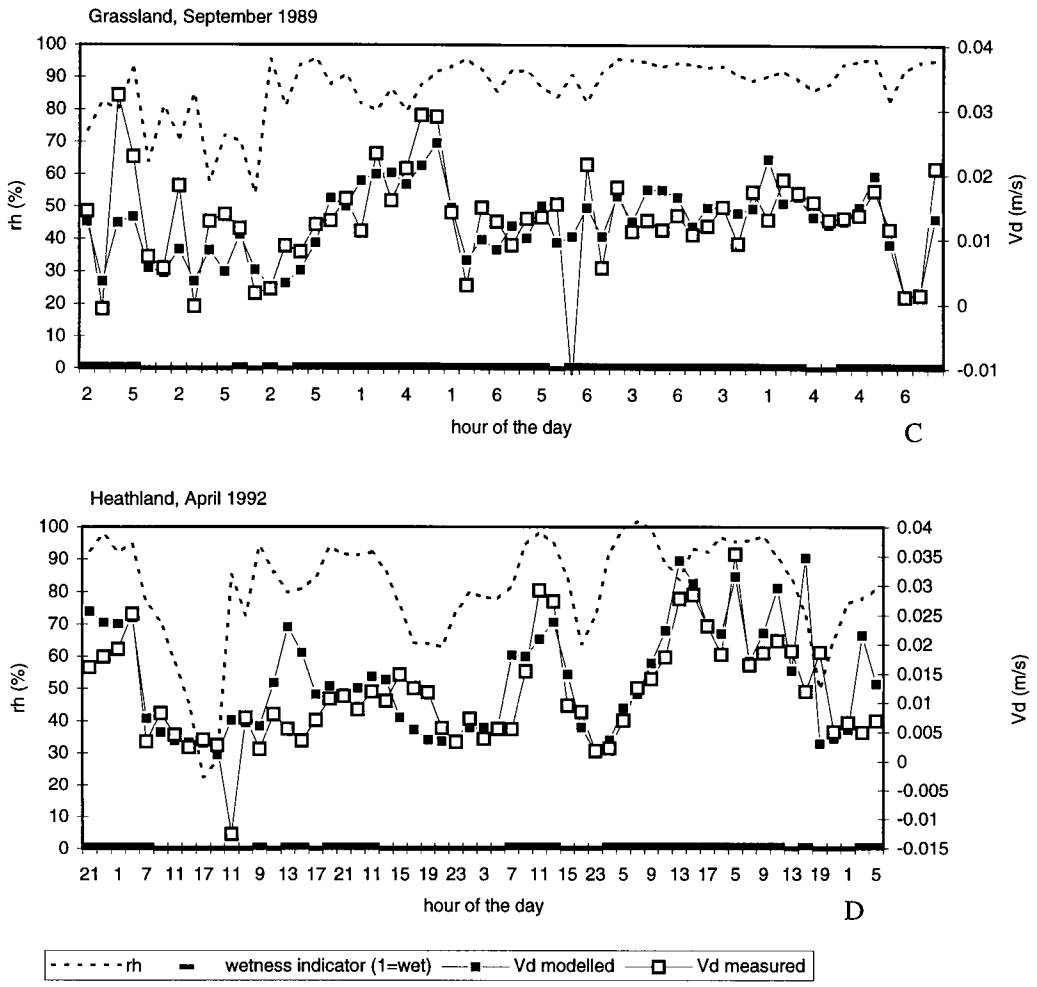


**FIGURE 6.2** (*continued*). Examples of time series of modelled and measured $V_d$: C. Grassland and D. Heathland.

## 6.1.4 DISCUSSION

The comparison analysis was conducted for dry deposition velocities instead of surface resistances, as it is the most important parameter and because $R_c$ values show large scatter with no general distribution, making comparison difficult. Furthermore, $R_c$ values are very

sensitive to measurement errors, especially at small $V_d$'s. Small $V_d$'s are the result of either large values of $R_a$+$R_b$ or a large resistance to surface uptake. Small measurement errors might result in very large positive or negative values of $R_c$, introducing enormous scatter in the dataset. Measurement errors lead to a normal distribution of errors in $V_d$, but to an unknown distribution in $R_c$ (see section on uncertainties below). By only comparing modelled with measured $V_d$ values there is the danger of ignoring differences between modelled and measured values. These differences can result from surface processes occurring during periods showing very high values of $R_a$+$R_b$ (i.e. stable conditions), which yield low $V_d$. In general, these processes do not influence agreement between model and measurements and may therefore be ignored. However, in cases where they dominate, this can introduce a large systematic bias.

*Uncertainties*

The measured and modelled deposition parameters are subject to several uncertainties. During periods when the fluxes or concentrations are small, measurements usually show a high uncertainty due to the relative high error in the concentration gradient. Systematic errors are excluded as much as possible through the selection procedure. However, a random measurement error can lead to random errors in $V_d$, which might lead to negative values. These might be interpreted as emission rather than small deposition. On the other hand, at zero resistance to uptake at the surface ($R_c$~0), random errors can yield $V_d$ values that are larger than the maximum possible $V_d$. Large random errors cause frequency plots of measured $V_d$ to look like normal distributions (the distribution of the random error), while the 'real' distribution of $V_d$ is logarithmic. Figures 6.3 A to D give the frequency distributions of measured and modelled $V_d$. As expected from the results presented in Figure 6.1, the modelled and measured distributions of $V_d$ over the coniferous forest and heathland are similar. Moreover, the distributions approach the logarithmic form, as expected. Thus, measured $V_d$ is not influenced to a large extent by a random error.

The distribution for the grassland is logarithmic, but the peaks for the modelled and measured distributions are different, suggesting an incorrect $R_c$ parametrisation. An investigation of individual measurements, revealed that by using 4-h averages, the surface wetness parametrisation yielded an underestimate of the time the surface was wet (see also Table 6.2). It was observed in the field that the surface was wet nearly all of the time, whereas results in Table 6.1 suggest that this was only true for about 50% of the cases.

The distribution for the deciduous forest follows the shape of a normal distribution. This suggests that the measurement results are dominated by a random error. Concentrations during the measurements are relatively low, with an average value of 3.1 $\mu g\ m^{-1}$ (Table 6.1). The lower the concentration, the higher the error in the concentration gradient as a result of random errors. This can be seen by introducing an extra selection criterion on concentration. If

measurements at concentrations below 2 μg $m^{-1}$ are rejected, the shape of the frequency distribution becomes logarithmic. Furthermore, the correlation coefficient between modelled and measured values increases to 0.6 (36% of variance accounted for), with no systematic differences between the averages. Also, comparison between modelled and measured values for dry/wet conditions during daytime and night-time shows improvement.

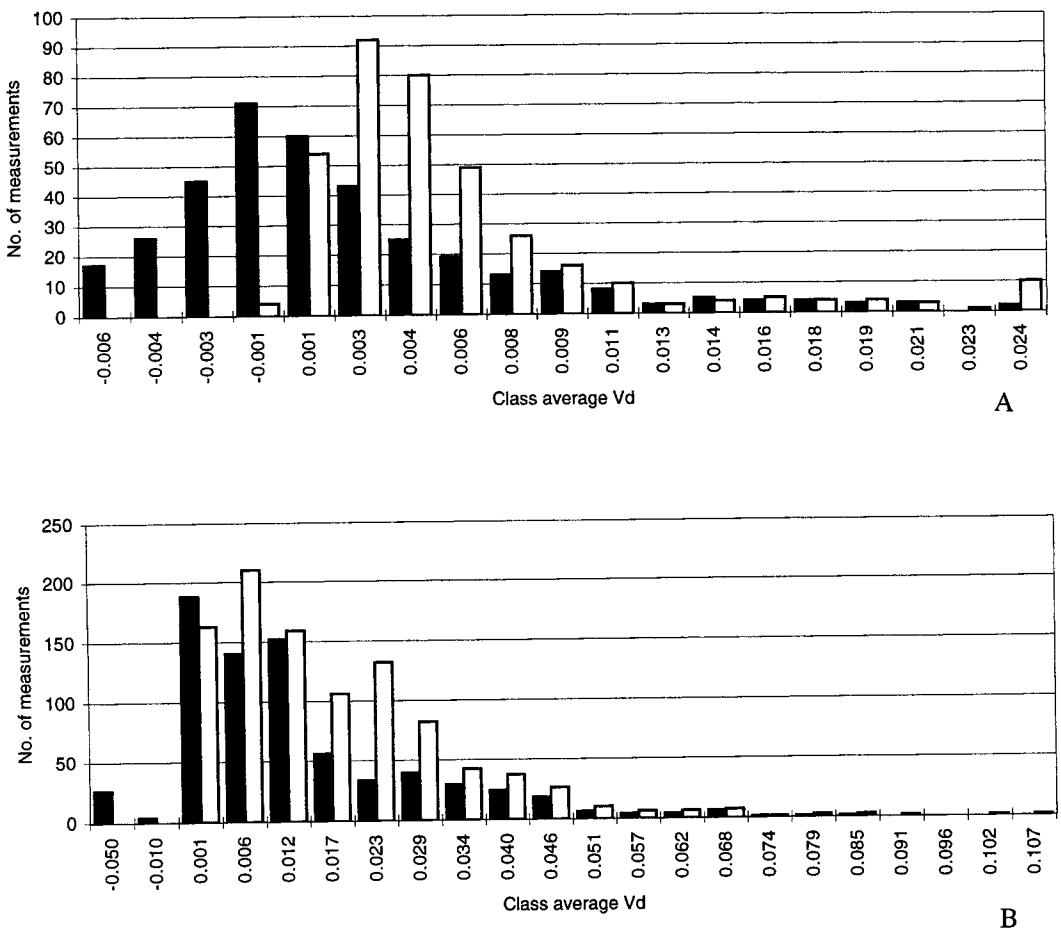


**FIGURE 6.3** Histograms of modelled (open columns) and measured (dark columns) $V_d$ (m $s^{-1}$): A. Deciduous forest; B. Coniferous forest.

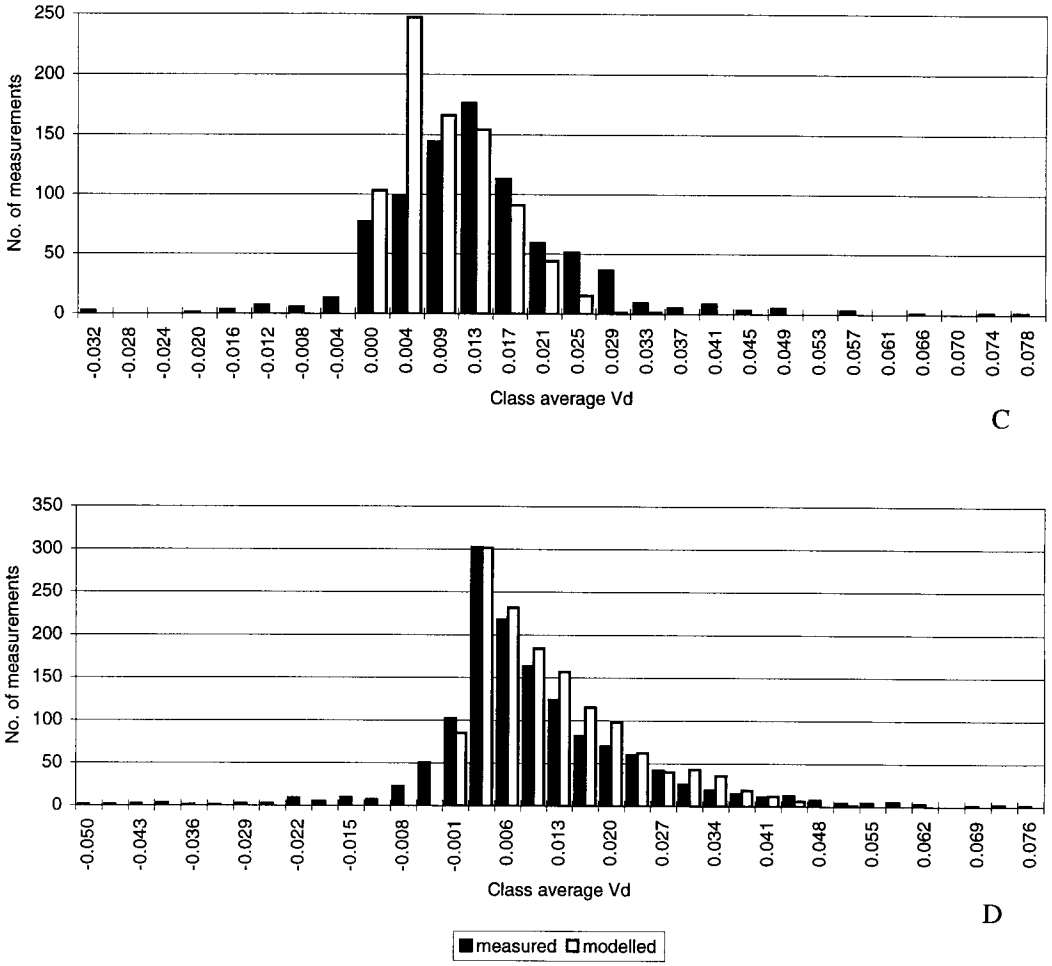


**FIGURE 6.3** (*continued*) Histograms of modelled (open columns) and measured (dark columns) $V_d$ (m $s^{-1}$): C. Grassland and D. Heathland

*Comparison with other parametrisations*

Much early work done on parametrisation of the surface resistance to gaseous dry deposition comes from the USA (Hicks *et al.*, 1987; 1989; Wesely, 1989), the UK (Garland, 1977; 1978; Fowler, 1978; 1985) and Canada (Voldner *et al.*, 1986; Padro *et al.*, 1993). Wesely (1989) recently derived a scheme for the RADM model representative for North American conditions (see Section 4). Padro *et al.* (1993) used this scheme and the scheme presently used in the ADOM model to compare $SO_2$ $V_d$ values with those obtained from measurements in the Borden forest, the same dataset as used here. They found that ADOM's estimates were much larger than the measured values, whereas Wesely's parametrisation yielded smaller estimates than were measured. These results are comparable to those found in the present study. Wesely's parametrisation yields much lower $V_d$ values than measured for each of the four types of vegetation. This is mainly caused by the surface resistance description for periods during or after rain. Wesely assumes that $R_c$ values increase during or after rainfall as a result of sufficient S(IV) saturation of the rain, which prevents further uptake of $SO_2$. This assumption is based on unpublished measurements by the Argonne National Laboratory (Wesely, 1989). Before Wesely's parametrisation is used, this assumption must be tested since it will have serious implications, especially in those areas where the surface is frequently wetted by rain. It could lead to an underestimate of the surface uptake of $SO_2$ by a of factor of 2 (low vegetation) to 8 (forests)! Testing the assumption on S(IV) saturation can be done using short-term precipitation measurements of S(IV), base cations and pH, as well as ambient $NH_3$ and base cation concentrations.

*Representativeness of parametrisation for European pollution climates*

As the surface resistance parametrisation is derived from the measurements made at the heathland site of Elspeetsche Veld (Erisman *et al.*, 1993c), it might only be representative for the Dutch pollution climate. This pollution climate is different from other climates common in Europe, and might therefore not be useful for models used to estimate deposition in Europe. However, from Table 6.1 it is obvious that the measured parameters (*C*, *T*, *u*, *Q* and *rh*) cover a very wide range, representative for large areas in Europe. The ratio of hours for which vegetation was assumed to be wet to those for which the vegetation was assumed to be dry is larger than for most areas in Europe because of the Dutch marine climate. However, there were sufficient measurements made during very dry periods to allow a valid study of the parametrisation under such conditions. In any case, during these periods deposition velocities and fluxes tend to be very low and therefore not too important.

A major concern in the Netherlands is the relatively high neutralisation capacity caused by large ammonia emissions from intensive livestock breeding. This is not representative for large areas of Europe (and USA, see discussion on comparison to Wesely's parametrisation), where $NH_3$ emissions and concentrations are much lower (Buijsman *et al.*, 1987; Asman and Van Jaarsveld, 1992). In the Netherlands the annual average ammonia concentration is about

equal to that of $SO_2$: 5 ppb and 4 ppb, respectively. This is also the case at the three Dutch measuring sites. It has been suggested that the presence of ammonia enhances sulphur deposition (Van Breemen *et al.*, 1982; Adema *et al.*, 1986). However, Erisman and Wyers (1993) showed that this so called co-deposition is important only in extreme conditions, i.e. when there is a very high ratio of $NH_3$ concentration to that of $SO_2$. They found that surface wetness was most important for enhancing dry deposition, but they did not demonstrate that $NH_3$ does not play a role under wet conditions.

### 6.2.5 SYNTHESIS

This section has described the testing of a surface resistance parametrisation for surface uptake of $SO_2$ using eddy correlation measurements over a deciduous forest in Canada and vertical gradient measurements over a coniferous forest, a grassland and a heathland in the Netherlands. The surface resistance parametrisation includes the stomatal resistance, the resistance for wet surfaces caused by precipitation and relative humidity, the resistance to in-canopy aerodynamic transport, and the resistance to soil and to snow-covered surfaces. It is concluded that the modelled $V_d$ compare reasonably well with the measurements, yielding no systematic differences for the coniferous forest and heathland (more than 40% of variance accounted for). There is much less agreement with the measurements for the deciduous forest and grassland, where systematic differences are shown. However, it was concluded that the errors were not due to the surface resistance parametrisation, but rather to possible random errors in the (low) concentration measurements over the deciduous forest and for the grassland measurements to underestimating the time the surface was assumed wet. The parametrisation was tested for four different classes (dry and wet conditions for day and night). No systematic error could be detected from this comparison other than what is described above.

The surface resistance parametrisation developed by Wesely (1989) was also tested using the same dataset. Results show a systematic underestimation of $V_d$ values when compared to measured values. The underestimate is mainly the result of the parametrisation of $R_c$ during and after precipitation. Wesely assumes an increase in $R_c$, whereas measurements show a decrease to values close to zero. This can lead to an underestimation of $V_d$ $SO_2$ by a factor of 2 for low vegetation to a factor of 8 for forests.

The parametrisation demonstrated for the Netherlands may be representative for large parts of Europe. Other types of vegetation can be modelled by adjusting the stomatal resistance. The parametrisation might not be representative for those areas which have a completely different pollution climate from that occurring during the measurements. This might be the case for very dry areas or areas where ammonia concentrations are negligibly low compared to those for $SO_2$. Unfortunately, there is a lack of long-term measurements for such areas. It is

therefore recommended to perform such measurements over these areas to evaluate and/or improve surface resistance parametrisations.

## 6.2 RELATION BETWEEN ATMOSPHERIC DEPOSITION AND SOIL LOADS

*Introduction*

There are no long-term micrometeorological measurements of other components available than those for $SO_2$. It is therefore not possible to do similar tests of the parametrised deposition parameters with measurements. Modelled fluxes might be tested with throughfall measurements. However, the relation between throughfall fluxes and atmospheric deposition is not in all cases very clear. Wash-off processes from leaf and bark surfaces due to water passing through the canopy can increase concentrations relative to open field precipitation. The net-throughfall flux is determined by the net contribution of washed-off dry deposited gases and particles, interception of cloud water and re-evaporation of gases from the canopy. The kinetics of removal by wash-off may be as complex as the kinetics of dry deposition itself. Canopy interaction is, next to dry deposition, regarded as one of the most important factors influencing throughfall and stemflow composition for several ions. Both leaching from the canopy as well as canopy uptake of nutrients and gases have been found (Parker, 1983).

In several attempts to compare throughfall fluxes with atmospheric deposition estimates, large differences between the two estimates for deposition were found (e.g. Ivens, 1990, Draaijers and Erisman, 1993; Erisman, 1993b). Establishing a link between the two is useful because it provides a way to estimate soil loads from atmospheric deposition estimates and allows the use of the relatively simple and cheap throughfall method to determine atmospheric deposition. The link between atmospheric deposition and soil loads is important because critical loads refer to soil loads and atmospheric deposition estimates provide a link with emissions. Thus if critical load exceedances are used to estimate emission reductions, the relation between atmospheric deposition and soil load should be known.

The data used in published comparisons between the two are of varying quality, for both atmospheric deposition estimates and throughfall estimates. Ivens (1990), Draaijers (1993) and Beier and Rasmussen (1989) have addressed the uncertainty in throughfall measurements and proposed sampling methods, which should reduce most of it. Furthermore, Erisman (1993a) provided a method to estimate atmospheric deposition on the required scale (stand level), which enabled a good comparison. Draaijers and Erisman (1993) compared throughfall estimates with atmospheric deposition estimates of SOx for 30 different forest stands on the Utrechtse Heuvelrug in the Netherlands. They assessed the uncertainty in the two methods and found that by changing the surface resistance parametrisation of $SO_2$ in the inference model to that derived from more recent dry deposition measurements in the Netherlands (Erisman *et al.*, 1994), the agreement between the two estimates was reasonable without any systematic differences. This would mean that canopy exchange of sulphur species is negligible in the long term (one year).

In this section throughfall measurements and deposition estimates will be compared on two levels: at the site, using experiments done at the Speulder forest in the Netherlands (described in section 7.3) and on the national level (The Netherlands), using throughfall measurements made at 51 sites throughout the Netherlands for several years. First, some theoretical considerations on canopy exchange processes will be given.

### 6.2.1 THEORETICAL CONSIDERATIONS ON CANOPY EXCHANGE

Draaijers *et al.* (1994) provide a literature overview of field and lab experiments on canopy exchange. The most important factors determining canopy exchange are listed. Here, only a summary of the most important processes will be given.

Concentrations in water layers covering leaves and needles are found to be influenced by passive diffusion and ion exchange between the surface water and the underlying apoplast of canopy tissues (i.e. aqueous layer outside cell membranes). Diffusion is found to be the major cause of elevated (leached) anionic concentration in throughfall, while both diffusion and ion exchange contribute to (leached) cationic concentrations in throughfall (Schaefer and Reiners, 1990). Diffusion is controlled by the (ion-specific) resistance of the cuticle and epicuticular wax, and by the concentration gradient between leaf-surface water and apoplast (Reiners and Olson, 1984). Ion exchange can take place for both anions and cations, but cuticular anion exchange sites are far fewer in number than cation exchange sites. Cations, especially those abundant in the foliar apoplast, are released from cuticular ionic binding sites in exchange for hydrogen or ammonium ions retained by the foliage (Roelofs *et al.*, 1985; Parker, 1990). Cations can also be released from foliage along with weak organic acid anions, or along with inorganic anions (Cronan and Reiners, 1983). Canopy uptake of gases through stomata is governed by gas concentrations and ion equilibrium concentrations in the apoplast, the dissolved gas in apoplast liquid and stomatal opening.

The rate of canopy exchange depends on tree physiology, pollution climate and ecological setting. As deciduous trees are leafless in winter, canopy exchange is little during this season. Coniferous trees stay green all year and continue to lose or gain nutrients throughout the dormant season. In general, however, deciduous trees tend to lose more nutrients than coniferous trees (Smith, 1981). The age distribution of leaves also affects the magnitude of leaching; young immature needles tend to lose fewer nutrients compared to older ones (Parker, 1990). Senescent leaves lose more nutrients than green leaves. Leaf wetness is important as the liquid on the outside of the foliage comprises the medium for canopy exchange. The wettability of foliage is found to differ considerably among tree species (Boyce *et al.*, 1991). Moreover, an increasing rate of foliar wax degradation caused by, for example, exposure to air pollutants is thought to lead to a decrease in water repellency, which in turn will lead to longer retention of moisture (Cape, 1983). Biotic stresses such as insect plagues

and diseases may initiate canopy leaching (Bobbink *et al.*, 1990). The same holds for abiotic stresses such as drought and temperature extremes (Tukey and Morgan, 1963). Soil fertilisation is found to increase canopy leaching (Cape, 1983). The presence of pollutants might enhance canopy leaching; concentrations of, for example, ozone might enhance the permeability of cell membranes in foliage, thereby increasing ion leakage (Evans and Ting, 1973). Moreover, the amount and timing of precipitation is found to be relevant with respect to canopy leaching. Relatively long residence times during drizzle account for relatively high leaching fluxes compared to short rain periods with large rainfall intensities.

### 6.2.2 RESEARCH RESULTS FROM THE SPEULDER FOREST SITE

*Throughfall fluxes at the Speulder forest*

During the experiments in the Speulder forest, the same throughfall method was used as that by Draaijers (1993) for the comparison reported in Draaijers and Erisman (1993) (see also section 7.3). The number of samplers (gutters) was increased to 25 in order to determine the optimum for deducing a soil-load flux representative for the whole forest stand (Van Leeuwen *et al.*, 1994). The results of the throughfall measurements have been reported in Van Leeuwen *et al.* (1994) and in Draaijers *et al.* (1994). Stemflow was not measured in the Speulder forest. It is expected that stemflow fluxes for Douglas fir are negligible compared to throughfall fluxes, accounting for a maximum of 6% of the total flux (Van Leeuwen *et al.*, 1994). Net throughfall fluxes are calculated for 30 different periods. Not all periods ended with showers with enough precipitation to wash off all the dry deposited material from the canopy. It was estimated that this would take about 15 mm of precipitation (Van Leeuwen *et al.*, 1994). This occurred only in four periods, thus the November '92-May '93 period was split in four periods. This, however, represents a small base for statistical analysis when comparing with atmospheric deposition estimates. Therefore another 12 periods were selected in which it is supposed that at least most of the dry deposited material was washed off and thus the whole period could be split into 16 periods. The net throughfall fluxes averaged over the period of 23 November 1993 to 10 May 1993 are listed in Table 6.3. The estimated uncertainty is given in parentheses. The contribution of canopy exchange to net throughfall was estimated using the Ulrich model (1983), as outlined in Draaijers *et al.* (1994).

*Atmospheric deposition at the Speulder forest*

Wet deposition is measured on a routine basis at the Speulder Veld, about 3 km from the Speulder forest site. Wet deposition data for 1993 are given in Table 6.3. As it is not possible to determine atmospheric deposition solely with micrometeorological measurements, the resistance analogy is used as supplement. Dry deposition fluxes are inferred from measured concentrations (gases and particles) and estimated dry deposition velocities for those periods in which gradient measurements could not be used for estimating deposition. $V_d$ is estimated using meteorological measurements and a component specific surface resistance. This surface

resistance is determined using a parametrisation outlined in Chapter 4. The resistance analogy is applied to determine gas, particle and fog deposition for the period that throughfall was measured in order to compare throughfall fluxes with atmospheric deposition (see section 7.3).

**TABLE 6.3** Average net throughfall fluxes, and dry and fog deposition estimates for the Speulder forest, along with wet deposition at Speulder Veld (mol $ha^{-1}a^{-1}$)

| Component | Net throughfall | Dry deposition based on net throughfall and model results (Draaijers *et al.*, 1994) | Dry deposition based on concentration and meteorological measurements | Wet deposition Speulder Veld | Difference between net throughfall and atmospheric deposition (%)[a] |
|---|---|---|---|---|---|
| $SO_2$ | | | 660 (30) | | |
| Fog | | | 35 (30) | | |
| $SO_4^{2-}$ aerosol | | | 215 (60) | | |
| SOx | 925(30) | 925 (30) | 910 (40) | 270 (20) | -1 |
| $NH_3$ | | | 1440 (40) | | |
| Fog | | | 100 (30) | | |
| $NH_4^+$ aerosol | | | 645 (60) | | |
| NHx | 1730 (30) | 1980 (40) | 2185 (50) | 680 (25) | 10 |
| $HNO_2$ | | | 105 (40) | | |
| $HNO_3$ | | | 135 (40) | | |
| $NO_2$ | | | 115 (40) | | |
| Fog | | | 25 (30) | | |
| $NO_3^-$ aerosol | | | 410 (60) | | |
| NOy | 395 (30) | 395 (40) | 790 (40) | 290 (25) | 67 |
| $Cl^-$ | 800 (30) | 800 (30) | 890 (50) | 535 (20) | 10 |
| $K^+$ | 305 (30) | 35 (50) | 35 (50) | 40 (30) | 0 |
| $Na^+$ | 690 (30) | 690 (30) | 600 (50) | 465 (20) | -14 |
| $Ca^{2+}$ | 160 (30) | 85 (40) | 100 (50) | 45 (30) | 17 |
| $Mg^{2+}$ | 140 (30) | 100 (40) | 120 (50) | 65 (30) | 19 |

[a] Calculated as $[(AD\text{-}NT)/(AD+NT)]*200\%$; *AD*=atmospheric deposition; *NT*= dry deposition based on net throughfall and a model by Van der Maas *et al.* (1991). Estimated uncertainty (expert judgement) is given in parentheses in %.

Gas deposition

The dry deposition of $SO_2$, $NO_2$ and $NH_3$ was estimated using the gradient technique (Erisman *et al.*, 1993; Wyers *et al.*, 1993). The performance of the $SO_2$ and $NO_2$ instruments used and the monitoring system as a whole are extensively described in Zwart *et al.* (1994). First, data were selected to meet theoretical demands and to reduce errors in deposition parameters. Second, a parametrisation of the surface resistance for the different gases was derived from the selected data and tested. Finally, meteorological and concentration measurements and

estimated surface conditions for the rejected periods were used, together with the surface resistance parametrisation and the resistance analogy, to estimate fluxes for individual periods that throughfall measurements were available. Results are reported in Draaijers *et al.* (1994). In the same period, dry deposition of $HNO_3$, $HNO_2$ and HCl was inferred from measured air concentrations and parametrised $V_d$ values (Erisman *et al.*, 1994). Gas deposition estimated for the total throughfall measuring period is given in Table 6.3. Estimates of the uncertainty from expert judgement (Zwart *et al.*, 1994; Mennen *et al.*, 1995) are given in parentheses. Part of the uncertainty is the result of low-time coverage of the measurements: for example, only 48% of the time measurements for $NH_3$ and 42% for $NO_2$ are available. For $SO_2$, a relatively large time coverage of 79% was obtained. The average dry deposition velocities over the period November 1992 to May 1993 are $1.8 \pm 2.5$ cm $s^{-1}$ for $SO_2$, $2.6 \pm 8.0$ cm $s^{-1}$ for $NH_3$, and $0.1 \pm 1.4$ cm $s^{-1}$ for $NO_2$.

Particle input

Dry deposition of acidifying aerosols and base cations was inferred from measured air concentrations and the model described in Chapter 4. The input was estimated using the continuous aerosol concentration measurements and an integrated dry deposition velocity over the size distribution of the components (Ruijgrok *et al.*, 1994). The average fluxes for the November 1992 to May 1993 period are listed in Table 6.3. The uncertainty in the fluxes is taken from Ruijgrok *et al.* (1994). The time coverage of the flux estimates was about 70% due to technical problems.

Fog input

Deposition of fog to the Speulder forest was estimated by Vermeulen *et al.* (1994). Input by fog was estimated by parametrisation of *LWC* on visibility measurements and a parametrisation of $V_d$ based on $u_*^2$ (see section 7.3). It was found that the water flux measured with throughfall was larger than that measured using the eddy correlation method. This is probably due to the cut-off diameter used by the droplet spectrum measurements (45 μm). This means that periods with drizzle are not taken into account in the fog deposition estimates using micrometeorological methods. The chemical composition of fog droplets was measured by Römer and Te Winkel (1994) using a CWP string collector. Concentrations in fog are taken as the average over a number of samples obtained in the Netherlands over several years (Van Aalst and Erisman, 1991; Vermeulen *et al.*, 1994) because of lack of measured data representative for the six months. Vermeulen *et al.* (1994) concluded that the $SO_4^{2-}$ and $NH_4^+$ fluxes estimated with the two methods did not differ by more than a factor of two. Differences were higher for $NO_3^-$.

The total fog deposition estimated for the November 1992 to May 1993 period is given in Table 6.3. The contribution of fog to the total dry deposition in this period is very low: 4% for SOx, 5% for NHx and 3% for NOy. Even on an annual basis fog input is small compared to dry deposition of gases and aerosols (Vermeulen *et al.*, 1994).

*Comparison of throughfall fluxes with atmospheric deposition estimates*
Averaged for the whole measurement period, the dry and fog deposition estimate for $SO_x$ derived from micrometeorological measurements and inferential modelling almost equal the measured net throughfall flux of $SO_4^{2-}$. Dry and fog deposition estimates for NHx and NOy are higher than net throughfall fluxes of $NH_4^+$ and $NO_3^-$, respectively. Dry and fog deposition estimates and net throughfall of $Na^+$ and $Cl^-$ are more or less equal. Dry and fog deposition estimates for $Ca^{2+}$, $K^+$ and $Mg^{2+}$ are lower than corresponding net throughfall fluxes. If net throughfall of $NH_4^+$ and base cations is corrected for canopy exchange by using the canopy exchange model of Ulrich (1983) (Draaijers *et al.*, 1994), good agreement is found with dry and fog deposition estimates (Table 6.3 and Draaijers *et al.*, 1994).

No significant relationships are found when dry and fog deposition estimates are compared to net throughfall fluxes from all the 16 measuring periods between November 1992 and May 1993. This may be explained to a large extent by incomplete wash-off of dry deposition from the canopy by rain, through which no independent samples are obtained. Moreover, in several periods concentration measurements had a relatively small time coverage through which dry deposition estimates were subject to large potential error. Four periods could be distinguished in which complete wash-off of dry deposition was expected (Van Leeuwen *et al.*, 1994). For these four periods, the SOx dry and fog deposition estimate agrees with the net throughfall flux of $SO_4^{2-}$ ($r=0.997$; $p=0.002$). Levels are also about equal. For other components, larger differences are found and relationships are not significant ($p<0.05$). Results are shown in Table 6.4.

**TABLE 6.4** Comparison of net throughfall fluxes with atmospheric deposition (% difference calculated as in Table 6.1) for four periods for which complete wash-off of deposited material was expected

| Period | $SO_4^{2-}$ | $NO_3^-$ | $NH_4^+$ | $Na^+$ | $Cl^-$ | $Ca^{2+}$ | $K^+$ | $Mg^{2+}$ |
|---|---|---|---|---|---|---|---|---|
| 1 | 4 | -84 | 18 | 83 | 47 | 78 | 170 | 55 |
| 2 | 9 | -39 | -16 | 23 | 0 | 59 | 169 | 86 |
| 3 | 5 | -87 | -33 | 8 | -16 | 58 | 154 | 6 |
| 4 | -6 | 4 | -22 | 47 | 62 | -86 | 153 | 0 |

*Canopy exchange processes in the Speulder forest*
The results of the comparison between throughfall and atmospheric deposition in Table 6.3 is in line with the expected differences resulting from canopy exchange processes. For sulphur, sodium and chloride no net canopy exchange is observed, whereas nitrogen components are taken up by the canopy and base cations are leached. Ammonium seems to be taken up by the canopy to a larger extent than nitrate. Draaijers *et al.* (1994) tried to assess the influence of canopy exchange processes on the difference between throughfall and atmospheric deposition

using the results of the Speulder forest experiments and the comparison in Table 6.3. Their results are summarised in Table 6.5.

No significant differences were found between the dry and fog deposition estimates of SOx and the net throughfall fluxes of $SO_4^{2-}$. Moreover, no significant differences were found between the amount of $SO_4^{2-}$ rinsed from Douglas fir and artificial twigs. A $S^{35}$ nutrition experiment performed by ECN at Speulder forest, indicated that leaching of soil-derived sulphur contributes only about 3% (80 mol $ha^{-1}$ $a^{-1}$) to the throughfall flux of $SO_4^{2-}$ in the Speulder forest (Wyers *et al.*, 1994). Stomatal uptake of $SO_2$ was estimated to constitute 5% (36 mol $ha^{-1}$ $a^{-1}$) of the total dry deposition of $SO_2$ (Erisman *et al.*, 1994; Draaijers *et al.*, 1994). It may be concluded that in the Speulder forest sulphur shows a more-or-less conservative behaviour, with $SO_2$ uptake balancing leaching of soil-derived sulphur.

Differences found between NOy dry and fog deposition estimates and $NO_3^-$ net throughfall fluxes would suggest that approximately 50% (400 mol $ha^{-1}$ $a^{-1}$) of the total NOy deposition is irreversibly retained within the canopy. Canopy foliage is capable of absorbing and incorporating gaseous $NO_2$, $HNO_2$ and $HNO_3$, as well as $NO_3^-$ in solution. In the Speulder forest, stomatal uptake was estimated to constitute 100%, 11% and 0% of the total $NO_2$, $HNO_2$ and $HNO_3$ dry deposition, respectively (Erisman *et al.*, 1994; Draaijers *et al.*, 1994). The sum of the stomatal uptake of $NO_2$ and $HNO_2$ was 130 mol $ha^{-1}$ $a^{-1}$. Uptake of $NO_3^-$ from the water layer solution is probably of no importance. Subtracting stomatal N uptake from the atmospheric deposition estimate leaves a gap between net throughfall and NOy dry and fog deposition of 30% (270 mol $ha^{-1}$ $a^{-1}$). This difference is well within the overall uncertainty of the $NO_3^-$ net throughfall fluxes, and NOy dry and fog deposition estimate and fluxes, although the difference is systematic.

Differences found between dry and fog deposition estimates of NHx and net throughfall fluxes of $NH_4^+$ were not statistically significant. According to the canopy exchange model of Ulrich (1983) and Van der Maas *et al.* (1990) canopy uptake of $NH_4^+$ in the Speulder forest amounts to 255 mol $ha^{-1}$ $a^{-1}$. This is considerably larger than the amount of $NH_3$ estimated to be taken up through stomata (140 mol $ha^{-1}$ $a^{-1}$) i.e. 10% of the total dry deposition of $NH_3$. The difference (115 mol $ha^{-1}$ $a^{-1}$) may be due to uptake of $NH_4^+$ from the water layer solution. However, results from a rinsing experiments showed no significant differences between $NH_4^+$ amounts rinsed from Douglas fir and artificial twigs (Römer and te Winkel, 1994). The difference is well within the uncertainty of the two estimates.

Dry and fog deposition estimates of $Na^+$, $Cl^-$ and $Mg^{2+}$ were not found to be significantly different from corresponding net throughfall fluxes. Moreover, no significant differences existed between the amounts of $Na^+$, $Cl^-$ and $Mg^{2+}$ rinsed from Douglas fir and artificial twigs, respectively (Römer and te Winkel, 1995). Rinsing experiments indicate some leaching of $Mg^{2+}$ during periods when the canopy is wet but this effect could not be quantified. The

canopy exchange model of Ulrich (1983) and Van der Maas *et al.* (1990) suggests that $Mg^{2+}$ leaching equals 41 mol $ha^{-1}$ $a^{-1}$ but it is assumed that the model slightly overestimates leaching of $Mg^{2+}$. All in all, it may be concluded that in the Speulder forest, canopy exchange of $Na^+$ and $Cl^-$ is negligible and canopy leaching of $Mg^{2+}$ is small (<40 mol $ha^{-1}$ $a^{-1}$).

In the Speulder forest leaching of $K^+$ is considerable. A comparison with dry and fog deposition estimates reveals that 89% (270 mol $ha^{-1}$ $a^{-1}$) of the net throughfall flux of $K^+$ results from canopy leaching. This is in good agreement with the leaching of $K^+$ calculated with the canopy exchange model of Ulrich (1983) and Van der Maas *et al.* (1990) (270 mol $ha^{-1}$ $a^{-1}$) and in reasonable agreement with results obtained by Draaijers *et al.* (1994) using the multiple regression model of Lovett and Lindberg (1984) (190 mol $ha^{-1}$ $a^{-1}$). Surface wash experiments indicate a $K^+$ leaching of only 104 mol $ha^{-1}$ $a^{-1}$. This large deviation from the other estimates (around a factor of 2.5) is probably due to the relatively small time coverage of these experiments so that results may not be representative for the whole measurement period (Römer and te Winkel, 1994).

**TABLE 6.5** Canopy uptake or leaching in Speulder forest estimated using results of different experiments (+ = uptake; - = leaching; 0 = inert or negligible; x = not estimated)

| Experiments | $SO_4^{2-}$ | $NO_3^-$ | $NH_4^+$ | $Na^+$ | $Cl^-$ | $Mg^{2+}$ | $Ca^{2+}$ | $K^+$ | $H^+$ |
|---|---|---|---|---|---|---|---|---|---|
| Comparison atm. dep. / throughfall | 0 | -400 | 0 | 0 | 0 | 0 | -55 | -270 | - |
| Stomatal resistance modelling | 35[a] | 130[b] | 140[c] | x | x | x | x | x | x |
| Model - Ulrich and $V_d$ Maas | 0 | 0 | 255 | 0 | 0 | -40 | -75 | -270 | 180 |
| Model - Lovett/Lindberg | x | x | x | x | x | x | x | -190 | 195 |
| Surface wash experiments (twigs) | 0 | 0 | 0 | 0 | 0 | 0 | -30 | -105 | x |
| $S^{35}$ nutrition experiment | -80 | x | x | x | x | x | x | x | x |

[a] stomatal uptake of $SO_2$
[b] stomatal uptake of $NO_2$ and $HNO_2$
[c] stomatal uptake of $NH_3$

Comparing dry and fog deposition estimates with net throughfall fluxes reveals that 36% (55 mol $ha^{-1}$ $a^{-1}$) of the net throughfall flux of $Ca^{2+}$ may be the result of canopy leaching. This corresponds reasonably well with the $Ca^{2+}$ leaching amount calculated with the model of Ulrich (1983) and Van der Maas *et al.* (1990) (73 mol $ha^{-1}$ $a^{-1}$), especially taking into account that this model probably overestimates leaching of $Ca^{2+}$. As for $K^+$, the $Ca^{2+}$ leaching calculated from surface wash experiments (30 mol $ha^{-1}$ $a^{-1}$) is probably too low. It is estimated that leaching of $Ca^{2+}$ in the Speulder forest is found between 50 and 75 mol $ha^{-1}$ $a^{-1}$ (Draaijers *et al.*, 1994).

Canopy retention of $H^+$ estimated with the exchange model of Ulrich (1983) and Van der Maas *et al.* (1990) (181 mol $ha^{-1}$ $a^{-1}$) agrees well with the $H^+$ canopy uptake calculated with

the Lovett and Lindberg (1984) multiple-regression model (200 mol $ha^{-1}$ $a^{-1}$). Field experiments were mainly performed in the winter period (November until May) when the vegetation is physiologically less active and frequently wetted. By scaling measurement results to a whole year, stomatal uptake is probably underestimated. The effect of measuring only in the winter period on uptake and leaching in solution is more difficult to assess. Due to the frequent occurrence of water films, uptake and leaching will be relatively intense in the winter period, which may to a certain extent counterbalance the effect of the low physiological status of the vegetation. During the measurement period no episodes with winter smog, frost, drought, or an insect plague occurred. Such stress factors are found to intensify canopy exchange processes considerably.

It is relevant to note that canopy exchange rates for the Speulder forest may not automatically be considered representative for other forests in the Netherlands. Canopy exchange is found to depend on tree species and ecological setting (Draaijers *et al.*, 1994).

*Synthesis*

It has been shown that for canopy exchange most of the Speulder forest experiments point in a similar direction. Although the estimates of the absolute amounts of components retained or leached in the canopy may differ, depending on the experiment (see Table 6.5), the average values give a good picture of the situation in the Speulder forest. The average values are given in Table 6.5. It shows that $H^+$ is taken up by the canopy; this is accompanied by leaching of $Mg^{2+}$, $Ca^{2+}$ and especially K. $SO_2$ taken up by stomata is eventually leached again, whereas $NH_3$ taken up via stomata is almost completely retained by the canopy. Oxidised nitrogen components, especially $NO_2$, are taken up by the canopy. Whether $NO_3$ and $NH_4$ aerosols are taken up directly or via solution is uncertain. We assume from the results of the experiments that $NO_3$ uptake is negligible, whereas $NH_4$ is taken up in exchange with $K^+$ and $Ca^{2+}$. $Na^+$ and $Cl^-$ are considered inert. The highest uncertainty in canopy exchange estimates relates to estimates of the nitrogen components.

Observed differences between dry and fog deposition estimates from micrometeorological measurements and inferential modelling, on the one hand, and net throughfall fluxes on the other cannot be seen as exclusively due to canopy exchange. Dry deposition estimates from micrometeorological measurements and inferential modelling are uncertain due to errors in the air concentration measurements (Arends *et al.*, 1994), their sometimes low time coverage and the uncertainties associated with the parametrisation of the dry deposition velocities (Erisman *et al.*, 1994; Ruijgrok *et al.*, 1994). Fog deposition estimates are uncertain due to uncertainties associated with the estimation of water fluxes and the measurement of the average chemical composition of the fog droplets (Vermeulen *et al.*, 1994). Uncertainties associated with the throughfall method when used for estimating dry and fog deposition include the dry deposition to the forest floor and understorey vegetation, dry deposition directly onto the throughfall gutters, the representativeness of the throughfall sampling, the

wet deposition estimate, and the stemflow contribution and canopy exchange processes (Draaijers and Erisman, 1993). However, with canopy exchange processes being the only exception, the above-mentioned factors probably contributed only to a very small extent to the uncertainty in the throughfall dry and fog deposition estimates in this study.

### 6.2.3 THROUGHFALL FLUXES COMPARED TO DEADM DEPOSITION ESTIMATES

*Acidifying components*

DEADM results were obtained for the locations and time periods in which throughfall was sampled as listed in Erisman (1993a) and Draaijers and Erisman (1993). For each measuring site an inventory of local forest characteristics was made. These data were used in DEADM to calculate the site-specific fluxes. In total, 51 sites were used in the comparison. The first 20 sites, operated in 1987 and 1988 by the University of Nijmegen ( *KUN)* (Houdijk and Roelofs, 1991) and the Winand Staring Centre for Integrated Land Soil and Water Research (*SC-DLO*) (De Vries *et al.*, 1990), are scattered over the country (Erisman, 1993b), whereas the other 30 are concentrated in an area of about 3 x 3 km. Table 6.6 gives the average and standard deviations of the throughfall estimates of the different sets of data. Also listed in this table are the average and standard deviations of the total deposition estimates obtained with DEADM. Throughfall fluxes were corrected for canopy exchange by using the Ulrich model, (1983) (Draaijers *et al.*, 1994). Figures 6.4A to D shows throughfall estimates compared to DEADM results for SOx, NOy, NHx and total potential acid, respectively, for the first dataset consisting of 21 sites. Figures 6.5A to D show the same comparison for the dataset consisting of 30 sites. Two different comparisons are made because the throughfall measurements were made in different periods using different methods.

**TABLE 6.6** Throughfall estimates and total deposition estimates averaged over different locations (mol $ha^{-1}$ $a^{-1}$)

| | | KUN/SC-DLO data (Houdijk and Roelofs, 1991; de Vries *et al.*, 1991) (21 sites) | | | | Utrecht Univ. data (Draaijers, 1993) (30 sites) | | | |
|---|---|---|---|---|---|---|---|---|---|
| | | SOx | NOy | NHx | pot. acid | SOx | NOy | NHx | pot. acid |
| Deposition estimates | average | 1792 | 1262 | 2853 | 7700 | 1265 | 1209 | 2892 | 6710 |
| | sd | 599 | 127 | 1172 | 1323 | 93 | 63 | 225 | 900 |
| Throughfall estimates | average | 2090 | 959 | 4232 | 9371 | 1170 | 820 | 2356 | 5566 |
| | sd | 966 | 316 | 1889 | 3921 | 250 | 242 | 722 | 1409 |
| Correlation coefficient ($R^2$) | | 0.04 | 0.02 | 0.17 | 0.10 | 0.30 | 0.50 | 0.01 | 0.43 |

On average the estimates are not significantly different, except for NOy fluxes for both datasets and NHx fluxes for the 30 sites. The NHx DEADM estimates are based on 5 x 5 km values. The 30 forests are located in only two 5 x 5 km grid squares, therefore do not show the

same variations as the measurements. The systematic difference between the two estimates for NOy deposition (with atmospheric deposition estimates higher than throughfall estimates), are in line with the results obtained at Speulder forest (section 6.2.2).

In general, the scatter in the graphs displaying the results for the 21 sites is larger than that for the 30 sites. This is the result of the difference in throughfall sampling and handling of samples applied to the two sets. Measurements of throughfall have to meet criteria related to representativeness, contamination, etc. (Draaijers *et al.,* 1994). The measurements made at the 30 sites meet these criteria better than those taken at the 21 sites. The agreement between DEADM and throughfall estimates for the 21 and 30 sites is good, with data scattering around the 1:1 line.

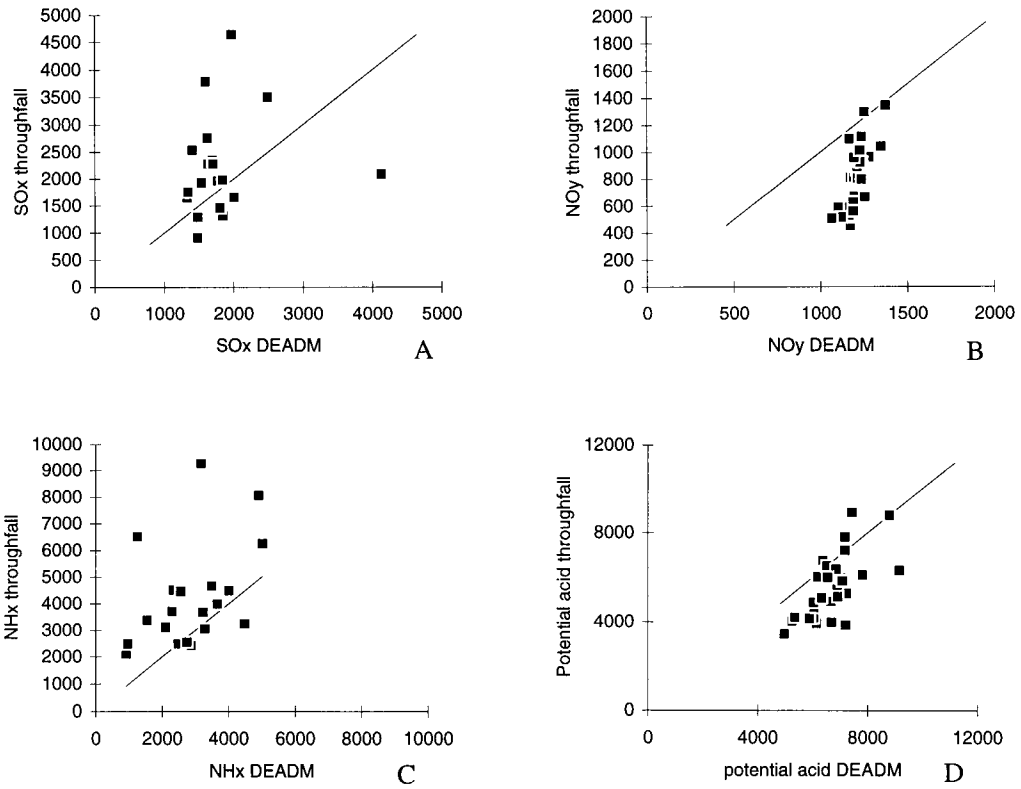


**FIGURE 6.4** Throughfall estimates compared to DEADM results for SOx (A), NOy (B), NHx (C) and total potential acid (D) (mol $ha^{-1}$ $a^{-1}$ ) for 21 sites. The 1:1 line is also shown.

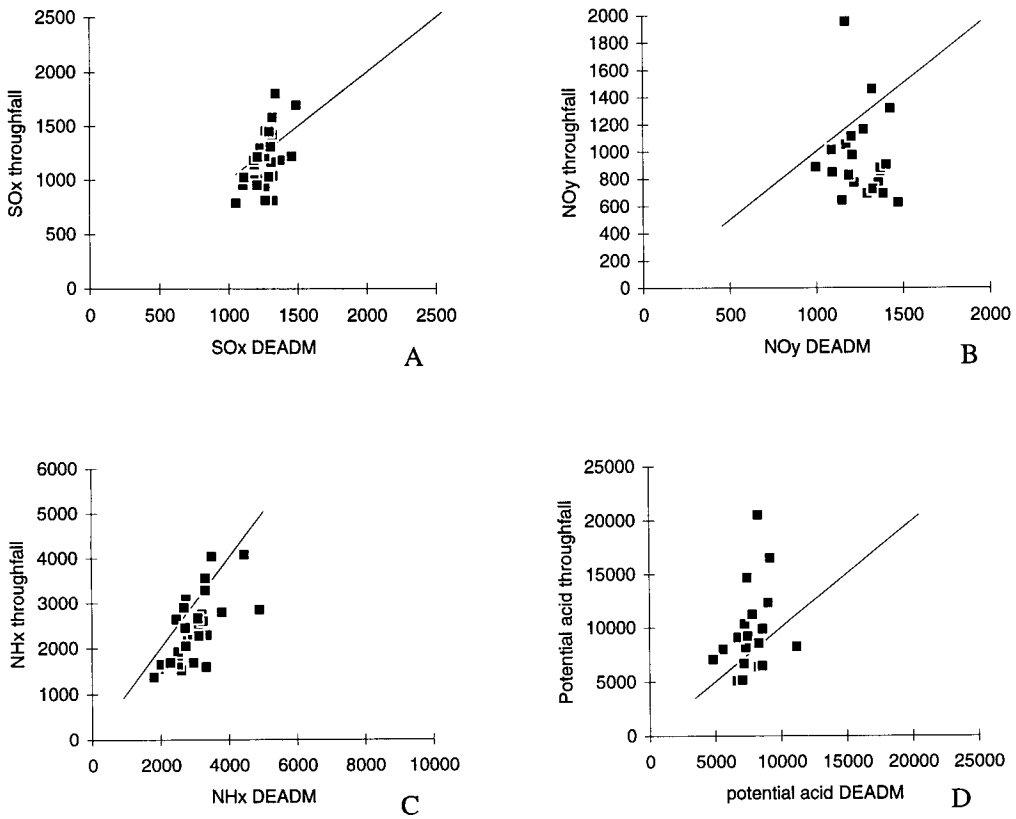


**FIGURE 6.5** Throughfall estimates compared to DEADM results for SOx (A), NOy (B), NHx (C) and total potential acid (D) (mol $ha^{-1}$ $a^{-1}$ ) for 30 sites. The 1:1 line is also shown.

Considering the sites are situated in one 10 x 10 km grid used in DEADM with constant $SO_2$, $NO_2$, wind speed, radiation, temperature, relative humidity and surface wetness data at 50 m high, the agreement for the 30 sites is remarkable. This shows that the blending height method is a good approach for estimating local fluxes (Draaijers and Erisman, 1993; Erisman, 1992).

*Base cations*

For comparison of base cation deposition estimates using DEADM and throughfall only the dataset containing the 30 sites is used. For the other dataset it was not possible to achieve the

ion balance, either through lack of data or errors in the data. There must be an ion balance made for applying the Ulrich model (Draaijers *et al.*, 1994).

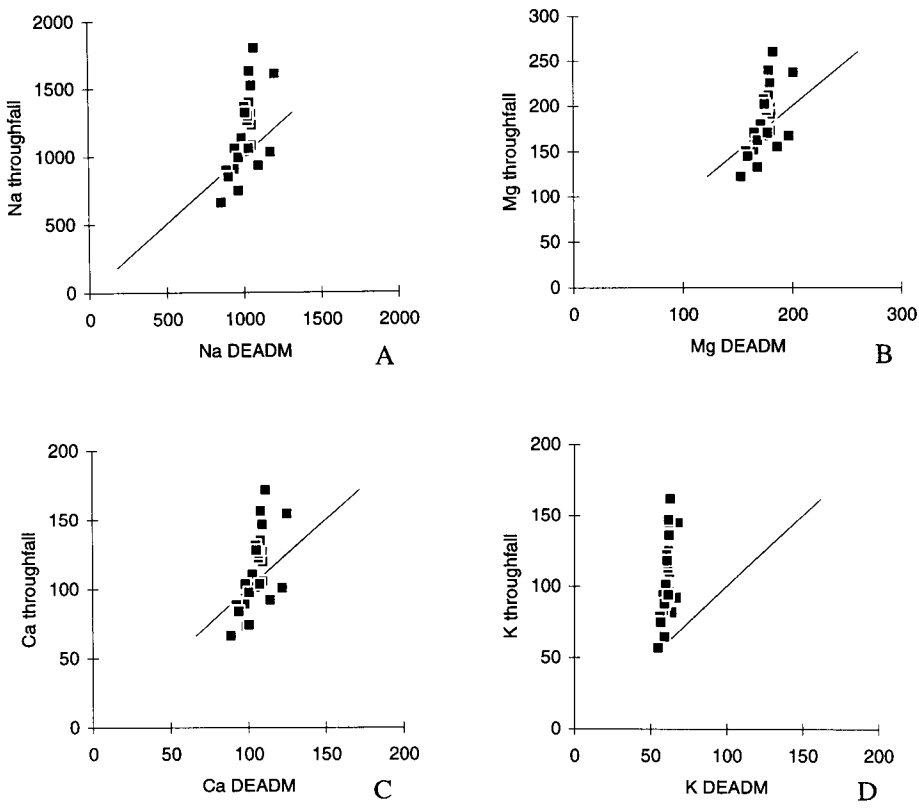


**FIGURE 6.6** Net throughfall estimates compared to DEADM dry deposition estimates for 30 sites for $Na^+$ (A), $Mg^{2+}$ (B), $Ca^{2+}$ (C) and $K^+$ (D) (mol $ha^{-1}$ $a^{-1}$ ). The 1:1 line is also shown.

Figure 6.6 displays the comparison between net throughfall estimates, corrected for canopy exchange using the Ulrich model, and dry deposition estimates using DEADM. Average fluxes and standard deviations are given in Table 6.7. The concentrations of base cations used to estimate dry deposition are derived from wet deposition measurements and scavenging coefficients (see Chapter 5). The agreement between the two estimates is very good, given the uncertainty in the two methods. The throughfall estimates are somewhat higher than deposition estimates; this may be due to the uncertainty in the Ulrich model (Draaijers *et al.*,

1994) or uncertainty in *Vd* estimates (Erisman *et al.*, 1994). However, the strong correlation (see Table 6.7) suggests that the modelled deposition of base cations leads to accurate values and/or that the throughfall method might be used for estimating atmospheric deposition for base cations, provided the Ulrich model is applied to estimate canopy exchange.

**TABLE 6.7** Net throughfall estimates and dry deposition estimates averaged over 30 different locations (mol $ha^{-1}$ $a^{-1}$)

| | | $Na^+$ | $Mg^{2+}$ | $Ca^{2+}$ | $K^+$ |
|---|---|---|---|---|---|
| Dry deposition estimates | average | 534 | 74 | 55 | 20 |
| | sd | 75 | 10 | 8 | 3 |
| Net throughfall estimates | average | 683 | 82 | 63 | 63 |
| | sd | 292 | 35 | 27 | 27 |
| | $R^2$ | 0.381 | 0.382 | 0.381 | 0.383 |

## 6.3 UNCERTAINTY IN DEADM RESULTS

The objective of the uncertainty analysis is to define confidence intervals for the results obtained and to identify gaps in the applied methods or procedures. A comparison of results obtained from a preliminary version of the DEADM model with measurements at a heathland site (Asselse heide) showed good agreement, especially for the deposition parameters $u_*$ and $V_d$ (Duyzer *et al.*, 1989; Erisman (1993a; 1993b). Although the model concept has been changed since then at several points, these results supported confidence in the approach. In this section the uncertainty analysis comprises the comparison of DEADM results with results from other estimates for the Netherlands and an error propagation analysis. Results are compared with flux measurements on a local scale made in the Netherlands and with fluxes calculated with another regional scale model.

### 6.3.1 DRY DEPOSITION MEASUREMENTS

The two main problems in comparing model results with flux measurements are, first of all, the local character of the measurements and, secondly, the large uncertainty in the measurements. The flux measurements available for different types of vegetation and gases are listed in Table 6.8, along with the year and measuring height. The latter can be taken as a measure of the surface area covered by the measurements (roughly a radius of 100 times the height). The same table presents the estimated fluxes for the 1 x 1 km and 5 x 5 km ($NH_3$) grids, where the locations are situated, being obtained from calculations from the model for the same year. The uncertainty in flux measurements is not given in the table. The uncertainty in yearly average fluxes is about 50-100% (Erisman *et al.*, 1992; Erisman 1993a).

From Table 6.8 it is obvious that the inference estimates of the $NH_3$ dry deposition flux over heathland are higher than fluxes obtained from the measurements. At the Speulder forest site, $NH_3$ fluxes as estimated by the model are lower than measured fluxes. However, the uncertainty in the measurements is large and the values presented here are median values (Van Aalst and Erisman, 1991; Duyzer *et al.*, 1991). It must be emphasised that the model resolution for $NH_3$ fluxes is 5 x 5 km. Variations of the flux within such a grid can be large, about a factor of 4 (Asman *et al.*, 1989; Asman and Van Jaarsveld, 1992). The location of the area where measurements are made relative to the $NH_3$ sources in the grid determines whether the depositions will be higher or lower than the average over the grid. The table probably gives an indication of this variation rather than a real comparison. Therefore no conclusions can be drawn on uncertainty in modelled $NH_3$ fluxes from this comparison.

The estimated $HNO_3$ and $SO_2$ dry deposition fluxes to low vegetation are slightly lower than those measured. However, agreement is reasonable. Estimates of dry deposition to the Douglas fir forest located near Speuld show a systematic overestimate for NOx. $SO_2$ fluxes

are underestimated by the model. Generally, it can be concluded that fluxes obtained using the model and those derived from measurements show differences of 20 % or more.

**TABLE 6.8** Flux measurements and estimates for different locations in the Netherlands in mol $ha^{-1}$ $a^{-1}$ using different methods

| Location | Component | Height (m) | Year | Reference | Measured flux | Estimate (this study) |
|---|---|---|---|---|---|---|
| Speuld | $SO_2$ | 30 | 1988 | Duyzer *et al.* (1994) | 590 | 530 |
| | NOx | 30 | | Duyzer *et al.* (1994) | 360 | 400 |
| Speuld | $SO_2$ | 30 | 1989 | Duyzer *et al.* (1994) | 540 | 584 |
| | NOx | 30 | | Duyzer *et al.* (1994) | 270 | 440 |
| | $NH_3$ | 30 | | Duyzer *et al.* (1994) | 1860 | 1645 |
| Elspeet | $SO_2$ | 4 | 1989 | Erisman *et al.* (1993a) | 350 | 510 |
| | $NH_3$ | 4 | | Erisman *et al.* (1993a) | 810 | 980 |
| Assel | $NH_3$ | 1.5 | 1987 | Duyzer *et al.* (1989) | 550 | 975 |
| Cabauw | $HNO_3$ | 200 | 1986 | Erisman *et al.* (1988) | 220 | 180 |
| Zegveld | $SO_2$ | 4 | 1988 | Erisman *et al.* (1993a) | 590 | 484 |

The estimates have been presented in more significant figures than those consistent with their accuracy for intercomparison.

Monthly mean concentrations obtained by measurements at a height of 30 m at Speuld (Vermetten *et al.* 1990), and concentrations obtained by extrapolation to 50 m from the LML measuring sites and interpolation over the 10 x 10 km grid, agree reasonably well, as can be seen in Figure 6.7. The most extreme outlier is a month with only a limited set of measurements (Vermetten *et al.*, 1990). These results suggest that the procedure to calculate concentrations at 50 m height from monitoring network observations can be used to estimate concentrations over the Netherlands accurately enough on a monthly basis and that the differences for $SO_2$ fluxes are the result of uncertainty in deposition parameters.

Figure 6.8 shows a comparison between monthly average dry deposition velocities of $SO_2$, $NH_3$, $NO_2$ and $SO_4$ aerosol measured at Speuld (36 m above ground level) in 1993 and calculated with DEADM (50 m above ground level). The agreement is reasonable, with an average deviation of about ±25%. Calculated $SO_4$ aerosol *Vd* values are somewhat higher than those derived from measurements. This is the result of a combination of a difference in height (36 m compared to 50 m) and a difference in roughness length estimates used locally ($z_0$ = 2 m) and from land-use data and forest statistical information in DEADM ($z_0$ = 1.3 m). The parametrisation of aerosol dry deposition velocities appears to be sensitive to the roughness length because the wind speed at canopy height used in the parametrisation is sensitive to $z_0$ values (Ruigrok *et al.*, 1994; Erisman *et al.*, 1994a). This influence is larger for $V_d$ of coarse particle than that of fine particles, DEADM average $V_d$ for coarse particles in Speulder forest amounts to 3.3 cm $s^{-1}$, whereas $V_d$ based on measurements equals 5.0 cm $s^{-1}$ (Erisman *et al.*, 1994a; section 7.3).

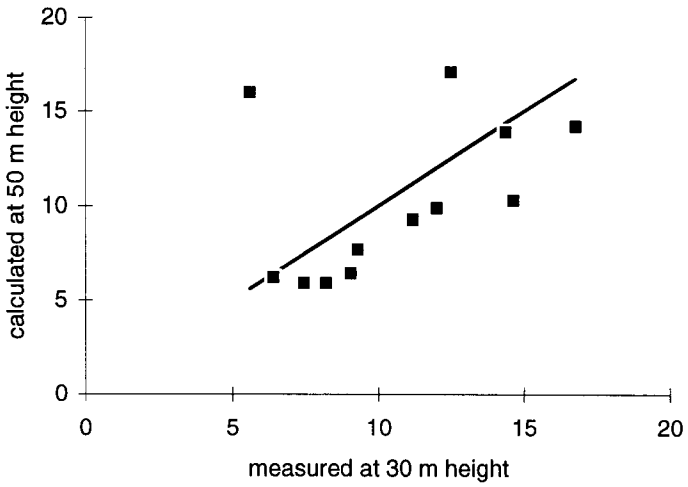


**FIGURE 6.7** Comparison of measured concentrations in Speulder forest (30 m) and those obtained from the model's calculations (50 m).

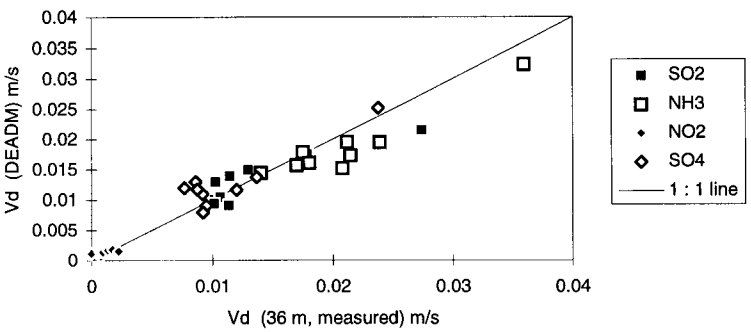


**FIGURE 6.8** Comparison of monthly $V_d$ values calculated with DEADM (50-m height) and measured in Speulder forest (36-m height) (m $s^{-1}$).

Monthly average modelled *Vd* values of $SO_2$ and $NO_2$ are in good agreement with those based on measurements with no systematic differences. $NH_3$ dry deposition velocities calculated with DEADM are smaller than those derived from measurements at the Speulder forest. DEADM calculations are representative for the 5 x 5 km area surrounding the Speulder forest, whereas measurements are representative for local surface characteristics. It must be noted that the comparison of modelled *Vd* with those derived from measurements in Speulder forest is not independent because parametrisations of *Vd* used in DEADM are partly based on data

from Speulder forest. Annual average fluxes derived from measurements and calculated using DEADM for the Speulder forest are listed in Table 6.9 (Erisman *et al.*, 1994a).

Agreement is reasonable, keeping in mind that DEADM results are 1 x 1 km grid averages, calculated with parameters such as land use, forestry statistics, etc. derived from long-term statistics. Furthermore, DEADM results for $NH_3$, $NH_4$ and base cations are estimated on a 5 x 5 km, whereas fluxes derived from the measurements/model are representative for more local conditions.

**TABLE 6.9** Average dry deposition fluxes ) for the Speulder forest (mol $ha^{-1}$ $a^{-1}$) based on measurements (November 1992 - September 1993) and calculated using DEADM (January 1993 - September 1993

| Component | Measurements | DEADM results |
|---|---|---|
| $SO_2$ | 488 | 509 |
| $SO_4^{2-}$ aerosol | 189 | 146 |
| Dry SOx | 677 | 655 |
| $NH_3$ | 1409 | 816[a] |
| $NH_4^+$ aerosol | 563 | 685[a] |
| Dry NHx | 1972 | 140[a] |
| $NO_2$ | 136 | 190 |
| $HNO_2$ | 96 | 109 |
| $HNO_3$ | 144 | 126 |
| $NO_3^-$ aerosol | 388 | 216 |
| Dry $NO_3$ | 764 | 614 |
| $K^+$ | 30 | 47[a] |
| $Na^+$ | 574 | 759[a] |
| $Ca^{2+}$ | 94 | 135[a] |
| $Mg^{2+}$ | 113 | 122[a] |

[a] 5 x 5 km estimates

## 6.3.2 COMPARISON WITH OTHER MODEL RESULTS

The DEADM results have been compared to results calculated with the TREND model. The TREND model calculates yearly average dry and wet deposition of SOx, NOy and NHx based on yearly meteorology statistics and detailed emission inventories for Europe (Van Jaarsveld, 1990; Van Jaarsveld and Onderdelinden, 1992; Asman and Van Jaarsveld, 1992). The most accurate emission inventory is that of 1980. Calculations using TREND for the 1980 emissions are compared to results obtained in this study for the year 1980. The Netherlands has been divided into 20 so-called acidification areas (Figure 5.2). In Figure 6.9, the estimates

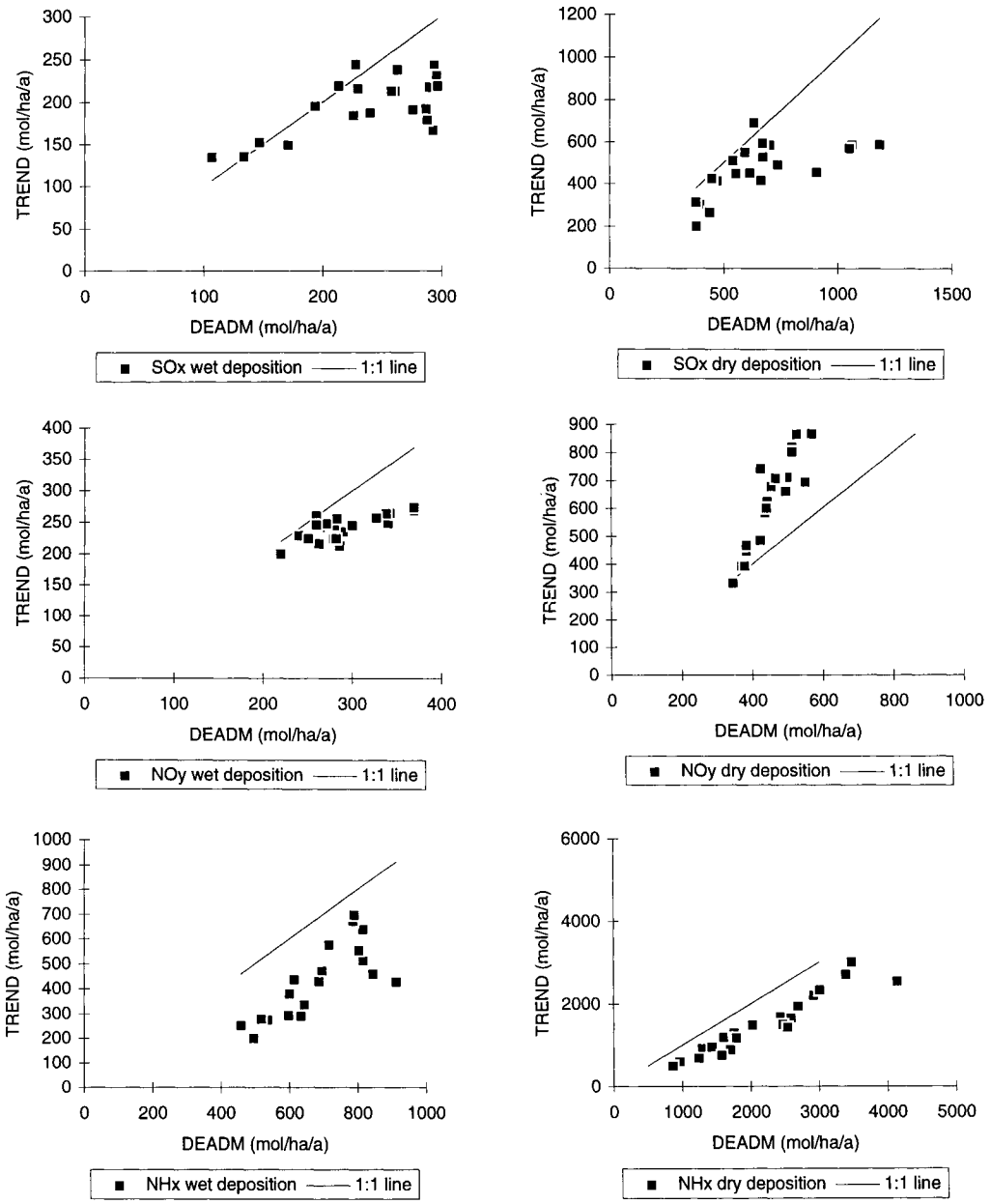


**FIGURE 6.9** Comparison of TREND model results with estimates from this study (mol $ha^{-1}$ $a^{-1}$). The 1:1 line is shown for comparison.

from TREND calculations per acidification region for dry and wet SOx, NOy and NHx deposition are compared to results from this study. From these figures it can be concluded that estimates from both models agree well on this scale. Differences in SOx and NHx dry deposition estimates are mainly a consequence of different assumptions for the roughness length. The TREND model uses a uniform $z_0$ field. The average $z_0$ value in the Netherlands used in TREND (0.15 m) is lower than that obtained in this study (0.22 m).

### 6.3.3 ESTIMATION OF UNCERTAINTY RANGES

Uncertainties in the deposition flux estimates are the result of random and systematic errors. Random errors could be the result of a certain variability in measured quantities and parameters used, as a result of e.g. measuring errors, correction procedures or parametrisations. Random errors in the total deposition will be a function of number of measurements and of averaging time intervals and the spatial scales under consideration. Systematic errors result from neglecting processes or variables on which knowledge is insufficient. Examples of systematic errors might be neglecting: 1) the difference in $R_c$ values for different receptor surfaces, 2) neglecting the spatial variability in concentrations of $HNO_3$, $HNO_2$, HCl and aerosols, 3) neglecting occult deposition, errors in $NH_3$ emission factors (and resulting errors in $NH_3$ and $NH_4^+$ concentrations), and 4) neglecting roughness transition zones and correlations which are not taken into account (e.g. the influence of $NH_3$ concentrations on the $SO_2$ dry deposition rate and vice versa). Systematic errors can be reduced only partly as a result of averaging in time and space. The difference between random and systematic errors is not always very clear. Certain corrections or assumptions can lead to both types of errors.

The propagation of errors in the process of estimating fluxes on different scales can be determined by error propagation methods. The most difficult part in the uncertainty analysis is the definition of the uncertainty ranges in the basic measured or theoretically derived parameters. Lack of reference or validation measurements necessitates assumptions on error or uncertainty ranges. Furthermore, poor understanding of physical, biological or chemical processes lead to the introduction of extra uncertainty, next to the mathematical uncertainty. This is of special importance in extrapolation and interpolation procedures. For some parameters the uncertainty can be determined directly from intercomparison studies (section 6.3.1).

The mathematical procedure followed for the error propagation can be so summarised:
- the individual absolute errors (random or systematic) for variables are squared and added;
- the square root of the result is the resulting absolute error ($S_a$) in the result when the variables are added or subtracted.

This is only valid if one assumes no correlation between the variables. When the variables are multiplied or divided the same procedure is followed, however, relative ($Q_a$) rather than absolute errors are considered. Again no correlation between the variables is assumed. If the variables are correlated an extra term must be added: $R$ times the product of individual errors, where R is the correlation coefficient between the variables:

$$\begin{aligned} a &= b + c \qquad S_a = \sqrt{S_b^2 + S_c^2 + 2\,R\,S_b\,S_c} \\ a &= b * c \qquad Q_a = \sqrt{Q_b^2 + Q_c^2 + 2\,R\,Q_b\,Q_c} \end{aligned} \qquad [6.1]$$

For many cases the correlation coefficient is unknown. Therefore two cases were considered: first, a propagation of errors without correlation (conservative), and second, a propagation with full positive correlation (worst case). In the following sections the random and systematic errors in the basic parameters will be discussed. Then the propagation of errors and the associated uncertainty in the final results will be described and summarised in a table for the conservative and the worst-case estimates. Numbers are presented as percentages reflecting the relative deviation from the estimated value for an average grid cell in terms of one standard deviation ($\sigma$), implying that the probability is 68% that the real value is the estimated value $\pm\, x\%$.

*Wet deposition*

Random errors

Random errors in wet deposition are determined by the uncertainty in the determination of the concentration in the precipitation samples and the determination of the precipitation amount. Random errors in individual samples have been investigated by comparison studies with more than one sampler at a location (Slanina *et al.*, 1988; Buijsman, 1990). Furthermore, analytical errors have been determined by reproducibility tests. The accuracy by which yearly average wet deposition can be estimated (reproduced) for an individual LML station is 1% for $SO_4^{2-}$, 5% for $NO_3^-$ and 11% for $NH_4^+$ (Van Egmond and Onderdelinden, 1981; van Egmond *et al.*, 1985). By interpolating the wet deposition fluxes over a 10 x 10 km grid, an extra uncertainty is introduced. The random errors on this scale can be obtained through theoretical considerations. This was done by Van Egmond and Onderdelinden (1981). They estimated the uncertainty in the spatial distribution of concentrations (and depositions) obtained from interpolation of monitoring network data and theoretical considerations. They concluded that the relative interpolation error for monthly mean $SO_4^{2-}$, $NO_3^-$ and $NH_4^+$ deposition is 17, 14 and 20%, respectively, in a monitoring network of 12 stations. Combined with the uncertainty in the fluxes due to measuring errors, this will lead to total random errors in the yearly wet deposition flux of 5% for $SO_4^{2-}$, 6% for $NO_3^-$ and 13% for $NH_4^+$. The results for the different

components on a local scale (10 x 10 km) and for the Netherlands as a whole are listed in Table 6.10. The uncertainty due to random errors in wet deposition flux is relatively low.

Systematic errors

Systematic errors in the wet deposition flux are introduced by dry deposition of gases and aerosols onto the funnels of the measuring devices, by the influence of local sources through below-cloud scavenging processes, terrain irregularities or differences in shower patterns and by measuring artefacts (e.g. the efficiency of collecting the amount of precipitation and small drops and fog, systematic sampling and analytical errors). Collectors often show systematic differences in the collection of the amount of water (e.g. Stedman *et al.*, 1990; Sevruk *et al.*, 1991). In this study the amount of water is obtained from the official rain gauges of the meteorological institute KNMI and not from the chemical collectors themselves.

Before 1988 open samplers were used in the monitoring network. Corrections had to be applied to the dry deposition in these samplers. For these data systematic errors may have been introduced through the application of correction factors. Application of dry deposition correction factors for fluxes before 1988 introduces an extra 10-20% uncertainty, depending on the location of the station (see, for example, Buijsman, 1990). The uncertainty introduced by the $Ca^{2+}$ correction is negligible for these errors and will be small for wet-only samples (< 5%) on a yearly basis. For the calculation of wet deposition, amounts of rain measured by KNMI using official rain gauges are used. It was found that the amount of rain collected by the (chemical) samplers could be either more-or-less that found in the official KNMI samplers (Buijsman, personal communication). A systematic error of about 20% was found in this comparison.

Systematic errors can be estimated by comparing results of measurements in a local network to those obtained by interpolation. This method was applied using data from a local precipitation network (six stations) in the province of Limburg in the southeast of the country (RIVM, 1990). From the comparison it was concluded that the agreement between $SO_4^{2-}$ and $NO_3^-$ fluxes is reasonable, usually within 20%. Agreement between $NH_4^+$ fluxes, however, is poor. The difference can be the result of different analytical procedures used by the two measuring institutes, scavenging through a strong variability in $NH_3$ concentrations and/or local disturbance at the measuring sites. Interpolation results heavily rely on the only LML station in the region. This one LML station is situated about 10 m from a station in the local network. The wet deposition fluxes at this location differ by about 15% for $NH_4^+$ and $SO_4^{2-}$ and 5% for $NO_3^-$, which can be taken as a measure of the uncertainty introduced by a difference in sampling and analytical procedures.

It was assumed that systematic errors are 25% for $SO_4^{2-}$ and $NO_3^-$, and 40% for $NH_4^+$. This assumption is based on the comparison study and on the systematic errors which result from dry deposition to open samplers and differences in the collecting efficiency of amounts of

rain. For the Netherlands as a whole, local influences are assumed to be of less importance. Systematic errors on this scale have been estimated at 20% for $SO_4^{2-}$ and $NO_3^-$, and 30% for $NH_4^+$. The overall systematic errors for 10 x 10 km grids and the Netherlands as a whole are presented in Table 6.10.

**TABLE 6.10** Total systematic uncertainty (%) in yearly average total deposition flux on different spatial scales for all individual components (1993)

| Component | F (mol $ha^{-1}$ $a^{-1}$) | 5 x 5 km | | | Country average | | |
|---|---|---|---|---|---|---|---|
| | | c/c | *Vd/Vd* | F/F | c/c | *Vd/Vd* | F/F |
| Dry $SO_2$ | 530 | 20 | 30 | 36 | 15 | 20 | 25 |
| Dry $SO_4^{2-}$ | 45 | 20 | 40 | 45 | 15 | 30 | 34 |
| Wet $SO_4^{2-}$ [a] | 195 | | | 25 | | | 20 |
| Total SOx | 770 | | | 25 | | | 15 |
| Dry NO | 0 | 30 | 200 | 200 | 20 | 100 | 102 |
| Dry $NO_2$ | 210 | 30 | 50 | 58 | 20 | 50 | 54 |
| Dry $HNO_2$ | 50 | 50 | 60 | 78 | 40 | 40 | 57 |
| Dry $HNO_3$ | 100 | 50 | 60 | 78 | 40 | 30 | 50 |
| Dry $NO_3^-$ [a] | 65 | 40 | 40 | 57 | 25 | 30 | 39 |
| Wet $NO_3$ | 320 | | | 25 | | | 20 |
| Total NOy | 745 | | | 40 | | | 25 |
| Dry $NH_3$ | 1250 | 40 | 30 | 58 | 30 | 20 | 36 |
| Dry $NH_4^+$ | 60 | 40 | 40 | 71 | 40 | 30 | 50 |
| Wet $NH_4^+$ [a] | 680 | | | 40 | | | 30 |
| Total NHx | 1990 | | | 50 | | | 30 |
| Total acid | 4270 | | | 35 | | | 15 |

[a] Wet deposition is calculated on a 10 x 10 km scale.

*Dry deposition*

The uncertainty ranges in dry deposition fluxes were determined on different scales by applying the error propagation method and the inferential framework. The random and systematic errors in the dry deposition fluxes of the components considered were calculated by defining uncertainty ranges in hourly concentrations, in $R_c$ values and in meteorological parameters. Via these ranges uncertainty ranges in the concentration field and wind field were calculated and accordingly in $u_*$, $R_a$, $R_b$, $V_d$ and $F$. In the cases where uncertainty ranges are not known, these are based on expert judgement.

Random errors

The random error in $R_a$ is mainly determined by the uncertainty in the wind speed values and accordingly in $u_*$. The hourly measured $u$ values usually exhibit an error of about 10% (Beljaars, 1988; Erisman and Duyzer, 1991). The wind field at 50 m height can be estimated

relatively accurately in situations where the assumption of the constant flux layer is valid, under near neutral conditions. In times of non-neutrality, stability corrections have to be made. This is the case more than 50% of the time during the year in the Netherlands. Especially when stability corrections are large, the extrapolated wind field will be very uncertain. The largest errors will be made at night when ground temperature inversions occur, and a decoupling between the layers separated through these inversions occurs. In these situations, however, fluxes will be low because of the low surface-exchange rates (stable conditions). These uncertainties can be considered systematic. However, because the uncertainty in the final results due to these uncertainties will be a function of averaging time intervals, they are processed as random errors. They will, however, not decrease due to spatial averaging. The uncertainty in the stability corrections $\psi(z/L)$ is assumed to be 100%.

The $z_0$ maps are used for deposition calculations. The uncertainty is hard to describe because of lack of any references or measurements. Furthermore, the uncertainty in the roughness length concept itself is hard to quantify; see the discussion in Beljaars (1988). It is assumed that the uncertainty in the $z_0$ maps is about 40-60% (Erisman, 1990; 1993a). Locally, however, the uncertainty can be more than 100%.

Under neutral conditions uncertainty of 60% in $z_0$ leads to a maximum error of 15% in $u_*$ values. The overall error in $u_*$ due to $z_0$, $u$ and stability corrections is estimated to be 20% in near-neutral conditions, and 50% in very stable or unstable conditions. If averaging the stability classes for one year, the average uncertainty in $u_*$ would lie somewhere between 20% and 50%. This value is assumed to be 30%. This leads to a random error of about 70% in $R_a$, calculated from Eqn.(6.1).The $R_b$ concept is generally used, but uncertainties are found to be large (Hicks *et al.*, 1989). The uncertainty in the $R_b$ concept can be considered systematic. However, it is assumed that the uncertainty can act both ways, i.e. it can lead to an overestimation or an underestimation. This uncertainty is therefore processed as random errors. The random error in $u_*$, combined with an overall error due to the uncertainty in the concept, leads to an uncertainty range of 50% in $R_b$.

The uncertainty in $R_c$ is much larger than in either $R_a$ or $R_b$. This, however, is due to systematic errors (see Section 6.3.3, Dry deposition). The random error in $R_c$ values was arbitrarily taken as 100% for the 1 x 1 km grids for forests, heathland and agricultural areas in the Netherlands.

The random errors in concentrations on a 1 x 1 km scale are assumed to range from 40% for $SO_2$ to 120% for $HNO_2$ , $HNO_3$, and HCl, and the random error on the 5 x 5 km scale is 120% for $NH_3$. These values are related only to the quantity of available measurements for each component (in time and space), and to the expected local variation due to, for example, the difference in source height, source strength and amount of sources. The random error in F for each component per 1 x 1 km grid can be calculated from the random errors in $R_a$, $R_b$ and $R_c$

and in $c$ by the error propagation chain. These random errors are very large for 1 x 1 km grids, ranging from about 70% for the $SO_2$ flux to 225% for aerosols. For $NH_3$, random errors in the flux on 5 x 5 km are calculated at 130%. Random errors can be neglected for most components when considered for the flux in the Netherlands as a whole. Random errors for 5 x 5 km grids and as country averages are listed in Table 6.10.

Systematic errors

Systematic errors in the dry deposition fluxes are much harder to quantify. Systematic errors have been estimated for the fluxes on a 5 x 5 km scale and for the Netherlands as a whole. The difference between systematic errors for the two scales considered is due only to the contribution of processes influencing the dry deposition flux on a local scale. This can be, for example, many roughness transition zones and/or forest edges within one grid, or a grid mainly composed of arable land where several crops are grown during one year, local sources within a grid, etc. The influence of transition in roughness in forests to the deposition is assessed using throughfall measurements. This study is summarised in section 7.2. Apart from these local contributions, errors will be independent of the scale considered.

An uncertainty in $R_c$ is introduced through differences in $R_a$ and $R_b$ calculation schemes. From parallel measurements of $u_*$ in the Netherlands at the Elspeetsche Veld (Erisman and Duyzer, 1991) and in Scotland at Halvergate (Duyzer *et al.*, 1990) using different methods, up to a 20% difference in averages of $u_*$ has been observed. This leads to differences in $R_a$ of 30-40% and in $R_b$ of about 20%. This difference is directly reflected in the $R_c$ values obtained from these measurements, leading to different estimates by different methods for the same location (receptor surface). The systematic error in $R_c$ was estimated separately for forest, heather and agricultural land-use categories. These estimates are based on results obtained from measurements of $HNO_3$, $SO_2$ and $NH_3$ over grassland and moorland, reported in Erisman (1993A), and on literature values, as listed in Table 6.11

**TABLE 6.11** Range in annual average $R_c$ values (s $m^{-1}$) for forests, heathland and agricultural areas

| Component | Forests | | Heathland | | Agricultural areas | |
|---|---|---|---|---|---|---|
| | min | max. | min | max. | min | max. |
| $SO_2$ | 40 | 200 | 40 | 200 | 20 | 100 |
| $NH_3$ | 10 | 100 | 10 | 60 | 10 | 100 |
| NO | 1000 | 4000 | 1000 | 4000 | 1000 | 4000 |
| $NO_2$ | 150 | 700 | 150 | 700 | 150 | 700 |
| $HNO_2$ | 40 | 200 | 40 | 200 | 20 | 100 |
| $HNO_3$ and HCl | -20[a] | 20 | -20[a] | 20 | -20[a] | 20 |

[a] Formally, negative surface resistance has no meaning. The data here reflect a range of uncertainty in total deposition velocity.

The systematic errors in $V_d$ can be calculated from the ranges of $R_c$ in Table 6.11 and the uncertainty in $R_a$ and $R_b$ based on the results of the intercomparison experiment on $u_*$ (Erisman and Duyzer, 1991).

Over very rough areas, the interpolated wind speed at 50-m height might be overestimated because of the increased surface drag relative to the smoother areas where wind speeds are routinely monitored. In areas with the highest $z_0$ values this may lead to overestimations of $u_*$ values of about 30%.

The systematic error in concentration values is rather different for different components. Overall, the systematic error in local concentration is determined by: systematic measuring artefacts, extrapolation and interpolation errors. The systematic errors in concentrations on different spatial resolutions are listed in Table 6.10. The possible measuring artefacts are greatest for aerosols and $NH_3$ (the latter used for testing model results). The systematic error in $SO_2$ concentrations is mostly determined by the interpolation procedure, whereas the error in NO and $NO_2$ concentrations is largely determined by the extrapolation procedure. This is due to the emissions of NOx from low-level sources (traffic) and the photostationary equilibrium, both of which can have a large impact on the vertical gradient (Duyzer *et al.*, 1990). The systematic errors in concentration as listed in Table 6.10 have been estimated following discussions with experts in the field of monitoring and modelling air pollution.

From the yearly average absolute values in concentration and deposition parameters, and corresponding systematic errors, the systematic error in $F$ was calculated using the inference method and the error propagation method. The estimated errors in $c$ and the calculated errors in $V_d$ and $F$, averaged over the Netherlands and 5 x 5 km grids are listed in Table 6.10.

*Total deposition*
The random and systematic errors in the total deposition are calculated from the errors in the wet and dry deposition fluxes for the different components by the error propagation theory. The random and systematic errors in the total depositions for different spatial scales have been listed in Table 6.10. From this table it is obvious that both for the Netherlands and for 5 x 5 km scale, random errors, compared to systematic errors, can be neglected, except for the random error in the total $NH_x$ deposition on a 5 x 5 km basis.

The uncertainty in the total potential acid deposition can be estimated from the errors in the individual fluxes for SOx, NOy and NHx. The estimated uncertainty in the yearly average total potential acid deposition flux is 35% for the 5 x 5 km grids (random errors taken for NHx) and 30% for the Netherlands as a whole.

Most processes in the atmosphere are correlated to some extent, e.g. the dry deposition of gases is linked by surface exchange processes, stomatal behaviour, etc.. Furthermore, co-

deposition can occur, for instance, between acid-forming and base-forming gases ($SO_2$ and $NH_3$). Also some correlation is expected between dry and wet deposition, and total deposition of SOx, NOy and NHx. All these correlations are implicitly accounted for in the uncertainty analysis. However, by assuming 100% correlation in all these processes a worst-case uncertainty estimate can be obtained. If 100% correlation is assumed between systematic errors, the resulting uncertainty is much larger, leading to 70% for total potential acid deposition for each 5 x 5 km grid and 30% for the Netherlands on the whole (Erisman, 1995). The best estimate for the errors in total fluxes will probably be found somewhere between the non-correlated and fully correlated estimates.

For SOx the main uncertainties are in the deposition velocities of $SO_2$ and sulphate. For grassland and heathland, deposition studies have provided much information on $SO_2$ deposition velocity, resulting in rather small error ranges (Erisman *et al.*, 1992). Budget calculations also support present estimates of deposition fluxes (Van Jaarsveld, 1990). In the case of $SO_x$, emissions, export, wet deposition and total air concentration are sufficiently accurate to estimate dry deposition as the only remaining unknown with reasonable accuracy. Unfortunately, this is not possible for NOy and NHx. For NOy, the uncertainty in concentrations of reaction products (e.g. organic nitrates, $HNO_2$) and their fate is large. For NHx the emission uncertainty is at least 40% (Erisman, 1989). Moreover, due to high spatial variability in the concentration, it is hard to obtain an experimental estimate of total content of NHx in air. These two factors preclude a budget estimate of NHx dry deposition.

The uncertainty in the total potential acid deposition is dominated by the uncertainty in NHx and NOy fluxes on a 5 x 5 km scale. For the country average the uncertainty in the total potential acid flux is dominated by the uncertainty in NHx.

## 6.4 UNCERTAINTY IN THE EDACS RESULTS

For the EDACS model (European deposition estimates), no uncertainty study has been more extensive than the one performed for the Netherlands (section 6.3). The method described here will be applied both to the model and its results in the near future. It can be hypothysed that, as a result of the data available for The Netherlands are much more accurate and numerous than for Europe, that the uncertainty ranges presented here for The Netherlands can be assumed to be equal to or the lower boundary of the uncertainty in European estimates. The aim of the deposition maps is to show the variations of the deposition of acidifying components on a small scale in Europe and to demonstrate the possibilities of the method used. The maps presented here are considered as preliminary and of limited accuracy (van Pul *et al.*, 1995). Several uncertainties and shortcomings will be discussed here.

### 6.4.2 WET DEPOSITION

The wet deposition maps are subject to several sources of uncertainty. This section contains an estimation of these uncertainties. The uncertainties are divided into three main categories: *(1)* uncertainty associated with the measurements, *(2)* uncertainty associated with assumptions and simplifications in the methods used, and *(3)* uncertainty caused by the interpolation procedure.

The first source of uncertainty consists of measurement errors and other uncertainties associated with the original data. This can be caused by errors in the field when the samples are collected and in the laboratory when the chemical composition of the samples is analysed. Furthermore, different chemical analytical methods were used by the laboratories in different countries to analyse the chemical composition of the samples, hampering intercomparison of data. De Ridder *et al.*, (1984) reported systematic differences of approximately 10% between the same samples analysed at three different laboratories in the Netherlands. Mosello *et al.* (1994) report an experiment in which 98 laboratories from 18 different countries participated in a study to reveal the magnitude of systematic differences between results analysed in different laboratories. They found differences of about 10% for $SO_4^{2-}$, $NH_4^+$ and $Ca^{2+}$, 15% for $NO_3^-$, $Na^+$ and $K^+$, 25% for $Cl^-$ and even up to 50% for $Mg^{2+}$.

Besides, data at about 500 locations originated from 1989, while at other locations data from other years or an average of several years were used. For the acidifying components Kovar and Puxbaum (1992) showed that in the Alps the yearly variability in concentration only adds an uncertainty of approximately 10% to the overall uncertainty.. In the United Kingdom the annual mean of the acidifying components at individual sites varied by ± 10-20% over the years (UK Review Group on Acid Rain, 1990). The variability in the average European concentrations is smaller than that for individual sites because the variability is smoothed by

the averaging over Europe in the interpolation procedure. Concentrations of the base cations, however, appear to be more variable than acidifying components. In 1987 the network mean concentration in the United Kingdom was approximately 40% lower than in 1986, probably due to meteorological conditions (particularly wind speed) (UK Review Group on Acid Rain, 1990). The uncertainty introduced by these factors collectively for an average 50 x 50 km grid cell is assumed to be 40%.

The second source of uncertainty consists of errors caused by simplifications and assumptions in the methods used. Major error sources might be *(a)* the representativeness of the sites and *(b)* the use of long-term mean precipitation amounts instead of year-specific data. Besides, *(c)* the seeder-feeder mechanism and *(d)* problems in high rainfall areas were not taken into account, because there is a lack of relevant information on a European scale. Furthermore, the influence of *(e)* topography (altitude), as well as the uncertainty introduced by *(f)* not capturing snow in the precipitation samplers and *(g)* the derivation of correction factors for the contribution of dry deposition to bulk precipitation samplers are considered. And at last, *(h)* uncertainty in sulphate concentration introduced by correction for the influence of sea salt through the use of interpolated sodium concentrations is taken into account.

*a)* The representativeness of the sites is determined by two components. First, it is questionable whether results obtained at a particular measurement site are representative for the area surrounding that point. This might lead to uncertainties, e.g. when a sample is taken near sources, whereas it should represent a large area where sources are sparse. Second, although the rainfall measurement technique is not a very complex one, the collection of representative rainfall measurements for a specific area can have an uncertainty factor, because nearby objects like trees, houses and hills can change rainfall amounts systematically through their influence on turbulent transport of rain drops. For this reason it is recommended to position rainfall samplers at a distance of at least four times the height of the nearest porous obstacle and at a distance of at least eight times the height of the nearest stationary obstacle. Furthermore, it is recommended to measure precipitation amounts using a standard meteorological device situated 40 cm above the ground (WMO, 1971). The uncertainty in representativeness for an average 50 x 50 km grid cell is assumed to approximate 50%.

*b)* The usage of long-term mean precipitation amounts instead of year-specific data introduces an uncertainty of 45% on average. However, locally large deviations can occur. Of all 867 stations, 19 ODS stations deviate from EPA more than ±200% and 90 stations deviate to more than ±100%. Over the whole of Europe the precipitation amount balance is fairly correct as the summed total of all positive deviations almost equals the summed total of all negative deviations (the average deviation is 3%). However, strictly these values can not be regarded as average relative uncertainties, as ODS is not a correct standard for average precipitation amounts in 1989. Deviations between ODS and EPA are therefore caused by uncertainty in ODS as well as uncertainty in EPA. The values can thus be considered as 'maximum average

uncertainties' introduced by the usage of long-term mean data instead of year specific data. The uncertainty introduced in the interpolation procedure performed by EPA is thought to be of minor importance.

*c)* In upland areas in north-west Europe a substantial proportion of rainfall originates from scavenging of cap cloud by the seeder-feeder process (Browning *et al.*, 1974). The effect of orography on rainfall composition has been investigated experimentally in the Great Dun Fell in the United Kingdom. The work showed that concentrations of major ions in rain increased with altitude by between a factor of 2 to 3 over the range of 200 to 850 m above sea level (UK Review Group on Acid Rain, 1990). The four major ions $SO_4^{2-}$, $NO_3^-$, $NH_4^+$ and $H^+$ behaved in approximately the same way. Over this height range the amount of rain roughly doubled due to orographic effects, so that wet deposition increased by a factor of 4 to 6 (Dollard *et al.*, 1983; Fowler *et al.*, 1988 and Mourne *et al.*, 1990). The increase in concentration of major ions at high altitude occurs when the cap cloud (feeder) droplets contain larger concentrations than rain from higher levels (seeder). In this process, aerosols containing elements mentioned above (and all other ions) are lifted by hills and activated into orographic clouds. Cloud droplets in the orographic (feeder) cloud are efficiently scavenged by precipitation falling from a higher level. For upland areas where orographic enhancement of rainfall is an important contributor to wet deposition, the additional scavenging of pollutant from orographic cloud is therefore expected to increase wet deposition above the values that would be predicted when chemical composition is assumed to be constant with altitude. Large uncertainties remain, and the values mentioned should be regarded as providing an initial estimate and applicable only to regions with a similar climate, precipitation and topography to the United Kingdom. Dore *et al.* (1992) mapped wet deposition in the United Kingdom, incorporating the seeder-feeder effect over mountainous terrain. Over high ground they found an increase in wet deposition of 41 to 76% compared to the situation when ion concentrations are considered to be constant with height. The areas with large enhancements represent a relatively small fraction of the land area and have therefore only a small impact on the total pollutant budget. The uncertainty introduced by ignorance of the seeder-feeder process in the concentration mapping in this study is smaller than the values reported by Dore *et al.* (1992), as local wet deposition enhancements will be smoothed out when data are interpolated to a grid with 50 x 50 km blocks. If in areas where wet deposition is enhanced by the seeder-feeder process measurement sites are located at high altitudes then, of course, there is no problem at all. However, in practice sites are mostly located in lowland areas.

*d)* In high rainfall areas (e.g. in mountainous areas and near coasts) dilution of precipitation by condensation is likely to occur. To obtain wet deposition fluxes, interpolated concentration fields were multiplied by rainfall amounts from EPA. In this way there is no physical coupling between concentration and precipitation amount. As a result, precipitation amounts are multiplied by a constant concentration, leading to an overestimation in high rainfall areas. This is the case when (high) concentrations from areas with low precipitation amounts are

interpolated to areas with large precipitation amounts. The opposite, i.e. underestimation in low rainfall areas, is possible as well. However, the former is more likely to occur, as most high rainfall areas are located at large distances from major anthropogenic pollution sources (background areas). In areas where sampler density is low, underestimation is expected to be largest. In the areas concerned this uncertainty is assumed to be about 20%.

*e)* Unlike the uplands of north west Europe, concentrations in precipitation in the Alps generally decrease with increasing altitude. In regions with large mountains, snow and rain chemistry reveal marked vertical gradients in composition (Ronseaux and Delmas, 1988; Delmas *et al.*, 1988; Puxbaum *et al.*, 1988). For these regions the very high elevation snows (>2000 m) are, in general, less polluted than those on lower slopes because the majority of the pollutant burden is restricted to the boundary layer. This effect might lead to an overestimation, which is assumed to approximate 20%. Besides, because of the differentiated topography in mountainous areas, the spatial variability of annual precipitation amounts is rather large. To calculate accurate wet deposition fluxes in these areas it is therefore necessary to use precipitation amount maps based on a large number of measurements (Kovar *et al.*, 1991). However, at high altitudes sampler density is, in general low due to large maintenance costs. A better result might be obtained by using a digital terrain model (DTM) in combination with an empirically obtained relationship between altitude and annual rainfall (Behr, 1990). In the Alps, the highest rainfall is observed in the pre- and high Alpine areas along the northern and southern Alps, whereas in the valleys in the centre of the Alps the smallest rainfall amounts are measured (Kovar *et al.*, 1991). Generally, concentrations in the Alps are lower than outside the Alps. Concentrations increase to the north, south and especially the south-east (Kovar *et al.*, 1991).

*f)* High wind velocities prevent snowfall being captured by the funnels of samplers. Especially in the winter season, this leads to an underestimation of rainfall amounts in mountainous areas. Depending on altitude and wind conditions of the sites, the underestimation will vary between 0 and 30% (Kovar *et al.*, 1991). For snow, good data can be obtained by using specially designed snow collectors situated at ground level (Lövblad *et al.*, 1994).

*g)* The uncertainty introduced by the method to derive correction factors for the contribution of dry deposition to bulk precipitation samplers is a combination of *(1)* uncertainty in the measurements and *(2)* uncertainty in the derivation method itself. Buijsman (1990) reports that application of dry deposition correction factors introduces 10-20% uncertainty in the Netherlands, depending on the location of the station. Together with uncertainty introduced by *(2)*, total uncertainty is estimated to be 30%.

*h)* For sulphate, additional uncertainty is added in the non-marine sulphate calculation procedure, as for about 200 locations interpolated sodium values were used to correct for the contribution of sea salt. This uncertainty is assumed to be of minor importance as *(1)* only 200

sites are concerned, and *(2)* the correction causes a decrease in sulphate concentration of 25% at a maximum. Only at high sodium concentration levels will the interpolation error caused by the interpolation procedure have some impact. Besides, the 200 locations are distributed over Europe randomly, hampering quantification of the introduced uncertainty.

The third source of uncertainty is a result of uncertainties inherent to the interpolation procedure, because derived values are nothing more than an estimation of the expected value at locations where no measurements were made. This uncertainty is expressed as Kriging variances. As the original values were transformed to their common logarithms, all subsequent analyses were performed on the transformed values. Retransformation of the data (from log to original values) was performed by taking the exponent. In this way the median value of the block is obtained (Journel and Huijbregts, 1978). Because the original data were distributed skewly, with some large outliers of high concentrations, the median gives a more representative block value than the mean does. Interpolation errors can be quantified in kriging standard deviation maps or can be used to map confidence intervals to give an idea about the reliability of the interpolation. The smallest errors occur where data are numerous and the largest where data are sparse. Because interpolation was performed on concentration data, kriging variances were only available for interpolated concentrations and not for fluxes. Kriging variances cannot be transformed back to the original values by just taking the exponent. A cumbersome procedure is needed and interpretation of the results will be difficult (Journel and Huijbregts, 1978). Therefore, to investigate the error information, 68% confidence intervals (the estimation ±1 standard deviation) were calculated and mapped (i.e. upper and lower boundary maps) for non-marine sulphate, nitrate and ammonium concentrations. When upper and lower boundary maps of a particular element are compared, the probability is 68% that at a particular location the actual value will fall within the range between the values on the lower- and upper boundary maps at that location. For non-marine sulphate the average relative error for an average 50 x 50 km grid cell varied from 15% in Western Europe to 40% in the largest part of the southwest and southeast of Europe. (only very locally in the former Soviet Union ). For nitrate, interpolation errors varied from 10 to 30%, and for ammonium between 15 and 40%. For all elements, only very locally in the former Soviet Union did uncertainties exceed 50%. A wide interval (i.e. large uncertainties) may be caused by *(1)* small-scale differences in the concentration field (so that even in areas with a large number of measurement sites the estimation of the average block value is more variable), *(2)* a lack of measurement sites (so that even in areas with only large-scale differences the average block value is based on too few measurements to derive a confident result) or *(3)* a combination of these factors. For all components, confidence intervals are rather large in (south)east Europe and the former Soviet Union, because of a lack of data. In these areas the interpolation error is by far the largest source of uncertainty. For ammonium, large intervals might also be caused by characteristics of emission sources of $NH_3$, i.e. many local sources showing strong variation.

*Total uncertainty in the wet deposition maps*

To assess the total uncertainty in the wet deposition maps obtained in this study is very difficult and therefore the estimates themselves are uncertain as well. The numbers presented here should therefore be regarded as a best guess based on expert judgement. To assess the total uncertainty a division into three categories is made, i.e. *(a)* West, northwest and Central Europe as 'good quality areas' where data quality is assumed to be good and sufficient (representative) data is present, *(b)* areas on edges of the maps, i.e. East, southeast and southwest Europe as 'poor quality areas', where less data is available of which the representativeness and quality can be questionable and *(c)* mountainous areas (e.g. the Alps) and upland areas (e.g. United Kingdom and Scandinavia), even though located in areas with many data, as 'complex terrain areas with additional uncertainties'. Total uncertainty in concentrations and in rainfall amounts have been estimated separately. For both variables the most dominating uncertainty (which could be quantified either in this study or by literature) was taken to represent total uncertainty, as all uncertainties are distributed around the same mean. The mathematical procedure followed for the error propagation is that of Eqn (6.1). In the case of calculation of the wet deposition fluxes the correlation coefficient is unknown. Therefore, two cases are considered: first a propagation of errors without correlation (conservative), and second, a propagation with full positive correlation (worst case). The numbers of total uncertainty are also presented as percentages, which show the total relative deviation from the estimated value in terms of 1 standard deviation, i.e. the probability is 68% that the real value is the estimated value $\pm$ $x$%. As the estimates are rather crude, no distinction between different components was made. In the conservative case *(1)*, the overall uncertainty for an average 50 x 50 km grid cell is estimated to be 50% in West, north-west and Central Europe, whereas in the worst case *(2)* the overall uncertainty is estimated to be 70% here. In areas on the edges of the maps, i.e. East, southeast and southwest Europe, *(1)* is estimated to be 65% and *(2)* 90%, whereas in complex terrain areas *(1)* is estimated to be 85% and *(2)* 120% (Table 6.12).

**TABLE 6.12** Summary of total uncertainty in wet deposition per average grid cell of 50 x 50 km for different areas in the conservative and the worst cases.

| Area | Conservative case | Worst case |
|---|---|---|
| West, northwest and Central Europe | 50% | 70% |
| East, southeast and southwest Europe | 65% | 90% |
| Mountainous and upland areas | 85% | 120% |

## 6.4.2 DRY DEPOSITION

Probably the highest uncertainty contribution is the result of the using the simple resistance formulation for such a complex process as dry deposition, and, more specifically, the surface resistance parametrisations used to determine the surface exchange of gases and particles. The resistance model represents a simple approach to a highly variable process. It assumes a constant flux layer, i.e. there are no surface inhomogeneities, edge effects or chemical reactions. How much these simplifications contribute to the total uncertainty in the annual average deposition fluxes has not been quantified. The uncertainty in the surface resistance parametrisation is the largest uncertainty in this simplified scheme. Therefore more and more accurate parametrisations are needed for various vegetation species and surface types. Moreover, there is a lack of measurements which can be used to test these parametrisations, especially for southern and eastern European climates and surfaces. The vegetation and land use classes used in EDACS should be expanded when more parametrisations become available. Surface wetness is found to be one of the major factors influencing the deposition process of soluble gases. In the present version of EDACS only rain and indication of dew are used. Because of the great influence of surface wetness, processes leading to surface wetness should be taken into account in greater detail. The overall uncertainty in the surface resistance due to these factors is different for each component and surface type. This uncertainty varies on an annual basis, between 20 percent or more to more than 100%.

In the current version of EDACS, the EMEP-LTRAP modelled concentrations on a 150 x 150 km grid are used. The uncertainty in the concentrations are estimated to amount 40 - 70% using a statistical analysis with the EMEP measurements (Krüger, 1993). These concentrations represent the background situation in Europe. In source areas the uncertainty can be even higher. It is assumed that the concentration distribution within a grid is homogeneous. This is not the case in a grid which contains industrialised areas or many scattered sources such as with $NH_3$ and NOx. For such conditions, sub-grid concentration variations are present and will lead to underestimates of the deposition in that grid. To obtain an indication of the errors, a small-scale, short range model can be useful here to resolve sub-grid concentration gradients for dense source areas. The uncertainty in the deposition in an EDACS grid cell due to these gradients is estimated at 25% (Berg and Schaug, 1994).

The deposition in EDACS is based on the EMEP-LTRAP concentrations which in turn are dependent on EMEP deposition parametrisations. The deposition in the EMEP model and in EDACS are parametrised in different ways. By using other dry deposition velocities in EDACS, a mass inconsistency between EMEP-calculated deposition and the small-scale maps of EDACS might be introduced. However, if the differences in the deposition descriptions used between the two models are not very large and non-systematic over a larger region, this will not lead to large mass inconsistencies. Figure 6.10 shows a comparison between the sulphur dry deposition per country estimated by EMEP and EDACS. It can be seen that on the

average there is a good agreement, indicating that for the model area the mass inconsistency is not violated to a large extent. However, for some countries the deviations can be as large as 50%. To avoid the mass inconsistency, implementation of the deposition module used in EDACS in the EMEP-LTRAP model it is planned. In this way, the calculated concentration fields are consistent with the EDACS deposition description.

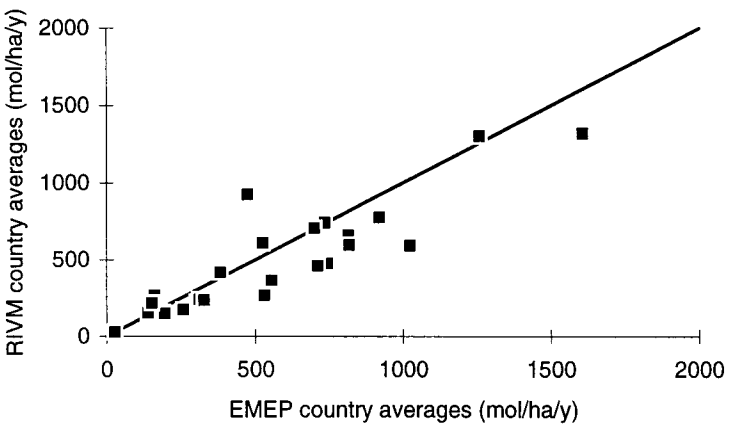


**FIGURE 6.10** Comparison of the country average calculated dry deposition of sulphur using EMEP and EDACS (mol $ha^{-1}$ $a^{-1}$).

The accuracy of the presented results depends on the availability and quality of the input data, such as the land-use map and the meteorological observations. In the gridded version of the RIVM land-use database, forest is not subdivided into deciduous and coniferous forest. All forest is classified as coniferous forest. This will probably lead to overestimates of the deposition velocity to deciduous forests for all components during winter. However, the stomatal resistance in winter will generally be large due to the low temperatures. This overestimate will therefore not be very large.

The dry deposition is calculated on a daily basis. However, due to the daily averaging of the concentration and deposition velocity, a loss in temporal interpolation is introduced. This error is component-specific and estimated to be smaller than 20% (van Pul *et al*, 1993).

### 6.4.3 TOTAL DEPOSITION

The uncertainty in regional scale deposition estimates strongly depends on the pollution climate and on landscape complexity of the area under study. The uncertainty is determined by the uncertainty in wet, dry or cloud and fog deposition. Furthermore, deposition estimates

yield higher uncertainty in areas built up by complex terrain and with strong horizontal concentration gradients. In section 7.3 the influence of roughness transition zones and forest edges to the deposition in the Netherlands is quantified. It shows that there is a systematic underestimation of the dry deposition in the order of 5 - 10% as the result of these factors. Estimates for other types of complex terrain, such as mountainous regions, are not available.

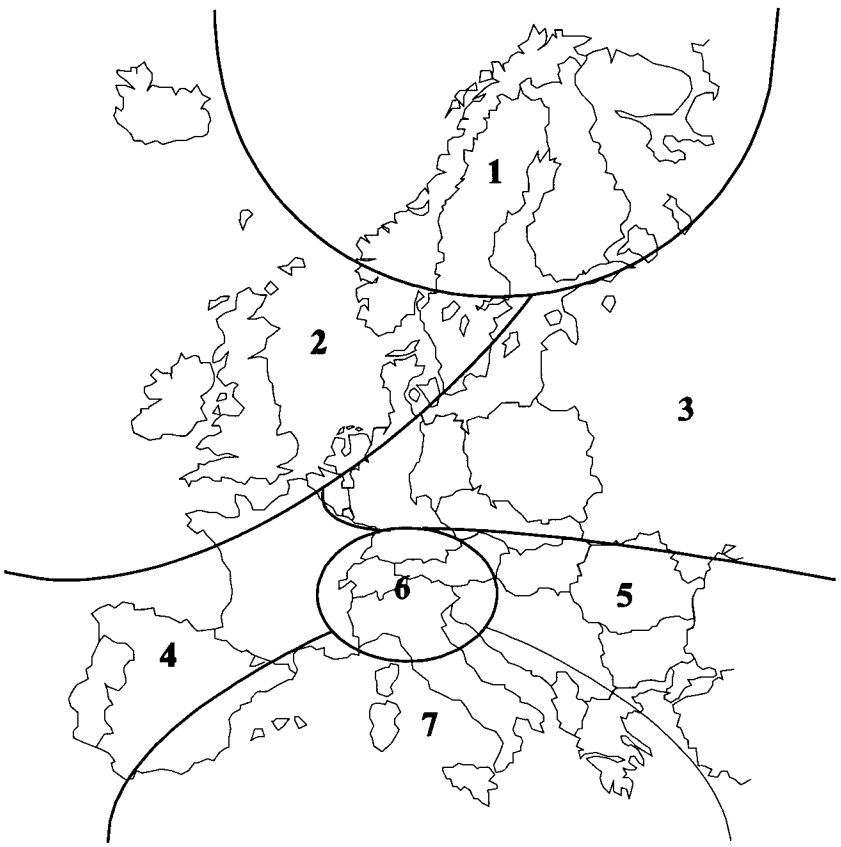


**FIGURE 6.11** Distribution of the pollution regions in Europe in Table 6.13 (see text for explanation).

Table 6.13 shows the uncertainties associated with major key factors in deposition for seven (pollution) regions in Europe. The seven regions are shown on a European map in Figure 6.11. These regions are chosen because there is a marked difference in dominating deposition process: region 1: main input is wet deposition: region 6: main input is fog or cloud

deposition; or there is a marked difference in climate: region 2 exhibits a sea climate, whereas region 7 exhibits a Mediterranean sea climate and region 4 mainly an inland climate; or there is a marked difference in industrial activity: region 1 is remote, region 3 is mainly dominated by large old industrial complexes and region 2 exhibits high reduced nitrogen emission densities. This is only a crude classification. Furthermore, Table 6.13 shows only a crude estimate of uncertainty. Because of the strong local variations in dry deposition and the associated uncertainty, as discussed in section 6.4.1, local scales should be considered.

**TABLE 6.13** Uncertainty of key factors influencing deposition estimates of S and oxidised and reduced N in different pollution regions in Europe

| Key Factors | NOy | | | | | | | NHx | | | | | | | SOx | | | | | | |
|---|---|---|---|---|---|---|---|---|---|---|---|---|---|---|---|---|---|---|---|---|---|
| Regions[a]: | 1 | 2 | 3 | 4 | 5 | 6 | 7 | 1 | 2 | 3 | 4 | 5 | 6 | 7 | 1 | 2 | 3 | 4 | 5 | 6 | 7 |
| emission/type of | - | ++ | ++ | + | ++ | + | + | - | ++ | + | + | + | + | - | - | + | ++ | + | + | + | - |
| source | 2 | 2 | 2 | 2 | 2 | 2 | 2 | 2 | 3 | 3 | 3 | 3 | 3 | 2 | 1 | 1 | 3 | 1 | 3 | 1 | 1 |
| concentration | ++ | ++ | ++ | ++ | ++ | ++ | ++ | ++ | ++ | ++ | ++ | ++ | ++ | ++ | ++ | ++ | ++ | ++ | ++ | ++ | ++ |
| | 2 | 2 | 3 | 3 | 3 | 3 | 2 | 1 | 3 | 3 | 3 | 3 | 3 | 2 | 1 | 2 | 3 | 3 | 3 | 2 | 2 |
| wind speed | - | + | + | - | - | + | - | + | ++ | ++ | + | ++ | ++ | - | + | ++ | ++ | + | ++ | ++ | - |
| | 1 | 1 | 1 | 1 | 1 | 1 | 1 | 1 | 1 | 1 | 1 | 1 | 1 | 1 | 1 | 1 | 1 | 1 | 1 | 1 | 1 |
| roughness length | - | + | + | + | + | + | - | + | + | + | + | + | + | + | + | + | + | + | + | + | + |
| | 1 | 1 | 2 | 2 | 2 | 2 | 2 | 1 | 1 | 2 | 2 | 2 | 2 | 2 | 1 | 1 | 2 | 2 | 2 | 2 | 2 |
| surface wetness | - | - | - | - | - | - | - | + | ++ | ++ | + | ++ | + | + | + | ++ | ++ | + | ++ | ++ | + |
| | 1 | 1 | 1 | 1 | 1 | 1 | 1 | 3 | 2 | 3 | 2 | 3 | 3 | 3 | 3 | 2 | 3 | 2 | 3 | 3 | 3 |
| orography | - | - | - | - | - | ++ | - | ++ | - | - | + | + | ++ | - | + | - | + | + | + | ++ | - |
| | 1 | 1 | 1 | 1 | 1 | 1 | 1 | 2 | 1 | 1 | 2 | 2 | 2 | 1 | 2 | 2 | 2 | 2 | 2 | 2 | 1 |
| co-deposition | - | - | - | - | - | - | - | - | ++ | ++ | + | + | + | - | - | ++ | ++ | + | + | + | + |
| | 1 | 1 | 1 | 1 | 1 | 1 | 1 | 3 | 2 | 3 | 3 | 3 | 3 | 3 | 3 | 2 | 3 | 3 | 3 | 3 | 3 |
| surface | ++ | ++ | ++ | ++ | ++ | ++ | ++ | ++ | ++ | ++ | + | ++ | + | + | ++ | ++ | ++ | + | ++ | + | - |
| resistance | 2 | 2 | 2 | 2 | 2 | 2 | 2 | 3 | 3 | 3 | 3 | 3 | 3 | 3 | 3 | 3 | 3 | 3 | 3 | 3 | 3 |
| dry deposition | - | + | + | + | + | + | - | - | ++ | ++ | + | ++ | + | - | - | ++ | ++ | + | ++ | + | - |
| | 3 | 3 | 3 | 3 | 3 | 3 | 3 | 3 | 3 | 3 | 3 | 3 | 3 | 3 | 3 | 3 | 3 | 3 | 3 | 3 | 3 |
| wet deposition | ++ | + | + | + | + | ++ | + | ++ | + | + | + | + | ++ | + | ++ | + | + | + | + | ++ | + |
| | 1 | 1 | 1 | 1 | 2 | 2 | 2 | 1 | 1 | 1 | 1 | 2 | 2 | 2 | 1 | 1 | 1 | 1 | 2 | 2 | 2 |
| cloud and fog | + | ++ | - | - | + | ++ | - | + | ++ | - | - | + | ++ | - | + | ++ | - | - | + | ++ | - |
| | 3 | 3 | 3 | 3 | 3 | 3 | 3 | 3 | 3 | 3 | 3 | 3 | 3 | 3 | 3 | 3 | 3 | 3 | 3 | 3 | 3 |

legend:

importance of key factors:
++ dominating
+ important
- neutral
-- unimportant

uncertainty:
1 low <30%
2 median 30-70%
3 high > 70%

[a]the distribution of these regions is given in Figure 6.11

## 6.5 GENERAL SYNTHESIS

In this section the work described in this book will be evaluated. This book describes the current state of knowledge on atmospheric deposition of acidifying components to ecosystems. Methods and their limitations are described in Chapter 1 to 6 to come to a generalised description of deposition in the Netherlands and Europe. Chapter 7 gives an extensive summary of three case studies on deposition which have been executed in a multidisciplinary cooperation during recent years in the Netherlands. The results of these studies have been used in the methods and results described in Chapter 1 to 6.

The historical overview in section 1.3 has shown that the need for receptor or ecosystem specific deposition estimates is fairly new. Up to now deposition was treated as a loss term from the atmosphere and not as a highly variable spatial input parameter to sensitive systems. In this book we tried to quantitatively assess the actual atmospheric input of acidifying compounds to ecosystems in Europe. The emphasis is on the methodology development and on the application and evaluation of resulting current loads. The results can be used to estimate critical load exceedances and to determine where ecosystems are at risk. The method can be used with long-range transport models which are used in assessments. Such models are used for the determination of critical loads exceedances in scenario studies and to optimise abatement strategies in order to protect the most sensitive ecosystems by implementing the most effective measures on emission reduction. The inferential method is a good alternative for the combination of large-scale deposition estimates and filtering factors and percentile values of critical loads which are currently used for policy development. The method applied here for acidifying components which play a role in the issue of acidification can easily be used for other components related to other issues, such as heavy metals, persistent organic components, etc.

The methodology which is used to assess the loads is based on the coupling of measurements and models. Measurements are used to explore and understand processes and to derive parameters which are used in models for generalisation. Measurements are also used to evaluate model results and to determine long-term trends. Models are used for generalising experimental results and to extrapolate them in space and time. For this, the parameters derived from experiments are used. For the Netherlands this methodology has proved its value already. Also in other countries as the UK (RGAR, 1990), Sweden (Lövblad *et al.*, 1994) and the USA (Hicks *et al.*, 1991) similar methods have been applied. In this book, the method is applied here for the first time for Europe as a whole.

In this chapter (no. 6) the uncertainty in the estimates in the Netherlands and Europe are assessed. Especially the uncertainty in small scale European estimates are large. This has to do with the concentration estimates, which are calculated on a coarse grid (150 x 150), and with the surface resistance estimates. Although surface resistance parametrisations are based on

measurements, the number and accuracy of most of these measurements is not enough to be representative for all receptor types and pollution climates in Europe. Measurements of dry deposition fluxes of different components are therefore needed for different areas of Europe. Currently a pilot project is executed in Europe, which aims at developing and implementing deposition monitoring sites in three different areas at three different receptors, i.e. over moorland near Edinburgh (UK), over semi-natural grassland near Leipzig (Germany) and over Douglas fir forest, the Speulder forest (the Netherlands). The project is financed by the EC Life programme. Three deposition monitoring stations are equipped with methods to continually determine vertical gradients of $SO_2$, $NH_3$ and NOx, together with meteorological instruments and equipment to monitor particle concentrations in two size classes and concentrations of acid gases such as $HNO_3$, $HNO_2$ and HCl. The gradient measurements are used to determine the fluxes of the three gases and to determine receptor specific surface resistances. The three gases are chosen because they represent three different types of surface uptake. From the surface resistance parametrisations derived for the three gases, parametrisations for other gases might be derived. In this way, dry deposition of all gases and particles can be determined using the inferential technique. Wet deposition is measured using wet-only samplers and cloud and fog deposition is determined by the inferential technique: concentrations are determined from fog and cloud droplets sampled with a string collector and fog and cloud occurrence is registered with optical instruments. The project is running for one year now, and continuous measurements are available for three months. It appears that the methods are suitable for determining the deposition and continuos application is possible. More of such sites should be established at several other locations in Europe. These so-called intensive monitoring sites can serve as reference stations for deposition. Trends in deposition can be determined at these sites to evaluate abatement strategies. Furthermore, the stations can serve as reference stations for testing more simple low cost deposition monitoring methods, which can be implemented at a large number of sites in Europe to determine the spatial variability of deposition and to test parametrisations and models at different receptors in different pollution climates. In combination with the methodology to determine deposition, as outlined in Chapter 5, such monitoring activities can serve as the measuring/modelling strategy which is suggested at the end of Chapter 3 (section 3.4.4). In this way, process oriented studies, evaluation of models and detection of trends can be established.

Regarding the cheap and low cost deposition monitoring methods for forests, the throughfall method is often suggested (e.g. Johnson and Lindberg, 1992, Ivens, 1990, Lövblad *et al.*, 1994, Draaijers *et al* 1995). Throughfall measurements have been used in several places in this book and it has proven to be of great value. An important achievement regarding the application of throughfall measurements for estimating deposition has been the simultaneous measurements of deposition and throughfall, and the testing of the canopy exchange model by Ulrich and Van der Maas at the Speulder forest. These comparisons show that at Speulder forest, throughfall estimates are as accurate as inferred deposition estimates, except for nitrogen components. When using the critical load concept, it is inevitable to consider soil

loads and establish the relation between soil loads (throughfall) and atmospheric deposition. Furthermore, throughfall can be helpful in understanding the canopy uptake and/or exposure. Finally, as demonstrated in section 7.2, throughfall measurements can serve to study the influence of deposition processes which cannot easily be studied by micrometeorological techniques, i.e. the influence of complex terrain. For sulphur, atmospheric deposition to forests may usually be considered more-or-less equal to the forest soil load. For inorganic nitrogen, however, atmospheric deposition will always be larger than the forest soil load as a result of canopy retention. Canopy uptake of inorganic nitrogen may be partly compensated by canopy leaching of organic nitrogen. Forest soil loads may also be estimated from simple regression models with canopy structure characteristics obtained (see section 7.2). Information on the situation of the forest stand within the landscape will make it possible to also account for edge effects. The throughfall method has to be further tested and parameters for the canopy exchange model have to be derived for other tree species and pollution climates, before general application can be advised.

A relatively large chapter in this book is about uncertainties, and in several subsections uncertainties are addressed also. We feel that uncertainty is an essential part of assessments. Especially in this kind of research where the resulting numbers can have large economic and political impact. The uncertainty analysis is in first instance used to check the results: how do they compare with other, independent estimates: modelled or measured. Moreover, it can help to trace errors in procedures. Furthermore, it is useful to determine what uncertainty of subparts contribute most to the total uncertainty, in order to focus future research on. Finally, it is a good way of showing the value of the research results and the chance that newest insights will produce data that are far from or close to your estimate.

*Summary of gaps in knowledge*
Based on information presented in this synthesis several gaps in our knowledge regarding deposition monitoring and estimation of deposition can be identified. The most important ones leading to uncertainty in deposition estimates in the Netherlands and Europe can be summarised as follows:

There is a great need to increase our understanding of the factors of importance for the spatial and temporal variability in deposition in order to take such factors into account in the design of monitoring programmes, in modelling, and in the assessment and evaluation of deposition measurements.

There is a great need for further knowledge about canopy processes, especially for nitrogen components, in order to distinguish the deposition and the in-canopy contribution to the throughfall flux. This may involve further use of radioactive tracers, more detailed canopy sampling in both time and space, and comparisons of surface sampling techniques with micrometeorological methods. In general, there is a need for direct method intercomparisons.

There is a general need for further development of sensors (especially for $NH_3$ and particles) and micrometeorological methods to be used for process studies. Furthermore, micrometeorological methods should be developed for routine application. Process-oriented studies need to be extended to obtain parametrisations of parameters such as size specific $V_d$ for particles and $R_c$ for gases for different land uses, meteorological circumstances and pollution climates. These parametrisations have to be incorporated in deposition estimates using inference to improve accuracy.

Cloud and fog deposition measuring methods need further development and testing.

Existing monitoring programs (EMEP, NADP) should be extended with dry, and cloud and fog deposition measurements or with measurements needed for the application of inferential techniques. Furthermore, monitoring programmes should be extended with several extensive monitoring locations and with many simple and cheap routine monitoring sites (e.g. throughfall sampling). Network design and representativeness of sites with regard to homogeneity, type of vegetation, and pollution climate need special attention.

Emissions, concentrations and atmospheric behaviour of base cations and other components relevant in the issue of acidification, such as HF, HCl, organic acids, PAN, etc. need to be quantified.

Extrapolating these fluxes or derived deposition parameters to larger areas is still a great problem, because of varying surface properties and roughness characteristics and accordingly non-homogeneous turbulent behaviour. There is a need to develop methods to extrapolate point measurements to regions, especially in complex terrain.

Deposition may vary within grids as the result of differences in land use, but also as the result of roughness transitions within a specific land use class, or because of edge. It should be realised that if measures to reduce atmospheric deposition are based on average deposition values within grids, deposition reductions will not be enough for preventing adverse effects. Therefore, it is recommended to determine a subgrid frequency distribution of deposition values for each land-use category, and take this frequency distribution into account when assessing the emission reduction required.

This Page Intentionally Left Blank

# CHAPTER 7 THREE CASE STUDIES

*Introduction*

In this chapter three experiments will be described which were aimed at determining deposition parameters for different receptors, a heathland, a Douglas fir forest and complex terrain, to be used for generalisation. The first study id the Elspeetsche Veld experiment, conducted at a heathland in the centre of The Netherlands. Micrometeorological measurements of $SO_2$, $NH_3$ and $NO_2$ were made together with throughfall measurements of $SO_4^{2-}$, $NO_3^-$ and $NH_4^+$ to determine the annual input to the heathland, to derive deposition parameters and the interrelations between parameters for different gases to be used for generalisation (see Chapter 4) and to study the relation between atmospheric deposition and the soil load (throughfall). The second field study deals with a large scale measurement program in the forested area the Utrechtse Heuvelrug in the centre of the Netherlands to determine the influence of canopy structure and complex terrain (forest edges and roughness transitions) to the deposition of acidifying components and base cations, using the throughfall method. The third field experiment described in this chapter has been conducted in the Speulder forest in the middle of the Veluwe, the largest forested area in the centre of The Netherlands. Micrometeorological measurements were combined with concentration measurements and meteorological measurements to determine the exposure to and input of gases and particles to the forest. Also throughfall measurement were made to determine the soil load and to relate the soil load to the atmospheric load. At this site also long-term measurements of changes in effect parameters were made, together with manipulation experiments. The results of these experiments and those of the inputs are used to evaluate dose - effect relations and to determine the most serious impact at the forest.

# 7.1 THE ELSPEETSCHE VELD EXPERIMENT ON SURFACE EXCHANGE OF TRACE GASES

## 7.1.1 INTRODUCTION

A three-year experiment was conducted at the Elspeetsche Veld heathland in the Netherlands (Veluwe). The aim of this experiment was to quantify atmospheric fluxes and to derive deposition parameters for heathland vegetation to use for generalisation. Gradients of $SO_2$ (RIVM), $NH_3$ (KEMA and ECN) and $NO_2$ (TNO) have been measured together with throughfall and bulk precipitation fluxes (RUU). A second aim of this study was to investigate the co-deposition of $NH_3$ and $SO_2$ and the relation between throughfall and atmospheric deposition for acidifying components.

In this chapter a summary of the results of this integrated study is given. Detailed descriptions of the measuring methods, equipment and results can be found in the reports and papers published by the individual research groups, i.e. for $NH_3$ by van den Beld and Römer (1990) and by Wyers *et al.* (1992, 1993), Erisman and Wyers (1993), for $SO_2$ by Erisman *et al.* (1993), Erisman (1992), Mennen *et al.* (1992) and by Erisman and Duyzer (1991), for $NO_2$ by Duyzer *et al.* (1991) and for the throughfall measurements by Bobbink *et al.* (1990; 1992). For an extensive description of the experiments the reader is referred to Erisman et. al. (1991) and Erisman (1992).

## 7.1.2 STUDY AREA AND METHODS

*Study area*
The experiment was carried out at a heathland nature reserve in the central part of the Netherlands: Elspeetsche Veld (52° 16' N, 5° 45' E), near the village Elspeet. The heathland is located in a region with moderate ambient concentrations of $SO_2$ (6 $\mu g\ m^{-3}$) and NOx(20 ppb) (RIVM, 1989). The ammonia emission density in this area is about equal to the average $NH_3$ emission in the Netherlands (Erisman, 1989). The vegetation at the site belongs to the GENISTO-CALLENETUM (dry inland heath, characterised by Calluna (Heather)). At the site Calluna vulgaris (L.) Hull completely dominates the dwarf-shrub layer. Approximately 20% of the soil surface is not covered by vegetation. The age of the Calluna plants is 4 - 5 years and the height of the canopy is 20 - 30 cm (Bobbink *et al.*, 1990). Subsoil is nutrient-poor fluvio-glacial sand with a well developed podzolic soil profile.

The heathland vegetation is surrounded by agricultural grasslands with livestock farms in the South and West at $\geq$ 1 km distance. The ideal fetch to fulfil the demands of steady state

homogeneous flow over the heathland is obtained at about 120-270°. In all other directions the fetch is disturbed by roughness elements too close to the measuring site.

A small part of the field was enclosed for the equipment. Just outside the fence three meteorological towers were erected, one for the $NO_2$ gradients (during two months), one for the $NH_3$ gradients using the continuous flow denuders (during three months) and the third for the $SO_2$ and $NH_3$ (thermodenuder) gradients. The monitors for $SO_2$ and $NO_2$ were stored together with the other sensors and data acquisition equipment in special low boxes within 2 m North of the towers. The $NH_3$ thermodenuders were stored in a caravan at 15 m North of the towers. Three open rain samplers were placed at 40 cm above the soil surface within the fence. Throughfall and stemflow devices were placed randomly at 5 places outside the fence within a radius of 50 m. In the next section a brief overview of the equipment is presented. Details are given in the references mentioned earlier.

*Measurement methods and approach*

In Table 7.1, an overview is presented of the different methods and equipment used during the experiment. In order to monitor dry deposition fluxes on a routine basis, dry deposition monitoring systems for $SO_2$, $NO_2$ and $NH_3$ have been developed based on the micrometeorological gradient technique. The $SO_2$ system was previously tested during a two year feasibility at Zegveld, a grassland location in the centre of the Netherlands (Erisman *et al.*, 1993). Selection criteria have been derived to select measuring periods fulfilling the demands of the flux-profile theory. Furthermore, a scheme has been developed to calculate yearly average fluxes from the selected and rejected measuring periods. After the first year of measurements at Elspeet, the system was considerably improved by using more accurate $SO_2$ monitors, with a lower detection limit.

**TABLE 7.1** Overview of methods and equipment used during the Elspeetsche Veld experiment.

| Method | Period | Flux averaging time | Meteorological measurements | Gas analysers | Reference |
|---|---|---|---|---|---|
| $SO_2$ gradients (4, 2, 1 and 0.5 m) | 1-4-1989 28-7-1992 | 30 minute | $u$, $\theta$, $\sigma_\theta$, at 5 m; net radiation; 1.5m $T$ and rh at 2.5m height | Thermo Environmental Instruments model 43S | Haan (1988), Mennen *et al.* (1992; 1993) Erisman *et al.*, (1993) |
| $NH_3$ gradients (4 and 1 m) | 1-4-1989 1-4-1990 | 30 minute | (meteo of $SO_2$ gradients used) | thermodenuder | van den Beld and Römer (1990) |
| $NH_3$ gradients (4, 2 and 1 m) | 6-9-1991 6-12-1991 | 6 minute | (meteo of $SO_2$ gradients used) | continuous flow denuders | Wyers *et al.* (1992; 1993) |
| $NO_2$ gradients (4, 2, 1 and 0.5 m) | 1-10-1989 24-12-1989 | 1 minute | sonic anemometer | Scintrex LMA3 luminol $NO_2$ monitor | Duyzer *et al.* (1991) |
| throughfall, stemflow and bulk precipitation | 27-4-1989 27-4-1990 | bi-weekly | | polythene funnels (165 $cm^2$) | Bobbink *et al.*, (1990); Bobbink *et al.*, (1992) |

## 7.1.3 CALCULATION OF DEPOSITION PARAMETERS

The standard deviation of the wind direction $\sigma\theta$, the wind speed $u$, temperature $T$ and net radiation $R_n$ are used to estimate the friction velocity $u_*$ and the sensible heat flux (Hicks *et al.*, 1987, Erisman *et al.*, 1993). During a period of six weeks, simultaneous measurements using an automated eddy correlation system were made at this site. $u_*$ values calculated from measurements by the monitoring system agreed very well with the directly measured $u_*$ values (Erisman and Duyzer, 1991). The average stability-corrected concentration gradients of $SO_2$, $NO_2$ and $NH_3$ are calculated as the slope of the regression line of the concentrations as a function of the stability-corrected logarithm of the height (see e.g. Erisman *et al.*, 1993). The flux $F$, deposition velocity $V_d$, aerodynamic resistance $R_a$, quasi-laminar layer resistance $R_b$ and the surface resistance $R_c$ are calculated as 2 hour averages according to the equations given e.g. in Hicks *et al.*, 1987 and Erisman *et al.* (1993).

*$SO_2$*

For measurements of the $SO_2$ dry deposition flux, two periods can be distinguished, 1989 to 1991 and 1991 to half 1992. During 1989 to 1991, measurements were made with the 'old' monitors. Results for this period are given in Erisman *et al.* (1993). These results are summarised in the tables below. For the interpretation of the measurements from the period 1991 to 1992, using the more accurate monitors, rejection criteria have been applied to assure high quality results. These criteria differ somewhat from those given in Erisman *et al.* (1993). The criteria for acceptance are listed in Table 7.2.

**TABLE 7.2** Criteria for acceptance of observations and no. of observations rejected (total no. of measurements: 5298 two hourly average periods).

| Criteria | 'New' monitors | Number of remaining periods after application of criteria |
|---|---|---|
| Flux profile relation valid; wind speed at 10 m height: | $> 1$ m s$^{-1}$ | 1031 |
| Non-disturbing fetch; wind direction between: | 120° and 270° | 1936 |
| Concentration (detection limit) | $> 1$ µg m$^{-3}$ | 604 |
| Concentration difference of two monitors measuring simultaneous at 4 m level: | $\Delta c < 3$ µg m$^{-3}$ | 125 |
| $\|V_d\| < 2\,[R_a + R_b]^{-1}$ | $\|V_d\| < 2*[R_a + R_b]^{-1}$ | 50 |
| Error in $R_c$: | $< 1000$ s m$^{-1}$ | 161 |

Deposition parameters for selected periods

The rejected data in 1991 and 1992 contain 74% of the total number of measurements, 10% less than the measurements during the first period using the 'old' monitors. The average $SO_2$ concentration at 4 m height for this period was 6.9 µg m$^{-3}$ (ranging from 0.1 to 120 µg m$^{-3}$). The average $SO_2$ concentration for the selected dataset was 7.2 µg m$^{-3}$ (ranging from 0.5 to

120 μg $m^{-3}$). The yearly average $z_0$ value for the wind direction sectors used in the selected dataset is about 4 cm. This value agrees with those obtained from the eddy correlation measurements (Erisman and Duyzer, 1991). The average $R_c$ values for dry and wet conditions and for daytime and night time are listed in Table 7.3. In this table uncertainty estimates are given based on error propagation calculations using uncertainties in measured quantities (Erisman *et al.*, 1990; 1993; Erisman and Duyzer, 1991; Mennen *et al.*, 1992). The uncertainty in $R_c$ values is given here as if $R_c$ is normally distributed. This is not the case. However, uncertainties should be interpreted as a measure of the accuracy of the mean.

**TABLE 7.3** Average $SO_2$ $R_c$ (4 m) values (± uncertainty estimates) for selected daytime and night-time and dry and wet conditions at Elspeetsche Veld.

| Condition | $R_c$ (s $m^{-1}$) day | $R_c$ (s $m^{-1}$) night |
|---|---|---|
| | old monitors (1989/1991) | |
| Dry | 55 ± 115 | 95 ± 95 |
| Wet | 10 ± 15 | 25 ± 25 |
| | new monitors (1991/1992) | |
| Dry | 150 ± 245 | 85 ± 130 |
| Wet | 35 ± 35 | 15 ± 25 |

$R_c$ values show strong variations with time; when the surface becomes wet, $R_c$ values drop to zero, whereas at very dry conditions $R_c$ values can easily increase up to values of 10000 s $m^{-1}$ at night. By the use of average $R_c$ values for only four different classes, this large variation with time is not accounted for. An $R_c$ parameterization derived from a sub-set of the measurements was tested. This parameterization is given in Section 4.7. of this book. Hourly $R_c$ values were parametrised and accordingly $V_d$ values estimated using $R_a$ and $R_b$ estimates. It was found that with this parameterization, 44% of the variance in parametrised $V_d$ versus the measured $V_d$ was accounted for, with no systematic differences. An example of the comparison between parametrised and measured $R_c$ is given in Figure 7.1. This parameterization is probably representative for Dutch environmental conditions. At Elspeetsche Veld annual average $NH_3$ concentration equals that of $SO_2$ (see also Section 3.5 about co-deposition). The parameterization might be improved with better information about surface wetness, its origin (dew, fog, rain, etc.) and its chemical composition, and about stomatal behaviour of heather plants.

Hicks *et al.* (1987) and Wesely (1989) presented parameterizations of $R_c$ $SO_2$ for North American conditions. When these parameterizations are applied for the heathland dataset, too low $V_d$ values are calculated in comparison to measured values. $R_c$ values resulting from their parameterizations are much higher than those obtained from measurements and from Eqn (4.1). The main differences are found for periods with wet surfaces due to rainfall.

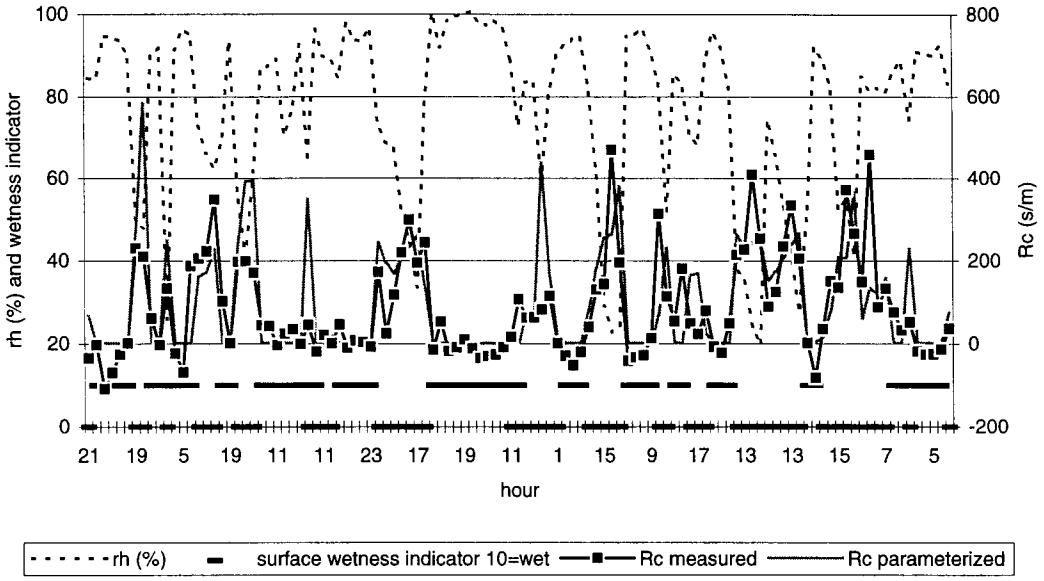


**FIGURE 7.1** Time series of parametrised and measured $R_c$ for $SO_2$ at Elspeetsche Veld.

Annual averages

There is a problem in estimating annual averages because by selection most data have been rejected (over 70%). Application of the rejection criteria results in overestimation of the annual average dry deposition velocity and dry deposition flux, since only periods with concentrations above the detection limit and with appreciable turbulence present were selected. However, it was found that data rejection does not leads to bias in $R_c$ values. This was investigated by comparing the relative frequency distributions of the most relevant parameters used to derive surface conditions for the selected and the rejected dataset (Erisman *et al.*, 1990). $R_c$ values are therefore expected to be similar for both the selected and total dataset.

The annual average dry deposition flux and $V_d$ can be obtained from the resistance analogy by calculating $R_a$ and $R_b$ from the observations of $u$, $T$ and $R_n$ and taking the parameterization for $R_c$ (Equation 4.1) corresponding the appropriate conditions. The annual average flux and deposition velocities for the complete datasets calculated using the parametrised $R_c$ are listed in Table 7.4. In Table 7.4 uncertainties in deposition parameters are given. The estimate of the uncertainty in $R_c$ is based on error propagation using uncertainties in all measured quantities to determine its value (see Section 3.1.1. and Erisman *et al.*, 1990; 1993; Erisman and Duyzer, 1991; Mennen *et al.*, 1992,. It is shown that the improved system (new monitors) yields more

accurate deposition parameters than the system with 'old' $SO_2$ monitors (i.e. smaller uncertainties). Differences in $R_a$ and $R_b$ are the result of the different conditions during the years.

**TABLE 7.4** Annual average dry deposition parameters for $SO_2$ at Elspeetsche Veld (4 m height). For the resistances the harmonic averages (± uncertainty estimates) are presented.

| Parameter | 'Old' monitors | 'New' monitors | Dimension |
|---|---|---|---|
| $z_0$ | 4 | 4 | cm |
| $C$ | 7.5 | 6.9 | $\mu g\ m^{-3}$ |
| $R_a$ | 43 ± 62 | 36 ± 45 | $s\ m^{-1}$ |
| $R_b$ | 23 ± 15 | 20 ± 28 | $s\ m^{-1}$ |
| $R_c$ | 47 ± 65 | 6 ± 8 | $s\ m^{-1}$ |
| $V_d$ | 0.8 ± 0.4 | 1.0 ± 0.1 | $cm\ s^{-1}$ |
| $F$ | 300 ± 270 | 250 ± 125 | $mol\ ha^{-1}\ a^{-1}$ |

*$NO_2$*

The fully automated instrumentation to monitor the $NO_2$ flux was operated for a two month period (Duyzer, 1991). Some measurements during periods with easterly winds over a nearby road were rejected because of a possible interference due to $NO_2$ emissions from the traffic. Nevertheless, a large dataset consisting of some 1100 twenty-minute averages remains.

The deposition velocity obtained from these measurements ranged from 0.1 to 0.4 cm $s^{-1}$. A weak diurnal cycle was observed. The $R_c$ values correspond to those estimated based on stomatal behaviour, and ranged from 100 to 200 s $m^{-1}$ during the day to 700 s $m^{-1}$ at night (see Figure 7.2). These results are consistent with those found in the literature (e.g. Duyzer *et al.*, 1990; Fowler *et al.*, 1991). The $NO_2$ flux for this two month period was estimated 500 mol $ha^{-1}$ $a^{-1}$. No annual average flux can be obtained from these measurements because conditions cannot be regarded representative for a year.

*$NH_3$*

Thermodenuder measurements

From April 1989 to April 1990, $NH_3$ gradients at the heathland were measured by KEMA at two levels with an automatic analyser equipped with two thermodenuder instruments. A description of the apparatus and the measuring set-up is given in van den Beld and Römer (1990), Erisman *et al.* (1991) and Erisman (1992). In order to eliminate systematic differences in the concentration gradient, a quality programme was initiated (van den Beld and Römer, 1990; Erisman, 1992). During several days of the year, both thermodenuders measured at the same height (1 m). In this way, correction factors can be obtained for systematic differences between concentrations measured with the two thermodenuders. Furthermore, every two

weeks the two thermodenuders were exchanged in order to measure at the other height. From the quality control tests, it was concluded that the error in the individual measurements was too large to use single gradients obtained with the two denuders for flux estimates (Erisman *et al.*, 1991; Erisman, 1992). Individual measurements could not be used for estimation of deposition parameters. However, deposition parameters were obtained by using yearly average diurnal variations of the concentration gradient and of meteorological data. Because of the regular exchange of the tubes between two heights, the corrections obtained from the quality control tests and a de-trending procedure, the errors were minimised when the gradients were averaged over the whole year (Erisman *et al.*, 1991; Erisman, 1992).

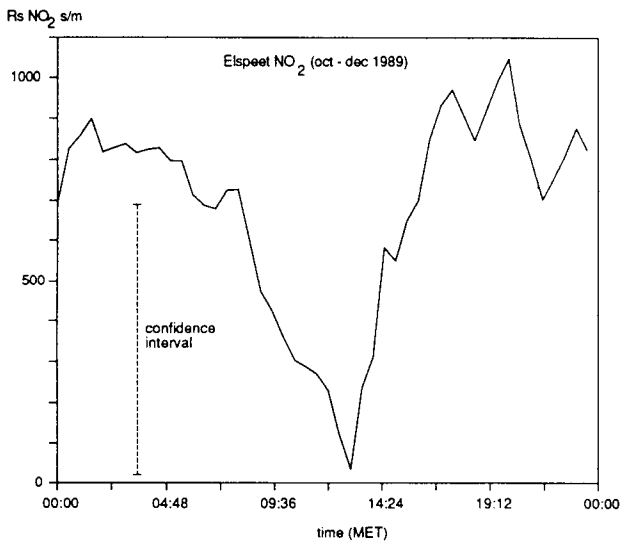


**FIGURE 7.2** Averaged $R_c$ for $NO_2$ over heathland (Elspeetsche Veld) in autumn 1989 (Duyzer *et al.*, 1991).

From the annual average diurnal variation of the concentrations and the annual average meteorological data the stability corrected concentration gradient $c_*$ has been calculated based on the method described by Erisman (1992). From $u_*$ and $c_*$ the annual average diurnal variation of the flux and deposition velocity at a height of 4 m can be calculated for $NH_3$. By using annual averages instead of data for each measuring period an error is introduced because of correlation's between some parameters (between e.g. $V_d$ and $c$). The magnitude of this error for $NH_3$ is unknown, because of lack of measurements to test the influence of these correlation's. For $SO_2$, this error was found to be small (Erisman *et al.*, 1990). The annual

average diurnal variations of $F$ and $V_d$ are presented in Figure 7.3. A strong diurnal variation can be observed for both $F$ and $V_d$. The annual average flux is 850 mol $ha^{-1}$ $a^{-1}$ and the annual average $V_d$ is 0.8 cm $s^{-1}$. This is in agreement with similar measurements over heat land (Duyzer *et al.*, 1987; Sutton *et al.*, 1992). It must be emphasised that despite the minimisation of the errors, the uncertainty in these values is very large. Furthermore, separate averaging of meteorological data and concentration gradients over the year increases the uncertainty in the annual average $F$ and $V_d$.

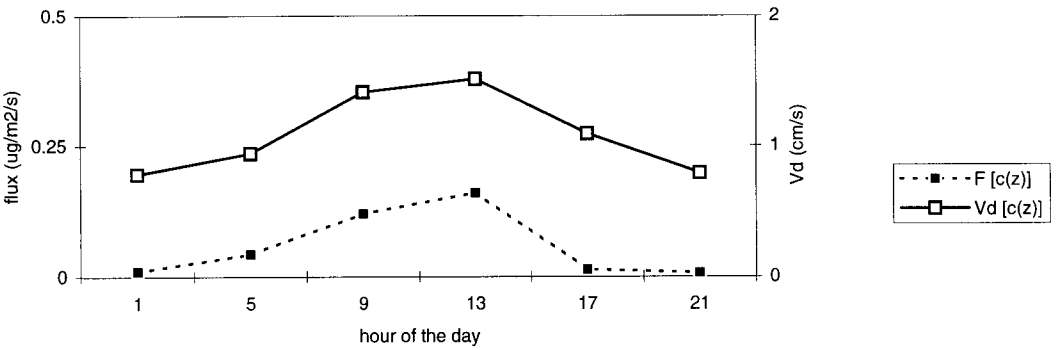


**FIGURE 7.3** Annual average diurnal variations of $F$ and $V_d$ for $NH_3$.

Continuous flow denuder measurements

During three months at the end of 1991, continuous $NH_3$ gradients were monitored using continuous flow denuders (Wyers *et al.*, 1992; Erisman and Wyers, 1993). The measurements were attuned to the $SO_2$ gradients to yield average $NH_3$ concentration gradients for the same time intervals. The results of the simultaneous measurements of the two gases were used to derive indications for their possible interaction in the deposition process (see Section 3.5 and Erisman and Wyers, 1993). It was found that dry deposition of $NH_3$ is generally determined by turbulent transport with low $R_c$ values of 15 s $m^{-1}$ on average. The low $R_c$ values are related to surface wetness which occurred most of the time. Surface wetness can be the result of either precipitation, fog or dew (visible or macroscopic wetness) or of high (>80%) relative humidity (microscopic surface wetness).

The changes in surface resistances of $NH_3$ match changes in relative humidity (see Figure 7.4). During very dry periods with rh<60%, high positive (deposition) or negative (emission) $R_c$ values for $NH_3$ were observed. Upward fluxes of $NH_3$ were observed only during daytime. At higher relative humidities the surface resistances for $NH_3$ become small. An increase in rh from 30% to 95% was accompanied by a change from negative (emission) to near-zero values.

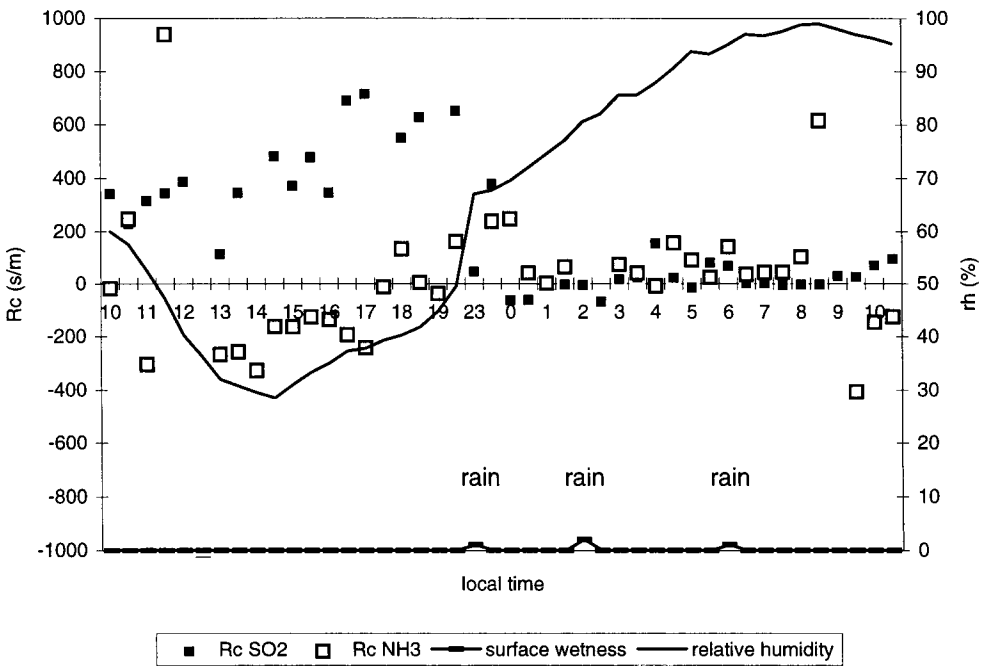


**FIGURE 7.4** Surface resistance for $SO_2$ and $NH_3$, relative humidity and surface wetness indicator for the Elspeetsche Veld site, 14-15 September 1991 (Erisman and Wyers, 1993).

After rain or fog events volatilisation of $NH_3$ from water layers was sometimes observed. At temperatures below zero degrees centigrade at ground level, $R_c$ values were observed to increase to several hundreds s $m^{-1}$.

*Throughfall and stemflow*

Bulk precipitation, throughfall and stemflow were sampled from 17 April 1989 to 17 April 1990 (Bobbink *et al.*, 1990; 1992). Rainfall was recorded until the end of 1989 with a pluviograph. Throughflow fluxes, defined as the sum of throughfall and stemflow, were found to be higher than bulk precipitation for all measuring periods. Throughflow fluxes of nitrate were relatively high in dry periods in May and in July. These periods corresponded with observed smog episodes of nitrogen dioxide in the summer of 1989 (RIVM, 1990). Throughflow fluxes of sulphate and ammonium were relatively high in autumn (October and November). This is probably related to wet Calluna canopies in this period leading to increased deposition (Bobbink *et al.*, 1992). In January and February 1991 high fluxes of sea-salt components were measured. Strong north-westerly winds, transporting marine air over the country, were observed in these months.

The annual bulk and throughflow fluxes of sulphate, ammonium and nitrate are shown in Table 7.5. The two-weekly fluxes of throughflow and bulk precipitation are given in Bobbink *et al.* (1990). Since foliar uptake or loss of sulphate was found to be negligible in heathland vegetation, the annual throughflow flux of $SO_4^{2-}$ is considered to represent the total atmospheric deposition of sulphur to the vegetation. Furthermore, it was demonstrated that ammonium and nitrate in throughflow did not leach from the Calluna canopy. In contrast, foliar uptake of $NH_4^+$ by Calluna has been observed (Bobbink *et al.*, 1990; 1992).

**TABLE 7.5** Annual average $SO_4^{2-}$, $NO_3^-$ and $NH_4^+$ throughflow fluxes and bulk deposition (mol $ha^{-1}$ $a^{-1}$). The standard deviation is given between brackets (Bobbink *et al.*, 1990).

| | $SO_4^{2-}$ | $NH_4^+$ | $NO_3^-$ |
|---|---|---|---|
| Bulk deposition | 355 (9) | 845 (42) | 380 (3) |
| Throughflow | 1035 (108) | 2145 (311) | 935 (145) |
| Interception deposition | 680 | 1300 | 550 |

Comparison of atmospheric deposition estimates and throughfall measurements
The comparison is made for throughfall fluxes of $SO_4^{2-}$ and $NH_4^+$ (Bobbink *et al.*, 1991). These fluxes comprise wet deposition and dry deposition of gases and aerosols. Only micrometeorological measurements of $SO_2$ and $NH_3$ fluxes were made. Aerosol data are lacking. Fluxes for $SO_4^{2-}$ and $NH_4^+$ aerosol deposition were estimated by inference from concentrations obtained from the National Air Quality Monitoring Network and $V_d$ estimates from $u_*$ values (Wesely *et al.*, 1985; Erisman, 1992; 1993A). These aerosol measurements represent the fraction with small particle diameter (0.5 - 2.5 μm). The large particle fraction is not measured. However, this fraction is included in the throughfall. Thus throughfall fluxes have to be corrected for the contribution of this fraction according to Erisman (1992; 1993B). The throughfall data were also corrected for the dry deposition of gases and aerosols to the funnels of the devices (Erisman, 1993B).

The yearly average (corrected) net throughfall flux for $SO_4^{2-}$ was 500 mol $ha^{-1}$ $a^{-1}$ and the dry deposition flux amounted to 350 mol $ha^{-1}$ $a^{-1}$. The yearly average net throughfall flux for $NH_4^+$ corrected for foliar uptake (Bobbink *et al.*, 1992) was 1180 mol $ha^{-1}$ $a^{-1}$ and the dry deposition flux amounted to 930 mol $ha^{-1}$ $a^{-1}$. The correlation between the two estimates on a monthly basis is significant ($R$=0.50 for $SO_4^{2-}$ and $R$=0.52 for $NH_4^+$, $p$<0.05). The atmospheric deposition estimates tend to be somewhat lower. The agreement between net throughfall and dry deposition estimates is reasonable, provided that the corrections are made for the contribution of neutral salt deposition and of dry deposition on the sampling surfaces (Erisman, 1993B). Net-throughfall was somewhat higher for both $SO_4^{2-}$ as well as for $NH_4^+$.

*Co-deposition of $SO_2$ and $NH_3$*
Simultaneous measurements of $SO_2$ and $NH_3$ concentration gradients were made (Erisman and Wyers, 1993). Furthermore, throughfall measurements of $SO_4^{2-}$ and $NH_4^+$ were collected. These data might provide information on the process of co-deposition between $SO_2$ and $NH_3$.

Throughfall fluxes compared to atmospheric deposition
Bobbink *et al.* (1992) concluded from their throughfall measurements made at Elspeetsche Veld that stoichiometric co-deposition for $SO_4^{2-}$ and $NH_4^+$ occurred. The conclusion was based on the observation that the slope of the regression equation of the throughflow fluxes of $NH_4^+$ and $SO_4^{2-}$ is near to 2 with a regression coefficient of 0.91. In the net-throughfall fluxes this ratio is also found. Monthly mean dry deposition estimates of $SO_2$ and $NH_3$ were calculated using the resistance analogy, together with concentration measurements. Aerosol deposition was estimated as described in Section 7.3. The ratio of monthly mean dry SOx to dry NHx fluxes (aerosols included) obtained from the micrometeorological measurements does not differ from 2 (Erisman *et al.*, 1991; Erisman, 1992). However, the scatter is larger than that in throughfall.

The correlation that was found for the atmospheric fluxes of SOx and NHx is, in the present model formulation, not resulting from the co-deposition between $SO_2$ and $NH_3$ through pH coupling; neither the $R_c$ parameterization of $NH_3$ nor that of $SO_2$ used for the calculation of these fluxes takes the pH coupling effect into account (see Chapter 4). The deposition velocities, however, are correlated because of the low $R_c$ values used for both gases. $V_d$ values are therefore determined by aerodynamic behaviour ($R_a$+$R_b$). The high correlation can thus be largely ascribed to the aerodynamic behaviour of the two gases. The calculated flux is the result of a concentration and a deposition velocity. The monthly average concentrations of $NH_3$ and $SO_2$ show a low correlation, although the annual average $NH_3$ concentration is twice that for $SO_2$. This might explain the 1:2 ratio found in throughfall.

The low $R_c$ values for $SO_2$ and $NH_3$ are assumed to be caused by vegetation wetness. Furthermore, $R_c$ values are different for day and night probably because of stomatal behaviour. An interdependence of $R_c$ values for both gases will probably only have some influence on the fluxes under extreme conditions, i.e. very dry conditions, absence of $NH_3$ for $R_c$ of $SO_2$, absence of $SO_2$ for the $R_c$ for $NH_3$ or a large excess of $NH_3$ causing saturation of the surface and therefore increasing $R_c$ for $NH_3$. The exact 2:1 relation found in throughfall samples might be the consequence of other processes such as evaporation of excess $NH_4^+$ in the samples.

Micrometeorological measurements of $SO_2$ and $NH_3$
So far there have only been a limited number of simultaneous micrometeorological measurements of $NH_3$ and $SO_2$, which are needed to test the importance of this process in the field. With the recent development of dry deposition monitoring systems for $SO_2$ and $NH_3$ (Erisman *et al.*, 1993; Mennen *et al.*, 1992; Wyers *et al.*, 1993), continuous measurement of the fluxes over extended periods and with sufficient accuracy has become possible.

The results of the simultaneous measurements performed in the autumn of 1991 clearly show the importance of surface wetness in the dry deposition process (Erisman and Wyers, 1993). However, the water layer composition affects the surface resistance of both gases. Under the environmental conditions prevailing in the Netherlands - commonly wet surface conditions - $SO_2$ and $NH_3$ are deposited with negligible surface resistances. A high flux of one gas relative to the other can increase its surface resistance through saturation of the surface and lower the resistance for the other gas. When $NH_3$ is present in excess over acid or acid-forming species, the surface resistance for $NH_3$ is mostly higher than zero, usually round 100 s $m^{-1}$, which is due to an increase in the pH of surface water layers. Analogous behaviour has been observed for $SO_2$ as a result of a decrease in the pH of surface water layers.

During dry periods (low *rh*), $SO_2$ and $NH_3$ surface resistances are determined by stomatal uptake. In very dry periods, small emission fluxes of $NH_3$ are observed. However, such conditions are not frequently observed in the Netherlands. At temperatures below zero, when the surface is frozen, $R_c$ values of the two gases increase up to several hundreds s $m^{-1}$. Fog composition has a large influence on $R_c$ values, resulting in both high and low values.

It is concluded that under the environmental conditions prevailing in the Netherlands, co-deposition is not an important process in the dry deposition of both gases. However, if the low $R_c$ values found from independent measurements of $SO_2$ and $NH_3$ are the result of both gases being present in approximately the same concentrations during the measurements, then co-deposition is always important in the Netherlands. In those areas where there is a large excess of one gas over the other, co-deposition might certainly play an important role.

### 7.1.4 CONCLUSIONS

A three year experiment for the determination of deposition fluxes to heathland was conducted at the Elspeetsche Veld involving several research groups. From these measurements, annual average deposition parameters for $SO_2$ were estimated. Two extensive series of measurements resulted in estimates of $V_d$ (4 m height) of 0.8 and 1.0 cm $s^{-1}$ respectively. An $R_c$ parameterization for $SO_2$ was derived which corresponds well with observed resistances. $R_c$ values are usually low, related to surface wetness. A clear difference in $R_c$ values between day and night and dry and wet conditions was observed. Changes in $R_c$ values match changes in relative humidity in dry conditions.

From $NO_2$ concentration gradient measurements (TNO), deposition parameters were derived, yielding $V_d$ values between 0.1 and 0.4 cm $s^{-1}$. $R_c$ values generally followed stomatal behaviour.

$NH_3$ dry deposition was measured using different methods, which were evaluated. The annual average flux measured using thermodenuders (KEMA) was 850 mol $ha^{-1}$ $a^{-1}$ and the annual average $V_d$ (4 m height) was 0.8 cm $s^{-1}$. It must be emphasised that despite minimisation of errors, the uncertainty in these values is large. During three months continuous $NH_3$ concentration gradients were monitored using continuous flow denuders (ECN). The measurements were made for the same time intervals as the $SO_2$ gradient measurements. It was found that dry deposition of $NH_3$ is generally determined by turbulent transport with low $R_c$ values. These low $R_c$ values were related to surface wetness which occurred most of the time. Surface wetness can be the result of either precipitation, fog or dew (macroscopic wetness) or of high (>80%) relative humidity (microscopic surface wetness). The changes in $R_c$ of $NH_3$ match changes in relative humidity. During very dry periods with rh<60%, high positive (deposition) or negative (emission) $R_c$ values were observed. Upward fluxes were only observed during daytime.

The influence of deposition of $NH_3$ to the deposition of $SO_2$ and vice verse was investigated. The deposition velocities of the two gases are correlated because $V_d$ values are generally determined by turbulent transport, with low $R_c$ values. The high correlation can thus be ascribed to the aerodynamic behaviour of the two gases. Also the annual average $NH_3$ concentrations were twice that for $SO_2$. This might explain the 1:2 ratio in throughfall studies. It could not be established whether the low $R_c$ values for both gases are the result of surface wetness or a combination of surface wetness and the fact that concentrations of both gases were approximately equal.

Fluxes of $SO_4^{2-}$ and $NH_4^+$ measured with the throughfall method were compared with fluxes derived using micrometeorological measurements. The yearly average (corrected) net throughfall flux for $SO_4^{2-}$ was 500 mol $ha^{-1}$ $a^{-1}$ and the dry deposition flux ($SO_2$ and $SO_4^{2-}$ particles) amounted 350 mol $ha^{-1}$ $a^{-1}$. The yearly average net throughfall flux for $NH_4$ was 1180 mol $ha^{-1}$ $a^{-1}$ and the dry deposition flux ($NH_3$ and $NH_4^+$ particles) amounted 930 mol $ha^{-1}$ $a^{-1}$. The correlation between the two on a monthly basis is significant ($R$=0.50 for $SO_4^{2-}$ and $R$=0.52 for $NH_4^+$, $n$=12, $p$<0.05). The atmospheric deposition estimates tend to be somewhat lower.

## 7.2 THE UTRECHTSE HEUVELRUG EXPERIMENT ON THE IMPACT OF CANOPY STRUCTURE AND FOREST EDGE EFFECTS ON DEPOSITION

### 7.2.1 INTRODUCTION

Dry deposition depends heavily on the aerodynamic properties of the underlying surface. The supply of gases and particles from the free atmosphere to the receptor surface will be relatively high in case of 'rough' forest canopies exerting a large drag force on moving air masses. Especially tall forest canopies will exert a large drag force. Open and very dense canopies, caused by sheltering effects, will exert relatively small drag forces. Somewhere between these two extremes one might expect an optimum canopy density in the sense that maximum turbulent exchange occurs. Actual dry deposition amounts onto forest canopies depend on the efficiency of individual canopy elements to capture or absorb gases and particles. Small, needle-like structures are found to be more efficient in collecting particles and cloud droplets compared to larger leaf-like structures. Forest stands with small canopy density experience high in-canopy wind speeds which may enhance transport considerably.

Results from surface wash experiments (Van Dam *et al.*, 1987; Lindberg *et al.*, 1988; Draaijers *et al.*, 1992) and deposition modelling (Lovett and Reiners, 1986; Meyers *et al.*, 1989) suggest that dry deposition of various constituents increases linearly with increasing *LAI*. However, model results in particular indicate that this increment may level off or even be slightly reduced at higher *LAI* values. The *LAI* of forest canopies is found to influence transport from the free atmosphere to the receptor surface, as well as quasi-laminar layer transport and surface resistance.

In northern and western parts of Europe, extensive uniform forested areas are not common. In Scandinavia, for example, forest landscapes usually consist of a spatial mosaic of several subsystems: forest stands of different composition, height and canopy structure, logging areas, peat bog areas and lakes (Wiman, 1988). In the Netherlands and several other parts of Europe, forests are usually relatively small and surrounded by vast agricultural areas (Bleuten *et al.*, 1989). Consequently, many forest edges and other transition zones exist which are found to be important in affecting the exchange of momentum and mass between atmosphere and forest vegetation on both local (Wiman and Ågren, 1985; Li *et al.*, 1990) and regional scales (Klaassen, 1992).

Compared to forest interiors, atmospheric deposition in forest edges will be larger due to local advection and enhanced turbulent exchange. Wind entering a forest edge induces a pressure gradient of which the magnitude will be determined by the drag force introduced by the edge. This drag force will largely depend on the leaf area density of the forest edge. Relatively high in-canopy wind speeds significantly increase transport in forest edges, through which

especially the deposition of super-micron particles and cloud and fog water droplets will be enhanced (Wiman and Ågren, 1985). Particle resuspension through bounce-off or blow-off processes may be relatively intense near the very edge of a forest at extremely high wind speeds and low stickiness of the collecting surface (Slinn, 1971; Wu *et al.*, 1992).

As explained in Chapter 4, for gases like $NO_2$ and $SO_2$ stomatal resistance is known to be one of the controlling factors for dry deposition. Enhanced solar radiation and daytime temperatures in forest edges (Ranney *et al.*, 1978) may reduce stomatal resistance and consequently promote dry deposition. At the same time, enhanced evapotranspiration (Miller, 1980) and the additional water consumption by dense understory vegetation usually present in forest edges, may reduce the availability of soil moisture through which stomata close and stomatal resistance increases. Surface wetness is also found to be an important feature with respect to dry deposition, especially for $NH_3$ and $SO_2$ (Adema *et al.*, 1986; Erisman and Wyers, 1993). It may be hypothesised that trees in forest edges are less frequently covered with a water film due to enhanced evaporation (Ranney *et al.*, 1978). However, interception of fog and cloud water is more efficient in forest edges than in forest interiors (Weathers *et al.*, 1992), which again could increase the occurrence of water films.

Existing models describing transport and deposition of pollutants in forest edges suggest a very large horizontal depletion of super-micron particles downwind of a forest edge (Wiman and Ågren, 1985; Bosveld and Beljaars, 1987; Van Pul *et al.*, 1991). The associated horizontal deposition patterns show distinct maxima around the forest wall. Submicron particles and gases are found subject to relatively small depletion and edge effects. This is in agreement with ambient air concentration measurements (Dasch, 1987; Wiman and Lannefors, 1985), and deposition measurements in forest edges using surface wash methods (Potts, 1978; Hasselrot and Grennfelt, 1987; Draaijers *et al.*, 1988; Beier and Gundersen, 1989). Little is known on the deposition enhancement in forest edges in relation to the forest structure and the exposition of the edge to prevailing wind directions.

Regional scale and receptor-oriented deposition models (see Chapter 5) treat deposition as an one-dimensional (vertical) transfer to homogeneous surfaces with infinite length. By determining turbulent exchange parameters at a height of 50 m above the receptor surface, it is believed that enhanced turbulent exchange induced by local roughness transitions is sufficiently taken into account in the deposition estimates (Erisman, 1992; 1993). Advection processes are not considered in these models. To date, there is no technique available to adequately compensate for 'edge effects' as the underlying processes are still scarcely studied and the land-use data necessary are usually not available.

This section presents results of an extensive field study on the effects of canopy structure and edge aspects on deposition gradients in forest edges. On the basis of these results and information gathered on forest fragmentation in the Netherlands, the deposition to Dutch forests is estimated taking edge effects into account.

## 7.2.2 METHODS

*Study area*
To study the relationship between atmospheric dry deposition and canopy structure, an extensive throughfall monitoring programme was performed in the middle of 30 different forest stands (1-30, Figure 7.5). Forest edge effects were assumed negligible as the distance to the nearest stand edge always exceeded 50 m (five edge heights). Nine measurement sites were situated in Douglas fir (*Pseudotsuga menziesii* Mirb. Franco) stands, 10 sites in Scots pine (*Pinus sylvestris* L.) and 11 sites in oak (*Quercus robur* L.) stands. To study the spatial deposition variability within forest stands, very detailed throughfall monitoring was performed in one Douglas fir, one Scots pine and one oak stand. Bulk precipitation was measured in five clearings scattered over the study area.

To study edge effects, throughfall was monitored at eight forest edges (A-H, Figure 7.6). Forest edge measurements were conducted in three European larch (*Larix decidua* Mill) stands, three Scots pine (*Pinus sylvestris* L.), one Corsican pine (*Pinus nigra* var. maritima) and one Norway spruce (*Picea abies* L.) stand. All edges were exposed to the prevailing southwesterly winds. More-or-less undisturbed fetch over heather, grassland or arable land was found in front of the edges. Bulk precipitation was measured in the vicinity of each forest edge.

All forest stands and forest edges investigated were located in a forested area in the central part of the Netherlands, called the 'Utrechtse Heuvelrug'. The Utrechtse Heuvelrug is an approximately 50-m high ice-pushed morainic ridge with dry, sandy and nutrient-poor podzolic soils. Large source areas of $SO_2$ and $NO_x$ are located 200 km to the southeast (industrial Ruhr area) and 100 km to the southwest (Rotterdam port) of the Utrechtse Heuvelrug. $NO_x$ also originates from local traffic on small roads crossing the Utrechtse Heuvelrug. The forested area is enclosed by two relatively large agricultural areas, which are called the 'Gelderse Vallei' and the 'Kromme Rijn area'. These areas are large sources of $NH_3$ due to ammonia volatilisation from animal manure. Within the forested area, some scattered farms with intensive animal husbandry also act as a source of ammonia.

It was expected that the 30 measurement sites used to study the relationship between atmospheric dry deposition and canopy structure were expected to be exposed to more-or-less similar air concentrations as they were situated within a radius of 1.4 km of each other. However, it was recognised that some local $NH_3$ air concentration gradients may have existed due to the location of the study area near two large ammonia emission areas and the situation of some intensive livestock farms within the study area. Moreover, small NOx air concentration gradients were expected near few thoroughfares crossing the study area, along with local air concentration gradients of $Ca^{2+}$ and other base cation-containing particles near arable land and small unmetalled forest roads.

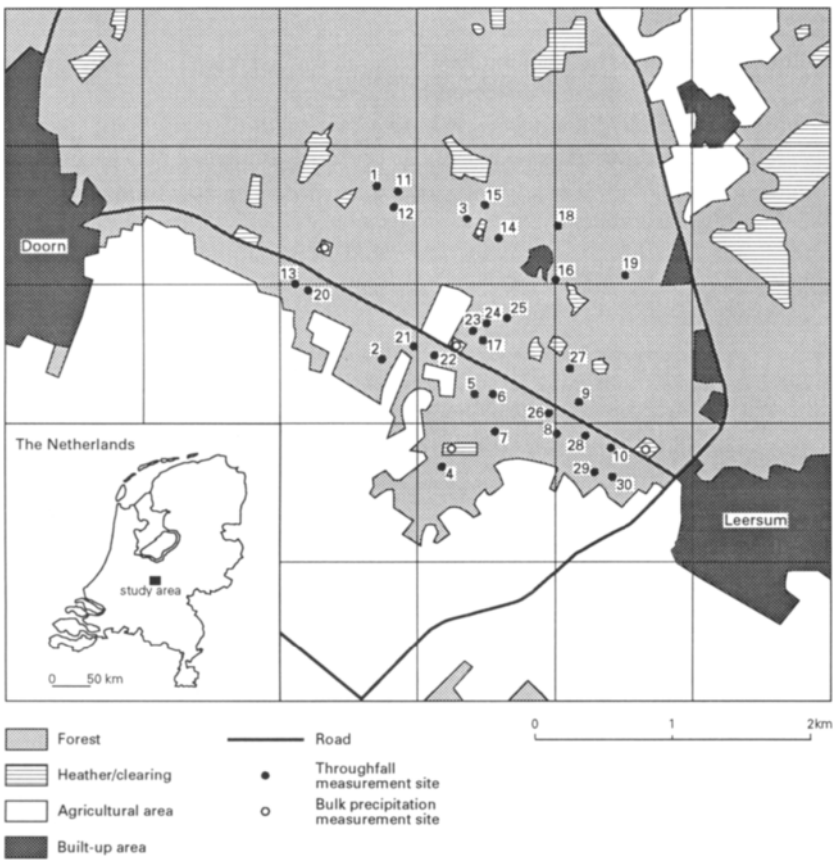


**FIGURE 7.5** Location of the study area with the 30 throughfall measurement sites and five bulk precipitation measurement sites used to study the impact of canopy structure on dry deposition amounts.

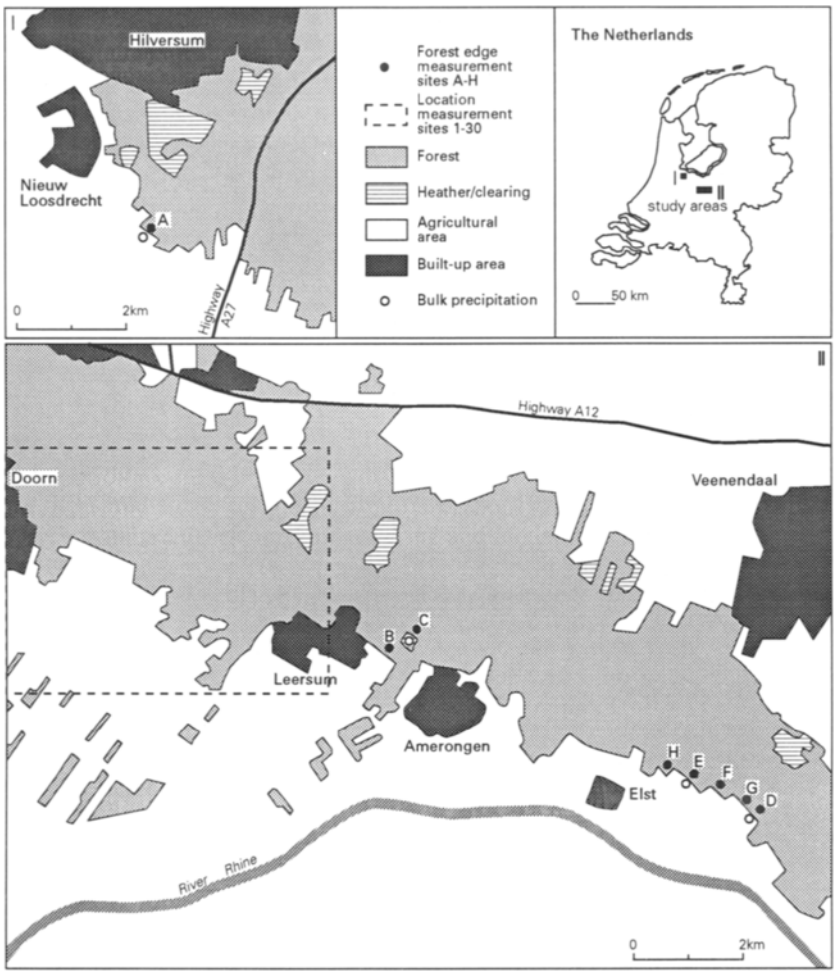


**FIGURE 7.6** Location of the study area with the eight forest edge measurement sites and four bulk precipitation measurement sites used to study the impact of edge effects on dry deposition amounts.

*Throughfall and bulk precipitation sampling procedure*

Field procedures
In each of the 30 forest stands two throughfall gutters were placed near the stand centre. Each throughfall gutter was 5 m long and had a total collecting area of 0.054 $m^2$. They were placed at a slight angle of approximately 15° to the horizontal. Throughfall gutters were preferred to funnels because they integrate over a larger canopy area, yielding more representative estimates of the throughfall flux (Duijsings *et al.*, 1986; Beier and Rasmussen 1989; Ivens, 1990). A large number of funnels would have been needed to obtain similar results (Kimmins, 1973; Draaijers *et al.*, 1995). The spatial variability of throughfall fluxes in the middle of three different forest stands was studied by means of eight throughfall gutters. In the eight forest edges, throughfall gutters were placed at a distance of 5, 10, 20, 30, 40, 60, 80 and 150 m from each edge (up to 6.0-11.4 edge heights from the edge). Gutters at 150 m from the edge were only placed when the depth of the forest stand exceeded 200 m to be sure other roughness transitions had negligible impact on throughfall fluxes. Bulk precipitation was measured by two funnels positioned at a distance of at least three times the height of the nearest obstacle. Nearby obstacles will most probably still have had a certain impact on the air flow around the funnels and, consequently, on their collecting efficiency. The funnels were placed approximately 1.5 m above the ground surface to prevent soil splash. Each funnel had a collecting surface area of 0.017 $m^2$.

To avoid contamination, e.g. by insects and coarse litter fragments, throughfall and bulk precipitation were filtered (mesh width of filter = 250 μm) before entering a 10-*l* and 2-*l* reservoir, respectively. Only opaque reservoirs were used to avoid light penetration, which could promote algae growth. The materials used for sampling (principally polyethylene) were all chemically inert as far as ions were concerned. Gutters, funnels, reservoirs and filters were cleaned with de-ionised water after each sampling period. Throughfall and bulk precipitation samples were stored in the field no longer than one week to prevent biochemical transformations (Slanina *et al.*, 1990).

Throughfall and bulk precipitation at the 30 measurement sites and eight forest edges were measured continuously for one year. For the 30 measurement sites collection started on 17 May 1990 and ended on 30 April 1991. During that time period 18 throughfall and matching bulk precipitation collections were made in total. At locations B, C and D, collection started on 27 September 1989 and ended on 27 September 1990; 23 collections were performed, while at the locations E, F, G, and H, collection starting on 15 October 1990 and ended on 1 October 1991, with 16 collections in total. At location A, throughfall and bulk precipitation was measured continuously for two years (from 27-09-89 to 01-10-91; 39 collections). To achieve complete removal of dry deposited material from the canopy, water was collected, as far as possible, after showers bringing large amounts of rain (preferably >10 mm). However, the fact that such rain amounts are not common in the Netherlands and the condition that

samplers were not allowed to stay in the field longer than one week regularly prevented this. The matching deposition periods were assumed to start immediately after the end of the last rain event of the previous collection. This information was gathered from results of a pluviograph situated near the measurement sites.

Laboratory procedures and data management

After collection, samples were stored in darkness at 5 °C. Samples were analysed for acidity (pH) and electric conductivity (EC) within 24 hours of sampling. Ion concentrations were measured within one week of sampling. Samples were analysed by colorimetry using a Skalar autoanalyser for ammonium ($NH_4^+$), nitrate ($NO_3^-$), sulphate ($SO_4^{2-}$), chloride ($Cl^-$), magnesium ($Mg^{2+}$), calcium ($Ca^{2+}$), orthophosphate ($PO_4^{3-}$) and bicarbonate ($HCO_3^-$). Furthermore, ion concentrations of potassium ($K^+$) and sodium ($Na^+$) were determined by flame photometry. In the period 7 January 1991 to 1 October 1991, Kjeldahl-N analyses were also performed on throughfall samples from the forest edges A, E, F, G, and H, collected at 5, 30 and 80 m distance from each edge, respectively. In this way, information was gathered on the organic nitrogen content in throughfall, as organic N was assumed equal to Kjeldahl-N minus $N\text{-}NO_3^-$ and $N\text{-}NH_4^+$.

Directly after the laboratory analysis, measured ion concentrations were entered into the data management programme, DAVER (Klein Tank, 1990), in order to calculate ion balances. Through this approach, ion concentrations were directly verified and repeated within 24 hours, if necessary. Analytical errors were found to be small (< 5%). However, concentration measurements were less reliable when concentrations were below the detection limit of the analysing equipment; this sometimes occurred for $SO_4^{2-}$, $PO_4^{3-}$, $HCO_3^-$, $Mg^{2+}$ and $Ca^{2+}$ in bulk precipitation (analytical error ± 20%). All chemical analyses were performed at the Laboratory of Physical Geography at Utrecht University. The laboratory regularly participates in interlaboratory tests to ensure good quality concentration measurements.

Interpolation of missing values

Approximately 10% of all throughfall and bulk precipitation data (concentrations and/or amounts) were missing because of damaged collecting equipment due to vandalism (humans and/or rabbits) or gales, or was not usable due to bird droppings onto the collectors. Bird droppings were detected in the field or could be ascertained by unusually high pH, $PO_4^{3-}$, $K^+$ and/or $HCO_3^-$ concentrations in the samples. These missing values were interpolated using the remaining data set through the very strong spatial correlations observed between two throughfall gutters or two bulk precipitation funnels situated close to each other. Due to the large size of the dataset, an interpolation method using ratios was preferred to the more time-consuming method using linear regressions between two gutters or funnels. Moreover, a comparison between the ratio method and the regression method using a small subset of the data did not yield significantly different results.

Hail and snowfall occurred from 20 January until 15 February 1991, and no single reliable throughfall and bulk precipitation collection could be made. For this reason, the method of spatial interpolation could not be applied. Precipitation volumes during this period were measured using slightly heated pluviographs. Bulk precipitation concentrations were interpolated using the fairly strong (temporal) correlation observed between precipitation concentrations and volume. Throughfall volumes were estimated from the strong (temporal) correlation found between throughfall and bulk precipitation volumes, whereas throughfall concentrations were assumed equal to the mean ratio between throughfall and bulk precipitation concentrations in the winter period. The latter interpolation procedure probably yields an underestimate of the throughfall concentrations as, compared to winter averages, relatively high air concentrations were observed in the dry period preceding the snowfall (RIVM, 1991). All round, this interpolation procedure does not seem very reliable, but there was no better alternative available; the error introduced in the annual mean bulk precipitation and throughfall fluxes was assumed to be smaller than 5%.

Calculation of deposition fluxes

After interpolation procedures, bulk precipitation fluxes for each sampling period were calculated by multiplying rainfall concentrations with rainfall amounts. Similarly, throughfall fluxes were calculated by multiplying throughfall concentrations with throughfall volumes. To obtain wet deposition amounts, bulk precipitation fluxes were corrected for dry deposition onto the collectors using the correction factors of Ridder *et al.* (1984) (see Table 3.1). The dry deposition amounts were subsequently estimated by subtracting wet deposition amounts from throughfall fluxes (= net throughfall). Throughfall fluxes were not corrected for dry deposition directly onto the gutters because the amount of dry deposition is expected to be relatively small. By using net throughfall as an indicator for dry deposition, the contribution of cloud and fog water deposition and canopy exchange to net throughfall was neglected. Annual mean wet and dry deposition fluxes were computed by aggregating the fluxes calculated for single periods. Total deposition was calculated by summing wet and dry deposition fluxes.

*Canopy and edge structure measurements*

Around each throughfall gutter, an inventory of relevant canopy structure characteristics was made in order to determine the aerodynamic roughness of the canopy, the collecting efficiency of individual canopy elements and the total collecting surface area. From each tree of which the crown was (partially) located within a 100 $m^2$ plot around the gutter (Figure 7.7), the following information was gathered through field measurements or model calculations using the canopy structure model TREE especially designed for this purpose (Van der Zanden and Sluyter, 1990):

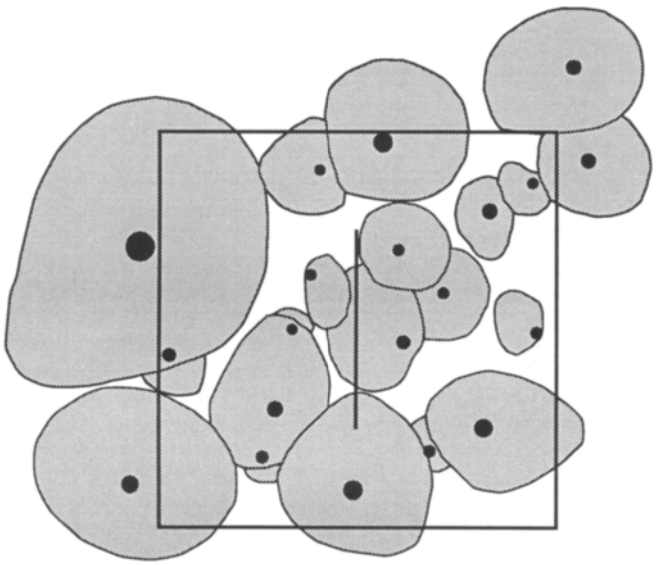

**FIGURE 7.7** An example of a measurement site showing the area (10 x 10 m) around the throughfall gutter in which tree and stand structure characteristics were determined. The throughfall gutter, indicated as a black bar, is located in the centre of the plot. Grey areas mark the vertical crown projection of individual trees, whereas stem bases are indicated as black circles. The thick line indicates the boundary of the 100 $m^2$ plot.

Location of stems, stem density and stem diameter
The exact location of the stem base within (or outside) the plot was measured with help of a measuring tape (measurement error ± 10 cm). The number of trees within the 100 $m^2$ plot was computed as the sum of stems weighted for the amount of the crown volume of each tree located within the plot. The stem diameter at breast height was measured in two directions perpendicular to each other using a large marking gauge (measurement error ± 0.5 cm).

Crown top, crown base and periphery height, and crown radius
The height of the crown top, living crown base and periphery height (where the crown has its maximum horizontal radius) was measured in the field using a standard tree-height measuring device based on goniometry (measurement error ± 5 %). The crown depth was defined as the crown top minus the crown base. The radius of the crown at periphery height was measured in eight wind directions with help of a compass, a long pole and a measuring tape (measurement error ± 10-20 cm).

Crown volume and crown silhouette area
To compute the crown volume and silhouette area (= frontal crown area) of each individual tree, field information on the height of the crown top, crown base and periphery was used together with field information on the eight crown radii, and so-called 'crown shape exponents' describing the concavity or convexity of the crown above and below the periphery height, respectively (Koop, 1989). These shape exponents were selected in such a way that the resulting crown model best reflected the shape of the crown as observed in the field.

Leaf/needle area and leaf/needle area density
Several workers have reported a functional relationship between the total needle area of a tree and the water-conductive capacity of the stem (e.g. Waring *et al.*, 1982). To express this water-conductive capacity, usually sapwood area is used, although some workers have pointed out that also wood density, hydraulic conductivity and the number of annual rings must be taken into account (e.g. Espinosa Bancalari *et al.*, 1987). The slope of the relationship between needle area and sapwood area is found to differ with growing conditions (Whitehead, 1978) and tree species (Waring *et al.*, 1982). For the measurement sites in this study, growing conditions were similar since all trees were growing on poor, sandy podzolic soils with deep groundwater table and were exposed to equal climatic conditions.

A small tree borer was used to determine the sapwood area of Douglas fir, Scots pine, Corsican pine and Norway spruce trees. Two opposite wood cores in the direction of the thickest stem diameter were taken into account for possible asymmetrical positioning of the sapwood. For Scots pine, Corsican pine and Norway spruce trees, sapwood appeared as glassy tissue if the core was held towards the light. For Douglas fir trees, a clear colour distinction could be made between heartwood and sapwood. Except for sapwood, the number of annual rings was also counted to compute tree age. The sapwood area was calculated according to $\pi^*$ (total stem radius from centre to phloem)$^2$ minus $\pi^*$ (mean radius covering heartwood)$^2$.

In January 1991 needles were destructively sampled from three Scots pine, three Corsican pine, three Norway spruce and three Douglas fir trees to determine the relationship between sapwood and needle areas. Special care was taken to ensure that the trees destructively sampled covered the range of tree heights present at the measurement sites. Due to practical reasons only 20% of all needles were sampled and weighed after drying at 70°C for 48 h. Weight of the remaining 80% was extrapolated on the basis of a count of branches left intact on the trees sampled. To compute specific needle area (i.e. surface area of fresh needle divided by its corresponding dry weight), a subsample of fresh foliage was used, as foliage was found to shrink as much as 25% in drying (Waring *et al.*, 1982). Total needle area was calculated by multiplying dry weight of all needles by specific needle area. The needle area density of an individual tree was computed by dividing total needle area by crown volume.

Although only three trees were destructively analysed from each species, clear and significant relationships were found between total needle area (*TNA*, in $m^2$) and sapwood area (*SA*, in $cm^2$):

| | | |
|---|---|---|
| Scots pine: | [*TNA*] = 18.85 + 0.230 * [*SA*] | (*R*=0.9996; *R*= 0.018) |
| Corsican pine: | [*TNA*] = -3.20 + 0.388 * [*SA*] | (*R*=0.9979; *R*= 0.041) |
| Norway spruce: | [*TNA*] = -8.16 + 0.895 * [*SA*] | (*R*=0.9989; *R*= 0.030) |
| Douglas fir: | [*TNA*] = 2.67 + 0.603 * [*SA*] | (*R*=0.9970; *R*= 0.049) |

For deciduous trees, the relationship between surface area and sapwood area is found to be less exact (Rogers and Hinckley, 1979). Therefore, the leaf area of oak and European larch was estimated by litterfall collections. Litterfall collections were made using three litter traps per 100-$m^2$ plot. Each littertrap had a collecting surface area of 1 $m^2$ arranged in a row in the centre of a plot beneath the throughfall gutter. Litterfall collections were made during the autumn until no more leaves remained on the tree branches. Total leaf area collected with the litter traps was calculated by multiplying specific leaf area by the total dry weight. This value was multiplied by 100/3 to compute total leaf area per 100-$m^2$ plot. Thus, a mean plot leaf area was obtained but no information was gathered on leaf areas of individual trees. Unfortunately, this method could not be applied near forest edges. At forest edges, leaf collection will not be representative for the canopy leaf area right above the gutter due to relatively high horizontal wind speeds within and under the canopy. For this reason, the leaf litter collection method for forest edges was only applied at 150 m from the edge.

Internal crown cover, crown area and crown projection area

The internal crown cover of individual trees was visually estimated and expressed in percentage classes of 5%. Although this technique is rather subjective, repeated estimates showed fairly consistent results, even when the observations were made by different observers. Most estimates differed only by 10% percentage class. For oak and European larch trees, the internal crown cover was estimated for both foliated and unfoliated conditions. The crown area of each individual tree was computed using the eight crown radii measured in the field. This was done by interconnecting the ends of the eight crown radii by a straight line, thereby forming a polygon with eight corners. The area of this polygon was assumed to equal the crown area. The crown projection area was calculated by multiplying calculated crown area by the internal crown cover measured in the field.

Crown projection area estimated from scanned images

Because the visual estimation of the internal crown cover was rather subjective, panchromatic images by means of photography were also used to determine crown projection areas. For the oak and European larch stands, both winter and summer images were taken to account for the seasonal variability of the crown cover. Images were only made on days when the sky had a uniform cloud cover. These weather conditions made the canopy appear as black against a white background. Days with clear skies were not useful because direct sunlight illuminated

canopy foliage, causing an underestimation of the total canopy projection area. An image of the canopy right above the middle of each throughfall gutter was made using a 28-mm standard lens pointing vertically, making sure the zenith angle of the camera equalled 0°. Such a wide-angle lens has longitudinal and latitudinal recording angles of 37.5° and 25°, respectively. Images were scanned using ERDAS digital processing techniques. The number of black pixels divided by the total number of pixels was used as an estimate of the crown projected area. Three rectangular areas of different size were scanned from each image, namely the full-size image, a medium-size image (corresponding to longitudinal and latitudinal recording angles of 27.5° and 15°, respectively) and a small-size image (corresponding to recording angles of 22.5° and 10°, respectively). Thus, no information was gathered on crown projection areas of individual trees. The actual canopy area scanned differed for each image. Except for recording angles, the actual canopy area scanned depends on the mean tree height. The actual canopy area scanned can be computed as [2 $h$ tan($\alpha$)] by [2 h tan($\beta$)], in which $\alpha$ and ß represent recording angles and $h$ the mean tree height.

Computations for the whole 100-$m^2$ plot
Besides the mean stem diameter and mean height of the crown top, crown base and periphery for each 100 $m^2$ plot, the total crown volume, total silhouette area, total crown projection area and total leaf/needle area of each 100 $m^2$ plot were also computed with the restriction that overlapping crown volumes, silhouette areas and projection areas were only counted once. Moreover, crown volumes, silhouette areas, crown projection areas and leaf/needle areas located outside the 100 $m^2$ plot were excluded.

Estimation of the aerodynamic roughness of the canopy
The roughness length is often used to characterise the aerodynamic roughness of a forest canopy (Thom, 1971). Due to the large number of measurement sites, it was impossible to estimate the roughness length in practice from measurements on the logarithmic wind profile. For this reason, the roughness length of the forest canopy above each throughfall gutter was estimated using the geometrical model of Lettau (1969). For Douglas fir, Scots pine, Corsican pine and Norway spruce trees, a drag coefficient of 0.35 was assumed (Leonard and Federer, 1973). For foliated conditions in the summer period, the drag coefficient of oak and European larch trees was also assumed to be equal to 0.35, whereas for unfoliated conditions in the winter period, a drag coefficient of 0.13 was assumed (Kruijt, 1986). The effective height in Lettau's model is calculated by $h$-$d$ with $h$ equal to the mean tree height and $d$ the zero plane displacement. The zero plane displacement varied between 0.57 $h$ and 0.87 $h$, depending on the total crown projection area ($cpa$) within the 100 $m^2$ plot:

$$d/h = 0.57 + 0.3 * (cpa/100) \qquad [7.1]$$

To compute the roughness length of a canopy according to the geometrical model of Lettau, information on silhouette areas and number of trees within the 100 $m^2$ plot was also used.

Estimation of the collecting efficiency of individual canopy elements
Parameters expected to influence the collecting efficiency of individual leaves/needles include mean projected surface area and diameter (width). For this reason, 150 Douglas fir and 150 Scots pine needles were sampled and measured as accurately as possible using a small marking gauge. As the shape of Douglas fir needles was found to be practically flat, only the length and the maximum diameter were recorded. The shape of Scots pine needles was regarded as a half-cylinder lengthwise of which length, minimum diameter, and maximum diameter were recorded. The dimensions of oak leaves were not measured because the difference in collecting efficiency with Douglas fir and Scots pine needles was obvious.

Other parameters related to the collecting efficiency, such as 'stickiness' or 'hairiness' of the leaf/needle surface, were also recorded. However, the clustering of leaves/needles was not quantified although it was recognised that this may be an important parameter with respect to the collecting efficiency of individual leaves/needles.

Estimation of the collecting surface area of the canopy
The most direct measure for the total collecting surface area of a canopy is the *SAI*. Because leaves/needles usually contribute more than 85% to the total surface area of trees (Halldin, 1985), the LAI was used in this study. A lower percentage will probably hold for trees with leaf/needle loss as a result of reduced vitality. The total crown projection area may be regarded as an indirect measure for the collecting surface area. Besides the field estimates, estimates from the scanned photographs were also used. Total crown volume and mean crown depth also reflect to some extent the collecting surface area of a canopy.

Estimation of edge structure characteristics
Parameters important for the aerodynamic properties of forest edges include relative height, edge porosity, and fetch and roughness of the upwind terrain. The relative height of the eight forest edges was computed as the mean tree height of the forest minus the height of the vegetation in front of the edge. Special attention was paid to irregular tree height with distance to the forest edge because this was also to some extent supposed to influence edge aerodynamics.

The porosity of a forest edge (i.e. the proportion of open area (background sky) to the total edge area) was estimated by scanning panchromatic images made at both one- and two-edge heights into the forest interior, looking outside. Forest edge images were processed in a similar manner as described for canopy images. Edge porosity was also estimated visually, in a way comparable to the estimation of the internal crown cover of trees. Edge porosity was determined 2 m above the forest floor, in this way it was more representative for the lower levels of the edge (trunk area). This method for characterising edge porosity turns the forest edge in a two-dimensional plane, through which objects in the foreground look larger than those in the background. Moreover, only the two-dimensional gaps, and not all the spaces through which the wind flows across the forest edge, are determined. Therefore the optical

porosity estimated is not similar to the real porosity of the forest edge (Nord, 1991). Edge porosity was also characterised by the stand leaf/needle area density defined as the total leaf/needle area divided by the total stand volume (i.e. plot area times mean tree height). The drag force a forest canopy exerts on moving air masses may also be characterised by the stand silhouette area density computed as the total silhouette area divided by the total stand volume. Crown leaf/needle area densities and crown silhouette area densities were similarly computed. For this, total canopy volumes (i.e. plot area times mean crown depth) were used instead of total stand volumes.

Recording of the land use in front of the forest edge allowed a rough estimate of the fetch and the roughness length of the upwind terrain to be made. A terrain classification made by Wieringa (1992) was adopted to obtain roughness lengths. In this classification, the roughness length of fallow ground is averaged to 0.0025 m, that of short grass to 0.019 m, that of long grass and heather to 0.04 m, that of low mature agricultural crops to 0.065 m, and that of high mature agricultural crops to 0.15 m.

### 7.2.3 THE IMPACT OF CANOPY STRUCTURE: RESULTS AND DISCUSSION

*Evaluation of canopy structure parametrisation*

Results of the canopy structure measurements are summarised for the 30 measurement sites in Table 7.6. A discrimination has been made between parameters related to the aerodynamic roughness, and parameters reflecting the collecting surface area of the canopy. The classification of a single parameter into a particular category was sometimes arbitrary. The roughness length as estimated with the geometrical model of Lettau (1969) was, on average, 2.1 m and ranged from 1.1 m to 4.0 m. Input parameters for the geometrical model of Lettau revealed large spatial variability: mean tree height was between 12.4 m and 24.1 m, stem density between 340 and 1300 trees per ha and silhouette area between 7100 and 20,900 $m^2$ $ha^{-1}$. Uncertainties in the estimate of the roughness length were primarily associated with the rather badly calibrated drag coefficient.

The leaf area index was, on average, 6.7 and ranged from 2.4 to 12.0. Other parameters related to the collecting surface area of a canopy also showed wide ranges: crown projection (field estimates): 17.7%-71.8%, crown projection (estimated from scanned 'full-sized' images): 48.1%-86.5%, crown volume: 13,700-85,200 $m^3$ $ha^{-1}$ and crown depth: 3.9-18.8 m. Crown projection estimates from scanned 'full-sized' images were similar to crown projections estimates from scanned medium-sized' and 'small-sized' images. A strong relationship was observed between crown projection estimated from scanned images and field estimates ($R$=0.79; $p<0.001$; n=30) but estimates from scanned images were significantly larger than field estimates. This was most probably the result of including the stem areas in the estimates of scanned images, whereas in the field estimates stem areas were neglected. A strong relationship was found between the difference of both estimates and stem density ($R$=0.67;

$p<0.001$; $n=30$). Because the 30 measurement sites had rather low vitality indices (section on Canopy...measurements), trunks, branches and twigs may have contributed significantly to the total collecting surface area of the canopy. This introduces an uncertainty when using *LAI* as a measure for the collecting surface area of the canopy.

**TABLE 7.6** Overview of stand structure characteristics of the 30 forest stands

| | *x* | *sd* | *cv* | max | min | max/min |
|---|---|---|---|---|---|---|
| *Aerodynamic roughness* | | | | | | |
| $z_o$ (m)[a] | 2.1 | 0.6 | 0.30 | 4.0 | 1.1 | 3.62 |
| Tree height (m) | 18.0 | 2.6 | 0.14 | 24.1 | 12.4 | 1.95 |
| Silhouette area ($m^2$ $ha^{-1}$) | 13040 | 3538 | 0.27 | 20896 | 7096 | 2.94 |
| Stem density ($ha^{-1}$) | 686 | 243 | 0.35 | 1302 | 341 | 3.82 |
| *Collecting surface area* | | | | | | |
| *LAI* (-) | 6.7 | 2.8 | 0.41 | 12.0 | 2.4 | 5.00 |
| Crown projection[b], field (%) | 40.9 | 12.9 | 0.31 | 71.8 | 17.7 | 4.05 |
| Crown projection[b], image (%) | 64.5 | 9.7 | 0.15 | 86.5 | 48.1 | 1.80 |
| Crown volume ($m^3$ $ha^{-1}$) | 35510 | 16383 | 0.46 | 85160 | 13740 | 6.20 |
| Crown depth (m) | 9.0 | 4.4 | 0.49 | 18.8 | 3.9 | 4.82 |

*x* = mean, *sd* = standard deviation, *cv* = coefficient of variation

[a] For $z_o$, *LAI* and crown projection of oak, annual mean values are presented which were computed by averaging summer and winter values.

[b] For crown projection, field estimates and estimates from scanned 'full sized' images are presented.

The roughness length, leaf area and crown projection of oak stands differed greatly with the seasons (Table 7.6). This contradicted observations made by Dolman (1986), who reported negligible impact of leaf shedding on the roughness length of an oak stand. The drag coefficient used to compute the roughness length of the oak stands in the summer period was based on experiments done by Kruijt (1986), and equalled the drag coefficient used for Douglas fir and Scots pine trees (0.35). However, it may be hypothesised that the drag coefficient for oak trees will be smaller than that of coniferous trees because per unit surface area individual leaves initiate smaller drag forces compared to needles (Thom, 1968; Monteith, 1973). Assuming that a correct drag coefficient was used for the computation of the roughness length in the winter period, a summer drag coefficient of 0.20 should have been used to obtain summer roughness length values comparable to those in the winter period. However, the drag coefficient used for the winter period (0.13) was also subject to considerable uncertainty. The leaf area of Douglas fir and Scots pine stands will also show some variability with time but this variability was not quantified. Measurements at Speuld have indicated that the leaf area of Douglas fir stands may deviate up to 30% from the annual mean (Steingröver, 1993, personal communication).

**TABLE 7.7** Overview of stand structure characteristics of single tree species

| | *x* | *sd* | *cv* | max | min | max/min |
|---|---|---|---|---|---|---|
| *Douglas fir (n=9)* | | | | | | |
| $z_o$ (m)[a] | 2.7 | 0.8 | 0.28 | 4.0 | 1.8 | 2.22 |
| Tree height (m) | 19.5 | 2.6 | 0.13 | 24.1 | 14.8 | 1.63 |
| Silhouette area ($m^2$ $ha^{-1}$) | 14941 | 4011 | 0.27 | 20896 | 8755 | 2.39 |
| Stem density ($ha^{-1}$) | 662 | 271 | 0.41 | 1302 | 433 | 3.01 |
| *LAI* (-) | 9.4 | 1.6 | 0.17 | 12.0 | 7.5 | 1.60 |
| Crown proj. field (%) | 54.1 | 11.0 | 0.20 | 71.8 | 39.9 | 1.80 |
| Crown proj. image (%) | 76.0 | 8.8 | 0.12 | 86.5 | 59.2 | 1.46 |
| Crown volume ($m^3$ $ha^{-1}$) | 49491 | 18293 | 0.37 | 85160 | 22950 | 3.71 |
| Crown depth (m) | 8.3 | 1.8 | 0.22 | 10.5 | 5.9 | 1.78 |
| *Scots Pine (n=10)* | | | | | | |
| $z_o$ (m)[a] | 1.9 | 0.4 | 0.18 | 2.4 | 1.3 | 1.85 |
| Tree height (m) | 17.1 | 1.1 | 0.06 | 18.3 | 15.1 | 1.22 |
| Silhouette area ($m^2$ $ha^{-1}$) | 9545 | 1442 | 0.15 | 11205 | 7096 | 1.58 |
| Stem density ($ha^{-1}$) | 717 | 265 | 0.37 | 1112 | 407 | 2.73 |
| *LAI* (-) | 7.9 | 1.2 | 0.15 | 9.9 | 6.3 | 1.57 |
| Crown proj. field (%) | 31.2 | 9.0 | 0.29 | 44.9 | 17.7 | 2.53 |
| Crown proj. image (%) | 59.9 | 3.7 | 0.06 | 65.0 | 50.9 | 1.28 |
| Crown volume ($m^3$ $ha^{-1}$) | 23584 | 8771 | 0.37 | 45200 | 13740 | 3.29 |
| Crown depth (m) | 4.9 | 0.7 | 0.14 | 6.0 | 3.9 | 1.54 |
| *Pedunculate oak (n=11)* | | | | | | |
| $z_o$, summer (m)[a] | 2.2 | 0.5 | 0.23 | 3.2 | 1.4 | 2.23 |
| $z_o$, winter (m)[a] | 1.3 | 0.3 | 0.24 | 1.8 | 0.8 | 2.32 |
| $z_o$, annual (m) | 1.8 | 0.4 | 0.23 | 2.5 | 1.1 | 2.25 |
| Tree height (m) | 17.6 | 3.1 | 0.18 | 23.3 | 12.4 | 1.88 |
| Silhouette area ($m^2$.$ha^{-1}$) | 14663 | 1786 | 0.12 | 17239 | 11598 | 1.49 |
| Stem density ($ha^{-1}$) | 677 | 218 | 0.32 | 1031 | 341 | 3.02 |
| *LAI*, summer (-) | 7.1 | 1.0 | 0.15 | 8.0 | 4.7 | 1.70 |
| *LAI*, winter (-) | 0.0 | 0.0 | -- | 0.0 | 0.0 | -- |
| *LAI*, annual (-) | 3.5 | 0.5 | 0.15 | 4.0 | 2.4 | 1.70 |
| Crown proj. field, summer (%) | 60.8 | 11.7 | 0.19 | 75.9 | 44.2 | 1.72 |
| Crown proj. field, winter (%) | 17.1 | 4.1 | 0.24 | 24.2 | 12.1 | 2.01 |
| Crown proj. field, annual (%) | 39.0 | 7.6 | 0.19 | 49.7 | 28.1 | 1.77 |
| Crown proj. image, summer (%) | 83.0 | 5.5 | 0.07 | 88.2 | 66.3 | 1.33 |
| Crown proj. image, winter (%) | 39.4 | 6.0 | 0.15 | 49.5 | 30.0 | 1.65 |
| Crown proj. image, annual (%) | 61.2 | 4.8 | 0.08 | 67.1 | 48.1 | 1.40 |
| Crown volume ($m^3$.$ha^{-1}$) | 34913 | 11084 | 0.32 | 53790 | 20255 | 2.66 |
| Crown depth (m) | 13.5 | 3.8 | 0.28 | 18.8 | 5.7 | 3.31 |

*x* = mean, *sd* = standard deviation, *cv* = coefficient of variation

[a] For $z_o$, *LAI* and crown projection of oak, summer, winter and annual mean values are presented.

Douglas fir stands were characterised by relatively large roughness lengths and crown projections compared to those of Scots pine and oak stands (Table 7.7). Roughness lengths of Scots pine and oak stands were not significantly different. Annual mean *LAI* values of oak

stands were significantly smaller compared to those of Douglas fir and Scots pine stands. Leaf areas of Douglas fir and Scots pine stands were not significantly different. Scots pine stands were characterised by significantly smaller crown projections, crown depths, crown volumes, and silhouette areas compared to Douglas fir and oak stands. In contrast to Scots pine, oak revealed relatively large crown depths due to the frequent occurrence of stem shoots.

Table 7.8 summarises dimensions of Douglas fir and Scots pine needles. Douglas fir needles can be characterised as short and flat, whereas Scots pine needles were found to be long and (half-) cylinder shaped. Compared to Scots pine needles, the diameter of Douglas fir needles was large, while their mean total surface area was small. No hairs were present on the needles of either species. Considering these findings, it was assumed that the efficiency of Douglas fir needles to collect particles and cloud droplets was more-or-less equal to that of Scots pine needles. The collecting efficiency of oak leaves was assumed to be small compared to that of Douglas fir and Scots pine needles.

**TABLE 7.8** Mean dimensions of needles from Douglas fir and Scots pine trees, with *SD* in parentheses (n = 150)

| | Douglas fir | Scots Pine |
|---|---|---|
| Shape | flat | (half-)cylinder |
| Diameter (cm) | 0.112 (0.013) | 0.054 (0.011) - 0.117 (0.019)* |
| Length (cm) | 2.038 (0.309) | 5.384 (1.218) |
| Surface area ($cm^2$) | 0.458 (0.097) | 1.610 (0.539) |

* Minimum and maximum diameter of the cylinder

*Relationships between dry deposition and canopy structure*

Relationships between net throughfall and canopy structure characteristics
Pearson's correlation coefficients between annual net throughfall fluxes and canopy structure characteristics of the 30 forest stands are presented in Table 7.9. Net throughfall fluxes of $SO_4^{2-}$, $NO_3^-$, $NH_4^+$ and $H^+$ were found to relate well with parameters reflecting the aerodynamic roughness as well as collecting surface area of the canopy. For $SO_4^{2-}$, $NO_3^-$ and $NH_4^+$, high correlation coefficients were observed with the roughness length of the canopy and for $NO_3^-$ and $NH_4^+$, also with leaf area. The dependency of $SO_4^{2-}$ and $NH_4^+$ net throughfall on the roughness length may be explained in the Netherlands by the small surface resistance of $SO_2$ and $NH_3$ (see Chapter 4). Dry deposition of these compounds is mainly controlled by the aerodynamic roughness of the canopy surface. Large leaf areas contribute to small aerodynamic resistances. For $NO_3^-$, the strong dependency on *LAI* and roughness length may be explained by assuming that the surface resistance of $NO_2$ was inversely related to the leaf area of the forest stand, and/or (in the case of irreversible canopy uptake of $NO_2$) by considering net throughfall of $NO_3^-$ to be controlled to a large extent by dry deposition of

$HNO_3$ and $NO_3^-$ aerosol. Dry deposition of $HNO_3$ compounds is believed to be controlled by atmospheric transfer to the receptor surface (see Chapter 4) and hence by the aerodynamic roughness (length) of the canopy. Dry deposition velocities of $NO_3^-$ above forests are also found to be determined by aerodynamic roughness of the surface, for very rough surfaces (see section 7.3). Net throughfall of $H^+$ is to a large extent controlled by dry deposition of acids, such as $HNO_3$ and $H_2SO_4$, as well as by the ability of the canopy to retain protons. Dry deposition velocities of acids will be determined to a large extent by the aerodynamic properties of the canopy, whereas the ability of the canopy to retain protons will be influenced, for instance, by its total surface area (e.g. nutrient status of the leaves).

**TABLE 7.9** Correlation matrix between net throughfall fluxes and canopy structure characteristics for the 30 forest stands

| | $SO_4^{2-}$ | $NO_3^-$ | $NH_4^+$ | $H^+$ | $Na^+$ | $Cl^-$ | $Mg^{2+}$ | $Ca^{2+}$ | $K^+$ | $HCO_3^-$ | $PO_4^{3-}$ | mm |
|---|---|---|---|---|---|---|---|---|---|---|---|---|
| $z_o$ | *0.76* | *0.73* | *0.77* | *-0.63* | *0.55* | *0.54* | 0.45 | *0.65* | - | - | -0.39 | *-0.72* |
| Tree height | *0.64* | 0.44 | *0.51* | *-0.52* | 0.43 | 0.40 | *0.52* | 0.64 | - | - | - | -0.42 |
| Silh. area | *0.56* | - | - | *-0.50* | - | - | - | - | *0.56* | 0.44 | - | -0.40 |
| Stem density | - | - | - | - | - | - | - | - | - | - | - | - |
| LAI | - | *0.78* | *0.73* | *-0.50* | *0.56* | *0.56* | - | 0.38 | *-0.59* | *-0.62* | *-0.82* | *-0.72* |
| Cr. pr. field | *0.51* | *0.47* | *0.46* | *-0.72* | - | - | - | - | - | - | - | *-0.55* |
| Cr. pr. image | *0.52* | *0.56* | *0.56* | *-0.86* | - | - | - | - | - | - | - | *-0.74* |
| Cr. volume | *0.66* | *0.49* | *0.52* | *-0.64* | - | - | 0.37 | 0.40 | - | - | - | *-0.52* |
| Crown depth | - | - | - | - | - | - | 0.40 | - | *0.85* | *0.81* | *0.72* | - |

Figures in italics indicate correlation coefficients with $p<0.01$.
Correlation coefficients with $p>0.05$ were excluded from the table.

Compared to acidifying compounds, net throughfall of $Na^+$ and $Cl^-$ showed weaker but still significant relationships with the roughness length and leaf area of the canopy. Next to aerodynamic properties and the total collecting surface area of the canopy, collecting efficiency of individual canopy elements and in-canopy wind speeds also determine the amount of dry deposition of sea salt particles (see section 7.3). Because net throughfall of $K^+$, $HCO_3^-$ and $PO_4^{3-}$ is mainly controlled by canopy leaching, positive relationships with parameters reflecting the canopy collecting surface area were expected. Such relationships were indeed observed with mean crown depth, but at the same time strong negative relationships were recorded with leaf area. Relationships between net throughfall of $K^+$, $HCO_3^-$ and $PO_4^{3-}$, and canopy structure characteristics, were strongly influenced by extremely large fluxes observed in the oak stands and, for this reason, should be interpreted with caution. Tree species seems to be the major controlling factor for these fluxes.

Non-linear regression models were not any better able to explain a larger fraction of the variation in net throughfall than linear regression models. Often an unimodal relationship between dry deposition and *LAI* has been suggested in the literature (Meyers *et al.*, 1989; Lovett and Reiners, 1986; Ivens, 1990), but in this study relationships between net throughfall

and *LAI* turned out to be linear in the *LAI* range of 2.4 to 12.0. Relationships between net throughfall and other canopy structure characteristics were also found to be linear.

Relationships between net throughfall (corrected for canopy exchange) and canopy structure characteristics

To obtain more insight into the relation between dry deposition and canopy structure, net throughfall was corrected for the contribution of canopy exchange by using the Ulrich (1993) and Van der Maas and Pape (1991) model before relating them to the canopy structure characteristics. Correlation coefficients between corrected net throughfall fluxes of $SO_4^{2-}$, $NO_3^-$, $Na^+$, $Cl^-$, $Mg^{2+}$, $Ca^{2+}$, $K^+$, and $PO_4^{3-}$ on the one hand, and canopy structure characteristics on the other, were found equal to those computed with uncorrected net throughfall fluxes (Table 7.9). For $Cl^-$, $Mg^{2+}$, $Ca^{2+}$, $K^+$, and $PO_4^{3-}$, this can be attributed to the method used in the model to compute the contribution of canopy exchange to net throughfall, and for $SO_4^{2-}$, $NO_3^-$ and $Na^+$ to the assumption that canopy exchange is negligible (Draaijers *et al.*, 1994). Corrected net throughfall fluxes of $NH_4^+$ related fairly well with roughness length ($R$=0.71; $p$<0.001), LAI ($R$=0.66; $p$<0.001) and crown projection estimated from scanned images ($R$=0.71; $p$<0.001). Corrected net throughfall fluxes of $H^+$ were found to relate well with LAI ($R$=-0.85; $p$<0.001) and crown projection estimated from scanned images ($R$=-0.75; $p$<0.001).

Impact of season on relationships between net throughfall and canopy structure characteristics

Relationships between net throughfall of $SO_4^{2-}$, $NO_3^-$ and $NH_4^+$, and canopy structure characteristics, were strongly influenced by season. Stronger relationships were observed in the winter period, which may be attributed to the relatively low physiological activity at this time, giving canopy exchange processes minor influence on the composition of throughfall. More than 70% of the variation in winter net throughfall of $SO_4^{2-}$, $NO_3^-$ and $NH_4^+$ could be explained by differences in aerodynamic roughness length of the canopy (Figure 7.8 - 7.10) but strong relationships were also observed with *LAI* ($R$=0.59, 0.77 and 0.76, respectively), crown projection estimated in the field ($R$=0.69, 0.78 and 0.76, respectively) and crown projection estimated from scanned images ($R$=0.64, 0.75 and 0.74, respectively).

Relationships between net throughfall and multiple canopy structure characteristics

Multiple regression was used to see if multiple canopy structure characteristics regulated annual net throughfall. Strong interrelationships were found between most canopy structure characteristics (Table 7.10). The roughness length, for example, related significantly to tree height, silhouette area, leaf area, crown projection and crown volume. To determine whether combinations of two likely factors explain a larger amount of the variance in net throughfall than single factors, multiple regression was performed using all possible pairs of independent variables. Roughness length and crown depth were found to explain large parts of the variance in net throughfall of $NO_3^-$ ($R$=0.84), $NH_4^+$ ($R$=0.83), $Na^+$ ($R$=0.62) and $Cl^-$ ($R$=0.61). Similar correlation coefficients were obtained using tree height and leaf area as explanatory variables. Other combinations of two independent canopy structure variables were not able to explain a larger amount of the variance than single variables.

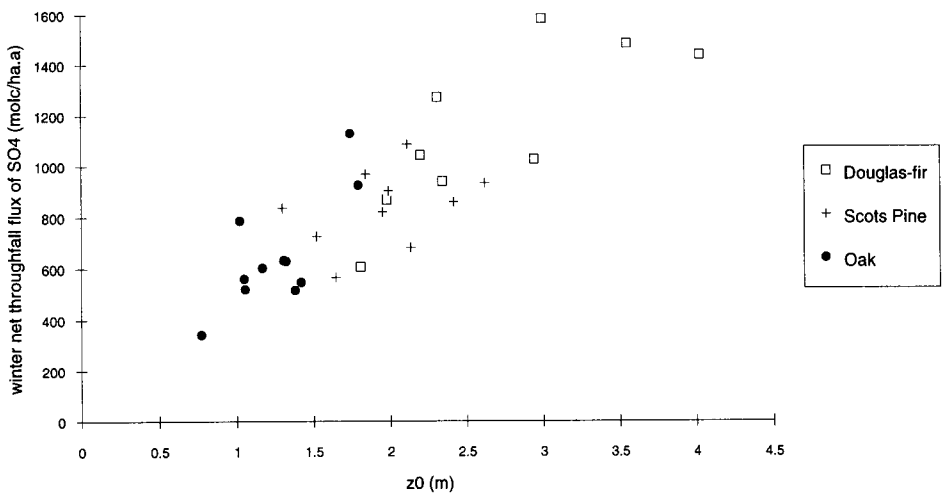


**FIGURE 7.8** Relationship between winter net throughfall fluxes of $SO_4^{2-}$ and the aerodynamic roughness length of the canopy. Douglas fir is indicated by squares, Scots pine by plus signs and oak by dots. The following relationship is valid: $[NTF\text{-}\ SO_4^{2-}]=344.9[z_o]$ +201.3 ($R$=0.84; $p$<0.001).

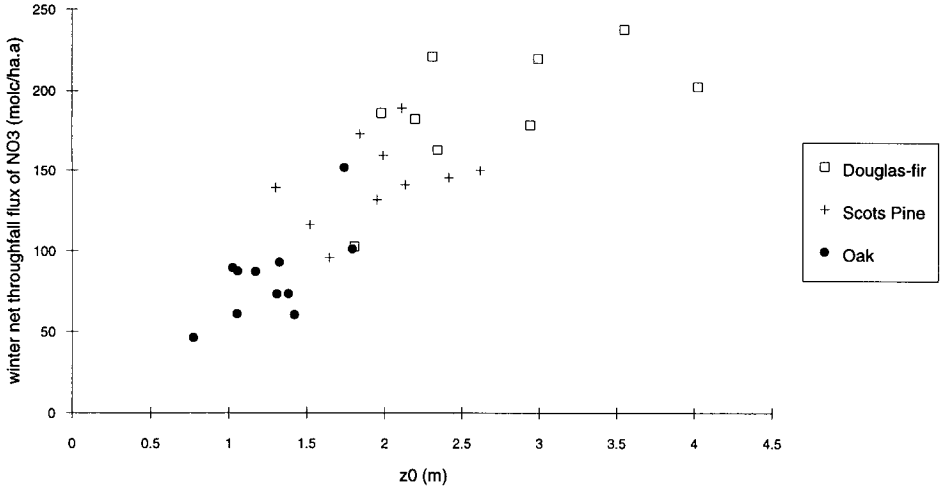


**FIGURE 7.9** Relationship between winter net throughfall fluxes of $NO_3^-$ and the aerodynamic roughness length of the canopy. Douglas fir is indicated by squares, Scots pine by plus signs and oak by dots. The following relationship is valid: $[NTF\text{-}NO_3^-]=59.6[z_o]$ +21.5 ($R$=0.84; $p$<0.001).

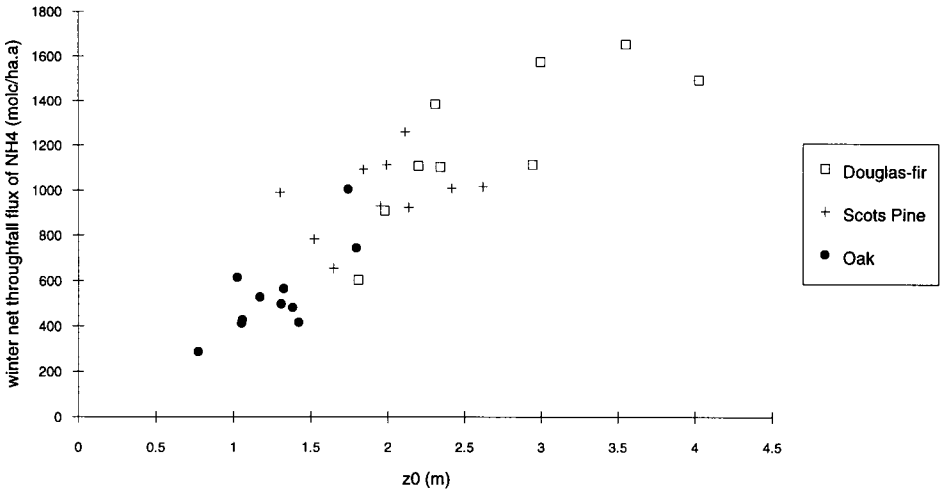


**FIGURE 7.10** Relationship between winter net throughfall fluxes of $NH_4^+$ and the aerodynamic roughness length of the canopy. Douglas fir is indicated by squares, Scots pine by plus signs and oak by dots. The following relationship is valid: $[NTF\text{-}NH_4^+]=431.0[z_o]$ +65.5 ($R$=0.88; $p$<0.001).

**TABLE 7.10** Interrelationships between the individual canopy structure characteristics of the 30 forest stands

| | $z_0$ | Tree height | Silhouette area | Stem density | *LAI* | Crown proj., field | Crown proj., image | Crown volume | Crown depth |
|---|---|---|---|---|---|---|---|---|---|
| $z_0$ | *1.00* | *0.63* | *0.63* | -- | *0.55* | 0.45 | *0.59* | *0.68* | -- |
| Tree height | | *1.00* | 0.39 | *-0.50* | -- | *0.52* | -- | *0.60* | 0.44 |
| Silhouette area | | | *1.00* | -- | -- | *0.58* | *0.60* | *0.79* | *0.61* |
| Stem density | | | | *1.00* | -- | -- | -- | -- | -- |
| *LAI* | | | | | *1.00* | -- | 0.46 | -- | *-0.64* |
| Crown proj., field | | | | | | *1.00* | *0.79* | *0.85* | -- |
| Crown proj., image | | | | | | | *1.00* | *0.67* | -- |
| Crown volume | | | | | | | | *1.00* | -- |
| Crown depth | | | | | | | | | *1.00* |

Italics indicate correlation coefficients with p<0.01.
Correlation coefficients with p>0.05 were not considered significant and thus were excluded from the table.

Relationships between net throughfall and canopy structure characteristics for single tree species

To avoid differences in surface resistance, collecting efficiency, canopy exchange and uncertainties in drag coefficients, relationships between annual net throughfall and canopy structure characteristics were also examined for single tree species. Essentially, similar relationships were found between net throughfall and canopy structure characteristics to those observed considering all the 30 stands together (Table 7.10). However, many relationships were somewhat weaker, which may be attributed to the limited range in canopy structure characteristics observed within single tree species. For example, for all the stands collectively the ratio between maximum and minimum roughness length was 3.62 (Table 7.6), whereas within single tree species this ratio was only 1.85-2.23 (Table 7.7). For *LAI*, the difference was even more extreme. Whereas the ratio between maximum and minimum *LAI* was 5.00 for all the stands collectively, it was only 1.57-1.70 within single tree species.

*Predicting net throughfall using simple regression models with canopy structure and information on pollution climate*

To see if it was possible to predict net throughfall fluxes using simple linear regression models with canopy structure characteristics, winter net throughfall fluxes of $SO_4^{2-}$, $NO_3^-$ and $NH_4^+$ for each of the 30 stands were predicted by using regression equations with a roughness length based on the data of the remaining 29 stands. Predicted and measured fluxes are presented in Figures 7.11-13. Reasonable agreement was observed ($R$=0.60, 0.50 and 0.58 for $SO_4^{2-}$, $NO_3^-$ and $NH_4^+$, respectively) although the regression models were found to overestimate net throughfall fluxes at low values and tended to underestimation at higher values. Using annual net throughfall fluxes and/or other canopy structure characteristics (e.g. *LAI* or crown projection) as a basis for the regression models yielded similar conclusions, though differences between predicted and measured net throughfall fluxes were larger.

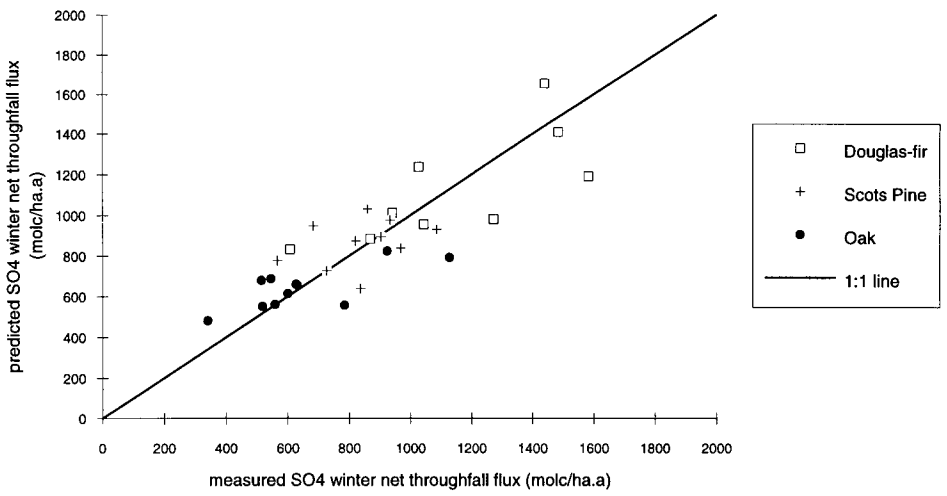


**FIGURE 7.11** Winter net throughfall fluxes of $SO_4^{2-}$ predicted from linear regression models with the roughness length of the canopy, compared to measured winter net throughfall fluxes. Douglas fir is indicated by squares, Scots pine by plus signs and oak by dots.

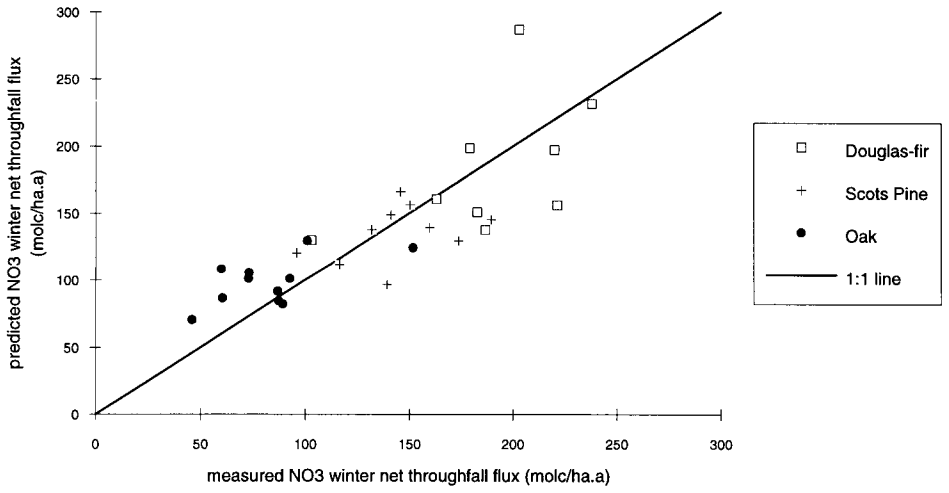


**FIGURE 7.12** Winter net throughfall fluxes of $NO_3^-$ predicted from linear regression models with the roughness length of the canopy, compared to measured winter net throughfall fluxes. Douglas fir is indicated by squares, Scots pine by plus signs and oak by dots.

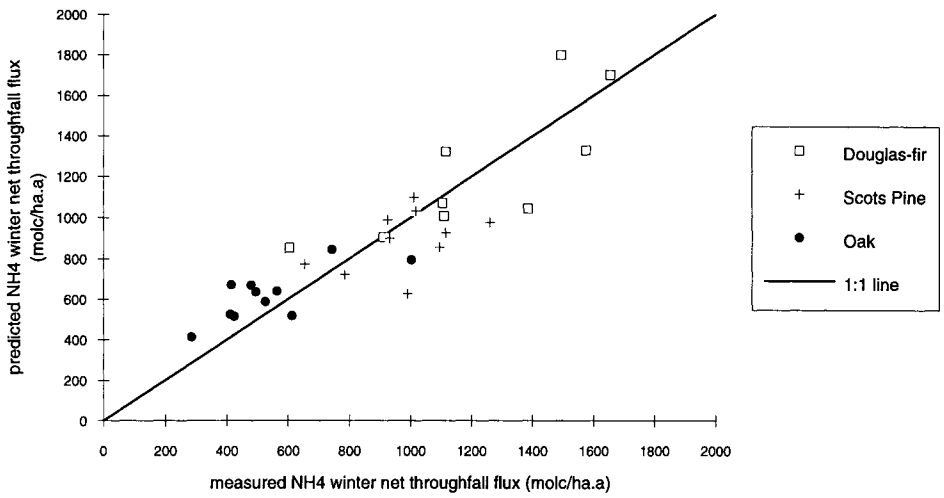


**FIGURE 7.13** Winter net throughfall fluxes of $NH_4^+$ predicted from linear regression models with the roughness length of the canopy, compared to measured winter net throughfall fluxes. Douglas fir is indicated by squares, Scots pine by plus signs and oak by dots.

## 7.2.4 THE IMPACT OF FOREST EDGES: RESULTS AND DISCUSSION

*Evaluation of canopy structure parametrisation*

Table 7.11 presents mean canopy and edge structure data of the eight forest edges. Stem density, *LAI*, leaf-area density and silhouette area density were found to differ greatly among the edges. Relatively large values for these structure characteristics were recorded for location F, and to a lesser extent for location C. Forest edges consisting of European larch trees (locations A, E and G) have relatively large crown depths as a result of the frequent occurrence of stem shoots. The roughness length of the upwind terrain as estimated from the terrain classification of Wieringa (1992) was found to range between 0.03 m and 0.08 m, indicating rather 'smooth' conditions of the upwind terrain for all edges. The roughness length of the forest canopy as estimated from the geometrical model of Lettau (1969) has no physical meaning because the Lettau model only yields roughness lengths comparable to micrometeorologically derived roughness lengths for homogeneous canopy surfaces with an 'infinite' length.

Within an individual forest edge, canopy and edge structure characteristics showed only small spatial variability. Coefficients of variation were nearly always less than 0.20 (not shown in Table 7.11). For location A, the tree height was found to increase from 16 m to approximately

24 m within the first two edge heights. Tree height increment with distance from the edge was less, though still significant for location E (12 m to 15 m) and location G (13 m to 17 m). Only European larch stands showed such an increment. Probably, European Larch trees are probably relatively susceptible to reduced growth as a result of wind exposure. Other canopy or edge structure characteristics did not show significant gradients with distance from the edge. At the very edge of the forest edges A, B, C, F and H, relatively dense understorey vegetation (shrubs and/or small trees) was present.

**TABLE 7.11** Canopy and edge structure characteristics of the eight forest edges, showing averages of 7 or 8 recordings (structure characteristics were determined around each throughfall gutter) with the exception of porosity and the roughness length of the upwind terrain

| Forest edge[a]: | A | B | C | D | E | F | G | H |
|---|---|---|---|---|---|---|---|---|
| Canopy structure characteristics | | | | | | | | |
| $z_o$, canopy (m) | 1.6 | 1.3 | 1.4 | 1.0 | 1.8 | 2.4 | 1.3 | 1.3 |
| Tree height (m) | 22.3 | 12.7 | 9.0 | 13.7 | 14.1 | 9.9 | 16.0 | 13.7 |
| Silhouette area ($m^2$ $ha^{-1}$) | 8771 | 8351 | 13453 | 5432 | 15145 | 25124 | 10413 | 7348 |
| Stem density ($ha^{-1}$) | 630 | 1264 | 2490 | 531 | 830 | 2533 | 329 | 653 |
| *LAI* (-) | 2.8 | 6.9 | 8.8 | 5.4 | 2.3 | 15.7 | 2.6 | 5.2 |
| Crown proj., field (%) | 21.3 | 18.0 | 29.6 | 17.7 | 12.7 | 49.2 | 15.5 | 23.0 |
| Crown proj., image (%) | 63.6 | 65.3 | 67.7 | 59.3 | 62.1 | 87.2 | 60.7 | 58.3 |
| Crown volume ($m^3$ $ha^{-1}$) | 33159 | 13763 | 18847 | 10775 | 26721 | 35489 | 30133 | 16260 |
| Crown depth (m) | 13.1 | 3.4 | 4.1 | 4.2 | 7.2 | 6.6 | 7.8 | 4.3 |
| Edge structure characteristics | | | | | | | | |
| Relative height (m) | 21.5 | 12.6 | 8.5 | 13.0 | 13.8 | 9.7 | 15.3 | 13.0 |
| Porosity, 1 edge height (%) | 39.3 | 41.8 | 29.7 | 57.5 | 45.8 | 43.3 | 45.5 | 45.0 |
| Porosity, 2 edge heights (%) | 36.3 | 34.3 | 28.8 | 42.3 | 39.4 | 15.4 | 43.6 | 33.7 |
| Stand leaf area d. ($m^2$ $m^{-3}$) | 0.13 | 0.54 | 0.98 | 0.40 | 0.16 | 1.58 | 0.16 | 0.38 |
| Stand silh. area d. ($m^2$ $m^{-3}$) | 0.04 | 0.07 | 0.15 | 0.04 | 0.11 | 0.26 | 0.07 | 0.05 |
| Crown leaf area d. ($m^2$ $m^{-3}$) | 0.22 | 2.03 | 2.14 | 1.27 | 0.32 | 2.38 | 0.33 | 1.21 |
| Crown silh. area d. ($m^2$ $m^{-3}$) | 0.07 | 0.25 | 0.33 | 0.13 | 0.21 | 0.38 | 0.13 | 0.17 |
| $z_o$, upwind terrain (m) | 0.08 | 0.03 | 0.07 | 0.08 | 0.04 | 0.03 | 0.08 | 0.08 |

[a]Tree species: *Larix decidua* for forest edge A, E and G; *Pinus sylvestris* for forest edge B, D and H. *Pinus nigra* for forest edge C and *Picea abies* for forest edge F.

For $z_o$ 'canopy', *LAI*, crown projection, relative height, porosity, leaf area density and $z_o$ 'upwind terrain', annual mean values are presented which were calculated by averaging summer and winter values.

*Dry deposition gradients in the forest edges*

Horizontal net throughfall flux gradients for the eight forest edges are presented in Figure 7.14. In general, an exponential increase with decreasing distance to the edge was found, with in most cases a considerable scatter around the curve. To a large extent this may be the result of non-representative throughfall sampling as net throughfall at each distance from the edge was measured by means of only one fixed throughfall gutter. Because of this the mean flux at that distance may be underestimated or overestimated by 32%-45%. depending on the ion under consideration (Van Ek and Draaijers, 1991). The observed scatter could not be explained by the variability in canopy structure characteristics in the edge. From Figure 7.14 it is also clear that the width of the zone with enhanced net throughfall fluxes was usually five edge heights at most. This is in agreement with throughfall studies performed in other forest edges (Hasselrot and Grennfelt, 1987; Draaijers *et al.*, 1988; Beier and Gundersen, 1989).

A schematical presentation of a mean net throughfall flux gradient in a forest edge is shown in Figure 7.15. Discrimination is made here between basic net throughfall and edge-net throughfall. The basic net throughfall is defined as the net throughfall flux which would have been measured without the edge effect; edge-net throughfall is defined as the net throughfall flux resulting from the edge effect. Using the data from Figure 7.14, edge net throughfall fluxes were computed by calculating best-fitting decay curves using a power-law relationship ($NTF=a(x/h)^b$ in which $NTF$ = net throughfall flux, $x/h$ = distance to forest edge divided by edge height, with a and b as regression coefficients), and subsequent computing of the area under this curve through integration. Edge net throughfall fluxes were determined between x/h=0.25 and x/h=5.0. The zone between $x/h$=0 and $x/h$=0.25 was not included because net throughfall fluxes in this zone were not measured in the field, and infinitely high edge net throughfall fluxes would be obtained, otherwise (at $x/h$=0, $NTF$ equals $\infty$ for $b$<0). This area could be included by fitting other curves (for example, $NTF=a(e^{-x/h})+b$), but then usually considerable smaller amounts of variance were explained. For this reason, power-law decay curves were preferred. Basic net throughfall in the zone between $x/h$=0.25 and x/h=5 was assumed equal to the net throughfall flux at $x/h$=5 multiplied by 4.75 (= 5 minus 0.25). Dividing edge + basic net throughfall by basic net throughfall yielded whole-edge integrated net throughfall enhancement factors (*WEINTE* factors). If no significant power-law decay curve was found, edge net throughfall fluxes were assumed to be zero, and the *WEINTE* factor equal to 1.

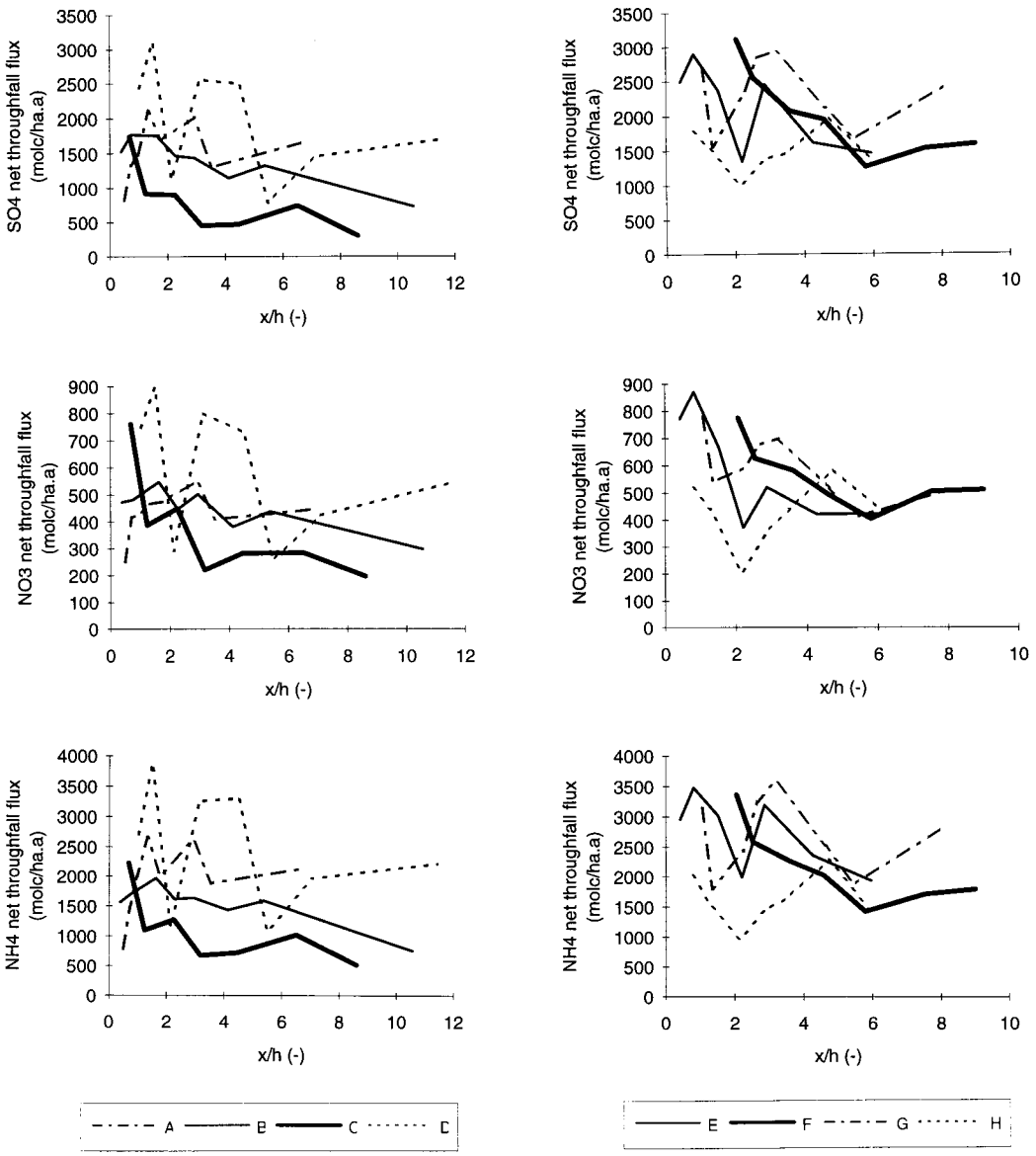


**FIGURE 7.14** Net throughfall flux gradients of $SO_4^{2-}$, $NO_3^-$ and $NH_4^+$ for the eight forest edges. Distance to edge divided by edge height is *x/h*

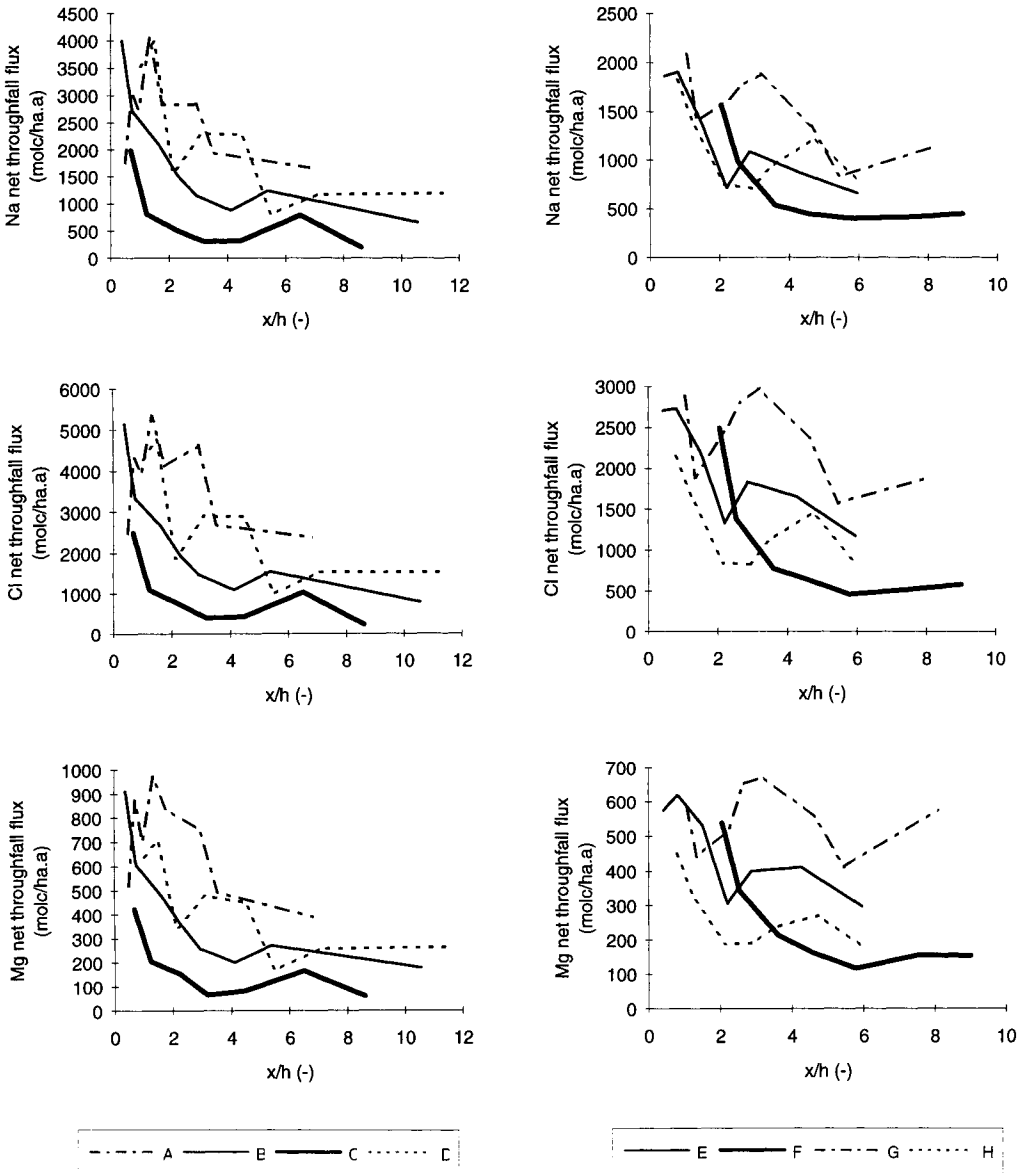


**FIGURE 7.14** *(continued)* Net throughfall flux gradients of $Na^+$, $Cl^-$ and $Mg^{2+}$ for the eight forest edges. Distance to edge divided by edge height is *x/h*

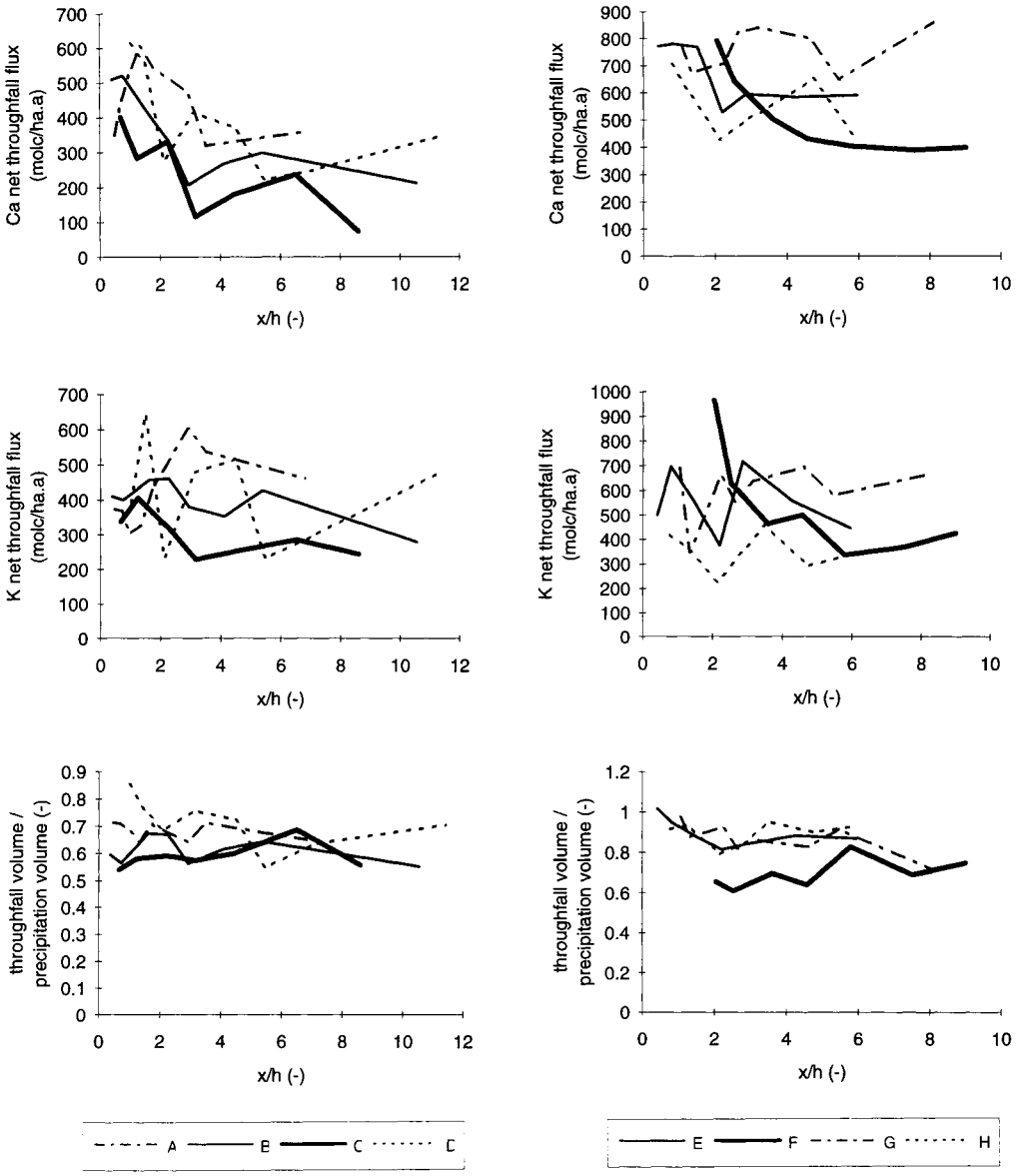


**FIGURE 7.14** *(continued)* Net throughfall flux gradients of $Ca^{2+}$ and $K^{+}$, and gradients of the ratio between throughfall volume and precipitation volume for the eight forest edges. Distance to edge divided by edge height is *x/h*

*WEINTE* factors for the eight forest edges are shown in Table 7.12. A significant net throughfall enhancement was observed for $Na^+$, $Cl^-$ and $Mg^{2+}$ in all edges. Net throughfall fluxes at location A also decreased with distance from the edge but the decrease only started at approximately two edge heights from the forest edge. A gradually increasing tree height with distance from the edge (16 up to 24 m) and the dense understorey vegetation present at the very edge of this forest may have resulted in a smooth roughness transition zone. Air entering such a roughness transition will tend to be lifted over, rather than to penetrate into the forest edge. It must be noted, however, that the net throughfall pattern observed for location A and its large deviation from the 'ideal' power-law decay curve may also be explained by non-representative throughfall sampling.

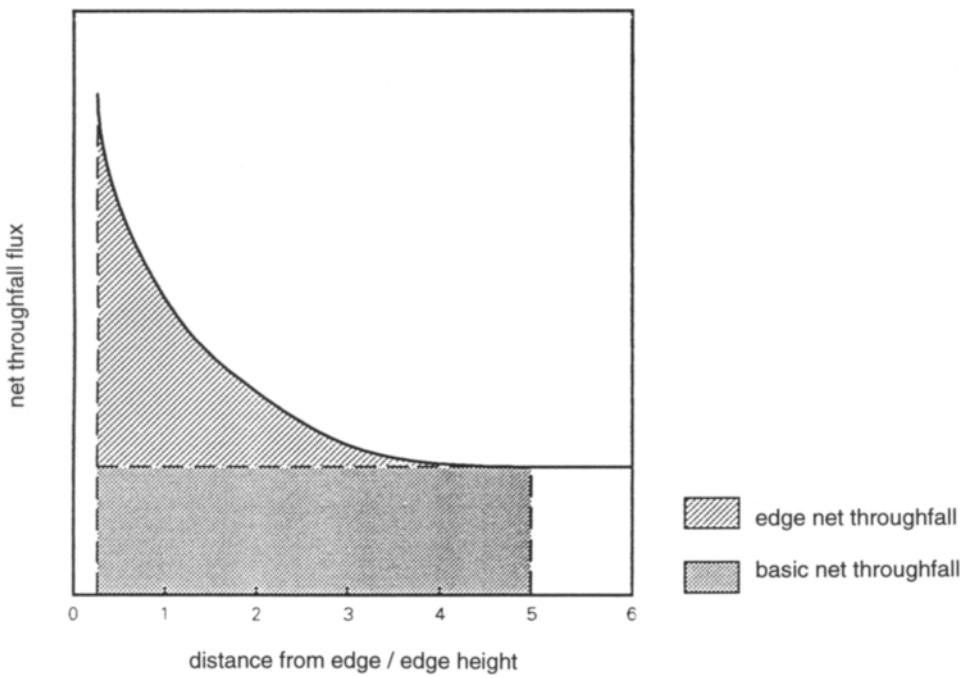


**FIGURE 7.15** 'Ideal' net throughfall flux gradient in a forest edge.

The *WEINTE* factors for $SO_4^{2-}$, $NO_3^-$ and $NH_4^+$ were considerably smaller than those for $Na^+$, $Cl^-$ and $Mg^{2+}$ (Table 7.12). This may be attributed to the different sources for these ions in throughfall. Net throughfall of $SO_4^{2-}$, $NO_3^-$ and $NH_4^+$ is controlled to a large extent by dry deposition of gases and fine (sub-micron) particles, whereas net throughfall of $Na^+$, $Cl^-$ and $Mg^{2+}$ is mainly controlled by dry deposition of coarse sea salt particles. Deposition of coarse particles is very much enhanced in forest edges as a result of high in-canopy wind speeds,

which enhances impaction efficiencies considerably. Edge effects seem to have only minor impact on the deposition of gases and fine particles. For the locations A, D, G and H, net throughfall fluxes of $SO_4^{2-}$, $NO_3^-$ and $NH_4^+$ were not significantly enhanced.

**TABLE 7.12** Whole-edge integrated net throughfall enhancement (*WEINTE*) factors for the eight forest edges ($x$ = mean of all edges)

| | A | B | C | D | E | F | G | H | $x$ |
|---|---|---|---|---|---|---|---|---|---|
| $SO_4^{2-}$ | 1.00 | 1.20 | 1.73 | 1.00 | 1.23 | 1.64 | 1.00 | 1.00 | 1.23 |
| $NO_3^-$ | 1.00 | 1.11 | 1.54 | 1.00 | 1.31 | 1.31 | 1.18 | 1.00 | 1.18 |
| $NH_4^+$ | 1.00 | 1.16 | 1.54 | 1.00 | 1.15 | 1.55 | 1.00 | 1.00 | 1.18 |
| $Na^+$ | 1.00 | 1.71 | 2.00 | 1.73 | 1.48 | 2.50 | 1.32 | 1.35 | 1.64 |
| $Cl^-$ | 1.00 | 1.74 | 2.07 | 1.66 | 1.33 | 3.11 | 1.00 | 1.39 | 1.66 |
| $Mg^{2+}$ | 1.00 | 1.66 | 1.88 | 1.58 | 1.26 | 2.57 | 1.00 | 1.39 | 1.54 |
| $Ca^{2+}$ | 1.00 | 1.31 | 1.65 | 1.33 | 1.13 | 1.58 | 1.00 | 1.00 | 1.25 |
| $K^+$ | 0.82 | 1.00 | 1.16 | 1.00 | 1.00 | 1.74 | 1.00 | 1.00 | 1.09 |
| Volume | 1.00 | 1.00 | 1.00 | 1.09 | 1.05 | 1.00 | 1.09 | 1.00 | 1.03 |

Although $Ca^{2+}$ and $K^+$ net throughfall fluxes were also likely to be influenced by dry deposition of coarse particles (e.g. soil dust, pollen), *WEINTE* factors for these ions were much lower compared to those of $Na^+$, $Cl^-$ and $Mg^{2+}$ (Table 7.12). This was a surprising result, given the fact that these fluxes are probably strongly influenced by canopy leaching (Van Ek and Draaijers, 1993). Canopy leaching was assumed to be relatively intense in forest edges due to vigorous transpiration of trees in wind-exposed forest edges through which the supply of $Ca^{2+}$ and $K^+$ from the soil to the foliage was expected to be relatively high. However, the nutrient status of trees at the forest border may have been lowered as a result of extensive leaching of $Ca^{2+}$ and $K^+$ out of the topsoil due to the high acid inputs of the last decades. The significantly reduced $K^+$ net throughfall fluxes measured near the edge of location A may be an indication of this. For most other locations, this reduced leaching at the edge apparently counterbalanced enhanced dry deposition of $K^+$-containing particles, resulting in no net throughfall flux enhancement. Only for locations C and F were significantly enhanced net throughfall fluxes of $K^+$ observed. These locations also showed the highest *WEINTE* factors for $Na^+$, $Cl^-$ and $Mg^{2+}$.

For the locations D, E and G, throughfall volumes were slightly, though significantly, enhanced (Table 7.12). For location E, throughfall volumes very close to the edge were even found to exceed precipitation volumes. Enhanced throughfall volumes near the forest edge may to a large extent be attributed to the horizontal influx of rain droplets through the trunk area. In the trunk area of the forest edges D, E and G, no understorey vegetation taller than 1 m was present and the height of the living crown base exceeded 7 m. Other locations showed relatively high and dense understory vegetation near the very edge of the forest, limiting the

horizontal influx of rain droplets. Relatively large turbulence intensities in forest edges, through which interception and capture of (small) rain droplets and cloud and fog water droplets is efficient (Weathers *et al.*, 1992), may also have contributed to the enhanced throughfall volumes observed in some forest edges.

On average, ratios of net throughfall fluxes at x/h=0.25 and x/h=5 (Table 7.13) were similar to those found by Potts (1978), Hasselrot and Grennfelt (1987), Draaijers *et al.* (1988) and Beier and Gundersen (1989). At the very edge of the forest, net throughfall fluxes of $Na^+$, $Cl^-$ and $Mg^{2+}$ were, on average, approximately five times larger than net throughfall fluxes in the interior forest. For the locations C and F extremely large ratios were computed, where net throughfall fluxes of $Cl^-$ at x/h=0.25 was up to 20 times larger than those at x/h=5.0. Net throughfall fluxes of $SO_4^{2-}$, $NO_3^-$ and $NH_4^+$ were, on average, doubled at the very edge of the forest.

**TABLE 7.13** Ratio between the net throughfall flux at x/h = 0.25 and that at *x*/h = 5 for the eight forest edges

| | A | B | C | D | E | F | G | H | *x* |
|---|---|---|---|---|---|---|---|---|---|
| $SO_4^{2-}$ | 1.00 | 1.86 | 5.18 | 1.00 | 1.98 | 4.53 | 1.00 | 1.00 | 2.19 |
| $NO_3^-$ | 1.00 | 1.43 | 3.83 | 1.00 | 2.42 | 2.41 | 1.76 | 1.00 | 1.86 |
| $NH_4^+$ | 1.00 | 1.63 | 3.78 | 1.00 | 1.63 | 3.89 | 1.00 | 1.00 | 1.87 |
| $Na^+$ | 1.00 | 5.06 | 7.44 | 5.15 | 3.45 | 12.31 | 2.44 | 2.64 | 4.94 |
| $Cl^-$ | 1.00 | 5.26 | 7.98 | 4.67 | 2.53 | 19.39 | 1.00 | 2.85 | 5.59 |
| $Mg^{2+}$ | 1.00 | 4.64 | 6.42 | 4.07 | 2.16 | 13.09 | 1.00 | 2.87 | 4.41 |
| $Ca^{2+}$ | 1.00 | 2.42 | 4.55 | 2.50 | 1.51 | 4.11 | 1.00 | 1.00 | 2.26 |
| $K^+$ | 0.47 | 1.00 | 1.64 | 1.00 | 1.00 | 5.22 | 1.00 | 1.00 | 1.54 |
| Volume | 1.00 | 1.00 | 1.00 | 1.36 | 1.20 | 1.00 | 1.33 | 1.00 | 1.11 |

*x*/*h* = distance to edge divided by edge height; *x* represents the mean of all edges.

*Impact of canopy/edge structure and edge aspect*

Pearson's correlation coefficients between *WEINTE* factors and canopy/edge structure characteristics are presented in Table 7.14. Enhancement factors correlated positively with parameters, reflecting the density of the canopy/edge. For $Na^+$, $Cl^-$ and $Mg^{2+}$, very strong relationships were observed with leaf area and leaf-area density. Such relationships were already predicted by Wiman and Ågren (1985) using a modelling approach and suggest that in-canopy wind speeds determine, to a large extent, differences between forest edge and forest interior dry deposition. *WEINTE* factors of $SO_4^{2-}$, $NO_3^-$ and $NH_4^+$ correlated best with silhouette area density and stem density. This suggests that for these ions the differences between forest edge and forest interior dry deposition can be explained by differences in drag forces and, thus, turbulence intensities. Furthermore, strong relationships were found between throughfall volume enhancement factors on the one hand, and crown projection and edge

porosity on the other. This is in agreement with the hypothesis that enhanced throughfall volumes were largely the result of horizontal influx of rain droplets.

**TABLE 7.14** Correlation matrix between whole-edge integrated net throughfall enhancement (*WEINTE*) factors and canopy/edge structure characteristics for the eight forest edges

| | $SO_4^{2-}$ | $NO_3^-$ | $NH_4^+$ | $Na^+$ | $Cl^-$ | $Mg^{2+}$ | $Ca^{2+}$ | $K^+$ | mm |
|---|---|---|---|---|---|---|---|---|---|
| *Canopy structure characteristics* | | | | | | | | | |
| $z_o$, canopy | - | - | - | - | - | - | - | 0.75 | -0.81 |
| Tree height | -0.74 | - | -0.74 | *-0.86* | -0.75 | -0.79 | -0.80 | - | - |
| Silhouette area | 0.75 | - | 0.79 | 0.71 | 0.75 | - | - | *0.88* | -0.78 |
| Stem density | *0.98* | 0.76 | *0.99* | *0.85* | *0.87* | *0.87* | *0.90* | 0.78 | 0.76 |
| *LAI* | 0.77 | - | *0.83* | *0.92* | *0.98* | *0.97* | 0.81 | *0.93* | *-0.86* |
| Crown proj., field | 0.72 | - | 0.78 | 0.78 | 0.77 | *0.89* | - | *0.90* | *-0.92* |
| Crown proj., image | 0.75 | - | 0.81 | 0.81 | *0.89* | *0.85* | - | *0.93* | *-0.91* |
| Crown volume - | - | - | - | - | - | - | - | - | |
| Crown depth | - | - | - | - | - | - | - | - | - |
| *Edge structure characteristics* | | | | | | | | | |
| Relative height -0.73 | - | -0.73 | *-0.85* | -0.74 | -0.78 | -0.79 | - | - | |
| Porosity, one edge h. | - | - | - | - | - | - | - | - | - |
| Porosity, two edge h. | -0.78 | - | *-0.83* | -0.77 | *-0.89* | *-0.87* | - | *-0.87* | *0.97* |
| Stand leaf area dens. | *0.85* | - | *0.89* | *0.94* | *0.98* | *0.97* | *0.86* | *0.93* | *-0.84* |
| Stand silh. area dens. | *0.87* | 0.71 | *0.90* | *0.86* | *0.88* | *0.84* | 0.72 | *0.94* | *-0.80* |
| Crown leaf area dens. | 0.72 | - | 0.75 | *0.86* | *0.86* | *0.90* | *0.86* | - | - |
| Crown silh. area dens. | *0.93* | 0.76 | *0.94* | *0.91* | *0.89* | *0.89* | *0.85* | *0.83* | -0.71 |
| $z_o$, upwind terrain | - | - | - | - | - | - | - | - | - |

Italic values indicate correlation coefficients with $p<0.01$. Correlation coefficients with $p>0.05$ were excluded from the table.

The impact of edge aspect on dry deposition gradients in forest edges could not be assessed directly in this experiment because all edges had the same southwest exposition. However, to obtain some insight on the impact of edge aspect, the percentage to which a particular wind direction contributed to the total pollutant dose and the total air mass supply were computed (Figure 7.16). The pollutant dose of a particular wind direction was calculated by multiplying air mass supply (= mean wind speed multiplied by the duration) and average pollutant concentration during the measurements. Information on air mass supply was gathered from hourly based data on wind direction and wind speed from the meteorological-station 'De Bilt', located approximately 20 km northwest of Leersum. These data were made available by the Royal Netherlands Meteorological Institute (KNMI). Concentrations of $SO_2$, $NO_2$, NO gas, and $SO_4^{2-}$, $NO_3^-$, $NH_4^+$ and $Cl^-$ aerosol, were gathered from respective hourly and daily measurements taken by RIVM at Bilthoven (near 'De Bilt'). Air concentrations of $Na^+$, $Mg^{2+}$, $Ca^{2+}$ and $K^+$ were not measured, but gathered from results of an observational study in the western part of the Netherlands on precipitation chemistry as function of the surface wind

direction (Weijers and Vugts, 1990). The concentrations were estimated using the concentrations in precipitation and scavenging ratios presented by Eder and Dennis (1990). Unfortunately, no information was available on the percentage a particle wind direction contributed to the total dose of $HNO_3$, $HNO_2$, $NH_3$ and HCl.

It can be observed from Figure 7.16 that southern, southwesteren and westeren wind directions contributed the bulk (50-70%) of the dose of each pollutant. This may be attributed to the fact that these are the prevailing winds in the Netherlands; they also show the largest mean wind speeds. For $SO_2$, $NO_2$, NO gas and $SO_4^{2-}$, $NO_3^-$ and $NH_4^+$ aerosol, the contribution of winds from the east to the total pollutant dose was also relatively large. This was due to the highly polluted air masses coming from the Ruhr area and Eastern Europe. The contribution of western, northwestern and northern winds was reasonably high for $Na^+$, $Cl^-$ and $Mg^{2+}$, due to the supply of air masses which traversed the North Sea and/or the Atlantic Ocean. These air masses are rich in sea salt particles. Compared to the locations E-H, locations A-D showed relatively large percentages of the total pollutant dose contributed by wind directions exposed to the forest edge.

Assuming that dry deposition is only enhanced when the wind enters the forest edge, *WEINTE* factors for edges with other than southwestern aspects can be computed by:

$$WEINTE_x = [DOSEEXP_x/DOSEEXP_{sw} * (WEINTE_{sw}-1)]+ 1 \qquad [7.2]$$

in which $WEINTE_x$ is the whole-edge integrated net throughfall enhancement factor for an edge with aspect $x$; $DOSEEXP_x$ is the percentage of the total pollutant dose supplied with wind directions exposed to the forest edge (e.g. for a forest edge with western aspect, $DOSEEXP_w$ is equal to the sum of the percentages for southwestern, western, northwestern, half of the southern and half of the northern wind direction); $DOSEEXP_{sw}$ is the percentage of the total pollutant dose supplied with wind directions exposed to the forest edge with a southwestern aspect; and $WEINTE_{sw}$ equals the whole-edge integrated net throughfall enhancement factor for an edge with a southwestern aspect. The latter was assumed equal to the mean of the forest edges A-H (Table 7.12). For the computation of $DOSEEXP_x$, two yearly averaged percentages for each wind direction were used. Moreover, computed $DOSEEXP_x$ values were weighted to the relative contribution of the pollutant to the net throughfall flux (Draaijers, 1993). For the computation of *WEINTE* factors of $NO_3$ and $NH_4$, only wind direction-related doses of $NO_2$, NO, $NO_3^-$ and $NH_4^+$ aerosols could be used because data for $HNO_3$, $HNO_2$ and $NH_3$ were lacking. For the computation of whole-edge integrated enhancement factors of throughfall volumes, essentially the same procedure was followed but, instead of the percentage of the total pollutant dose, the percentage of the total air mass supply was used. Besides the percentage of the total pollutant dose supplied with wind directions exposed to the edge, the actual dry deposition in forest edges is also dependent on the 'deposition climate'. The latter will most probably change with edge exposition but these changes are not considered in the calculation of $WEINTE_x$ factors.

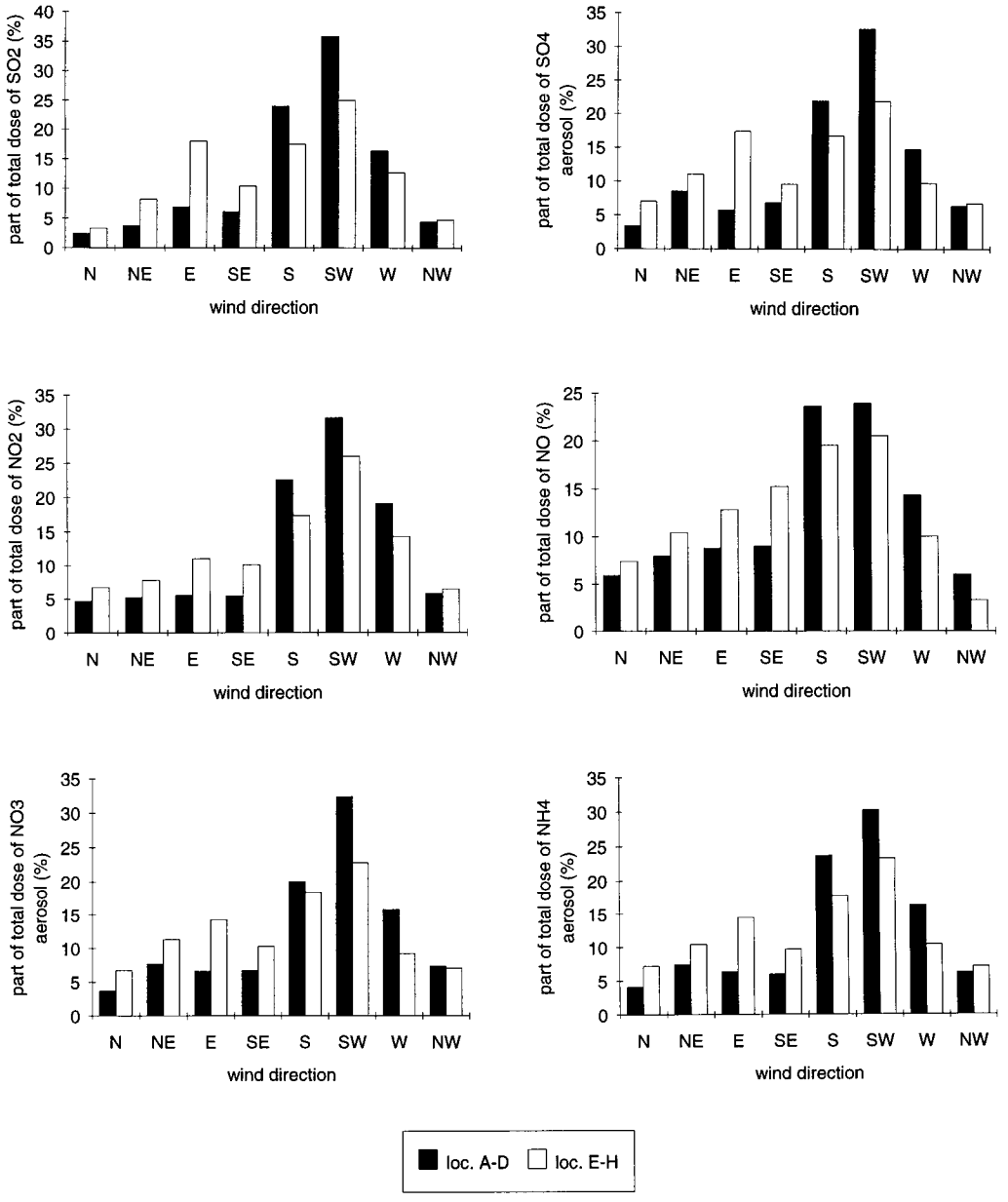


**FIGURE 7.16** The percentage to which a particular wind direction contributed to the total pollutant dose of $SO_2$, $SO_4^{2-}$, $NO_2$, NO, $NO_3^-$, and $NH_4^+$ during the measurements, respectively

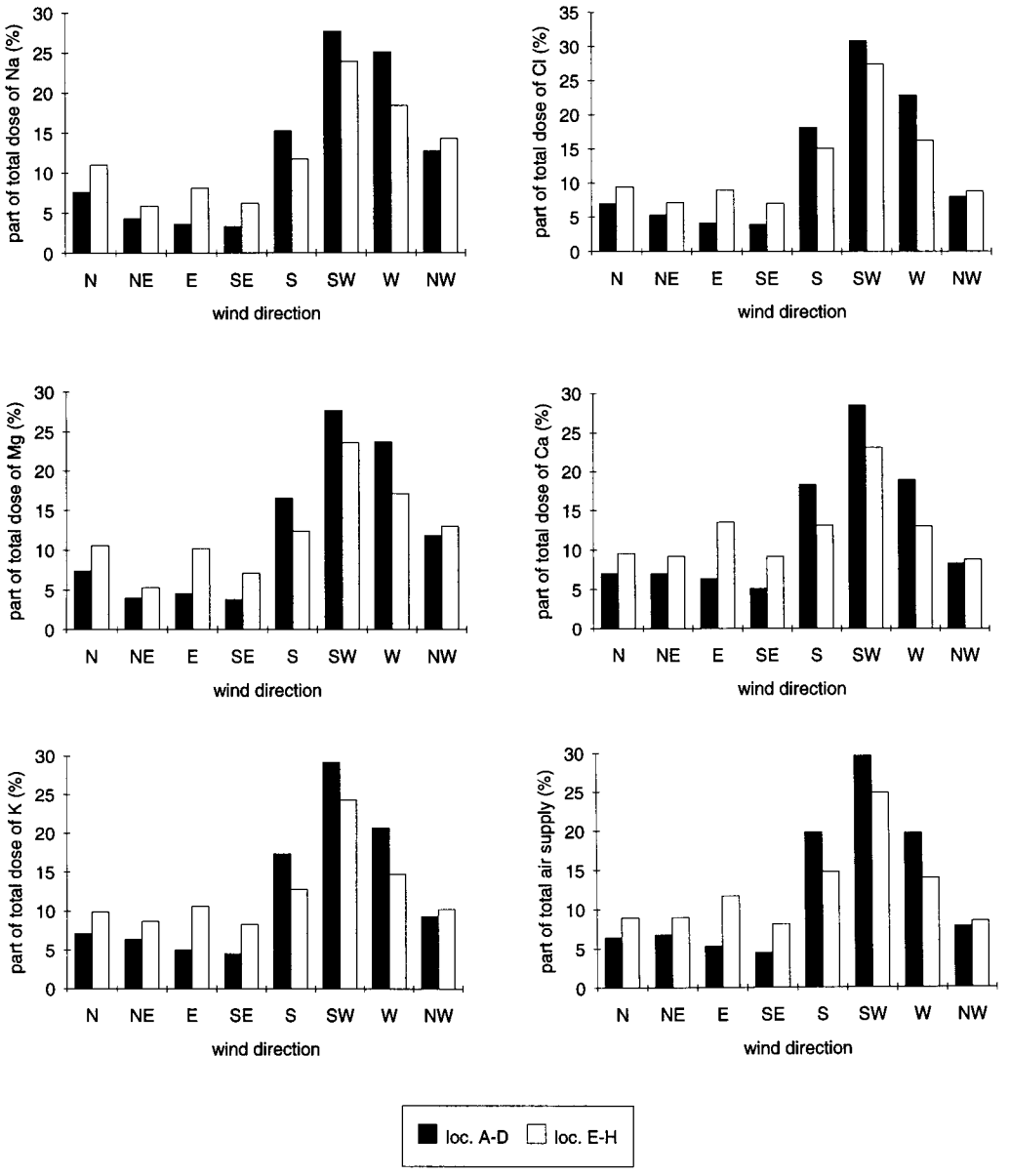


**FIGURE 7.16** *(continued)* The percentage to which a particular wind direction contributed to the total pollutant dose of $Na^+$, $Cl^-$, $Mg^{2+}$, $Ca^{2+}$ and $K^+$, and total air supply during the measurements, respectively

The computed *WEINTE* factors in relation to edge aspect are presented in Table 7.15. For $SO_4^{2-}$, $NO_3^-$ and $NH_4^+$, the enhancement factors were found to range between 1.08 and 1.23. Edges with southeastern, southern, southwestern and western aspects showed the highest values. Enhancement factors for $Na^+$, $Cl^-$ and $Mg^{2+}$ were found to range between 1.23 and 1.66, where edges with southern, southwestern, western and northwestern aspects showed the highest values. Values presented in Table 7.15 rely on the assumption that representative mean enhancement factors were measured for forest edges with a southwestern aspect. However, mean structure characteristics of the eight forest edges ($z_o$ = 1.5m, height = 13.9m and *LAI* = 6.2) may be considered more-or-less representative for an average Dutch forest. Moreover, the computation of *WEINTE* factors in relation to edge aspect was based on data (percentages to which particular wind directions contribute to the total pollutant dose) which most probably only hold for the central part of the Netherlands and at great distances from local sources. Finally, *WEINTE* factors presented only hold for linear forest edges. In case of non-linear edges, larger enhancement factors will occur as the disturbance of the wind profile will be larger. In the Netherlands linear forest edges are typical.

**TABLE 7.15** Whole-edge integrated net throughfall enhancement (*WEINTE*) factors in relation to the edge aspect. $x$ = mean of all aspects

| | N | NE | E | SE | S | SW | W | NW | $x$ |
|---|---|---|---|---|---|---|---|---|---|
| $SO_4^{2-}$ | 1.09 | 1.09 | 1.13 | 1.19 | 1.23 | 1.23 | 1.18 | 1.13 | 1.16 |
| $NO_3^-$ | 1.08 | 1.08 | 1.10 | 1.14 | 1.18 | 1.18 | 1.16 | 1.11 | 1.13 |
| $NH_4^+$ | 1.09 | 1.09 | 1.11 | 1.15 | 1.18 | 1.18 | 1.15 | 1.11 | 1.13 |
| $Na^+$ | 1.38 | 1.27 | 1.25 | 1.36 | 1.52 | 1.64 | 1.66 | 1.54 | 1.45 |
| $Cl^-$ | 1.33 | 1.25 | 1.28 | 1.42 | 1.59 | 1.66 | 1.64 | 1.49 | 1.46 |
| $Mg^{2+}$ | 1.31 | 1.23 | 1.23 | 1.33 | 1.46 | 1.54 | 1.55 | 1.45 | 1.39 |
| $Ca^{2+}$ | 1.15 | 1.13 | 1.14 | 1.19 | 1.24 | 1.25 | 1.24 | 1.19 | 1.19 |
| $K^+$ | 1.05 | 1.04 | 1.04 | 1.06 | 1.08 | 1.09 | 1.09 | 1.07 | 1.07 |
| Volume | 1.02 | 1.01 | 1.01 | 1.02 | 1.03 | 1.03 | 1.03 | 1.02 | 1.02 |

*The impact of edge effects on dry deposition amounts to forests in the Netherlands*

A rough assessment of the percentage of Dutch forests influenced by edge effects was made with help of information available in the Dutch Forest Statistics (CBS, 1985). Two kinds of forest edges were distinguished, namely edges between forest complexes (defined as coherent sets of forest stands) and non-forested areas, and edges situated within forest complexes between forest stands of different heights. In Figure 7.17, the number and total area of forest complexes as well as individual forest stands in the Netherlands are presented by size class. In total, 23,871 forest complexes and 213,691 individual forest stands were present during the recording period 1980-1985. The total forested area in the Netherlands approximated 334,027 ha. Almost 80% of all forest complexes were found to be smaller than 5 ha; only 18 complexes were larger than 2000 ha. More than 70% of all forest stands were found to be

smaller than 1.5 ha. These figures clearly indicate that Dutch forests are considerably fragmented.

Considering forest complexes as squares, their edge area was computed by:

$$EA_{fc} = TA_{fc} - (TA_{fc}^{0.5} - 2L)^2 \qquad [7.3]$$

in which $EA_{fc}$ is the edge area of the forest complex, $TA_{fc}$ the total area of the forest complex, and $L$ the edge width. With an average height of forest stands in the Netherlands of 11.7 m (Meijers, 1990), and an edge zone which approximate five edge heights, L equals, on average, 58.5 m. The percentage edge area [= $(EA_{fc}/TA_{fc})$ * 100%] of each size class was computed using the average $TA_{fc}$ values for each size class. By weighting these percentages for the contribution of each size class to the total area of Dutch forests, it was calculated that 24% of the total forested area in the Netherlands consisted of forest edges bordering a non-forested area.

Similarly, the edge area between forest stands of different height was computed by:

$$EA_{fs} = 0.5 * (TA_{fs} - (TA_{fs}^{0.5} - 2L)^2) \qquad [7.4]$$

in which $EA_{fs}$ and $TA_{fs}$ are the edge area and the total area of the forest stand, respectively. A factor of 0.5 was added because it was assumed that a transition between two forest stands of different heights will cause enhanced dry deposition amounts in the highest stand only. From the frequency distribution of forest stand heights (Figure 7.18), it was computed that the average height difference between two forest stands equalled 8.0 m. A random distribution of forest stands was assumed. In reality, however, forest stands of the same age will be grouped together, resulting in a somewhat lower mean height difference. Because this effect could not be quantified, a mean height difference of 8.0 m was used for the computation of $L$ (= 40 m). The percentage edge area [= $(EA_{fs}/TA_{fs})$ * 100%] of each size class was, similar to above, computed using average $TA_{fs}$ values for each size class. By weighting these percentages for the contribution of each size class to the total area of Dutch forests, it was calculated that 28% of the total forested area in the Netherlands consisted of edges between two forest stands.

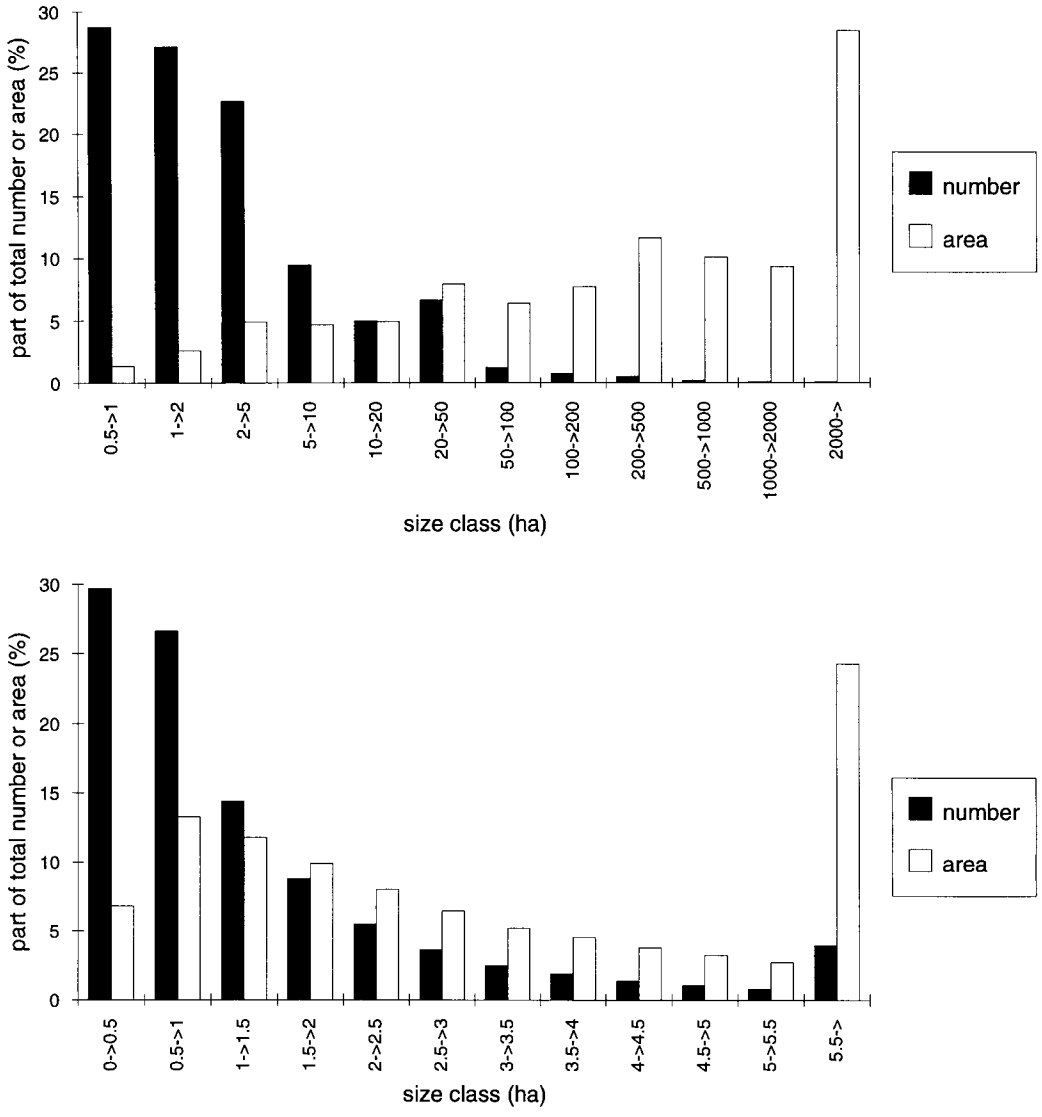


**FIGURE 7.17** The percentage to which different size classes contribute to the total number (and area) of forest complexes (above), and to the total number (and area) of individual forest stands in the Netherlands (below).

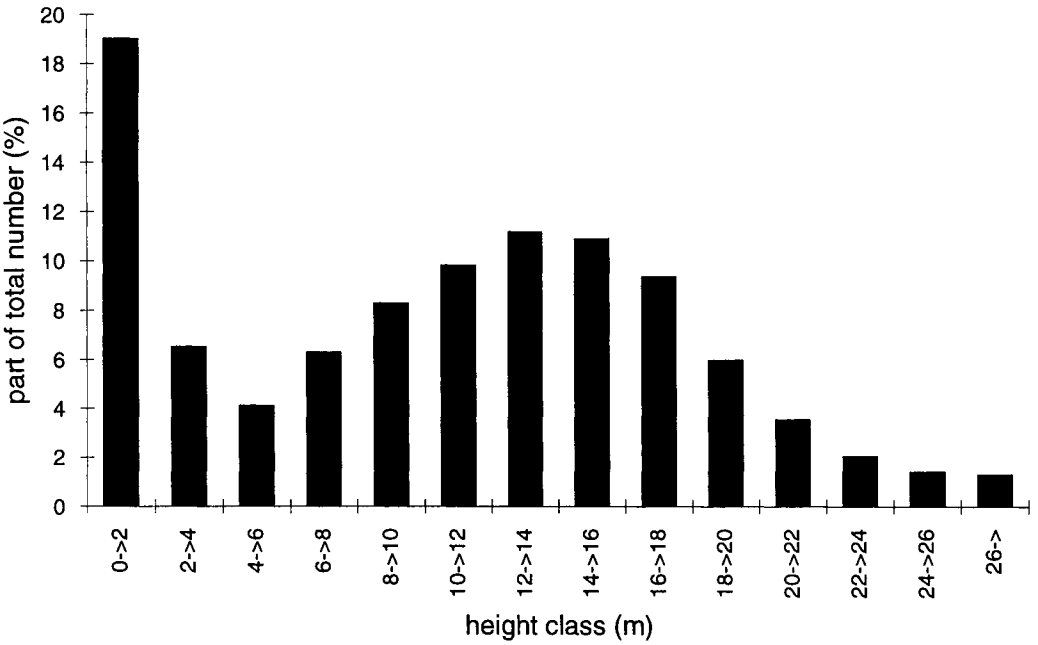


**FIGURE 7.18** Frequency distribution of forest stand heights in the Netherlands. The relatively high percentage observed for height class 0-2 m is the result of the relatively high fraction of timber felling areas and non-afforested silvicultural areas in the Netherlands.

When an edge width of five edge heights is applied, the total percentage of Dutch forests influenced by edge effects thus amounts 52% (if other values for edge width are used the total percentage calculated will change according to Figure 7.19). This percentage is probably too low, because small forest roads, fire lanes and canopy gaps, also expected to cause edge effects, have not been considered in the calculations. Moreover, forests are considered as squares in the calculations, whereas in reality irregular-shaped forest complexes and rectangular-shaped forest stands also occur frequently. However, taking this 52% for granted, and assuming that *WEINTE* factors for $SO_4^{2-}$, $NO_3^-$ and $NH_4^+$ presented in Table 7.15 are valid all over the Netherlands and representative for all kind of forest edges, it can be computed that by neglecting edge effects, dry deposition of acidifying compounds to forests in the Netherlands may be underestimated by approximately 5-10%. Similarly, it can be computed that dry deposition of sea salt particles may be underestimated by 20-25%. Most probably, these are upper limits of underestimation because enhanced dry deposition in a forest edge may lead to a significant downwind depletion of gases and particles, resulting in a relatively reduced deposition in the forest interior. Significant negative relationships found between *WEINTE* factors of $Na^+$, $Cl^-$ and $Mg^{2+}$ on the one hand, and their basic net throughfall fluxes on the

other ($R$=-0.75, $p$<0.05; $R$=-0.72, $p$<0.05 and $R$=-0.75, $p$<0.05, respectively) may be an indication for this. Such relationships were not observed for $SO_4^{2-}$, $NO_3^-$ and $NH_4^+$.

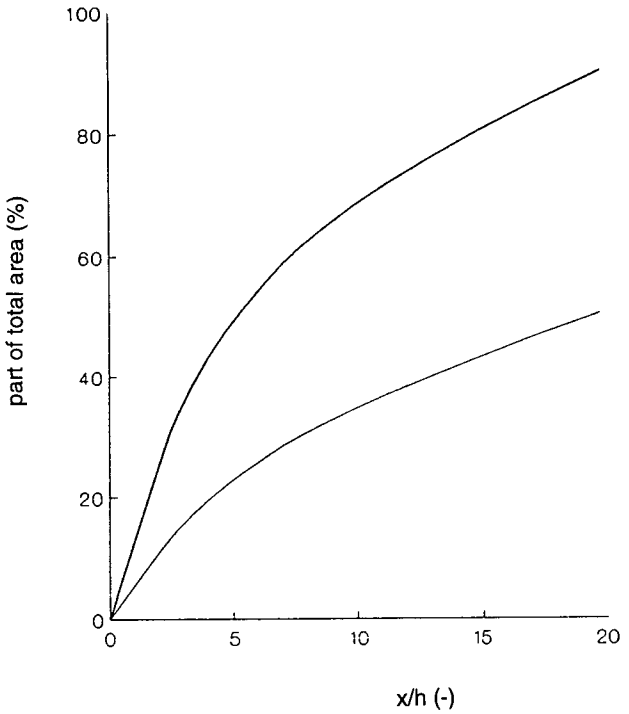


**FIGURE 7.19** Relationship between the part of the total area of Dutch forests influenced by edge effects and edge width. The thin line represents this relationship when only edges between forested areas and non-forested areas are taken into account.

## 7.2.5 CONCLUSIONS

*The impact of forest canopy structure on deposition amounts*

Strong relationships exist between net throughfall fluxes of $SO_4^{2-}$, $NO_3^-$, $NH_4^+$, $Na^+$ and $Cl^-$ on the one hand, and the roughness length and leaf area of the canopy on the other. For $SO_4^{2-}$ and $NH_4^+$ this was explained by the relatively small surface resistance to $SO_2$ and $NH_3$ in the Netherlands, whereby dry deposition is controlled to a large extent by the aerodynamic roughness (length) of the canopy. For $NO_3^-$ it was assumed that the surface resistance of $NO_2$ is inversely related to the leaf area of the forest stand, and/or that the net throughfall flux of $NO_3^-$ was mainly determined by dry deposition of $HNO_3$ and $NO_3^-$ aerosol. Dry deposition of these

compounds depends largely upon atmospheric transfer to the receptor surface. Compared to acidifying compounds, net throughfall of $Na^+$ and $Cl^-$ show weaker, but still significant, correlation with the roughness length and leaf area of the canopy. Net throughfall of these compounds is largely controlled by dry deposition of sea salt particles which, in turn, depends on, in addition to aerodynamic properties and the collecting surface area of the canopy, the canopy density and the collecting efficiencies of individual canopy elements. Relationships between net throughfall of $SO_4^{2-}$, $NO_3^-$, $NH_4^+$, $Na^+$ and $Cl^-$ on the one hand, and *LAI* on the other, are linear in the *LAI* range of 2.4 to 12.0.

The impact of forest canopy structure on deposition amounts is very complex and must be separately considered for each component. Aerodynamic transport, quasi-laminar layer transport and surface resistance are influenced by canopy structure characteristics. Atmospheric transport from the free atmosphere to the forest canopy depends heavily on tree height and leaf area (determining the roughness length); transport through the quasi-laminar layer is influenced, for instance, by the leaf area density (controlling in-canopy wind speeds) and tree species (determining the collecting efficiency of individual canopy elements); the surface resistance is, among other factors, influenced by tree species and leaf area.

Incorporating detailed information on tree height, leaf area (density) and tree species in present-day inferential deposition models offers prospects for estimating deposition fluxes to individual forest stands more accurately. Such detailed information may be obtained through forest inventories or by using remote sensing techniques. Approximately every 15 years in the Netherlands a detailed forest inventory is made through which information on tree species, mean tree height and crown projection is available on stand level (CBS, 1985). In the near future this information will become available in a Geographical Information System (Stuurman, personal communication). Recent applications of remote sensing in air pollution research have focused on directly visible effects of atmospheric pollution, such as defoliation and yellowing of vegetation (e.g. Westman and Price, 1988; Vogelmann and Rock, 1986). However, reasonable relationships have also been found between reflection values of Landsat Thematic Mapper (TM) images and *LAI* (Peterson *et al.*, 1987). Tree species can also be detected from satellite data. Remote sensing seems to be a potentially useful tool for determining canopy structure characteristics from the viewpoint of deposition modelling (Heil *et al.*, 1992), especially when a combination of multi-temporal Landsat and Spot-images is used (Meijers *et al.*, 1993).

*The impact of forest edge effects on deposition amounts*

In general, net throughfall fluxes inside forests increase exponentially towards forest edges. The width of the zone with enhanced net throughfall fluxes approximates five edge heights. Net throughfall enhancement of $SO_4^{2-}$, $NO_3^-$ and $NH_4^+$ near forest edges (on average, a factor of 2) is smaller than that of $Na^+$, $Cl^-$ and $Mg^{2+}$ (on average, a factor of 5). Differences are attributed to the sources for these ions in throughfall. Net throughfall of $SO_4^{2-}$, $NO_3^-$ and $NH_4^+$ in the Netherlands is determined to a large extent by dry deposition of gases and submicron

particles, and net throughfall of $Na^+$, $Cl^-$ and $Mg^{2+}$ largely by dry deposition of supermicron sea salt particles.

Net throughfall enhancement in forest edges also strongly depends upon forest density and edge aspect. For $SO_4^{2-}$, $NO_3^-$ and $NH_4^+$, very strong relationships were observed between net throughfall enhancement factors and silhouette area density, suggesting that drag forces (influencing aerodynamic transport) mainly determine the differences between forest edge and forest interior dry deposition. For $Na^+$, $Cl^-$ and $Mg^{2+}$, the largest correlation coefficients were found with leaf area density, which suggest that for these ions in-canopy wind speeds largely determine the differences between forest edge and forest interior dry deposition. Forest edges exposed to prevailing wind directions and/or high pollutant doses are especially subject to enhanced dry deposition. For $SO_4^{2-}$, $NO_3^-$ and $NH_4^+$, the largest net throughfall enhancement factors were found in forest edges with SE, S, SW or W aspect. This was in agreement with results from an extensive survey of the groundwater quality under forests in the Netherlands (Bouwmans and Beltman, 1991). The largest $SO_4^{2-}$ and $NO_3^-$ concentrations in groundwater were found in forest edges exposed to SE, S, SW and W wind directions. For $Na^+$ and $Cl^-$, the largest net throughfall enhancement factors were observed in forest edges exposed to S, SW, W and NW wind directions.

In large parts of Europe, extensive uniform forests are more the exception than the rule and also Dutch forests are considerably fragmented. Almost 80% of all forest complexes in the Netherlands are smaller than 5 ha, and more than 70% of all individual forest stands smaller than 1.5 ha. For an edge width of five edge heights, it was computed that at least 50% of the total forested area in the Netherlands is influenced by edge effects. By neglecting edge effects, dry deposition of acidifying compounds to forests in the Netherlands as a whole may be underestimated by approximately 5-10%. Similarly, dry deposition of (sea salt) particles may be underestimated by 20-25%. These are upper limits of underestimation because it may be expected that enhanced dry deposition in a forest edge leads to a downwind depletion of gases and particles, resulting in relatively reduced dry deposition in the forest interior. Therefore it is desirable to obtain more insight on the impact of edge effects on regional deposition amounts. A combination of modelling and measuring surface fluxes in heterogeneous landscapes seems most promising for this purpose. Incorporating edge effects in present-day deposition models may offer prospects to estimate regional deposition amounts and deposition to individual forest stands more accurately. Most probably this will require the use of detailed geographical information on the length and exposition of existing edges, the height difference between edges, and the ratio between edge area and total area of forest stands (Meijers *et al.*, 1990). Such information should be available in a Geographical Information System (Burrough, 1986). Remote sensing techniques also seem useful for detecting forest edges and for quantifying landscape heterogeneity (Heil *et al.*, 1992).

## 7.3 THE SPEULDER FOREST EXPERIMENTS TO DETERMINE THE INPUT AND RELATED IMPACTS TO DOUGLAS FIR

### 7.3.1 INTRODUCTION

During the past nine years (1986-1994) research has been conducted at the Speulder forest at the Hoge Veluwe in the centre of the Netherlands. Most research was part of the Dutch National Programme on Acidification, which has now reported its third and probably final phase (Heij and Schneider, 1995). The results of the first two phases were summarised in Schneider and Bresser (1988) and Heij and Schneider (1991). The main emphasis of the research at the Speulder forest was on acidification. The research and monitoring programmes aimed: *i)* to estimate current loads and levels of air pollutants such as sulphur and nitrogen compounds, but also base cations, *ii)* to determine forest characteristics and follow growth parameters in time, *iii)* to determine the effects or risks in relation to exposure of high pollutant loads and levels and *iv)* to determine the effects of reduction in these loads and levels.

*Deposition research*
In 1990 a large project was initiated to develop and evaluate a monitoring method for measurement of deposition of acidifying components onto forests. This project represents the continuation of the successful development of monitoring methods for $SO_2$, $NO_2$ and $NH_3$ deposition to low vegetation (Erisman, 1992; Mennen *et al.*, 1992; Erisman *et al.*, 1993a, 1993b; Wyers *et al.*, 1993a; Erisman and Wyers, 1993; see also Section 7.1). The Speulder forest was chosen because most of the infrastructure was already present after the site had been used for a three-year experiment. Dry deposition estimates were derived from these measurements by Vermetten *et al.* (1992). However, several problems were encountered in the analysis of the data because the accuracy of the measured gradients was too small. This was the consequence of an experimental set-up which was not aimed at accurate measurement of deposition. Duyzer (1992) made a systematic analysis of possible errors and recommended improvements for dry deposition monitoring onto forests.

From January to August 1992 tests were done over low vegetation on the heathland, Elspeetsche Veld (Zwart *et al.*, 1994) with the monitoring equipment. The purpose was *i)* to determine effects of obstacles (monitor housing) to be installed in the mast above the forest on the momentum and heat flux measurements, *ii)* optimisation of the gradient system for $NO_2$ and $SO_2$, *iii)* comparison of $SO_2$ dry deposition parameters with those measured with another dry deposition monitoring system (Mennen *et al.*, 1995), and *iv)* tests of eddy correlation measurements of the $NO_2$ flux. At the end of 1992 the optimised monitoring systems for $SO_2$, $NO_2$ (RIVM) and $NH_3$ (ECN) were installed at the forest site. Since then continuous vertical concentration gradient measurements of these components have been available. In June 1992 eddy correlation measurements of $NO_2$ were also started. From that time on, direct $NO_2$ flux

measurements have been available. These data, however, have not yet been validated and evaluated.

Next to gaseous deposition measurements, a project was run for six months to determine the particle flux at Speulder forest and to compare atmospheric deposition with throughfall measurements (Erisman *et al.*, 1994). The three main research issues addressed in this project were:

- What is the contribution of 'acidifying' aerosols to the total acid input of nature areas?
- What is the relation between atmospheric deposition estimates and throughfall measurements and what is the contribution of aerosol deposition to the difference between the two estimates?
- How important is the coarse particle flux (base cations) to the nutrient cycle in nature conservation areas?

The research required for satisfying answers to the three research issues was defined by a project group, in which research institutes and universities with experience in the field of aerosol research in the Netherlands participated. The work on the 'aerosol project' was a joint initiative of the *National Institute of Public Health and Environmental Protection (RIVM), KEMA (Laboratory for Environmental Research), TNO (Institute of Environmental Sciences), ECN (Netherlands Energy Research Foundation), RUU-FG (Utrecht University, Department of Physical Geography)* and *WAU-AQ (Wageningen Agricultural University, Department of Air Quality)*. First, a model was selected from existing models of aerosol deposition to forests (Ruijgrok *et al.*, 1994). The model was to be representative for the Dutch situation (pollution climate). Insight from model simulations into the most important processes involved in aerosol deposition was gained. The main processes were tested by means of experimental research in the field (at the Speulder forest). The results of the experiments led to a verification of the model description and a basis for a parametrisation of $V_d$ in terms of routinely available data. The parametrisation was used for the generalisation of aerosol deposition to other nature conservation areas in the Netherlands. It was anticipated in the project that by executing all available experimental techniques in combination with a large modelling effort, a more accurate estimation of particle dry deposition velocities for rough surfaces would be obtained. In June 1993, TNO organised an international field campaign in the Speulder forest. The University of Manchester (UMIST) and RISOE National Laboratory (Denmark) participated in a three-week campaign. During the campaign particle fluxes were measured by UMIST using an eddy correlation method. The preliminary results have been kindly made available for use.

*Assessment of relations between loads/levels and effects*

The main focus of this section will be on the determination of atmospheric input and soil loads at Speulder forest. However, at the end, the major findings of the research at the Speulder forest will be used to assess the causal relations between loads and levels on the one hand and effects on the other. First, the atmospheric loads and levels at the Speulder forest will be presented. The uncertainty in the atmospheric load and level estimates will be

discussed along with their evolution during the past years. Subsequently, critical loads and levels derived for the Speulder forest and exceedances determined will be outlined. Critical levels and loads refer to thresholds, which can serve as a tool in assessing the occurrence of effects in natural ecosystems (Nilsson and Grennfelt, 1986; Hettelingh *et al.*, 1991; see Chapter 1 for definitions).

Finally, effects observed at the Speulder forest will be discussed and the concept of critical loads and critical levels evaluated. Effects are defined as ecosystem changes due to environmental impacts. Risks for adverse effects in the future are indicated. Results from manipulation experiments are used to show the recovery of forests after reducing soil loads to pre-industrial levels. At the end of this section, the research programme carried out at the Speulder forest since 1985 will be critically evaluated on its merits and shortcomings.

### 7.3.2 SITE DESCRIPTION

The Speulder forest is located in the Veluwe, a large undulating area with forests and heathlands in the central part of the Netherlands. The measuring site covers an area of 2.5 ha, planted with 2 year old Douglas fir trees (*Pseudotsuga menziessi* (Mirb.) Franco L.) of the provenance Arlington in 1962. Gaps caused by windthrow and diseases were filled with Douglas fir of unknown provenance. The canopy is well closed, with the exception of some gaps due to windthrow caused by the heavy storms in February 1991. The one-sided LAI was between 13.9 and 9.7 for the measuring years 1987-1993 (Steingröver and Jans, 1995). The stand is surrounded by a forested area of approximately 50 $km^2$. The stand itself is surrounded by Larix, birch, Pedunculate oak, Scotch pine and Douglas fir stands, with mean tree heights varying between 12 and 25 m. A small clearing of 1 ha is situated to the north of the stand.

In 1986, when the stand was selected, the mean number of needle year classes on an average first-order branch in the sun-adapted crown level of a tree was four. According to European Community vitality parameters, the vitality of the stand was better than the nationwide average for Douglas fir (Steingröver and Jans, 1995). The stem density varies between 765 trees $ha^{-1}$ in the eastern part of the stand and 812 trees $ha^{-1}$ in the western part. Unless stated otherwise, all measurements took place in the eastern part of the stand. At the end of 1993 the average *DBH* was 25 cm and the trees were approximately 22 m height (Jans *et al.*, 1994).

Soil chemical and texture data are given in Table 7.16. The forest stand is situated on top of an ice-pushed ridge. The groundwater is found at a depth of about 40 m. The soils are well drained. The soil is a Typic Dystochrept on sandy loam and loamy sand-textured Rhine sediments of Middle Pleistocene age. The soil can also be classified as an Orthic Podzol (FAO, 1988) or as a Holtpodzol (Van Breemen and Verstraten, 1991). The soil is rather heterogeneous. The texture of the soil shows a strong spatial variability related to the elongated, parallel outcrops of layers of different textures typical of an ice-pushed ridge.

**TABLE 7.16** Soil chemical and texture data for the Speulder forest (Van Breemen and Verstraten, 1991)

| Depth (cm) | pH $H_2O$ | pH KCl | %C | %N | *CEC*[a] mmol/kg | Texture (%) <2 µm | 2-16 µm | 16-2000 µm | > 2000µm |
|---|---|---|---|---|---|---|---|---|---|
| 0 - 5 | 3.63 | 2.83 | 7.3 | 0.30 | 59 | 1 | 3 | 70 | 1 |
| 5 - 10 | 3.70 | 3.00 | 2.9 | 0.11 | 39 | 0 | 3 | 87 | 0 |
| 15 - 20 | 3.87 | 3.70 | 2.0 | 0.07 | 42 | 0 | 4 | 94 | 1 |
| 30 - 35 | 4.15 | 4.27 | 0.8 | 0.04 | 21 | 0 | 3 | 95 | 2 |
| 50 - 55 | 4.22 | 4.38 | 0.3 | 0.02 | 13 | 0 | 2 | 97 | 0 |
| 90 - 95 | 4.22 | 4.28 | 0.2 | 0.01 | 24 | 0 | 2 | 95 | 0 |

[a] *CEC*: calculated as the sum of 0.5 M $BaCl_2$ extractable $Ca^{2+}$, $Mg^{2+}$, $K^+$, $Na^+$, plus 1 M KCl extractable $Al^{3+}$, $H^+$ and $NH_4^+$.

The climate is moderately humid with an average precipitation of around 800 mm $a^{-1}$ Large sources of $SO_2$ and NOx are located 200 km to the southeast (industrial Ruhr area) and 100 km to the southwest (Rotterdam port). The distance to $NH_3$ sources varies from a few kilometres to the south to some 10 kilometres to the north of the stand.

### 7.3.3 RESEARCH PROJECTS

Several investigations were conducted at the Speulder forest. Until 1990, these were co-ordinated by ACIFORN, established to analyse and quantify the effects of air pollution and soil acidification on forest growth and vitality (Evers *et al.*, 1991). The results of the projects conducted within the framework of ACIFORN have been reported in Heij and Schneider (1991) and in Evers *et al.* (1991). After 1990 research at Speulder forest was not co-ordinated, but the location was extensively used for different kinds of investigations. One of the research topics since 1990 has been the investigation of deposition of acidifying pollutants and base cations. The research activities at the Speulder forest site related to deposition research are summarised in Figure 7.20 (section 7.3.4).

At the Speulder forest research was also conducted on: *i)* boundary-layer clouds and vegetation-atmosphere exchange (KNMI), *ii)* the physiology of Douglas fir trees (IBN-DLO), *iii)* the effects of manipulation of nutrient inputs, (see Figure 7.20, KUN-NITREX), *iv)* mono-terpene emissions from trees, chlorine formation in the soil and chloroform emission from the soil (TNO) and *v)* the hydrological cycle in the forest and the forest soil (UvA FGBL). The primary aim of the physiology project was to analyse and quantify the physiological effects of air pollution, drought and nutrient supply/availability on trees under field conditions (Steingröver and Jans, 1995). The project descriptions of these studies can be found in Heij and Schneider (1992).

## 7.3.4 DEPOSITION MONITORING OF GASEOUS COMPONENTS

*Introduction*

Erisman *et al.* (1993) evaluated the deposition measurements made between November 1992 and September 1993. The main emphasis was on the evaluation of the dry deposition measurements for routine application, estimation of fluxes and their accuracy, and deriving a parametrisation for the surface resistance to deposition on forest. Dry deposition parameters were derived from the results of the hourly average measurements. Following the recommendations reported by Erisman *et al.* (1993), the system configuration and the measurement scheme were adjusted. The system configuration, several tests, and the calibration and quality control procedures are extensively described in Mennen *et al.* (1995). In this section, a summary of the evaluation of the deposition monitoring methods and the interpretation of data will be described along with the results of two years of monitoring.

*Experimental procedure*

The Speuld location was equipped with two towers and measuring facilities. One tower was used for gas deposition measurements. The second tower was used for the so-called 'Aerosol project' (Erisman *et al.*, 1994; see section 7.2.5). A schematic representation of the monitoring system at the Speulder forest is shown in Figure 7.20. Most of the equipment is put on a tower consisting of a mast, a scaffolding and two hoists, both provided with a suspension frame. One of the hoists is used for transport of material, whereas the other is used to carry two boxes containing the monitors, which can be transported downwards for calibration or maintenance. Both mast and scaffolding are 36 m high and have a triangular cross-section (Zwart *et al.*, 1993; Mennen *et al.*, 1995).

A sonic anemometer (Kaijo Denki DAT-310) mounted on the top of the scaffolding at 36.5 m height was used to measure the horizontal and vertical wind velocity, wind direction and friction velocity, and the sensible heat flux. A net radiation meter (Thies 8110) and a temperature and relative humidity sensor (Vaisala HMP121B) were mounted 1.5 m outside the scaffolding towards the south, at heights of 35 and 33 m, respectively. The two boxes housed the gas monitors, two pulsed fluorescence $SO_2$ analysers (Thermo Environmental Instruments Inc., Model 43S) and two Luminox $NO_2$ analysers (Scintrex Ltd., LMA-3). The performance of the instruments and the monitoring system as a whole was thoroughly tested by Zwart *et al.* (1993). This work also contains an extensive description of the system. Zwart *et al.* concluded that the performance of the $SO_2$ monitors is sufficient for dry deposition monitoring. For $NO_2$ they demonstrated that the performance to be questionable; it should be further tested in the field.

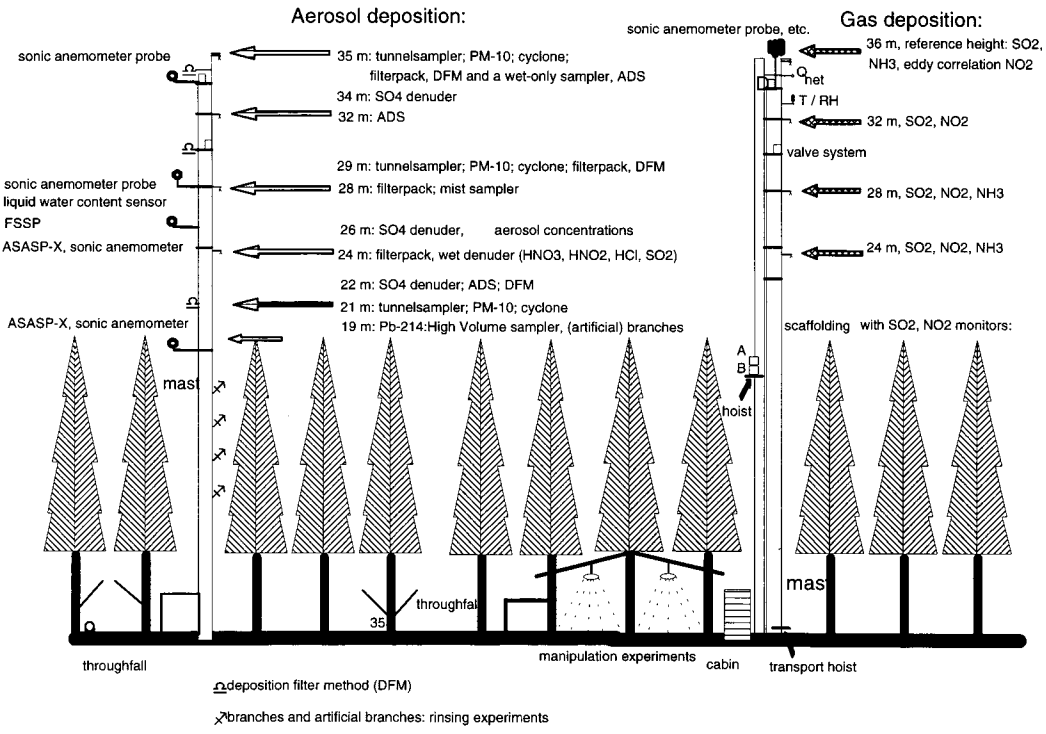


**FIGURE 7.20** Deposition research at the Speulder forest site.

*Theory and interpretation*

Dry deposition of gases can be calculated from concentration gradients and meteorological parameters. The calculation of $c_*$, $F$, $V_d$ and $Rc$ is outlined in Chapter 3. $c*$ is obtained from the weighted regression between $c$ and the stability corrected height (4 levels). Weights are obtained from the standard deviation of the 1-min concentration measurement at each height. The concentrations of $SO_2$ and $NO_2$ are corrected by variations in time using the concentrations measured with the reference monitor ($M_r$) by:

$$c(M_s,t_1,z) = c(M_s,t_i,z)\frac{c(M_r,t_1,36)}{c(M_r,t_i,36)} \qquad [7.5]$$

$t_i$ denotes the successive four measuring periods for determination of the gradient by the scanning monitor ($M_S$).

During the experiments in 1989 at the Speulder forest, the Royal Netherlands Meteorological Institute (KNMI) compared gradients of temperature and wind speed above the forest with directly measured fluxes of heat and momentum in order to test the commonly used flux profile relations (Dyer and Hicks, 1970). From these experiments systematic differences were found between the Dyer and Hicks relations and those obtained above the Speulder forest (Bosveld, 1991; Duyzer *et al.*, 1992). This can be accounted for by introducing $\alpha_h$, a height-dependent correction factor. In the roughness layer the following relations were proposed for the flux profile relations for heat (Bosveld, 1991):

$$\begin{aligned} \phi_h &= \alpha_h \, \phi_h, \text{ for unstable conditions} \\ \phi_h &= \phi_h - (1 - \alpha_h), \text{ for stable conditions} \end{aligned} \qquad [7.6]$$

**TABLE 7.17** Correction factor for flux profile functions over the Speulder forest (Bosveld, 1991).

| Height intervals (m) | $\alpha_h$ |
|---|---|
| 18-24 | 0.65 |
| 24-31 | 0.80 |
| 31-36 | 0.95 |

$\alpha_h$ is a function of height and equals unity at the height where the influence of the individual roughness elements inducing extra turbulence has become small (for the Speulder forest this is at z≈36 m). The correction factors $\alpha_h$ for the flux profile function for heat are given in Table 7.17.

It is assumed here that these factors can also be applied for trace gas flux profile relations. The method of application proposed by Bosveld (1991) and Duyzer *et al.* (1992) is adopted here. Flux profile relations for ozone and heat were evaluated at the Speulder forest by TNO. They showed that similar alpha factors can be applied for ozone (Westrate and Duyzer, 1994).

*Dry deposition parameters for the Speulder forest*
Measurements of $SO_2$, $NO_2$ and $NH_3$ and meteorological parameters have been recorded ever since the end of November 1992. Because of problems with the $NO_2$ monitors, very little data are available to evaluate the gradients and to obtain fluxes. The main focus in this section is therefore on $SO_2$ and $NH_3$.

Constant flux layer assumption
The eddy correlation measurements of $u*$ and $H$ at 30 m height by TNO and those at 36 m height by RIVM were compared to evaluate the constant flux layer assumption. Figures 7.21 and 7.22 show scatter plots of hourly average $u*$ and $H$ values measured at the two heights in

December - June. A selection is made because during several weeks in December, February and March, the eddy correlation measurements by TNO were disturbed by an interfering signal on the datalogging system. Another selection was made for measurements with wind coming from the north through the clearing in the forest. Finally, $u*$ values below 0.1 $m^{-1}$ were not taken into account. About 50% of the dataset remains after selection. There is a reasonable agreement between the 30-m and 36-m $u*$ values; most scatter is due to local influence on the fetch and to scatter in the data as a result of differences in averaging time. The difference between the heat fluxes measured at the two levels was much larger. The reason for this large difference is that during and after rain or fog, heat flux measurements might be contaminated as a result of droplets on the sensors. Furthermore, at very low heat flux values (very stable conditions) the change on temperature inversions and thus decoupling of the air in and above the forest increases. Therefore, hours with differences larger than 25 W $m^{-2}$ between the heat fluxes measured at the two heights were not taken into account. About 40% of the data remain; see plotted in Figure 7.22. From the two figures it is obvious that during these months the constant flux layer assumption for momentum and sensible heat fluxes is valid.

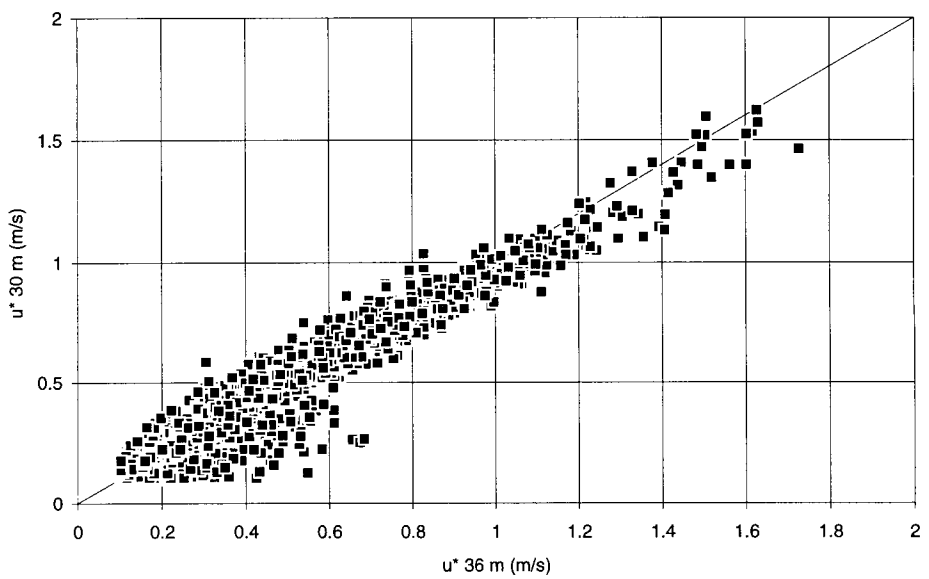


**FIGURE 7.21** Eddy correlation $u*$ measurements at 30 m compared to those measured at 36 m.

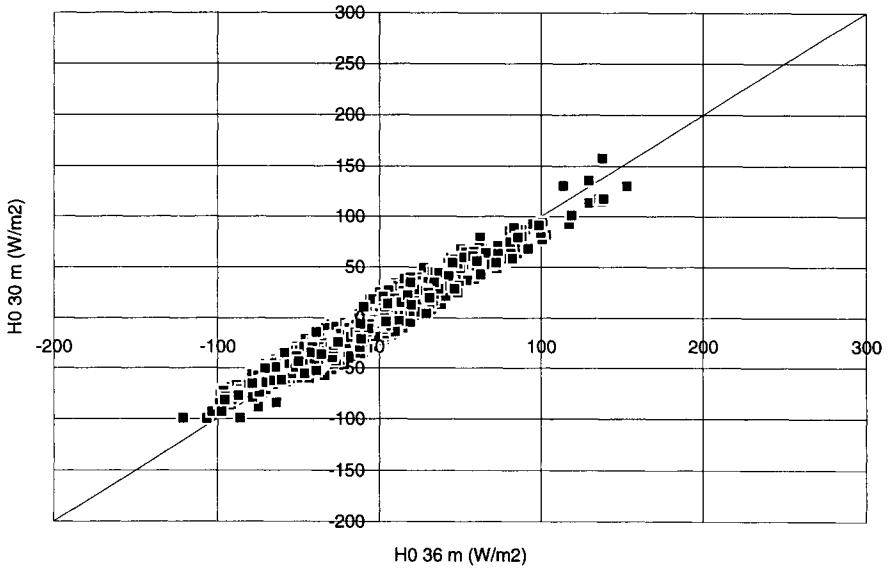


**FIGURE 7.22** Eddy correlation $H$ measurements at 30 m compared to those measured at 36 m.

Averages for selected periods

The three vertical $SO_2$ and $NO_2$ gradients were averaged for each hour and $c*$, $F$, $V_d$, $R_a$, $R_b$ and $R_c$ were calculated. The 10 $NH_3$ gradients measured within one hour were also averaged and the deposition values were calculated accordingly. The dataset thus obtained has to be 'cleaned' by selecting the hours during which: 1) the theoretical demands for the gradient technique were fulfilled; 2) the concentrations were well above the detection limit, and 3) there was no loss of necessary measurements due to technical problems. Selection criteria for $SO_2$ derived from measurements over a heathland (Erisman *et al.*, 1993a,b) were adjusted and applied here. These criteria are listed in Table 7.18. In this table the per cent of the total number of hourly averaged measurements remaining after applying the selection criteria is also given. For $SO_2$ about 42% survived the selection criteria. Most of the data were rejected as a result of measuring errors due to moisture in one of the sampling tubes (36-m height) and due to the random error in individually measured concentrations. It was found that by loss of one of the filters during a storm, the inside of the tubes had become moist, leading to adsorption and desorption of $SO_2$. This problem has now been overcome by heating the tubes. At concentrations below 5 $\mu g\ m^{-3}$ the random error is the dominating error in deposition parameters.

**TABLE 7.18** Selection criteria for gradients measured over the Speulder forest and the percentage of measurements left after selection (total remaining: 2345 hours of continuous $SO_2$ measurements, 220 hours of $NO_2$ measurements and 756 hours of continuous $NH_3$)

| Criteria | Percentage of remaining $SO_2$ data | Percentage of remaining $NO_2$ data | Percentage of remaining $NH_3$ data |
|---|---|---|---|
| Validity of flux profile relations $u$>1or $u*$>0.1 m/s, plus $NH_3$ instrumental failure due to freezing | 95 | 95 | 30 |
| Fetch requirements: $\theta$<330 and $\theta$> 30° | 89 | 89 | |
| Deviation between two monitors: $\|\Delta C\| < 3$ μg m$^{-3}$ | 78 | 21 | - |
| No gradient: $c* > 0$ | 77 | - | - |
| Moisture in the tubes: 5-25 January 1993 | 59 | - | - |
| High concentration fluctuations in time: $dC/dt$ | 58 | - | 28 |
| High $u*$ fluctuations in time: $du*/dt$; $\sigma_{u*}$ | 57 | - | - |
| Detection limit and random errors: $C > 5$ μg m$^{-3}$ | 48 | - | 27 |
| Stability range (errors in $R_a$ and $R_b$): $\|[z-d]/L\|$<0.5 | 42 | - | 26 |

Most $NO_2$ data (80%) were rejected as a result of instrumental failure. It is obvious from this large amount of data lost that monitoring of $NO_2$ deposition with the current system is impossible. The Scintrex monitors are not suitable for routine application. In the meantime eddy correlation measurements with the Scintrex monitors have been started. Evaluation of these measurements is currently being carried out.

For $NH_3$, data from the period 28 November 1992 - 31 March 1993 have so far been processed. About 26% of the data remained after selection, see Table 7.18. Most data were rejected as a result of incorrect operation of instrumentation due to freezing of the solutes in the denuders. Application of this criteria and of the last two selection criteria in Table 7.18 may have lead to a bias in the dataset towards larger deposition velocities.

$SO_2$

Figure 7.23 shows the average daily variation in $R_c$ values for selected hours for wet and dry leaf surfaces. During dry conditions a weak daily variation can be seen following stomatal behaviour. It must be emphasised that the standard deviations in the values presented in Figure 7.23 are very large (see Table 7.19). This has a large influence on the variation shown in Figure 7.24. During wet conditions $R_c$ values are generally low. The average $V_d$ and $R_c$ values for dry and wet conditions, and for daytime and night-time are listed in Table 7.19.

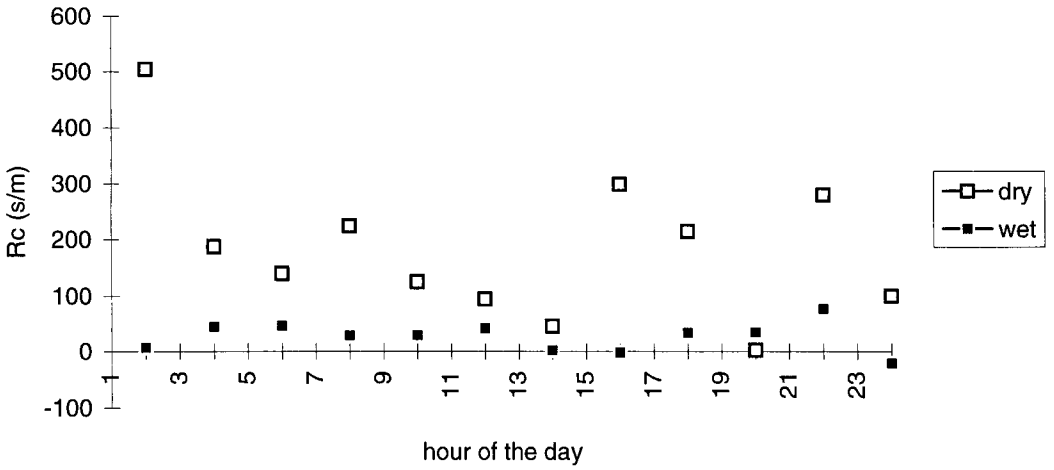


**FIGURE 7.23** Daily variations of $SO_2$ in $R_c$ for dry and wet surface conditions.

**TABLE 7.19** Average deposition parameters for $SO_2$, with standard deviations in parentheses

| | $R_c$ (s m$^{-1}$) | | $V_d$ (m s$^{-1}$) | |
|---|---|---|---|---|
| Conditions | Observations | Modelled | Observations | Modelled |
| Night, dry canopy | 250 (900) | 90 (60) | 0.008 (0.012) | 0.012 (0.009) |
| Day, dry canopy | 290 (2520) | 150 (320) | 0.007 (0.018) | 0.011 (0.006) |
| Night, wet canopy | 20 (120) | 5 (10) | 0.024 (0.021) | 0.030 (0.017) |
| Day, wet canopy | 20 (80) | 5 (10) | 0.030 (0.020) | 0.027 (0.014) |

*Surface resistance parametrisation for $SO_2$* An $R_c$ parametrisation derived from analogous measurements over a heathland during a three-year period (Erisman *et al.*, 1993a,b; section 7.1 and Chapter 4) was tested. This parametrisation is evaluated in section 6.1. Figure 7.24 shows 'measured' and parameterised $SO_2$ $R_c$ values, and measured $NH_3$ $R_c$ values for four successive days. Also shown in this figure are the concentrations of the two gases, the relative humidity and information on surface wetness. Parameterised and 'measured' $R_c$ values for $SO_2$ show reasonable agreement, with high values during dry periods at night, low values during daytime and values approaching zero during wet surface conditions. $R_c$ values for $NH_3$ show similar variations. For both this period and the whole dataset no influence of $NH_3$ on deposition parameters for $SO_2$ and vice versa was observed. This is in contrast to the

observations of Erisman and Wyers (1993) who demonstrated influence of both gases on each other's deposition under extreme conditions. The explanation is that during November 1992 to April 1993 these extreme conditions did not occur. $NH_3$ is therefore not included in the parametrisation. For the dataset with the selected measuring periods, 40% of the variance in parameterised $V_d$ versus the 'measured' $V_d$ was accounted for with no systematic differences. These results are similar to those found for heathland vegetation using the same parametrisation (Erisman *et al.*, 1993a,b). A plot of the parameterised and measured $V_d$ is given in Figure 6.1.

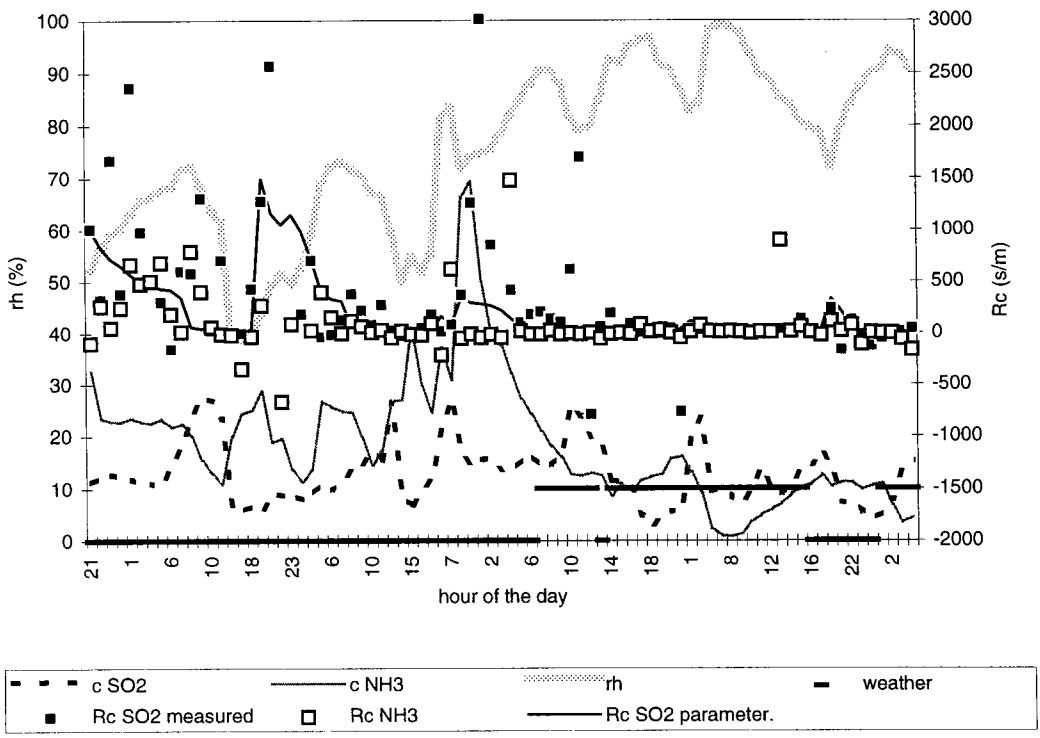


**FIGURE 7.24** $R_c$ values for $SO_2$ and $NH_3$ from continuous measurements of vertical gradients over the Speulder forest ('Weather' provides information on precipitation: 0 = dry; 10 = rain).

The surface resistance parametrisation will be used to estimate deposition parameters for measurements which did not satisfy the selection criteria. In this way, it is possible to estimate annual average deposition parameters using both the selected and the rejected data. One condition, however, is that this selection does not lead to a systematic bias in the parametrisation as a result of omitting an important deposition regulating process. When one

year of monitoring data become available, this will be investigated by comparing surface conditions and measured parameters in selected and rejected periods, and looking for systematic differences (Erisman *et al.*, 1993c).

$NO_2$

Very few $NO_2$ measurements satisfy the selection criteria (Table 7.18). Most of the data has been rejected due to instrumental failure. The Scintrex $NO_2$ monitors are not suitable for routine applications. Currently, this is the only instrument which can measure $NO_2$ concentration with enough accuracy and speed for eddy correlation and gradient measurements (Zwart *et al.*, 1993). In 1994 results of laboratory tests with two new instruments which might be suitable would become available.

This section presents the first results of an analysis of the selected measuring periods. Figure 7.25 shows the average diurnal variation of $V_d$ derived from the $NO_2$ concentration measurements satisfying the selection criteria. Also plotted in this figure is an estimate of the average diurnal variation of the deposition velocity as a result of stomatal uptake. The latter is calculated using Eqn. (4.4). Flux measurements over low vegetation and forests have shown that $NO_2$ dry deposition is determined by stomatal uptake (Hicks *et al.*, 1989; Duyzer 1992; Hargreaves *et al.*, 1992). A positive correlation between the $V_d$ for stomatal uptake and the dry deposition velocity would therefore be expected. In Figure 7.25, however, an anti-correlation is observed with negative 'measured' values during daytime and positive (deposition) values at night, in contrast to positive stomatal values during daytime and zero values at night (stomata closed). The anti-correlation might be the result of NO emissions out of the forest, reacting with $O_3$ during daytime, forming $NO_2$ and thus establishing a net upward flux (Duyzer, 1992).

$NH_3$

The results of the $NH_3$ measurements have been reported in Wyers *et al.* (1993b). It is found that the surface resistance to ammonia deposition disappears when the canopy becomes wet (e.g. Figure 7.24). Emission of $NH_3$ was observed on several occasions and seemed to be strongly related to drying of the canopy. For the four-month period considered here (wintertime), it is estimated that as much as 20% of the deposited $NH_3$ was re-emitted from the canopy. Emission was observed mainly during the day at a relative humidity decreasing below 80%. So far, no relation is apparent between occurrence of emission and low or sharply decreasing ambient $NH_3$ concentrations. When the canopy is dry and the flux is towards the surface, this flux is higher than the inferred stomatal flux (Eqn. 4.4), indicating that the external leaf surface is also an important receptor for $NH_3$.

When the canopy is continuously wet, the surface resistance derived from the measurements is consistently negative with a typical value of -20 m $s^{-1}$. This indicates that the derived dry deposition velocities exceed the maximum possible $V_d$ given by: $(R_a+R_b)^{-1}$. It is possible that $R_a$ and/or $R_b$ are overestimated under these conditions.

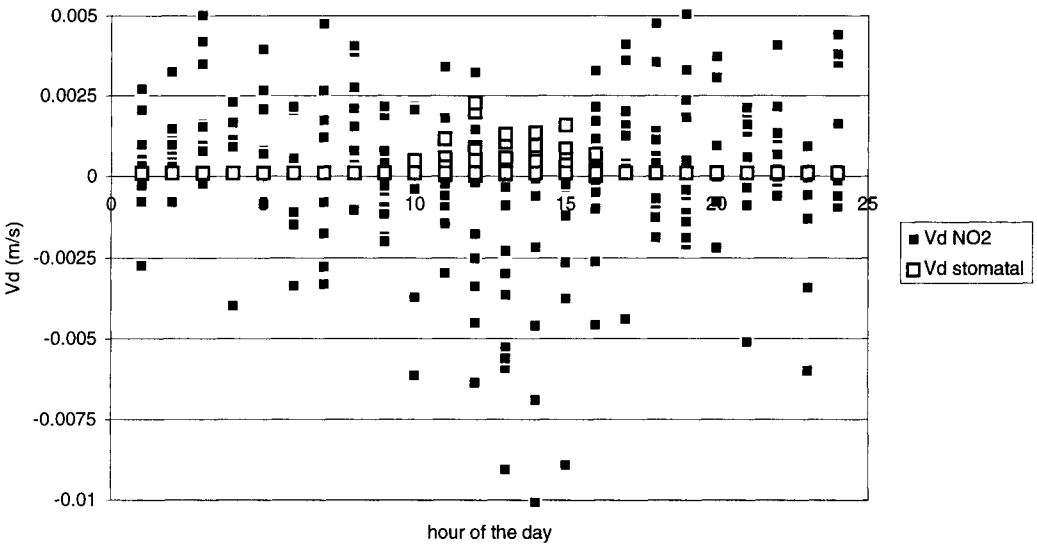


**FIGURE 7.25** Diurnal variation of $V_d$ $NO_2$ and $V_d$ for stomatal uptake for selected measuring periods.

Measurements made at this site by Bosveld (personnel communication) suggest that $R_b$ for water vapour is negligibly small. This might also be the case for $NH_3$ as its behaviour is similar. Another possibility is the presence of an additional sink above the canopy caused, for example, by chemical reactions or deposition to acid particles (Erisman and Wyers, 1993). Erisman and Wyers (1993) estimated that when using simulated water vapour, temperature, nitric acid and $NH_4NO_3$ aerosol gradients over heathland, negative $R_c$ values could be the result of a shift in the equilibrium between gas phase and aerosol concentration between one height and the other above the surface.

*Surface resistance parametrisation* A start was made with the derivation of a parameterised description for $NH_3$ surface exchange (Wyers *et al.*, 1993b). Under conditions of deposition it was assumed that $R_c$ could be described by:

$$R_c = \frac{1}{\frac{1}{R_{stom}} + \frac{1}{R_{ext}}} \qquad [7.7]$$

in which the stomatal resistance is described with Eqn. (4.4) and $R_{ext}$ is the resistance to deposition for external leaf surfaces. For a wet canopy the $R_{ext}$ is zero; for a dry canopy, $R_{ext}$ is empirically derived as 20 s $m^{-1}$. The deposition velocity is calculated using Eqn. (3.3).

For a description of periods with $NH_3$ emission, related to evaporation of water films on the canopy, it is necessary to have an accurate description of canopy wetness and canopy drying. Unfortunately, this is not yet available. For the moment, emission is simply assumed to occur at global radiation above 0 W $m^{-2}$ (daytime) and at a relative humidity below 80% during dry weather conditions. The resistance concept is not applicable for emission fluxes. However, as a first approximation, the 'emission' velocity is simply estimated using Eqn. (3.3) in a revised form:

$$V_e = \frac{-1}{R_a + R_b + R_{c,e}} \qquad [7.8]$$

with $R_{c,e}$ empirically derived as 10 s $m^{-1}$. Figure 7.26 shows the comparison between measured and modelled $V_d$. The prediction of occurrence of emission is still inadequate, as expected from the poor parametrisation for drying the canopy. Under conditions of deposition there is reasonable agreement between modelled and 'measured' $V_d$ values, with 25% of variance accounted for.

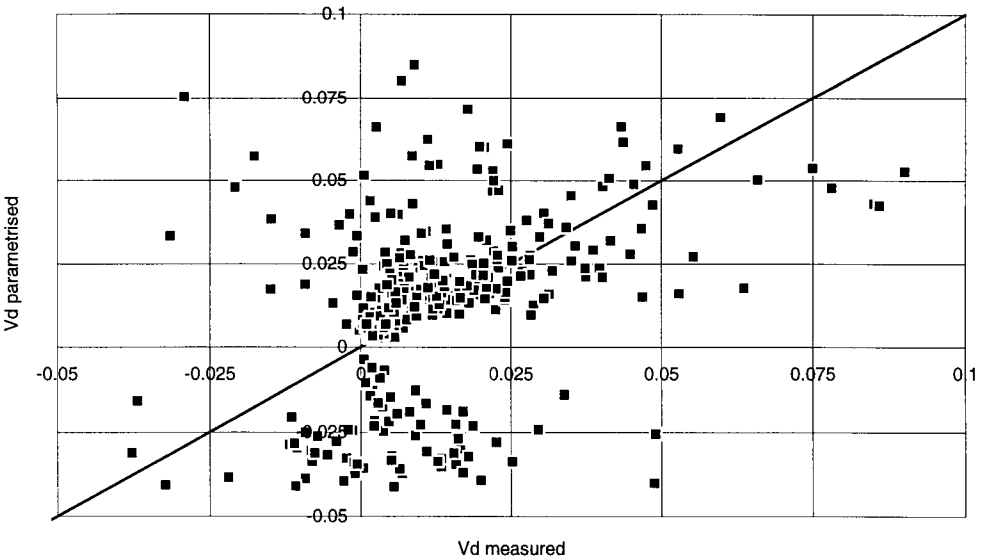


**FIGURE 7.26** Parameterised values of $V_d$ compared to $V_d$ derived from $NH_3$ gradients for selected measuring periods ($R^2$=0.25 for positive values)

**TABLE 7.20** Average deposition parameters for $NH_3$, with standard deviations in parentheses

| | $R_c$ (s m$^{-1}$) | | $V_d$ (m s$^{-1}$) | |
|---|---|---|---|---|
| Conditions | Observations | Modelled | Observations | Modelled |
| Night, dry canopy | 20 (100) | 20 (0) | 0.02 (0.03) | 0.02 (0.01) |
| Day, dry canopy | 10 (40) | 10 (0) | 0.01 (0.05) | -0.01 (0.03) |
| Night, wet canopy | 0 (30) | 0 (0) | 0.04 (0.05) | 0.04 (0.02) |
| Day, wet canopy | 0 (40) | 0 (0) | 0.04 (0.06) | 0.04 (0.04) |

In Table 7.20 observed and modelled averages of $V_d$ and $R_c$ are listed for the entire dataset. In general, there is good agreement between averages of observed and modelled values of the two parameters. An important discrepancy is observed for exchange over a dry canopy during the day, when net emission is modelled in contrast with the observed average deposition velocity of 0.01 m s$^{-1}$. From this table it is again obvious that canopy wetness is a dominating factor in the dry deposition of $NH_3$.

### 7.3.5 THE AEROSOL PROJECT

*Introduction*

Particle, which are responsible for the atmospheric load to ecosystems consist of aerosols such as sulphate, nitrate, chloride, ammonium and base cations such as calcium, magnesium, sodium and potassium. Deposition of particles containing $SO_4^{2-}$, $NO_3^-$, $Cl^-$ and $NH_4^+$ might contribute to the potential acidification and eutrophication (nitrogen components) of ecosystems. Compared to gaseous deposition of acidifying compounds, particle deposition velocities and fluxes are usually found to be small. However, accurate knowledge on particle deposition is necessary for areas far from sources since this might be the major atmospheric pathway of deposition, together with wet deposition, and because the long-range transport of particles is determined by a combination of their deposition velocity and scavenging ratio. Furthermore, it is believed that the dry deposition velocity of small particles and, with this, the fluxes, is currently underestimated for very rough surfaces like forests (Wiman *et al.*, 1990; Erisman, 1992; 1993a). Current knowledge is therefore insufficient to give an adequate assessment of the dry deposition of particulate sulphur and nitrogen over the Netherlands and Europe. There is a need for quantification to evaluate critical load exceedances and abatement strategies for atmospheric pollution.

Base cation deposition may be of importance for nutrient cycling in soils and ecosystems and may also neutralise acid input. Base cation input is therefore important in the determination of critical loads and/or critical load exceedances. Ecosystems receiving a high atmospheric input of base cations have higher critical loads than those receiving smaller inputs (Hettelingh *et al.*,

1991). Base cations are usually found in the coarse fraction of ambient aerosols. Their deposition velocities are therefore large.

In several studies where throughfall fluxes are compared with atmospheric deposition estimates, large differences have been found (e.g. Ivens, 1990, Draaijers and Erisman, 1993; Erisman, 1993b, see also Chapter 6). Establishing a link between the two is useful because it provides a way to estimate soil loads from atmospheric deposition estimates on the one hand, and allows the use of the relatively simple and cheap throughfall method to determine atmospheric deposition on the other. The link between atmospheric deposition and soil loads is important because critical loads refer to soil loads and because atmospheric deposition estimates provide a link with emissions. Thus, if critical load exceedances are used to estimate emission reductions, the relation between atmospheric deposition and soil load should be known. It was suggested by Draaijers and Erisman (1993) that besides canopy exchange processes, aerosol and/or fog and cloud-water deposition might be important processes contributing to the observed differences between atmospheric deposition estimates and throughfall measurements.

This section will summarise the results of the project. It is based on subprojects executed by the participating institutes (Ruigrok *et al.*, 1994; Römer and Te Winkel, 1994; Hofschreuder *et al.*, 1994; Duyzer *et al.*, 1994; Draaijers *et al.*, 1994; Vermeulen *et al.*, 1994; Van Leeuwen *et al.*, 1994; Arends *et al.*, 1994). First, the outline of the measurements and the model's development is explained. Results of the measurements and the model's application are then presented, followed by a discussion on canopy exchange, fog-water input, modelling and experimental validation and a generalisation of results. Detailed descriptions of subprojects are reported by the participating institutes. The main emphasis in this section is on the integration of subproject results.

*Experimental set-up*

The Speuld location was equipped with two towers and measuring facilities (see Figure 7.20). One tower was used for gas deposition measurements (Zwart *et al.*, 1994; Erisman *et al.*, 1993b,c; 1994e; see section 7.3.4). During the experiments, meteorological data and dry deposition data for $SO_2$, $NH_3$ and $NO_2$ obtained from this tower were available from the concurrent project on trace gas deposition (Erisman *et al.*, 1993b,c; 1994d; Wyers *et al.*, 1993, see section 7.3.4). The second tower was used for the aerosol project only. The tower is 34 m high and has a rectangular cross-section of 2.0 m x 1.5 m. An overview of the experimental set-up is shown in Figure 7.20. The measurements will only be described briefly in this section. A summary of the measurements is given in Table 7.21. For detailed descriptions of the equipment, sampling, analytical methods, selection of data, etc., please refer to the literature cited.

Micrometeorological experiments

*Gradient measurements* Gradients were determined by concentration measurements of $(NH_4)_2SO_4$ and $NH_4HSO_4$ at three heights (22, 26 and 34 m) by ECN using thermodenuders (Wyers *et al.*, 1994). Concentrations of total $SO_4^{2-}$ and $NO_3^-$ were measured at four heights (23, 26, 30 and 34 m) by TNO using filterpacks (Duyzer *et al.*, 1994). Concentrations of $Cu^{2+}$, $Ti^{3+}$, $Ca^{2+}$, $Mg^{2+}$, $Na^+$ and $K^+$ were measured at three heights (21, 29 and 35 m) using tunnel samplers (total particle mass), PM-10 devices (MD-50 of 10 μm) and cyclones (fine particles, MD-50 of 2.5 μm) by WAU (Hofschreuder *et al.*, 1994).

*Eddy correlation measurements* During a number of fog events, high frequency measurements (20.8 Hz) were made of turbulent characteristics and the liquid water content of fog (Vermeulen *et al.*, 1994; Wyers *et al.*, 1994). To characterise the droplet distribution function additional measurements were made with a Forward Scattering Spectrometer Probe (FSSP). Liquid water content fluxes were averaged over 10-min intervals. During the entire event, fog water was sampled actively with a string collector and analysed in the lab for its chemical composition (Römer and Te Winkel, 1994). More details can be found in Vermeulen *et al.* (1994).

Two Active Scattering Aerosol Spectrometer Probes (ASASP-X, Particle Measuring Systems, Boulder, Colorado, USA) were mounted in the tower at 18- and 25-m height by UMIST (UK). The instrument at 18 m was used in conjunction with a Gill Solent ultrasonic anemometer and at 25 m with a Kaijo-Denki ultrasonic anemometer (Beswick *et al.*, 1994). An ASASP-X measures particle sizes in the range of 0.1–3.0 μm diameter, this being split into 31 size bins plus an oversize channel. Both probes sampled through 4-m tubes. The equipment set-up allowed use of both the eddy correlation and the gradient technique for determining particle $V_d$. Data was logged at a frequency of 10 Hz (Beswick *et al.*, 1994). Measurements reported here were made between 29 June and 1 July.

Accumulation experiments

*Accumulation of $^{214}Pb$* The $^{214}Pb$ activity accumulated on needles and the corresponding $^{214}Pb$ activity in air were measured simultaneously over a three-hour period for several days in 1993-1994. The dry deposition velocity for $^{214}Pb$ can be obtained from these measurements; which are expected to be representative for submicron particles since $^{214}Pb$ activity is attached to these particles. The experiments, based on the method previously used by Bondietti *et al.* (1984), are described in Wyers *et al.* (1994).

*Deposition Filter Method (DFM)* At three heights above the canopy (21, 29 and 35 m) deposition plates (DFM) were mounted to measure the accumulation of $Cu^{2+}$, $Ti^{3+}$, $Ca^{2+}$, $Mg^{2+}$, $Na^+$ and $K^+$ (Hofschreuder *et al.*, 1994). This method uses a horizontal paper filter as depositing surface. The filter was placed in a petri-dish with a 3-mm high edge which, in turn,

was placed on a plate with a diameter of 30 cm. The filter was protected against precipitation by a roof mounted to the plate. Accumulation of particles was measured in the week before analysing. Between February and May 1993, about 14 weekly average samples were collected.

*Washing Douglas fir and artificial branches* Another series of accumulation experiments was carried out with needles from natural and artificial (polythene) branches (Römer and Te Winkel, 1994). Both Douglas fir and artificial branches were used in order to determine the influence of canopy exchange on the observed fluxes. Four Douglas fir branches were selected from near the mast at 11, 15, 17 and 19 m. Artificial branches were mounted on the tower at three heights (15, 17 and 19 m). The artificial branches were tested in the lab for chemical inertness. The needle surface was estimated beforehand using twig characteristics. Furthermore, the branches were taken into the lab and examined after the last experiment. The material accumulated during dry periods of several days was rinsed from the branches using a polypropylene bag filled with demineralised water.

*Precipitation and throughfall measurements* Rainfall and throughfall were collected in the Speulder forest for 10 months (Van Leeuwen *et al.*, 1994). Rainfall was measured with a wet-only device placed on top of the mast (35 m) and with four funnels in a clearing approximately 300 m from the mast. Two of the funnels were used for the mechanical sequential sampler. This sampler collects every 23 ml of volume rainwater (equivalent to 0.36 mm precipitation). Bulk throughfall was measured in 25 PVC gutters placed at an angle of approximately 24° from the horizontal. The gutters were placed in a regular pattern of two rows within a square of 250 $m^2$. For the sake of comparison, throughfall was also measured with 25 open samplers placed next to the gutters. A wet-only gutter, similar in size and form, and developed by the ECN, was placed near the gutters to determine wet-only throughfall. Throughfall was sampled sequentially during several events with two gutters connected to a shielded Campbell tipping bucket rain gauge. The minimum recording quantity was 0.04 mm and the maximum was set at 0.12 mm, after which sampling took place. Bulk rainfall and throughfall was collected in 30 periods. Samples were analysed within 24 hours of sampling for $NH_4^+$, $PO_4^{3-}$, $Cl^-$, $HCO_3^-$, $NO_3^-$, $SO_4^{2-}$, $Ca^{2+}$, $Mg^{2+}$, $Na^+$, $K^+$ and $H^+$.

Ambient concentration measurements

In addition to the measurements used for estimating deposition, concentrations of $SO_4^{2-}$, $NO_3^-$, $NH_4^+$, $Cl^-$, $Na^+$, $K^+$, $Ca^{2+}$ and $Mg^{2+}$ were measured in two size classes as 24-h averages (< 2.5 μm and > 2.5 μm) during a period of nine months (Römer and Te Winkel, 1994). Concentrations of $HNO_2$, $HNO_3$, HCl, $SO_4^{2-}$, $NO_3^-$, and $NH_4^+$ (< 2.5 μm) were determined for several days with annular denuders (Mennen (unpublished data); Arends *et al.*, 1994; Hofschreuder *et al.*, 1994) and once every week as hourly averages with wet rotating denuders (Wyers *et al.*, 1994).

**TABLE 7.21** An overview of experiments performed at the Speulder forest site to quantify particle dry deposition

| Technique | Species | Size range (μm) | Time resolution | Sampling heights (m) | Successful measurements | Random error flux (%) | Reference |
|---|---|---|---|---|---|---|---|
| *Gradient measurements:* | | | | | | | |
| Filterpacks | $NO_3/SO_4$ | < ?[a] | 2 h | 24, 30, 35 | 39 | 75 | Duyzer *et al.* (1994) |
| Thermodenuders | $(NH_4)_2SO_4$ | < ?[a] | 30 min | 22, 26, 34 | 202 | 100 | Wyers *et al.* (1994) |
| Cyclone, PM-10 tunnel sampler | Na, K, Ca, Mg | <2.5; <10; total | 48 - 72 h | 21, 29, 35 | 30 | - | Hofschreuder *et al.* (1994) |
| *Eddy correlation:* | | | | | | | |
| Gerber | LWC | 3 - 45 | 1 s | 28 | 1637 | 20 | Wyers *et al.* (1994) |
| FSSP | Fog droplets | 1 - 95 | 15 min | 28 | 1637 | 50 | Wyers *et al.* (1994) |
| ASASP-x | Particles | 0.1 - 3 | 0.1 s | 18, 25 | ?[a] | 50 - 150 | Beswick *et al.* (1994) |
| *Accumulation experiments:* | | | | | | | |
| Accumulation on branches | $^{214}Pb$ | < 1 | 3 h | 18 | 26 | 60 | Wyers *et al.* (1994) |
| Washing of branches | $SO_4$ ... Mg | 0 - ∞ | days | 11, 15, 17, 19 | 13 | 60 | Römer and Te Winkel (1994) |
| DFM | Na, K, Ca, Mg | 0 - ∞ | 7 days | 21, 29, 35 | 14 | >25 | Hofschreuder *et al.* (1994) |
| Throughfall | $SO_4$ ... Mg | 0 - ∞ | max. 1 week | 1.5 | 30 | 30 | Van Leeuwen *et al.* (1994) |
| *Concentrations measurements:* | | | | | | | |
| Wet denuder | $HNO_3$, $HNO_2$, HCl, $SO_2$ | - | 1 h | 24 | 1000 | 15 | Wyers *et al.* (1994) |
| ADS | $SO_4$ ... Mg | < 2.5 | 24 h | 34 | 35 | 40 | Hofschreuder *et al.* (1994); Mennen (unpublished data) |
| | $HNO_3$, $HNO_2$, HCl, $SO_2$ | | 12 h | 21, 34 | 16 | 30 | |
| Aerosol sampler | $SO_4$ ... Mg | <2.5, 2.5-15 | 24 h | 26 | ~280 | 5 | Römer and Te Winkel (1994) |

[a] unknown or no estimate available

*Experimental determination of the acidifying aerosol and base cation input onto Speulder forest*

In this section experimental deposition estimates of acidifying aerosol and base cations onto the Speulder forest will be summarised. The results are described extensively in Erisman *et al.* (1994d) and in a series of publications in *Atmospheric Environment* (Erisman *et al.*, 1995; Hofschreuder *et al.*, 1995; Ruigrok *et al.*, 1995; Wyers and Duyzer, 1995; Draaijers *et al.*, 1995; Gallagher *et al.*, 1995). The project aimed at validation of different processes in the particle deposition model. Results of this validation are described in section 7.3.5. In this section an outline of the assessment of aerosol deposition based purely on the measurements will be attempted.

As was previously known, it is obvious from the experimental results that determining particle deposition with measurements is very difficult. Even the most direct measurement technique, the eddy correlation measurements, sometimes shows controversial results with a large uncertainty. The most important factors leading to uncertainty are the measuring errors, the uncertainty in representativeness of measurement size distribution, the scaling factors for accumulation experiments, the influence of chemical conversion and the influence of humidity on particle growth. In general, the results show a distinct influence of the size distribution and $u_*$ on the dry deposition velocity of particles. Figure 7.27 shows the relation between $V_d$ and $u_*$ for different experiments. The results are representative for different size distributions; see Table 7.22 (next section), showing $V_d$ ($^{214}$Pb) < $V_d$ ($SO_4$) < $V_d$ ($NO_3$) < $V_d$ (fog). $V_d$ of fog is proportional to $u_*^2$, indicating that impaction is the most important process determining $V_d$. Sedimentation is also important. $V_d$ values of other compounds are proportional to $u_*$ or a weak function of $u_*^x$, with $0 < x < 1$, indicating no distinct dominating process but rather a mixture of processes occurring simultaneously (Van Aalst, 1986).

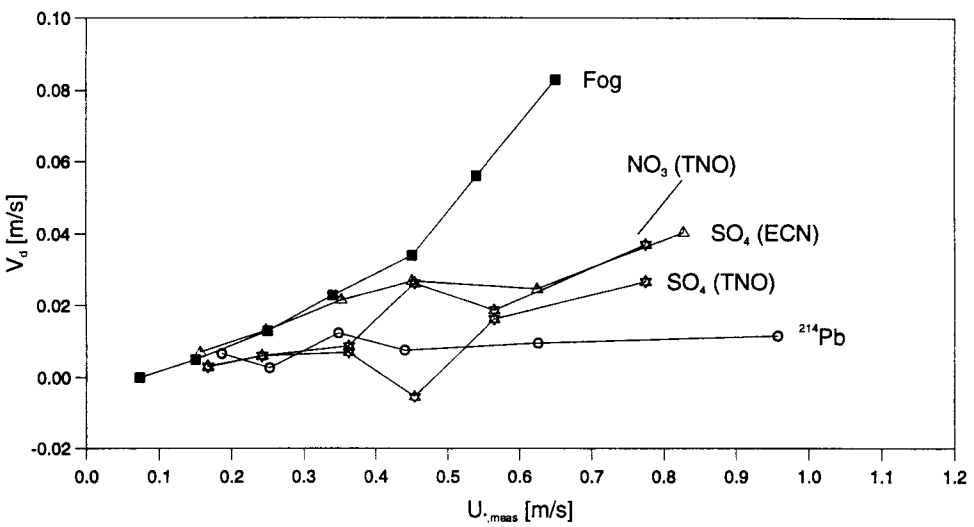


**FIGURE 7.27** Experimentally determined $V_d$ versus $u_*$. $V_d$ values were estimated at the following heights: fog at 28 m; $NO_3^-$ and $SO_4^{2-}$ (TNO) at 35 m; $SO_4^{2-}$ (ECN) at 22 m and $^{214}$Pb at 19 m.

Results are in line with other investigations, showing that particle deposition to forests can be considerable, with dry deposition velocities of several cm $s^{-1}$ (Hicks *et al.*, 1982; Waraghai and Gravenhorst, 1989; Sievering *et al.*, 1994). The relationships with $u_*$ found for different particle size classes provide confidence in the experimental results. This can only be

considered as an indication as errors in deposition estimates usually show a high correlation with $u_*$; this is because factors influencing the error in the deposition estimates are highly correlated to $u_*$.

*Modelling particle deposition*

A separate project dealing with modelling particle deposition was executed by KEMA (Ruijgrok *et al.*, 1994). First, the selection of the model and the sensitivity analysis for this project will be briefly described. Next, the results of the model evaluation with experimental results will be described and, finally, the suggested parametrisations will be discussed.

**TABLE 7.22** Characteristic features of some models describing the dry deposition of particles to vegetation and water surfaces (Ruijgrok *et al.*, 1994)

| Model | Surface | Type | Diameter range | Processes included in the model | | | | | | | |
|---|---|---|---|---|---|---|---|---|---|---|---|
| | | | | Turbulent transport | Sedimen-tation | Impaction | Intercep-tion | Brownian diffusion | Rebounce | Humidity growth | Capture by waves |
| Sehmel and Hodgson (1980) | any | A/I | $10^{-3}$-$10^{2}$ | + | + | and | and | + | - | - | - |
| Haynie (1986) | any | A | $10^{-3}$-$10^{2}$ | +• | + | + | - | + | - | - | - |
| Schack *et al.* (1985) | water/ vegetation | A | $10^{-3}$-$10^{2}$ | +• | + | and | and | and | - | - | - |
| Ibrahim *et al.* (1983) | snow/ forest | A | $10^{-3}$-$10^{2}$ | +• | +/- | + | + | + | - | - | - |
| Wiman and Ågren (1985) | forest | N | $10^{-3}$-$10^{2}$ | + | + | + | - | + | +/- | - | - |
| Peters and Eiden (1992) | forest | A/I | $10^{-3}$-$10^{2}$ | +• | + | + | + | + | - | - | - |
| Davidson *et al.*. (1982) | grass | N | $10^{-3}$-$10^{2}$ | +• | + | + | + | + | +/- | - | - |
| Legg and Price (1980) | vegetation | A/I | 10- $10^{2}$ | +• | - | - | - | - | - | - | - |
| Bache (1979) | vegetation | N | 10- $10^{2}$ | +• | + | + | - | - | - | - | - |
| Slinn (1982) | vegetation | A | $10^{-3}$-$10^{2}$ | +• | + | + | + | + | + | - | - |
| Slinn and Slinn (1980) | water | A | $10^{-3}$-$10^{2}$ | +• | + | + | + | + | - | + | - |
| Williams (1982) | water | A | $10^{-3}$-$10^{2}$ | +• | + | + | + | + | - | + | + |
| Hummelshøj *et al.* (1992) | water | A | $10^{-3}$-$10^{2}$ | +• | + | + | + | + | - | + | + |

| | | | |
|---|---|---|---|
| A | Analytical model | + | Mechanism included |
| N | Numerical model | - | Mechanism not included |
| A/I | Analytical with iterative solving for some parts | and | Mechanism included by empirical data |
| | | +/- | Mechanism considered, not included |
| | | • | Neutral conditions only |

Selection of models

A number of process-oriented particle deposition models were considered for an intercomparison study of models to measurement. The report by Ruijgrok *et al.* (1994) presents an overview of the models currently available for particle deposition. They consider

two types of models, i.e. process-oriented and bulk-resistance models. The main characteristics of different process-oriented models are given in Table 7.22.

Bulk resistance models describe deposition in terms of resistances or deposition velocities applied over the entire size range of depositing particles. The EMEP model uses a uniform value for $V_d$ of 0.1 cm $s^{-1}$ (Iversen *et al.*, 1991). In the TREND model the resistance analogy is used with an adapted value for $R_c$. Voldner *et al.* (1986) used the same method; however, in their model $R_b$+$R_c$ values were assumed to differ for receptor surfaces, seasons and day and night. Wesely *et al.* (1985) derived a parametrisation for $V_d$ on $u_*$. This relation was modified by Erisman (1993a) and used for mapping particle deposition in the Netherlands. The results of these different methods display large differences in $V_d$ (Ruijgrok *et al.*, 1994).

Current knowledge on the dry deposition process of particles is mainly qualitative. Only a small number of direct comparisons of particle deposition models with experimental data have been made. Results of most models, both process-oriented and bulk-resistance, indicate low values of $V_d$ for small particles. This also applies to the dry deposition over very rough surfaces such as forests. Current process-oriented models for particle deposition require too many (unknown) parameters and are too uncertain for mapping dry deposition over large areas. On the other hand, no well-established and validated bulk resistance model exists for particle deposition.

From these models, the Slinn model (1982) was selected based on following criteria: it had to include the main processes with fundamental process descriptions and vegetation characteristics. Furthermore, it had to be easy to implement. In order to improve the model, four additions were made to the model, i.e.: 1) inclusion of growth in particle size at high relative humidity; 2) gravitational settling and impaction to include the Cunningham slip correction factor; 3) correction factors in the flux profile relations to account for deviations found from the original Dyer and Hicks (1970) relationships above the Speulder forest (Bosveld, 1991; Westrate and Duyzer, 1994); and 4) along with size-specific deposition velocities, an integration of $V_d$ over the size distribution function, assuming values for *MMD* and the geometric standard deviation.

The uncertainty in model results was investigated using a Monte Carlo method (Janssen *et al.*, 1993). It was found that model results exhibit a large sensitivity to input conditions, especially for modelled $V_d$ in the submicron size range. The upper limit of the central 95% of variation around the median $V_d$ is several orders of magnitude larger than the lower limit. $V_d$ for acidifying aerosols, integrated over the entire particle size distribution, was found to range from 1 mm $s^{-1}$ to 5 cm $s^{-1}$. This range reflects natural variability (wind speed and roughness length) and uncertainty. For alkaline particles, in which most of the aerosol mass is concentrated between 1 and 20 μm, sensitivity to wind speed and roughness length is much

smaller than that for acidifying aerosols. However, ranges in $V_d$ are still substantial (Ruijgrok *et al.*, 1994).

Validation of the model using experiments
In order to simulate experimental results, the forest characteristics of the Speulder forest were estimated as accurately as possible. Ruijgrok *et al.* (1994) list the model input parameters used. Meteorological parameters such as wind speed, wind direction, Monin-Obukhov length, temperature and relative humidity were directly derived from measurements made in the Speulder forest. Model simulations were made for exactly the same times as for the micrometeorological experiments, and for the same measuring levels ($V_d$). For the results of accumulation experiments, averages over longer periods were calculated. To assess the model performance, the correspondence between modelled and measured values ($V_d$ or $F$) is expressed in four measures: the correlation coefficient ($R$), the fractional bias ($FBM$) of mean observed and calculated values, ($FBV$) of the variances of observed and calculated values and the normalised mean square error ($NMSE$), which is a standardised measure of deviation between observed and calculated values (Ruigrok *et al.*, 1994). These measures are further explained in Ruijgrok *et al.* (1994). The values of these measures for the different comparisons are summarised in Table 7.24. In this table, averages, standard deviations and test results showing significant differences are also given.

Size distributions for particles were determined using values from the literature, measurements of the distribution of $^{214}Pb$ (Wyers *et al.*, 1994), measurements of alkaline particles in three classes (Hofschreuder *et al.*, 1995), measurements of 24-h average particle concentrations in two classes (Römer and Te winkel, 1994) and from a dataset of the size distribution of acidifying aerosols in 1983 and 1984 (Wyers *et al.*, 1994). The distributions thus obtained and used by Ruijgrok *et al.* (1994) are listed in Table 7.23.
For each experiment model calculations were made using the modified Slinn (1982) model with forests characteristics estimated for the Speulder forest, size distributions from Table 7.23, actual meteorology and concentrations measured above the forest, and the exact periods the experiments lasted. The individual model results are compared to measurements in (Ruijgrok *et al.*, 1994).

The experimental work was aimed at evaluating different aspects or process descriptions of the model. Most processes in particle deposition differ in their dependency on particle size. The best way to evaluate individual processes is to use measurements representative of different particle size classes. As discussed in Ruijgrok *et al.* (1994), the size distribution for which experiments are representative are uncertain. Furthermore, uncertainty in measurement results is usually so large that it is difficult to draw conclusions from a comparison. The experiments done here for evaluation of the modelled deposition mechanisms can be divided into four categories:

- $^{214}Pb$ measurements and eddy correlation measurements of particle deposition representative for small particles with diameters smaller than 1 μm
- $NO_3^-$ and $SO_4^{2-}$ measurements representative for particles with a bimodal distribution, with most of the total mass under 1 μm
- measurements of total base cation deposition representative for large particles
- fog deposition measurements representative for large particles.

Even though the *MMD* for which the four categories are representative differ considerably, none of these is representative for a single deposition mechanism. All four are determined mainly by impaction and interception. Sedimentation may play an important role in fog deposition, depending on the size of droplets.

**TABLE 7.23** Component specific-size distributions (mass median diameter, *MMD*, and geometrical standard deviation, $\sigma_g$) derived from measurements in the Netherlands

| Component | *MMD* (μm) | $\sigma_g$ |
|---|---|---|
| $^{214}Pb$ | 0.35 | 2.0 |
| $Ca^{2+}$ | 7.73 | 3.47 |
| $Mg^{2+}$ | 5.92 | 2.73 |
| $K^+$ | 2.64 | 1.84 |
| $Na^+$ | 5.12 | 2.64 |
| $SO_4^{2-} < 2.5$ μm | 0.6 | 2.2 |
| $SO_4^{2-} > 2.5$ μm | 4.5 | 1.6 |
| $NH_4^+ < 2.5$ μm | 0.6 | 2.2 |
| $NH_4^+ > 2.5$ μm | 4.0 | 1.6 |
| $NO_3^- < 2.5$ μm | 0.6 | 2.3 |
| $NO_3^- > 2.5$ μm | 4.5 | 1.6 |
| Fog droplets (December) | 19.4 | |
| Fog droplets (February) | 7.4 | |

The next factor which is important for particle deposition is the friction velocity. Similar size dependencies and $u_*$ dependence of the dry-particle deposition velocity for the measurements and the model results, might serve as some sort of validation of the most determining processes. However, one has to be careful in drawing firm conclusions from such a comparison. Errors in deposition estimates usually show a high correlation with $u_*$, because factors influencing the error in the deposition estimates are highly correlated to $u_*$, e.g. the stability corrected gradient. For the $u_*$ dependence of $V_d$, Figures 7.27 and 7.28 need to be compared. In these figures, the measured or modelled $V_d$ is averaged for each class of $u_*$. For base cations, the $u_*$ dependence cannot be compared because only total fluxes have been compared. The figures show that the three other categories distinguished above show different dependencies on $u_*$, as might be expected. Furthermore, the figures show similar relations between $V_d$ and $u_*$ for the three categories, although the variation in measured $V_d$ per $u_*$ class can be very high.

Evaluation of the integral model results can only be done with statistical parameters, as displayed in Table 7.24, when the uncertainty in modelled and measured values is taken into account. The uncertainty in model results and the sensitivity of model results on input and model parameters has been extensively described in Ruijgrok *et al.* (1994). The overall random error in modelled $V_d$ integrated over the size distribution representative for acidifying aerosols (Table 7.23) is estimated at about 65% (Ruijgrok *et al.*, 1994). For base cations this error is somewhat smaller (60%) because of the contribution of the relatively well-parameterised description of sedimentation. The uncertainty in model estimates is lower than or about equal to the uncertainty in measurement results, with the exception of the fog deposition measurements, which are estimated to have smaller errors (20%). The fractional bias of the means (the relative difference between the mean calculated and observed values) falls within these limits (Table 7.24). The relatively large sensitivity of the model and an inaccuracy of the same order of magnitude in measuring results mean that a perfect 1:1 correspondence cannot be expected. Statistical testing of the difference between modelled and measured values is done using the non-paramatric sign and Wilcoxon tests for paired samples (Table 7.24). Both tests revealed no significant differences between the mean values of modelled and measured fluxes or $V_d$'s (Ruijgrok *et al.*, 1994). This is of course mainly the result of the large standard deviations in measuring and modelling results.

**TABLE 7.24** Model performance indicators[a] and averages for the different comparison studies

| Intercomparison | *R* | *FBM* | *FBV* | *NMSE* | $V_d$ model | σ model | $V_d$ meas. | σ meas. | *n* | Remarks[b] |
|---|---|---|---|---|---|---|---|---|---|---|
| Fog | 0.57 | 0.18 | 0.71 | 1.12 | 2.9 | 1.8 | 2.8 | 2.3 | 116 | |
| $^{214}Pb$ | 0.15 | -0.37 | -0.66 | 1.01 | 0.5 | 0.3 | 0.7 | 0.5 | 26 | ** & |
| $NO_3^-$ (filterpacks) | 0.55 | 0.02 | -1.06 | 1.75 | 1.2 | 1.1 | 1.2 | 1.9 | 23 | |
| $SO_4^{2-}$ (filterpacks) | 0.42 | 0.55 | -0.60 | 2.66 | 1.1 | 1.0 | 0.7 | 1.4 | 23 | |
| $SO_4^{2-}$ (thermodenuders) | 0.33 | -0.08 | -1.54 | 1.94 | 2.1 | 1.2 | 2.3 | 3.4 | 169 | |
| $Ca^{2+}$ (DFM, scaled) | 0.78 | 0.62 | 0.93 | 0.59 | 4.1 | 2.5 | 2.4 | 0.9 | 14 | |

[a] Perfect agreement if $R$=1, $FBM$=0, $FBV$=0, $NMSE$=0; no agreement if $R$=0, $|FBM|$=2, $|FBV|$=2, $|NMSE|$=∞

[b] Non-significant differences between mean calculated and measured values of $V_d$ (cm $s^{-1}$) are denoted with ** ($p$<0.05 in a Wilcoxon paired sample test); Non-significant (<95%) correlation coefficients ($R$) are denoted with and.

In conclusion, there are no strong indications for a significant underestimation or overestimation of the modelled $V_d$ compared to measured values. The fact that the model is reasonably capable of describing a response of $V_d$ to $u_*$ similar to the measurements for different particle diameters provides confidence in the process descriptions.

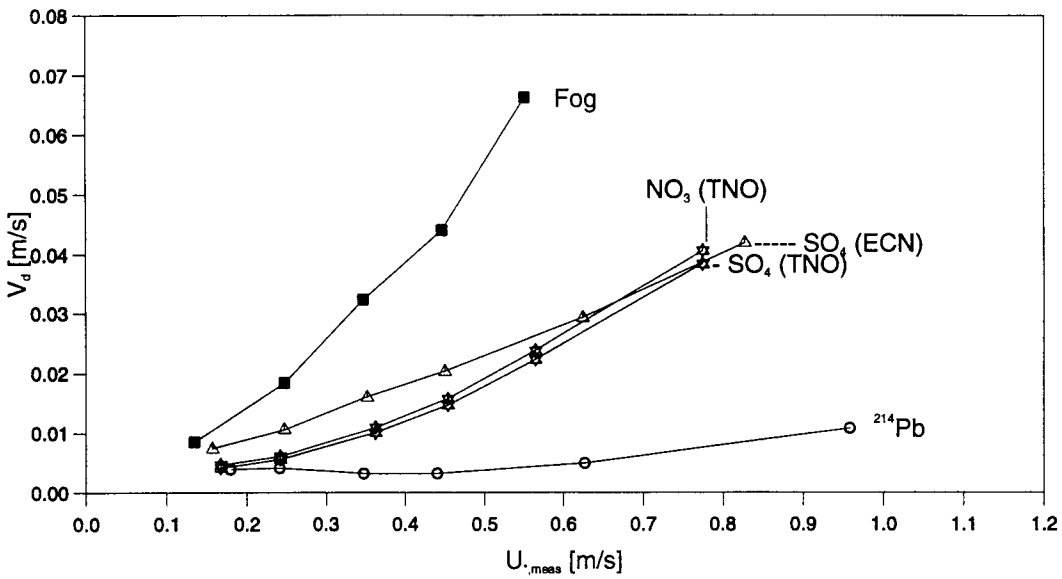


**FIGURE 7.28** Summary of modelled deposition velocities versus $u_*$. $V_d$ values were estimated at the following heights: fog at 28 m; $NO_3^-$ and $SO_4^{2-}$ (TNO) at 35 m; $SO_4^{2-}$ (ECN) at 22 m and $^{214}Pb$ at 19 m.

Validation of the model using accumulation experiments

Long-term experiments were executed to evaluate the balance of measured and modelled fluxes. It has been shown that most of the experiments at Speulder forest point in a similar direction regarding canopy exchange. Although the estimates of the absolute amounts of components retained or leached in the canopy may differ depending on experiment, the average values (Table 7.25) give a good picture of the situation at Speulder forest. The table shows that $H^+$ is taken up by the canopy, which is accompanied by leaching of $Mg^{2+}$, $Ca^{2+}$ and most of all $K^+$. $SO_2$ taken up by stomata is eventually leached again, whereas $NH_3$ taken up via stomata is almost completely retained by the canopy. Oxidised nitrogen components are taken up by the canopy, especially $NO_2$. Whether $NO_3^-$ and $NH_4^+$ aerosols are taken up directly or via solution is uncertain. We assume from the results of the experiments that $NO_3^-$ uptake is negligibly small, whereas $NH_4^+$ is taken up in exchange for $K^+$ or $Ca^{2+}$. $Na^+$ and $Cl^-$ are considered inert. The highest uncertainty in canopy exchange estimates relates to estimates of the nitrogen components and $Ca^{2+}$ and $Mg^{2+}$.

Observed differences between dry and fog deposition estimates from micrometeorological measurements and inferential modelling on the one hand and net throughfall fluxes on the other cannot be regarded exclusively due to canopy exchange. Dry deposition estimates from micrometeorological measurements and inferential modelling are uncertain through errors in

the air concentration measurements (Arends *et al.*, (1994), their sometimes low time coverage and the uncertainties associated with the parametrisation of the dry deposition velocities (Erisman *et al.*, 1994; Ruijgrok *et al*, 1994). Fog deposition estimates are uncertain due to uncertainties associated with the estimation of water fluxes and the measurement of the average chemical composition of the fog droplets (Vermeulen *et al.*, 1994). Uncertainties associated with the throughfall method when used for estimating dry and fog deposition include the dry deposition to the forest floor and understorey vegetation, dry deposition directly onto the throughfall gutters, the representativeness of the throughfall sampling, the wet deposition estimate, the stemflow contribution and canopy exchange processes (Draaijers and Erisman, 1993). With canopy exchange processes being the only exception, aforementioned factors probably contributed only to a very small extent to the uncertainty in the throughfall dry and fog deposition estimates in this study.

**TABLE 7.25** Average uptake and leaching amounts at the Speulder forest derived from field experiments and modelling (mol $ha^{-1}$ $a^{-1}$) (Draaijers *et al.*, 1994)

| Component | Uptake | Leaching |
|---|---|---|
| $SO_2$ | 35 | 0 |
| $SO_4^{2-}$ | 0 | 80 |
| $NO_2$ | 115 | 0 |
| $HNO_2$ | 15 | 0 |
| $HNO_3$ | 0 | 0 |
| $NO_3^-$ | 0 | 0 |
| $NH_3$ | 140 | 0 |
| $NH_4^+$ | 115 | 0 |
| $Na^+$ | 0 | 0 |
| $Cl^-$ | 0 | 0 |
| $Mg^{2+}$ | 0 | 40 |
| $Ca^{2+}$ | 0 | 50-75 |
| $K^+$ | 0 | 250 |
| $H^+$ | 190 | 0 |

## 7.3.6 ANNUAL AVERAGE GAS AND PARTICLE DEPOSITION AND CHANGES WITH TIME

Meteorological data and dry deposition data for $SO_2$, $NH_3$ and $NO_2$ were available from the continuous gradient and eddy correlation measurements for quantifying the input of acidifying gases and aerosols, and base cations, onto the Speulder forest (section 7.3.4, Erisman *et al.*, 1993a,b,d; Wyers *et al.*, 1993). Annual averages were determined by averaging the dry deposition parameters for the selected periods and those derived by the surface resistance parametrisation, concentration and meteorological data for the rejected periods. Particle input of acidifying aerosols and base cations, and fog-water deposition were estimated using measurements of concentrations, meteorological parameters and model results (section 7.3.5, Erisman *et al.*, 1994). Wet deposition is estimated using interpolated values from the National Air Quality Monitoring Network (e.g. RIVM, 1993). Table 7.26 summarises the results of the experiments and model calculations regarding fluxes of different compounds. In this table measurements and flux estimates made at the Speulder forest site during the first and second phase of the Dutch Programme on Acidification are also listed. These data have been taken from Van Aalst and Erisman (1991) and Duyzer *et al.* (1994). The estimates of the canopy uptake reflect the needle uptake of gases ($SO_2$, $NH_3$ and $NO_2$) through stomata and the uptake through cuticles from the water layer covering the needle surface. This is not the net uptake, because part of this flux might be leached or evaporated again. Above-ground uptake and leaching by the canopy (Table 7.25) was estimated by Draaijers *et al.* (1994) by *i)* comparing atmospheric deposition estimates with throughfall fluxes, *ii)* applying several canopy budget models; *iii)* comparing deposition estimates from surface wash experiments using real and artificial Douglas fir twigs and *iv)* using results from a $S^{35}$ nutrition experiment. Stomatal uptake of gases was estimated from concentration measurements and the stomatal conductance model of Bosveld and Bouten (1992).

**TABLE 7.26** Average fluxes at Speulder forest in 1987-1993 (mol $ha^{-1}$ $a^{-1}$)

| Compound | Year | Measurements and inferential modelling | Throughfall measurements[b] | Canopy uptake | Canopy leaching |
|---|---|---|---|---|---|
| SOx: | 1987 | | 1180 | | |
| ($SO_2$, $SO_4^{2-}$, wet $SO_4^{2-}$) | 1988 | 1220[c] | 1120 | | |
| | 1989 | 980[c] | 1020 | | |
| | 1992/1993 | 1180 | 1090 | 35 | 80 |
| NHx: | 1987 | | 2870 | | |
| ( $NH_3$, $NH_4^+$, wet $NH_4^+$) | 1988 | 2975[c] | 2740 | | |
| | 1989 | 2910[c] | 2630 | | |
| | 1992/1993 | 2865[a] | 2560 | 255 | 0 |
| NOy: | 1987 | | 820 | | |
| ($NO_2$, $HNO_2$ , $HNO_3$, | 1988 | 1105[c] | 720 | | |
| $NO_3^-$, wet $NO_3^-$) | 1989 | 1235[c] | 820 | | |
| | 1992/1993 | 1080 | 770 | 130 | 0 |
| $Cl^-$ | 1987 | | 1060 | | |
| | 1988 | | 1640 | | |
| | 1989 | | 1090 | | |
| | 1992/1993 | 1425 | 1290 | 0 | 0 |
| $Na^+$ | 1987 | | 850 | | |
| | 1988 | | 1160 | | |
| | 1989 | | 770 | | |
| | 1992/1993 | 1065 | 1040 | 0 | 0 |
| $Ca^{2+}$ | 1987 | | 380 | | |
| | 1988 | | 280 | | |
| | 1989 | | 250 | | |
| | 1992/1993 | 145 | 200 | 0 | 50-75 |
| $Mg^{2+}$ | 1987 | | 240 | | |
| | 1988 | | 310 | | |
| | 1989 | | 220 | | |
| | 1992/1993 | 190 | 270 | 0 | 0-40 |
| $K^+$ | 1987 | | 70 | | |
| | 1988 | | 40 | | |
| | 1989 | | 40 | | |
| | 1992/1993 | 75 | 80 | 0 | 270 |

[a] Net-flux, emissions accounted for (see text)

[b] Data are in very good agreement with KUN measurements (Boxman, 1994, personal communication). Throughfall is corrected for canopy exchange with a model as described by Draaijers *et al.* (1994).

[c] Data derived from Van Aalst and Erisman (1991); particle fluxes corrected for the underestimated $V_d$ of particles (see section 7.3.5).

Measurements of atmospheric loads and throughfall for the years before 1987 are not available. Deposition estimates for the acidifying components for the years between 1980 and 1987 are available from the DEADM model (Chapter 5, Erisman, 1993a) and presented in Table 7.27, along with estimates for the deposition before 1980. These are based on the data for 1980, scaled by the ratio of the deposition in the Netherlands between 1950 and 1980

estimated by the DAS model on the basis of emissions in these years (De Boer and Thomas, 1991). Deposition estimates for base cations are not available for the years before 1993.

**TABLE 7.27** Estimates of the deposition of acidifying components between 1950 and 1994 for the Speulder forest site (mol $ha^{-1}$ $a^{-1}$)

| Year | SOx | NHx | NOy | Total nitrogen | Potential acid |
|---|---|---|---|---|---|
| 1950 | 1700 | 1350 | 740 | 2090 | 5490 |
| 1955 | 2230 | 1410 | 770 | 2180 | 6640 |
| 1960 | 2320 | 1600 | 870 | 2470 | 7110 |
| 1965 | 3100 | 1790 | 980 | 2770 | 8970 |
| 1970 | 2710 | 2180 | 1190 | 3370 | 8790 |
| 1975 | 2030 | 2630 | 1440 | 4070 | 8130 |
| 1980 | 1940 | 2690 | 1470 | 4160 | 8040 |
| 1981 | 1940 | 2560 | 1600 | 4160 | 8040 |
| 1982 | 1700 | 2580 | 1540 | 4120 | 7520 |
| 1983 | 1510 | 2780 | 1560 | 4340 | 7360 |
| 1984 | 1590 | 2690 | 1580 | 4270 | 7450 |
| 1985 | 1530 | 2740 | 1560 | 4300 | 7360 |
| 1986 | 1570 | 2600 | 1470 | 4070 | 7210 |
| 1987 | 1190 | 2970 | 1490 | 4460 | 6840 |
| 1988 | 1220 | 2980 | 1110 | 4080 | 6520 |
| 1989 | 980 | 2910 | 1240 | 4150 | 6110 |
| 1990 | 1170 | 2830 | 1220 | 4050 | 6390 |
| 1991 | 1080 | 2820 | 1190 | 4010 | 6170 |
| 1992 | 1080 | 2890 | 1240 | 4130 | 6290 |
| 1993 | 1040 | 2740 | 1200 | 3940 | 6020 |

From Table 7.27 it is obvious that the highest input of potential acid was in the seventies. After 1965 the acid input gradually decreased from 9000 to 6000 mol $ha^{-1}$ $a^{-1}$. The nitrogen input increased from 1950 to 1987. In 1987 a maximum nitrogen input of 4500 mol $ha^{-1}$ $a^{-1}$ (63 kg $ha^{-1}$) was reached. After 1987 the nitrogen input decreased to 3900 mol $ha^{-1}$ $a^{-1}$ (~55 kg $ha^{-1}$). Throughfall measurements of $NH_4^+$ and $NO_3^-$ made between 1988 and 1993 show a slight decrease in soil N load (Table 7.26). The main contribution to the nitrogen input is formed by ammonia and ammonium (70%). Throughfall fluxes of base cations show strong year-to-year variation. Base cation input is mainly the result of dust emissions from nearby roads and emissions due to industrial and agricultural activities. The input of sodium is determined by sea salt deposition. High input occurs during periods with high wind speeds from a westerly or south-westerly direction.

## 7.3.7 ASSESSMENT OF THE EFFECTS OF ACIDIFICATION, EUTROPHICATION AND OZONE

*Critical levels and loads at the Speulder forest site*
Generally, critical levels are expressed in terms of exposure ($\mu g\ m^{-3}$ and exposure duration) while critical loads are expressed in terms of deposition (mol $ha^{-1}\ a^{-1}$ or kg $ha^{-1}\ a^{-1}$). Critical levels focus on no-effect thresholds for short-term exposures (one year or less) and critical loads focus on safe deposition quantities for the long term (10-100 years). Critical levels and loads are not aimed to completely protect vegetation against adverse effects. No-effect levels and loads are usually higher and lower than the critical level or loads, respectively (Steingröver *et al.*, 1995). Exceedances are determined by estimating the difference between actual levels and loads, and critical levels and loads, for the time and scales that the critical values were estimated.

Critical levels
In order to assess critical levels, information is needed on quantitative relationships between exposure and effect. In many cases this information is not available or based on only few experiments and therefore rather speculative. Specific critical levels for the Speulder forest can not be assessed with current knowledge.

*$SO_2$* In order to prevent visual damage (leaf discoloration and/or loss) to coniferous and deciduous forests on poor sandy soils the annual, daily and hourly average $SO_2$ concentration should not be higher than 25 $\mu g\ m^{-3}$, 70 $\mu g\ m^{-3}$ and 150 $\mu g\ m^{-3}$, respectively (Heij and Schneider, 1991; Table 7.28). Van der Eerden (1995) mentions a critical level of 20 $\mu g\ m^{-3}$ (winter and annual mean).

*NOx* To prevent effects on photosynthesis and growth, for example, the critical level for $NO_x$ (NO and $NO_2$, added in ppb and expressed as $NO_2$ in $\mu g\ m^{-3}$) is set to 30 $\mu g\ m^{-3}$ as an annual mean, and 75 $\mu g\ m^{-3}$ as a 24-h mean (Van der Eerden *et al.*, 1995). Interactive effects between $NO_2$ and $O_3$ and/or $SO_2$ have been reported frequently, but the lowest effective levels for $NO_2$ are about equal to those for combination effects. Generally, at concentrations near to its effect threshold, $NO_2$ causes growth stimulation if $NO_2$ is the only pollutant, while in combination with $SO_2$ and/or $O_3$ it results in growth inhibition (Van der Eerden, 1995).

*$NH_3$* Exposure to high $NH_3$ concentrations (>180 $\mu g\ m^{-3}$) or high $NH_4^+$ concentrations in canopy surface water (>5 mmol $l^{-1}$) is found to damage the crystalline structure of the epicuticular wax layer of the needles of Douglas fir (Van der Eerden *et al.*, 1992). Critical levels for adverse effects of $NH_3$ on plants were estimated by Van der Eerden *et al.* (1991). To protect 95% of the species at $p<0.05$ a 24-h and annual mean of 270 and 8 $\mu g\ m^{-3}$, respectively, was estimated.

*$O_3$* Recently, a threshold value for $O_3$ for forest ecosystems was set at 40 ppb. As a provisional critical level, an *AOT* (Accumulative exposure Over a Threshold concentration) has been defined. The *AOT40* represents the summed hourly concentrations in the growing season (April-September) with concentrations above 40 ppb (Fuhrer and Achermann, 1994). To protect 95% of the tree species against a growth reduction of more than 10%, the AOT40 should be lower than 10 ppm h (Van der Eerden, 1995). This *AOT40* value was derived from $O_3$ exposure experiments using juvenile trees in open-top chambers.

**TABLE 7.28** Critical levels for forests in Europe

| Gas | Effects | Critical level | Reference |
|---|---|---|---|
| $SO_2$ | Visual damage | yearly average: 20-25 μg $m^{-3}$<br>daily average: 70 μg $m^{-3}$<br>hourly average : 150 μg $m^{-3}$ | Schneider and Bresser (1988);<br>Van der Eerden (1995) |
| $NO_x$ | Photosynthesis and growth reduction | annual average: 30 μg $m^{-3}$<br>daily average: 75 μg $m^{-3}$ | Van der Eerden *et al.* (1994) |
| $NH_3$ | 95% of the species protected | hourly average: 3300 μg $m^{-3}$<br>daily average: 270 μg $m^{-3}$<br>monthly average: 23 μg $m^{-3}$<br>yearly average: 8 μg $m^{-3}$ | Van der Eerden *et al.* (1991) |
| | Damage to epicuticilar wax layer | $NH_3$ in air > 180 μg $m^{-3}$<br>$NH_4^+$ in water layer > 5 mmol $l^{-1}$ | Van der Eerden *et al.* (1992) |
| $O_3$ | Biomass reduction > 10% | AOT40 (growing season) = 10 ppm h | Fuhrer and Achermann (1994) |

Critical loads

Critical loads for acidity for the Speulder forest were derived using the steady-state mass balance model of De Vries (1993). The equations, basic assumptions and values used to estimate the critical loads are given in Erisman *et al.* (1995). It is of importance to notice that the newest insights are used to estimate the critical loads of acidity, i.e. a critical $Al^{3+}/(Ca^{2+} + Mg^{2+} + K^+)$ ratio of 1.0 mol $mol^{-1}$ for coniferous forest and 3.3 mol $mol^{-1}$ for Douglas fir is used instead of the usually used $Al^{3+}/Ca^{2+}$ ratio of 1.5 mol $mol^{-1}$. These ratios are also used for the root damage criteria instead of a critical $Al^{3+}$ concentration. The critical load values of acidity for the Speulder forest are listed in Table 7.29.

Critical acid loads for the Speulder forest are about 100% larger than average critical acid loads derived for coniferous forests on sandy soils in the Netherlands found by de Vries and Kros (1991) because of *i)* the different criteria used: $Al^{3+}/(Ca^{2+}+Mg^{2+}+K^+)$ ratio instead of $Al^{3+}/Ca^{2+}$ ratio, and $Al^{3+}$ concentration, *ii)* the high weathering rate at Speulder forest and *iii)* the high values for N uptake (actually, one should use values at critical N loads and not the current value).

**TABLE 7.29** Critical acid loads for Speulder forest based on different effects (mol $ha^{-1}$ $a^{-1}$)

| Effects | Criteria | Critical load |
|---|---|---|
| Inhibition of uptake/root damage | $Al^{3+}/(Ca^{2+} + Mg^{2+} + K^{+}) = 1.0$ mol $mol^{-1}$ | 2760[a] |
| | $Al^{3+}/(Ca^{2+} + Mg^{2+} + K^{+}) = 3.3$ mol $mol^{-1}$ | 5990 |
| $Al^{3+}$ depletion | $\delta Al(OH)_3 = 0$ mol $kg^{-1}$ | 2725 |
| $Al^{3+}$ pollution | $Al^{3+} = 0.02$ mol $m^{-3}$ | 915 |

[a] Using a critical molar $Al^{3+}/Ca^{2+}$ ratio of 1.0 yields a value of 1860 mol $ha^{-1}$ $a^{-1}$. A critical $Al^{3+}$ concentration, often used in critical load calculations to date, leads to a critical acid load of 1970 mol $ha^{-1}$ $a^{-1}$.

The critical N loads for the Speulder forest related to vegetation changes, increased sensitivity and $NO_3$ pollution of the groundwater were also derived with the steady-state mass balance model according to De Vries (1993). The derivation of the critical N loads is also given in De Vries (1993) and for Speulder forest in Erisman *et al.* (1995). Critical loads for N are listed in Table 7.30.

**TABLE 7.30** Critical N loads for Speulder forest based on different effects (mol $ha^{-1}$ $a^{-1}$)

| Effects | Criteria | Critical load |
|---|---|---|
| Vegetation changes | N = 0.1 mol $m^{-3}$ | 810 |
| Increased sensitivity | N = 1.8% | 1500 |
| $NO_3^-$ pollution | $NO_3^- = 0.4$-$0.8$ mol $m^{-3}$ | 1950-3190 |
| Inhibition of uptake[a] | $NH_4^+/K^+ = 5$ mol $mol^{-1}$ | 2460 |

[a] Refers to $NH_3$ only

The critical load for ammonia, related to the occurrence of nutrient imbalances in the soil solution, was also calculated with a steady-state model according to De Vries (1993). This critical load is also listed in Table 7.30. The critical $NH_3$ load derived for the Speulder forest is approximately three times as large as the lower value given by Bobbink *et al.* (1992) for coniferous forest growing on non-calcareous sandy soils in the Netherlands (800 mol $ha^{-1}$ $a^{-1}$). The latter value was derived in an experiment with trees with elevated N/K ratios in needles, as compared to those at critical loads, and a soil with very low (negligible) nitrification rate. For soils with increased cation rates, Bobbink *et al.* (1994) reports values up to 4000 mol $ha^{-1}$ $a^{-1}$.

Uncertainties in critical loads are due to uncertainties in the calculation method, the critical chemical values and criteria used, and the input data. The largest uncertainties in critical (acid) loads are likely to be due to the uncertainties in critical chemical values. Whether one uses a critical $Al^{3+}/(Ca^{2+}+Mg^{2+}+K^{+})$ ratio of 1.0 (for coniferous forest) or 3.3 mol $mol^{-1}$ (for Douglas fir) will change the critical acid load from less than 3000 to about 6000 mol $ha^{-1}$ $a^{-1}$. Furthermore, the uncertainties in input data may also lead to large uncertainties in the critical loads. The estimated weathering rate at the Speulder forest, for example, is based on an input - output budget and includes cation exchange as well. Generally, average weathering rates for

acid sandy soils are estimated at 200 mol $ha^{-1}$ $a^{-1}$, which is much lower than the value of 550 mol $ha^{-1}$ $a^{-1}$ used for Speulder forest. Furthermore, one has to be aware that the critical loads previously derived are all based on present data with respect to dry deposition, weathering, uptake, litterfall and throughfall. Actually one should use the values at critical loads. Elevated present N uptake rates cause an increase in critical loads for N and acidity, whereas elevated N/K ratios in needles decrease the critical load for $NH_3$ related to inhibition of uptake. In general, the uncertainty in criteria and input data may cause an uncertainty of more than 50% in most of the critical loads derived.

*Effect parameters and observed effects*

What are the effect parameters?
Before answering the question on what the observed effects are, we need to define what we mean by effects and what kind of effect parameters are taken into account. Effects are defined as ecosystem changes as a result of environmental impacts/stress. In general, direct and indirect effects are distinguished. Direct effects are the result of exposure to air pollutants, whereas indirect effects are the result of soil loads and changes in soil solution. On the other hand, direct and indirect effects are sometimes distinguished according to the time between cause and observed effect (i.e. effects on photosynthesis versus effects on growth).

In practice, the health (vitality) of trees and of entire forest ecosystems is their capacity to cope with stress: not only the result of the occurrence of air pollution but also natural stresses caused by changes in environmental conditions (drought, frost, windthrow, pests, diseases, etc.). Usually, it is difficult to derive mono-causal relations from the multiple stress to which forests are exposed.

An overview of possible effects on forests as a result of increased atmospheric acid and nitrogen deposition and/or exposure to air pollutants is presented in Table 7.31. Based on the processes and effects mentioned in this table, three ecosystem compartments can be distinguished: the trees, the understorey and the soil and litter layer. In these compartments we can distinguish between several effect indicators or parameters, which will be used to relate changes to environmental stresses. For the trees we distinguish growth, photosynthesis, transpiration and water stress, the nutrient composition of needles and vitality; for the understorey changes in composition of flora and fauna, and for the soil and humus layer we distinguish parameters such as water and nutrient fluxes, root and mycorrhiza parameters. The increased atmospheric acid and nitrogen load and air pollutant concentrations lead to changes in the aforementioned effect parameters and/or changes in sensitivity and thus increase the risk of damage due, for example, to plagues, diseases, storms, drought and frost sensitivity.

The changes in the effect parameters (underlined in Table 7.31) in the Speulder forest during the research period are discussed and evaluated in Erisman *et al.* (1995). Here the outcome will only be used in a synthesis.

**TABLE 7.31** Possible effects on forest ecosystems of increased atmospheric N+S loading and exposure to $SO_2$, NOx, $NH_3$ and/or $O_3$. Effect parameters are underlined.

| Ecosystem compartment | Effects chemistry | Ecosystem |
|---|---|---|
| Trees (including foliage and roots) | proton accumulation in foliage | - damage of epicuticular wax layer of foliage |
| | $O_3$ | - decrease of photosynthesis and respiration |
| | $SO_2$, $O_3$ , $NH_3$ | - enhanced transpiration and drought sensitivity by elevated stomatal control |
| | elevated N contents in foliage | - increased frost sensitivity<br>- increased parasite injury (insects, fungi, virus)<br>- increased ratio of foliage to roots (risk of drought and nutrient deficiency)<br>- increased biomass production<br>- increased water demand<br>- increased cell size in stems |
| | elevated arginine concentration | - growth reduction |
| | nutrient deficiency absolute or relative (to N) | - discoloration (defoliation) |
| Soil (solution) | elevated N contents in soil | - increase in nitrophilus species<br>- decrease in biodiversity |
| | depletion of secondary Al compounds | - possible root damage by pH decrease and nutrient deficiencies |
| | elevated concentrations (leaching) of H + Al | - root damage<br>- mycorrhiza decline |
| | elevated ratios of $NH_4$ and $Al^{3+}$ to base cations | - inhibition of uptake (nutrient deficiency) |

*Synthesis*

Exceedance of critical levels

At the Speulder forest critical levels for $SO_2$ were exceeded from 1955 up to 1975. In this period, annual average $SO_2$ concentrations were above 25 $\mu g\ m^{-3}$. From 1975 onwards, annual average $SO_2$ concentrations at the Speulder forest were lower than the critical level, and decreasing steadily. However, daily and hourly average critical levels of $SO_2$ may still have been exceeded during periods of winter smog. Annual average NOx concentrations at the Speulder forest have, since 1950, always been lower than the critical levels. As for $SO_2$, daily average critical levels of NOx may have been exceeded during smog periods. The critical levels for $NH_3$ probably have not been exceeded at the Speulder forest. The highest annual

mean concentration at the forest was estimated to be 4 $\mu g\ m^{-3}$ (Erisman *et al.*, 1995) whereas 24-h means never exceeded 10 $\mu g\ m^{-3}$ (Wyers *et al.*, 1993; Vermetten *et al.*, 1991). Concentrations of $NH_4^+$ observed in sequentially sampled throughfall water at the Speulder forest were as high as 4 $mmol\ l^{-1}$ (Van Leeuwen and Bleuten, 1994). As dilution of the water films covering the needle surface occurs during the wash-off process, it is likely that the foliage is exposed to larger concentrations than those measured in throughfall, thereby probably close to or even exceeding critical levels. The *AOT40* for $O_3$ has been exceeded since measurements started in 1979 and have probably been exceeded since planting the forest 33 years ago.

There is no hard evidence that the direct effects found at Speuld related to air pollutant exposure result in a significant decrease in vitality and or sustainability of the trees. Critical levels of $O_3$ have been exceeded continuously since $O_3$ measurements started in 1979. In 1992, total assimilation was reduced by 2.5%-7% at an *AOT40* of 39.1 ppm h. In 1993 the reduction found was approximately twice as large at an *AOT40* of 23.8 ppm h (Steingröver and Jans, 1995). Van der Eerden (1995) suggests that the *AOT40* of 10 ppm h set to protect tree species against a growth reduction of more than 10% may be too small. Mature trees under field conditions may have some kind of feedback mechanism through which they can cope with larger $O_3$ concentrations compared to juvenile trees in open-top chambers. Comparison of 3-, 17- and 33-year old trees at the Speulder forest revealed that the youngest trees had relatively more reactive stomata and thus were more sensitive to ozone and vapour pressure deficits (Steingröver and Jans, 1995). This is in agreement with findings of Colls *et al.* (1993) and Pleijel *et al.* (1993). No direct effects of $SO_2$ and $NO_2$ were observed. This agrees with the observation that critical levels of these components have not been exceeded. Critical levels for $NH_3$ have not been exceeded either. Occasionally, $NH_3$ was found to stimulate the net assimilation rate. Exposure to high $O_3$ and/or high $NH_3$ concentrations was suggested as the cause of stomata remaining open even at low shoot-water potentials and/or high vapour pressure deficits, through which trees become more vulnerable to drought. $NH_4^+$ concentrations in water layers covering the needle surface were sometimes (especially after long dry periods and/or during fog episodes) such that damage of the epicuticular wax layer was likely to occur. Such effects have, however, not been investigated at Speulder forest.

Exceedance of critical loads

The critical loads related to most effects are exceeded since planting the trees some 33 years ago. Table 7.32 gives information on the exceedances of the critical loads and whether the effects related to these exceedances have been observed at Speulder forest. Comparison of current acid loads (ca. 6000 $mol\ ha^{-1}\ a^{-1}$; Table 7.27) with critical acid loads (Table 7.29) shows that the critical loads are exceeded since the trees were planted, especially those related to the pollution of phreatic groundwater (see Table 7.32). The critical load for inhibition of uptake and root damage are exceeded since planting whenever both a critical $Al^{3+}/(Ca^{2+}+Mg^{2+}+K^+)$ ration of 1.0 $mol\ mol^{-1}$ is used and when the value for Douglas fir is used (3.3 $mol\ mol^{-1}$).

Comparison of current N loads (ca 3900 mol $ha^{-1}$ $a^{-1}$) with critical N loads (Table 7.26) shows that $NO_3^-$ pollution above the EC drinking-water standard may occur in the long term when N immobilisation becomes negligible. The exceedance of N loads related to vegetation changes is irrelevant for this production forest because it is a monoculture with no understorey vegetation. The critical load for increased sensitivity is exceeded since the trees were planted. The critical load for inhibition of uptake ($NH_3$) is also exceeded since the trees were palnted, but only by a few hundreds of moles. This is due to the relatively high nitrification rate at the Speulder forest. The present N input does, however, not preclude nutrient imbalances in the foliage. It may cause too high N contents related to $Ca^{2+}$, $Mg^{2+}$ and/or $K^+$.

**TABLE 7.32** Critical loads, exceedances and effects observed at Speulder forest

| Effects | Criteria | Exceedance[b] | Observed effects at Speulder forest |
|---|---|---|---|
| Inhibition of uptake/root damage | $Al^{3+}/(Ca^{2+}+Mg^{2+}+K^+) = 1.0$ mol $mol^{-1}$ | always | inhibition of base cation and phosphorus uptake; decrease in mycorrhiza |
| | $Al^{3+}/(Ca^{2+}+Mg^{2+}+K^+) = 3.3$ mol $mol^{-1}$ | always | |
| $Al^{3+}$ depletion | $\delta Al(OH)_3 = 0$ mol $kg^{-1}$ | always | aluminium depletion |
| $Al^{3+}$ pollution | $Al^{3+} = 0.02$ mol $m^{-3}$ | always | aluminium leaching |
| Vegetation changes | $N = 0.1$ mol $m^{-3}$ | always | non, no understorey |
| Increased sensitivity to drought, storms, frost and fungal diseases | N = 1.8% | always | large growth stimulation; high foliage N concentration and N/K ratio (frost, fungal diseases); high foliage/fine root ratio high water demand; high foliage/coarse root ratio (-> storms) |
| $NO_3^-$ pollution of groundwater | $NO_3^- = 0.4$-$0.8$ mol $m^{-3}$ | always - 1970 | decrease in mycorrhiza; nitrogen saturation; nitrate leaching |
| Inhibition of uptake[a] | $NH_4^+/K^+ = 5$ mol $mol^{-1}$ | always | P, K , N/P and N/Mg deficient, increase in arginine |

[a] Refers to $NH_3$ only
[b] Always refers to 'since the plantation of the forest in 1961'

There are several uncertainties associated with the estimates of exposure and loads, but also with the estimates of the critical levels and loads (De Vries, 1995; Erisman *et al.*, 1995). Furthermore, critical loads should evolve during time, which is not taken into account. This might all have an effect on the exceedance and thus the determination whether the forest is at risk or which effects are expected. The critical loads are defined in such a way that there is an increased risk when both the exceedance or the time of exceedance increases. The expected effects related to exceedance and exceedance time are thus related to $Al^{3+}$ depletion and leaching, deviation from optimal growth, increased sensitivity to drought, storms, frost and fungal diseases, and to some extent to inhibition of uptake and root damage. Considering the changes in effect parameters, it can be concluded that the evolution of loads at the Speulder

forest has already lead to *i)* a decrease in mycorrhiza through which base cation and phosphorus uptake is inhibited, leading to a relative base cation and phosphorus deficiency in the foliage, *ii)* a high foliage/fine root and foliage/coarse root ratio through which the forest becomes increasingly sensitive to drought and windthrow; *iii)* depletion of readily available $Al^{3+}$ compounds, causing a further pH decline in the future (De Vries, 1993), and *iv)* leaching of $Al^{3+}$ and $NO_3^-$ to the groundwater. It can thus be concluded that the critical load exceedances and the related effects are indeed to a some extent observed.

Despite these effects, the Speulder forest grows well and can be classified as moderately vital, using needle loss and needle discoloration as vitality parameters (Steingröver and Jans, 1994). Compared to other Dutch forests in the Netherlands, the vitality of the trees at the Speulder forest decreased from 1986 to 1994. Besides the postponed thinning, the gradual decline of the nutrient status of the trees may be the cause for this. The N content in the needles is at its optimum for biomass production, but indications of excess N were found: poor mycorrhization, high foliage/fine root ratios and high arginine contents in the needles. The foliage/fine root ratio and arginine content exceeded the values found in clean areas by a factor 2 and 5-10, respectively.

No relation was found between the vitality class of an individual tree and its total needle surface area (Steingröver and Jans, 1995), suggesting that, at least at the Speulder forest, needle loss is not a good indicator of tree vitality. There is a natural variation in tree vitality in monoculture forests as a result of local stand conditions (soil, soil water potential, mychorriza, etc.) and genetic differences. Local stand conditions are very variable at Speulder forest (see section 7.3.4). The ecological principle of competition assumes that all organisms in a forest differ genetically in resistance and susceptibility to all types of stress (Woodman and Cowling, 1987). This natural variation in forest condition makes it difficult to detect additional changes induced, for example, by airborne chemicals.

Reference situation

Effects may also be hard to detect because of a lack of a reference: how would the Speulder forest look if it had not been exposed to the levels of anthropogenic pollution, as it has been during the past decades, and/or when thinning had not been postponed. A clue for a reference may be found in old statistics of the forestry service, which were used to estimate wood production expectations. The Speulder forest can be classified as fast growing according to the predictions of yields for production forests in the Netherlands, based on growth data recorded in the fifties (LaBastide and Faber, 1972). This is not expected since the stand was not thinned in the last decade and may be an indication that high nitrogen loads lead to higher growth rates. A negative effect of nitrogen availability and growth stimulation is the increase in the foliage/fine root ratio. At the Speulder forest, this ratio is high compared to similar Douglas fir stands in non-polluted areas. In the future the N utilisation efficiency will probably decrease and the primary production will be limited by other essential resources than nitrogen. This is shown by the decreasing $K^+$ concentration and increasing $N/K^+$ ratio in the needles from 1987

onwards, the already existing $K^+$ and P deficiency, the deficient N/P and $N/Mg^{2+}$ ratio and the arginine accumulation in the needles. The relative low root/mycorrhiza density will reinforce the effect of drought and/or nutrient deficiency as a result of increased N availability and/or soil acidification ($Al^{3+}$ toxification). Dry years or a sequence of dry years may enhance the effects of air pollutants and soil acidification on tree health. Furthermore, a relatively low root density will increase the risk of windthrow.

Manipulation experiments

Another method to introduce a reference situation in some way is by using the results of the manipulation experiments. Within the framework of the NITREX programme, manipulation experiments have been conducted in the Speulder forest by covering an area under the Douglas canopy by a roof and applying pre-industrialised and collected rainwater under the roof to the soil (Boxman *et al.*, 1995a,b). These experiments are focused on recovering the quality of the soil, needles and vitality of the trees by reducing soil loads to pre-industrialised levels. Unfortunately, the exposure of the canopy to air pollutants cannot be reduced. The nitrogen and sulphur concentrations in the soil solution were found already decreased within several months, improving the nutrient balance considerably (Boxman *et al.*, 1995a,b). To date, the nitrogen content in the needles and the vitality of the trees have remained similar for the trees exposed to both pre-industrialised and current loads. This could be the result of the above-ground uptake of nitrogen by the trees. Above-ground N uptake is probably enhanced when the supply from the soil is lowered (Perez Soba and Van der Eerden, 1992). The arginine content of the needles was, however, significantly reduced, indicating that trees react first to the reduced nitrogen availability in the soil by producing less arginine (Boxman *et al.*, 1995b). In the more polluted southeastern part of the Netherlands at a similar manipulation plot, an even higher reduction of arginine in needles was found for these years (Boxman *et al.*, 1995b). The difference between the two sites might be the result of a difference in nitrogen exposure in recent years. In the southeastern part of the Netherlands larger ammonia emission reductions are reported than in the surroundings of the Speulder forest (Van der Hoek, 1994). $NH_x$ deposition at the Speulder forest measured as throughfall showed only a small decrease in recent years (Van Leeuwen and Bleuten, 1994).

As a result of the reduction in nitrogen en sulphur inputs during the manipulation experiment, the species diversity of microarthropods was found to be increased. Moreover, the nutrient balance in the forest has improved; this was suggested to be related to an enhanced root quality, a favourable $NH_4^+/NO_3^-$ ratio in the soil solution and decreased leaching of base cations. The nitrogen concentrations in older needles were found to be lower than in current needles, which is the normal situation in nitrogen-limited coniferous ecosystems. This points to a re-allocation of nitrogen from the older to younger needles and is consistent with the decreasing arginine concentration in the needles (Boxman *et al.*, 1995).

N budget of the Speulder forest
In 1992, the Speulder forest experienced an atmospheric N deposition of about 55 kg $ha^{-1}$ $a^{-1}$. Moreover, every year about 73 kg N $ha^{-1}$ is released due to mineralisation of the litter layer (Heij and Schneider, 1991). Since the need for this essential nutrient is great, plants have evolved very efficient mechanisms to gather and retain it. Consequently, almost no nitrogen is present in the drainage water that leaves the rooting zone of pristine forests (Vitousek *et al.*, 1979; Grennfelt and Hultberg, 1986). Unfortunately, no information on the chemical composition of drainage water in the Netherlands is available for the time period before air pollution started to increase. However, Minderman and Leeflang (1968) showed that almost no nitrogen leached from a lysimeter planted with black pine trees in the period 1947-1961. At the moment, approximately 31 kg N $ha^{-1}$ $a^{-1}$ is found to leach from the rooting zone in the Speulder forest (Van der Maas and Pape, 1991), indicating nitrogen saturation (Aber *et al.*, 1989). The nitrogen uptake by the needles is probably regulated by uptake of $NH_3$, $NH_4^+$, $NO_2$ and $HNO_2$ from the atmosphere. It is estimated that 5.4 kg $ha^{-1}$ $a^{-1}$ of nitrogen is taken up by the canopy through this route. Total below-ground uptake of N in the Speulder forest amounts to 92 kg $ha^{-1}$ $a^{-1}$ (Hey and Schneider, 1991). The total amount of N stored in the needles equals 344 kg $ha^{-1}$ (Van der Maas and Pape, 1991; Steingröver and Jans, 1995). According to data from the literature this is very high. For instance, in a Douglas fir stand with trees of equal age and heavily fertilised for nine years only 115 kg N $ha^{-1}$ was found to be stored in the needles (Pang *et al.*, 1978). This is probably the result of the very large foliage biomass in the Speulder forest.

### 7.3.8 CONCLUSIONS

*Gaseous deposition*
Continuous measurements of $u*$ and $H$ for one month show that the constant flux layer assumption for momentum and heat above the Speulder forest seems valid. The results of the deposition parameters obtained from the continuous measurements of $SO_2$ and $NH_3$ vertical gradients and meteorological parameters indicate that deposition monitoring of $SO_2$ and $NH_3$ onto forest is possible. For future monitoring activities, investigation of how to reduce random errors in individual concentration measurements is recommended. Possibilities for reducing random errors are minimising tube length, enlarging the averaging time for concentration measurements and averaging gradients for estimating deposition parameters. Deposition monitoring of $NO_2$ with the currently used monitors is concluded to be impossible as a result of instrumental failure

Values of $R_c$ of $SO_2$ for the Douglas fir forest are generally low, differences between day and night, and wet and dry conditions have been observed. An $R_c$ parameterisation derived for heathland vegetation yields reasonable results for forests. Further improvements of the $R_c$ parametrisation is possible by minimising errors in measured quantities, improving the

parametrisation for surface wetness, and extending the parametrisation with information on buffering capacities (of leaves or the atmosphere).

Surface exchange of ammonia over a coniferous forest has been measured continuously since November 1992. Canopy wetness has been observed to have a very strong influence on the dry deposition of ammonia: the surface resistance for a wet canopy is negligible. Over a dry canopy, the observed flux generally exceeds the estimated stomatal flux, indicating that deposition to external leaf surfaces is also important. Emission of ammonia was observed to occur during the daytime at low ambient humidity (<80%), and is thought to be related to evaporation of water films on the canopy. It is estimated that up to 20% of the deposited ammonia was re-emitted during the period November 1992-March 1993. An initial surface resistance parametrisation for surface exchange of ammonia over coniferous forest was derived. Modelled deposition velocity values have been found to compare reasonably to observed values.

*Deposition of particles*
The state of knowledge on particle deposition is relatively uncertain. Two contradicting opinions have been aired in the literature: 1) deposition of fine particles is negligible and 2) deposition of fine particles might contribute to a large extent to acid loads in forests. The main uncertainty is in the dry deposition velocity. The aim therefore was to use all available means and combined efforts to reduce this uncertainty to more accurately determine particle deposition to forests. It was assumed that by using the results of different kinds of measurements, in combination with a large modelling effort, at least a choice could be made between the two statements. Results would then likely point in one direction despite the large uncertainty.

The most important factors leading to uncertainty in particle deposition are the measuring errors, the uncertainty in representativeness of size distribution of the measurements, the scaling factors for accumulation experiments, and the influence of chemical conversion and humidity on particle growth. In general, the experimental and modelled results show a distinct influence of the size distribution and $u_*$ on the dry deposition velocity of particles. They show that $V_d$ ($^{214}$Pb) < $V_d$ ($SO_4$) < $V_d$ ($NO_3$) < $V_d$ (base cations) < $V_d$ (fog), in line with the size distributions. The deposition velocity of fog and base cations is proportional to $u_*^2$, indicating that impaction is the most important process determining $V_d$. Sedimentation is also important. The $V_d$ values of other compounds are proportional to $u_*^x$, with $0 < x < 1$, indicating that no distinct process has precedence a mixture of processes.

Size- and $u_*$ dependence of the dry particle deposition velocity is similar for both the measurements and the modelled results. This serves as some sort of validation of the most determining processes. The overall error in modelled $V_d$ integrated over the size distribution representative for acidifying aerosols equals about 65%. For base cations, this error is somewhat smaller (60%) because of the contribution of the relatively well-parametrised

sedimentation description. The uncertainty in model estimates is lower than or about equal to the uncertainty in measurement results, with the exception of the fog deposition measurements, which are estimated to have smaller errors (20%). The fractional bias of the means (the relative difference between the mean calculated and observed values) falls within these limits. The relatively high sensitivity of the model and an inaccuracy of the same order in measuring results mean that a perfect 1:1 correspondence between calculated and observed values cannot be expected. The Wilcoxon tests for paired samples, however, revealed no significant differences between the mean values of modelled and measured fluxes or $V_d$'s, showing that they are in good agreement.

From the results obtained in this project the deposition of fine particles can be concluded to be an important pathway for acid input to forests. Dry deposition velocities of particles to forests and probably other rough surfaces have been confirmed to be high. Six months average $V_d$ values for fine particles in the Speulder forest range from 1 to 2 cm $s^{-1}$ ($K^+$, $SO_4^{2-}$, $NO_3^-$, and $NH_4^+$), with daytime velocities at 1.3 ± 1.2 cm $s^{-1}$ and night-time velocities at 1.0 ± 1.4 cm $s^{-1}$ ($SO_4^{2-}$). $V_d$ values for coarse particles are about 5 cm $s^{-1}$, with daytime values of 5.1 ± 3.9 cm $s^{-1}$ and night-time values of 4.8 ± 4.0 cm $s^{-1}$. In comparison, $V_d$ values for $SO_2$, $NH_3$ and $NO_2$ for the same period were 1.5, 2.5 and 0.1 cm $s^{-1}$, respectively. This means that the deposition of aerosols to forest canopies in the Netherlands is to date underestimated by a factor of 2 to 3. For forests in Europe, this is even higher for the EMEP model results.

The answers to the three main research questions which were formulated in the introduction can be now be formulated:
1. Total deposition of SOx amounted 1185 mol $ha^{-1}$ $a^{-1}$ in the Speulder forest in 1993. The contribution of $SO_4^{2-}$ aerosols to the total deposition of SOx amounted to 18%; fog deposition contributed 3% and dry deposition of $SO_2$, 56%. Total deposition of NHx amounted to 2865 mol $ha^{-1}$ $a^{-1}$; dry $NH_4$ aerosols contributed 23%; fog deposition, 3% and dry deposition, 50%. Total deposition of NOy amounted to 1085 mol $ha^{-1}$ $a^{-1}$; dry $NO_3$ aerosols contributed 38%; fog deposition, 2% and dry deposition of NOy, 33%. Aerosol input for SOx and NHx is significant and forms a major input for $NO_3$. These results are representative for nature conservation areas in the Netherlands which are classified as rough terrains i.e. with many, isolated trees, scattered hedges, etc. For nature conservation areas consisting mainly of low vegetation, such as large areas of heathland, the aerosol deposition is much less (about 5-10% for $SO_4$, 10-15% for $NH_4$ and 5-10% for $NO_3$).

2. The results of the comparison study of atmospheric deposition and throughfall fluxes, and the experiments to determine canopy exchange (rinsing of artificial and Douglas fir branches, $^{35}S$ experiments), show that $H^+$ and $NH_4^+$ are taken up by the canopy. Uptake of $H^+$ and $NH_4^+$ is compensated for by the leaching of $Mg^{2+}$, $Ca^{2+}$, and most of all, K. $SO_2$ taken up by stomata is eventually leached again, whereas $NH_3$ taken up via stomata is probably not leached from the canopy. Oxidised nitrogen components, especially $NO_2$,, are taken up by the stomata in the

canopy. Whether $NO_3^-$ is taken up is uncertain. $Na^+$ and $Cl^-$ are considered inert. The highest uncertainty is found in the estimates of the nitrogen components. The contribution of particle deposition to the throughfall flux is considerable for base cations. Along with leaching from root-derived nutrients (except for $Na^+$), the throughfall flux of base cations is the result of particle deposition. The deposition of acidifying aerosols to rough forests has been, to date, underestimated, thereby closing the gap between throughfall fluxes of sulphur and atmospheric deposition estimates; there is no net uptake or loss of $SO_4^{2-}$. Throughfall fluxes of $NH_4^+$ and atmospheric deposition are in reasonable agreement; aerosol fluxes of $NH_4^+$ appear in the order of uncertainty found in the two methods. For $NO_3^-$, however, the systematic difference between atmospheric deposition and throughfall fluxes has increased with the new estimates of aerosol input. There is still a large uncertainty in canopy exchange processes for oxidised nitrogen and in deposition estimates of the different gases contributing to the total oxidised nitrogen flux.

The throughfall method can be concluded to be applicable for monitoring deposition of $SO_4^{2-}$, $Na^+$ and $Cl^-$. Uncertainty in the results obtained with throughfall is in the same order of magnitude as that in atmospheric deposition estimates on an annual basis. The throughfall, however, has to be representatively collected for the whole canopy (e.g. by using gutters) and samples must not remain in the field longer than one week. For the Speulder forest it has been shown that throughfall measurements might also be used for $Mg^{2+}$, $K^+$ and $Ca^{2+}$, provided the model of Van der Maas (1990) is used to correct for canopy exchange. It is uncertain whether the model can be used for measurements in other pollution climates and/or for other tree species. Results for nitrogen components are uncertain. It seems that for conditions found in the Speulder forest, the throughfall method can also be applied for $NH_4^+$; this leads to estimates similar to atmospheric deposition. For $NO_3^-$, it is not advisable to use the throughfall method until uncertainty in canopy exchange processes is reduced.

3. Sulphur is estimated to be deposited at 1185 mol $ha^{-1}$ $a^{-1}$ on the canopy and the forest soil., while 3950 mol $ha^{-1}$ $a^{-1}$ of nitrogen is deposited onto the canopy, of which 3565 mol $ha^{-1}$ $a^{-1}$ reaches the soil surface. For $Na^+$ and $Cl^-$, about 1220 and 1425 mol $ha^{-1}$ $a^{-1}$, respectively, deposit on the canopy and reaches the soil unchanged. For $K^+$, 325 mol $ha^{-1}$ $a^{-1}$ reaches the soil surface; 75 mol $ha^{-1}$ $a^{-1}$ is of atmospheric origin, whereas 250 mol $ha^{-1}$ $a^{-1}$ is root derived $K^+$. Regarding $Mg^{2+}$, 225 mol $ha^{-1}$ $a^{-1}$ reaches the soil surface: of this 185 mol $ha^{-1}$ $a^{-1}$ is of atmospheric origin. For $Ca^{2+}$, these numbers are 210 mol $ha^{-1}$ $a^{-1}$ and 150 mol $ha^{-1}$ $a^{-1}$ respectively. Total base cation input ($Ca^{2+}+K^+ +Mg^{2+}$), 390 mol $ha^{-1}$ $a^{-1}$, represents about 6% of the total potential acid deposition of 6320 mol $ha^{-1}$ $a^{-1}$. The base cation deposition forms therefore an important input in forests in the Netherlands.

*Assessment of the relation between loads/levels and effects*

The Speulder forest is a well growing forest, exceeding production forest yield predictions based on data observed in the fifties. This large growth rate is the result of high nitrogen exposure and loads during the last few decades. The high foliage/fine root and foliage/large

root ratio observed is also the result of high nitrogen loads, making the forest increasingly sensitive to drought, storms, frost and parasite injury (insects, fungi, virus). Mycorrhiza are poorly developed in the Speulder forest. There are indications that this is also caused by excess nitrogen availability but more information is needed to confirm this.

The elevated arginine concentrations in the needles indicate excessive nitrogen availability as do the disturbed balances between nitrogen and other nutrients. So far, it is not known whether arginine accumulation is detrimental to trees. In large concentrations it was found to affect cellular pH regulation and may be associated with increased parasite susceptibility. P and K are deficient in the needles. Ratios of most nutrients to nitrogen indicate that the nutrient status of the trees is far from optimal and gradually getting worse. The N utilisation efficiency of the Speulder forest will decrease in the future. The primary production will become limited by other essential resources than N. Nitrate is leaching from the rooting zone in large quantities and in this respect the Speulder forest ecosystem can be regarded as nitrogen saturated. Aluminium is also leaching in large amounts.

$NH_4^+$ concentrations in water layers covering the needle surface were sometimes such that damage of the epicuticular wax layer can be expected. However, this effect was not investigated in the Speulder forest. Over the period of a year, $CO_2$ assimilation was reduced as a result of ozone exposure and high vapour pressure deficits. The *AOT40* of 10 ppm h set to protect tree species against a growth reduction of more than 10% seems too small. Exposure to high $O_3$ and/or high $NH_3$ concentrations probably cause stomata to remain open, even at low shoot-water potentials and/or high vapour pressure deficits. In this way trees become more vulnerable to drought. Short periods with considerable water stress have occurred. As high aluminium concentrations are found in these periods, for example, the combination of drought stress and stress by unfavourable soil chemical conditions may cause adverse effects.

It is difficult to draw conclusions with respect to tree or stand vitality both now and in the future, as it depends on how vitality is defined. If vitality is defined in the traditional terms of needle loss and discoloration, no adverse effects are seen at the Speulder forest. However, poorly developed mycorrhiza may be regarded as an indication of reduced vitality as this implies a reduced capacity to take up water and nutrients. Besides the nutrient status of the needles, the high foliage/fine root and foliage/coarse root ratio may be regarded to indicate future risk for vitality reduction.

Exceedance of critical levels and loads means that there is a greater risk that adverse effects occur. The risk will be higher with larger exceedances and a longer duration of the exceedance. Whether such effects occur as a result of exceedances depends on the interaction with other stresses. The Speulder forest is under stress and, for this reason, more vulnerable to other stresses. The risk that adverse effects occur, cannot be properly quantified with current knowledge. A more quantitative risk assessment for forests should be developed in the near future by using results from experiments and by modelling (Van Grinsven *et al.*, 1994).

## 7.3.9 EVALUATION

The aim of the combined research in the Speulder forest was to determine the exposure and loads of acidifying and eutrophying pollutants, as well as their harmful influence on the vitality of Douglas fir trees and the forest ecosystem as a whole. The question is whether this research has succeeded. The success of a research project is related to the state of previous knowledge: is the research for validating known causal relations in the field, for investigation of unknown processes or for evaluating expectations of effects by measuring all that can be measured?

When research in the Speulder forest started in 1985, the state of knowledge on acidification was such that damage to ecosystems was observed in very highly polluted areas; also, in less polluted areas damage was expected to be forthcoming. The eutrophication problem had only been just recognised. It was not known at that time which combinations of stress was causing the damage and what local conditions could prevent or reduce damage.

The Speulder forest was at the time of selection a stand showing good growth. The criteria for selection of the stand were related to species, representativeness, conditions and surroundings, but also to the possibility of measuring the deposition using micrometeorological techniques (homogeneity of the stand and its surroundings, no sources in the neighbourhood, no advection problems, etc.). This limited the choice of forest stands in the Netherlands considerably. Furthermore, it appeared impossible to fulfil all criteria (Vermetten *et al.*, 1989).

Research of this kind should focus on both the causal relations and processes which might play a role in the cause - effect chain. Processes can be studied under controlled conditions in the laboratory or in open-top chambers, where process-related parameters can be manipulated. Field studies are always necessary to confirm the laboratory studies, e.g. to see if feedback mechanisms occur. The manipulation experiment is a good example of research on such processes.

Deriving mono-causal relations from the multiple stress to which the Speulder forests is exposed is difficult because of a lack of a proper reference and/or a lack of results from comparable investigations allowing comparison of temporal and spatial variations in (changes) in different effect parameters. This means that this kind of research should be carried out at more locations under different environmental circumstances as a combined effort of institutes and disciplinary-oriented bodies. Furthermore, as the observed effects are the result of multiple stress, all stress parameters should be investigated and not only those related to acidification, eutrophication and ozone.

The resilience of forests is high: relatively old ecosystems have large enough buffering capacities to cope with multiple stresses for several years. In an effort to determine effects of environmental stress, it is therefore advisable to continue research for several years.

Monitoring programmes should be established for effect and stress parameters, and process level investigations have to be repeated frequently during the monitoring programmes. Simultaneous research at different locations under different environmental conditions would enhance the chance of deriving mono-causal relations.

Manipulation experiments can serve in the introduction of a reference situation, so as to observe the difference between a polluted and non-polluted situation. The above-ground exposure, which is not reduced using a roof, presents a problem. The NITREX experiments were too short to see what the long-term recovery of the trees would be, or what the 'normal' growth (reference situation) would be. Extending the manipulation experiment at the Speulder forest site is therefore desirable. Another way of introducing a reference is using forest production yield predictions based on observations in the fifties.

Last but not least, in such large research programmes, where the experimental effort is enormous, more time should be reserved for interpretation of the large amount of experimental data.

# REFERENCES

Aalst, R.M. van (1983) Depositie van verzurende stoffen in Nederland. In: E.H. Adema and J. van Ham (Editors), Zure regen; oorzaken, effecten en beleid. Pudoc Wageningen, The Netherlands.

Aalst, R.M. van (1986) Dry deposition of aerosol particles. In: S.D. Lee, T. Schneider, L.D. Grant and P.J. Verkerk (Editors), Lewis Publ., Chelsea (MI) USA, pp. 933-949.

Aalst, R.M. van and Erisman, J.W. (1991) Atmospheric Input. In: G.J. Heij and T. Schneider (Editors), Acidification research in the Netherlands: Studies in Environmental Science 46, Elsevier, Amsterdam.

Aben, J. (1994) Luchtkwaliteit Jaaroverzicht 1993. Rapport No. 722101014, National Institute of Public Health and Environmental Protection, Bilthoven, The Netherlands.

Abrahamson, G., Bjor, K., Horntvedt, R. and Tveite, B. (1976) Effects of acid precipitation on coniferous forest. In: Impact of acid precipitation on forest and freshwater ecosystems in Norway. SNSF Project Report 6/76, Oslo, pp. 36-63.

Abrahamson, G., Seip, H.M. and Semb, A. (1989) Long-term acidic precipitation studies in Norway. In: S.E. Lindberg, A.L. Page and S.A. Norton (Editors), Acidic Precipitation. Vol. 3, Springer-Verlag, New York, pp.137-145.

Acharya, R.C. (1994) From emission to concentration: Analysis of ammonia predictions by the OPS model. Ph.D. Thesis, International Institute for Infrastructural, Hydraulic and Environmental Engineering, IHE, Delft, The Netherlands.

Adema, E.H., Heeres, P. and Hulskotte, J. (1986) On the dry deposition of $NH_3$, $SO_2$ and $NO_2$ on wet surfaces in a small scale wind tunnel. Proceedings of the Seventh World Clean Air Congress, Sydney, Australia, pp. 1-8.

Alcamo, J., Amann, M., Hettelingh, J.P., Holmberg, M., Hordijk, L., Kämäri, J., Kauppi, L., Kauppi, G. Kornai, G. and Mäkelä, A. (1989) Acidification in Europe: a simulation model for evaluating control strategies. Ambio, 16:232-245.

Alcock, M.R. and Morton, A.J. (1981) Nutrient content of throughfall and stem flow in woodland recently established on heathland. J. Ecol., 73:625-632.

Alens, I. and Skörby, L. (1988) Throughfall of plant nutrients in relation to crown thinning in a Swedish coniferous forest. Water, Soil Air Pollut, 38:223-237.

Allen, A.G., Harrison, R.M. and Erisman, J.W. (1989) Field measurements of the dissociation of ammonium nitrate and ammonium chloride aerosols. Atmospheric Environment, 23:1591-1599

Allerup, P. and Madson, H. (1980) Accuracy of Point Precipitation Measurements. Nordic Hydrol., 11: 57-70.

Alway, F.J. (1940) A nutrient element. J. Am. Soc. Agron. 32:913-921.

Andersen, H.V., Hovmand, M.F., Hummelshøj, P. and Jensen, N.O. (1993) Measurements of ammonia flux to a Spruce stand in Denmark. Atmospheric Environment, 27A:189-202.

Andreae, M.O. and Raemdonck, H. (1983) Dimethylsulfide in the surface ocean and the marine atmosphere. Science, 221:744-777

Andreae, M.O. and Andreae, T.W. (1988) The cycle of biogenic sulfur compounds over the Amazon basin. 1. Dry season. J. Geophys. Res., 93:1487-1497.

Andreae, M.O. (1991) Biomass burning: Its history, use and distribution and its impact on environmental quality and global climate. In: J.S. Levine (Editor), Global Biomass Burning: Atmospheric, Climatic and Biospheric implications. MIT Press, Boston, pp. 3-21.

Andreae, M.O. and Jaeschke, W.A. (1992) Exchange of sulphur between biosphere and atmosphere over temperate and tropical regions. In: R.W. Howarth, J.W.B. Stewart and M.V. Ivanow( Editors), Sulphur Cycling on the Continents. John Wiley and Sons Ltd., pp. 27-61.

Aneja, V.P., Rogers, H.H. and Stahel, E.P. (1986) Dry deposition of ammonia at environmental concentrations on selected plant species. J. Air Pollut. Control Assoc., 36: 1338-1341.

Arends, B.G., Wyers, G.P., Mennen, M.G., Erisman, J.W., Römer, F.G., Hofschreuder, P. and Duyzer, J.H. (1994) Comparison of concentration measurements for aerosols and gases using different techniques. Report No. ECN-C--94-058, ECN, Petten, The Netherlands.

Arens, K. (1934) Jahresbuch Wiss. Botanik, 80: 248-300.

Asman, W.A.H. (1985) De verhoging van de $NH_4$ koncentratie in regen in gebieden met hoge $NH_3$ emissie. Report R85-12, Institute for meteorology and oceanography, State University of Utrecht, The Netherlands..

Asman, W.A.H., Buijsman, E., Vermetten, A., Brink, H.M. ten, Heijboer, R.J., Janssen, A.J. and Slanina, J., (1986) Import and export of acid pollution in the Netherlands. Report No. ECN-186, Netherlands Energy Research Foundation, Petten, The Netherlands.

Asman, W.A.H., Pinksterboer, E.F., Maas, H.F.M., Erisman, J.W.and Horst, T.W. (1989) Gradients of the ammonia concentration in a nature reserve: model results and measurements. Atmospheric Environment, 23:2259-2265.

Asman, W.A.H. and Jaarsveld, J.A. van (1990) A variable-resolution statistical transport model applied for ammonia and ammonium. Report No. 228471007, National Institute of Public Health and Environmental Protection, Bilthoven, The Netherlands.

Asman, W.A.H. and Jaarsveld, J.A. van (1992) A variable-resolution transport model applied for NHx for Europe. Atmospheric Environment, 26A:445-464.

Asman, W.A.H. (1992) Ammonia emission in Europe: updated emission and emission variations. Report No. 228471008, National Institute of Public Health and Environmental Protection, Bilthoven, The Netherlands.

Asman, W.A.H., Sørenson, L. Berkowicz, R., Granby, K., Nielsen, H., Jensen, B., Runge, E.H., Lykkelund, C., Gryning., S.E. and Sempreviva, A.M. (1994) Processer for tørdeposition. Havforskning fra Miljøstyrelsen, nr. 35.

Bache, D.H. (1979) Particulate transport within plant canopies II. Prediction of deposition velocities. Atmospheric Environment, 13:1681-1687.

Bache, D.H. (1986) On the theory of gaseous transport to plant canopies. Atmospheric Environment, 20:1379-1388.

Baldocchi, D.D., Hicks, B.B., and Camara, P. (1987) A canopy stomatal resistance model for gaseous deposition to vegetated surfaces. Atmospheric Environment, 21:91-101.

Baldocchi, D.D., Hicks, B.B. and Meyers, T.P. (1988) Measuring biosphere-atmosphere exchanges of biologically related gases with micro meteorological methods. Ecology , 69:1331-1340.

Barral (1852) Mémoires sur les eaux de pluie recueillies à l'Observatoire de Paris. Compt. rend., 34:283-284, 35:427-431 and 36:184-187, Chapter 1, p.13.

Barrie, L.A. and Warmsley, J.L. (1978) A study of sulphur dioxide deposition velocities to snow in northern Canada. Atmospheric Environment, 12:2321-2322.

Barry, R.G. and Chorley, R.J. (1977) Atmosphere, weather and climate. Methuen and Co. Ltd, London.

Bary, E. and Junge, C. (1963) Distribution of sulfur and chlorine over Europe. Tellus, 15:370-381.

Bates, T.S., Cline, J.D., Gammon, R.H. and Kelly-Hansen, S.R. (1987) Regional and seasonal variations in the flux of oceanic dimethylsulfide to the atmosphere. J. Geophys. Res., 92: 2930-2938.

Beauchamp, E.G., Kidd, G.E. and Thurtell, G. (1982) Ammonia volatilization from liquid diary cattle manure in the field. Can. J. Soil Sci., 62:11-19.

Behra, P., Sigg, L. and Stumm, W. (1989) Dominating influence of $NH_3$ on the oxidation of aqueous $SO_2$: the coupling of $NH_3$ and $SO_2$ in atmospheric water. Atmospheric Environment, 23:2691-2707.

Beier, C. and Gundersen, P. (1989) Atmospheric deposition to the edge of a Spruce forest in Denmark. Environ. Pollut., 60:257-271.

Beier, C. and Rasmussen, L. (1989) Problems related to collection of rain and throughfall water. Proceedings of a workshop on Monitoring air pollution and forest ecosystem research, Bilthoven, The Netherlands, pp. 101-110.

Beier, C. (1991) Separation of gaseous and particulate dry deposition of sulphur at a forest edge. J. Environ. Qual., 20: 460-466.

Beier, C., Gundersen, P. and Rasmussen, L. (1992a) A new method for estimation of dry deposition of particles based on throughfall measurements. Atmospheric Environment, 26a:1553-1559.

Beier, C., Hansen, K. and Gundersen, P. (1992b) Spatial variability of throughfall fluxes in a spruce forest. Environmental Pollution, 81:257-267.

Beld, L.van den and Römer, F.G. (1990) Ammoniakmetingen op het Elspeetsche Veld in de periode van mei 1989 tot april 1990. Report No. 90389-MOC 90-3415, KEMA, Arnhem, The Netherlands.

Beljaars, A.C.M., Schotanus, P. and Nieuwstadt, F.T.M. (1983) Surface layer similarity under nonuniform fetch conditions. J. Climate Appl . Met., 22:1800-1810.

Beljaars, A.C.M., Holtslag, A.A.M. and Westrhenen, R.M. van (1987a) Description of a software library for the calculation of surface fluxes. Technical report TR-112, Royal Netherlands Meteorological Institute, De Bilt, The Netherlands.

Beljaars, A.C.M., Walmsley, J.L. and Taylor, P.A. (1987b) A mixed spectral finite-difference model for neutrally stratified boundary-layer flow over roughness changes and topography. Boundary-Layer Met., , 38:273-303.

Beljaars, A.C.M. (1988) The measurement of gustiness at routine wind stations. Contribution to the WMO Technical Conference on Instruments and Methods of Observation, Teco-1988, Leipzig, GDR, May 1988.

Beljaars, A.C.M. and Holtslag, A.A.M. (1990) Description of a software library for the calculation of surface fluxes. Environ. Software, 5:60-68.

Berg, T. and Schaug, J. (1994) Proceedings EMEP workshop on the accuracy of measurements, with sessions on determining the representativeness of measured parameters in a given grid square as compared to model calculations, 22-26 November 1993, Passau (Germany).

Berresheim, H., Andreae, M.O., Ayers, A.P., and Gillet, R.W. (1989) Distribution of biogenic sulfur compounds in the remote southern hemisphere. In: E.S. Saltzmann and W.J.Cooper (Editors), Biogenic Sulfur in the Environment. ACS Symposium Series, pp. 352- 366.

Beswick, K.M., Hargreaves, K.J., Gallagher, M.W., Choularton, T.W. and Fowler, D. (1991) Size-resolved measurements of cloud droplet deposition velocity to a forest canopy using an eddy correlation technique. Q. J. R. Met. Soc.,117:623-645.

Beswick, K.M., Gallagher, M.W., Hummelshoj, P., Pilegaard, K., Jensen, N.O. and Duyzer, J. (1994) Aerosol exchange to Speulder forest. In: Proc. EUROTRAC Symposium 94, Garmisch-Partenkirchen, FRG.

Bineau, A. (1855) Sur les eaux pluviales et sur l'atmosphère de Lyon, et quelques points des environs, pendant les années 1852 et 1853. Compt. rend., 38:272-274 and (1854) Ann.Chim. Phys.,42:428-484.

Bleeker, A. and Erisman, J.W. (1995) Temporal variations in ammonia concentrations described by measurements. Report No. 722108008, National Institute of Public Health and Environmental Protection, Bilthoven, The Netherlands.

Bleuten, W., Ertsen, A.C.D. and Draaijers, G.P.J (1989) Verzuring en eutrofiering in Nederland: gevolgen van versnippering van natuurgebieden, Geogr. Tijdschrift, 4:272-281.

Bobbink, R., Heil, G.W., Raessen, M.B.A.G. (1990) Atmospheric deposition and canopy exchange in heathland ecosystems. Report project 119, Dutch Priority Programme on

Acidification. Department of Plant Ecology and Evolutuonary Biology, University of Utrecht, The Netherlands.

Bobbink, R.; Heil, G.W. and Raessen, M.B.A.G. (1992). Atmospheric Deposition and Canopy Exchange Processes in Heathland Ecosystems. Environ. Pollut., 75:29-37.

Boermans, G.M.F. and Erisman, J.W. (1991) Meetstrategieontwikkeling voor het representativiteits-onderzoek als onderdeel van het additioneel meetprogramma ammoniak; fenomenologie van $NH_3$ en meetritsimulaties. Report No. 222105001, Laboratory of Air Research, National Institute of Public Health and Environmental Protection (RIVM), Bilthoven, The Netherlands.

Boermans, G.M.F. and Erisman, J.W. (1993) Final report in the Additional Programme on Ammonia. Report No. 222105002, Laboratory of Air Research, National Institute of Public Health and Environmental Protection (RIVM), Bilthoven, The Netherlands.

Boermans, G.M.F. and Pul, W.A.J. van (1993) SLAM, een transportmodel voor de korte termijn en de korte afstand met als toepassing de beschrijving van de verspreiding van ammoniak. Report No. 222105003, National Institute of Public Health and Environmental Protection (RIVM), Bilthoven, The Netherlands.

Bondietti, A., Hoffmann, F.O., Larsen, I.L. (1984) Air-to vegetation transfer rates of natural submicron aerosols, J. Environ. Radioact., 1:5-27.

Bosanquet, C.H. (1957) The rise of a hot waste gas plume. J. Inst. Fuel.,30:322-328.

Bosveld, F.C. and Beljaars, A.C.M. (1987) Complex terrain effects on dry deposition. In: H. van Dop (Editor), Air pollution modelling and its applications IV. Plenum Press, New York.

Bosveld, F.C. (1991) Turbulent exchange coefficients over a Douglas fir forest. Report WR-91-02, KNMI, De Bilt, The Netherlands.

Böttger, A., Ehhalt, D.H. and Gravenhorst, G. (1980) Atmosphärische Kreisläufe von Stickoxiden und Ammoniak. Kernforschungsanlage Jülich GmbH, Germany.

Boumans, L.J.M. and Beltman, W.H.J. (1991) Kwaliteit van het bovenste freatische grondwater in de zandgebieden van Nederland, onder bos en heideveld. Rijksinstituut voor Volksgezondheid en Milieuhygiëne, Bilthoven, rapport nr. 724901001.

Boussingault, J.B. (1858) Recherches sur la quantité de l'acide nitrique contenue dans la pluie, le brouillard, la rosée. Compt. rend.,46:1123-1130, 1175-1183.

Bouten, W., and Bosveld, F.C. (1993) Stomatal control in a partially wet Douglas fir canopy. Report No. 791302-1, Dutch Priority Programme on Acidification, RIVM, Bilthoven, The Netherlands.

Bowden, R.D. Geballe, G.T. and Bowden, W.B. (1989) Foliar uptake of $^{15}N$ from cloud water by red spruce (*Picea rubens* Sarg.) Can. J. Forest Res.,19:382-386

Bowman J. (1991) Acid Sensitive Surface Waters in Ireland, The impact of a major new sulphur emission on sensitive surface waters in an unacidified region. Report of the Environmental Research Unit, Dublin, Ireland.

Boyce, R.L., McCune, D.C., Berlyn, G.P. (1991) A comparison of foliar wettability of red spruce and balsam fir growing at high elevation. New Phytologist, 117:543-555.

Bredemeier, M. (1988) Forest canopy transformation of atmospheric deposition. Water Air Soil Pollut., 40:121-138.

Breemen, N.van, Burrough, P.A., Velthorst, E.J., Dobben, H.F. van, Wit, T. de, Ridder, T.B., Reinders, H.F.R. (1982) Soil acidification from atmospheric ammonium sulphate in forest canopy throughfall. Nature, 299:548-550.

Breemen, N. van, Visser, W.F.J. and Pape, Th. (1988) Biochemistry of an oak woodland ecosystem in the Netherlands affected by acid atmospheric deposition. Agr. Res. Report 930, Pudoc, Wageningen, The Netherlands.

Breemen, N. van and Verstraten, J.M. (1991) Soil acidification/N cycling. In: G.J. Heij and T. Schneider (Editors), Acidification research in the Netherlands. Studies in Environmental Science 46, Elsevier, Amsterdam, The Netherlands.

Bretschneider, P. (1872) Über die Quantitäten Ammoniak welche die hauptsten Ammoniak welche die hauptsächlichesten Konstituenten des Kulturbodens aus der Atmosphäre innerhalb eines Jahres auf gemessener Fläche absorbieren. Der Landwirt, 8:225-241.

Brimblecombe, P. (1978) Dew as a sink for sulphur dioxide. Tellus, 30:151-157.

Brimblecombe, P. and Stedman, D.H. (1984) Historical evidence for a dramatic increase in the nitrate component of acid rain. Nature, 298:460-462.

Brogger, W.C. (1881) Notes on a contaminated snowfall. Nature, 5:47.

Browning, K.A., Hill, F.F. and Pardoe, C.W. (1974) Structure and mechanism of precipitation and the effect of orography in a winter-time warm sector. Q. J. Roy. Met. Soc., 100:309-330.

Brost, R.A., Delany, A.C. and Huebert, B.J. (1988) Numerical modelling of concentrations and fluxes of $HNO_3$, $NH_3$ and $NH_4NO_3$ near the surface. J. Geophys. Res., 93:7137-7152.

Brüggemann, E. (1993a) Abschlußbericht zum Förderungsvorhaben BMfT: Wissenschaftliches Begleitprogramm zur Sanierung der Atmosphäre über den neuen Bundesländern (SANA), Aufbau und Betrieb eines Meßnetzes zur Bestimmung des flächenhaften Eintrags und der zeitlichen Trends von Schadstoffen durch Niederschläge; Projekt B. 2.1, Institut für Troposphärenforschung e.V., Leipzig, Germany (in German).

Brüggemann E. (1993b), Quantitativer Einfluß verschiedener Emissionsgebiete auf die chemische Zusammensetzung der nassen Deposition sowie Trendberechnungen anhand mehrjähriger Meßreihen; Auswirkungen lufthygienischer Sanierungs maßnahmen in den neuen Bundesländern, Abschlußbericht für den Zeitraum 1991/1992; Verbundprojekt SANA, Projekt: Nasse Deposition, prj. B 2.2 (in German).

Brutsaert, W.P. (1975) The roughness length of water vapour, sensible heat and other scalars. J. Atmos. Sci. 32:2028-2031.

Brydges, T.G. and Wilson, R.B. (1991) Acid rain since 1985 - times are changing. In: F.T. Last and R. Watling R. (Editors), Acid deposition, Its nature and impacts. Proc. Roy. Soc. Edinburgh, 97:1-15

Buijsman, E., Maas, J.F.M., Asman, W.A.H. (1984) Een gedetailleerde ammoniak-emissiekaart van Nederland. Report No.V-84-20, Institute for meteorology and oceanography, State University of Utrecht, Utrecht, The Netherlands.

Buijsman, E. and Erisman, J.W. (1988) Wet deposition of ammonium in Europe. J. Atmos. Chem., 6:265-280.

Buijsman, E. (1989) Onderbouwende informatie over het Landelijk Meetnet Luchtkwaliteit. I: Het Landelijk Meetnet Regenwatersamenstelling. Report No. 228703006, National Institute of Public Health and Environmental Protection, Bilthoven, The Netherlands.

Buijsman, E. (1990) De berekening van de natte, zure depositie: een vergelijking van een aantal berekeningswijzen. Report No. 228703011. National Institute of Public Health and Environmental Protection, Bilthoven, The Netherlands.

Buishand, T.A. (1989), Changes in the chemical composition of atmospheric precipitation in the Netherlands during the period 1978-1987. Wageningen Agricultural University, technical note 89-02.

Burkhardt, J.and Eiden, R. (1994) thin water films on coniferous needles. Atmospheric Environment, 28:2001:2017.

Burrough, P.A. (1986) Principles of geographical information systems, Monographs on soil and resources survey. Oxford University Press, UK.

Businger, J.A., Wyngaard, J.C., Izumi, Y. and Bradley, E.F. (1971) Flux-profile relationships in the atmospheric surface layer. J. Atmos. Sci., 28:181-189.

Businger, J.A. (1986) Evaluation of the accuracy with which dry deposition can be measured with current micrometeorological techniques. J. Climate Appl. Meteor., 25:1100-1124.

Caddle, S.H., Dasch, J.M. and Mulawa, P.A. (1985) Atmospheric concentrations and the deposition velocity to snow of nitric acid, sulphur dioxide, and various particulate species. Atmospheric Environment, 19:1819-1827.

Campbell G.W., Stedman J.R. and Irwin J.G. (1992) Acid Deposition in the United Kingdom. Report LR 865 (AP) Warren Spring Laboratory, Stevenage (UK).

Cape, J.N. (1983) Contact angles of water droplets on needles of Scotch pine (Pinus Sylvestrus) growing in polluted atmospheres. New Phytology, 293-299.

Cape, J.N., Fowler, D., Kinnaird, J.W., Nicholson, I.A. and Paterson, I.S. (1987) Modification of rainfall chemistry by a forest. In: P.J. Coughtrey, M.H. Martin and M.H. Undworth (Editors), Pollutant transport and fate in ecosystems. Blackwell Scientific Publications, London.

Cape, J.N. and Lightowlers, P.J. (1988) Review of throughfall and stemflow chemistry data in the United Kingdom. ITE project T07003e1, Institute of Terrestrial Ecology, Edinburgh.

Cape, J.N., Sheppard, L.J., Fowler, D., Harrison, A.F., Parkinson, J.A. and Dao, P. (1992) Contribution of canopy leaching to sulphate deposition in a Scotch pine forest. Environ. Pollut., 75:229-236.

Carleton, T.J. and Kavanagh, T. (1990) Influence of stand age and spatial location on throughfall chemistry beneath Black spruce. Can. J.For. Res., 20:1917-1925.

CBS (1985) Dutch Forest Statistics ('Vierde bosstatistiek'). Central Bureau of Statistics, Voorburg, The Netherlands.

CBS (1987) Soil Statistics ('Bodemstatistiek'). Central Bureau of Statistics, Voorburg, The Netherlands.

Chamberlain, A.C. (1960) In: E.G. Richardson (Editor), Aerodynamic capture of particles. Pergamon Press, New York, pp. 63-88.

Chamberlain, A.C. (1966) Transport of gases from grass and grass-like surfaces. Proc. R. Soc. Lond., A290:236-265.

Chamberlain, A.C. (1975) The movement of particles in plant communities. In: J.L. Monteith (Editor), Vegetation and the atmosphere - 1. Academic Press, New York.

Chamberlain, A.C. (1980) Dry deposition of sulphur dioxide. In: D.S. Sriner, C.R. Richmond and S.E. Lindberg (Editors), Atmospheric Sulphur deposition Environmental Impact and Health Effects. Ann Arbor Science Publishers, MI, USA, pp. 185-197.

Chamberlain, A.C. (1983) Deposition and resuspension. In: H.R. Pruppacher, R.G. Semonin and W.G.N. Slinn (Editors), Precipitation Scavenging, dry deposition and resuspension. Proc. 4th Conference, Santa Monica, New York.

Chameides, W.L. (1987) Acid dew and the role of chemistry in the dry deposition of reactive gases to wetted surfaces. J. Geophys. Res. 92:895-908.

Clarke, A.G. and Lambert, D.R (1987) Local factors affecting the chemistry of precipitation. In: R. Perry, R.M. Harrison, J.N.B. Bell and J.N. Lester (Editors), Acid rain: scientific and technical advances. Publications Divisions Selpter Ltd. London.

Clarke, J.F., Edgerton, E.S. and Boksleitner, R.P. (1992) Routine estimation and reporting of dry deposition for the USA Dry Deposition Network. In: S.E. Schwartz and W.G.N. Slinn (Editors), Proc. 5th IPSASEP conference, Richland, 15-19 June 1991. Hemisphere Publishing Corp., Washington.

Coddeville P., Guillermo R. and Houdret JL. (1993) Les Retombees Atmosferiques en France. Réseau MERA 1990; Ecole des Mines de Douai (in French).

Cogbill, C.V., Likens, G.E. and Butler, T.A. (1984) Uncertainties in historical aspects of acid precipitation: getting it straight. Atmospheric Environment, 10:2261-2270.

Collatz, G.J., Ball, J.T., Grives, C. and Berry, J.A. (1991) Regulation of stomatal conductance and transpiration: a physiological model of canopy processes. Agr. For. Met., 54:107-136.

Cronan, C.S. and Reiners, W.A. (1983) Canopy processing of acidic precipitation by coniferous and hardwood forests in New England. Oecologia, 59:216-223.

Cullis, C.F. and Hirschler, M.M. (1980) Atmospheric sulfur: Natural and man-made sources. Atmospheric Environment, 14:1263-1278.

Dabney, S.M. and Bouldin, D.R. (1990) Apparent deposition velocity and compensation point of ammonia inferred from gradient measurements above and through alfalfa. Atmospheric Environment, 24A:2655-2666.

Dam, D. van (1990) Atmospheric deposition and nutrient cycling in chalk grassland. Ph.D. thesis, Department of Plant Ecology and Evolutionary Biology, University of Utrecht, the Netherlands.

Dambrine E. (1992) Etablissement d'un réseau de collecte et d'analyse de la pluie et des pluviolessivats dans les Vosges; Rapport Technique Definitif, Commission des Communautes Europeennes, Direction Généreale VI, Décision no. 8960. Fr 005.0 (Code INRA 4278 B), INRA Centre de Nancy (in French).

Dasch, J.M. (1987) Measurement of dry deposition to surfaces in deciduous and pine canopies. Environ.Pollut., 44:261-277.

Davenport, A.G. (1960) Rationale for determining design wind velocities. J. Struct. Div. Am. Soc. Civ. Eng., 86:39-68.

Davidson, C.I., Miller, J.M. and Pleskov, M.A. (1982) The influence of surface structure on predicted particle dry deposition to natural grass canopies. Water Soil Air Pollut., 18:25-44.

Davidson, C.I., Lindberg, S.E., Schmidt, J., Cartwright, L. and Landis, L. (1985) Dry deposition of sulphate onto surrogate surfaces. J. Geophys. Res., 90:2121-2130.

Davidson, C.I. and Wu, Y.L. (1990) Dry deposition of particles and vapors. In: S.E. Lindberg, A.L. Page and S.A. Norton (Editors), Acidic Precipitation, Vol. 3. Springer-Verlag, New York.

Davies, T.D. and Mitchell, J.R. (1983) Dry deposition of sulphur dioxide onto grass in rural Eastern England (with some comparison with other forms of sulphur deposition). In: Pruppacher *et al.*, Precipitation Scavenging, Dry deposition and Resuspension. Elsevier Science Publishing Co., Inc.

Davies, T.D. and Wright, R.G. (1985) Sulphur dioxide deposition velocity by a concentration gradient measurement system. J. Geophys. Res., 90:2091-2095.

Denmead, O.T. (1983) Micrometeorological methods for measuring gaseous losses of nitrogen in the field. In: J.R. Freney and J.R. Simpson (Editors), Gaseous loss of nitrogen from plant-soil systems. Martinus Nijhoff/Dr W. Junk, The Hague, The Netherlands, pp. 133-158.

Derwent, R.G., Hov, O., Asman, W.A.H., Jaarsveld, J.A. van, Leeuw, F.A.A.M. de (1989) An intercomparison of long-term atmospheric transport models; the budgets of acidifying species for the Netherlands. Atmospheric Environment, 23:1893:1909.

Diederen, H.S.M.A. and Jansen, J. (1983) Eindrapportage van het deelprojekt 'Vergelijkingsmetingen' van het projekt Meetplan Aerosolen. Rapport No. G1155, TNO, Delft.

Dollard, G.J., Unsworth, M.H. and Harvey, M.J. (1983) Pollutant transfer in upland regions by occult precipitation. Nature, 302:241-243.

Dollard, G.J., Davies, T.J. and Lindstrom, J.P.C. (1986) Measurements of the dry deposition rates of some trace gas species. In: G. Angeletti and G. Restell (Editors), Proc. of the 4th European Symposium on Physico-chemical behaviour of atmospheric pollutants. Stresa, Italy, 23-25 September 1986.

Dollard, G.J., Jones, B.M.R. and Davies, T.J. (1990) Dry deposition of $HNO_3$ and PAN. AERE-Report R13780. Harwell, Oxfordshire, UK.

Dop, H. van, Ridder, T.B., Tonkelaar, J.F. den, Egmond, N.D. van (1980) Suphur dioxide measurements on the 213 metre tower at Cabauw, the Netherlands. Atmospheric Environment, 14:933-945.

Dop, H. van (1983) Terrain classification and derived meteorological parameters for inter-regional transport models. Atmospheric Environment 17:1099-1105.

Dop, H. van (1986) Models for deposition processes. In: S. Sandroni (Editor), Regional and Long-range transport of air pollution. Esevier Science Publishers, Amsterdam.

Dore, A.J., Choularton W. and Fowler D. (1992) An improved wet deposition maps of the United Kingdom incorporating the seeder-feeder effect over mountainous terrain. Atmospheric Environment, 8:1375-1381.

Draaijers, G.P.J., Ivens, W.P.M.F. and Bleuten, W. (1988) Atmospheric deposition in forest edges measured by monitoring canopy throughfall. Water, Air Soil Pollut., 42:129-136.

Draaijers, G.P.J., Ivens, W.P.M.F., Bos, M.M. and Bleuten W. (1989) The contribution of ammonia emissions from agriculture to the deposition of acidifying and eutrofying compounds onto forests. Environ. Pollut., 60:55-66.

Draaijers, G.P.J., Van Ek, R. and Meijers, R. (1992) Research on the impact of forest stand structure on atmospheric deposition. Environ. Pollut., 75:243-249.

Draaijers, G.P.J. and Erisman, J.W. (1993) Atmospheric sulphur deposition onto forest stands: throughfall estimates compared to estimates from inference. Atmospheric Environment, 27A:43-55.

Draaijers, G.P.J. (1993) The variability of atmospheric deposition to forests. Ph.D.thesis, University of Utrecht, The Netherlands.

Draaijers, G.P.J., Erisman, J.W., Leeuwen, N.F.M. van, Römer, F.G., Winkel, B.H. te and Wyers, G.P. (1994) Canopy exchange processes at the Speulder forest. Report No. 722108004, National Institute of Public Health and Environmental Protection, Bilthoven, The Netherlands.

Draaijers, G.P.J. and Erisman, J.W. (1994) De bijdrage van ammoniak aan de verzuringsproblematiek in Nederland, Vraagstelling, tijdschrift voor de gammawetenschappen, 3:71-88.

Draaijers, G.P.J., van Ek, R. and Bleuten, W (1994) Atmospheric deposition in complex forest landscapes. Boundary-Layer Met., 69:343-366.

Draaijers, G.P.J., Erisman, J.W., Potma, C., van Leeuwen, N.F.M. and van Pul, W.A.J. (1995) Mapping atmospheric deposition of base cations on a small scale over Europe. 5th International Conference on 'Acidic deposition', Gothenburg, Sweden, 26-30 June 1995.

Draaijers, G.P.J., Erisman, J.W., van Leeuwen, N.F.M., Römer, F.G., te Winkel, B.H., Wyers, G.P. and Hansen, K. (1995) The impact of canopy exchange on throughfall composition: results from a case study at the Speulder forest, the Netherlands. Atmospheric Environment (submitted).

Draaijers, G.P.J., Spranger, T., Erisman, J.W. and Wyers, G.P. (1995) The application of throughfall measurements for atmospheric deposition monitoring. Atmospheric Environment (submitted).

Driedonks, A.G.M., Dop, H. van, Kohsiek, W.H. (1978) Meteorological observations on the 213m mast at Cabauw in the Netherlands. 4th Symp. Meteor. Observ. Instr., Denver, CO, USA.

Droppo, J.G. Jr. (1985) Concurrent measurements of ozone dry deposition using eddy correlation and profile flux methods. J. Geophys. Res., 90:2111-2118.

Duijm, N.J. and Aalst, R.M. van (1984) Bijdrage van industrie en verkeer aan de verzuring van gevoelige gebieden in Nederland. Rapport 84-010176, TNO, Delft.

Duijsings, J.J.H.M., Verstraten, J.M. and Bouten, W. (1986) Spatial variability in nutrient deposition under an oak/ beech canopy. Zeitschrift für Pflanzenernährung und Bodenkunde, 149:718-727.

Durant, C.L. (1932) 'Bleeding' of trees. Malay Forester, 1:220.

Duyzer, J. H., Bouman, A.M.M., Aalst, R.M. van and Diederen, H.S.M.A. (1987) Assessment of dry deposition of $NH_3$ and $NH_4^+$ over natural terrains. In: Proc. of the EURASAP Symposium on Ammonia and Acidification. Bilthoven, The Netherlands, 13-15 April 1987.

Duyzer, J.H. and Bosveld, F.C. (1988) Measurements of dry deposition fluxes of $O_3$, $NO_X$, $SO_2$ and particles over grass/heathland vegetation and the influence of surface inhomogeneity. Report No. R 88/111, TNO, Delft, The Netherlands.

Duyzer, J.H. and Diederen, H.S.M.A. (1989) Measurements of dry deposition velocities of $NH_3$ over heathland and forest. Report P 89/023, TNO, Delft.

Duyzer, J.H., Verhagen, H.L.M. and Erisman, J.W. (1989) De depositie van verzurende stoffen op de Asselse heide. Report No. R 89/29, TNO/RIVM, Delft.

Duyzer, J.H., Fowler, D., Meixner, F., Dollard, G., Johanson, C. and Gallagher, M. (1990) The Halvergate trace gas experiment on surface exchange of oxides of nitrogen: preliminary results. Contribution to the COST 611 workshop: Field measurements and interpretation of species derived from $NO_X$, $NH_3$ and VOC emissions in Europe. Madrid, Spain, 12-14 March 1990.

Duyzer, J.H., Verhagen, H.L.M. and Weststrate, J.H. (1991) Monitoring deposition of nitrogen dioxide on the Elspeetsche Veld heathland. MT-TNO report in preparation.

Duyzer (1991) Inputs of nitrogen compounds and photo-oxidants as components of the pollution climate of Europe (progress report). Report No. R 91/005, TNO, Delft, The Netherlands.

Duyzer, J.H. (1992) The influence of chemical reactions on surface exchange of NO, $NO_2$ and $O_3$: results of experiments and model calculations. In: S.E. Schwartz and W.G.N. Slinn (Editors), Proc. of the 5th IPSASEP conference, Richland, USA, 15-19 June 1991. Hemisphere Publishing Corp., Washington.

Duyzer, J.H., Verhagen, H.L.M., Weststrate, J.H., Bosveld, F.C. and Vermetten, A.W.M. (1992) The dry deposition of ammonia onto a Douglas fir forest in the Netherlands. Environ. Pollut., 75:3-13

Duyzer, J.H.,Weststrate, J.H., Beswick, K. and Gallagher, M. (1994) Measurements of the dry deposition flux of sulphate and nitrate aerosols to the Speulderbos using micrometeorological methods. IMW-TNO report R94/255, Delft.

Duyzer J.H. and Westrate, J.H. (1994) Ozon gradienten boven het Speulderbos. IMW-TNO report P94/071, Delft.

Duyzer, J.H. (1994) Deposition of ozone and nitrogen dioxide to European forest. IMW-TNO report R94/060, Delft.

Duyzer, J.H., Weststrate, J.H., Diederen, H.S.M.A., Vermetten, A., Hofschreuder, P., Wyers, P., Bosveld, F.C. and Erisman, J.W. (1994) The deposition of acidifying compounds and

ozone to the Speulderbos derived from gradient measurements in 1988 and 1989. TNO report R94/095, Delft.

Duyzer, J.H. and Fowler, D. (1994) Modelling land atmosphere exchange of gaseous oxides of nitrogen in Europe. Tellus, 46B:353-372.

Dyer, A.J. and Hicks, B.B. (1970) Flux gradient relationships in the constant flux layer. Q. J. Roy. Met. Soc., 96:715.

Eder, B.K. and Dennis, R.L. (1990) On the use of scavenging ratios for the inference of surface-level concentrations and subsequent dry deposition of $Ca^{2+}$, $Mg^{2+}$, $Na^{+}$ and $K^{+}$. Water Air Soil Pollut., 52:197-215.

Egmond, N.D. van and Onderdelinden, D. (1981) Ruimtelijke betekenis van lucht verontreinigings-meetresultaten. Report No. 227905035, National Institute of Public Health and Environmental Protection, Bilthoven, The Netherlands.

Egmond, N.D.van, Kesseboom, H. and Onderdelinden, D. (1985) Statistische optimalisatie van het Landelijk Meetnet voor de Regenwaterkwaliteit. Report No. 218203001, National Institute of Public Health and Environmental Protection, Bilthoven, The Netherlands.

Ek, R. van and Draaijers, G.P.J. (1991) Atmospheric deposition in relation to forest stand structure. Report AD 1991-01.Department of Physical Geography, Utrecht University, The Netherlands.

Ek, R. van and Draaijers, G.P.J. (1994) Estimates of atmospheric deposition and canopy exchange for three common tree species in the Netherlands. Water Air Soil Pollut., 73:61-82.

Eliassen, A. and Saltbones, J. (1983) Modelling of long-range transport of sulphur over Europe: a two year model run and some model experiments. Atmospheric Environment, 17:1457-1473.

Elskamp, H.J. (1989) National Air Quality Monitoring Network, Technical description. Report No. 228702017, National Institute of Public Health and Environmental Protection, Bilthoven, The Netherlands.

Elzakker B.G. van, Aben J., Erisman J.W., Mennen M.G. (1995) Het interim meetnet ammoniak. Report in prep. National Institute of Public Health and Environmental Protection, Bilthoven, The Netherlands.

Enders G., Dlugi R., Steinbrecher R., Clement B., Daiber R., Eijk J.van, G,,b S., Haziza M., Helas G., Herrmenn U., Kessel M., Kesselmeier J., Kotzias D., Kourtidis K., Kurth H.H., McMillen R.T., Roider G., Schürmann W., Teichmann U., Torres L. (1992) Biosphere/atmosphere interactions: integrated research in a European coniferous forest ecosystem. Atmospheric Environment, 26A, 171-189.

Enger H. and Eriksson E. (1955) Current data on the chemical composition of air and precipitation. Tellus,7,134-139.

Erbrink J.J. (1986) Windfluctuaties en de relatie met de stabiliteit. III: Eindrapportage metingen te Deelen. Koppeling met het kortetermijn verspreidingsmodel (in Dutch). Report No. 60654-MOL 86-3015. KEMA, Arnhem, The Netherlands.

Erbrink J.J. (1989) A simple method for the determination of the stability class for application in dispersion modelling using wind fluctuations. In: Decision Aids to Offsite Emergency Management, EEG, Luxemburg, May 16-19, 1989.

Eriksson E. (1952a) Composition of atmospheric precipitation: A. Nitrogen compounds. Tellus, 4, 215-232.

Eriksson E. (1952b) Composition of atmospheric precipitation: II. Sulfur, chloride, iodine compounds. Bibliography. Tellus, 4, 280-303.

Erisman J.W., Vermetten A.W.M., Asman W.A.H., Mulder W., Slanina J. en Waijers-IJpelaan A. (1986) Concentrations of ammonia and ammonium over the Netherlands. Instituut voor Meteorologie en Oceanografie, Universiteit van Utrecht. Rapport R-86-3.

Erisman J.W., Leeuw F.A.A.M.de, Aalst R.M.van (1987) Depositie van de voor verzuring in Nederland belangrijkste komponenten in de jaren 1980 t/m 1986 (Deposition of the most important acidifying components in the Netherlands in 1980-1986, in Dutch with English summary). Report No. 228473001, National Institute of Public Health and Environmental Protection, Bilthoven, The Netherlands.

Erisman J.W., Vermetten A.W.M., Asman W.A.H., Slanina J. and Waijers-IJpelaan A. (1988) Vertical distribution of gases and aerosols: the behaviour of ammonia and related components in the lower atmosphere. Atmospheric Environment, 22:1153-1160.

Erisman J.W., Versluis A.H., Verplanke T.A.J.W., de Haan D., Anink D., van Elzakker B.G., Mennen M.G., van Aalst R.M. (1989a) Monitoring the dry deposition of $SO_2$ in the Netherlands. Report No. 228601002. National Institute of Public Health and Environmental Protection, Bilthoven, The Netherlands.

Erisman J.W., Leeuw F.A.A.M.de, and Aalst R.M.van (1989b) Deposition of the most acidifying compounds in the Netherlands during 1980-1986. Atmospheric Environment, 23, 1051-1062

Erisman J.W. (1989) Ammonia emissions in the Netherlands in 1987 and 1988. Report No. 228471006 National Institute of Public Health and Environmental Protection, Bilthoven, The Netherlands.

Erisman J.W. (1990) Atmospheric deposition of acidifying compounds onto forests in the Netherlands: throughfall measurements compared to deposition estimates from inference. Report No.723001001, National Institute of Public Health and Environmental Protection, Bilthoven, The Netherlands.

Erisman J.W., Elzakker B.G.van, Mennen M. (1990) Dry deposition of $SO_2$ over grassland and heather vegetation in the Netherlands. Report No. 723001004, National Institute of Public Health and Environmental Protection, Bilthoven, The Netherlands.

Erisman, J.W. (1990) Estimates of the roughness length at Dutch Air Quality Monitoring Network stations and on a grid basis over the Netherlands. Report No. 723001003, National Institute of Public Health and Environmental Protection, Bilthoven, The Netherlands.

Erisman, J.W. and Duyzer, J.H. (1991) A micrometeorological investigation of surface exchange parameters over heathland. Boundary-Layer Met., 57:115-128.

Erisman, J.W., Elzakker, B.G. van, Mennen, M.G., Beld, L. van den, Römer, F.G., Verhage, A., Rooth, R., Bobbink, R., Raessen, M., Duyzer, J.H. and Verhagen, H.L.M. (1991) Monitoring deposition fluxes and throughfall of acidifying components at the heathland

Elspeetsche Veld. Report No. 723001006, National Institute of Public Health and Environmental Protection, Bilthoven, The Netherlands.

Erisman, J.W. (1991) Acid deposition in the Netherlands. Report No. 723001002, National Institute of Public Health and Environmental Protection, Bilthoven, The Netherlands.

Erisman, J.W., Elzakker, B.G.van, Mennen, M.G. and Duyzer, J.H. (1992) Monitoring the dry deposition of $SO_2$ in the Netherlands. In: Proc. 5th IPSASEP conference, Richland, USA, 15-19 June 1991.

Erisman, J.W. (1992) Atmospheric deposition of acidifying compounds in the Netherlands. Ph.D. Thesis, Utrecht University, The Netherlands.

Erisman, J.W. (1993a) Acid deposition onto nature areas in the Netherlands; Part I. Methods and results. Water Soil Air Pollut.,71:51-80.

Erisman, J.W. (1993b) Acid deposition onto nature areas in the Netherlands; Part II. Throughfall measurements compared to deposition estimates. Water Soil Air Pollut., 71:81-99.

Erisman, J.W. and Wyers, G.P. (1993a) Continuous measurements of surface exchange of $SO_2$ and $NH_3$; implications for their possible interaction in the deposition process. Atmospheric Environment, 27A:1937-1949.

Erisman, J.W., Versluis, A.H., Verplanke, T.A.J.W., Haan D. de, Anink, D., Elzakker, B.G. van, Mennen, M.G. and Aalst, R.M van. (1993b) Monitoring the dry deposition of $SO_2$ in the Netherlands. Atmospheric Environment, 27:1153-1161.

Erisman, J.W., Mennen, M., Hogenkamp, J., Goedhart, D., Pul, A. van and Boermans, J. (1993c) Dry deposition over the Speulder forest. In: J. Slanina, G.Angeletti and S. Beilke (Editors), Air Pollution Report 47, CEC, Brussels.

Erisman, J.W., Mennen, M., Hogenkamp, J., Kemkers, E., Goedhart, D., Pul, A. van and Boermans, J. (1993d) Dry deposition over the Speulder forest. In: Proc. of the CEC/BIATEX workshop, Aveiro, Portugal, 4-7 May 1993.

Erisman, J.W., Jaarsveld, J.H. van, Pul, A. van, Fowler, D., Smith, R. and Lövblad, G. (1993e) Comparison between small scale and long-range transport modelling. In: G. Lövblad, J.W. Erisman and D. Fowler (Editors), Models and methods for the quantification of atmospheric input to ecosystems, Report No. 1993:573, Nordic Council of Ministers, Copenhagen, Denmark.

Erisman, J.W. (1994) Evaluation of a surface resistance parameterization of $SO_2$. Atmospheric Environment, 28:2583-2594.

Erisman, J.W. and Baldocchi, D.D. (1994a) Modelling dry deposition of $SO_2$. Tellus, 46B:159-171.

Erisman, J.W., Beier, C., Draaijers, G. and Lindberg, S. (1994b) Review of deposition monitoring methods. Tellus, 46B:79-93

Erisman, J.W., Pul, A. van and Wyers, P. (1994c) Parameterization of dry deposition mechanisms for the quantification of atmospheric input to ecosystems. Atmospheric Environment, 28:2595-2607.

Erisman, J.W., Draaijers, G.J.P., Duyzer, J.H., Hofschreuder, P., Leeuwen, N. van, Römer, F.G., Ruijgrok, W. and Wyers, G.P. (1994d) Contribution of aerosol deposition to atmospheric deposition and soil loads onto forests. Report No. 722108005, National Institute of Public Health and Environmental Protection, Bilthoven, The Netherlands.

Erisman, J.W., Mennen, M., Hogenkamp, J., Kemkers, E., Goedhart, D., Pul, A. van, Boermans, J. Duyzer, J.H. and Wyers, G.P. (1994e) Evaluation of dry deposition measurements for monitoring application over the Speulder forest. Report No. 722108002, National Institute of Public Health and Environmental Protection, Bilthoven, The Netherlands.

Erisman, J.W., Elzakker, B.G. van, Mennen, M. G., Hogenkamp, J., Zwart, E., Beld L. van den, Römer, F.G., Bobbink, R., Heil, G., Raessen, M., Duyzer, J.H., Verhage, H., Wyers, G.P., Otjes, R.P. and Möls, J.J. (1994f) The Elspeetsche Veld experiment on surface exchange of trace gases: summary of results. Atmospheric Environment, 28:487-496

Espinosa Banclari, M.A., Perry, D.A. and Marshall, J.D. (1987) Leaf area - sapwood area relationships in adjacent young Douglas-fir stands with different early growth rates. Canadian Journal for Forest Research, 17:174-180.

Evans, L.S. and Ting, I.P. (1973) Ozone-induced membrane permeability changes. Am. J. Botany, 60:115-162.

Farquhar, G.D., Firth, P.M., Wetselaar, R. and Wier, B. (1980) On the gaseous exchange of ammonia between leaves and the environment: determination of the ammonia compensation point. Plant Physiol., 66:710-14.

Fassbender, H.W. (1977) Modellversuch mit jungen Fichten zur Erfassung des internen Nährstoffenumsatzes. Ocologia Plantarum, 123:263-272.

Fassina, V. and Lazzarini, L. (1981) Sulphur dioxide atmospheric oxidation in the presence of ammonia. Water Air Soil Pollut., 15:343-352.

Fitzgerald, J.W. (1975) Approximation formulas for the equilibrium size of an aerosol particle as a function of its size and composition and the ambient relative humidity. J. Appl. Meteor., 14:1044-1049.

Finlayson-Pitts, B.J. and Pitts, J.M. (1986) Atmospheric chemistry. John Wiley and Sons, New York.

Fodor, J. (1881) Hygienische untersuchungen über Luft, Boden und Wasser. I. Die Luft. Braunschweig, Germany.

Fowler, D. (1978) Dry deposition of $SO_2$ on agricultural crops. Atmospheric Environment, 12:369-373.

Fowler, D. and Unsworth, M.H. (1979) Turbulent transfer of sulphur dioxide to a wheat crop. Q. J. R. Met. Soc. 105:767-783.

Fowler, D. (1981) Turbulent transfer of sulphur dioxide to cereals: a case study. In: Plants and Flux, pp. 139-146.

Fowler, D. (1984) Transfer to terrestrial surfaces. Phil. Trans. R. Soc. Lond., B30: 281-297.

Fowler, D. and Cape, J.N. (1984) The contamination of rain samples by dry deposition on rain collectors. Atmospheric Environment, 18:183-189.

Fowler, D. (1985) Dry deposition of $SO_2$ onto plant canopies. In: W.E. Winner, H.A. Mooney and R.A. Goldstein (Editors), Sulphur dioxide and vegetation. Stanford University Press, California, pp. 75-95.

Fowler, D, Cape, J.N., Leith, I.D., Choulartan, T.W., Gay, M.J. and Jones, A. (1988) The influence of altitude on rainfall composition at Great Dun Fell. Atmospheric Environment, 22:1355-1362.

Fowler, D., Cape, J.N. and Unsworth, M.H. (1989) Deposition of atmospheric pollutants on forests. Phil. Trans. R. Soc. Lond., B 324:247-265.

Fowler, D. and Duyzer, J.H. (1990) Micrometeorological techniques for the measurement of trace gas exchange. In: M.O. Andrae and D.S. Schimel (Editors), Exchange of trace gases between terrestrial ecosystems and the atmosphere. John Wiley and Sons, pp. 189-207.

Fowler, D., Duyzer, J.H., and Baldocchi, D.D. (1991) Inputs of trace gases, particles and cloud droplets to terrestrial surfaces. Proc. R. Soc. Edinburgh, 97B:35-59.

Fowler, D., Cape, J.N., Sutton, M.A., Mourne, R., Hargreaves, K.J., Duyzer, J.H. and Gallaghar, M.W. (1992) Deposition of acidifying compounds. In: T. Schneider (Editor), Acidification research: evaluation and policy applications. Elsevier, Amsterdam, pp. 553-572.

Freiesleben, N.E. von, Ridder, C. and Rasmussen, L. (1986) Patterns of acid precipitation to a Danish spruce forest. Water Air Soil Pollut., 30:135-141.

Galbally, I. (1979) Sulphur uptake from the atmosphere by forest and farmland. Nature, 280:49-50.

Galbally, I.E. and Roy, C.R. (1980) Destruction of ozone at the earth's surface. Q. J. R. Met. Soc., 106:599-620.

Gallagher, M.W., Choularton, T.W., Morse, A.P. and Fowler, D. (1988) Measurements of the site dependence of cloud droplet deposition at a hill site. Q.J. R. Met. Soc., 114:291-303.

Galloway, J.N. and Welphdale, D.M. (1980) An atmospheric sulfur budget for eastern North America. atmospheric Environment, 14:409:417.

Ganor, E., Foner, H.A., Brenner, S., Neeman, E. and Lavi, N. (1991) The chemical composition of aerosols settling in Israel following dust storms. Atmospheric Environment, 25A:2665-2670.

Garland, J.A. (1977) The dry deposition of sulphur dioxide to land and water surfaces. Proc. R. Soc. Lond., A354:245-268.

Garland, J.A. and Branson, J.R. (1977) The deposition of sulphur dioxide to pine forest assessed by a radioactive tracer method. Tellus, 29:445-454.

Garland, J.A. (1978) Dry and wet removal of sulfur from the atmosphere. Atmospheric Environment, 12:349.

Garten, C.T., Bondietti, E.A. and Lomax, R.D. (1988) Contribution of foliar leaching and dry deposition to sulfate in net throughfall below deciduous trees. Atmospheric Environment, 7:1425-1432.

Garratt, J.R. and Hicks, B.B. (1973) Momentum, heat and water vapour transfer to and from natural and artificial surfaces. Q. J. R. Met. Soc., 99:680-687.

Garsed, S.G. (1985) $SO_2$ uptake and transport. In: W.E. Winner, H.A. Mooney and R.A. Goldstein (Editors). Sulphur dioxide and vegetation, Stanford University Press, California, pp. 75-95.

Gaudichaud, C. (1841) Recherches generales sur l'organographie, la physiologie et l'organogenie. Fortin, Masson Cie.

Gay, D.W. and Murphy, C.E. (1985) Final report: The deposition of $SO_2$ on forests. EPRI Project R.P, 1813-2, Electric Power Research Institute, Palo Alto, California.

Georgii, H.W., Grosch, S. and Schmitt, G. (1986) Assessment of dry and wet pollutant deposition to forests in the Federal Republic of Germany. Final report: Institut für Meteorologie und Geophysik. J.W. Goethe Universität, Frankfurt, FRG.

Gilbert, O.L. (1968) Bryophytes as indicators of air pollution in the Tyne valley. New Phytol., 67:15-30.

Graham, R.C., Robertson, J.K., Schroder, L. and Lafemina, J. (1988) Atmospheric Deposition Sampler Intercomparison. Water Air Soil Pollut., 37:139-147.

Granat, L. and Johansson, C. (1983) Dry deposition of $SO_2$ and NOx in winter. Atmospheric Environment, 17:191-192.

Granat, L. (1989) Luft- och nederbördskemiska stationsnätet inom PMK. Stockholms Universitet, Meteorologiska institutionen. Rapport från verksamheten 1989, Naturvårdsverket Rapport 3789 (in Swedish).

Granat, L. and Hällgren, J.E. (1992) Relation between estimated dry deposition and throughfall in a coniferous forest exposed to controlled levels of $SO_2$ and $NO_2$. Environ. Pollut., 75:237-242.

Gravenhorst, G. and Böttger, A. (1982) Field measurements of NO and $NO_2$ to and from the ground. In: S.Beilke and A.J. Elshout (Editors), Acid deposition. CEC workshop, Berlin. Reidel Publishing Co., Dordrecht, The Netherlands, pp. 172-184.

Grennfelt, P., Larsson, S., Leyton, P. and Olsson, B. (1985) Atmospheric deposition in the Lake Gårdsjön area, SW Sweden. Ecol. Bull., 37:101-108.

Grennfelt, P. (1987) Deposition processes for acidifying compounds. Environ. Tech. Lett., 8:515-527

Haan, D. de (1988) Droge depositie: een geautomatiseerd gradient-meetsysteem (Dry deposition: an automatized gradient-measuring system, in Dutch). Internal Report No. 2286602008, National Institute of Public Health and Environmental Protection, Bilthoven, The Netherlands.

Hales, S. (1727) Vegetable Staticks. Innys and Woodward, London.

Hall, A.D. and Miller, N. H. J. (1911) On the absorption of ammonia from the atmosphere. J. Agr. Sci., 4:56-68.

Halldin, S. (1985) Leaf and bark distribution in a Pine forest. In: B.A. Hutchinson & B.B. Hicks (Editors), The forest-atmosphere interaction, Reidel, Dordrecht, the Netherlands.

Ham, J. van der (1977), Wij en het weer (in Dutch). Teleac.

Hanna, S.R. (1981) Diurnal variation of horizontal wind direction fluctuations in complex terrain at Geysers, Cal. Boundary-Layer Met., 21:207-213.

Hansen, D.A. and Hidy, G.M. (1982) Review of questions regarding rain acidity data. Atmospheric Environment, 16:2107-2126.

Hansen, K., Draaijers, G.P.J., Ivens, W.P.M.F., Gundersen, P. and Leeuwen, N.M.F. van (1994) Concentration variations in rain and canopy throughfall collected sequentially during individual rain events. Atmospheric Environment, .

Hanson, P.J., Rott, K., Taylor Jr. G.E., Gunderson, C.A., Lindberg, S.E. and Ross-Todd B.M. (1989) $NO_2$ deposition to elements representative of a forest landscape. Atmospheric Environment, 23:1783-1794.

Hanson, P.J. and Lindberg, S.E. (1991) Dry deposition of reactive nitrogen compounds: review of leaf, canopy and non-foliar measurements. Atmospheric Environment, 25A:1615-1634.

Hargreaves, K.J., Fowler, D., Storeton-West, R.L. and Duyzer, J.H. (1992) The exchange of nitric oxide, nitrogen dioxide and ozone between pasture and the atmosphere. Environm. Poll., 75:53-60.

Harrison, R.M. and Pio, C.A. (1983) An investigation of the atmospheric $HNO_3$- $NH_3$- $NH_4$-$NH_4NO_3$ equilibrium relationship in a cool humid climate. Tellus, 35B:155-159.

Harrison, R.M., Rapsomanikis, S. and Turnbull, A. (1989) Land-surface exchange in a chemically reactive system; surface fluxes of $HNO_3$, HCl and $NH_3$. Atmospheric Environment, 23:1795-800.

Harper, L.A., Sharpe, R.R., Langdale, G.W. and Giddens, J.E. (1987) Nitrogen cycling in a wheat crop: soil, plant and aerial nitrogen transport. Agron. J., 75;212-218.

Hasselhof, E. and Lindau, G. (1903) Die Beschädigung der Vegetation durch Rauch. Leipzig.

Hasselrot, B. and Grennfelt, P. (1987) Deposition of air pollutants in a wind-exposed forest edge. Water Air Soil Pollut., 34:135-143.

Hauhs, M. and Wright, R.F. (1988) Acid deposition: reversibility of soil and water acidification - a review. Air Pollution Report 11, CEC, Brussels.

Haynie, F.H. (1986) Theoretical model of soiling of surfaces by airborne particles. In: S.D. Lee, T. Schneider, L.D. Grant and P.J. Verkerk (Editors), Aerosols. Lewis Publ. Chelsea (MI), USA, pp. 951-959.

Hedin, L.O., Granat, L., Likens, G.E., Buishand, T.A., Galloway, J.N., Butler, Th. J., Rodhe, H. (1994) Steep declines in atmospheric base cations in regions of Europe and North America. Nature, 367:

Heeres, P. and Adema, E.H. (1989) A study of the dry deposition of $SO_2$, $NH_3$, $CO_2$, $O_2$ and $O_3$ on a water surface. In: Proc. 8th World Clean Air Congress, The Hague.

Heil, G.W., Bobbink, R., Dam, D.van and Heijne, B. (1989) LAI of grasslands: A measure for ammonium deposition from polluted air. In: Proc. 8th World Clean Air Congress, The Hague.

Heil, G.W., Deursen, W.P.A. van, Boxtel, A.M.J.V. van, Rijsberman, F.R., Erisman,, J.W., Jong, S.M. de, Draaijers, G.P.J., Addink, E., Keizer, V. and Ruyssenaars, P. (1992) Demonstration project: using remote sensing data on roughness length for modelling atmospheric deposition. Resource Analysis, Delft.

Heij, G.J., Vries, W. de, Posthumus, A.C. and Mohren, G.M.J. (1991) Effects of air pollution and acid deposition on forests and forest soils. In: G.J. Heij and T. Schneider (Editors), Acidification research in the Netherlands. Studies in Environmental Science 46, Elsevier, Amsterdam.

Heij, G.J. and Schneider, T. (1991) Final report, Dutch Priority Programme on Acidification, Second Phase. Report No. 200-09, National Institute of Public Health and Environmental Protection, Bilthoven, The Netherlands.

Heij, G.J. and Schneider, T. (1992) Dutch Priority Programme on Acidification, Third Phase (1992-1994). Report No. 300-01, National Institute of Public Health and Environmental Protection, Bilthoven, The Netherlands.

Heij, G.J. and Schneider, T. (1995) Final report, Dutch Priority Programme on Acidification, Third Phase. Report in prep. National Institute of Public Health and Environmental Protection, Bilthoven, The Netherlands.

Hettelingh, J.P., Downing, R.J. and Smet, P.A.M. de (1991) Mapping critical loads for Europe, Report No. 259101001. Coordination Centre for Effects, National Institute of Public Health and Environmental Protection, Bilthoven, The Netherlands.

Hicks, B.B., Wesely, M.L., Durham, J.L. and Brown, M.A. (1982) Some direct measurements of atmospheric sulphur fluxes over a pine plantation. Atmospheric Environment, 16:2899-2903.

Hicks, B.B., Wesely, M.L., Coulter, R.L., Hart, R.L., Durham, J.L., Speer, R.E. and Stedman, D.H. (1983a) An experimental study of sulphur deposition to grassland. In: Pruppacher et al. (Editors), Precipitation Scavenging, Dry deposition and Resuspension. Elsevier Science Publishing, Amsterdam, pp. 933-942.

Hicks, B.B., Wesely, M.L., Coulter, R.L., Hart, R.L., Durham, J.L., Speer, R.E. and Stedman, D.H. (1983b) An experimental study of sulphur and $NO_X$ fluxes over grassland. Boundary-Layer Met., 34:103-121.

Hicks, B.B., Baldocchi, D.D., Meyers, T.P., Hosker Jr., R.P. and Matt, D.R. (1987) A preliminary multiple resistance routine for deriving dry deposition velocities from measured quantities. Water Air Soil Pollut., 36:311-330.

Hicks, B.B. and Meyers, T. (1988) Measuring and modelling deposition in mountain environments. In: M. Unsworth and D. Fowler (Editors), Process of acidic deposition in mountainous terrain. Kluwer Academic Publishers, London.

Hicks, B.B., Draxler, R.R., Albritton, D.L., Fehsenfeld, F.C., Hales, J.M., Meyers, T.P., Vong, R.L., Dodge, M., Schwartz, S.E., Tanner, R.L., Davidson, C.I., Lindberg, S.E. and Wesely, M.L. (1989a) Atmospheric processes research and procecess model development. State of Science/Technology, Report No. 2. National Acid Precipitation Assessment Program.

Hicks, B.B., Matt, D.R. and McMillen, R.T. (1989b) A micrometeorological investigation of surface exchange of $O_3$, $SO_2$ and $NO_2$ : a case study. Boundary-Layer Met., 47:321-336.

Hicks, B.B., Hosker, R.P., Meyers, T.P. and Womack, J.D. (1991) Dry deposition inferential measurement techniques - I. Design and tests of a prototype meteorological and chemical system for determining dry deposition. Atmospheric Environment, 25A:2345-2359.

Hillamo, R.E., Pacyna, J.M., Semb, A. and Hanssen, J.E. (1992) Size distribution of inorganic ionst in atmospheric aerosol in Norway. In: ....

Hoek, K.W. van der (1994) Berekeningsmethodiek ammoniakemissies in Nederland voor de jaren 1990, 1991 en 1992. Report No. 773004003, National Institute of Public Health and Environmental Protection, Bilthoven, The Netherlands.

Hofschreuder, P., Bogaard, A.J. and Hartog, K.D. (1994) Aerosol deposition in forests. Report No. R 637, Agricultural University Wageningen, Wageningen, The Netherlands.

Holtslag, A.A.M. and Ulden A.P. van (1983) A simple scheme for daytime estimates of the surface fluxes from routine weather data. J. Climate Appl. Met., 22:517-529.

Holtslag, A.A.M. and Bruin, H.A.R. de (1988) Applied modelling of the nighttime surface energy balance over land. J. Appl. Met., 27:689-704.

Horn, R., Schulze, E.-D. and Hantschel, R. (1989) Nutrient balance and element cycling in healthy and declining Norway Spruce stands. In: E.D. Schulze, O.L. Lange and R. Oren (Editors), Forest decline and air pollution - A study of Spruce Picea Abies. on acid soils. Ecological Studies 77, pp. 444-455.

Horvath, L. (1982) On the vertical flux of gaseous ammonia over water and soil surfaces. In: Deposition of atmospheric pollutants. (Eds. Georgii, H.W. and Pankrath, J.), pp 17-22, D. Reidel Publishing Company.

Houdijk, A.L.F.M. (1990) Effecten van zwavel- en stikstof depositie op bos- en heide vegetaties (Effects due to sulfur and nitrogen deposition to forest and heather vegetation, in Dutch). University of Nijmegen, The Netherlands.

Houdijk, A.L.F.M. and Roelofs, J.G.M. (1991) Deposition of acidifying and eutrophycating substances in Dutch forests. Acta Botany Neerl., 40:245-255.

Hov, O., Allegrini, I., Beilke, S., Cox, R.A., Eliassen, A., Elshout, A.J., Gravenhorst, G., Penkett, S.A. and Stern, R. (1987) Evaluation of atmospheric processes leading to acid deposition in Europe. Report 10, EUR 11441, CEC, Brussels.

Hove, L.W.A.van (1989) The mechanism of $NH_3$ and $SO_2$ uptake by leaves and its physological effects. PhD Thesis. Wageningen Agricultural University, The Netherlands.

Hrcek, D. (1992) Air Pollution in Slovenia: April 1991 - March 1992. Ministry of Environment and Regional Planning; Hydrometeorological Institute of Slovenia.

Huebert, B.J. and Robert, C.H. (1985) The dry deposition of nitric acid to grass. J. Geophys. Res., 90:2085-2090.

Hughes, D.W. (1992) The meteorite flux. Space Science Reviews, 61:275-299.

Hultberg, H. and Grennfelt, P. (1992) Sulphur and seasalt deposition as reflected by throughfall and runoff chemistry in forested catchments. Environ. Pollut., 75:215-222.

Hummelshøj, P., Jensen, N.O. and Larsen, S.E. (1992) Particles dry deposition to a sea surface. In: W.G.N. Slinn and S.E. Schwartz (Editors), Precipitation scavenging and atmosphere-surface exchange processes. Hemisphere Publ., Washington D.C., pp. 829-840.

Ibrahim, M., Barrie, L.A. and Fanaki, F. (1983) An experimental and theoretical investigation of the dry deposition of particles to snow, pine trees and artificial collectors. Atmospheric Environment, 17:781-788.

IHE (1991) Regennet 01/04/90-31/3/91. Rapport Instituut voor hygiëne en epidemiologie, afdeling lucht, Brussel.

Ingham, G. (1950) Effects of materials absorbed from the atmosphere in maintaining soil fertility. Soil Sci., 70:205-212.

INMG (1989) InvestigaÇao Meteorologica de Apoio à Defesa de Ambiente. Instituto Nacional de Meteorologia e geofisica, Estudos do Clima, Divisao de ProtecÇao do Ar, Boletim do Projecto I2 do Piddac, nos 61, 62, 63, 64 (I, II, III, IV Trim., 1989).

Ivens, W., Tak, A.K., Kauppi, P. and Alcamo J. (1988) Atmospheric deposition of sulphur, nitrogen and basic cations onto European forests: observation and model calculations. In: Proc. Aulanko-meeting on Models to describe the geographic extent and time evolution of acidification and air pollution damage. Hmeenlina, Finland, 5-8 July 1988.

Ivens, W., Løvblad, G., Westling, O. and Kauppi, P. (1989) Throughfall monitoring as a means of monitoring deposition to forest ecosystems - Evaluation of European data. UN-ECE.

Ivens, W.P.M.F. (1990) Atmospheric deposition onto forests: an analysis of the deposition variability by means of throughfall measurements. PhD Thesis, Utrecht University, The Netherlands.

Ivens, W., Tak, A.K., Kauppi, P. and Alcamo, J. (1988) Atmospheric deposition of sulphur, nitrogen and basic cations onto European forests: observation and model calculations. In: Proceedings of Aulanko meeting on Models to describe the geographic extent and time evolution of acidification and air pollution damage. Hmeenlina, Finland, 5-8 July 1988.

Iversen, T., Halvorsen, N., Mylona, S. and Sandnes, H. (1991) Calculated budgets for airborne acidifying components in Europe, 1985, 1987, 1988 and 1990. MSC-West, Norwegian Meteorological Institute, Oslo.

Jaarsveld, J.A. van and Onderdelinden, D. (1986) Modelmatige beschrijving van concentratie en depositie van kolenrelevante componenten in Nederland, veroorzaakt door emissies in Europa. RIVM Rapport No. 228202002, National Institute of Public Health and Environmental Protection, Bilthoven, The Netherlands.

Jaarsveld, H.J.A. van (1989) A model approach for assessing transport and deposition of acidifying components on different spatial scales. In: Changing composition of the troposphere. Special Environmental Report No. 17, WMO, Geneva.

Jaarsveld, H.J.A.van (1990) A quantative model analysis of year to year changes in concentration and deposition. Presented at the NATO CCMS meeting, Vancouver, Canada.

Jaarsveld, H.J.A. and Onderdelinden, D. (1992) TREND: An analytical long term deposition model for multi-scale applications. Report No. 228603009, National Institute of Public Health and Environmental Protection, Bilthoven, The Netherlands.

Jaarsveld, H.J.A. (1995), modelling the long-term atmospheric behaviour of pollutants on various spatial scales. Ph.D. thesis, University of Utrecht, the Netherlands.

Jans, W.W.P., Roekel, G.M. van, Orden, W.H. van and Steingröver, E.G. (1994) Above ground biomass of adult Douglas fir. A dataset collected in Garderen and Kootwijk from 1986 onwards. IBN-DLO Research Report No. 94/1, 58 pp.

Janssen, L.H.J.M., Visser, H., Vaessen, R.J., Römer, F.G. and Rietbergen, J.M. (1987) Aerosolconcentraties in Nederland. Resultaten van het aerosolmeetnet van de elektriciteitsbedrijven over de periode 1979-1986. KEMA Report No. 98371-MOL 86-3075, Arnhem, The Netherlands.

Janssen, P.H.M., Heuberger, P.S.C. and Sanders, R. (1992) UNCSAM 1.1: A software package for sensitivity and uncertainty analysis: Manual. Report No. 95101004, National Institute of Public Health and Environmental Protection, Bilthoven, The Netherlands.

Järvinen, O. and Vänni, T. (1990) Sadeveden Pitoisuus- ja Laskeuma- Arvot Soumessa Vuonna 1989. Nro 236, Vesi- ja Ympäristöhallituksen Monistesarja, Helsinki (in Finnish).

Jarvis, P.G. (1976) The interpretation of the variations in leaf water potential and stomatal conductance found in canopies in the field. Phyl. Trans. R. Soc. Lond., B273:593-610.

Jarvis, S.C., Hatch, D.J. and Lockyer, D.R. (1989) Ammonia fluxes from grazed grassland: annual losses from cattle production systems and their relation to nitrogen inputs. J. Agric. Aci. Camb., 113:99-108.

Johansson, C. and Granat, L. (1986) An experimental study of the dry deposition of gaseous nitric acid to snow. Atmospheric Environment, 20:1165-1170.

Johansson, C. (1987) Pine forest; a negligible sink for atmospheric $NO_X$ in rural Sweden. Tellus, 39B:426-438.

Johnson, D.W. and Lindberg, S.E. (1992) Atmospheric deposition and forest nutrient cycling. Ecological Studies 91, Springer, New York.

Joslin, J.D. and Wolfe, M.H. (1992) Tests of the use of net throughfall sulfate to estimate dry and occult sulfur deposition. Atmospheric Environment, 26A:63-72.

Junge, C.E. (1974), Residence time and variability of tropospheric trace gases. Tellus, 26A: 477-488.

Kallaste, T., Roots, O., Saar J. and Saare, L. (1992) Air Pollution in Estonia 1985-1990. Environmental Report 3, Environment Data Centre, National Board of Waters and the Environment, Helsinki.

Kerfoot, O. (1968) precipitation on vegetation. Forestry Abstr., 29:8-20.

Keuken, M.P., Mallant, R.K.A.M., Woittiez, J.R.W., Das, H.A. and Slanina, J. (1989) Verzuringsonderzoek bij ECN. Report No. ECN-PB-89-7, ECN, Petten, The Netherlands.

Khlystov, A., Ten Brink, H.M., Wyers, G.P. (1993) Hygroscopic growth rates of aerosols at high relative humidities. Report No. ECN-C--93-011, ECN, Petten, The Netherlands.

Kimmins, J.P. (1973) Some statistical aspects of sampling throughfall precipitation in nutrient cycling studies in British Columbian coastal forests, Ecology, 54:1008-1019.

Klaassen, W. (1992) Average fluxes from heterogeneous vegetated regions. Boundary-Layer Met., 58:329-354.

Klein Tank, A. (1990) DAVER, een dataverwerkingsprogramma voor neerslag-, doorval-, bodemvocht- en grondwaterkwaliteitsgegevens. Vakgroep Fysische Geografie, Universiteit Utrecht.

Klockow, D. and Wintermeyer, D. (1990). Erstellung von Depositionskarten für die Bundesrepublik Deutschland. Abschlußbericht zum Vorhaben Nr. 0339232 A, Gefördert durch das Bundesministerium für Forschung und Technologie, Dortmund (in German).

KNMI (1979) Luchtverontreiniging en weer. Staatsuitgeverij, The Hague.

KNMI/RIVM (1988) Chemische samenstelling van de neerslag over Nederland, Annual Report 1987. KNMI Report No. 156-10; RIVM report No. 228703005, De Bilt, The Netherlands.

Koenigswald, G.H.R. von (1964) The problem of tektites. Space Sci., Rev., 3:433-446.

Koop, H. (1989) Forest dynamics. Ph.D. thesis, Agricultural University of Wageningen, the Netherlands.

Kovar, A., Kasper, A., Puxbaum, H., Fuchs, G., Kalina, M. and Gregori, M. (1991) Kartierung der deposition von $SO_X$, $NO_X$, $NH_X$ und basischen kationen in Österreich. Technische Universität Wien, Institut für Analytische Chemie, Vienna (in German).

Kovar, A. and Puxbaum, H. (1992) Nasse Deposition im Ostalpenraum, Untersuchung der nassen deposition atmosphärischer spurenstoffe im bereich der arge Alp und der arbeitsgemeinschaft Alpen-Adria. Institut für Analytische Chemie der Technischen Universität Wien, Vienna (in German).

Kramm, G. (1989) A numerical method for determining the dry deposition of atmospheric trace gases. Boundary-Layer Met., 48:157-176.

Krüger, O. (1993) The applicability of the EMEP-code to estimate budgets for airborne acidifying components in Europe. In: proceedings CEC/BIATEX Workshop 4-7 May 1993, Aveiro, Portugal.

Kruijt, B. (1986) Oak forest description for the estimation of aerodynamic roughness parameters. Department of Physical Geography, University of Groningen, the Netherlands, report no. 20.

Lang, G.E., Reiners, W.A. and Heier, R.K. (1976) Potential alteration of precipitation chemistry by epiphytic lichens. Oecologica Berl., 25:229-241.

Langford, A.O., Fehsenfeld, F.C., Zachariassen, J. and Schimel, D.S. (1992) Gaseous ammonia fluxes and background concentrations in terrestrial ecosystems of the United States. Global Biochem. Cycl., 6:459-483.

Last, F.T. (1991) Critique, In: F.T. Last and R. Watling Last (Editors), Acid Deposition; Its Nature and Impacts. (eds. R.) Roy. Soc. of Edinburgh, UK, pp. 273-324.

Last, F.T. and Watling, R. (1991) Acid deposition, Its nature and impacts. Proc. Roy. Soc. Edinburgh 97,UK.

Lawes, J.B. and Gilbert, J.H. (1851) On agricultural chemistry. J. Roy. Agr. Soc., 12:1-40.

LeClerc, J.A. and Breazeale, J.F. (1908) Yearbook U.S. Department of Agriculture, 1908, pp. 389-402.

Lee, Y. and Schwartz, S.E. (1981) Evaluation of the rate of uptake of nitrogen dioxide by atmospheric and surface liquid waters. J. Geophys. Res., 86:11971-11983.

Leeuwen, N.P.M. van, Bleuten, W., Hansen, K. (1994) Deposition of acidifying and basic compounds measured at the Speulder forest by means of the throughfall method. Report of the Department of Physical Geography, University of Utrecht, The Netherlands.

Leeuwen, E.P. van, Potma, C., Draaijers, G.P.J., Erisman, J.W. and Pul, W.A.J. van (1995) European wet deposition maps based on measurements. RIVM Report 722108006, National Institute for Public Health and Environmental Protection, Bilthoven, The Netherlands.

Legg, B.J. and Price, R.I. (1980) The contribution of sedimentation to aerosol deposition to vegetation with a large leaf area index. Atmospheric Environment, 14:305-309.

Leinonen, L. and Junto, S. (1991) Ilmanlaadun Tuloksia Tausta-Asemilta, Results of Air Quality at Background Stations January - June 1989 and July - December 1989. Finish Meteorological Institute - Air Quality Department, Helsinki (in Finnish).

Lemon, E. and Van Houtte, R. (1980) Ammonia exchange at the land surface. Agron. J., 72:876-883.

Lenschow (1982) Reactive trace species in the boundary layer from a micrometeorological perspective. J. Met. Soc. Japan, 60:

Leonard, R.E. and Federer, C.A. (1973) Estimated and measured roughness parameters for a pine forest. Journal of Applied Meteorology, 12:302-307.

Lettau, H. (1969) Note on aerodynamic roughness-parameter estimation on the basis of roughness-element description. J. Appl. Met., 8:828-832.

Leuning, R., Neumann, H.H. and Thurtell, G.W. (1979) Ozone uptake by corn: a general approach. Agri. Met. 20:115-135.

Li, Z., Lin, J.D. and Miller, D.R. (1990) Air flow over and through a forest edge: a steady state numerical simulation. Boundary-Layer Met., 51:179-197.

Liebig, Von (1827) Sur la nitrification. Ann. Chim. Phys.,35:329.

Liesegang, W. (1927) Chemische Ermittlungen auf dem Gebiete der Lufthygiene. Kleine Mitt. Mitgl. Ver. Wasser-, Boden und Lufthygiene, 3:9.

Lightowlers, P.J. and Cape, J.N. (1988) Sources and fate of atmospheric HCL in the UK and Western Europe. Atmospheric Environment, 22:7-15.

Likens, G.E., Bormann, F.H., Hedin, L.O., Driscoll, C.T. and Eaton. J.S. (1990) Dry deposition of sulphur: a 23 year record for the Hubbard Brook Forest ecosystem. Tellus, 42B:319-329.

Lindberg, S.E., Lovett, G.M., Richter, D.D. and Johnson, D.W. (1986) Atmospheric deposition and canopy interaction of major ions in a forest. Science, 231:93-102.

Lindberg, S.E., Lovett, G.M., Schaefer, D.A. and Bredemeier, M. (1988) Coarse aerosol deposition velocities and surface-to-canopy scaling factors from forest canopy throughfall. J. Aeros. Sci., 19:1187-1190.

Lindberg, S.E. and Garten, C.T. (1989) Sources of sulphur in forest canopy throughfall. Nature, 336:148-151.

Lindberg, S.E., Lovett, G.M., Knoerr, K. and Ragsdale H. (1990) The integrated forest study: Atmospheric deposition and canopy interactions of sulphur, nitrogen and cations. NAPAP Int. Conf. on 'Acidic deposition: State of science and technology', February 1990, Hilton Head Island, USA.

Lindberg, S.E., Bredemeier, M., Schaefer, D.A. and Qi, L. (1990) Atmospheric concentrations and deposition of nitrogen and major ions in conifer forests in the United States and Federal Republic of Germany. Atmospheric Environment, 24:2207-2220.

Lindberg, S.E., Cape, J.N., Garten,C.T. Jr and Ivens, W. (1992) Can sulphate fluxes in forest canopy throughfall be used to estimate atmospheric sulphur deposition?. In: S.E. Schwartz

and W.G.N. Slinn W.G.N. (Editors), Proc. 5th IPSASEP conference, Richland, USA, 15-19 June 1991. Hemisphere Publishing Corporation, Washington.

Lindberg, S.E. and Lovett, G.M. (1992) Deposition and forest canopy interactions of airborne sulphur: results from the integrated forest study. Atmospheric Environment, 26A:1477-1492.

Lindner, L. and Welten, K.C. (1994) Meteorieten voor het oprapen. Zenith, 5:196-201.

Locht, J.V. and Aalst, R.M.van (1988) Depositie van verzurende stoffen op de Nederlandse bodem van niet antropogene herkomst. TNO Report R 88/458, Delft.

Lockyer, D.R. and Whitehead, D.C. (1986) The uptake of gaseous ammonia by the leaves of Italian Rygrass. J. Experim. Botany, 37:919-927

Lorenz, R. and Murphy, C.H. Jr. (1985) Sulphur dioxide, carbon dioxide, and water vapout flux measurements utilizing a microprocessor-controlled data acquisition system in a pine plantation. In: B.A. Hutchison and B.B. Hicks (Editors), The Forest-Atmosphere Interaction. Kluwer, Dordrecht, The Netherlands, pp. 133-148.

Lövblad, G. and Erisman, J.W. (1992) Deposition of nitrogen in Europe. In: P. Grennfelt and E. Thörnelöf (Editors), Proc. on Critical loads for nitrogen, Report No. Nord 1992:41, Lökeberg, Sweden, 6-10 April 1992. Nordic Council of Ministers, Copenhagen, Denmark.

Lövblad, G., Erisman, J.W. and Fowler, D. (1993) Models and methods for the quantification of atmospheric input to ecosystems. Report No. Nord 1993:573 Göteborg, Sweden, 3-7 November 1992. Nordic Council of Ministers, Copenhagen, Denmark.

Lovett, G.M. and Reiners, W.A. (1983) Cloud water: an important vector of atmospheric deposition. In: H.R. Pruppacher, R.G. Semonin & W.G.N. Slinn, eds., Precipitation scavenging, dry deposition and resuspension, Kluwer, Dordrecht, the Netherlands, pp. 84-106.

Lovett, G.M. and Lindberg, S.E. (1984). Dry deposition and canpopy exchange in a mixed oak forest as determined by analysis of throughfall. J. Appl. Ecol., 21:1013-1027.

Lovett, G.M. and Reiners, W.A. (1986) Canopy structure and cloud water deposition in subalpine coniferous forests. Tellus, 38B:319-327.

Lovett, G.M., Lindberg, S.E., Richter, D.D. and Johnson, D.D. (1988) Can. J. For. Res., 15:1055-1060.

Lovett, G.M. (1988) A comparison of methods for estimating cloud water deposition to a New Hampshire USA. subalpine forests. In: M.H. Unsworth and D. Fowler (Editors), Acid deposition at high elevation sites. Kluwer, Dordrecht, The Netherlands, pp. 309-320.

Lovett, G.M. and Kinsman, J.D. (1990) Atmospheric pollutant deposition to high-elevation ecosystems. Atmospheric Environment, 24A:2767-2786.

Lovett, G.M. (1992) Nitrogen cycle. In: D.W. Johnson and S.E. Lindberg (Editors), Atmospheric deposition and nutrient cycling in forest ecosystems. Springer, Berlin.

Lovett, G.M., Likens, G.E. and Nolan, S.S. (1992) Dry deposition of sulphur to Hubard Brook Experimental Forest: A preliminary comparison of methods. In: S.E. Schwartz and W.G.N.Slinn (Editors), Proc. 5th IPSASEP conference, Richland, USA, 15-19 June 1991, USA. Hemisphere Publishing Corporation, Washington.

Lovett, G.M. and Lindberg, S.E. (1992). Atmospheric deposition and canopy interactions of nitrogen in forests. Can. J. For. Res., 23:1603:1616.

Ludwig, H. (1862), Die natürlichen Wasser in ihren chemischen Beziehungen zu Luft und Gesteinen. Atmosphärwasser, 1-29.

Ludwig, J. and Klemm, O. (1990) Acidity of size-fractionated aerosol particles. Water Soil Air Pollut., 49:35-50.

Maas, M.P.van der (1990) Hydrochemistry of two Douglas fir ecosystems in the Veluwe, The Netherlands. Final report No. 102.1

Maas, M.P. van, Breemen, N. van, Langenvelde, I. van (1991) Estimation of atmospheric deposition and canopy exchange in two Douglas fir stands in the Netherlands. Department of Soil Science and Geology, Agricultural University of Wageningen, The Netherlands.

Madgewick, H.A.I. and Ovington, J.D. (1959) The chemical composition of precipitation of adjacent forest and open plots. Forestry, 32:14-22.

Mallant, R.K.A.M. and Kos, G.P.A. (1990) An optical device for the detection of clouds and fog. Aerosol Sci. Technol., 13:196-202.

Malo, B.A. and Purvis, E.R. (1964) Soil absorption of atmospheric ammonia. Soil Sci., 97:242-247.

Masuch, G., Kettrup, A., Mallant, R.K.A.M. and Slanina, J. (1986) Effects of $H_2O_2$ containing acidic fog on young trees. Int. J. Environ. Anal. Chem., 27:183-213.

Matt, D.R., McMillen, R.T., Womack, J.D. and Hicks, B.B. (1987) A comparison of estimated and measured $SO_2$ deposition velocities. Water Air Soil Pollut., 36:331-347.

Matzner, E., Khanna, P.K., Meiwes, K.J. and Ulrich, B. (1983) Effects of fertilization on the fluxes of chemical elements through different ecosystems. Plant and Soil, 74:343-358.

Mayer, R. and Ulrich, B. (1978) Input of atmospheric sulfur by dry and wet deposition to two central European forest ecosystems. Atmospheric Environment, 12:375-377.

Mallant, R.K.A.M. and Kos, G.P.A. (1990) An optical device for the detection of clouds and fog. Aerosol Sci. Technol., 13:196-202.

McMillen, R.T., Matt, D.R., Hicks, B.B. and Womack, J.D. (1987) Dry deposition measurements of Sulphur dioxide to a Spruce-Fir forest in the Black forest: A data report. NOAA Technical Memorandum, ERL ARL-152.

Meetham, A.R. (1950) Natural removal of pollution from the atmosphere. Q. J. R. Met. Soc., 76:359-371.

Meijers, R. (1990) Parametrisatie van de structuur van Nederlandse natuurgebieden, Vakgroep Fysische Geografie, Utrecht University, The Netherlands.

Meijers, R., Draaijers, G.P.J. and Ek, R. van (1990) Predicting atmospheric deposition onto forests using remote sensing techniques: a local scale model. In: Proceedings of the international conference on Acidic Deposition: its Nature and Impacts, Glasgow, Scotland.

Meijers, R., Draaijers, G.P.J. and Ek, R. van (1995) Assessment of forest structure characteristics from monotemporal Landsat TM for application in atmospheric deposition monitoring, to be published.

Meixner, F.X., Franken, H.H., Duyzer, J.H. and Aalst, R.M. van (1988) Dry deposition of gaseous $HNO_3$ to a pine forest. In: H. van Dop (Editor), Air Pollution Modelling and its application VI. Plenum Publishing Corp., New York.

Meixner, F.X., Böswald, F., Buck, C., Eiblmeier, K. and Müller, H. (1990) Measurement of $HNO_3$ dry deposition by gradient techniques. Proc. of the CEC workshop, COST 611, Working group 3. Madrid, 12-16 March 1990.

Mennen, M.G., Erisman, J.W., Elzakker, B.G.van and Zwart, E. (1992) A monitoring system for continuous measurement of the $SO_2$ dry deposition flux above low vegetation. In: Air Pollution Report 39. CEC, Brussels, Belgium.

Mennen M.G., Hogenkamp J.E.M., Zwart H.J.M.A., Erisman J.W. (1995) Monitoring dry deposition fluxes of $SO_2$ and $NO_2$: Analysis of errors. In: Erisman, J.W. and Hey, B.J. (Editors), Acid Rain; do we have all the answers?, 10-12 October 1994, Den Bosch, The Netherlands.

Mészáros, E. (1981), Atmospheric chemistry, fundamental aspects. Studies in Environmental Science 11, Elsevier Scientific Publishing Company, Amsterdam, 1981).

Meyers, T.P. (1987) The sensitivity of modelled $SO_2$ fluxes and profiles to stomatal and boundary layer resistance. Water, Air Soil Pollut., 35:261-278.

Meyers, T.P. and Baldocchi, D.D. (1988) A comparison of models for deriving dry deposition fluxes of $O_3$ and $SO_2$ to a forest canopy. Tellus, 40B:270-284.

Meyers, T.P., Huebert, B.J. and Hicks, B.B. (1989) $HNO_3$ deposition to a deciduous forest. Boundary-Layer Meteorology, 49:395-410.

Meyers, T.P., Hicks, B.B., Hosker, R.P., Womack, J.D. and Satterfield, L.C. (1991) Dry deposition inferential measurement techniques-II. Seasonal and annual deposition rates of sulphur and nitrate. Atmospheric Environment, 25A:2361-2370.

Meyrac, V. (1852) Observations sur les eaux de pluie, des neiges et de rosées. Compt. Rend., 34:714-717.

Milford, J.B. and Davidson, C.I. (1985) The sizes of particulate trace elements in the atmosphere - A review JAPCA, 35:1249-1260.

Milford, J.B. and Davidson, C.I. (1985) JAPCA, 37:124-134.

Miller, D.R. (1980) The two-dimensional energy budget of a forest edge with field measurements at a forest-parking lot interface. Agr. Met., 22:53-78.

Miller, H.G., Miller, J.D. and Cooper, J.M. (1987) In: Pollutant transport and fate in ecosystems. Blackwell Scientific Publications, London.

Miller, N.H.J. (1905) The amounts of nitrogen as ammonia and as nitric acid, and of chlorine in the rainwater collected at Rothamsted. J. Agr. Sci., 1:280-303.

Milne, J.W., Roberts, D.B. and Williams, D.J. (1979) Atmospheric Environment, 13:373-379.

Mitchell, M.J., Fitzgerald, J.W., Harrison, R.B. and Lindberg, S.E. (1990) The integrated forest study: sulphur cycle. NAPAP Int. Conference on 'Acidic deposition: State of science and technology', February 1990, Hilton Head Island, USA.

Mohnen, V.A. (1988) Mountain cloud chemistry project - wet, dry and cloud water deposition. EPA-600/3-89-009, U.S. Environmental Protection Agency, Research Triangle Park, N.C., USA.

Möller, D. and Schieferdecker, H. (1985) A relationship between agricultural $NH_3$ emissions and the atmospheric $SO_2$ content over industrial areas. Atmospheric Environment, 19:695-700.

Montheith, J.L. (1975; 1976) Vegetation and the atmosphere. Academic Press, London, UK.

Morgan, J.A. and Parton, W.J. (1989) Characteristics of ammonia volatilization from spring wheat. Crop. Sci., 29:726:731.

Mosello, R., Marchetto, A and Tartari, G.A. (1988) Bulk and wet atmospheric deposition chemistry at Pallanza N. Italy. Water Air Soil Pollut., 42:137-151.

Mosello, R., Bianchi, M., Geiss, H., Marchetto, A., Tartari, G.A., Serrini, G., Serrini Lanza, G. and Muntau, H. (1994) Acid Rain Analysis: Results of the third interlaboratory exercise, Aquacon-Medbas-Subproject N.6 (Analytical Quality Control and Assessment Studies in the Mediterranian Basin).

Mosello, R. and Morselli, L. (1992) Situazione degli Srudi Sulla Chimica delle Deposizioni Atmosferiche Umide nel 1989 in Italia. Documenta dell'Istituto Italiano de Idrobiologia Dott. Marco De Marchi, N.33, Pubblicazione n.5, Consiglio Nazionale delle Richerche, Pallanza (in Italian).

Mueller, S.F. (1992) Estimating cloud water deposition to subalpine spruce forests. I. Modificatuions to an existing model. Atmospheric Environment, 25A:1093-1104.

Murphy, C.E., Sinclair, T.R. and Knoerr, K.R. (1977) An assessment of the use of forests as sinks for the removal of atmospheric sulphur dioxide. J. Environ. Qual., 6:388-396.

Murphy, C.E. and Sigmon, J.T. (1989) Dry deposition of sulphur and nitrogen oxide gases to forest vegetation. In: S.E. Lindberg, A.L. Page and S.A. Norton (Editors), Acidic precipitation, Volume 3. Springer-Verlag, Berlin, pp. 217-238.

Mylona, S. (1993) Trends od sulphur dioxide emissions, air concentrations and depositions of sulphur in Europe since 1880. EMEP/MSC-W Report 2/93, The Norwegian Meteorological Institute, Oslo.

Nagel, J.F. (1956) Fog precipitation on Table Mountain, Q. J. R. Met., Soc., 82:452-460.

NABEL (1992) Luftbelastung 1992. Schriftenreihe umwelt nr. 207, BUWAL, Bern, Switzerland (in German).

NAPAP (1990) Acid Deposition: State of Science and Technology, NAPAP, Washington DC., USA.

Neumann, H.H. and Hartog, C.D. (1985) Eddy correlation measurements of atmospheric fluxes of ozone, sulphur, and particles during the campaign intercomparison study. J. Geophys. Res., 90:2097-2110.

Nicholson, K.W. and Davies, T.D. (1987) Field measurements of the dry deposition of particulate sulphate. Atmospheric Environment, 21:1561-5171.

Nicholson, K.W. (1988) The dry deposition of small particles: a review of experimental measurements. Atmospheric Environment, 22:2653-2666.

Nicholson, K.W. and Davies, T.D. (1988) Letter to the editors: The dry deposition of sulphur dioxide at a rural site. Atmospheric Environment, 22:2885-2889.

Nilsson, J. and Grennfelt, P. (1988) Critical loads for sulphur and nitrogen. Proceedings of the workshop in Skokloster, Sweden.

Nord, M. (1991) Shelter effects of vegetation belts - results of field measurements. Boundary-Layer Meteorology, 54:363-385.

Northolt, J., Hjorth, J. and Raes, F. (1992) Formation of $HNO_2$ on aerosol surface during foggy periods in the presence of NO and $NO_2$. Atmospheric Environment 26A:211-217.

O'Dell, R.A., Taheri, M. and Kabel, R.L. (1973) A model for uptake of pollutants by vegetation. JAPCA, 27:1104-1109.

Odén, S. (1967) Stockholm Newspaper, Dagens Nyheter, October 24, 1967.

Olsen, R.A. (1957) Absorption of sulphur dioxide from the atmosphere by cotton plants. Soil Sci., 84:107-111.

Onderdelinden, D., Jaarsveld, J.A. van, and Egmond, N.D. van (1984) Bepaling van de depositie van zwavelverbindingen in Nederland. RIVM Report 842017001, Bilthoven, The Netherlands.

Padro, J., Hartog, G. den, and Neumann, H.H. (1991) An investigation of the ADOM dry deposition module using summertime $O_3$ measurements above a deciduous forest. Atmospheric Environment 25A:1689-1704.

Padro, J., Neumann, H.H. and Hartog, G. den (1992) Modelled and observed dry deposition velocity of $O_3$ above a deciduous forest in the winter. Atmospheric Environment 26A:775-784.

Padro, J., Puckett, K.J. and Woolridge, D.N. (1993) The sensitivity of regionally averaged $O_3$ and $SO_2$ concentrations to ADOM dry deposition velocity parametrizations. Atmospheric Environment, 27A:2239:2242.

Pandis, S.N. and Seinfeld, J.H. (1990) On the interaction between equilibrium processes and wet or dry deposition. Atmospheric Environment, 24A:2313-2327.

Pannekoek, A.J. (1976) Algemene geologie. H.D. Tjeenk Willink bv, Groningen, The Netherlands.

Parker, G.G. (1983) Throughfall and stemflow in the forest nutrient cycle. In: A. McFadyen and E.D. Ford (Editors.), Advances in Ecological Research, Vol. 13.

Parker, G.G. (1990) Evaluation of dry deposition, pollutant damage, and forest health with throughfall studies. In: A.A. Lucier and S.G. Haines (Editors) Mechanisms of forest response to acidic deposition. Springer Verlag, New York.

Parton, W.J. Morgan, J.A., Altenhofen, J.M. and Harper, L.A. (1988) Ammonia volatilization from spring wheat plants. Agron. J., 80:857:861.

Pasquill, F. (1971) Atmospheric dispersion of pollutants. Q. J. R. Med. Soc.,97:369-395.

Pasquill, F. and Smith, F.B. (1983) Atmospheric diffusion. John Wiley and Sons, New York.

Payrissat, M. and Beilke, S. (1974) Laboratory measurements of the uptake of sulphur dioxide by different European soils. Atmospheric Environment, 9:211-217.

Pedersen, L.B. (1992) Throughfall chemistry of Sitka spruce stands as influenced by tree spacing. Scan. J. For. Res., 8:

Peterson, D.L., Spanner, M.A., Running, S.W. and Teuber, K.B. (1987) Relationship of Thematic Mapper Simulator data to leaf area index of temporate coniferous forests. Remote Sensing and Environment, 22:323-341.

Perry, J.H. (Editor) (1950) Chemical Engineers Handbook, Third ed., McGraw - Hill Comp. Inc.

Persson, K., Lövblad, G. and Munthe, J. (1993). Luft- och nederbördskemiska stationsnätet inom PMK. IVL, Göteborg, Sweden (in Swedish).

Peters, K. and Eiden, R. (1992) Modelling the dry deposition velocity of aerosol particles to a spruce forest. Atmospheric Environment, 26A:2555-2564.

Petit, C., Ledoux, M. and Trinite, M. (1976) Transfer resistance to $SO_2$ capture by some plane surfaces, water and leaves. Atmospheric Environment, 11:1123-1126.

Pierre, J. (1860) Note relative a l'emploi du sel sur terres. Du sel contenu dans les terres non réputées terres sallées et dans les eaux de pluie. Ann. Agron.,1:466-475.

Pio, C.A. and Harrison, R.M. (1987) The equilibrium of ammonium chloride aerosol with gaseous hydrochloric acid and ammonia under tropospheric conditions. Atmospheric Environment, 21:1243:1246.

Pitts, B.J. and Pitts, J.M. (1986) Atmospheric chemistry. John Wiley and Sons, New York.

Plantaz, M. A. H. G., Vermeulen, A. T. and Wyers, G.P. (1994) Surface exchange of ammonia over grazed pasture. In: F.G. Römer and B.W. te Winkel, Droge depositie van aerosolen op vegetatie: verzurende componenten en basische kationen. Report 63591-KES/MLU 93-3243, KEMA, Arnhem, The Netherlands.

Platt, U. (1978) Dry deposition of $SO_2$. Atmospheric Environment, 12:363-367.

Porter, L.K., Viets, F.G.J. and Hutchinson, G.L. (1972) Air containing nitrogen-15 ammonia: foliar absorption by corn seedlings. Science, 175:759:761.

Potts, M.J. (1978) 'The pattern of deposition of air-borne salt of marine origin under a forest canopy', Plant Soil, 50:233-236.

Pul, W.A.J. van, Aalst, R.M. van and Erisman, J.W. (1991) Deposition of air pollution at a forest edge: a simple approach, In: J. Slanina (Editor), Eurotrac-Biatex annual report, Garmisch Partenkirchen, FRG.

Pul, W.A.J. van (1992) The flux of ozone to a maize crop and the underlying soil during a growing season. PhD Thesis. Wageningen Agricultural University, The Netherlands.

Pul, W.A.J. van, Erisman, J.W., Jaarsveld, J.A. van and Leeuw, F.A.A.M. de (1992) High resolution assessment of acid deposition fluxes. In: T. Scneider (Editor), Acidification research: evaluation and policy application. Studies in Environmental Science. Elsevier, Amsterdam.

Pul, W.A.J. van, and Jacobs, A.F.G. (1993) The conductance of a maize crop and the underlying soil to ozone under various environmental conditions. Boundary-layer Met., 69:83-99

Pul, W.A.J., Potma, C., Leeuwen, E.P. van, Draaijers, G.P.J. and Erisman, J.W. (1994) EDACS: European Deposition maps of Acidifying Compounds on a Small scale. Model description and results. RIVM Report 722401005.

Puxbaum, H. and Kovar, A. (1991) Seasonal trend of snowfall composition at the high alpine observatory Sonnblick (3106 m a.s.l., eastern alps). In: P. Borell et al. (Editors), Proc. of EUROTRAC symposium '90. SPB Academic Publishing bv, pp. 61-66.

Pyatt, F.B. and Haywood, W.J. (1989) Air borne particulate distributions and their accumulation in tree canopies, Nottingham. UK. Environmentalist, 9:291-298.

Quinn, P.K., Charlson, R.J. and Zoller, W.H. (1987) Ammonia, the dominant base in the remote marine troposphere: a review. Tellus, 39b:413-425.

Ranney, J.W., Bruner, M.C. and Levenson, J.B. (1978) The importance of edge in the structure and dynamics of forest islands, In: R.L. Burgess and D.M. Sharpe, Forest island dynamics in man-dominated landscapes, Springer, New York, pp. 67-95.

Raupach, M.R. and Thom, A.S. (1981) Turbulence in and above plant canopies. Ann. Rev. Fluid Mechanics, 13:97-129.

Reiners, W.A. and Olson, R.K. (1984) Effects of canopy components on throughfall chemistry: An experimental analysis. Oecologia, 63:320-330.

ReVelle, D.O. (1979) J. Atmos. Terres. Phys., 41:453.

Rich, S., Waggoner, P.E. and Tomlinson, H. (1970) Ozone uptake by bean leaves. Science, 169:79-80.

Richter, A. and Granat, L. (1993) Dry deposition of sulphur dioxide at low ppb concentration (unpublished data).

Richter, D.D. and Lindberg, S.E. (1988) Wet deposition estimates from long-term bulk and event wet-only samples of incident precipitation and throughfall. J. Environ. Qual., 17:619-622.

Ridder, T.B. Over de chemie van de neerslag; vergelijking van meetresultaten. Scientific Report W.R. 78-4, KNMI, De Bilt, The Netherlands.

Ridder, T.B., Baard, J.H. and Buishand, T.A. (1984) The impact of sample strategy and analysis protocol on concentrations in rainwater (in Dutch). Royal Netherlands Meteorological Institute, Report No. TR-55.

RIVM (1986) Jaarrapport 1985. Report No. 228702015., National Institute of Public Health and Environmental Protection, Bilthoven, The Netherlands.

RIVM (1988) Jaarrapport 1987. Report No. 228702015., National Institute of Public Health and Environmental Protection, Bilthoven, The Netherlands.

RIVM (1989) Jaarrapport 1988. Report No. 228702015., National Institute of Public Health and Environmental Protection, Bilthoven, The Netherlands.

RIVM (1990) Jaarrapport 1989. Report No. 222101006., National Institute of Public Health and Environmental Protection, Bilthoven, The Netherlands.

RIVM (1994) Jaarrapport 1993. Report No. 222101006, National Institute of Public Health and Environmental Protection, Bilthoven, The Netherlands.

Rodhe, H. and Granat, L. (1984) An evaluation of sulphate in European precipitation. Atmospheric Environment,18:2627-2639.

Roelofs, J.G.M., Kempers, A.J., Houdijk, A.L.F.M. and Jansen, J. (1985) The effect of air-borne ammonium sulphate on *Pinus nigra* var. maritima in the Netherlands. Plant Soil, 84:45-56.

Rogers, R. and Hinckley, T.M. (1979) Foliar weight and area related to current sapwood area in Oak. Forest Science, 25(2):298-303.

Römer, F.G, Winkel, B.H. te, Ruigrok, W., Steenkist, R. and Wakeren, J.H.A.van (1990) The chemical composition of dew and the deposition flux of water vapour: field measurements and modelling. Final Report No. 50583-MOC90-3411, KEMA, Arnhem, The Netherlands.

Römer, F.G. and Winkel, B.W. te (1994) Droge depositie van aerosolen op vegetatie: verzurende componenten en basische kationen. Report 63591-KES/MLU 93-3243, KEMA, Arnhem, The Netherlands.

Ronseaux, F. and Delmas, R.J. (1988) Chemical composition of bulk atmospheric deposition to snow at Col de la Brevna (Mt Blanc). In: M.H. Unsworth and D. Fowler (Editors), Acid deposition at high elevation sites.

Rooth, R.A., Verhagen, A.J.L. and Wouters, L.W. (1990) Photoacoustic measurement of ammonia in the atmosphere, influenced by water vapour and carbon dioxide. Appl. Optics., 29:3643-3653.

Ruijgrok, W., Visser, H. and Römer, F.G. (1989) Comparison of bulk and wet-only samplers for trend detection in wet deposition. N.V. Kema, Arnhem, The Netherlands.

Ruijgrok, W. and Davidson, C.I. (1992) Particle deposition. In: G. Lövblad, J.W. Erisman and D. Fowler (Editors), Models and methods for the quantification of atmospheric input to ecosystems. Nordiske Seminar- of Arbejdsrapporter 1993:573. The Nordic Council of Ministers, Copenhagen, pp.145-162.

Ruijgrok, W. and Davidson, C.I. (1993) Particle deposition. Background document to the Workshop of 3-6 November 1992, Göteborg, Sweden.

Ruijgrok, W., Tieben, H. and Eisinga, P. (1994) The dry deposition of acidifying and alkaline particles on Douglas fir. Report No. 20159-KES/MLU 94-3216, KEMA, Arnhem, The Netherlands.

Russel, E.J. and Richard, E.H. (1919) The amounts and composition of rain and snow falling at Rothamsted. J. Agr. Sci., 9:309-337.

Sachs, J. (1892) Lehrbuch der Pflanzenphysiologie, Leipzig.

Sandnes, H. and Styve, H. (1992) Calculated budgets for airborne acidifying components in Europe, 1985, 1987, 1988, 1989, 1990 and 1991. EMEP Report 1/92. MSC-West, Oslo, Norway.

Saussure, N.T. de (1804) Recherches chimiques sur la végétation. Gauthier-Villars, Paris.

Savoie, D.L. and Prospero, J.M. (1982) Particle size distribution of nitrate and sulphate in the marine atmosphere. Geophys. Res. Lett., 9:1207-1210.

Schack, C.J., Sotiris, E.P. and Friedlander, S.K. (1985) A general correlation for deposition of suspended particles from turbulent gases to completely rough surfaces. Atmospheric Environment, 19:953-960.

Schaefer, D.A. and Reiners, W.A. (1990). Throughfall chemistry and canopy processing mechanisms. In: S.E. Lindberg, A.L. Page and S.A. Norton (Editors), Acid precipitation, Vol. 3: sources, deposition and canopy interactions. Springer Verlag.

Schaug, J., Pedersen, U. and Skjelmoen, J.E. (1991). EMEP Co-operative programme for monitoring and evaluation of the long-range transmission of air pollutants in Europe, Data Report 1989, part 1: Annual Summaries, Norwegian Institute for Air Research, EMEP/CCC-Report 2/91.

Schemenauer, R.S. (1986) Acidic deposition to forests: the 1985 Chemistry of High Elevation Fog CHEF. Project. Atmos. Ocean, 24:303-328.

Schjörring, J.K. and Byskov-Nielsen, S. (1991) Ammonia emission from barley plants: field investigations 1989 and 1990. In: Nitrogen and phosphorus in soil and air., pp 249-265. national Agancy of Environmental Protection, Ministry of Environment, Denmark.

Schlösing, T. (1874) Sur l'Ammoniaque de l'atmosphère. Compt. Rend., 80:175-178.

Schneider, T. and Bresser, A.H.M. (1988) Evaluatierapport Verzuring. Report No. 00-06. National Institute of Public Health and Environmental Protection, Bilthoven, The Netherlands.

Schutter, M.A.A. and Leeuw, F.A.A.M. de (1991) Zure depositie in Nederland: scenarioresultaten voor 1994 en 2000. Report No. 222101008. National Institute of Public Health and Environmental Protection, Bilthoven, The Netherlands.

Schwela, D. (1977) Die trockene Deposition gasförmiger Luftverunreinigungen. Schriftenreihe de Landesanstalt für Immissionsschutz, Heft, 42:46-85.

Sehmel, G.A. (1980) Particle and gas dry deposition: a review. Atmospheric Environment, 14:983-1011.

Sehmel, G.A. and Hodgson, W.H. (1980) A model for predicting dry deposition of particles and gases to environmental surfaces. AICHE Symp.Series, 76:218-230.

Sehmel, G.A. (1983) Particle dry deposition measurements with dual tracers in field experiments. In: Pruppacher et. al. (Editors), Precipitation scavenging, Dry deposition and Resuspension. Elsevier Science Publishing Co., Inc., Amsterdam.

Seinfeld, J.H. (1986) Atmospheric chemistry and physics of air pollution. John Wiley and Sons, New York.

Sevruk, B. (1993) Checking precipitation gauge performance. In: S. Couling (Editor), Measurement of Airborne pollutants. Butterworth Heinemann, Oxford, pp. 89-107.

SFT (1991) Overvåking av langtransportert forurenset luft og nedbor, Årsrapport 1989. Statlig program for forurensningsovervåking, Rapport 437/91 (in Norwegian).

Shaw, R.H., Hartog G. den and Neumann, H.N. (1988) The influence of foliar density and thermal stability on profiles of reynolds stress and turbulence intensity in a deciduous forest. Boundary-Layer Met., 45:391-409.

Sievering, H., Enders, G., Kins, L., Kramm, G., Ruoss, K., Roider, G., Zlger, M., Anderson, L. and Dlugi, R. (1994) Nitric acid, particulate nitrate and ammonium profiles at the Bayerischer wald: evidence for large deposition rates of total nitrate. Atmospheric Environment, 28:311-315.

Sisteron, D.L., Bowersox, V.C., Olsen, A.R., Meyers, T.P. and Vong, R.L. (1989) Deposition monitoring: methods and results. State of Science/Technology Report No. 2. National Acid Precipitation Assessment Program.

Slanina, J. Römer, F.G. and Asman, W.A.H. (1982) Investigation of the source regions for acid deposition in the Netherlands. Proc. CEC Workshop on Physic-Chemical behaviour of atmospheric pollutants, 9 September, Berlin, 1982.

Slanina, J. (1985) Achtergrondmetingen in Neerslag. Report No. ECN-85-40. ECN, Petten, The Netherlands.

Slanina, J., Möls, J.J. and Baard, J.H. (1988) The influence of outliers on results of wet deposition measurements as a function of measurement strategy. Report No. ECN-88-006, ECN, Petten, The Netherlands.

Slanina, J., Keuken, M.P., Arends, B., Veltkamp, A.C. and Wyers, G.P. (1990) Report on the contribution of ECN to the second phase of the Dutch priority programme on acidification. ECN, Petten, The Netherlands.

Slinn, S.A. and Slinn, W.G.N. (1980) Predictions for particle deposition on natural waters. Atmospheric Environment, 14:1013-1016.

Slinn, W.G.N. (1982) Predictions for particle deposition to vegetative surfaces. Atmospheric Environment, 16:1785-1794.

Smith, R.A. (1872) Air and Rain, The Beginnings of Chemical Climotology. Longmans Green, London.

Smith, F.B. and Carson, J.B. (1977) Some thoughts on the specification of the boundary-layer relevant to numerical modelling. Boundary-layer Met., 12:307-330.

Smith, W.H. (1981) Forest vegetation as a sink for gaseous contaminants. Springer Verlag, New York.

Spedding, D.J. (1969) Uptake of sulphur dioxide by barley leaves at low sulphur dioxide concentrations. Nature, 224:1229-1234.

Spranger, T. (1992) Erfassung und ökosystemare der atmosphärischen Deposition und weitere oberirdischer Stofflüsse im Bereich der Bornhöveder seen Kette. PhD Thesis, Kiel University, Germany.

Stanners, D. and Bourdeau, Ph. (1995), Europe's Environment, The Dobrís Assessment. Report prepared by the European Environmental Agency Task Force, Copenhagen.

Stedman, J.R.; Heyes, C.J. and Irwin, J.G. (1990) A comparison of bulk and wet-only precipitation collectors at rural sites in the United Kingdom. Water Air Soil Pollut., 52:377-395.

Steingröver, E.G. and Jans, W.W.P. (1994) Physiology of forest-grown Douglas-fir trees. Effects of air pollution and drought. Final Report, APV III project 793315. IBN-DLO Research Report No. 94/3.

Stelson, A.W. and Seinfeld, J.H. (1982) Relative humidity and temperature dependence of the ammonium nitrate dissiciation constant. Atmospheric Environment, 16:983-992.

Stull, R.B. (1988) An introduction to Boundary-layer meteorology. Kluwer Academic Publishers, Dordrecht, The Netherlands.

Sutton, M.A., Fowler, D. and Moncrieff J.B. (1989) Measurements of atmospheric ammonia and the assessment of its exchange with vegetative surfaces. In: Changing composition of the troposphere, Special environmental Report No. 17, WMO, Geneva.

Sutton, M.A. (1990) The surface/atmosphere exchange of ammonia. PhD Thesis. University of Edinburgh, UK.

Sutton, M.A., Moncrieff, J.B. and Fowler, D. (1992) Deposition of atmospheric ammonia to moorlands. Environ. Pollut., 75:15-24.

Sutton, M.A., Pitcairn, C.E.R. and Fowler, D. (1993) The exchange of ammonia between the atmosphere and plant communities. Advances in Ecological Research Vol. 24, 301-393.

Swap, R.M., Garstang, M. and Greco (1992) Saharan dust in the Amazon Basin. Tellus, 44B:133-149

Tanner, R.L. (1989) Sources of acids, bases, and their precursors in the atmosphere. In: S.E. Lindberg, A.L. Page and S.A. Norton (Editors), Acidic Precipitation,Vol. 3. Springer-Verlag, New York.

Taylor, G.E., McLaughin, S.B., Shriner, D.S. and Selvidge, W.J. (1983) The flux of sulphur containing gases to vegetation. Atmospheric Environment, 17:789-796.

Taylor, G.E. and Tingley, D.T. (1983) Sulphur dioxide flux into leaves of Geranium carolinianum L. Plant Physiol., 72:237-244.

Thom, A.S. (1971) Momentum absorption by vegetation. Quarternary Journal of the Royal Meteorological Society, 97:414-428.

Thom, A.S. (1975) Momentum, mass and heat exchange of plant communities. In: J.L. Monteith (Editor), Vegetation and Atmosphere. Academic Press, London, pp. 58-109.

Thomas, M.D., Hendricks, R.H., Collier, T.R. and Hill, G.R. (1943) The utilization of sulphates and sulphur dioxide for the sulphur nutrition of alfalfa. Plant Physiol., 18:345-371.

Thomas, R., Arkel, W.G. van, Baars, H.P., Ierland, E.C., Boer, K.F. de, Buijsman, E., Hutten, T.J.H.M. and Swart, R.J. (1988) Emissions of $SO_2$, VOC and $NH_3$ in the Netherlands and in Europe in the period 1950-2030. Report No. 758472002. National Institute of Public Health and Environmental Protection, Bilthoven, The Netherlands.

Thorne, P.G., Lovett, G.M. and Reiners, W.A. (1982) Experimental determination of droplet impaction on canopy components of Balsem fir. J. Appl. Met., 23:1413-1416.

Tiegs, E. (1927) Pflanzen und Giftgase, inbesondere Schweflige Säure. Kleine Mitt. Mitgl. Ver. Wasser-, Boden und Lufthygiene, 3:314-328.

Tukey, H.B. and Morgan, J.V. (1963) Injury to foliage and its effect upon the leaching of nutrients from above-ground plant parts. Plant Physiol., 16:557-564.

Tukey, H.B. (1970) The leaching of substances from plants. In: L. Machlis (Editor), Annual review of plant physiology, Vol. 21.

Tuovinen, J.P., Barrett, K. and Styve, H. (1994) Transboundary acidifying pollution in Europe: Calculated fields and budgets 1985 - 1993. EMEP/MSC-W, Report 1/94, Norwegian Meteorological Institute, Oslo.

Turner, N.C., Waggoner, P.E. and Rich, S. (1973) Removal of ozone by soil. J. Environ. Qual. 2:259-264.

Turner, N.C., Waggoner, P.E. and Rich, S. (1974) Removal of ozone from the atmosphere by soil and vegetation. Nature, 250:486-489.

UK Review group on acid rain (1990) Acid deposition in the United Kingdom 1986-1988. Warren Spring Laboratory, UK.

Ulden, A.P. van and Holtslag ,A.A.M. (1985) Estimation of atmospheric boundary layer parameters for diffusion applications. J. Climate. Appl. Meteor., 24:1196-1207.

Ulrich, B. (1983) Interaction of Forest Canopies with Atmospheric Constituents: $SO_2$, Alkali and Earth Alkali Cations and Chloride. In: B. Ulrich and J.Pankrath (Editors), Effects of Accumulation of Air Pollutants in Forest Ecosystems. D. Reichel Publ. Co., pp. 33-45.

Ulrich, E. and Williot, B. (1993) Les depot atmospheriques en France de 1850 a 1990. L'Office National de Forêt, Fontainebleau, France.

Valdez, M.P., Bales, R.C., Stanley, D.A. and Dawson, G.A. (1987) Gaseous deposition to snow 1. Experimental study of $SO_2$ and $NO_2$ deposition. J. Geophys. Res. 92:9779-9787.

Vermetten, A.W.M., Hofschreuder, P., Duyzer, J.H., Bosveld, F.C. and Bouten, W. (1992) Dry deposition of $SO_2$ onto a stand of Douglas fir: The influence of canopy wetness. In: S.E. Schwartz and W.G.N. Slinn (Editors), Proc. 5th IPSASEP conference, Richland, USA, 15-19, June 1991. Hemisphere Publishing Corporation, Washington.

Vermetten, A.W.M., Hofschreuder, P., Versluis, A.H., Bij, E.S. van der, Tongeren, J. van, Molenaar, E., Houthuyzen, J.D. and Veld, F. in 't (1990) Air pollution in forest canopies. Report No. R-424, Wageningen Agricultural University, The Netherlands.

Vermeulen, A.T., Wyers, G.P., Römer, F.G., Leeuwen, N.P.M. van, Draaijers, G.P.J. and Erisman, J.W. (1994) Fog deposition on Douglas fir forest, ECN Report RX-94-100, Petten, The Netherlands.

Verver, G.H.L. (1986) Terreinclassificatie voor regionale verspreidingsmodellen. Technical Report TR-81, Royal Netherlands Meteorological Institute, De Bilt, The Netherlands.

Ville, G. (1850) Note sur l'assimilation de l'azote du l'air, par les plantes, et sur l'influence qu'excerce l'ammoniaque dans la végétation. Compte Rendus Acad. Sci., Paris, 31:578-580 (in French).

Vogelmann, J.E. and Rock, B.N. (1986) Assessing forest decline in coniferous forests of Vermount using NS-001 Thematic Mapper Simulation data. International Journal of Remote Sensing, 7:1303-1321.

Voldner, E.C., Barrie, L.A. and Sirois, A. (1986) A literature review of dry deposition of oxides of sulfur and nitrogen with emphasis on long-range transport modelling in North America. Atmospheric Environment, 20:2101-2123.

Walcek, C.J., Brost, R.A., Chang, J.S. and Wesley, M.L. (1986) $SO_2$, sulfate and $HNO_3$ deposition velocities computed using regional landuse and meteorological data. Atmospheric Environment, 20:949-964.

Waldman, J.M., Munger, J.W., Jacob, D.J., Flagan, R.C., Morgan, J.J. and Hoffman, M.R. (1982) Chemical composition of acid fog. Science, 218:677-680.

Walmsey, J.L., Taylor, P.A and Keith, T. (1986) A simple model of neutrally stratified boundary-layer flow over complex terrain with surface roughness modulations MS3DJH/3R.. Boundary-Layer Met., 36:157-186.

Walpole, R.E. and Myers, R.H. (1978) Probability and statistics for engineers and scientists. Macmillan Publishing Co. Inc., New York.

Waranghai, A. and Gravenhorst, G. (1989) Dry deposition of atmospheric particles to an old spruce stand. In: H.W. Georgii (Editor),Mechanisms and effects of air pollutant transfer into forests. Kluwer Academic Publishers, Dordrecht, The Netherlands.

Waring, R.H., Schroeder, P.E. and Oren, R. (1982) Application of the pipe model to predict canopy leaf area. Canadian Journal for Forest research, 12:556-560.

Warneck, P. (1988) Chemistry of the natural atmosphere. Academic Press, San Diego.

Way, J.T. (1855) The atmosphere as a source of nitrogen to plants being an account of recent researches on this subject. J. Roy. Agr. Soc. Engl., 16:249-267.

Weathers, K.C., Lovett, G.M. and Likens, G.E. (1992) The influence of a forest edge on cloud deposition, In: S.E. Schwartz and W.G.N. Slinn (Editors), Precipitation scavenging and atmosphere-surface exchange. Hemisphere, Washington, pp. 1415-1424.

Weathers, K.C., Likens, G.E., Bormann, F.H., Eaton, J.S., Bowden, W.B., Anderson, J.L., Cass, D.A., Galloway, J.N., Keene, W.C., Kimball, K.D., Huth, P. and Smiley, D. (1986) A regional acidic cloud/fog water event in the eastern United States. Nature, 319:657-658.

Weijers, E.P. and Vugts, H.F. (1990) An observational study on precipitation chemistry data as a function of surface wind direction. Water Air Soil Pollut., 52:115-133.

Welphdale, D.M. and Shaw, R.W. (1974) Sulphur dioxide removal by turbulent transfer over grass, snow, and water surfaces. Tellus, 26:196-204.

Welphdale, D.M. (1987) Atmospheric deposition of acidic pollutants. In: Int Symp. on Acidification and Water Pathways, Bolkesjø, Norway, 4-8 May, 1987.

Wernicke, E. (1927) Lufthygienisches, Kleine Mitt. Mitgl. Ver. Wasser-, Boden und Lufthygiene, 3:257-313.

Wesely, M.L. and Hicks, B.B. (1977) Some factors that affect the deposition rates of Sulfur Dioxide and similar gases on vegetation. J. Air Pollut. Contr. Assoc., 27:1110-1116.

Wesely, M.L., Eastman, J.A., Cook, D.R. and Hicks, B.B. (1978) Daytime variation of ozone eddy fluxes to maize. Boundary-layer Met., 15:361-373.

Wesely, M.L., Cook, D.R. and Williams, R.M. (1981) Field measurements of small ozone fluxes to snow, wet bare soil, and lake water. Boundary-layer Met., 20:459-471.

Wesely, M.L., Cook, D.R., and Hart, R.L. (1985) Measurements and parameterization of particulate sulphur dry deposition over grass. J. Geophys. Res., 90:2131-2143.

Wesely, M.L., Sisteron, D.L., Hart, R.L., Drapapcho, D.L. and Lee, I.Y. (1989) Observations of nitric oxide fluxes over grass. J. Atmos. Chem., 9:447-463.

Wesely, M.L. and Lesht, M. (1989) Comparison of RADM dry deposition algorithms with a site-specific method for inferring dry deposition. Water Air Soil Pollut., 44:273-293.

Wesely, M.L. (1989) Parametrization of surface resistances to gaseous dry deposition in regional-scale numerical models. Atmospheric Environment, 23:1293-1304.

Wesely, M.L., Sisteron, D.L. and Jastrow, J.D. (1990) Observations of the chemical properties of dew on vegetation that affect the dry deposition of $SO_2$. J. Geophys. Res. , 95:7501-7514.

Westman, W.A. and Price C.V. (1988) Detection of air pollution stress in southern California vegetation using Landsat Thematic Mapper band data. Photogrammetric Engineering and Remote Sensing, 54:1305-1311.

Weston, K. and Fowler, D. (1991) The importance of orography in spatial patterns of rainfall acidity in Scotland. Atmospheric Environment, 25A:1517-1522.

Westrate, H. and Duyzer, J.H. (1994) Evaluation of the gradient method for use in monitoring of dry deposition at Speuld based on measurements for ozone. TNO-IMW Report No. R94/104, TNO, Delft.

Whipple, F.L. (1950) Proceedings of the National Academy of Science, Washington, 36:687.

Whipple, F.L. (1951) Proceedings of the National Academy of Science, Washington, 37:19.

Whitby, K.T. (1978) Physical characteristics of sulphur aerosols. Atmospheric Environment, 12:135-160.

White, E.J. and Turner, F. (1970). A method of estimating income of nutrients in a catch of air-borne particles by a woodland canopy. J. Appl.Ecol., 7:441-461.

Whitehead, D. (1978) The estimation of foliage area from sapwood basal area in Scots pine. Forestry, 51(2):137-149.

Wieringa, J. (1981) Estimation of mesoscale and local-scale roughness for atmospheric transport modelling. In: C. Wispelaere (Editor), Air pollution modelling and its application. Plenum Publishing Corp., New York, pp. 279-295.

Wieringa, J. (1992) Updating the Davenport roughness classification. J. Wind Engin. Indust. Aerodynamics, 41.

Wiliams, R.M. (1982) A model for the dry deposition of particles to natural water surfaces. Atmospheric Environment, 17:1933-1938.

Williams, E.J., Parish, D.D. and Feshenfeld, F.C. (1987) Determination of nitrogen oxide emissions from soils: results from a grassland site in Colorado, United States. J. Geophys. Res., 92:2173-2179.

Will, G.M. (1955) Removal of mineral nutrients from tree canopies by rain. Nature, 176:1180.

Wiman, B.L.B. (1988) Aerosol capture by complex forest architecture. In: J.T.A. Verhoeven, G.W. Heil and M.J.A. Werger (Editors),Vegetation structure in relation to carbon and nutrient economy, Academic Publishing, The Hague. pp. 157-183.

Wiman, B.L.B. and Ågren, G.I. (1985) Aerosol depletion and deposition in forests - a model analysis. Atmospheric Environment, 19:335-347.

Wiman, B.L.B. and Lannefors, H.O. (1985) Aerosol characteristics in a mature coniferous forest: methodology, composition, sources and spatial concentration variations, Atmospheric Environment, 19:349-362.

Wiman, B.L.B., Unsworth, M.H., Lindberg, S.E., Bergkvist, B., Jaenicke, R. and Hansson, H.C. (1990) Perspectives on aerosol deposition to natural surfaces: interactions between aerosol residence times, removal processes, the biosphere and global environmental change. J. Aerosol Sci., 21(3):313-338.

Winkel, B.H.de (1990) Onderzoek naar de chemische samenstelling van mist. Report No. 50583-MOC 90-3392, KEMA, Arnhem, The Netherlands.

Witz, G. (1885) Sur la presence de l'acide sulpureux dans l'atmosphère des villes. Compt. Rend., 100:1385-1388.

WMO (1971) Guide to meteorological instrument and observing practices. WMO- No. 8, TP. 3, Geneva.

Wu, Y.L., Davidson, C.I., Dolske, D.A. and Sherwood, S.I. (1992) Dry deposition of atmospheric contaminants to surrogate surfaces and vegetation. Aerosol Sci. Technol., 16:65-81.

Wyers, G.P., Otjes, R.P., Vermeulen, A.T., Wild, P.J. de and Slanina, J. (1992). Measurement of vertical concentration gradients of ammonia by continuous-flow denuders. In: G. Angeletti, S. Beilke, J. Slanina (Editors), Air Pollution Report 39. CEC, Brussels.

Wyers, G.P., Otjes, R.P. and Slanina J. (1993) A continuous-flow denuder for the measurement of ambient concentrations and surface exchange fluxes of ammonia. Atmospheric Environment, 27A:2085-2090.

Wyers, G.P., Veltkamp, A.C., Vermeulen, A.T., Geusebroek, M., Wayers, A. and Möls, J.J. (1994) Deposition of aerosol to coniferous forest. Report No. ECN-C--94-051, ECN, Petten, The Netherlands.

Zanden, D.J. van der and Sluyter R.J.C.F. (1990) Handleiding bij het bosstructuur model TREE. Vakgroep Fysische Geografie, Universiteit Utrecht.

Zeller, K.W., Massman, D., Stocker, D.G., Stedman, D. and Hazlett, D. (1989) Initial results from the Pawnee eddy correlation system for dry acidic deposition research. U.S.D.A. Forest Service Research Paper RM-282.

Zwart, H.J.M.A., Hogenkamp, J.E.M. and Mennen, M.G. (1994) Performance of a monitoring system for measurement of $SO_2$ and $NO_2$ dry deposition fluxes above a forest. Report No. 722108001, National Institute of Public Health and Environmental Protection, Bilthoven, The Netherlands.

This Page Intentionally Left Blank

# INDEX


—A—

Abatement, 18, 19, 23, 26, 325
Ablation, 94, 95
Absorption, 11, 50, 59, 80, 86, 98, 101
Accumulation, 18, 59, 72, 82, 91, 98, 327, 328, 329, 330, 333, 336, 345, 349, 351, 354
Accumulation experiments, 327, 328, 329, 330, 333, 336, 351
Acid gases, 91
Acidification, 1, 3, 4, 5, 6, 7, 12, 16, 19, 23, 38, 40, 56, 97, 310, 313, 325, 338, 341, 349, 355
ACIFORN, 313
Advection, 19, 267, 355
Aerodynamic resistance, 58, 76, 98, 104, 256, 283
Agriculture, 8, 13
Air pollution, 1, 3, 14, 16, 18, 20, 23, 30, 31, 36, 38, 40, 308, 310, 313, 344, 349, 350
Alfalfa, 14, 91
Alkaline particles, 38, 333
Alkalinity, 88
Altitude, 51, 76
Aluminium, $Al^{3+}$, 4, 96, 97, 313, 342, 343, 345, 347, 348, 349, 354
Ammonia, $NH_3$, 5, 6, 8, 9, 10, 11, 13, 24, 25, 26, 27, 28, 29, 30, 31, 32, 33, 34, 41, 42, 43, 44, 47, 51, 56, 69, 79, 81, 87, 88, 91, 92, 93, 94, 99, 101, 102, 103, 253, 254, 255, 256, 257, 259, 260, 261, 262, 263, 264, 265, 266, 268, 269, 283, 300, 307, 310, 313, 316, 318, 319, 320, 321, 322, 323, 324, 325, 326, 336, 338, 339, 340, 341, 342, 343, 344, 345, 346, 347, 349, 350, 351, 352, 354
Ammonium chloride, $NH_4Cl$, 33, 91
Ammonium nitrate, $NH_4NO_3$, 33, 91, 92, 93, 323
Ammonium, $NH_4^+$, 5, 10, 24, 32, 33, 43, 44, 48, 56, 91, 262, 263, 273, 325, 340
Analytical techniques, 12, 17, 53
Anemometer, 69, 255, 314, 327
AOT40, 342, 346, 354
Apoplast, 73, 79
Arable land, 82, 269
Arginine, 345, 347, 348, 349, 354
Artificial branches, 328
Atmospheric chemistry, 21, 30, 32, 38
Atmospheric deposition, 1, 7, 8, 10, 15, 16, 17, 18, 19, 20, 30, 72, 73, 81, 82, 253, 254, 263, 264, 311, 326, 338, 352, 353
Austria, 44, 54

—B—

Balsam Fir, 82
Bare soil, 85
Base cation dry deposition, 74

Base cation total deposition, 334
Belgium, 2, 16, 29, 43, 44, 54
BIATEX, 7
Biomass, 24, 26, 38, 74, 80, 342, 345, 348, 350
Black triangle, 28
Boundary layer, 23, 35, 36, 38, 40, 55, 56, 57, 58, 59, 60, 61, 68
Bowen ratio, 63
Brownian diffusion, 60, 61, 331
Bulgaria, 54
Bulk precipitation, 52, 78, 254, 262, 263, 272, 273, 274
Bulk sampler, 328
Bulk sampling, 52, 53, 54, 58, 78, 99, 254, 262, 263, 270, 271, 272, 273, 274, 300, 332
Buoyancy, 34, 56, 58

## —C—

Cabauw, 67
Calcium, $Ca^{2+}$, 20, 39, 52, 53, 56, 74, 78, 82, 94, 273, 284, 285, 295, 297, 298, 299, 302, 303, 313, 325, 327, 328, 334, 335, 336, 339, 342, 343, 347, 353
Calluna, 254, 262, 263
Canopy exchange, 15, 20, 72, 73, 81, 82, 274, 285, 288, 326, 328, 336, 337, 339, 352, 353
Canopy leaching, 73, 82, 284, 297
Canopy structure, 269, 274, 280, 283, 284, 285, 287, 288, 290, 292, 307, 308
Canopy uptake, 79, 338
Catchment areas, 51, 74
Causal chain, 4, 6
Cell membranes, 73, 79
Chamber methods, 74
Chemical composition, 51, 52, 53, 56, 93, 96, 257, 327, 337, 350
Chloride, $Cl^-$, 9, 15, 16, 20, 39, 43, 56, 73, 74, 84, 94, 273, 284, 285, 294, 296, 297, 298, 299, 300, 302, 303, 307, 309, 325, 328, 336, 339, 353
Climatic change, 1, 84
Cloud droplets, 51, 267, 283
Cloud occurrence, 76
Cloud water deposition, 76
Compensation point, 92, 102
Complex terrain, 20, 69, 72, 80, 83, 85, 90, 253
Concentration gradient, $c_*$, 260, 315, 318, 319
Condensation nuclei, 34, 39, 50, 51
Conditional sampling, 63
Coniferous forest, 85, 342, 343, 351
Conservation areas, 3, 311, 352
Constant flux layer, 30, 58, 63, 69, 89, 317, 350
Continuous flow denuder, 255, 261, 266
Convection, 36, 38, 58
Correlation coefficient, R, 283, 287, 298, 299, 309, 333, 335
Corsican pine, 269, 276, 277, 278
Country average, 43, 44
Critical level, 4, 50, 312, 341, 342, 345, 346, 347, 354
Critical load, 4, 18, 19, 312, 325, 326, 341, 342, 343, 346, 347
Crops, 3, 20, 85, 93, 105, 280
Crown projection, 275, 277, 278, 279, 280, 281, 282, 285, 291, 308
Cuticle, 56, 86, 88, 90, 98, 101, 104
Cuticle resistance, 86, 101
Cyclone, 329
Czech Republic, 28, 44, 54

## —D—

DEADM, 339
Deciduous forest, 85, 88, 105, 341
Deliquescent, 51
Denmark, 19, 29, 43, 51, 311

Density, 19, 53, 62, 63, 65, 72, 94, 254, 267, 275, 276, 280, 281, 282, 284, 287, 290, 291, 298, 299, 308, 309, 312, 349
Denuders, 44, 255, 260, 261, 266, 319, 329
Deposition Filter Method, DFM, 327, 329, 335
Deposition models, 18, 21, 30, 82, 98, 267, 268, 308, 329, 331, 332
Deposition velocity, 30, 32, 39, 57, 58, 61, 62, 74, 86, 90, 91, 93, 94, 104, 256, 258, 259, 260, 264, 322, 324, 325, 327, 330, 334, 351
Dew, 5, 10, 38, 76, 77, 87, 90, 257, 261, 266
Diffusion, 33, 35, 50, 56, 57, 59, 60, 61, 73, 99, 331
Diffusion coefficient, 99
Direct ffects, 2, 4, 344, 346
Displacement height, 58, 65
Dissociation, 33, 92
Douglas fir, 85, 253, 269, 276, 277, 278, 279, 281, 282, 283, 286, 287, 289, 290, 310, 312, 313, 328, 342, 348, 349, 350, 352, 355
DPA, 3, 4, 5, 7
Drag coefficient, 278, 280, 281
Drag force, 65, 267, 280, 281, 309
Droplet size, 76, 87
Drought, 1, 73, 344, 345, 346, 347, 348, 349, 354
Dry deposition measurements, 11, 17, 55, 80, 85, 98, 314
Dunes, 91
Dustfall buckets, 72

—E—

EACN, 14
ECN, 254, 266, 311, 327, 328, 330, 336
Ecological setting, 73
Ecosystem, 1, 4, 18, 20, 23, 38, 39, 56, 74, 78, 80, 81, 83, 84, 91, 103, 312, 325, 342, 344, 345, 349, 354, 355
Ecosystem response, 84
Eddy correlation measurements, 63, 64, 68, 256, 257, 310, 311, 316, 319, 322, 327, 330, 334, 338
Eddy size, 65
Elspeetsche Veld, 71, 85, 253, 254, 255, 257, 258, 259, 260, 262, 264, 265, 310
EMEP, 14, 16, 18, 28, 29, 40, 43, 45, 46, 47, 48, 52, 53, 54, 84, 332, 352
Enclosure technique, 89, 101
Environment, 1, 34
Epicuticular wax layer, 341, 345, 346, 354
Epiphytic lichens, 80
Equilibrium, 30, 33, 34, 39, 59, 70, 87, 89, 92, 93, 98, 323
Error, 10, 52, 53, 68, 257, 258, 260, 266, 273, 274, 275, 310, 318, 319, 329, 330, 331, 333, 334, 335, 350, 351, 352
Error propagation, 257, 258
Estonia, 54
Eucalyptus, 61, 62
Eulerian model, 39
EUROTRAC, 7, 31, 43
Eutrophication, 1, 4, 23, 56, 325, 341, 355
Evaporation, 51, 87, 264, 324, 351
Evaporation rate, 87
Exchange rates, 33, 69
Exposure, 1, 3, 4, 8, 11, 19, 52, 86, 91, 94, 99, 253, 291, 310, 341, 342, 344, 345, 346, 347, 349, 354, 355, 356
External resistance, 98, 100, 101, 103, 104, 324

—F—

Fertiliser, 9
Fertilisers, 25
Fetch, 63, 69, 72, 255, 256, 269, 279, 280, 317

Filterpacks, 327, 329, 335
Fine particles, 93, 297, 327, 351, 352
Finland, 54
Flux profile relations, 316, 319, 332
Fog deposition measurements, 18, 334, 335, 352
Fog droplets, 76, 337
Fog water deposition, 49, 274
Foliage, 73, 76, 80, 276, 278, 297, 345, 346, 347, 348, 350, 354
Forest edges, 19, 51, 82, 88, 90, 253, 267, 268, 269, 271, 272, 273, 277, 279, 280, 290, 291, 292, 293, 294, 295, 296, 297, 298, 299, 300, 303, 304, 306, 308, 309
Forest floor, 20, 72, 82, 88, 89, 96, 105, 279, 337
Forest structure, 268
Fragmentation, 94
France, 3, 9, 12, 14, 15, 29, 43, 44, 51, 54
Friction velocity, $u_*$, 59, 61, 62, 65, 66, 67, 68, 256, 260, 263, 314, 317, 319, 330, 331, 332, 334, 336, 350, 351
Frost, 100, 344, 345, 347, 354
FSSP, 327, 329
Fungal diseases, 347

—G—

Gaseous deposition, 38, 57, 311, 325
Gaussian plume, 31, 40
Gelderse Vallei, 29
Germany, 2, 3, 4, 8, 9, 11, 13, 14, 28, 43, 44, 51, 52, 54
Global radiation, 98, 99, 324
Glutamine, 93
Gradient measurements, 14, 69, 70, 71, 92, 266, 322
Grassland, 85, 88, 102, 255, 269
Gravitational settling, 57, 332
Greece, 54
Groningen, 52
Groundwater, 276, 309, 312, 343, 346, 347, 348
Growth, 3, 8, 93, 272, 291, 310, 313, 330, 331, 332, 341, 342, 344, 345, 346, 347, 348, 351, 354, 355, 356

—H—

Hail, 49, 50
Heat flux, 63, 64, 67, 256, 310, 314, 317
Heathland, 7, 73, 79, 85, 88, 101, 253, 254, 255, 257, 259, 260, 263, 265, 310, 318, 320, 323, 352
Henry's law, 93
Hill cloud, 51
$HNO_2$ deposition, 104
$HNO_3$ deposition, 90
Homogeneous surface, 51, 57, 69
Horizontal gradients, 48, 83
Hungary, 11, 54
Hydrochloric acid, HCl, 2, 5, 6, 7, 9, 16, 24, 33, 41, 43, 70, 91, 93, 104, 300, 329
Hydrogen peroxide, $H_2O_2$, 32, 87
Hydrogen, $H^+$, 7, 283, 284, 285, 313, 328, 336

—I—

IFS, 79, 80, 82
Impaction, 57, 60, 61, 76, 297, 330, 331, 332, 334, 351
In-canopy resistance, 98
Incinerators, 5
In-cloud scavenging, 50
Increased sensitivity, 343, 347
Indirect ffects, 4, 6, 12, 344
Industry, 5, 16, 25, 30, 96, 97
Inert surface, 72, 82
Inferential model, 79, 81, 339
Inferential technique, 19, 74, 79
Inorganic nitrogen, 73, 80, 81
Interception, 57, 60, 76, 263, 334
Internal resistance, 99, 100, 104

Interpolation, 274
Ion exchange, 73
Ireland, 54
Italy, 44, 52, 54

—K—

KEMA, 254, 259, 266, 311, 331

—L—

Lagrangian model, 39
Land use, 19, 83, 280
Larch, 291
Latvia, 54
Leaching, 15, 20, 73, 79, 80, 82, 87, 284, 297, 336, 337, 338, 339, 345, 347, 348, 349, 353, 354
Leaf area density, 291, 308, 309
Leaf area index (LAI), 99, 267, 279, 280, 281, 282, 283, 284, 285, 287, 288, 290, 291, 299, 303, 308, 312
Litterfall, 15, 73, 344
Livestock breeding, 5, 25, 29, 30, 87, 269
Local scale, 17
Long-range transport, 39, 45, 46, 47, 48, 80, 83
Low vegetation, 57, 61, 69, 94, 102, 104, 310, 322, 352
Lowlands, 76
Luxembourg, 43

—M—

Magnesium chloride, $MgCl_2$, 93
Magnesium, $Mg^{2+}$, 20, 39, 52, 56, 74, 78, 82, 94, 96, 273, 284, 285, 294, 296, 297, 298, 299, 300, 302, 303, 309, 313, 325, 327, 328, 334, 336, 339, 342, 343, 347, 349, 353
Maize, 105
Manipulation experiments, 312, 313, 349, 355, 356
Manure, 9, 24, 29, 102, 269
Mass balance, 74, 80, 81, 82, 342, 343
Mass distribution, 93
Mass flux, 64, 65, 66
Mass median diameter, 61, 62, 93, 332, 334
Mesophyl resistance, 98
Meteorites, 6, 38, 94, 95, 96, 97
Meteorology, 31, 35, 40, 63, 83, 333
Micrometeorological measurements, 76, 79, 81, 84, 88, 89, 253, 263, 264, 266, 336
Mineral dust, 39
Mineralisation, 350
Models, 7, 16, 18, 19, 20, 21, 23, 28, 30, 31, 39, 40, 41, 43, 44, 45, 46, 47, 48, 59, 67, 74, 79, 80, 81, 82, 83, 94, 98, 102, 255, 264, 267, 268, 274, 276, 278, 280, 285, 288, 289, 290, 308, 309, 311, 314, 326, 331, 332, 333, 334, 335, 336, 338, 339, 342, 343, 352, 353
Molecular diffusivity, 59
Momentum flux, 56, 58, 59, 63, 64, 65, 67, 76, 267, 310, 316, 317, 350
Monin Obukhov length, 59, 66
Monitoring network, 14, 53, 54, 84
Montsouris, 10
Mountains, 35
Multiple regression model, 82
Mycorrhiza, 348

—N—

$Na^+$ deposition, 82
National Air Quality Monitoring Network (LML), 28, 41, 43, 44, 52, 263, 338
Natural sources, 6, 23, 24, 25, 38
Natural surfaces, 72
Needle loss, 279, 348, 354
Net radiation, 67, 255, 256, 314
Net throughfall, 72, 79, 81, 82, 263, 266, 283, 284, 285, 286, 287, 288, 289, 290,

292, 293, 294, 295, 296, 297, 298, 299, 300, 303, 307, 308, 309
Neutral stability, 13, 56, 65, 66, 68, 69
Neutralising species, 87
$NH_3$ concentration, 11, 42, 43, 92, 93, 101, 257, 261, 264, 266, 322, 341, 346, 354
$NH_3$ deposition, 81, 92, 310
$NH_3$ dry deposition, 81, 266
$NH_3$ emission, 25, 28, 29, 51, 88, 254, 324
$NH_3$ surface resistance, 265
$NH_4^+$ concentration, 92, 341, 346, 354
NHx dry deposition, 81
Nitrate, $NO_3^-$, 5, 6, 10, 20, 24, 32, 33, 41, 43, 44, 47, 51, 52, 53, 56, 73, 74, 76, 78, 80, 81, 92, 93, 94, 253, 262, 263, 273, 283, 284, 285, 286, 288, 289, 293, 296, 297, 298, 299, 300, 301, 303, 306, 307, 308, 309, 325, 327, 328, 329, 330, 334, 335, 336, 339, 340, 343, 347, 348, 349, 351, 352, 353
Nitric acid, $HNO_3$, 5, 8, 9, 10, 11, 24, 30, 32, 33, 34, 41, 43, 44, 46, 51, 56, 60, 70, 74, 80, 90, 91, 92, 93, 94, 104, 284, 300, 323, 329, 337, 339
Nitrogen dioxide, $NO_2$, 5, 24, 28, 32, 33, 41, 42, 43, 44, 48, 60, 64, 70, 80, 89, 90, 91, 104, 253, 254, 255, 256, 259, 260, 262, 265, 268, 299, 300, 301, 307, 310, 314, 315, 316, 318, 319, 322, 323, 326, 336, 337, 338, 339, 341, 346, 350, 352
Nitrogen oxide, NO, 5, 24, 25, 26, 27, 28, 33, 41, 42, 43, 44, 60, 64, 70, 80, 89, 90, 91, 104, 253, 254, 255, 256, 259, 260, 265, 268, 299, 300, 301, 307, 310, 314, 315, 316, 318, 319, 322, 323, 326, 336, 337, 338, 339, 341, 346, 350, 352
Nitrogen oxides, NOx, 5, 6, 24, 25, 26, 27, 28, 29, 30, 31, 32, 33, 34, 43, 44, 46, 81, 89, 104, 254, 269, 313, 341, 342, 345
Nitrous acid, $HNO_2$, 5, 24, 32, 41, 43, 90, 104, 300, 337, 339, 350
NO emission, 322
$NO_2$ concentration, 41, 42, 43, 265, 322
$NO_2$ concentration measurements, 322
$NO_2$ deposition, 89, 319
$NO_2$ dry deposition, 322
$NO_2$ emission, 259
Norway, 16, 35, 43, 54, 269, 276, 277, 278
NOx concentration, 43, 345
NOx deposition, 81
NOx dry deposition, 81
NOx emission, 26, 28
NOy dry deposition, 81, 352
Nutrients, 15, 20, 73, 254, 269, 284, 297, 311, 313, 325, 343, 344, 345, 347, 348, 349, 350, 354
Nutrition, 8, 10, 86, 99

## —O—

Optimal gowth, 8
Organic acids, 5, 7
Organic nitrogen, 273
Orographic clouds, 51
Overijssel, 29
Oxidants, 32, 87
Ozone, $O_3$, 1, 4, 16, 24, 30, 32, 33, 43, 44, 60, 64, 70, 73, 87, 89, 99, 104, 105, 316, 322, 341, 342, 345, 346, 354, 355

## —P—

PAN deposition, 91, 104
Particle deposition, 57, 80, 94, 325, 329, 330, 331, 332, 333, 334, 338, 351, 353
Pasquill, 34, 65, 66
Pastures, 91
Pb, 327, 330, 333, 334, 335, 336, 351
Petri dishes, 72
pH, 2, 3, 14, 32, 86, 87, 88, 91, 98, 101, 102, 104, 264, 265, 273, 313, 345, 348, 354
Phoretic mechanism, 57
Photostationary equilibrium, 70
Pine, 282, 283

Poland, 28, 44, 54
Pollution climate, 20, 84, 288, 311, 353
Portugal, 54
Potassium, $K^+$, 20, 39, 56, 74, 78, 82, 94, 273, 284, 285, 295, 297, 298, 299, 302, 303, 313, 325, 327, 328, 334, 336, 339, 342, 343, 347, 349, 352, 353
Potential acid total deposition, 7, 353
Potential temperature, 64
Power plants, 5, 24
Prandtl number, 59, 60
Precipitation amount, 53
Precursor, 32, 34, 87, 91

—R—

Ra, 58, 59, 90, 98, 256, 257, 258, 259, 264, 318, 319
RADM, 80
Rain gauge, 328
RAINS, 19, 79, 81
Random errors, 318, 319, 335, 350
Range land, 100
Rb, 59, 60, 90, 98, 256, 257, 258, 259, 264, 318, 319, 323, 332
Reaction rate, 32, 33, 38
Reduced nitrogen, NHx, 7, 11, 41, 81, 264, 339, 340, 349, 352
Refineries, 5, 24, 25
Relative humidity, 33, 34, 50, 86, 88, 91, 98, 101, 102, 103, 255, 261, 262, 265, 266, 314, 320, 322, 324, 332, 333
Remote sensing, 308
Residence time, 32, 33, 41, 81
Resistance analogy, 57, 60, 74, 98, 258, 264, 332
Rijnmond area, 28
RIVM, 36, 41, 43, 44, 54, 254, 262, 274, 311, 338
Root, 3, 73, 342, 343, 344, 345, 347, 348, 349, 353, 354
Rothamsted, 10
Rotterdam, 313
Rough surface, 57, 59, 284, 311, 325, 332, 352
Roughness length, 58, 62, 67, 68, 278, 280, 281, 282, 283, 284, 285, 286, 287, 288, 289, 290, 291, 307, 308
Roughness transitions, 253, 268, 272, 296
Royal Netherlands Meteorological Institute (KNMI), 36, 53, 299, 313, 316
Russian Federation, 54
RUU, 254, 311

—S—

Sahara dust, 15
Saturation, 92, 264, 265, 347, 350
Scavenging, 49, 50, 51, 325
Scavenging ratio, 325
Scotts pine, 269, 276, 277, 278, 279, 281, 282, 283, 286, 287, 289, 290
Sea or oceans, 6, 13, 15, 24, 25, 26, 32, 36, 37, 38, 76, 82, 89, 91, 93, 94, 96, 284, 300, 306, 308, 309, 340
Sea salt, 24, 32, 284, 300, 306, 308, 309, 340
Seaspray, 38
Sedimentation, 62, 76, 78, 330, 334, 335, 351, 352
Selection criteria, 318, 319, 321, 322
Senescence, 92
Silhouette area, 276, 278, 280, 283, 298
Silicium, 96, 97
small scale, 19
Smog, 8, 31, 262, 345
Snow cover, 9, 10, 11, 13, 15, 16, 35, 38, 49, 50, 56, 85, 89, 90, 100, 274, 331
$SO_2$, 2, 5, 6, 8, 12, 14, 21, 24, 25, 26, 27, 33, 43, 79
$SO_2$ concentration, 14, 43, 341, 345
$SO_2$ conentration, 14
$SO_2$ deposition, 88, 101

$SO_2$ dry deposition, 14, 80, 85, 86, 87, 101, 256, 310
$SO_2$ emission, 26, 28
Sodium chloride, NaCl, 15, 93
Sodium, $Na^+$, 9, 20, 39, 52, 53, 56, 73, 74, 78, 82, 84, 273, 284, 285, 294, 296, 297, 298, 299, 300, 302, 303, 306, 307, 309, 313, 325, 327, 328, 334, 336, 339, 340, 353
Soil, 3, 5, 7, 9, 14, 20, 24, 25, 82, 88, 89, 90, 104, 269, 276, 312, 325, 341, 342, 343, 344
Soil derived sulphate, 79
Soil dust, 10, 93, 97, 297
Soil loads, 15, 19, 20, 72, 311, 312, 326, 344, 349
Soil resistance, 86, 98
Source contribution, 18, 25
Sources, 5, 10, 12, 14, 16, 17, 23, 24, 25, 26, 30, 31, 34, 38, 40, 48, 51, 52, 53, 56, 69, 78, 81, 84, 89, 96, 97, 269, 296, 303, 313, 325, 355
SOx dry deposition, 57, 79
SOx total deposition, 352
Spatial variability, 18, 72, 81, 84, 272
Specific heat, 63, 64
Speulder forest, 57, 70, 71, 76, 81, 82, 85, 253, 281, 310, 311, 312, 313, 314, 315, 316, 319, 321, 326, 328, 329, 332, 333, 336, 337, 338, 339, 340, 341, 342, 343, 344, 345, 346, 347, 348, 349, 350, 352, 353, 354, 355, 356
Spruce, 81, 82, 269, 276, 277, 278
Stability classes, 40
Stability correction, 66, 67, 68, 69
Stability function, 59, 66
Stable conditions, 36, 38, 65, 66, 67, 68, 73, 317
Standard deviation of wind direction, 67, 68, 69
Statistical errors, 68
Stem density, 72, 275, 280, 312
Stemflow, 5, 15, 20, 72, 79, 255, 262, 337
Stomata, 56, 59, 79, 86, 98, 99, 103, 104, 268, 322, 336, 338, 346, 354
Stomatal conductance, 72
Stomatal control, 89, 104, 345
Stomatal resistance, 86, 90, 98, 99, 100, 101, 103, 268, 324
Stress, 63, 65, 344, 348, 354, 355, 356
Sub-grid effects, 39
Submicron, 41, 57, 327, 332
Substomatal cativity, 92
Sulphate, $SO_4^{2-}$, 5, 9, 12, 13, 20, 24, 33, 39, 41, 43, 44, 45, 51, 52, 53, 56, 73, 76, 78, 79, 80, 82, 87, 88, 93, 94, 253, 262, 263, 264, 266, 273, 283, 284, 285, 286, 288, 289, 293, 296, 297, 298, 299, 300, 301, 303, 306, 307, 308, 309, 325, 327, 328, 330, 334, 335, 336, 337, 339, 352, 353
Sulphur dioxide, $SO_2$, 5, 6, 12, 14, 24, 25, 26, 28, 29, 30, 31, 32, 34, 41, 42, 43, 44, 45, 51, 56, 60, 74, 79, 80, 85, 86, 87, 88, 89, 90, 91, 99, 101, 102, 103, 104, 105, 253, 254, 255, 256, 257, 258, 259, 261, 262, 263, 264, 265, 266, 268, 269, 283, 299, 300, 301, 307, 310, 313, 314, 315, 316, 318, 319, 320, 321, 326, 329, 336, 337, 338, 339, 341, 342, 345, 346, 350, 352
Sulphur oxides, SOx, 7, 57, 79, 264, 339, 340, 352
Sulphuric acid, 2, 8, 9, 11, 12, 13, 16, 24, 30, 32, 33, 34, 284
Surface accumulation, 18, 72, 82
Surface drag, 35
Surface resistance parametrisation, 79, 320, 321, 338, 351
Surface temperature, 88, 99
Surface wash methods, 267, 268, 338
Surface water, 73, 98, 265, 341
Surface wetness, 38, 77, 87, 257, 261, 262, 265, 266, 268, 320, 351

Sweden, 35, 52, 54, 74, 80, 101
Switzerland, 44, 54

—T—

Target loads, 18
Temperature, 33, 34, 35, 36, 38, 48, 53, 63, 64, 67, 73, 78, 88, 90, 92, 98, 99, 101, 256, 314, 316, 317, 323, 333
Temperature inversion, 35, 317
Thermodenuder, 255, 259, 266, 327, 335
Throughfall deposition estimates, 20
Throughfall measurements, 71, 73, 76, 79, 80, 81, 253, 254, 263, 264, 311, 326, 328, 353
Throughflow, 263, 264
TNO, 254, 311, 313, 316, 317, 327, 330, 336
Topography, 51
TOR, 43
Trace gases, 12, 23, 39, 56, 57, 59, 254
Traffic, 5, 24, 25, 259, 269
Trajectories, 40
Transformation, 23, 31, 53
Transpiration, 104, 268, 297, 344, 345
TREND, 18, 28, 40, 41, 43, 44, 80, 332
Trends, 10, 18, 26, 28, 43, 83, 84
Tunnel sampler, 327, 329
Turbulence, 34, 35, 51, 52, 56, 57, 58, 59, 68, 90, 258, 316
Turbulent exchange, 65, 267, 268

—U—

Ukraine, 54
Uncertainties, 280, 337, 343
Understorey, 291, 296, 337, 344, 347
United Kingdom, 19, 44, 52, 54
Unstable conditions, 38, 56, 65, 66, 67, 68
Urban areas, 51, 100
Utrecht, 9, 52, 269, 273, 311
Utrechtse Heuvelrug, 85, 253, 269

—V—

Variance, 63, 257, 286, 292, 321, 324
Vegetation, 2, 3, 4, 5, 7, 8, 12, 14, 16, 19, 24, 39, 49, 57, 59, 61, 69, 72, 74, 76, 77, 84, 85, 86, 88, 89, 90, 91, 92, 93, 94, 98, 99, 100, 101, 102, 103, 104, 254, 263, 264, 267, 268, 279, 291, 296, 310, 313, 321, 322, 331, 337, 341, 343, 347, 352
Veluwe, 253, 254, 310, 312
Vertical gradients, 321, 350
Visual damage, 342
Vitality, 20, 279, 281, 312, 313, 344, 346, 348, 349, 354, 355
Volcanoes, 6, 15, 24, 38
Von Karman constant, 65

—W—

Water bodies, 85
Water layers, 56, 86, 88, 91, 92, 102, 262, 265, 338, 342, 346, 354
Water resistance, 98
WEINTE factor, 292, 296, 297, 298, 299, 300, 303, 306
Wet denuder, 329
Wet deposition measurements, 17, 84
Wetlands, 26, 100
Wheat, 92
Wind direction, 2, 12, 16, 36, 38, 68, 69, 256, 257, 299, 300, 301, 302, 303, 309, 314, 333
Wind profile, 66, 68, 69, 278, 303
Wind shear, 35, 56
Wind speed, 8, 16, 36, 38, 58, 59, 61, 63, 64, 68, 69, 90, 92, 93, 98, 256, 267, 268, 277, 284, 298, 299, 300, 308, 309, 316, 333
Windthrow, 312, 344, 348, 349

—Z—

Zegveld, 255

This Page Intentionally Left Blank